UNIVERSITY OF SOUTHAMPTON

FACULTY OF NATURAL AND ENVIRONMENTAL SCIENCES

Centre for Biological Sciences

Unravelling zinc homeostatic mechanisms in the crop plant barley

by

Ahmad Zulhilmi Bin Nazri

Thesis for the degree of Doctor of Philosophy

September 2016

UNIVERSITY OF SOUTHAMPTON

ABSTRACT

FACULTY OF NATURAL AND ENVIRONMENTAL SCIENCES

Cellular and Molecular Biology

Thesis for the degree of Doctor of Philosophy

Unravelling zinc homeostatic mechanisms in the crop plant barley

Ahmad Zulhilmi Bin Nazri

Zinc (Zn) is an essential micronutrient in plants but becomes toxic when present in excess, with nutritional extremes leading to agricultural yield losses. Homeostatic mechanisms are in place to control cellular Zn levels with transcription factors and membrane transport proteins playing vital roles. In *Arabidopsis thaliana*, two F-group bZIP transcription factors, bZIP19 and bZIP23, are proposed to sense and respond to Zn deficiency by regulating the expression of particular Zn membrane transporters, ZIPs (ZRT/IRT-like proteins). In this thesis, four unique *bzip19 bzip23* knockout mutants with different combinations of T-DNA insertion sites were generated and shown to be hypersensitive to Zn-deficiency. To understand the role of F-group bZIPs in the economically important crop *Hordeum vulgare* (barley), HvbZIP1, 10, 56, 57, 58, and 61 were cloned and characterized to various extents. *HvbZIP56, HvbZIP57, HvbZIP62* but not *HvbZIP1* partially rescue the hypersensitive phenotype of the *A. thaliana bzip19-4 bzip23-2* mutant. HvbZIP56 was localised to the cytoplasm and nucleus when expressed in *A. thaliana* and tobacco. Promoter analysis demonstrates that barley ZIP transporters that are up-regulated under Zn deficiency contain cis Zn-deficiency response elements (ZDREs), similarly to *A. thaliana*. Overall, these results indicate that the mechanisms operating in controlling Zn levels in barley are conserved.

Two transporters, AtHMA3 (a P_{1B-2}-type ATPase) and AtMTP1 (a Metal tolerance protein) have been implicated in sequestering Zn in Arabidopsis vacuoles to alleviate Zn toxicity. In this study, only the *mtp1* mutant and not the *hma3* mutant showed hypersensitivity to high Zn levels. HvHMA3 (a barley P_{1B-2}-ATPase) when expressed in *mtp1* rescued this hypersensitivity indicating a role in Zn transport, although this could not be confirmed by expression in *S. cerevisiae*. This study represents a significant step forward in understanding the mechanisms controlling Zn responses in cereal crops, and will aid in developing strategies for crop improvement.

Table of Contents

Table of Contents ..... **i**

List of Tables ..... **vii**

List of Figures ..... **ix**

DECLARATION OF AUTHORSHIP ..... **xv**

Acknowledgements ..... **xvii**

Definitions and Abbreviations ..... **xix**

Chapter 1: General Introduction **1**

1.1 Zn is an essential heavy metal micronutrient 1

1.1.1 Cereals are the staple food in many countries but are low in Zn 4

1.2 Zn and Cd toxicity to plants 6

1.3 Cu, Fe, and Mn 7

1.4 Plant biotechnology strategies related to Zn and Cd 9

1.4.1 Biofortification 10

1.4.2 Phytoremediation 11

1.5 Zn homeostatic mechanisms in plants 12

1.5.1 Sensors 13

1.5.2 Membrane-bound transporters involved in Zn homeostasis 18

1.5.2.3 The cation diffusion facilitator (CDF) transporters 27

1.5.3 The role of Zn binding proteins/chelators in Zn homeostasis 31

1.5.4 miRNA regulation of Zn homeostasis in plants 33

1.6 Cd sensing in plants 33

1.7 Tools for studying protein function 34

1.7.1 Bioinformatics 34

1.7.2 *A. thaliana* T-DNA insertional mutants 36

1.7.3 Heterologous expression in *S. cerevisiae* 36

1.8 Aims 38

Chapter 2: Materials and Methods **41**

2.1 Gene and protein nomenclature 41

2.2 Plant material and growth conditions 41
2.2.1 Growth of *A. thaliana* for metal-tolerance assays on plates 42
2.2.2 Growth of *A. thaliana* seedlings in hydroponic assays 42
2.2.3 Growth of barley in hydroponic assays 42
2.3 *A. thaliana* transformation using the floral dip method 44
2.4 *A. thaliana* fresh weight measurement 46
2.5 Growth of *S. cerevisiae* 46
2.5.1 Culturing *S. cerevisiae* strains 46
2.5.2 *S. cerevisiae* transformation 47
2.5.3 *S. cerevisiae* drop testing for growth assays 47
2.6 Standard molecular biology methods 47
2.6.1 Bacterial cells preparation 47
2.6.2 Plasmid Transformation by Heat Shock 50
2.6.3 Plasmid Transformation by Electroporation 50
2.6.4 Plasmid Purification from bacterial cells 51
2.6.5 Genomic DNA Isolation from plant material 51
2.6.6 RNA Isolation 52
2.6.7 cDNA Synthesis 53
2.6.8 DNA Sample Quality Check 53
2.6.9 DNA Amplification by RT-PCR 54
2.6.10 Colony PCR 54
2.6.11 Quantitative RT-PCR (qPCR) 54
2.6.12 Gel Extraction 59
2.6.13 GATEWAY® cloning to introduce barley genes of interest into expression vectors 59
2.6.14 Diagnostic restriction enzyme analysis of plasmids 60
2.6.15 DNA sequencing and analysis 60
2.7 Transient expression in tobacco 60
2.8 Confocal fluorescent microscopy 63
2.9 Bioinformatic analyses 63
2.10 Statistical analysis 66

Chapter 3: Identification and characterization of additional mutant alleles for *A. thaliana* bZIP transcription factors..... 67

3.1 Introduction 67

3.1.1 Reverse genetics and *A. thaliana* 67

3.1.2 *A. thaliana* bZIP19 and bZIP23 are important for the Zn deficiency response .67

3.1.3 Aims 70

3.2 Results 71

3.2.1 Isolation of T-DNA insertion *bzip19 bzip23* double mutants 71

3.2.2 *bzip19 bzip23* double mutants are adversely affected by Zn deficiency 82

3.2.3 *bzip19-4 bzip23-2* and its corresponding single mutants had similar phenotype to *bzip19-1 bzip23-1* and its respective single mutants 82

3.2.4 Double *bzip19 bzip23* T-DNA insertion mutants are adversely affected by Zn deficiency when grown hydroponically 90

3.2.5 Zn-concentration dependency of the *bzip19-4 bzip23-2* double mutant.....90

3.2.6 Other micronutrient deficiencies (Mn, Cu and Fe) do not impact the response of the *bzip19-4 bzip23-2* double mutants compared to WT. 95

3.3 Discussion 102

Chapter 4: Exploring the role of barley bZIP transcription factors in the Zn-deficiency response mechanism 105

4.1 Introduction 105

4.1.1 Barley as a model organism for cereals 105

4.1.2 The binary vector system for *A. thaliana* transformation 105

4.1.3 The regulation of the Zn homeostatic network in plants 106

4.1.4 Localisation of bZIPs 107

4.1.5 Aims 109

4.2 Results 110

4.2.1 Finding F-group bZIPs in barley.....110

4.2.2 Phylogenetic analyses of the F-group bZIPs.....112

4.2.3 Cloning F-group *bZIP* genes from barley cv. Golden Promise 115

4.2.4 Barley bZIP56, bZIP62, bZIP57 but not bZIP1 rescues the Zn-deficiency phenotype of *A. thaliana bzip19-4 bzip23-2* 130

4.2.5 Identifying HvbZIP1b 134
4.2.6 The expression of *HvbZIP56* rescues the *bzip19-4 bzip23-2* double mutant on high Cu and Fe at 1µM Zn supply 142
4.2.7 Localisation of HvbZIP56 in plant cells 142
4.2.8 Regulation of barley bZIPs 149
4.2.9 Expression level of barley F-group *bZIPs* in different tissues 154
4.2.10 Investigating the presence of ZDRE and other core motifs in promoters of barley *ZIPs* and *bZIPs* 154
4.2.11 Investigating the presence of ZDRE and other core motifs in promoters of barley *Asparagine synthetases* (*ASNs*) 158
4.3 Discussion 161
4.3.1 Seven F-group bZIPs were identified in barley using bioinformatics analyses and shown to be expressed 161
4.3.2 Functional complementation as a tool for demonstrating a role for bZIPs in Zn deficiency 162
4.3.3 The presence of ZDRE motifs supports a conserved mechanism for responding to Zn deficiency although they are unlikely to be the sole determinant. 163
4.3.4 Regulation of F-group bZIPs 165
4.3.5 Micronutrient effects at low Zn 166
Chapter 5: Functional Analyses of the barley P_{1B-2}-ATPase, HvHMA3 169
5.1 Introduction 169
5.1.1 Aims 171
5.2 Results 172
5.2.1 Identifying P_{1B-2}-ATPases in barley and wheat 172
5.2.2 Percentage identity of P_{1B-2}-ATPases 172
5.2.3 Membrane topology of P_{1B-2}-ATPases 175
5.2.4 Polymorphism in the coding region of HvHMA3 179
5.2.5 Phylogenetic analyses of P_{1B}-ATPases 179
5.2.6 Isolation of T-DNA insertion *hma3 mtp1* double mutants 186
5.2.7 Single *mtp1-1*, double *mtp1-1 hma3-2* and double *hma3-2 mtp1-1 A. thaliana* mutants are sensitive to Zn toxicity using a plate assay 192

5.2.8 Single *mtp1-1* and double *mtp1-1 hma3-2 A. thaliana* mutants are sensitive to Zn toxicity using a hydroponic system 197
5.2.9 Response of *hma3-2* and *mtp1-1* mutants to Cd 197
5.2.10 Cloning *HvHMA3* gene into *A. thaliana* and *S. cerevisiae* destination vectors 200
5.2.11 Expressing *HvHMA3* gene in *A. thaliana* and *S. cerevisiae* for functional analyses 204
5.2.12 HvHMA3 rescues the Zn-dependent phenotype of the *A. thaliana mtp1-1* mutant 207
5.2.13 Functional analyses of HvHMA3 in *S. cerevisiae* 207
5.2.14 Expression level of barley *P_{1B-2}-ATPases* in different tissues 210
5.3 Discussion 212
5.3.1 Sequence analyses of HvHMA3 and other members of barley and wheat P_{1B-2}-ATPases 212
5.3.2 The effect of knocking out both *AtMTP1* and *AtHMA3* on Zn and Cd sensitivity in *A. thaliana* 214
5.3.3 Functional analyses of HvHMA3 215
Chapter 6: General Discussion 219
6.1 Resolving Zn homeostatic mechanisms in plants 219
6.2 The role of bZIP transcription factors in the Zn-deficiency sensing mechanism 220
6.2.1 Are F-group bZIPs the primary sensors for Zn deficiency? 220
6.2.2 Interaction with the ZDRE 223
6.2.3 Further Post-translational regulation of bZIPs 225
6.3 Downstream targets of F-group bZIPs 227
6.3.1 Zn-regulated genes 227
6.3.2 Broader roles for F-group bZIPs (oxidative stress response) 228
6.4 Other responses to Zn stress 230
6.4.1 The role of miRNA 230
6.4.2 Micronutrient and macronutrient imbalances and cross talk 230
6.5 The vacuole is a crucial compartment for Zn and Cd homeostasis 231
6.6 Potential for agriculture and human nutrition 233
6.7 Conclusion 234

Reference.. 237

Appendix 1 271

Appendix 2 273

Appendix 3 277

List of Tables

Table 1.1 The functions of Zn in plant cells.....3

Table 1.2 Selected references on effect of Cd on plant physiology. 8

Table 1.3 Function of eleven bZIP groups.....17

Table 1.4 Function of barley ZIP membrane transporters.....21

Table 1.5 P_{1B}-ATPase subclasses and their biochemically established substrates 24

Table 1.6 T-DNA insertion collections by various groups 37

Table 2.1 The contents of basal 0.5 MS media. 43

Table 2.2 SC-ura media composition for *S. cerevisiae* culture (liquid assay).....48

Table 2.3 *S. cerevisiae* strains used in this study 48

Table 2.4 Bacterial strains used in this study.....48

Table 2.5 PCR reagent concentrations used for different reactions 55

Table 2.6 Cycling conditions used for different PCR reactions.....55

Table 2.7 Primer purpose, nomenclature and sequences. 56

Table 2.8 Tools used for bioinformatics analysis in this project.....65

Table 3.1 *bzip19* and *bzip23* mutant alleles used in three different studies.....72

Table 3.2 Plant lines crossed to generate heterozygotes and the double *bzip19 bzip23* plants with their mutant allele designation. 78

Table 3.3 Sequencing analysis of the T-DNA insertion site for different mutant lines. (The T-DNA insertion site is indicated by '^'). 81

Table 3.4 Statistical analysis of two-way ANOVA for evaluating interaction between genotype and Zn concentration for experiment given in Figure 3.9 85

Table 3.5 Statistical analysis of two-way ANOVA for evaluating interaction between genotype and Zn concentration for experiment given in Figure 3.11 94

Table 4.1 Sequence information for the barley F-group bZIP. 113

Table 4.2 Percentage identity for barley and *A. thaliana* F-group bZIPs..... 116

Table 4.3 The Gateway-compatible entry vectors constructed 122

Table 4.4 The expression vectors generated for expressing *HvbZIP* genes in plants (*A. thaliana*) in this study 125

Table 4.5 The transgenic *A. thaliana* lines created for expressing *bZIP* genes. Each plasmid was transformed into WT and *bzip19-4 bzip23-2* plants. 127

Table 4.6 Eight barley tissues available for gene expression analyses. The data were extracted from the Morex barley RNA-seq database (Mayer et al., 2012). 156

Table 4.7 ZDRE and the A-, T-, C-, G-box positions in barley *ZIP* (non-shaded) and *bZIP* (shaded) promoters..... 157

Table 4.8 ZDRE and the A-, T-, C-, G-box positions in barley *ASNs* promoters..... 160

Table 5.1 Barley and wheat P_{1B-2}-ATPases identified from bioinformatics analyses..... 173

Table 5.2 Percentage identity/similarity of *A. thaliana*, rice, barley and wheat P_{1B-2}-ATPase protein sequences..... 174

Table 5.3 The number of HvHMA2/3 and HvHMA3 TMs obtained from different programmes.176

Table 5.4 The expression vectors generated for expressing *HvHMA3 gene* in *A. thaliana* and *C. cerevisiae* in this study 202

Table 5.5 The transgenic *A. thaliana* lines created for expressing *HvHMA3* gene..... 206

Table 5.6 Transgenic *S. cerevisiae* strains generated. *S. cerevisiae* strains transformed with yeast expression constructs (Table 5.3)..... 206

List of Figures

Figure 1.1 Elements present in all plants. 3

Figure 1.2 Zn deficiency response network in *A. thaliana*, mediated by the TFs bZIP19 and bZIP23. 14

Figure 1.3 A Zn-sensing model showing the mechanisms of AtbZIP19 and AtbZIP23 TFs under Zn deficiency. 14

Figure 1.4 Phylogenetic tree of barley bZIPs. 16

Figure 2.1 Scheme used to generate transgenic *A. thaliana* lines. 45

Figure 2.2 Vectors used in this study. 61

Figure 3.1 Amino acid multiple alignment of *A. thaliana* F-group bZIPs. 69

Figure 3.2 Steps in isolating *bzip19 bzip23* double mutants 72

Figure 3.3 The relevant sequence information for (A) *AtbZIP19* and (B) *AtbZIP23*. 73

Figure 3.4 Schematic diagrams of *AtbZIP19* and *AtbZIP23* gene structure. 75

Figure 3.5 Genotyping potential *bzip19* and *bzip23* single mutant lines 77

Figure 3.6 Genotyping the progeny from the crosses: 79

Figure 3.7 The screening of potential homozygous:homozygous *bzip19*/bzip23 F2 plants: 80

Figure 3.8 Confirmation of the double mutant alleles at the RNA level 84

Figure 3.9 All four unique *bzip19 bzip23* double mutants show an adverse effect to Zn deficiency. 86

Figure 3.10 Direct comparison of single and double mutant bZIP alleles. 88

Figure 3.11 All four unique *bzip19 bzip23* double mutants show an adverse effect under Zn deficiency. 91

Figure 3.12 Zn-concentration dependency of the *bzip19-4 bzip23-2* double mutant. 96

Figure 3.13 Mn deficiency does not affect the phenotype of Zn deficient seedlings. 98

Figure 3.14 Cu deficiency does not specifically affect *bzip19, bzip23* and *bzip19 bzip23* mutants compared to WT. 99

Figure 3.15 Increasing Fe concentrations does not affect *bzip19-2 bzip23-2* mutants. 100

Figure 4.1 Schematics of the pMDC32 and pMDC83 Gateway-compatible *A. thaliana* destination vectors. 108

Figure 4.2 Six barley *ZIP* genes are up-regulated by Zn deficiency. 108

Figure 4.3 Phylogenetic analyses of F-group bZIP proteins from barley including HvbZIP61 and a range of other species. 111

Figure 4.4 Phylogenetic analyses of F-group bZIP proteins from barley excluding HvbZIP61 and a range of other species. 114

Figure 4.5 Amino acid multiple alignment of *A. thaliana* and barley F-group bZIPs including HvbZIP61. 117

Figure 4.6 Amino acid multiple alignment of *A. thaliana* and barley F-group bZIPs excluding HvbZIP61. 118

Figure 4.7 Seven F-group bZIP products amplified from barley cDNA with Pfu. 119

Figure 4.8 Cloning of *HvbZIP56* into entry vector pENTR and *A. thaliana* expression vector pMDC32. 120

Figure 4.9 Multiple sequence alignment of HvZIP58 from different barley cultivars. 123

Figure 4.10 Multiple sequence alignment of HvbZIP62 from different barley cultivars. 124

Figure 4.11 *A. tumefaciens* transformed with pMDC32 *HvbZIP56*. 126

Figure 4.12 Expression of *HvbZIP56* in *A. thaliana* WT T_3 lines. 128

Figure 4.13 Expression of *HvbZIP56* in *A. thaliana bzip19-4 bzip23-2* T_3 lines. 129

Figure 4.14 Expression of *HvbZIP62* in *A. thaliana bzip19-4 bzip23-2* T_3 lines. 131

Figure 4.15 Expression of *HvbZIP56*, *HvbZIP57*, *HvbZIP62* but not *HvbZIP1* partially rescue Zn-deficiency phenotype of *A. thaliana bzip19-4 bzip23-2* double mutants. 133

Figure 4.16 *HvbZIP56* expressing *bzip19-4 bzip23-2* lines grow to a similar level to *bzip19-4* single mutant under Zn deficiency. 135

Figure 4.17 Expression of *HvbZIP56-GFP* partially rescue Zn-deficiency phenotype of *A. thaliana bzip19-4 bzip23-2* double mutants. 136

Figure 4.18 HvbZIP56 has little influence on the *A. thaliana bzip19-4 bzip23-2* mutant at elevated Zn. 137

Figure 4.19 *HvbZIP56* expression in WT *A. thaliana* does not influence their response to Zn deficiency or Zn excess. 138

Figure 4.20 HvbZIP1b amino acid alignment with *A. thaliana* and barley F-group bZIPs..... 139

Figure 4.21 Cloning of *HvbZIP1b* into *A. thaliana* expression vectors. 141

Figure 4.22 High Cu concentrations influence the response of *bzip19-4 bzip23-2* mutants when supplied with 1µM Zn and the expression of *HvbZIP56* in *bzip19-4 bzip23-2* mutants rescues the phenotype. 143

Figure 4.23 High Fe concentrations influence the response of *bzip19-4 bzip23-2* mutants when supplied with 1µM Zn and the expression of *HvbZIP56* in *bzip19-4 bzip23-2* mutants rescue the phenotype. 144

Figure 4.24 High Mn concentrations do not influence the response of *bzip19-4 bzip23-2* mutants when supplied with 1µM Zn and the expression of *HvbZIP56* in *bzip19-4 bzip23-2* mutants does not have any effect on the mutants. 145

Figure 4.25 Subcellular localisation of bZIP56-GFP in cotyledons. 146

Figure 4.26 Subcellular localisation of bZIP56-GFP in roots. 147

Figure 4.27 Localisation of HvbZIP56-GFP in tobacco..... 148

Figure 4.28 Barley displays deficiency symptoms when grown under Zn-deficient conditions. 150

Figure 4.29 Regulation of *ZIPs* following imposition of Zn-deficiency conditions. 152

Figure 4.30 Real-time PCR to determine gene expression of barley *bZIPs* in roots and shoots of barley over time in response to Zn deficiency..... 153

Figure 4.31 *HvbZIP56* and *HvbZIP62* show no marked changes in response to Zn deficiency measured over a shorter time period. 155

Figure 4.32 Expression pattern of barley F-group *bZIPs* in different tissues. 156

Figure 5.1 Alignment of HvHMA3 with barley, wheat, rice and *A. thaliana* P_{1B-2}-ATPases showing the predicted TMs. 178

Figure 5.2 The predicted membrane protein topology of P_{1B-2}-ATPAses in barley and rice. 180

Figure 5.3 Alignment of HMA3 amino acid sequences from different barley and rice cultivars.183

Figure 5.4 The predicted membrane protein topology of the Haruna Nijo HvHMA3 used in this study. 184

Figure 5.5 Phylogenetic analyses of P_{1B}-ATPases from a range of plant species. 185

Figure 5.6 Phylogenetic analyses of the P_{1B-2}-ATPases family. 187

Figure 5.7 Genotyping potential *hma3-1* (A) and *hma3-2* (B) mutant lines..... 189

Figure 5.8 Genotyping crossed progenies: *hma3-1 x mtp1-1* (A), and *mtp1-1 x hma3-1* amplified with three sets of primer to determine their genotype..... 190

Figure 5.9 The screening of potential homozygous: homozygous *hma3-1 mtp1-1* (A) and *mtp1-1 hma3-2* (B) F2 plants. 191

Figure 5.10 Sequencing analyses of the T-DNA insertion site for *hma3-2* mutant line. 193

Figure 5.11 Mutant alleles for *HMA3* and *MTP1*. 194

Figure 5.12 The two unique *hma3 mtp1* double mutants and *mtp1-1* single mutants but not *hma3* single mutants show an adverse effect to Zn toxicity. 196

Figure 5.13 Zn toxicity phenotype of the *mtp1-1 hma3-2* double mutants in hydroponic assays.198

Figure 5.14 Cd toxicity does not specifically affect *mtp1-1*, *hma3-2* and *mtp1-1 hma3-2* mutants compared to WT..... 199

Figure 5.15 Cloning of *HvHMA3* into the entry vector, pENTR. 201

Figure 5.16 Diagnostic restriction analysis of the pENTR *HvHMA3withstop* entry vector..... 202

Figure 5.17 Cloning of *HvHMA3* into *A. thaliana* expression vector pMDC32 and *S. cerevisiae* expression vector pAG426GAL-ccdB-GFP. 203

Figure 5.18 Expression of *HvHMA3* in *A. thaliana mtp1-1* T_3 lines..... 205

Figure 5.19 HvHMA3 rescues the Zn-toxicity phenotype of the *A. thaliana mtp1-1* single mutant up to 150µM Zn. 208

Figure 5.20 *HvHMA3* expression under a Gal-inducible promoter in *S. cerevisiae*. 209

Figure 5.21 Expression pattern of barley P_{1B-2}-*ATPases* in different tissues.....211

Figure 6.1 Three models of Zn uptake regulation in plant roots. 221

Figure 6.2 Zn homeostasis model in barley 232

DECLARATION OF AUTHORSHIP

I, Ahmad Zulhilmi Bin Nazri

declare that this thesis and the work presented in it are my own and has been generated by me as the result of my own original research.

Unravelling zinc homeostatic mechanisms in the crop plant barley

I confirm that:

1. This work was done wholly or mainly while in candidature for a research degree at this University;
2. Where any part of this thesis has previously been submitted for a degree or any other qualification at this University or any other institution, this has been clearly stated;
3. Where I have consulted the published work of others, this is always clearly attributed;
4. Where I have quoted from the work of others, the source is always given. With the exception of such quotations, this thesis is entirely my own work;
5. I have acknowledged all main sources of help;
6. Where the thesis is based on work done by myself jointly with others, I have made clear exactly what was done by others and what I have contributed myself;
7. None of this work has been published before submission.

Signed: .....

Date: .....

Acknowledgements

I would like to express my sincere appreciation to my supervisor, Dr. Lorraine Williams with her constant guidance and encouragement throughout my four years here at the University of Southampton, without which this work would not have been possible. For her unwavering support, I am truly grateful. I am also grateful to all past and present LEW lab members (especially Kerry, Emily, Nick, Nancy, Jon, Franz, Ilectra, Tania, and Emma) who provide a conducive work environment. Thank you to the Malaysian Rubber Board (MRB) for a Scholarship to me to study at the University of Southampton. Without the MRB financial support, this work would not have been possible. Thank you to Dr. John Runions (Oxford-Brookes University, UK) for tobacco seed and the LTI6b-mOrange2 construct. To Dr. Mark Willett for help with the confocal microscopy. It is my privilege to thank my parents (Nazri Bin Ahmad and Rusmawati Binti Mohd Abd Kadir) and family who relentlessly supporting me with everything they possibly can.

This thesis is dedicated to the loving memory of my beloved grandfather, Muhd Abd Kadir. His humour, love, and care, always bring joy to me and people around him. I love you and always miss you. Thank you for everything atuk.

Definitions and Abbreviations

ºC	degrees Celsius
2D	two-dimensional
TM3	third transmembrane segment
TM6	sixth transmembrane segment
ABC	ATP-Binding Cassette protein
ABRC	Arabidopsis Biological Resource Center
Al	aluminium
ANOVA	analysis of variance
Arg	arginine
As	arsenic
ATP	adenosine triphosphate
B	boron
BAC	bacterial artificial chromosome
bp	basepair
BSA	bovine serum albumin
bZIP	basic leucine zipper transcription factor
C	carbon
CA	carbonic anhydrase
Ca	calcium
CAX	Cation/proton exchanger protein
Car ^{r}	carbenicillin resistance gene
Cd	cadmium
CDF	Cation Diffusion Facilitator

cDNA	complementary DNA
CDS	coding sequence
ChIP	chromatin immunoprecipitation
Cl	chlorine
Co	cobalt
Col	Columbia
CSD	Cu/Zn superoxide dismutase
Cu	copper
Cys	cysteine
dATP	2′-deoxyadenosine-5′-triphosphate
dCTP	2′-deoxycytidine-5′-triphosphate
ddH_2O	double-distilled water
d.f.	degrees of freedom
dGTP	2′-deoxyguanosine-5′-triphosphate
dicot	dicotyledon
DMSO	dimethyl sulfoxide
DNA	deoxyribose nucleic acid
dNTPs	2′-deoxynucleotide-5′-triphosphate
dTTP	2′-deoxythymidine-5′-triphosphate
ECR	environmentally controlled room
e.g.	*exemplī grātiā*, “for example”
EGFP	enhanced green fluorescence protein
EMS	ethyl methyl sulphonate
EMSA	electrophoretic mobility shift assay

EST	expressed sequence tag
et al.	*et alii* meaning “and others”
F_1	first generation
F_2	second generation
Fe	iron
g	unit of gravitational acceleration
G	glycine
Gal	galactose
Gbp	giga base pairs
GDP	guanosine-5’-diphosphate
GFP	green fluorescent protein
GHMM	the generalized hidden Markov model
Gln	glutamine
Glu	glucose
Gly	glycine
GUS	β-glucuronidase
h	hour
H	hydrogen
H^+	proton
H_2O	water
H_2O_2	hydrogen peroxide
HCl	hydrogen chloride
HEPES	4-(2-hydroxyethyl)-1-piperazineethanesulfonic acid
Hg	mercury

His	histidine
HMA	heavy-metal ATPase
Hyg ^{r}	hygromycine resistance gene
IBSC	The International Barley Sequencing Consortium
i.e.	*id est*, "that is"
IWSG	The International Wheat Genome Sequencing Consortium
K	potassium
K^+	potassium ion(s)
kb	kilobase(s)
K_D	dissociation constant
kDa	kilodalton
KH_2PO_4	monopotassium phosphate
KOH	potassium hydroxide
L	litre(s)
Leu	leucine
LB medium	Luria-Bertani broth medium
LB	left border
Mb	megabases
MES	2-(N-morpholino)ethanesulfonic acid
Mg	magnesium
Mg_2Cl_2	magnesium chloride
$MgSO_4$	magnesium sulphate
min (unit)	minute(s)
Mn	manganese

$MnCl_2$	manganese chloride
Mo	molybdenum
monocots	monocotyledons
MOPS	3-(N-morpholino)propanesulfonic acid
mRNA	messenger RNA
MS medium	Murashige and Skoog medium
MTP1	metal tolerance protein 1
mV	millivolts
N	nitrogen
N.A.	numerical aperture
Na^+	sodium ion(s)
NaAc	sodium acetate
NaCl	sodium chloride
Na_2 EDTA	ethylenediaminetetraacetic acid, disodium salt
Na_2HPO_4	disodium phosphate
NaOH	sodium hydroxide
NASC	Nottingham (European) Arabidopsis Stock Centre
Ni	nickel
NMR	nuclear magnetic resonance
NO	nitric oxide
NRAMP	The plant Natural Resistance Associated Macrophage protein
O	oxygen
OD	optical density
ORF	open reading frame

P	phosphorus
PAPS	3’-phosphoadenosine 5’-phosphosulfate
Pb	lead
PBS	Phosphate buffered saline
PCR	polymerase chain reaction
PCR1	Plant Cadmium Resistance 1 protein
PCR2	Plant Cadmium Resistance 2 protein
PCS	phytochelatin synthase
PEG	polyethylene glycol
PIPES	piperazine-1,2-bis[2-ethanesulfonic acid]
PLATE solution	PEG, lithium acetate and TE buffer solution
Pro	proline
qRT-PCR	quantitative reverse-transcriptase polymerase chain reaction
QTL	quantitative trait locus
RB	right border
Rif ^{r}	rifampicin resistance gene
ROS	reactive oxygen species
rpm	rotations per minute
RISC	RNA-independent Silencing Complex
RNA	ribonucleic acid
RNAi	RNA interference
RNA-seq	high-throughput mRNA sequencing
s	second(s)
S	sulphur

SC medium	synthetic complete medium
SC-ura medium	SC medium without uracil
SDS	sodium dodecyl sulfate
Se	selenium
Ser	serine
Si	silicon
siRNA	short interfering RNA
SNP	single nucleotide polymorphism
S.O.C. medium	Super Optimal Broth with Catabolite repression medium
T_0	parental plant
T_1	first-generation (plant/seed)
T_2	second-generation (plant/seed)
T_3	third-generation (plant/seed)
TAE	Tris-acetate-EDTA
TAIR	The Arabidopsis Information Resource
T-DNA	transfer-DNA
TE	Tris-EDTA
TFs	transcription factors
Ti plasmid	tumour-inducing plasmid
TM	transmembrane
URGI	Unité de Recherches en Génomique Info
UTR	untranslated region
UV/TMP	utraviolet/trimethylpsoralen
V	volts

Val	valine
V-ATPase	vacuolar-type H^+-ATPase
v/v	volume/volume
WGS	whole genome shotgun
w/o	without
w/v	weight/volume
WL	white light
Ws	Wassilewskija
YSL	The Yellow Stripe-Like protein
ZDRE	Zinc Deficiency Response Element
ZIFL	The Zinc-Induced Facilitator-Like
ZIP	Zinc-Regulated Transporter, Iron-Regulated Transporter (ZRT-IRT-like) Protein
Zn	zinc

Chapter 1: General Introduction

Micronutrients are chemical element or substances required in trace amounts for the proper growth and development of living organisms (Food and Board, 2001). There is now a growing awareness of the vital importance of micronutrients (many of which are heavy metals) to agriculture because in soils worldwide micronutrient availability limits crop production and influences nutritional quality (Allen et al., 2001, Marschner, 2012). Producing enough nutritious food to support the world's population is a major global issue and thus preventing losses in crop yield, associated with micronutrient deficiency, will contribute to a more sustainable food supply. The micronutrient content of food affects human nutrition and health with micronutrient imbalances leading to disease (White and Broadley, 2009). Plants are the basis of all foodstuffs that we ingest, therefore understanding the processes of plant micronutrient nutrition is highly relevant and improving nutritional aspects is an important breeding and biotechnological goal. Equally, heavy metal pollution is a serious problem worldwide with potentially dangerous bioaccumulation through the food chain (Huang et al., 2008, Dai et al., 2012). There is great interest in approaches aimed at either generating plants which can extract metals more efficiently from the soil and can accumulate and tolerate higher levels of metals or conversely producing crops with superior detoxification properties allowing them to be grown on a wider range of soils (White and Broadley, 2009, Lee et al., 2011, Sharma et al., 2016). To achieve these goals, a clear understanding of heavy metal homeostasis in plants is required. This project investigates transporter proteins and key regulators in order to understand their role in heavy metal homeostasis and potential for biotechnological application.

1.1 Zn is an essential heavy metal micronutrient

Seventeen elements are known to be essential to all plants (Figure 1.1). Those required in relatively large amounts (>0.1% of dry mass) are called macronutrients (Maathuis, 2009) while those required in trace amounts (<0.01% of dry mass) are known as micronutrients (Hansch and Mendel, 2009). Macronutrients include: carbon (C), hydrogen (H), oxygen (O), nitrogen (N), phosphorus (P), potassium (K), calcium (Ca), sulphur (S), and magnesium (Mg). Micronutrients are: boron (B), chlorine (Cl), manganese (Mn), iron (Fe), zinc (Zn), copper (Cu), molybdenum (Mo), nickel (Ni), cobalt (Co). Certain elements that promote growth and may be essential to some taxa are referred to as beneficial elements and include sodium (Na), cobalt (Co), aluminium (Al), selenium (Se) and silicon (Si). The heavy metal micronutrients and beneficial elements are Mn, Fe, Zn, Cu, and Co. Micronutrients can limit the growth of living organisms when they are present in

insufficient quantity (deficiency) or in excessive concentrations, causing toxicity (Alloway, 2008). In addition, there are other heavy metals that have no biological function, but are detrimental to plant growth when present in the environment. These include cadmium (Cd), arsenic (As), lead (Pb) and, mercury (Hg). Heavy metals have been defined as metal elements having a density of greater than 5g cm^{-3} (Weast et al., 1988).

This thesis is concerned mainly with the heavy metal micronutrient Zn. It is important in all living organisms including plants where it is integral to growth and development being required for gene expression and replication (Broadley et al., 2012). Generally, plants with Zn concentrations below 15µg per gram of dry leaf tissue are considered to be Zn-deficient plants (Broadley et al., 2007). Insufficient Zn supply to plants can cause stunted growth due to disturbance of auxin biosynthesis (Henriques et al., 2012) and as a result of increased oxidative stress (Brown et al., 1993). Auxin is required by plants for cell elongation and growth (Fu and Harberd, 2003), however, during Zn deficiency, the auxin concentration decreases, thereby reducing plant growth. A reduction in shoot biomass is usually the first obvious physiological response to Zn deficiency (Cakmak et al., 1996) and the effect is more pronounced in shoots than roots at the later stage (Lombnes and Singh, 2003). Zn-deficient plants can also be characteristically associated with chlorosis and necrosis of the leaves. This phenotype is the result of chlorophyll reduction (Krämer and Clemens, 2006) due to disrupted enzymes especially CA, which is involved in photosynthesis. The main substrate for CAs is Zn and during Zn deficiency CAs cease to function properly (Salama et al., 2006). Application of Zn to a soil deficient in available Zn increased the CA activity in wheat (*Triticum aestivum*) indicating the importance of Zn to CAs in combating Zn deficiency (Singh et al., 2014). Other roles of Zn in plants include plant defence as many defence proteins of *A. thaliana* and rice (*Oryza sativa*) containing Zn finger proteins have been shown to regulate plant cell death (Maldonado-Bonilla et al., 2013, Zhang et al., 2014). In addition, Zn finger proteins are involved in seedling establishment as shown in *A. thaliana* AtTZF1 controlling abscisic acid and gibberellin hormones that affect seedling growth (Lin et al., 2011). Table 1.1 presents some of the varied function of Zn in plants cells.

Zn is vital to human health as around 10% of the human proteome comprises Zn-binding proteins (Andreini et al., 2006). Cellular metabolism could not function properly without Zn; it mediates the catalytic activity of approximately 300 enzymes, acting as a cofactor (McCall et al., 2000, Pedas et al., 2009) and has a structural role in a large number of proteins (Tapiero and Tew, 2003) stabilising their conformation and therefore binding capabilities (Berg and Shi, 1996). Zn deficiency is a widespread problem to human health and well-being, with insufficient dietary intake leading to a magnitude of health problems and diseases (Roohani et al., 2013). This

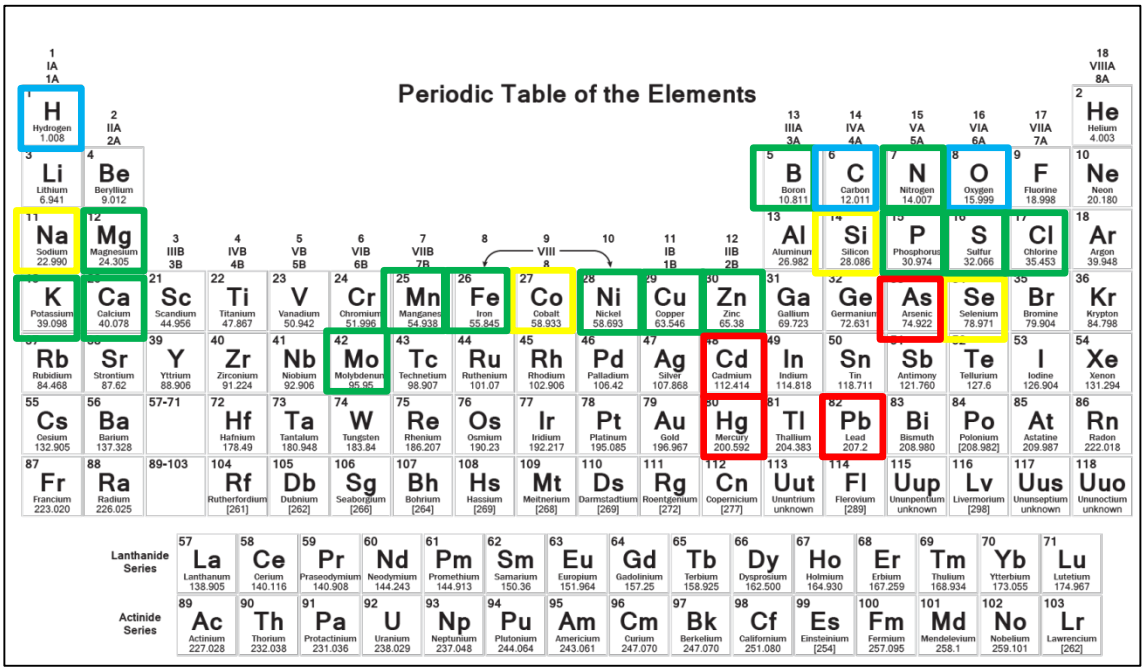

Figure 1.1 Elements present in all plants.

Green, yellow, blue, and red boxes represent essential, beneficial, non-mineral elements, non-essential elements respectively.

Table 1.1 The functions of Zn in plant cells

Function	**Reference**
Stabilize the structure of plant enzymes in all six classes of enzymes (oxidoreductases, transferases, hydrolases, lyases, isomerases and ligase)	Auld (2001), Weisany et al. (2012)
Structurally important for carbonic anhydrase (CA) that catalyses the reversible hydration of carbon dioxide; CA activity is important for photosynthesis. Without efficient photosynthesis, carbohydrate metabolism will be affected	Rengel (1995), Ohki (2006)
Bound to the most abundant form of SOD in higher plant cells, Cu/Zn superoxide dismutase (SOD)	Cakmak (1997)
Involved in regulation of gene expression by forming a specific loop (Zn-finger motif)	Englbrecht et al. (2004)
Maintains the integrity and function of cellular membranes by controlling generation and detoxification of reactive oxygen species	Cakmak (2000)
Maintains RNA polymerase I stability by binding to the enzyme	(Chanfreau, 2013)

includes immune dysfunction (Chasapis et al., 2012), cognitive impairment and developmental retardation (Bhatnagar and Taneja, 2001), psychological disorders, skin lesion and hair loss (Blindauer, 2015). Even mild Zn deficiency is a key factor in malnutrition, contributing significantly to the many deaths annually worldwide from malaria, diarrhoea, measles and pneumonia (Caulfield et al., 2004). This issue is particularly prevalent in developing countries where cereal crops are staple to many civilian diets, yet are inherently low in their nutritional quality due to the low bioavailability of micronutrients within the soil and poor portioning to the edible grain tissue (Cakmak, 2008). According to the world health report (WHO, 2002), 0.8 million deaths a year are attributable to Zn deficiency, ranking it amongst the top 20 global threats to health. As a result, there is a lot of clinical interest into enhancing the amount of Zn incorporated into the diet as a way of treating health problems globally (Galetti et al., 2015, Brnić et al., 2016).

1.1.1 Cereals are the staple food in many countries but are low in Zn

At the base of all food webs, plants have a vast influence on our nutrition. Cereals serve as the main staple food for a large proportion of the world's population but have the shortcoming from a nutrition perspective of having low essential trace elements such as the micronutrient Zn in their edible tissues (Broadley et al., 2007, Zhao et al., 2009, Wessells and Brown, 2012). This is a major issue for global human nutrition. In the past, the focus has been on strategies to increase crop yield; however since micronutrient malnutrition affects around a third to one-half of the world's population, especially women and pre-school children (Gibson et al., 2006), we now recognize that enhancing the micronutrient element content of edible plant foodstuffs is an urgent objective (Center, 2008). Biofortification is the use of traditional breeding approaches and modern biotechnology to enrich the nutritional content of crops (discussed in Section 1.4.1) but for this to be successful, we need to understand the underlying mechanisms controlling micronutrient content.

A further major concern is that, crops yield less and have a lower nutritional quality when grown in soils where Zn availability is low, further jeopardising global food security (Ramesh et al., 2004a, Genc et al., 2009). The level of Zn present within different types of soil can vary considerably and Zn must be present in a soluble form to allow uptake by plants. There are several factors affecting Zn solubility and availability to plants such as total Zn content, soil pH, organic matter, soil temperature and moisture regimes, root distribution, and rhizosphere effects (Sadeghzadeh and Rengel, 2011). A low total Zn concentration in soils such as sandy soils often produces Zn-deficient cereals (Singh et al., 2005). It has been reported that high pH decreases Zn availability to plants when it is adsorbed to the surfaces of various soil constituents, such as metal oxides and clay minerals (Brümmer et al., 1988, Barrow, 1993). A low content of organic matter in

soils can also affect the efficiency of Zn uptake. This was seen as clearly shown in the United States, where the removal of surface soil by land levelling caused poor availability of Zn to the crops (Alloway, 2004) as the subsoil has lower organic matter and, in many cases, also has a higher pH than topsoil (Alloway, 2008).

Soil moisture and low temperature are other factors that cause poor Zn availability to plants by altering the diffusion rate of Zn from soil to the root surface of the plants (Tack et al., 2006). It is important to keep soil moisture at the optimum level. High water content in soil by waterlogging or flooding usually leads to low Zn availability to plants (Saleh et al., 2013), while Li et al. (2015) has reported that soil drying from flooded conditions to 50% maximum water holding capacity has reduced metals availability including Zn. As for temperature related factors, low temperature has been observed to cause low Zn availability in plants. The availability of Zn together with Fe, Mn, and Cu have been reported to be decreased as soil temperature increases in the Eastern Tibetan Plateau of China (Li et al., 2014). Estimates suggest that up to half of all soils used for cereal crop production worldwide do not contain adequate levels of bioavailable Zn to meet plant requirements (Guerinot, 2000).

Zn availability is not only affected by features of the soil but also by its interactions with other soil nutrients. P and N are two common elements to interact with Zn in the soils, which results in Zn-deficiency symptoms in plants. Once again, bad agricultural practices can be the reason for the perilous interaction between Zn and other soil nutrients. The application of N fertilizers is good for enhancing protein production and plant growth but the excessive application of N onto the soil may increase the Zn requirement due to the increased growth and changing rhizosphere pH (Loneragan and Webb, 1993, Alloway, 2004). Meanwhile, it has been well documented that high levels of inorganic phosphate can induce Zn deficiency in plants. For example, CA activity in *Zea mays* decreased with increasing P supply (Soltangheisi et al., 2014) and CA activity has been one way to indicate Zn nutritional status (Soltangheisi et al., 2014). In cereals, a study has shown that high P supply can decrease Zn concentrations in wheat shoots (Imtiaz et al., 2006). Other cation macronutrients can also interact with Zn in soil and consequently decrease the availability of Zn to plants. For example, K, ammonia (NH_4), and Mg have been shown to cause a strong inhibition of Zn absorption and wheat seedlings that are treated with increasing Ca exhibit decreasing Zn concentration in their tissues (Loneragan and Webb, 1993).

Deficiency of Zn on cultivated soils is a worldwide problem so developing crops that can maintain growth and yields under low soil Zn (Zn-efficiency) without the input of costly fertilizers would have clear benefits for sustainable agriculture. Certainly, progress is being made in breeding programmes with the implementation of molecular markers. QTL is extremely valuable

in studying complex traits such as this, but ultimately genetic engineering probably has the most potential in increasing yield and nutritional quality under stress conditions (Sadeghzadeh et al., 2015). To achieve this, more in-depth knowledge of the underlying mechanisms is required.

1.2 Zn and Cd toxicity to plants

As mentioned previously, Zn is an essential heavy metal (Section 1.1) but can be toxic in excess. Although uncommon, Zn toxicity can occur when the soil pH is low (Beyer et al., 2013). Human activity can also cause Zn accumulation in soils. Contamination by smelters and mining waste, incinerators, excessive applications of fertilizers and pesticides, burned rubber residues, galvanized materials, livestock manures and biosolid sewage sludge can elevate Zn concentration in soils (Chaney, 1993). The response to Zn toxicity in plants is generally stunted growth and chlorosis. Root elongation and growth is reduced in the presence of excess Zn and chlorosis can be due to excess Zn displacing Fe in cells (Fukao et al., 2011) and causing oxidative stress (Lin and Aarts, 2012, Remans et al., 2012). Plants require Fe as a cofactor for metabolising the chlorophyll precursor compound, protochlorophyllide, during chlorophyll biosynthesis (Chaney, 1993, Tottey et al., 2003). Excess Zn can also lead to oxidative stress by producing reactive oxygen species (ROS), resulting in nucleic acid and pigment damage (Morina et al., 2010)

Plants also encounter other non-essential transition metals, such as Cd, Pb and Hg. Cd is at a far greater bioavailability in the soil than other non-essential elements (Reeves and Chaney, 2007) acting as a powerful Zn mimic to highjack importing machinery for cellular accumulation (Palmgren et al, 2008). These elements have the potential to be highly toxic, due to their displacement of essential cofactors and high reactivity with sulfhydryl groups, causing protein inactivation (Clemens, 2001; Palmgren et al, 2008). Transfer of these toxic metal into the food chain has serious ecological and human health consequences (Huang et al., 2008, Dai et al., 2012).

Cd can enter the environment through geogenic (geological process) and anthropogenic (human activities) pathways. In the geogenic pathway, Cd occurs mainly in association with Zn ores. Common soil-forming rocks such as igneous rocks, sandstones, and limestones have low Cd concentration and so entry via this route is low (Loganathan et al., 2012). Meanwhile, in the anthropogenic pathway, the emission of Cd into the atmosphere occurs by various processes including smelting of metals; combustion of coal, oil and wood; incineration of wastes; production of paints; electroplating; and manufacturing and disposal of batteries (Liu et al., 2012b). A major contribution of Cd contamination in soil has been the use of P fertilisers which can contaminate the soil environment with 54–58% of Cd (Tirado and Allsopp, 2012). Malidareh et al. (2014) reported that the application of P fertilizers in paddy field increased the Cd content in soils to

0.045–0.052 mg kg^{-1}. Sewage sludge application, manure application, cement industries, and emissions from power stations are other source of Cd contamination (Ok et al., 2010, Ok et al., 2011, Bolan et al., 2013).

Major food crops such as wheat and rice have been shown to accumulate Cd in their grains (Greger and Löfstedt, 2004, Jafarnejadi et al., 2011, Meharg et al., 2013). Thus, it poses health risks to the consumers, as they become the source of Cd entry to humans through the food chain. Cd consumption can cause kidney damage and deteriorate the pulmonary, cardiovascular and musculoskeletal systems (Faroon et al., 2012).

Cd has negative effects on plant growth and development with detrimental effects on the uptake and transport of water and nutrients, photosynthesis, and respiration (Arasimowicz-Jelonek et al., 2011). Cd induces water stress symptoms such as a decrease in stomatal conductance, transpiration rate, and leaf relative water content (Chen and Huerta, 1997), which is the result of physiological alterations in the plasma membrane properties (Astolfi et al., 2012). The effect of toxic Cd level in plants could also result in a decrease in the size and the number of xylem vessels, cellular spaces, and chloroplast (Sandalio et al., 2001). In addition to those changes, toxic levels of Cd can cause: cell wall impregnation by phenolic compounds (Vollenweider et al., 2006); degeneration of phloem sieve tubes (Günthardt-Goerg et al., 1993); thickening of cell wall support tissues (Vollenweider et al., 2006); reduced cambial activity, stomatal closure, and dysfunction of the photosynthetic apparatus in chloroplasts (Sandalio et al., 2001, da Cunha et al., 2008) (Table 1.2). At the metabolic level, Cd-induced signal transduction triggers ROS production (Ranieri et al., 2005), which may damage membrane and destroy cellular organelles and biomolecules (Ekmekci et al., 2008). Most plants accumulates Cd in the root system; the exceptions are the hyperaccumulators which can transfer Cd to the shoot where it is accumulated to high levels (Kramer, 2010, Cappa and Pilon-Smits, 2014).

1.3 Cu, Fe, and Mn

In this thesis, Cu, Fe, and Mn were also investigated to a lesser extent. These elements are essential micronutrients necessary for healthy plant growth and development (Hansch and Mendel, 2009). Cu is required by plants for a range of processes including: photosynthesis and mitochondrial respiration; carbon and N metabolism; oxidative stress protection, and cell wall synthesis (Hansch and Mendel, 2009, Cohu and Pilon, 2010). In plant cells, Cu can be in the oxidation states Cu^{1+} and Cu^{2+}, which can be potentially toxic as Cu ions can catalyse the production of free radicals through Fenton chemistry thereby causing damage to proteins, DNA, and other biomolecules (Gaetke and Chow, 2003). Toxic Cu levels in plants is commonly

Table 1.2 Selected references on effect of Cd on plant physiology.

Plant	Part of the plant affected	Observation	Reference
Rice	Roots	Root elongation is inhibited by the presence of Cd in the rhizosphere	Xiong et al. (2009)
Barley (*Hordeum vulgare*)	Roots/ Shoots	Reduced vigour index, root length, α-amylase, acid phosphatase, alkaline phosphatase activities in endosperms and mitotic index of the root tip.	Kalai et al. (2016)
Arabidopsis thaliana	Roots/ Shoots	350 mmol L^{-1} Cd concentration delayed the growth of roots and shoots.	Dauthieu et al. (2009)
Indian mustard (*Brassica juncea*)	Leaves	Photosynthetic parameters were significantly decreased with Cd treatment, and chlorophyll (total) decreased with increasing concentrations of Cd in soil.	Mobin and Khan (2007)
Wheat	Roots/Shoots	Low germination rate when seeds were exposed to 20 mg L^{-1} Cd	Ahmad et al. (2012)
Wheat	Leaves	Photosynthetic pigments in wheat leaves such as chlorophyll a, chlorophyll b and carotenoid concentrations were reduced when treated with Cd.	Ci et al. (2010), Chen et al. (2014)

associated with Fe-deficiency as many Cu-proteins have a functional counterpart that uses Fe as a cofactor (Patsikka et al., 2002, Burkhead et al., 2009, Festa and Thiele, 2011). Because of that, there are similarities between phenotypes associated with Cu toxicity and phenotypes associated with Fe deficiency (Printz et al., 2016).

Fe is the most abundant heavy metal in living organisms, especially plants. There are two strategies (Strategy I and Strategy II) utilised by plants to take up Fe. In Strategy I, plants reduce Fe^{3+} to Fe^{2+} prior to the uptake by transporter proteins (Eckhardt et al., 2001). Meanwhile, Strategy II requires plants to release mugineic acid (MA) to chelate Fe^{3+} before it can be transported into plants (Negishi et al., 2002). Fe is mostly required by chloroplasts, and 80% of Fe taken up by the plant is localised and stored in the plastids as the compound ferritin (Yruela, 2013). Fe is necessary for chloroplast biogenesis and also photosynthetic reactions (Hindt and Guerinot, 2012). It also serves as a cofactor for the electron transport chain reactions that occur during respiration (Hindt and Guerinot, 2012).

Mn can function to catalyse important cellular reactions (Hansch and Mendel, 2009). For example, in photosystem II Mn, existing as Mn_4CaO_5, is essential to catalyse the splitting of water (Szilard et al., 2007, Hou and Hou, 2013). Mn also plays a role in activating other enzymes such as phosphoenolpyruvate carboxykinase (Hansch and Mendel, 2009). Like the other micronutrients, Mn is only required in small amounts and an imbalance of Mn can disrupt the plants' health and growth. Therefore, plants contain mechanisms to regulate the transport and homeostasis of Mn (Pittman, 2005). Several studies have suggested that Mn and Zn have an antagonistic interaction (Imtiaz et al., 2003, Tariq et al., 2007, Hasani et al., 2012). However, it is unknown whether the stress of Mn deficiency influences the symptoms of Zn deficiency.

1.4 Plant biotechnology strategies related to Zn and Cd

Heavy metals can cause various problems to living organisms. In agriculture, the low availability of essential heavy metal micronutrients results in low quality agricultural products. The most common way that has been used to achieve sufficient essential micronutrients is by applying Zn fertiliser to seeds and soil. However, plant biotechnological applications relevant to biofortification may provide a more long-term solution (discussed below).

In contrast, when the concentrations of heavy metals are very high, they can be toxic. One common way to reduce the concentration of heavy metals is through the conventional soil removal, which is very expensive. Alternatives to combat these problems have emerged and they have better prospects than the conventional methods. Phytoremediation (discussed below) has been shown to have exciting potential for removing toxic heavy metals from soils.

1.4.1 Biofortification

Intensive breeding for yield has exacerbated the micronutrient deficiencies in staple cereal crops and elevated CO_2 levels in the future could intensify the problem (Hogy et al., 2009, Fernando et al., 2012). This is a particular problem in populations relying heavily on cereals in their diets. One of the traditional strategies to overcome micronutrient deficiency in susceptible populations is the use of supplementation or food fortification programmes. Unfortunately, these approaches have not always been successful. For example, there is mixed progress of the Millennium Development Goals (MDGs) set up by the United Nation in 2001 in which its ultimate goal was to eradicate the world's greatest health and poverty issues by 2015 (Nations, 2000). Part of the strategy is to fight micronutrient malnutrition by supplying micronutrients and applying industrial fortification (common cooking foods such as flour, oil, etc.) to those who are affected. Despite major progress in countering micronutrient deficiencies, greater efforts are needed to reach the initial target as suggested by the latest report (Lomazzi et al., 2014).

An alternative solution for combatting micronutrient deficiency is biofortification, which can be defined as a process of increasing the content ('density') of micronutrients in food crops, especially cereals (Alloway, 2004). This can be achieved by traditional breeding programmes or modern biotechnology approaches. Biofortification is still developing, thus many studies need to be performed to make it a feasible solution in food crops. The use of fertilizers, plant breeding and genetic modification are several strategies that have been adapted to achieve biofortification. The application of fertilisers could be a rapid solution to the problem but it is expensive and not always effective (Shaver et al., 2007). The plant breeding strategy appears to be a more sustainable and cost-effective approach in improving the micronutrient status of plants and their concentrations in grains. At present, however, this approach has some limitations; it is a long-term process requiring a variety of breeding activities and huge resources (Cakmak, 2008).

The genetic modification strategy offer a more focussed approach and has led to some impressive progress in developing transgenic plants with increased concentrations of micronutrients. One of the examples of this strategy is the Fe and Zn accumulation in genetically engineered wheat using the Sickle Alfalfa (*Medicago falcata*) ferritin gene (Liu et al., 2016). The transgenic wheat had 73% and 44% higher Fe and Zn contents respectively compared to the WT plants (Liu et al., 2016). However, the constitutive expression of sickle alfalfa ferritin gene did have an effect on the homeostasis of other minerals in the grain (Liu et al., 2016).

When attempting to increase the content of cereal grain with micronutrients the accumulation of toxic metals such as Cd does need consideration as some of the biofortification approaches could result in Cd accumulation. There is already concern in Asia about the

accumulation of Cd in rice, which is a staple there, and so developing technologies to reduce Cd accumulation in grains is also an important objective (Ueno et al., 2010, Abe et al., 2011, Takahashi et al., 2011).

1.4.2 Phytoremediation

As mentioned earlier, heavy metals can be hazardous to living organisms when in excess. Too high a concentration of essential micronutrients e.g. Zn and Mn as well as non-essential heavy metals such as Cd and Hg can be detrimental to plants. Phytoremediation can be defined as the use of plants and their associated microbes for environmental cleanup (Pilon-Smits, 2005). Plants can act as “accumulators” or “excluders”. Accumulators are chosen for phytoremediation since they can survive in soils that are contaminated with heavy metals despite the fact that contaminants are concentrated in their aerial tissues. The excluders are not suitable for phytoremediation because heavy metals are not transported to their biomass.

The status of phytoremediation technology is still in preliminary stages, and full-scale applications are still limited. The efficiency of phytoremediation relies on biological processes including plant-microbe interaction and rhizosphere processes, plant uptake, translocation mechanisms and plant chelation (Pilon-Smits, 2005). Some of them have been utilised for current phytoremediation techniques. Phytoremediation seems more publicly acceptable and less disruptive than the conventional ways of heavy metals removal from soils. Some of the conventional ways such as incineration, thermal vaporization, solvent washing involve physical removal and chemical processes and can cause many problems such as high costs, high-energy requirement and low removal efficiency (Kurniawan et al., 2006, Abourached et al., 2014). Usually, conventional heavy metal removal requires heavy-duty machines, highly skilled workers, long periods of time, and detailed planning, all of which are not cheap. On the other hand, phytoremediation offers a low cost solution, which can be 60%-80% less than conventional physiochemical methods since it does not require heavy machines and highly skilled personnel (Erakhrumen and Agbontalor, 2007). However, there are limitations in the use of phytoremediation, which include the restricted ability to exploit plants for environmental remediation due to our limited understanding of plant’s metabolic pathways, the full range of enzymes involved and tolerance mechanisms. Another phytoremediation limitation is the inability of plants to metabolise and breakdown certain organic compound (Dowling and Doty, 2009).

The success of phytoremediation depends on suitable plant species, which can hyperaccumulate heavy metals and produce large amounts of biomass using established crop production and management practices (Rodriguez et al., 2005). Several studies have shown the

effectiveness of phytoremediation in combating heavy metals contamination. According to the study that has been done by Talano et al. (2014), tobacco (*Nicotiana tabacum*) hairy roots were able to accumulate As to about 32 mg As/kg dry weight in their tissues. In addition, *B. juncea* could accumulate more than 15mg Ni/g dry weight and 12mg Zn/g dry weight after eight weeks (Ismail and Theodor, 2012). The use of plant biotechnology has promise and some transgenic plants have been developed that show promising potential in phytoremediation. *N. tabacum* plants expressing yeast (*Saccharomyces cerevisiae*) *MTII* gene, allowed higher Cd accumulation in shoot tissues up to 457mg Cd/ kg dry weight (Daghan et al., 2013). The hybrid poplar (*Populus tremula × P. alba*) tolerance to Cd is increased by the constitutive expression of the *E. coli γ-glutamylcysteine synthetase* gene. This produced higher glutathione (GSH) concentrations in leaves, which subsequently lead to the induction of genes involved in Cd transport and detoxification (He et al., 2015).

1.5 Zn homeostatic mechanisms in plants

As both too low and too high levels of Zn within plants can have damaging effects, mechanisms have evolved to regulate the level of Zn. The maintenance of Zn homeostasis involves the coordination of several processes: acquiring Zn from the environment, accumulating Zn within the plant, transport around the plant and into cells and cellular compartments, and chelation and sequestration to prevent toxic build up (Clemens, 2001). To ensure an appropriate concentration is maintained within all cells it is vital that these processes are precisely controlled and we are starting to uncover the regulatory mechanisms (Assuncao et al., 2010, Assuncao et al., 2013). Plants also encounter other non-essential transition metals, such as Pb, Cd and Hg. As already mentioned, Cd is at a far greater bioavailability in the soil than other non-essential elements (Reeves and Chaney, 2008) and can highjack importing machinery for cellular accumulation (Palmgren et al., 2008). These elements have the potential to be highly toxic, due to their displacement of essential cofactors and high reactivity with sulfhydryl groups, causing proteins inactivation (Clemens, 2001; Palmgren et al, 2008).

Understanding the mechanisms underlying efficiency of Zn uptake into the plant, distribution to the shoot tissue and partitioning of Zn to the grain is vital in developing plant biotechnology strategies to address global food security issues. Zn efficiency (the ability of plants to maintain growth and yield in soils with low Zn availability) is complex and the underlying mechanisms are not well understood in cereals, but new evidence has suggested that Zn homeostasis is maintained by the coordinated expression of Zn transporters, which are highly regulated themselves by a complex network of transcription factors (TF) (Assuncao et al., 2010).This interaction is ultimately responsible for maintaining equilibrium between acquisition of

Zn from the soil, transportation within the plant system and sequestration within tissues (Assuncao et al., 2010). In this way, plants can respond to their environment appropriately to avoid the lethal effects of Zn toxicity or starvation. This sensory-response mechanism is likely to be very sensitive and tightly regulated due to the narrow tolerance range of many plant species to Zn (Claus and Chavarria-Krauser, 2012). Major components of Zn homeostasis include membrane transporters and ligands, which can be regulated by a complex network of TFs and micro RNAs (miRNAs).

The transport of Zn across apoplastic barriers in plant tissues does not only require membrane transporters, but also chelating agents especially for the intercellular and long-distance transport of Zn. Zn has very low solubility at neutral and alkaline pH. Therefore, Zn is not present as free ions but will bind to ligands or binding proteins. Ligands can also bind to Cd as a means of Cd detoxification in plants (Graham and Stangoulis, 2003). Based on the present state of knowledge, nicotianamine (NA), phytochelatin, glutathione, metallothioneins, and histidine are involved in this type of Zn-homeostatic mechanism (Tennstedt et al., 2009, Yang et al., 2009, Deinlein et al., 2012, Barrameda-Medina et al., 2014, Kozhevnikova et al., 2014). Phytochelatin and glutathione have been implicated in Cd homeostatic mechanisms (Guo et al., 2008, Yang et al., 2015). In the following sections, some of the key mechanisms involved in Zn homeostasis are discussed.

1.5.1 Sensors

Zn homeostasis has been linked to the family of Zn-responsive type/Fe-response type protein transporters (ZIPs), which facilitate Zn entry into the cell (Assuncao et al., 2013). While various other classes of transporters also have the capacity to transport Zn, the ZIP transporters play a key role in Zn uptake at the roots as well as translocation and sequestration in organelles (Guerinot, 2000). In *A. thaliana*, some of these transporters together with a range of other Zn-responsive genes are regulated by members of the basic leucine zipper (bZIP) family of TFs, to coordinate Zn uptake and translocation (Assuncao et al., 2013).

Based on the current model proposed by Assuncao et al. (2013), two bZIP TFs of the F-group (bZIP19 and bZIP23) sense and respond to Zn deficiency (Figure 1.2). Cysteine/histidine (Cys/His) rich motifs at the N-terminal of the basic region of these bZIPs are proposed to act as Zn sensors (Assuncao et al., 2013). Under normal Zn conditions, free Zn ion in the cytosol binds to the Cys/His motifs inactivating bZIP19 and bZIP23 and preventing their movement to the nucleus to up-regulate Zn-responsive genes (Figure 1.3). Under Zn-deficient conditions there would be a “release” of coordinated Zn from the Cys/His-motif of bZIPs, thus allowing the TF to become

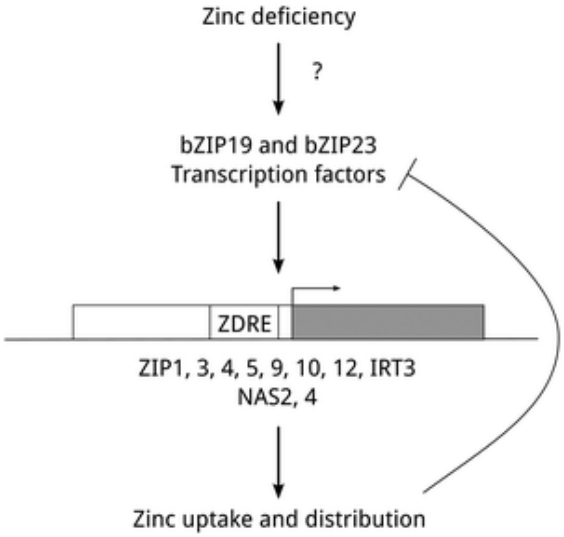

Figure 1.2 Zn deficiency response network in *A. thaliana*, mediated by the TFs bZIP19 and bZIP23.

The activation of AtbZIP19 and AtbZIP23 leads to the expression of *ZIP* and *NAS* genes. The figure is taken from Assuncao et al. (2013).

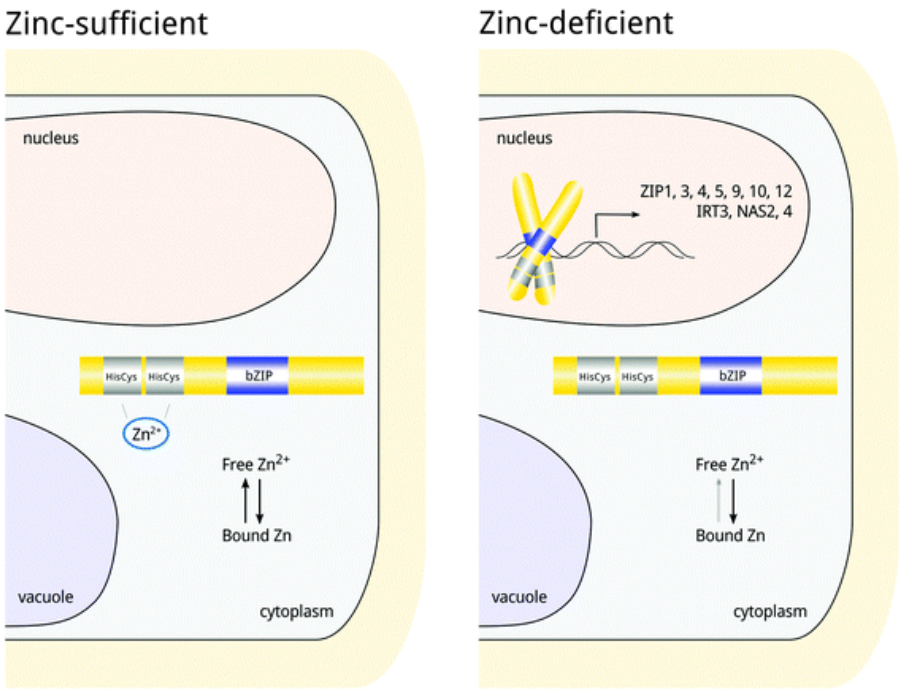

Figure 1.3 A Zn-sensing model showing the mechanisms of AtbZIP19 and AtbZIP23 TFs under Zn deficiency.

During normal Zn conditions, Zn is bound to the TFs in the cytosol, making them inactive. During Zn deficiency, Zn is released from Cys/His-motifs, allowing the TFs to enter nucleus and interact with the promoters of target genes. Blue bar represents bZIP domain and grey bars represent Cys/His -motif. The figure is taken from Assuncao et al. (2013).

functional (Figure 1.3) (Assuncao et al., 2013). This hypothesis remains to be tested as there is no direct experimental evidence, as yet, for this.

These TFs are proposed to bind to a 10 base pair cis element in the ZIP promoter, described as the Zn deficiency response element (ZDRE) to activate transcription and up-regulate gene expression (Assuncao et al., 2013). This ZDRE region is palindromic in nature corresponds to RTGTCGACAY where R=T/G/C/A and Y = A/C/G/T. This specific palindrome sequence is highly conserved amongst ZIP genes, which are responsive to Zn deficit in *A. thaliana* (Assuncao et al., 2010). The NA synthase genes *NAS2* and *NAS4* encoding enzymes that catalyse the synthesis of NA are also up-regulated by bZIP19 and bZIP23.

bZIP proteins are one of the largest families of TFs, widely distributed in all eukaryotes (Gao et al., 2014). They characteristically all contain a leucine zipper-dimerization motif and a highly conserved basic domain, which are capable of binding DNA in a sequence-specific manner. bZIPs bind to short palindromic or pseudopalindromic targets and can form homo- and/or heterodimers. In plants they regulate a diverse range of biological processes (eg. light and hormone signalling, organ and tissue differentiation, plant senescence and seed maturation (Gao et al., 2014). AtbZIP19 and AtbZIP23 are in the F-group of bZIP TFs. This grouping is based on phylogenetic analysis of a large number of angiosperm bZIP members that divided them into thirteen groups (Correa et al., 2008). Barley has eighty-nine bZIPs and they can be divided into eleven groups based on sequence homology (Figure 1.4) (Pourabed et al., 2015). Table 1.3 represent the eighty-nine barley bZIPs and their reported and inferred functions to date based on their well-studied orthologues in other species. As yet there is no direct functional evidence for a role in Zn deficiency in cereal crops for the F-group bZIPs and this thesis will investigate this further.

Yeast-one-hybrid screening originally identified AtbZIP19 and AtbZIP23 as TFs regulating the expression of the membrane transporter, AtZIP4, which is strongly induced under Zn deficiency and contains two copies of a specific Zn-deficiency response element (ZDRE) in its promoter (Assuncao et al., 2010). A double *A. thaliana* T-DNA insertion mutant, *bzip19-1* and *bzip23-1* showed a severe Zn-deficiency phenotype when grown under low-Zn conditions (Assuncao et al., 2010). Transcriptomics analysis comparing Zn-deficiency enhanced transcripts in the double mutant and WT revealed a cohort of genes that showed differential regulation in response to Zn. These genes contained one or more copies of the 10-bp imperfect palindrome in their promoter region (Assuncao et al., 2010). ZIP transporters and NAS genes were the main genes identified in this approach. A proteomics analysis using iTRAQ (isobaric Tags for Relative and Absolute Quantification) was recently implemented to identify proteins that showed AtbZIP19-dependent

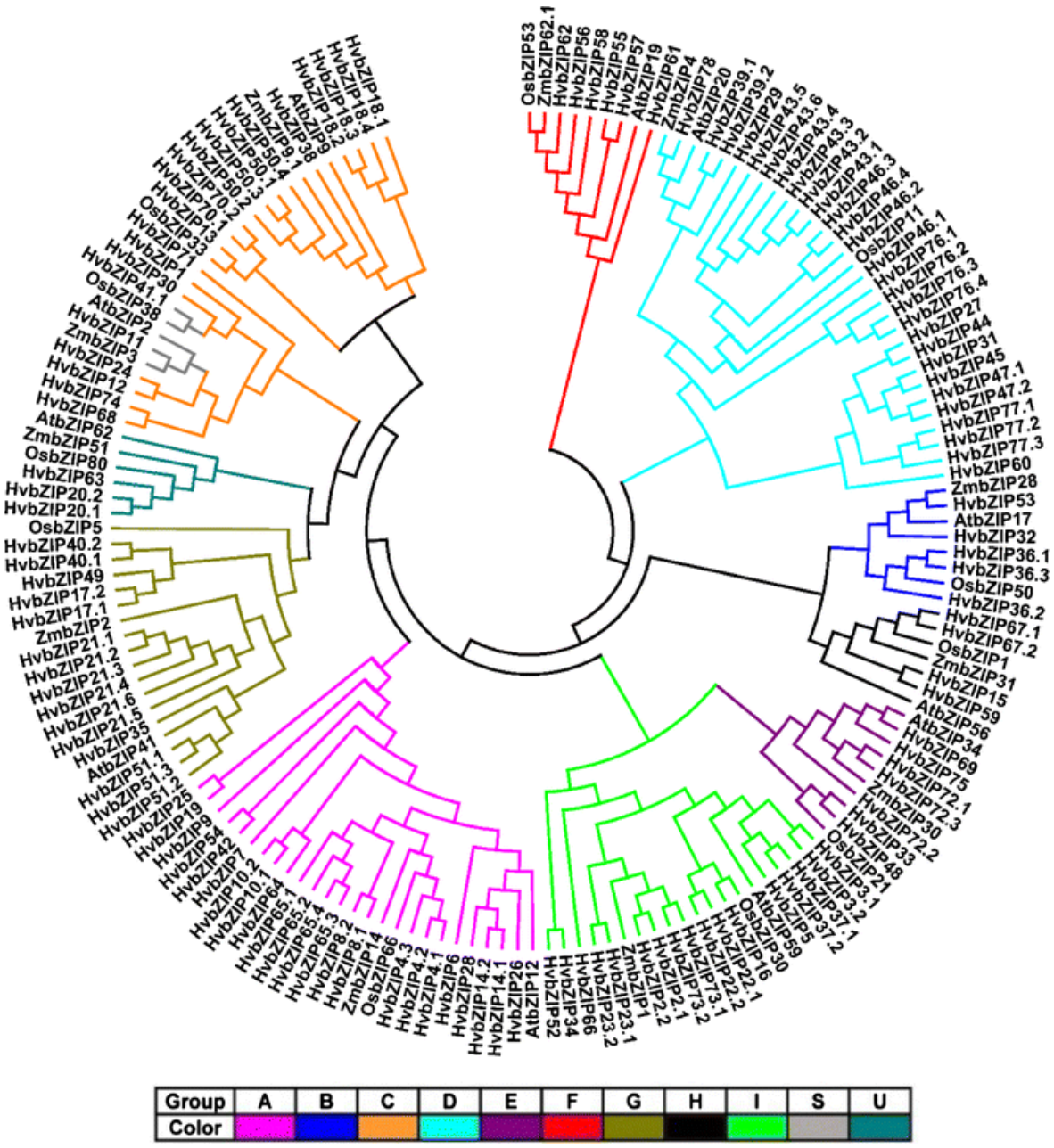

Figure 1.4 Phylogenetic tree of barley bZIPs.

The classification of eighty-nine *bZIP* genes in barley into eleven clades based on sequence homology. The diagram is taken from Pourabed et al. (2015).

Table 1.3 Function of eleven bZIP groups.

Where appropriate, the potential function of each group is outlined based on existing knowledge and functional comparison to respective bZIPs in other species. Nomenclature by Pourabed et al. (2015).

Group	Number	Members	Function
A	15	HvbZIP25, HvbZIP19, HvbZIP9, HvbZIP54, HvbZIP42, HvbZIP7, HvbZIP10, HvbZIP64, HvbZIP65, HvbZIP8, HvbZIP4, HvbZIP6, HvbZIP28, HvbZIP14, HvbZIP26	Abiotic stress response, ABA signalling (Choi et al., 2000, Uno et al., 2000, Jakoby et al., 2002)
B	3	HvbZIP53, HvbZIP32, HvbZIP36	
C	12	HvbZIP18, HvbZIP38, HvbZIP50, HvbZIP70, HvbZIP13, HvbZIP71, HvbZIP1, HvbZIP30, HvbZIP24, HvbZIP12, HvbZIP74, HvbZIP68	Cold/drought tolerance, ABA signalling, sugar signalling (Schmidt et al., 1992, Nakase et al., 1997, Liu et al., 2012a)
D	13	HvbZIP78, HvbZIP39, HvbZIP29, HvbZIP43, HvbZIP46, HvbZIP76, HvbZIP27, HvbZIP44, HvbZIP31, HvbZIP45, HvbZIP47, HvbZIP77, HvbZIP60	Defence, development(Despres et al., 2000, Singh et al., 2002)
E	5	HvbZIP69, HvbZIP75, HvbZIP72, HvbZIP33, HvbZIP48	
F	6	HvbZIP62, HvbZIP56, HvbZIP58, HvbZIP55, HvbZIP57, HvbZIP61	Zn deficiency response
G	6	HvbZIP40, HvbZIP49, HvbZIP17, HvbZIP21, HvbZIP35, HvbZIP51	Light response, defence, abiotic stress(Weisshaar et al., 1991, Schindler et al., 1992, Xiang et al., 1997)
H	3	HvbZIP67, HvbZIP15, HvbZIP59	stimulus-induced development of hypocotyl and root (Ang et al., 1998)
I	11	HvbZIP3, HvbZIP37, HvbZIP5, HvbZIP16, HvbZIP22, HvbZIP73, HvbZIP2, HvbZIP23, HvbZIP66, HvbZIP34, HvbZIP52	Vascular development, RSG (Yin et al., 1997, Ringli and Keller, 1998, Fukazawa et al., 2000)
S	2	HvbZIP41, HvbZIP11	Cold/drought tolerance (Kobayashi et al., 2008, Chen et al., 2012)
U	2	HvbZIP63, HvbZIP20	Sequestering other bZIP groups into inactive heterodimers (Nantel and Quatrano, 1996, Pourabed et al., 2015)

induction under Zn deficiency (Inaba et al., 2015). ZIP proteins were again identified (AtZIP3 and AtZIP9) but also members of the defensin-like family of proteins (Inaba et al., 2015). Although AtbZIP19 and AtbZIP23 TFs do have a clear involvement in the Zn-deficiency response in *A. thaliana*, we know little about the mechanisms existing in crop species and a thorough understanding of Zn-sensing mechanisms in plants is still far from complete.

1.5.2 Membrane-bound transporters involved in Zn homeostasis

Members of certain membrane-transporter families are thought to be involved in heavy metal influx into the cytosol while others are involved in efflux either to the outside of the cell or into compartments. Heavy metals are delivered to certain organelles for storage or detoxification e.g. the vacuole or to compartments where they are required for specific reactions (e.g. Golgi, chloroplast, mitochondria). For example, it is proposed that Mn is supplied to the Golgi for the action of glycosyltransferases (Mills et al., 2008) and Cu is transferred to the chloroplast for plastocyanin (Shikanai et al., 2003, Tapken et al., 2012). Some of the transporters that have been shown to be involved in Zn and Cd transport are discussed below. In particular, the focus will be on ZIPs, P_{1B}-ATPases, and CDFs/MTPs, which have been studied in this thesis. Where information is available their localisation is discussed together with their potential physiological roles. Some are thought to be involved in Zn uptake at the root, transfer into the vascular system for transport to the shoot, and there is evidence that some have specific roles in the grain.

1.5.2.1 The Zn-Regulated Transporter, Fe-Regulated Transporter (ZRT-IRT-like) Protein (ZIP)

The ZIP transporters have been reported now in many plant species as well as in bacteria (Grass et al., 2002), fungi (Zhao and Eide, 1996a, Zhao and Eide, 1996b), and animals (Gaither and Eide, 2001). The main function of these membrane transporters is to translocate divalent cations, specifically Zn, Fe, Mn and Cu across membranes (Guerinot, 2000). Cd has also been shown to be transported by certain members of ZIP family (Guerinot, 2000, Pence et al., 2000, Rogers et al., 2000). The followings are the characteristics of ZIP protein: (1) eight transmembrane domains (TMDs), (2) 309 to 476 amino acids in length, (3) a His-rich region found in the long loop between TMD3 and TMD4 (Eide, 2006), and (4) both amino (N)- and carboxyl (C)-terminus are located in the extra-cytoplasmic space (Guerinot, 2000).The ZIP mechanism of action is still unclear in plants but Pedas and Husted (2009) suggested that the transport capacity of barley ZIPs is influenced by proton activity. ZIP family members from other organisms have been shown to have a particular mode of action. For example, *S. cerevisiae* Zn transporter, ZRT1 ,requires energy (Zhao and Eide, 1996b). Meanwhile, its orthologue in human, SLC39A2, does not require energy but it is driven by the gradient of HCO_3^- (Gaither and Eide, 2001). In contrast, one member of ZIP family in

Bordetella bronchiseptica, ZIPB, has been indicated it forms a Zn-selective ion channel (Lin et al., 2010). There is no X-ray crystal structure of ZIP transporter to date. ZIPs substrate specificity varies for different family members, as does their regulation. Some *ZIPs* are regulated transcriptionally by Fe and/or Zn (Guerinot, 2000, Milner et al., 2013). *A. thaliana* has fifteen ZIPs and several of these have been reported to transport Zn (Grotz et al., 1998, Korshunova et al., 1999, Lin et al., 2009, Milner et al., 2013). Some assertions are based on assays conducted in *S. cerevisiae* while others are from studies carried out with T-DNA insertion mutants. The latter are particularly useful for providing evidence for a physiological role within the plant.

IRT1 was the first *A. thaliana* ZIP transporter to be characterised; it is localised to the plasma membrane and transports Fe, Zn, Mn, Co and Cd (Korshunova et al., 1999). AtIRT1 is subject to intricate metal-dependant transcriptional and post-translational regulation (Shin et al., 2013). The studies of IRT1 support the view that Zn and Fe can compete for the same uptake systems as excess Zn causes reduced Fe uptake and excess Fe alleviates Zn toxicity (Fukao et al., 2011, Shanmugam et al., 2013). This transporter is likely to be involved in Zn uptake into the plant, especially under Fe deficiency where it is up-regulated (Vert et al., 2002). IRT2 is another closely related broad affinity metal transporter expressed in epidermal cells (Vert et al., 2002). Its expression at internal membranes (Vert et al., 2009) suggests that it is not involved in direct uptake. IRT3 could have a role in the Zn-deficiency response as *IRT3* transcripts are strongly up-regulated after four days of treatment and constitutively high in roots of the Zn-hyperaccumulators *Arabidopsis halleri* and *Noccaea caerulescens* (Becher et al., 2004, van de Mortel et al., 2006). AtZIP1 and AtZIP2 are other members of the ZIP family of metal transporters that have been suggested to import Zn into roots (Lin et al., 2009). The constitutive expression of AtZIP1 in barley has resulted in higher Zn content in the seeds (Ramesh et al., 2004b). However, recent functional studies with plants mutated in *AtZIP1* and *AtZIP2* have questioned this assumption as the results suggest that these ZIP transporters are involved in Mn root to shoot transport (Milner et al., 2013). AtZIP1 may play a role in remobilizing Mn from the vacuole to the cytoplasm in root stellar cells, and contribute to the radial movement to the xylem parenchyma. ZIP2 on the other hand, may mediate Mn (and possibly Zn) uptake into root stellar cells, and thus may contribute to Mn/Zn movement in the stele to the xylem parenchyma, for subsequent xylem loading and transport to the shoot (Milner et al., 2013). Zn deficiency has also been shown to up-regulate the expression of *AtZIP1*, *AtZIP3*, *AtZIP4*, *AtZIP5*, *AtZIP9*, and *AtZIP12* (Assuncao et al, 2010). AtZIP4 could play some role in mediating cellular Zn uptake across the plasma membrane as it can complement the *zrt1 zrt2 S. cerevisiae* mutants (Assuncao et al, 2010). It also complemented the *S. cerevisiae ctr1* mutant defective in cellular Cu, indicating a potential role in Cu transport (Wintz et al., 2003). For AtZIP9 and AtZIP12, their roles in Zn transport are indicated

by significantly lower root Zn concentrations in their respective T-DNA mutants grown on high Zn medium compared to the WT plants (Inaba et al., 2015).

Concerning crop species, most information concerning the role of ZIPs has come from studies in rice and barley. In rice, there are sixteen ZIPs and five of them (*OsZIP1*, *OsZIP3*, *OsZIP4*, *OsZIP5*, and *OSZIP8*) are induced by Zn deficiency (Bashir et al., 2012). OsZIP1 have been implicated in root Zn uptake, whereas OsZIP4, OsZIP5, and OsZIP8 could be involved in root to shoot translocation (Ishimaru et al., 2007, Lee et al., 2010, Bashir et al., 2013). OsZIP3 is localised in the nodes where it mediates Zn transport from xylem to the developing tissues (Sasaki et al., 2015). OsIRT1 and OsIRT2 transport Fe (Ishimaru et al., 2006) but they can also transport Cd when expressed in yeast (Nakanishi et al., 2006). The overexpression of *OSIRT1* results in the accumulation of Cd in roots and shoots grown on medium containing excess Cd, however, the phenotype of the mutants are different in the field as they do not accumulate Cd (Lee and An, 2009). Based on the observation in the field, OsIRT1 is possibly implicated in root Cd uptake but its mechanism might be influenced by environmental conditions. OsZIP6 could also transport Cd as its expression in *Xenopus laevis* oocytes generate current across membrane on addition of Cd and the Cd concentration was also high within oocytes (Kavitha et al., 2015).

In barley, there are thirteen ZIP membrane transporters: HvIRT1, HvZIP1, HvZIP2, HvZIP3, HvZIP5, HvZIP6, HvZIP7, HvZIP8, HvZIP10, HvZIP11, HvZIP13, HvZIP14, HvZIP16 (Tiong et al., 2015). Various metal specificities have been assigned to these barley ZIPs and Table 1.4 summarises the reported function of barley ZIP members to date. The first to be identified was HvIRT1 and it is an important component in Mn transport. HvIRT1 may also transport Zn, Cd and Fe as suggested by yeast studies (Pedas et al., 2008). *HvIRT1* is up-regulated under Fe and Mn deficiency (Pedas et al., 2008). Three barley ZIPs isolated from roots, HvZIP3, HvZIP5 and HvZIP8, have been implicated in Zn transport and they seem selective for Zn, complementing *S. cerevisiae* cells defective in Zn but not Mn, Fe and Cu uptake (Pedas et al., 2009). *HvZIP3, 5,7,8,10* and *13* were induced in plants grown under with Zn deficiency (Tiong et al., 2015) . *HvZIP7* is strongly induced by Zn deficiency, primarily in vascular tissues of roots and leaves, and it is localised at the plasma membrane (Tiong et al., 2014). Overexpression of *HvZIP7* enhanced Zn accumulation in shoot and grains; suggesting it has a role in promoting root to shoot transport, and Zn loading (Tiong et al., 2014). ZIP transporters have been studied in other crop species including maize (Li et al., 2013a), soybean (Moreau et al., 2002), grape, (Gainza-Cortés et al., 2012), and a member of this family, shown to function in Zn transport, is present in wild emmer wheat (*Triticum turgidum*) (Durmaz et al., 2011).

Table 1.4 Function of barley ZIP membrane transporters

Barley ZIPs	Function
HvIRT1	Involved in Mn uptakes in barley roots and localised to the plasma membrane (Pedas et al., 2008).
HvZIP1	Contribute little to the enhanced uptake and root-to-shoot translocation of Zn when available Zn is in low to sub-micromolar concentration, and it was weakly induced in roots only (Tiong et al., 2015). No localisation study is found.
HvZIP2	Contribute little to the enhanced uptake and root-to-shoot translocation of Zn when available Zn is in low to sub-micromolar concentrations and it was weakly induced in the roots (Tiong et al., 2015). No localisation study is found.
HvZIP3	Involve in specific Zn uptake in barley roots (Pedas et al., 2009). Up-regulated with a nineteen days insufficient Zn supply in both shoots and roots and it was shown to be localised to the plasma membrane (Tiong et al., 2015).
HvZIP5	Involve in specific Zn uptake in barley roots (Pedas et al., 2009). In shoots, it was only up-regulated after thirteen days of Zn-deficient treatment, while in roots, its upregulation was increasing up to day 15 of Zn-deficient treatment, and it was shown to be localised to the plasma membrane (Tiong et al., 2015).
HvZIP6	Contribute little to the enhanced uptake and root-to-shoot translocation of Zn when available Zn is in low to sub-micromolar concentrations as it was weakly up-regulated in the roots only after thirteen days of treatment (Tiong et al., 2015). No localisation study is found.
HvZIP7	Mediate Zn accumulation at moderately high Zn supply and it was shown to be localised in the plasma membrane (Tiong et al., 2014). Express in barley grain (transfer cells and aleurone cells) (Tauris et al., 2009)
HvZIP8	Involve in specific Zn uptake in barley roots (Pedas et al., 2009) Up-regulated under Zn deficiency especially at day 13 of treatment in the shoots but the high expression levels stayed the same up to day 19 of treatment in the roots (Tiong et al., 2015).
HvZIP10	Up-regulated under Zn deficiency in both shoots and roots under Zn deficiency especially at day 13 of treatment, and it was shown to be localised in the plasma membrane (Tiong et al., 2015). Express in barley grain (all tissues) (Tauris et al., 2009)
HvZIP11	Contribute little to the enhanced uptake and root-to-shoot translocation of Zn when available Zn is in low to sub-micromolar concentrations as it was constitutively expressed in both treatments (Tiong et al., 2015). No localisation study is found.
HvZIP13	Up-regulated under Zn deficiency in both shoots and roots under Zn deficiency especially at day 13 of treatment, and it was shown to be localised in the plasma membrane (Tiong et al., 2015).
HvZIP14	Contribute little to the enhanced uptake and root-to-shoot translocation of Zn when available Zn is in low to sub-micromolar concentrations concentrations as it was constitutively expressed in both treatments (Tiong et al., 2015). No localisation study is found.
HvZIP16	Contribute little to the enhanced uptake and root-to-shoot translocation of Zn when available Zn is in low to sub-micromolar concentrations concentrations as it was constitutively expressed in both treatments (Tiong et al., 2015). No localisation study is found.

1.5.2.2 P_{1B}-ATPases

P_{1B}-ATPases or Heavy Metal ATPases (HMAs) are heavy metal pumps that belong to a super family of P-type ATPases(Møller et al., 1996). There are five major evolutionary subfamilies of P-type ATPases (P_1-P_5) and all of them are implicated in pumping different cations across the membrane except for the P_4 sub-family that has been reported to be involved in phospholipid flipping (Kuhlbrandt, 2004, Palmgren and Nissen, 2010). The catalytic cycle of P-type ATPases is initiated by the phosphorylation of a conserved aspartic acid residue (Axelsen and Palmgren, 1998). For some members of the HMA family, their attributes have suggested that they may show a good potential for biofortification and phytoremediation.

The main function of this membrane transporter family is to generate and maintain the crucial chemical gradient across cellular membranes, which can be done by translocating cations, heavy metals and lipids. P_{2A} and P_{2B} Ca-ATPases involve in maintaining Ca concentration in plant cells at the optimum level by pumping Ca out from the cytosol (Bose et al., 2011). Pollen development, stomatal opening/closing, reproductive and pollen tube growth, vegetative and inflorescence architecture, gibberellin signalling, and promoting salinity and drought stress tolerance are also associated with the functions of P_{2A} and P_{2B} Ca-ATPases (Schiøtt et al., 2004, George et al., 2008, Wang et al., 2011, Lucca and Leon, 2012, Huda et al., 2013). P_{3A}-H-ATPases in plants are implicated in energizing the electrochemical gradient used as the driving force for the active influx, efflux of ions and metabolites across the plasma membrane (Duby and Boutry, 2009). P_4-ATPases are well characterised in *S. cerevisiae*, and they are involved in phospholipid translocation and vesiculation involved in membrane vesicle budding (Poulsen et al., 2008a). In *A. thaliana*, one member of P_4-ATPases, ALA10, has been shown to be involved in taking up lysophosphatidylcholine (lysoPC), a signalling lipid involved in plant development (Poulsen et al., 2015).

P-type ATPases can be identified based on three conserved domains: (1) the transmembrane helix (TM) bundle that includes 6-10 TMs and provides the substrate translocation pathway; (2) the ATP-binding domain (ATPBD), which includes the nucleotide-binding domain (N-domain) and the invariant and transiently phosphorylated aspartate residue located in the phosphorylation domain (P-domain); (3) the actuator domain (AD), which is believed to transmit changes in the ATPBD to the transmembrane region and to drive dephosphorylation (Jorgensen et al., 2003, Toyoshima, 2009).

Structurally, P_{1B}-ATPases can be characterised by having a single subunit of six to eight transmembrane segments (Hussain et al., 2004, Williams and Mills, 2005), N- and C-termini exposed to the cytoplasm, and a large central cytoplasmic domain, including phosphorylation and

ATP binding sites (Olesen et al., 2004). N- and C-terminal metal binding (N-and C-MBDs) acts as putative metal binding domain since they contain metal-binding motifs including multiple interspersed Cys pairs and His residues in various motifs (Argüello, 2003, Wong et al., 2009, Laurent et al., 2016). The CPx/SPC motif is thought to function in heavy metal transduction (Arguello et al., 2007).

There are five different subclasses of P_{1B}-ATPases (P_{1B-1} to P_{1B-5}) based on substrate specificity, sequence similarity and overall architecture (Table 1.5). Two more P_{1B}-ATPases (P_{1B-6} and P_{1B-7}) have been identified but none of these were biochemically characterised beyond their sequence classification (Smith et al., 2014). In regard to the model plant *A. thaliana*, eight P_{1B}-ATPases have been identified, which can be classed into three groups: (1) P_{1B-1}, which is comprised of AtHMA5 to AtHMA8, is predicted to transport Cu/Ag; (2) P_{1B-2} that are predicted to be involved in Zn/Co/Cd/Pb transport; and (3) AtHMA1 in the P_{1B-4} (Axelsen and Palmgren, 1998, Arguello et al., 2007). Concerning Zn and Cd transport in *A. thaliana*, AtHMA2 and AtHMA4 have been reported to show some redundancy in their function. Both of these genes can mobilize Zn and Cd in plant vascular tissues to ensure subsequent xylem loading and transport to the shoot (Wong et al., 2009). When AtHMA2 and AtHMA4 are mutated independently as a single mutant, they show weak phenotypes, whereas a double mutant *hma2 hma4* shows a much more severe Zn-dependent phenotype and in this, Zn accumulates in root pericycle cells (Hussain et al., 2004, Verret et al., 2004, Wong and Cobbett, 2009). The ability of AtHMA4 to restore the growth of *E. coli* mutants, *zntA*, defective in the HMAs and to make S*. cerevisiae* more resistant to Cd when it was expressed in these two organisms indicated its roles as a Zn and Cd transporter (Mills et al., 2003).

As mentioned previously, the protein structure of P_{1B}-ATPases is very crucial for their function. AtHMA2 cannot function properly when its N-terminus is truncated (Wong et al., 2009). The C-terminus in AtHMA2 is predicted to be a binding site of Zn. It has been shown that the isolated C-domain of AtHMA2 can bind to Zn ions with very high affinity (Eren et al., 2006). The C-terminus of AtHMA4 is also a binding site of Zn and Cd. The removal of the C-terminus in AtHMA4 resulted in a pump protein that was superior compared with the wild-type (WT) membrane protein in rescuing Zn and Cd sensitivity of the *S. cerevisiae zrc1 cot1* strain, suggesting a regulatory function of C-domain (Baekgaard et al., 2010, Mills et al., 2010).

AtHMA3 has been reported to be involved in the detoxification of Zn and Cd by participating in vacuolar sequestration (Morel et al., 2009). Gravot et al. (2004) has reported that *AtHMA3* expression is able to rescue the Cd/Pb-hypersensitive phenotype of the *S. cerevisiae* mutant strain *ycf1* but unable to phenotypically complement the Zn-sensitive mutant *zrc1*.

Table 1.5 P_{1B}-ATPase subclasses and their biochemically established substrates

Subclass	Substrate(s)	References
1B-1	Cu, Ag	Fan and Rosen (2002), Mandal et al. (2002), Lowe et al. (2004), Gonzalez-Guerrero et al. (2008),
1B-2	Zn, Cd, Pb	Eren and Arguello (2004), Hussain et al. (2004), Liu et al. (2006), Kim et al. (2009), Morel et al. (2009), Mills et al. (2012)
1B-3	Cu	Mana-Capelli et al. (2003)
1B-4	Co, Cu	Kim et al. (2009), Raimunda et al. (2012), Zielazinski et al. (2012)
1B-5	Ni, Fe	Zielazinski et al. (2013)
1B-6	Unknown	Smith et al. (2014)
1B-7	Unknown	Smith et al. (2014)

AtHMA3 mRNA is present at a very weak level in all plant parts but with Zn or Cd treatments, its expression is slightly modulated (Gravot et al., 2004, Talke et al., 2006). In contrast, the AtHMA3 orthologue in the tolerant hyperaccumulator species *A. halleri* is strongly expressed and even up-regulated upon Zn exposure (Becher et al., 2004, Gravot et al., 2004, Talke et al., 2006). All the mentioned observations point out that AtHMA3 could be one of the membrane transporters that is involved in metal hyperaccumulation and/or metal tolerance. Further study by Morel et al. (2009) indicates that AtHMA3 participates in the vacuolar storage of Cd using the Zn/Cd fluorescent probe BTC-5N. In addition, a T-DNA insertional mutant was found to be more sensitive to Zn and Cd. Ectopic overexpression of *AtHMA3* improved plant tolerance to Cd, Co, Pb and Zn (Morel et al., 2009). AtHMA3 has high expression in guard cells, hydathodes (a type of secretory tissue in leaves) , vascular tissues, and the root apex (Morel et al., 2009). AtHMA3 has been identified as the sole major locus responsible for the variation in leaf Cd accumulation as some DNA polymorphisms in the protein coding region of the gene found in several *A. thaliana* accessions reduce the function of AtHMA3 (Chao et al., 2012). AtHMA3 is in the same group as AtHMA2 and AtHMA4 based on amino acid alignments, which shows that all three proteins exhibit a high degree of amino acid sequence similarities in their transmembrane domains, but they show divergent soluble C-terminal segments (Argüello, 2003). The C-terminus of AtHMA3 is shorter (around 60 residues) than AtHMA2 and AtHMA4.

AtHMA1 has been shown to transport a broad range of divalent cations including Zn. Seigneurin-Berny et al. (2006) has reported that AtHMA1 is implicated Cu and Zn based on the following results: (1) AtHMA1 can transport both heavy metals in *S. cerevisiae*; (2) chloroplast Cu level decrease when AtHMA1 was disrupted; and Cu enhanced AtHMA1 activity in the chloroplast envelope. *S. cerevisiae* experiments carried out by Moreno et al. (2008) concluded that AtHMA1 could effectively transport Cu and Zn but also Ca, Cd, and Co. Another study also suggested that it transported Zn but in an efflux mechanism from the chloroplast based on *in planta* and *S. cerevisiae* analysis (Kim et al., 2009).

In the P_{1B-1} subclass of *A. thaliana*, AtHMA5 is located in the pericycle cells of roots and it is implicated in Cu compartmentalisation and detoxification in root tissues. AtHMA6 can be found in the chloroplast inner envelope membrane and its function is to deliver Cu to Cu/Zn-SOD or to AtHMA8 that is localised to the thylakoid membrane where it supplies Cu to plastocyanin (Abdel-Ghany et al., 2005). Meanwhile, AtHMA7 has been reported to actively pump Cu into the post-Golgi compartment so that Cu can be used for the maturation of the ethylene receptor (Hirayama et al., 1999).

P_{1B-2}-ATPases of *A. thaliana* have been characterised intensively but less is known for this family in monocot plants. Elucidating P_{1B-2}-ATPases in monocots especially in cereals could be beneficial in improving the nutrient status of cereals by enriching them with essential-heavy metals and developing high-biomass phytoremediation plants. Ten P_{1B}-ATPases can be found in barley but only two have been characterised to date. Concerning Zn transport, HvHMA2 has been characterised by Mills et al. (2012), demonstrating its roles in Zn and Cd transport. The heterologous expression of *HvHMA2* in *S cerevisiae* confers Cd sensitivity to WT *S. cerevisiae*. The mutated version of HvHMA2, where the conserved aspartate was substituted with alanine failed to confer Zn sensitivity. HvHMA2 also conferred Zn resistance to the Zn-sensitive *S. cerevisiae* mutants, *zrc1 cot1,* indicating a role in Zn transport (Mills et al., 2012). Consistent with this, the Zn-deficient phenotypes of *A. thaliana hma2 hma4* mutants were suppressed with the introduction of HvHMA2 (Mills et al., 2012). HvHMA2 is localised predominantly in the plasma membrane when expressed in *A. thaliana*. The constitutive *HvHMA2* expression in tobacco showed that it can interfere with the Zn-Cd-Fe homeostasis and restrict Zn uptake in transgenic plants, resulting low Zn levels in the shoots (Barabasz et al., 2013).

TaHMA2 is the orthologue of HvHMA2 in wheat , displaying 92% identity (amino acids) (Mills et al., 2012). TaHMA2 is localised to the plasma membrane and it conferred Zn and Cd sensitivity to WT *S. cerevisiae* (Tan et al., 2013). The expression of *TaHMA2* in transgenic plants (rice, wheat, *A. thaliana* and tobacco) results in an improved root-shoot Zn/Cd translocation, which suggests it may function to pump Zn and Cd out of cells (Tan et al., 2013). The study also found that Zn concentrations were decreased in transgenic seeds of rice and wheat. When treated with high level of Zn and Cd, the transgenic plants had a decrease in Zn and Cd resistance. The Cd concentration in transgenic rice seedlings was dramatically increased under Zn deficiency (Tan et al., 2013). In this study, the transgenic monocots exhibit more obvious phenotypes than the transgenic dicots.

HvHMA1 is another barley gene that has been characterised. GFP tagging of HvHMA1 has suggested that it is localised to the periphery of chloroplast of leaves and intracellular compartments of grain aleurone cells (Mikkelsen et al., 2012). Unlike HvHMA2, HvHMA1 has a broad heavy metal sensitivity that is suggested to mobilise plastid Zn and Cu based on heterologous expression in *S. cerevisiae*. The expression of HvHMA1 in heavy metal-sensitive strains increases their sensitivity not only to Zn but also to Cu, Co, Cd, Ca, Mn, and Fe (Mikkelsen et al., 2012). In the same study, downregulation of *HvHMA1* by RNA interference results in a significant increase in grain Zn and Cu content. This indicates that HvHMA1 might also be implicated in mobilizing Zn and Cu from aleurone cells during the phases of grain filling and

germination. Based on the study on HvHMA1 and HvHMA2, barley could be a good model for studying metal transport in cereals.

Rice is another monocot that is extensively studied for metal transport. Baxter et al. (2003) have reported that rice has nine P_{1B}-ATPases based on a protein sequence database search. The phylogenetic analysis shows that OsHMA1 to OsHMA3 belong to the Zn cluster, whereas OsHMA4 to OsHMA9 are in the Cu cluster (Lee et al., 2007). OsHMA3 has been shown to be an important gene in controlling Cd accumulation in rice (Ueno et al., 2010, Miyadate et al., 2011). It can be found in the tonoplast and as yet there is no direct evidence that it transports Zn but it has been shown to function in Cd detoxification in the root vacuole (Ueno et al., 2010). Overexpression of OsHMA3 in rice was shown to enhance tolerance to Cd toxicity by sequestering it in the vacuole and reducing transfer to the shoots, whereas silencing it increased translocation (Ueno et al. 2010; Sasaki et al. 2014). Interestingly, in the over-expressing plants, Zn concentrations were increased in the roots but levels were maintained in the shoots, possibly by compensation from ZIP transporters, which were seen to be up-regulated in these plants. As yet there is no direct evidence demonstrating Zn transport by OsHMA3.

OsHMA2 is also indicated to be involved in Zn and Cd transport as suggested by a study which reports that a mutation in OsHMA2 causes decreased translocation of Zn and Cd from the roots to the shoots at the vegetative growth stage in rice (Sato-Nagasawa et al., 2012). However, Yamaji et al. (2013) have pointed out that the major role of OsHMA2 especially in nodes is to distribute preferential Zn as well as Cd through the phloem to the developing tissues. Also, the study has found out that this transporter was responsible for Cd distribution to the grains in rice. For the Cu cluster, only OsHMA5 and OsHMA9 has been studied. OsHMA5 functions as a transporter to load Cu to the xylem of the roots and other organs (Deng et al., 2013). Even though, OsHMA9 is clustered in the same group of P_{1B}-ATPase that is implicated in Cu transport, it has been shown to be a heavy metal transporter implicated not only in Cu efflux but also Zn and Pb efflux from the cells as the mutant plants have exhibited the phenotype of increased sensitivity to elevated Cu, Zn, and Pb (Lee et al., 2007).

1.5.2.3 The cation diffusion facilitator (CDF) transporters

CDF family members in plants are known as Metal Tolerance Proteins (MTPs). Various members of the MTP family have been cloned from a number of plant species and are shown to be involved in heavy metal transport (Blaudez et al., 2003, Kim et al., 2004, Kobae et al., 2004, Delhaize et al., 2007, Peiter et al., 2007, Kawachi et al., 2008, Podar et al., 2012). Twelve *MTP* genes have been identified in *A. thaliana* and the first MTP gene was identified as *ZAT* or Zn Transporter of *A. thaliana* (van der Zaal et al., 1999) and it was renamed *MTP1*. MTP3 is another

well-characterised CDF membrane protein in *A. thaliana.* A study has shown that both proteins can be found in root cells where MTP1 is highly expressed in the root tip including the meristematic and elongation zone (Kobae et al., 2004) whereas MTP3 expression in the root is undetectable until the Zn level becomes very high, which suggests its role as a Zn-stress response protein (Desbrosses-Fonrouge et al., 2005). The function of AtMTP1 as a Zn transporter is suggested from its ability to accumulate Zn when expressed in *Xenopus laevis* oocytes (Desbrosses-Fonrouge et al., 2005), and from the *A. thaliana mtp1-1* mutants that shows extreme sensitivity to excess Zn (Kobae et al., 2004). Also, *AtMTP3* has been shown to be up-regulated under Fe deficiency but this could be an indirect effect as the *AtIRT1* gene is up-regulated in this situation (Arrivault et al., 2006). The abundance of AtIRT1 increases Zn concentrations in the cell as the transporter can also transport Zn inwards (Baxter et al., 2008); this resulted in the induction of *AtMTP3* gene to prevent Zn toxicity.

Little is known regarding the CDF family in cereals, but a member of the CDF family in rice and barley MTP1 has been reported to be involved in Zn and Cd, and other heavy metal translocation (Podar et al., 2012, Yuan et al., 2012, Menguer et al., 2013). Rice OsMTP1 is able to complement the Zn and Cd-hypersensitive *S. cerevisiae* mutant strains but no other metals including Co and Mn (Yuan et al., 2012). The downregulation of *OsMTP1* using RNAi has resulted in Zn and Cd sensitivity (Yuan et al., 2012). A functional complementation analysis showed that when *OsMTP1* could rescue the Zn-toxicity phenotype of the *A. thaliana mtp1-1* mutant (Menguer et al., 2013). Based on these results, OsMTP1 is assumed a bivalent cation transporter that is necessary for efficient translocation of Zn and Cd. In barley, a member of the CDF family, HvMTP1, that is localised to the vacuolar membrane has exhibited selectivity for both Zn and Cd (Podar et al., 2012). Most of MTP family members seem to function as antiporters as shown by both *A. thaliana* and cucumber MTP1 that depends on the proton gradient to function properly when they were expressed in *S. cerevisiae* (Kawachi et al., 2008, Migocka et al., 2014).

1.5.2.4 The plant Natural Resistance Associated Macrophage protein (NRAMP)

The NRAMPs comprise a large family of transport proteins capable of transporting essential micronutrients such as Mn, Fe, Zn, Cu, Ni and non-toxic elements such as Cd across external and internal membranes (Colangelo and Guerinot, 2006, Nevo and Nelson, 2006). They contain 10 to 12 transmembrane domains (Cellier et al., 1995, Thomine et al., 2000) and are classified as secondary active transporters, thought to function via a proton cotransport mechanism (Mackenzie et al., 2006). In plants there are clear roles for NRAMPs in Fe (Thomine et al., 2000, Thomine et al., 2003, Lanquar et al., 2005) and Mn homeostasis (Cailliatte et al., 2010, Williams and Pittman, 2010) and some may also play a role in Zn homeostasis. The *A. thaliana* double

nramp3 nramp4 mutants exhibits impaired Fe, Mn and Zn mobilisation from the vacuole (Molin (Molins et al., 2013) and there is evidence for Zn transport by NRAMP4 when expressed in yeast (Curie et al., 2000, Thomine et al., 2000, Lanquar et al., 2005). There is also evidence that certain members function in Cd transport. For example, disruption of At*NRAMP6* results in enhanced Cd tolerance, whereas the overexpression causes Cd hypersensitivity (Cailliatte et al., 2009). There are seven *NRAMP* genes in rice and several of them have been implicated in Cd transport. *OsNRAMP1*, is implicated in Cd-influx at the plasma membrane (Takahashi et al., 2011). Transgenic rice overexpressing *OsNRAMP1* accumulated Cd in the shoots with lower levels in the roots (Uraguchi et al., 2009). The entry of Cd into rice root cells is mediated mainly by the Mn transporter OsNRAMP5 as the suppression of *OsNRAMP5* resulted in lower Cd content in both shoot and roots (Ishimaru et al., 2012).

1.5.2.5 The ZIF-like (ZIFL) family of transporters

The Zn-Induced Facilitator-Like (ZIFL) family of proteins is involved in Zn homeostasis. AtZIF1 is a root vacuolar protein that transports NA, which is a metal chelator. Overexpression causes Zn to be retained in roots with decreased Zn translocation to shoots (Haydon et al., 2012) (further discussion on NA in Section 1.5.3.1). *AtZIFL1* and *AtZIFL2* are two closely related genes to *AtZIF1* but none of them have been shown to be involved in Zn homeostasis (Ricachenevsky et al., 2011). On the other hand, the less related gene to AtZIF1 known as *AtZIF2* showed an ability to transport excess Zn into vacuoles (Remy et al., 2014). AtZIF2 is up-regulated by high Zn and also under these conditions, there is retention of a 5' UTR intron which leads to efficient translation (Remy et al., 2014). Overexpression of *AtZIF2* leads to enhanced Zn tolerance, while the knockout of *AtZIF2* leads to plant sensitivity to excess Zn (Remy et al., 2014). Rice OsZIFL4/TOM1 (for transporter of mugineic acid family) is the only related member in cereals that has been characterised in detail. The main function of OsZIFL4/TOM1 is to transport phytosiderophores, such as deoxymugineic acid, from the roots into the rhizosphere (Nozoye et al., 2011). Deoxymugineic acid can interact with Zn to form Zn(II)-deoxymugineic, which will then be transported by OsZIFL4/TOM1 (Suzuki et al., 2008). In barley, microarray analyses revealed that a *ZIF-1* like gene is expressed in the aleurone layer of grain and its transcription increases in the embryo upon foliar Zn application (Tauris et al., 2009). Thus, there is a possibility that *ZIFL* genes are involved in Zn translocation in grain.

1.5.2.6 The Yellow Stripe-Like (YSL) Transporter Family

YSL transporters are members of the Oligopeptide Transporter (OPT) superfamily and their name is derived from the maize Yellow stripe 1 protein (ZnYSI) that mediates Fe transport. In order to transport Zn or Cd, YSL transporters require Zn or Cd to form complexes with either

phytosiderophores or NA before they can be transported into the cytosol by proton-coupled symport (DiDonato Jr. et al., 2004, Schaaf et al., 2004). In dicots, only NA is present to form a complex with Zn since they cannot synthesize phystosiderophores (Schaaf et al., 2004). Most of the YSL transporters seem to function in the lateral movement of metals from the vasculature (DiDonato Jr. et al., 2004). Even though *A. thaliana* has eight YSL transporters, only YSL2 has been shown to be strongly regulated by plant Zn status. Under Zn deficiency, the transcript level of *YSL2* is repressed while the NAS2 transcript, which encodes one of the four isoforms of *NA synthase* (*NAS*), is strongly increased (Klatte et al., 2009). However, YSL transporters are not usually associated directly with Zn stress because most of the time, they affect the Zn level in plants indirectly, depending on the Fe or Cu status (Haydon et al., 2012). Further studies are necessary to improve our understanding of their functions especially in cereals. To date, only HvYSL5 in barley (Zheng et al., 2011) and OsYSL15 in rice (Inoue et al., 2009) have been characterised but they are suggested to transport Fe not Zn or Cd.

1.5.2.7 Plant Cd Resistance (PCR) Proteins

PCR1 and PCR2 are two members of the PCR protein family in *A. thaliana*, which are involved in Zn and Cd redistribution, translocation, and detoxification (Song et al., 2004, Song et al., 2010b). The structure of both proteins suggests that they are membrane associated or membrane intrinsic proteins. They are rich in Cys with only two TM helices. PCR1 localises at the plasma membrane in both *S. cerevisiae* and *A. thaliana*. Cd tolerance is enhanced in plants overexpressing *PCR1* by exporting Cd out of cells (Song et al., 2004). PCR2 functions as a Zn efflux transporter, which contributes to Zn distribution and detoxification in *A. thaliana* (Song et al., 2010b). AtPCR2 may also play in Zn xylem loading as *pcr2 hma4* double mutants and *pcr2 hma2 hma4* triple mutants had an additive effect compared to the individual single mutants (Song et al., 2010b). PCR2 is located mainly in epidermal cells and in the xylem of young root (Song et al., 2010b). Based on current available data, AtPCR1 and AtPCR2 could be involved in extruding Cd or Zn from cells to avoid the toxicity effects of Zn and Cd (Song et al., 2010b).

1.5.2.8 ATP-Binding Cassette (ABC) transporters

Certain ABC transporters have been implicated in cellular Cd detoxification. There are 132 ABC transporters in *A. thaliana* (Verrier et al., 2008). *ABCC1* and *ABCC2* contribute to the accumulation of Cd-phytochelatin (Cd-PC) complexes in the vacuole (Park et al., 2011). In addition, AtPDR8 has been shown to transport Cd and Pb. AtPDR8 can be found in the plasma membrane of *A. thaliana* root hair cells and epidermal cells and when overexpressed they confer Cd tolerance (Korenkov et al., 2007). In rice*, ABCG43* is induced by Cd (Oda et al., 2011) but Its role has not been determined in detail. There is no detailed study of ABC transporter in other

cereals but in *Z. mays*, ZmABCG3, ZmABCG1, ZmABCG4, and ZmABCG8 are in the same evolutionary branch as AtPDR8, indicating that these four members of ABC transporter family could be involved in Cd detoxification (Pang et al., 2013).

1.5.2.9 Cation/proton exchangers (CAXs)

The main function of this secondary energised transporter family is to sequester Ca from the cytosol into the vacuole by proton exchange. Some members of this family in plants have also shown broad substrate specificity including Cd and Mn (Hirschi et al., 2000, Pittman et al., 2009). Several studies have indicated the role of CAXs in Cd tolerance in plants. For example, the expression of *Sedum alfreddi* (a Zn/Cd hyperaccumulating plant) *CAX2*-like gene in tobacco increased Cd content in the transgenic plant (Zhang et al., 2016). A member of this family in *A. thaliana* known as *CAX4* has been shown to be highly expressed under Cd toxicity and its *A. thaliana* mutant, *cax4*, is affected by Cd toxicity (Mei et al., 2009). In barley, the protein level of CAX1 in highly purified tonoplast has been showed to be increased under Cd-toxicity treatment, indicating its role in Cd detoxification (Schneider et al., 2009).

1.5.3 The role of Zn binding proteins/chelators in Zn homeostasis

Other than transporters, Zn binding proteins/chelators are also vital components for Zn homeostasis in plants. These ligands can control Zn concentrations in the cell by acting independently or assisting by other Zn transporters such as ZIFL and YSL family transporters (discussed earlier). These low-molecular-weight chelators allow Zn to be trafficked into different parts of the cells or to facilitate Zn long-distance transport into different plant tissues. One of these ligands also have been shown to be up-regulated. Therefore, it is important to consider their roles when investigating Zn homeostatic mechanisms in plants.

1.5.3.1 Nicotianamine (NA)

NA is a major Zn and Mn chelator in plants but it also chelates Fe and other metals such as Cu (Klatte et al., 2009, Deinlein et al., 2012, Persson et al., 2016). NA functions in the symplastic mobility of Zn in the root toward the pericycle cells (Curie et al., 2009, Clemens et al., 2013) and in *A. halleri,* NA synthases (NAS) are highly expressed and NA has been shown to be involved in root-to-shoot translocation of Zn with a five-fold decrease in *NAS2*-silenced lines (Deinlein et al., 2012). The multi-bioimaging of *A. thaliana nas1 nas2 nas3 nas4* quadruple mutants has shown that Zn and Mn concentrations in leaves and xylem sap are very low, suggesting NA roles in the root-to-shoot transport of Zn and Mn (Persson et al., 2016). The same observation was also obtained in *A. halleri* RNAi lines where the suppression of NA content resulted in low Zn concentrations in xylem

(Cornu et al., 2015). In rice, several reports have shown that the constitutive overexpression of *NAS* is able to increase Zn concentration in the grain by two-fold (Lee and An, 2009, Johnson et al., 2011, Lee et al., 2011). Moreover, NA has been suggested to be the major Zn ligand in the phloem sap of rice (Nishiyama et al., 2012). Cd is not bound to NA as it is highly specific for Zn and, accordingly, rice plants overexpressing *OsNAS* do not show an increase in Cd (Lee et al., 2011).

1.5.3.2 Phytochelatins (PC) and Glutathione

Phytochelatins (PCs) are small peptides synthesized by an enzyme called phytochelatin synthase (PCS) from glutathione. The main function of PCs in plants is to bind Zn or Cd so that basal Zn and Cd are maintained in cells (Cobbett and Goldsbrough, 2002). The *PCS1*-defective *cad1* mutant of *A. thaliana* exhibits Cd and Zn-hypersensitive traits (Lee and Kang, 2005). The reduced version of PCs, glutathione, can also assist Zn transport in plant cells by acting as an Zn intracellular ligand, which is the key component in basal Zn tolerance in *A. thaliana* (Shanmugam et al., 2011). Glutathione is important for Fe-mediated Zn tolerance. This was shown when *A. thaliana zir1* mutant, which is defective in γ-glutamylcysteine synthetase (γ-ECS, γ-glutamylcysteine ligase, GSH1), could not tolerate a high level of Zn in the presence of additional Fe, as compared with the WT (Shanmugam et al., 2012). PC are also important for Zn and Cd tolerance in cereals. During P deprivation, the PCs content in rice seedling was decreased, resulting in Cd sensitivity to plants (Yang et al., 2015).

1.5.3.3 Metallothioneins (MTs)

Metallothioneins (MTs) are heavy metal binding ligands that are rich with Cys, important in essential metal homeostasis such as Zn and detoxification of non-essential heavy metals such as Cd. *A. thaliana* has seven genes that encode for MTs, and they fall into four different classes. MT4a and MT4b have been reported to be involved in Zn homeostasis especially in seeds; there is a correlation between the expression levels of both genes and the ability of seeds to germinate at low-Zn conditions (Ren et al., 2011). Most of the studies indicate that MTs frequently bind to Cu but there is a correlation between the MTs affinity for Cu with their binding with Zn. This has been suggested in a study of metal hyperaccumulator plants, *N. caerulescens*, which suggests that MT genes are required for efficient Cu homeostasis in the presence of elevated Zn and Cd levels (Roosens et al., 2004). In rice, *OsMTP1a* encodes a type 1 metallothionein. An increased Zn accumulation was observed in both leaves and grains when *OsMTP1a* was overexpressed in rice (Yang et al., 2009b). In barley, MT3 and MT4 are thought to play different physiological roles during grain filling and in mature seeds (Hegelund et al., 2012). MT3 is proposed to function as a Zn and Cu housekeeping protein maintaining metal homeostasis, whereas MTP4 coordinates Zn with a putative storage function (Hegelund et al., 2012).

1.5.3.4 Histidine (His) and organic acids

His is the second most abundant Zn-ligand species found in the Zn-hyperaccumulator *N. caerulescen*s as suggested by X-ray absorption fine structure studies (Krämer et al., 1999). In *N. caerulescen*s, exogenous His supply has been shown to enhance Zn xylem loading (Kozhevnikova et al., 2014). Organic acids such as citrate and malate can form organic acid complexes with Zn before being sequestered into subcellular compartments (Kramer, 2010, Samardjieva et al., 2015). Various organic acids have been shown to be increased in different developmental stages and plant tissues when treated with high Zn in the Zn accumulator plant, *Solanum nigrum* (Samardjieva et al., 2015).

1.5.4 miRNA regulation of Zn homeostasis in plants

The micro RNAs (miRNAs) are part of a widespread family of 20 to 24 nucleotides endogenous RNAs (Zhang, 2015) that act as post-transcriptional gene expression regulators. In plants, miRNAs regulate plant growth, development and metabolism along with their involvement in abiotic stress and pathogen responses (Yang et al., 2013, Xie et al., 2015). There are reports of miRNA involvement in Cu (Sunkar et al., 2006, Beauclair et al., 2010), Mn (Valdes-Lopez et al., 2010), and Fe homeostasis (Waters et al., 2012). The involvement of miRNA in Zn homeostasis was shown in *Sorghum bicolor*. Zn deficiency in *S. bicolor* triggers the upregulation of several miRNA families, such as *miR166*, *miR171*, *miR172*, *miR398*, *miR399*, and *miR319*, and some of them have at least one ZDRE in their promoter (Li et al., 2013b). C*SD* is one of the miRNA target genes, and interestingly, two of the miRNA family members regulate *CSD* expression in the opposite manner. Up-regulated *miR398* reduces *CSD* gene expression in the roots, whereas downregulation of *miR528* increases *CSD* gene expression in the leaves (Li et al., 2013b). The miRNA mechanisms involve endonucleolytic cleavage or translational inhibition (Song et al., 2010a). Generally, the miRNA mode of action starts with the recruitment of single-stranded miRNA to the RNA-induced silencing complex (RISC). This RISC contains the sense strand that has a perfect complementary nucleotide sequences to the target genes leading to regulation of gene expression level at the post transcriptional or transcriptional levels (Lee et al., 2004, Vazquez et al., 2010).

1.6 Cd sensing in plants

Cd sensing in plants starts with the accumulation of hydrogen peroxide (H_2O_2) as a result of Cd toxicity. Subsequently, H_2O_2 acts as signalling molecule and it activates mitogen-activated protein kinases (MAPK) pathways (Mittler et al., 2004, Colcombet and Hirt, 2008). In *A. thaliana*,

the two MAPKs, MPK3 and MPK6, have been reported to exhibit a higher activity after Cd treatment (Liu et al., 2010). The rice MPK3 and MPK6 activities were also increased during high Cd treatment suggesting the conservation of MAPK cascades in Cd sensing in cereals (Yeh et al., 2007). The activated MAPK cascades target various TFs including Zn finger (ZAT), WRKY, **N**o apical meristem **A**rabidopsis activation TFs **C**up-shaped cotyledons (NAC), the dehydration-responsive element-binding (DREB), bZIP and the myeloblastosis (MYB) family (Petrov and Van Breusegem, 2012). Soybean (*Glycine max*) *bZIP62* (C-group) is one example of many TFs to be up-regulated by MAPK cascades during Cd toxicity (Chmielowska-Bak et al., 2013). The MAPK cascades also interact with nitric oxide (NO) as part of the Cd-sensing mechanism in plants. In *G. max* roots exposed to Cd, NO production is increased and *MAKPK2* is also up-regulated, indicating a cross-talk between NO and MAPK cascades (Chmielowska-Bak et al., 2013). Plants also utilise miRNAs to regulate Cd. Using a microarray-based analysis, Ding et al. (2011) reported that a total of nineteen Cd-responsive miRNAs were identified in rice. These miRNA target genes encoding TFs and kinases (Ding et al., 2011).

1.7 Tools for studying protein function

1.7.1 Bioinformatics

A flood of data is being generated by genome sequencing projects and it is followed by experimental efforts to verify and establish the structure and function of biological molecules. These data have to be interpreted and bioinformatics is a powerful tool to do this. Luscombe et al. (2001) defined bioinformatics as conceptualising biology in terms of macromolecules (in the sense of physical-chemistry) and then applying "informatics" techniques (derived from disciplines such as mathematics, computer science, and statistics) to understand and organise the information associated with this molecules, on a large-scale. Bioinformatics analyses focus on macromolecular structures, genome sequences, and the results of functional genomics experiments (e.g. expression data) analyses. Bioinformatics requires a wide range of computational techniques including sequence and structural alignment, database design and data mining, macromolecular geometry, phylogenetic tree construction, prediction of protein structure and function, gene finding, and expression data clustering.

In this project, gene prediction will be the first step of *in silico* analyses since many, bZIPs, ZIPs and P_{1B-2}-ATPases members in cereals are not known. Gene prediction is the process of attaching biological information to sequences and the basic level of sequence annotation requires a computer analysis tool known as Basic Local Alignment Tool (BLAST). BLAST is used to find region of similarity between sequences (Altschul et al., 1997, Boratyn et al., 2013). There are

several sequence databases available for gene finding in barley and wheat. The International Barley Sequencing Consortium (IBSC) has generated the first genome sequence of barley by conducting bacterial artificial chromosome (BAC) fingerprinting, BAC end sequencing, whole genome shotgun (WGS) sequencing, RNA-Seq analysis and genetic mapping, and these data are integrated to develop a gene-based genome sequence of the North American six-row spring malting barley cultivar Morex (Mayer et al., 2012). Bowman, Barke and a Tibetan hulless are other barley cultivars that have been WGS sequenced (Mayer et al., 2012, Zeng et al., 2015). Another barley cultivar known as Haruna Nijo, has also been sequenced and its full-length cDNA database is publicly available (Matsumoto et al., 2011). Recently, a comparative analysis between Haruna Nijo and Morex gene information was made to find a better gene model in barley (Sato et al., 2016). Wheat genome databases are less complete compared to barley due to the fact that the wheat genome is more challenging to sequence as it is a hexaploid with three sub-genomes (A, B and D) (Lai et al., 2012). Wheat genome size is about 17Gbp (Brenchley et al., 2012). On the other hand, barley genome is less complex since it is only diploid with the haploid genome size of 5.1Gbp (Mayer et al., 2012). The WGS sequencing method was used to sequence the wheat cultivar Chinese Spring (Brenchley et al., 2012) and its draft sequence was further analysed by the International Wheat Genome Sequencing Consortium (IWGSC) producing a survey of the gene content, and composition of all 21 chromosomes and identified 124,201 gene loci, with more than 75,000 positioned along the chromosomes by comparing to other grass genomes (Mayer et al., 2014). The BAC sequencing method was used by Choulet et al. (2014) to sequence the largest wheat chromosome, 3B.

There are also gene prediction programmes that can help researchers to determine the sequence from the BLAST search to be functional. GeneMark was the first gene finding software developed in 1993 and its algorithm uses species-specific inhomogeneous Markov chain models of protein-coding DNA sequence as well as homogeneous Markov chain models of non-coding DNA. Parameters of the models are estimated from training sets of sequences of known type (Besemer and Borodovsky, 2005). GenScan is an online programme that can also be used to identify open reading frames (ORFs) in genomic DNA and its algorithm is based on generalized hidden Markov model (GHMM) (Burge and Karlin, 1997).

Multiple annotated sequences can be used to generate a phylogenetic tree. Phylogenetics is the science of estimating the evolutionary past, and in the case of molecular phylogeny, based on the comparison of DNA or protein sequences (Baldauf, 2003). The purpose of phylogenetic analysis is to provide valuable information on the origin, evolution and possible functions of genes and the protein they might encode. The molecular phylogenetic trees are based on multiple sequence alignments, starting with the most similar sequences and progressively adding the most

dissimilar ones. Programmes such as the Molecular Evolutionary Genetics Analysis version 7.0 (MEGA 7) can facilitate researchers in building sequence alignments and constructing phylogenetic trees (Kumar et al., 2016).

1.7.2 *A. thaliana* T-DNA insertional mutants

Reverse genetics is a strategy to investigate the function of a particular gene by studying the phenotypes of individuals with alterations in the gene of interest. The reverse genetic approach in *A. thaliana* is widely used because of the establishment of large insertion mutant collections (Krysan et al., 1999, Sussman et al., 2000). *A. thaliana* genome has high gene density (Bevan et al., 1999). Thus, there are reasonably good chances of finding a transgenic plant carrying a T-DNA insert within any gene of interest when a large population of T-DNA transformed lines is generated. Floral dipping with *Agrobacterium tumefaciens* suspensions is the common method for introducing T-DNA in *A. thaliana*. The T-DNA of *A. tumefaciens* can be used to create a loss of function in plants since the insertion of T-DNA of the order of 5 to 25 kb in length generally produces a disruption of gene function. As the sequence of the inserted T-DNA is known, the gene in which the insertion has occurred can be recovered, using various PCR-based strategies. One way to screen for T-DNA insertion is by sequencing regions flanking insertion sites in individual plants from large insertion mutant populations, thereby determining large numbers of insertion sites in advance (Parinov et al., 1999). Several *A. thaliana* stock centres such as Ohio State University (USA) and Nottingham (UK) have large collections of the T-DNA insertion lines. Table 1.6 represents the lists of T-DNA insertion lines generated by various groups and are available with different centres.

1.7.3 Heterologous expression in *S. cerevisiae*

Heterologous expression is a system in which genes of interest are transferred and translated into hosts other than the original source to provide a simpler system for studies on functions of proteins and for elucidation of their roles in complex mechanisms such as metabolic reactions and membrane transport (Yesilirmak and Sayers, 2009). This project utilised *S. cerevisiae* as a host organism for heterologous expression because it has well-documented genetics and physiology, and proteins are post-translationally modified through similar processes to those in plants (Goffeau et al., 1996). Another advantage of using *S. cerevisiae* as an expression system is that there are widely available mutants with disrupted genes (Giaever et al., 2002), which allow the expression of homologous or complementing genes from plants, thus providing indications about the functions and interactions of the genes. However, this host system can have several limitations such as low yields, cell stress due to the presence of the foreign gene and

Table 1.6 T-DNA insertion collections by various groups

Submitted by	Background	Selectable marker	Promoter/ reporter gene	Population size	Reference
GABI-Kat	Columbia-0	Sulfadiazine	-	59455	Rosso et al. (2003)
INRA Versailles	Ws, (Wassil-ewskija)	Basta	*GUS*	1480	Balzergue et al. (2001)
SALK	Columbia-0	Kanamycin	-	145589	Alonso et al. (2003)
Feldmann	Ws	Kanamycin	-	4900	Azpiroz-Leehan and Feldmann (1997)
Sussman and Amasino	Ws-2	Kanamycin	*Ap2::GUS*	37800	Sussman et al. (2000)

hyperglycosylation of secreted foreign proteins (Yesilirmak and Sayers, 2009). The *S. cerevisiae* mutants provide a convenient system for functional and kinetic studies of transporters (Dreyer et al., 1999). Several membrane transporters have been characterised using *S. cerevisiae* such as HvHMA2 of barley, which transports Zn and Cd (Mills et al., 2012), and HvZIP5 of barley that transports Zn (Pedas et al., 2009).

A gene of interest is introduced into *S. cerevisiae* by expression vectors. Certain expression vectors also have elements such as protein tags that facilitate identification, quantification, purification and localisation. Frequently used fusion proteins are FLAG epitope-tag, green fluorescent protein (GFP) and His-tag. In respect to localisation, several studies have successfully used fusion protein in *S. cerevisiae* for localisation investigations. For example, *A. thaliana* AtHMA3, a Zn and Cd transporter was fused with GFP protein and it was targeted to the vacuole of *S. cerevisiae* (Gravot et al., 2004).

1.8 Aims

This thesis aims to provide a deeper understanding of Zn homeostatic mechanisms in plants. In particular, it investigates the mechanisms operating in adapting to Zn deficiency in barley to determine whether Zn-sensing mechanisms operating in dicots are conserved in this monocot. Concerning other aspect of Zn homeostasis (Zn-toxicity response), this project also investigates the functionality P_{1B-2}-ATPases in barley. Barley was chosen for this project because it ranks fourth among cereals in farming acreage and is an economically important species. Therefore, findings here are relevant to future breeding and biotechnological strategies for crop improvement and sustainable agriculture. Moreover, being a diploid grass it is a natural model for the genetics and genomics of the Triticeae tribe, especially hexaploid wheat (Schulte et al., 2009). In addition, there are excellent genetic resources and tools for barley: genome sequence information, efficient transformation methods and germplasm availability (Mayer et al., 2012, Harwood, 2014, Barabaschi et al., 2016).

Specific aims to investigate bZIP TFs in regulating the Zn-deficiency response in cereals and the roles of P_{1B-2}-ATPases include:

1. To carry out a sequence analyses of the F-group bZIPs, ZIPs and P_{1B-2}-ATPases. This can provide preliminary information regarding the characteristics of the genes/proteins and can be useful for experimental design.

2. To determine the role of bZIPs in regulating the Zn-deficiency response using a novel set of T-DNA insertion mutants. Agarose plate assays and a hydroponic culture system will be used to induce Zn-deficient conditions for characterising the mutants.

3. To investigate if barley has similar mechanisms to *A. thaliana* for dealing with Zn deficiency by:

    a. Expressing barley *bZIP19* and *bZIP23* orthologues in *A. thaliana bzip19 bzip23* double mutants.

    b. Analysing barley F-group bZIP TFs responses to Zn deficiency at the transcriptional level

    c. Identifying putative ZDRE in the promoters of barley *ZIP* membrane transporters

    d. Analysing the cellular localisation of HvbZIP56

4. To elucidate function of one member of the barley P_{1B-2}-ATPases, HvHMA3, using complementation assays by:

    a. Cloning *HvHMA3* into *A. thaliana* and *S. cerevisiae* expression vectors

    b. Expressing *HvHMA3* in Zn-sensitive *S. cerevisiae* mutants to indicate its function in Zn transport and its localisation

    c. Expressing *HvHMA3* in *A. thaliana hma3-2* and *mtp1-1* mutants to investigate function

    d. Further characterising of *A. thaliana hma3-2*, *mtp1-1* and *mtp1-1 hma3-2* in Zn and Cd-toxicity conditions

Chapter 2: Materials and Methods

2.1 Gene and protein nomenclature

In this thesis, the gene and protein nomenclatures follow the New Phytologist guideline (http://onlinelibrary.wiley.com/journal/10.1111/(ISSN)1469-8137/homepage/ForAuthors.html). At the beginning of gene/protein nomenclature is the two-lettered prefixes referring the species origin with the first letter in uppercase only e.g. *Arabidopsis thaliana* (At). For the gene nomenclature, all of the letters are italicised in uppercase e.g. *AtbZIP19*; protein symbols are uppercase and are not italicised e.g. AtbZIP19, and mutant symbols are in all lowercase and italicised e.g. *bzip19-1*. The plasmid constructs generated in this thesis is indicated by lowercase "p", e.g. pMDC32. The promoters of the constructs can be identified with uppercase "P", e.g. *P35S* and it may be followed by a reporter, all italicised, e.g *P35S::HvbZIP56::gfp.*

2.2 Plant material and growth conditions

Soil grown *A. thaliana* Columbia-8/Wassilewskija, wild-type and mutant seed were grown using a 1:1:1 (v/v) mix of Vapogro seed modular (Vapogro Ltd, UK), John Innes No. 2 (John Innes Manufacturers Association, UK) and Sinclair Vermiculite Medium Grade (Scot Plants Direct, UK). The mixture was autoclaved for 30 min at 121^{o}C. After cooling, the insecticide Imidacloprid (Bayer Environmental Sciences SAS, UK) was added at a final concentration 0.28g/L. Four seeds were sown onto moist soil in 7 × 7 × 8 cm DESCH7B square black pots (Desch, UK). The pots were covered with the clear film and it was removed once the seeds were germinated. Also, only one seedling was left in the pot while the others were removed. The plants were bagged in 60 × 30 × 10 cm in flower sleeves when the first fluorescence appeared, with two wood rods to support the plants. All plants were placed on trays where they were bottom-watered with tap water. These plants were grown in environmentally controlled rooms (ECRs) – Fitotron Plant Growth Chambers (Weiss Gallenkemp, UK) with a day night cycle (23°C, 16 h light, 120 µmol m^{-2} s^{-1}; 18°C, 8 h dark). The source of the broad-band white light (W) was provided by fluorescent tubes (MASTER TL-D Reflex 58W/840 ISL, Netherlands). The seed were harvested after approximately two to three months and transferred to 30ml universal containers (Sterillin, UK). For transformation using floral dipping (Section 2.3), the first flowering inflorescence was snipped to the rosette level to encourage more bolting to increase the transformation efficiency.

2.2.1 Growth of *A. thaliana* for metal-tolerance assays on plates

A. thaliana seeds were sterilised with 15% bleach (Domestos, UK) for 15 min. The bleach was removed by washing the seeds with sterile ddH_2O before the seeds were plated using a sterile glass pasteur pipette inside a flow hood (Envair, UK). For round and square plate assays, seeds were plated on petri dishes (Thermo Fisher Scientific, UK) containing 30ml and 75ml respectively of 0.5 Murashige and Skoog (MS) medium (Table 2.1). The contents of this solution were modified as required. The addition of $ZnSO_4.7H_2O$ (Sigma, USA), $MnSO_4.H_2O$ (Sigma, USA), FeNaEDTA (Sigma, USA), $CuSO_4.H_2O$ (Sigma, USA), $CdSO_4$ were modified to produce media with different Zn, Mn, Fe and Cu concentrations. The pH was adjusted to 5.8 (Jenway 3505 pH meter, UK) using analytical grade 0.5M potassium hydroxide (KOH). Media was autoclaved to sterilise using the sugar media setting (Touchclave-lab LTE, UK). 1.25cm 3M™ Micropore™ (3M, UK) was used to seal the edge of the plates and the plates were wrapped in aluminium foil. Seed were stratified in the dark at 4°C for 48 h prior to transfer to a controlled-environment cabinet (22°C, 16 h light, 120 µmol m^{-2} s^{-1}; 18°C, 8 h dark). The plates were incubated vertically for the phenotyping experiments and horizontally for the segregation ratio analyses (Section 2.3).

2.2.2 Growth of *A. thaliana* seedlings in hydroponic assays

To grow *A. thaliana* hydroponically, seeds were placed in 1.5ml Eppendorf tubes with lids and bottom removed, containing 0.5% agarose (Melford, UK). They were placed in polyethylene foam floats, positioned on top of the nutrient solution in hydroponic tubs. Seeds were stratified at 4°C for 48 h prior to transfer to a controlled-environment room under short day conditions (23°C, 8h light 120 µmol m^{-2} s^{-1}; 18°C, 16 h dark). The nutrient solution was based on Maathius et al., (2003) containing the following composition for control conditions (1.25mM KNO_3, 500µM $Ca(NO_3)_2.4H_2O$, 0.5mM $MgSO_4.7H_2O$, 42.5µM FeNaEDTA, 0.625mM KH_2PO_4, 2mM NaCl, 0.16µM $CuSO_4.5H_2O$, 0.38µM $ZnSO_4.7H_2O$, 1.8µM $MnSO_4.H_2O$, 45µM H_3BO_3, 0.015µM $(NH_4)_6Mo_7O_{24}.4H_2O$, and 0.01µM $CoCl_2.6H_2O$). Zn was included or excluded from the media depending on the experiments. The media was changed once after two weeks, and once every week after that. The plants were harvested after 40 days in the growth chamber

2.2.3 Growth of barley in hydroponic assays

To grow hydroponically, barley (*Hordeum vulgaris* L. cv Golden Promise) seed was sterilized in 1% bleach for 15 min, rinsed in sterile water, germinated on wet tissue paper for five days, and then individual seedlings were grown in aerated 1L hydroponic culture pots (Thermo Fischer Scientific, UK) in a controlled environment room (21°C, 16 h light, 220 µmol $m^{-2}s^{-1}$, 55% humidity;

Table 2.1 The contents of basal 0.5 MS media.

Macroelements	**Final Concentration (mM)**
$CaCl_2$	1.495
KH_2PO_4	0.625
KNO_3	9.395
$MgSO_4$	0.75
NH_4NO_3	10.305
Microelements	**Final Concentration (µM)**
$CoCl_2.6H_2O$	0.055
$CuSO_4.H_2O$	0.05
FeNaEDTA	50
H_3BO_3	50.135
KI	2.5
$MnSO_4.H_2O$	50
$Na_2MoO_4.2H_2O$	0.515
$ZnSO_4.7H_2O$	14.955

16°C, 8 h dark, 65% humidity). Pots were filled with a nutrient solution as described in Lombnaes and Singh (2003) which contained 2mM $Ca(NO_3)_2$, 1mM KNO_3, 80µM KH_2PO_4, 0.5mM $MgSO_4$, 0.01mM H_3BO_3, 0.9mM NaOH, 75µM $Fe(NO_3)_3$, 8.0µM $ZnCl_2$, 0.6µM $MnCl_2$, 2.0µM $CuCl_2$, 0.1µM $NiCl_2$, 0.1µM Na_2MoO_4 and 1mM HEDTA buffered at pH 6.0 with 1.0mM 2-[N-Morpholino]ethanesulfonic acid (MES). For the Zn-deficient treatment, Zn was omitted from the media. The nutrient solution was replaced every three days and, at day 14, KH_2PO_4 was increased to 160µM, as described previously (Lombnaes and Singh, 2003). Root and shoot were harvested separately either for fresh weight determinations or for freezing in liquid N_2 for subsequent RNA extraction (Section 2.6.6).

2.3 *A. thaliana* transformation using the floral dip method

Prior to *A. thaliana* transformation, the *A. thaliana* expression vector carrying the gene of interest was transformed into *A. tumefaciens.* One µl of the expression clone was mixed gently with 50µl of electrocompetent *A. tumefaciens* GV3850 cells (Section 2.6.1.2). The mixture was transferred to pre-cleaned and prechilled 0.2 cm electroporation cuvettes (Bio-Rad Laboratories, CA, USA) and pulsed at 1.8 V for 5 ms using the Biorad MicroPulser™ Electroporation Apparatus (Bio-Rad, CA, USA). Immediately after that, 1ml of Luria-Bertani (LB) medium (1 % (w/v) tryptone, 0.5 % (w/v) yeast extract, 1 % (w/v) NaCl) was added to the cuvette. The bacterial suspension was then transferred to a chilled 15ml culture tube. Incubation for the culture was set at 30°C with vigorous agitation (250rpm) in a Innova ™ 4300 Incubator Shaker (New Brunswick Scientific Ltd., UK) for 2 h. The culture was spread on LB agar (LB medium with 1.5 % (w/v) agar) plates containing 50µM carbenicillin, 50µM kanamycin and 50µM rifampicin; these were incubated at 30°C for 3 d. Colony PCR was performed on a selection of colonies (Section 2.6.10).

A positive colony carrying the construct of interest was inoculated in 5ml LB medium containing 50µM carbenicillin, 50µM kanamycin and 50µM rifampicin and incubated at 30°C with gentle agitation (190rpm) overnight. The 5ml culture was then poured into 500ml LB medium containing the same antibiotic selections and incubation conditions as the previous culture. The next day, 100µM acetosyringone (3',5'-dimethoxy-4'-hydroxyacetophenone) was added to the culture and incubated for another 3 h before the cells were harvested by centrifugation at 3700 *g* for 15 min. The bacterial cells were resuspended in 250ml of ddH_2O containing 5 % (w/v) sucrose. Prior to floral dipping, Silwet L-77 (van Meeuwen Chemicals BV, Netherlands) was added to the suspension to a final concentration of 0.05 % (v/v). The six-week old plants (T_0) that had had their first inflorescence clipped were selected for the floral dipping adapted from Clough and Bent (1998). The aerial parts of the plants were dipped into the *A. tumefaciens* culture prepared earlier for 30 s with gentle agitation (Figure 2.1 step 1). The dipped plants were placed in high humidity

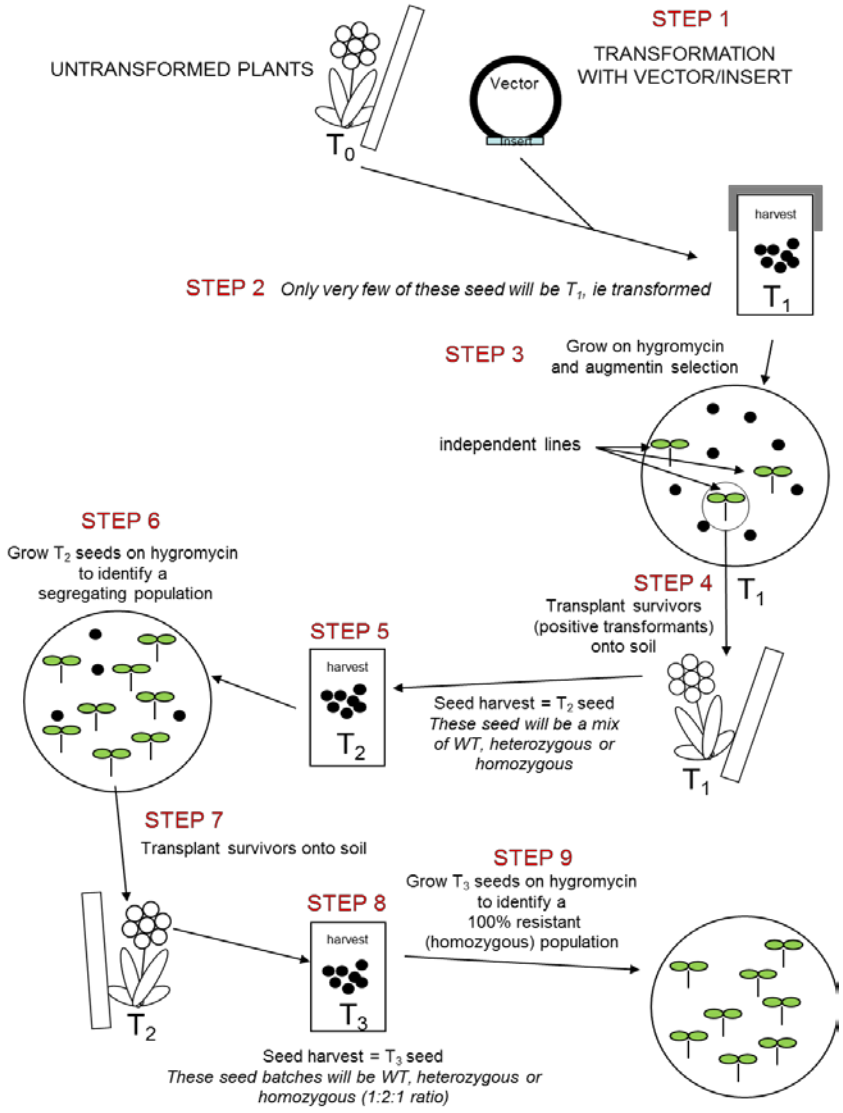

Figure 2.1 Scheme used to generate transgenic *A. thaliana* lines.

Three to four of each genotype e.g. *bzip19-4 bzip23-2* mutant plants was transformed with construct (**step 1**). T_1 seed was harvested (**step 2**). pMDC32 and pEG100 destination vectors used here have hygromycin and phosphinotricin resistance gene respectively as a positive selection marker. Grow T_1 seed grown on hygromycin and augmentin selection to identify independent transformants (**step 3**). Survivors were transplanted onto soil (**step 4**). T_1 plants were grown and their seed (T_2) was harvested; all T_2 seed are a mix of WT, heterozygous or homozygous for the insert (**step 5**). Segregation ratios was analysed by growing T_2 seeds on hygromycin to find ~75 % resistance lines indicating a single insert into the genome i.e. a segregating line (**step 6**). Transplant eight to ten survivors from each segregating line (independent lines) onto soil (**step 7**). T_2 plants were grown to mature for T_3 seed collection; all seed batches are either WT, heterozygous or homozygous for the insert (**step 8**). Homozygous T_3 seed batches were identified (indicated by 100% resistance to hygromycin) by growing seed on hygromycin (**step 9**). At least three independent lines for each construct transformed was identified in this way.

conditions by covering them with a plastic bag and sealing with tape in dimmed light for 24 h. The seeds were harvested once ripened.

In the first stage of selecting positively transformed plants, the T_1 seeds from T_0 plants were plated onto 0.5 MS media containing 1 % (w/v) sucrose and 1 % (w/v) agarose with the following antibiotic selections: 50µM hygromycin and 200µM augmentin (amoxicillin sodium and potassium clavulanate; Melford Laboratories Ltd., UK) (Figure 2.1 step 3). Seed were stratified in the dark at 4°C for 48 h prior to transfer to a controlled-environment cabinet (22°C, 16 h light, 120 µmol m^{-2} s^{-1}; 18°C, 8 h dark) and plates were incubated horizontally. The positive transformed seedlings were ready to be transplanted onto soil after two weeks (Figure 2.1 step 4). In the second stage, the T_2 seeds from T_1 plants were plated on on 0.5 MS media containing 1 % (w/v) sucrose, 1 % (w/v) agar and 50µM hygromycin for plants carrying pMDC32 or 15µM phosphinotricin (PPT) for plants carrying pEG100, and the survival ratio was recorded (steps 5 – 6). Eight to twelves T_2 seedlings from lines with a survival ratio of ~75% (±5%) were transplanted onto soil (Figure 2.1 step 7). In the last stage of selection, the T_3 seeds from T_2 plants were plated on 0.5 MS media containing selections mentioned earlier to find lines with 100% survival ratio, which were considered homozygous lines.

2.4 *A. thaliana* fresh weight measurement

A. thaliana seedlings were grown (as described in Section 2.2.1) on six plates for a range of different heavy metal concentrations. Each plate had an equal number of seedlings of WT, mutants, and transgenic lines, as appropriate. Following growth, the seedlings were removed from the plates using forceps and weighed (usually four to six seedlings per genotype, depending on experiment). The experiments were repeated at least two times in general and a representative experiment is shown.

2.5 Growth of *S. cerevisiae*

2.5.1 Culturing *S. cerevisiae* strains

Synthetic complete (SC) medium and SC medium without uracil (SC-ura) were the two types of media used for growing *S. cerevisiae* strains. Table 2.2 shows the compositions of these two media with pH adjusted to 5.3 before being autoclaved at 151°C for 15 min. Uracil (final concentration 0.68mM) was added into the media before either culturing on 90mm round plates or for inoculation for yeast drop testing (Section2.5.3)

2.5.2 *S. cerevisiae* transformation

A single colony of *S. cerevisiae* strain (Table 2.3) was selected from the cells that had been grown on agar for three days. The colony was dissolved in 1ml sterile ddH_2O and centrifuged at 15700*g* for 1 min. The cells were resuspended in 250µl of PLATE solution (8:1:1 ration of 50% polyethylene glycol (w/v), 1M lithium acetate pH 7.5 (w/v) and 10x TE buffer pH7.5 (w/v). Then, 5µl of boiled Herring sperm DNA was added. One µg of expression vector resuspended in 30µl of sterile ddH_2O) was added to the suspension. A heat shock at 42°C for 2 h was performed so that the *S. cerevisiae* cells could take up the expression vector. The cells were collected by centrifugation at 15700*g* for 1 min and resuspended in 200µl of sterile ddH_2O. The suspension was plated on SC Glucose minus uracil media and the transformed *S. cerevisiae* cells were incubated at 30°C for three days. The successful transformants were stored by inoculating them in 5ml SC Glucose minus uracil media at 28°C overnight in the shaking incubator and adding the overnight culture to 50% glycerol stock (v/v) to make final concentration of 15%. The stock was stored at -80°C until use.

2.5.3 *S. cerevisiae* drop testing for growth assays

Prior to the drop test, a single colony was inoculated in 10ml of SC glucose media containing uracil as in Table 2.2. The cells were grown with shaking at 200rpm at 30 °C in an Innova TM 4300 Incubator Shaker (New Brunswick Scientific Ltd., UK) overnight. The culture OD600 was adjusted between 0.42 – 0.45. Another two set of dilution was made, which were 1 in 10 and 1 in 100. All three sets of culture concentrations were inoculated onto SC agar assays containing the appropriate nutrients (any additional components for various growth assays are specified in the figure legends) by dropping 7µl of each concentration. The plates were incubated at 30°C for three days and photographs were taken to record growth.

2.6 Standard molecular biology methods

2.6.1 Bacterial cells preparation

Three *E. coli* and one *A. tumefaciens* were used in this study for cloning and gene expression (Table 2.4). These bacterial cells were prepared by making them competent for transformation before use (Section 2.6.1.1 and Section 2.6.3). In general, a sterile technique was carried out in handling these bacterial strains and the bacterial growth in liquid culture was facilitated by Innova ™ 4300 Incubator Shaker (New Brunswick Scientific Ltd., UK). The bacterial growth on plates was facilitated by Classic Incubator (LEEC, UK) and Gallenkamp Cooled

Table 2.2 SC-ura media composition for *S. cerevisiae* culture (liquid assay)

Reagent	SC Glucose	SC Galactose
Yeast nitrogen base w/o amino acids and ammonium sulphate (Difco 233520)	0.17 %	0.17 %
Ammonium sulphate (Sigma, USA)	0.5 %	0.5 %
Amino acids minus uracil (Sigma, USA)	0.192 %	0.192 %
Agar	2 %	2 %
Glucose (Sigma, USA)	2 %	-
Galactose (Sigma, USA)	-	2 %

Table 2.3 *S. cerevisiae* strains used in this study

#	Strains	Genotype
3	BY4741	*MAT a*; *his3*-Δ 1; *leu2*-Δ 0; *met15*-Δ 0; *ura3*-Δ 0
2	*Ycf1*	*MATα ura3-52 his6 leu2-3,-112 his3-Δ200 trp1-901 lys2-801 suc2-Δ, ycf1::hisG*
2	*zrc1*-Δ *cot1*-Δ	*MAT a*; *his3*-Δ 1; *leu2*-Δ 0; *met15*-Δ 0; *ura3*-Δ 0; *zrc1*::natMX *cot1*::*kanMX4*

Table 2.4 Bacterial strains used in this study

Bacterial strain	Usage	Source of competent cells
E. coli DB3.1	To propagate *ccdB* gene expressing vector	In-house (Section 2.6.1)
E. coli DH5α	To propagate expression vector	In-house (Section 2.6.1)
E. coli TOP10	To be transformed with TOPO entry vector	Invitrogen (USA)
A. tumefaciens GV3850	To be transformed with *A. thaliana* expression vector	In-house (Section 2.6.1)
A. tumefaciens GV3101	To expressed *HvbZIP56:GFP* in tobacco	In-house (Section 2.7)

Illuminated Incubator for *E. coli* strains and *A. tumefaciens* strain respectively. The LB media for growing these bacterial strains was prepared by mixing 1% (w/v) tryptone, 0.5% (w/v) yeast extract and 1 % (w/v) NaCl in ddH_2O with pH adjusted to 7.0. The LB media was sterilized by autoclaving (121 °C for 20 min). Antibiotic was added into melted LB agar when the temperature was around 55°C before pouring into 90mm plates. The collection of bacterial cells was performed using the Sorvall legend RT table-top centrifuge (Thermo Fisher Scientific, USA).

2.6.1.1 Preparing *E. coli* competent cells

Inoue transformation buffer was prepared first by making up 0.5M piperazine-1, 2-bis[2-ethanesulfonic acid] (PIPES). PIPES was dissolved in sterile ddH_2O and the pH was adjusted to 6.7 with 5M KOH. The solution was filter sterilised through a disposable Nalgene filter (0.45 µm pore size). The solution was stored at -20°C until use. The sterile PIPES was then added together with 55mM $MnCl_2.4H_2O$, 15mM $CaCl_2.2H_2O$, 250mM KCl and ddH_2O. The mixture then was sterilised by filtration through a pre-rinsed 0.45 µm filter. The sterilised transformation buffer was stored at -20°C.

DH5α *E. coli* strains were streaked on LB agar plate to obtain isolated colonies. The plates were incubated overnight at 37°C. A well-isolated colony was picked to be inoculated in 5ml LB broth and incubated in a shaking incubator (225rpm) at 37°C overnight. The inoculum was then transferred in a 1-L shaking flask containing 250ml LB medium. The bacterial cells in the flask were incubated up to OD600 of 0.5 at 22°C in the shaking incubator (160rpm). The incubation was stopped by putting the flask on ice for 10 min. The cells were collected using centrifugation at 2500×g for 10 min at 4°C, and resuspended in 20ml ice-cold transformation buffer, which had been prepared earlier. The cells were collected again using centrifugation at 2500×g for 10 min at 4°C, and resuspended in <1 ml ice-cold transformation buffer. Dimethyl sulfoxide (DMSO) was added to the bacterial suspension mix according to the volume of transformation used (1.5ml / 20ml transformation buffer). The cells became competent after the bacterial suspension mix stood on ice for 10 min. The bacterial suspension mix was dispensed (50µl) into chilled, sterile microfuge tubes, which were frozen immediately by immersing the microfuge tubes in liquid N_2. The cells were stored at -80°C.

2.6.1.2 Preparing *A. tumefaciens* competent cells

GSV3850 (C58) and GV3101 (pMP90) *A. tumefaciens* strains were used for *A. thaliana* and tobacco transformation respectively. The strain was streaked on LB agar plates with carbenicillin and rifampicin (both 50µM) and grown at 28°C for three days. An isolated colony from the plate was inoculated in 5ml LB with carbenicillin and rifampicin (both 50µM), and it was incubated at

28°C with vigorous agitation (225rpm) overnight. The next day the culture was transferred into 100ml LB with the same selective antibiotics and incubated overnight at 28°C with vigorous shaking until the cells had reached log phase (OD550 0.5 – 0.8). The cells growth was reduced by keeping them at 4°C and the cells were harvested by centrifugation at 4000*g* at 4°C for 10 min. The cells were resuspended with 100ml of ice-cold sterile ddH_2O. The volume of suspension was reduced to 40ml, 10ml and 1ml by centrifugation and resuspension in smaller volume of ddH_2O. The same centrifugation conditions were used. The final bacterial suspension mix was dispensed (50µl) into chilled, sterile microfuge tubes, which were then frozen by immersing the microfuge tubes in liquid N_2. The cells were stored at -80°C.

2.6.2 Plasmid Transformation by Heat Shock

One µl of plasmid was mixed with 50µl of chemically competent cells that had been prepared as in Section 2.6.1.1. The suspension was incubated on ice for 30 min, followed by a heat shock for 30 s in a water bath at 42°C, and transferred immediately to ice for 2 min. Thereafter, 800µl of LB medium was added to the mixture before it was incubated at 37°C for 1 h with vigorous agitation (225rpm). After incubation, 100 – 200µl of the culture was spread on LB agar plates containing the appropriate antibiotics (50µm kanamycin for pENTR, pMDC32, pMDC83, and pEG100; 50µm ampicillin for pAG426GAL-ccdB-EGFP) for selecting the successful transformed colonies. The resulting transformed colonies appeared after overnight incubation at 37°C.

2.6.3 Plasmid Transformation by Electroporation

Prior to the transformation, the 2 mm electroporation cuvettes were cleaned by soaking in 0.1M NaOH for 15 min. Reverse osmosis (RO) water was used to wash them afterwards before they were washed with 95% ethanol three times. One µl of plasmid was added into 50µl competent *A. tumefaciens*. The suspension was incubated on ice for at least 5 min before the electroporation was carried out using Gene Pulser Xcell™ Electroporation Systems (Bio-Rad, UK) with the following conditions: Capacitance = 25 µF, voltage = 2.4 kV, resistance = 200 Ohm, and pulse length 5 msec.

Immediately after electroporation, 1ml of LB was added to the cuvette containing the bacterial suspension and then it was transferred to a 15ml Falcon tube (Fisher Scientific, UK) and incubated at 28°C – 30°C for 2 h in a shaking incubator (250rpm). After incubation, 100 – 200 µl of the culture was plated on LB agar containing appropriate antibiotics. For *A. tumefaciens* that had been transformed with particular plasmids, three different selections were taken into account,

which were chromosomal marker and Ti plasmid marker for strain selection and foreign plasmid marker. The resulting transformed colonies appeared after 2 days incubation at 28-30^{o}C.

2.6.4 Plasmid Purification from bacterial cells

A well-isolated single colony from a freshly streaked selective plate was picked and inoculated into 5ml LB broth containing the appropriate selective antibiotic. The culture was kept in 20ml sterilin tube and it was incubated in the shaking incubator (225rpm) at 37^{o}C overnight. The next day, the glycerol stock was prepared by taking out and mixing 700µl of the culture with 300µl of 50% glycerol to make the final concentration of 15%. The glycerol stock of the bacterial culture was stored at -80^{o}C.

The remainder of the culture was used for plasmid minipreps using QIAprep Spin Minipreps kit (QIAGEN, UK) and a microcentrifuge. The bacterial cells were collected by centrifugation using the table-top centrifuge at 4550*g* for 10 min at 4^{o}C, and resuspended in 250µl of Buffer P1 (50 mM Tris-HCl pH 8.0, 10 mM EDTA, 100 µg/ml RNaseA). The bacterial cells in the suspension were lysed by adding and mixing 250µl Buffer P2 (200 mM NaOH, 1% SDS) into the suspension until a homogeneous suspension was achieved. Then, 350µl of Buffer N3, pH 4.8 (4.2M Gu-HCl, 0.9M potassium acetate) was added to the mixture to neutralize it and to make sure the efficient binding of plasmids to the silica membrane-based column. The precipitated proteins were removed by centrifugation at 15700*g* for 10 min at room temperature. The supernatant was applied into a QIAprep spin column before it was centrifuged at 15700*g* for 1 min. Once plasmids were bound to the QIAprep spin column, the wash was made using 500µl of Buffer PB, pH 6.6 (5M Gu-HCl, 30% ethanol) and 750µl of Buffer PE (10mM Tris-HCl pH 7.5, 80% ethanol). For each wash, a centrifugation at 15700*g* for 1 min was done and the flow through was discarded. However, a host strains such as DH5α did not require a wash with Buffer PB. An additional centrifugation at 15700*g* for 5 min was done to make sure the residual ethanol was completely removed from the plasmids. To elute plasmids from the column, 20µl of sterile distilled water was added into the column and it was centrifuged at 15700*g* for 1 min.

2.6.5 Genomic DNA Isolation from plant material

Genomic DNA was prepared using the DNAmite kit (MIcrozone, UK). The tissues were collected by taking a combination of one or two inflorescences and a few 1-2 cm^2 leaves into a 1.5 ml Eppendorf. For monocot plants, the tissue was ground in a pestle and mortar first using liquid N_2 to produce a powder. The tissue powder was allowed to warm up to room temperature before continuing to the next step. Three hundred µl of cell lysis solution (LA) was added into the

Eppendorf. The tissues were ground with sterile pestle thoroughly and vortexed briefly. Thirty µl of protein denaturation solution (PA) was added to the mixture and briefly vortexed to denature the protein. The isolation between the debris (denatured proteins and cell walls) and genomic DNA was carried out by centrifugation at 9300*g* for 15 min and 200µl of supernatant that contained genetomic material was centrifuged again to completely remove the debris. The purified supernatant (175µl) was added into 175µl of solution microCLEANg (CA) to capture, clean, and concentrate genomic DNA. The genomic DNA was pelleted by centrifugation at 15700*g* for 7 min. The supernatant was removed and the genomic DNA was rehydrated with 20µl of sterile distilled water and it was left in the room temperature overnight. The genomic DNA prep was stored at -20^{o}C until it was used for PCR reactions.

2.6.6 RNA Isolation

Fresh *A. thaliana* tissues were collected in 1.5ml Eppendorf tubes, frozen immediately in liquid N_2 and stored at -80^{o}C until use. The leaf tissues were ground using the pre-chilled pestle and mortar. The plant materials were kept frozen allowing easy grinding to a fine powder. A pre-chilled 1.5ml Eppendorf tube was filled with the fine powder and it was kept cold in dry ice to avoid RNA degradation. The breaking up of cells was done by adding 500µl of RNA miniprep buffer (1M NaCl, 1M Tris pH 7, disodium EDTA pH 8, 10% SDS, distilled water). Once proteins were denatured, the isolation of genetic material from denatured proteins was carried out by adding 150µl of phenol and 250µl of chloroform into the mixture. Centrifugation at 15700*g* for 5 min at 4^{o}C was done to create an aqueous phase and organic phase. The nucleic acids remained in the aqueous phase, while denatured protein remained in the organic phase. The aqueous phase was extracted and mixed with 450µl of 4M lithium chloride (LiCl). The nucleic acids were allowed to precipitate at 4^{o}C overnight and collected by centrifugation at 15700*g* for 20 min at 4^{o}C. The genomic DNA removal was done by resuspending the pellet in 300µl of DNAse buffer (1M Tris pH7, $MgCl_2$, $CaCl_2$, distilled water) and 1µl of DNAse was added to the suspension. The suspension was incubated at 37^{o}C for 60 min. Afterwards, the suspension was centrifuged at 15700*g* for 5 min at 4^{o}C, which resulted in the formation of two different phases. The aqueous phase was extracted and mixed with 2.5x volume of 100% ethanol containing 5% NaAc (3M, pH 5.5). RNA was allowed to precipitate in this mixture at -20^{o}C for 1 h and collected by centrifugation at 15700*g* for 5 min. The pellets were washed with 1ml of 75% ethanol twice, with a centrifugation at 7600*g* for 5 min between the washes. The supernatant was removed and the RNA pellet was air-dried before it was resuspended in 30µl of TE buffer (1M Tris pH 7, 0.5M Disodium EDTA pH 8, ddH_2O). The RNA was stored at -80^{o}C until use.

RNA isolation from barley samples was done using Guanidium thiocyanate phenol-chloroform (TRIZOL) reagent (Invitrogen Life Technologies, USA). Plant samples were ground into fine powder in liquid N_2 prior to RNA extraction. The grinding was carried out using a sterile, autoclaved pestle and mortar, pre-chilled using liquid N_2. Approximately, 500µl of fine powder was transferred into 1.5 ml Eppendorf tubes, which then was mix homogeneously with 1ml TRIZOL reagent to maintain RNA integrity, while at the same time disrupting and breaking down cells and cell components. To separate RNA from denatured proteins, 200µl of chloroform per 1ml TRIZOL was added to the solution and the aqueous phase was extracted after centrifugation at 12000g for 15 min at 4°C. RNA was recovered by precipitation with the addition of 500µl of isopropyl alcohol per 1ml TRIZOL into the aqueous phase. RNA was collected by centrifugation at 12000g for 15 min at 4°C. The RNA pellet was washed twice with the addition of 1ml of 75% ethanol. The dried pellet was resuspended in 30µl of 1X TE buffer and the suspension was stored at -80°C until use.

2.6.7 cDNA Synthesis

The isolated RNA was used to generate complementary DNA (cDNA) that can be used for normal PCR or quantitative reverse transcriptase-PCR (qRT-PCR). cDNA was produced using the Superscript III kit (Invitrogen, UK). Prior to the cDNA synthesis, the concentration of treated RNA sample was measured using the Nanodrop spectrophotometer (Thermo Scientific, UK) as in Section 2.6.8 so that the volume of RNA sample required to give 1000ng can be calculated. 1000ng RNA sample was denatured together with 5µM oligo dT18 primer (Sigma, Missouri, USA) in a total of 3.6µL sterile ddH_2O. This was incubated at 72°C for 5 min and then chilled to 4°C. In every 20µl reaction, 4µl of 5x buffer, 6.4µl of 25mM $MgCl_2$, 4µl of 10mM DNTPs consisting of adenine, thymine, cytosine and guanine, 1µl of reverse transcriptase (RT), 1µl of Oligo DTT and 1000ng of RNA sample in 3.6µl of SDW were mixed in a PCR tube. The sample was put through a cycle starting with the annealing of Oligo DTT primer to the 3'-end (Poly-A tail) of RNA strand at 25°C for 5 min. Then, 42°C for 60 min to extend the strand with the help of the reverse transcriptase and the cycle was finished with the inactivation of the enzyme at 70°C for 15 min. The resulting cDNA was stored at -20°C until use.

2.6.8 DNA Sample Quality Check

All DNA and RNA samples that had been prepared for cloning and sequencing underwent quality and quantity checks by nanodrop spectrophotometer (Thermo Scientific, UK) with the programme ND-1000 V3.7.7, to analyse the measurement made by the Nanodrop spectrophotometer. One µl of the RNA/DNA sample was loaded onto the sample pedestal and the

absorbance was measured over the range of 200 – 300 nm. The program utilises the Beer-Lambert equation (A = E x b x c) to correlate the absorbance reading at 260 nm to calculate nucleic acid concentration.

2.6.9 DNA Amplification by RT-PCR

DNA amplification was carried out by RT-PCR. DNA samples from genomic DNA or cDNA were amplified in a PCR tube and the reaction was performed using peqSTAR thermocylcer (PEQLAB, Germany). Table 2.5 provides the details on the PCR reagents and its concentration, while Table 2.6 provides the PCR conditions used in this project. Table 2.7 provides the primers information used in this project. For GATEWAY® cloning (Section 2.6.13), the gene amplification was performed with the proof-reading Pfu DNA polymerase (Promega, UK) to obtain a blunt end product. The other type of PCR used in this project was colony PCR, which was useful for checking colonies for successful bacterial transformation. The PCR products were run through 1% (w/v) agarose gels at 120V for 1 hour together with Hyperladder I (Bioline, UK) to predict the size of the amplified product. The visualization of the product was done using GelRed™ (Biotium, USA).

2.6.10 Colony PCR

The presence of constructs in the bacterial cells after transformation was confirmed using colony PCR. The reactions was carried out as in Section 2.6.9 but the 1µl DNA sample was replaced with one colony. The colony was lightly touched with a sterile pipette tip and it was dipped and swirled into 10µl PCR mix.

2.6.11 Quantitative RT-PCR (qPCR)

Quantitative RT-PCR (qPCR) was used to measure the expression level of genes of interest. The reaction was set up in 10µl reactions containing 2.5ng template DNA, 0.3µM forward primer, 0.3µM forward primers (Table 2.7), 1x SYBR-Green Master Mix (Primer Design, UK) and sterile ddH_2O. The mix was loaded into a 96-well plate and sealed with clear caps (MJ Research, USA). The solution was mixed by vortexing the whole plate and spun at 2000g for 2 min. The reaction was carried out on an Opticon DNA Engine Continuous Fluorescene Detector (GRI Braintree, UK) using the Opticon Monitor III program. PCR was generally performed at 95°C for 10 min followed by 40 cycles of 95°C for 15 s and 60°C for 1 min. Gene expression levels were calculated based on Pfaffl (2001), standardised by normalizing to *HvRNABP* expression (Mikkelsen et al., 2012). The results presented are from three biological reps with two technical reps for each and the

Table 2.5 PCR reagent concentrations used for different reactions

	Amplifying products for cloning using proofreader *Pfu*	**RT-PCR + Colony PCR using BioMix™**
Reagent	**Concentration**	
Template DNA	10nM	1nM /colony trace
2X BioMix Red™	-	1x
10X *Pfu* Buffer	1x	-
10 mM dNTPs	200µM	-
10 µM forward primer	1µM	200nM
10 µM reverse primer	1µM	200nM
Pfu polymerase	1.25 Units	-
Sterile 18 MΩ H2O	Up to 50µL	Up to 10µL

Table 2.6 Cycling conditions used for different PCR reactions

	Amplifying products for cloning using proofreader *Pfu*	**RT-PCR + Colony PCR using BioMix™**
Step	**Temperatures and Duration**	
Initial denaturation	95°C, 2 min	94°C, 2 min
Denaturation	95°C, 1 min	94°C, 30 s
Annealing	54-65°C*, 30 s	55°C, 1 min
Extension	72°C, 1 min/500 bases	72°C, 1 min
Repeat cycle	40 cycles	35 cycles
Final extension	72°C, 7 min	72°C, 3 min
Storage	4°C, indefinite	4°C, indefinite

*Annealing temperature is specific to primers used for cloning.

Table 2.7 Primer purpose, nomenclature and sequences.

Function: Genotyping *bzip19* and *bzip23 A. thaliana* mutants.		
No	**Primer name**	**Sequence (5' to 3')**
1	LBa	TGGTTCACGTAGTGGGCCATCG
2	LBb	GCGTGGACCGCTTGCTGCAACT
3	bZIP19F2	CTGTTTAGTGCGCCTTTAT
4	bZIP23R2	AAGGAACCTGAGCGAAGCTG
5	bZIP23F2	TCTTAAACCCTTCTCGCCGT
6	bZIP23R2	CAAACTGCTTTCGCTGCTCG
7	Actin2 F	GGTAACATTGTGCTCAGTGGTGG
8	Actin2 R	CTCGGCCTTGGAGATCCACATC
Function: *HvbZIP* genes GATEWAY cloning		
No	**Primer name**	**Sequence (5' to 3')**
9	HvbZIP1topo_F	CACCATGGACGACGGGCACCTC
10	HvbZIP1topo_S	CTAATGAAAACACGTATGAGG
11	HvbZIP10topo_F	CACCATGGACGACAACGGGGAC
12	HvbZIP10topo_S	TCACCTCTTTACATCATCTGGCA
13	HvbZIP55topo_F	CACCATGGACGACGGACTATAC
14	HvbZIP55topo_S	TTAGGCAACAGAGTTCACGAAGC
15	HvbZIP56topo_F	CACCATGGACGACGGGGACATC
16	HvbZIP56topo_S	TCATTATAGCATCCTAGCTAACG
17	HvbZIP56topo_NS	TTATAGCATCCTAGCTAACG
18	HvbZIP57topo_F	CACCATGGACGACGGGGTGGAC
19	HvbZIP57topo_S	TCAGCTAGGGAAGCAGAGCTC
20	HvbZIP58topo_F	CACCATGGACGACGGGGACCTG
21	HvbZIP58topo_S	CTAACGAAAACAGACAGGAGG

22	HvbZIP62topo_F	CACCATGGATGACGGGGACCTC
23	HvbZIP62topo_S	TCACTGCTTTTCGGAACTGGG
Function: Colony PCR for checking the positive clones		
24	M13F	TGTAAAACGACGGCCAGT
25	M13R	CAGGAAACAGCTATGACC
26	pMDC35S	CATTTGGAGAGGACCTCGACTCT
27	MDCnosR	AAGACCGGCAACAGGATTC
28	p426Gal1.F	GCGAAGCGATGATTTTTGATCTATT
29	p426Gal1.R	TCCTTCCTTTTCGGTTAGAGCG
30	pAG426FP.R	AGCTCGACCAGGATGGGCAC
31	AttL1B1NotI	GTACAAAAAAGCAGGCTCC
32	GFP R	CTGTTGACGAGGGTGTCTCC
33	HvH3rtF	GGTCGCTGGAGATGAGAAGG
Function: Real time RT PCR *H. vulgare bZIP* and *ZIP* expression analysis		
No	**Primer name**	**Sequence (5' to 3')**
34	HvRNABP F	CGCCCAGTTATCCATCCATCTA
35	HvRNABP R	AAAAACACCACAGGACCGGAC
36	HvGADPH F	GCTCAAGGGTATCATGGGTTACG
37	HvGADPH R	GCAATTCCAGCCTTAGCATCAAAG
38	HvZIP5rtF	ATCATCGGCATGTCCTTGGG
39	HvZIP5rtR	AAGAAAGACTTGTGGCGAAACC
40	HvZIP13rtF	GCTCGGCATCAACATCTCC
41	HvZIP13rtR	GTTGTAGGCTTGCGGCTAG
42	HvZIP14rtF	CACAGATGCACGATCAGAGAAC
43	HvZIP14rtR	CCACAATATCCACGGAACTCATA
44	HvbZIP1rtF	ACGACATCCTCATGGACACG

45	HvbZIP1rtR	TAATCTGGGCACCGCCCT
46	HvZIP10rtF	GACCTCATTGCTGCTGATTT
47	HvZIP10rtR	AGCTAGGCAACAGGTCGTAGT
48	HvbZIP55rtF	TCTGTCGTCTGTACTGCTGC
49	HvbZIP55rtR	ACAGCATCCACCACTTCAGG
50	HvbZIP56rtF	TGCCGGTGACACTATGGGTT
51	HvbZIP56rtR	TTACAGCATTTGGCCCCCA
52	HvbZIP57rtF	ATTGCGGGCTCGATGAAGAT
53	HvbZIP57rtR	GCTAGGGAAGCAGAGCTCAA
54	HvbZIP58rtF	GTCAGGGGCAGGATCGAAG
55	HvbZIP58rtR	TGAGCTCATCATGACCGGG
56	HvbZIP62rtF	CATTGGGGGTGCGAAATCTG
57	HvbZIP62rtR	GAACTGGGTAAACAGCCGGA
Function: Genotyping *hma3-1, hma3-2,* and *mtp1-1 A. thaliana* mutants.		
58	AtHMA3F	ACGTCGTTGGAATCTGCTGT
59	AtHMA3R	TATCCGCGATCACTGCCTTC
60	JL202	CATTTTATAATAACGCTGCGGACATCTAC
61	AtMTP1F	TCTTCAAGTCCCCACCATAGTCACA
62	AtMTP1F(Kobae)	GGGTGACTGTTACCACTCATCACCATC
63	AtMTP1R	TGACTAATGTTGTACTCCCTGCGGA
64	LBT-DNA	CTACAAATTGCCTTTTCTTATCGAC
65	FLAG TDNA fLB	CGTGTGCCAGGTGCCCACGGAATAGT
Function: *HvHMA3* gene GATEWAY cloning		
66	HvHMA3TopoF2	CACCATGACGGGCAGC
67	HvHMA3WithStop	CTACATGTTCCTACCTGTTTTTTCACGGGAGC
68	HvHMA3NoStop	CATGTTCCTACCTGTTTTTTCACGGGAGC

expression levels were expressed relative to expression at day 0 of the treatment, which was expressed as 1.

2.6.12 Gel Extraction

The extraction of DNA sample from the agarose gels was performed using QIAquick gel extraction kit (Qiagen, UK). In the dark room, the intended DNA fragment was excised with the help of UV transilluminator. The excised gel was weighed before adding three times volume of Buffer QG and the gel was solubilized in the buffer QG at 50°C for 10 min. The pH of the solution was checked by looking at the colour of the solution. 10µl of 3M sodium acetate, pH 5.0 was added when the colour was orange or violet until the solution turned yellow. The yield of DNA fragments was increased by adding 1x volume of 100% isopropanol to the solution. To bind DNA, the solution was poured into the column with a 2 ml collection tube and it was centrifuged at 15700*g* for 1 min. The DNA bounded on the column was washed with 750µl of Buffer PE and the column was centrifuged at 15700*g* for 5 min. The purified DNA molecule was collected in 1.5 ml Eppendorf by adding 20µl of sterile ddH_2O and the elution was achieved by centrifugation at 15700*g* for 1 min. The concentration of extracted DNA was measured using a Nanodrop spectrophotometer as in Section 2.6.8. The extracted DNA was stored at -20°C until it was used for Gateway cloning or sequencing.

2.6.13 GATEWAY® cloning to introduce barley genes of interest into expression vectors

The amplification with Pfu polymerase (Section 2.6.9) was performed with specific gene of interest primers to obtain a blunt-end PCR. The forward primers were designed starting with 'CACC'. Primer pairs used for cloning are outlined in Table 2.7. The PCR conditions were 1 cycle of 2 min at 95°C, followed by 38 cycles of 1 min at 95°C, 30 s at 65°C, and 2 min at 72°C, and finishing with 5 minutes incubation at 72°C. The resulting PCR product was run on 1% agarose gel (w/v) before it was purified as mentioned in Section 2.6.12. The DNA was topoisomerase-cloned into the TOPO® pENTR/D entry vector (Invitrogen, USA) according to the manufacturer's instructions (Invitrogen, USA) in 3 µl reaction containing 35ng of PCR product, 0.5µl salt solution, 0.5µl of TOPO® pENTR/D entry vector and sterile ddH_2O to a final volume of 3µl. The topoisomerase reaction was carried out at room temperature for 30 min facilitated by topoisomerase I. The resultant entry plasmids were transformed into chemically competent TOP10 *E. coli* (Invitrogen, USA) as in Section 2.6.2. The transformed cells were spread on LB containing 50 µM kanamycin and incubated at 37°C overnight. The verification of successful transformation was checked by colony PCR (Section 2.6.10) and the positive colonies were inoculated in the 5ml LB broth

containing the 50 µM kanamycin overnight. The plasmid purification was performed as in Section 2.6.4 prior to the restriction enzyme analyses (Section 2.6.14).

The successful entry vectors were introduced into several destination vectors such as pAG426GAL-ccdB-EGFP, pMDC32 and pMDC83 by carrying out the LR Clonase™ reaction based on the manufacturer's instructions (Invitrogen, USA): 75ng of entry vector was combined with 75ng of destination vector, TE buffer (pH 8.0) to a final volume of 4µl and 1 µl of LR Clonase ™ II enzyme. The mixture was incubated at 25°C for 16 h in the PCR machine. The recombination was stopped by adding 0.55µl of proteinase K followed by incubation at 37°C for 10 min. The confirmation of correct destination vectors was done by the same diagnostic tests that were performed on entry vectors. The plasmid was sequenced in both directions (Section 2.6.15) as the final check.

2.6.14 Diagnostic restriction enzyme analysis of plasmids

Plasmids were digested in a 10µl reaction containing 0.2µg of DNA, 1µl of restriction enzyme, 1µl of 100µM BSA, 1x buffer (Promega, USA) and ddH_2O to a final volume of 10µl. The mix was incubated at 37°C for 2 h followed by enzyme denaturation at 65°C for 15 min. The cut plasmid was run on the 1% agarose gel (w/v) for analysis. The size prediction of the reaction was carried out using pDRAW32 software (http://www.acaclone.com/).

2.6.15 DNA sequencing and analysis

Sequencing of plasmid DNA or DNA purified from gels were performed by Sanger sequencing service (Source Bioscience Life Sciences, UK). A pair reads (forward and reverse reactions) was requested and this was repeated twice. BioEdit 7.0.9.0 Sequence Alignment Editor Program (http://www.mbio.ncsu.edu/bioedit/bioedit.html) was used to visualise the sequence received. The actual sequence of the DNA was aligned with the sequence received using the EMBL-EBI EMBOSS Needle - Pairwise Sequence Alignment Program, which uses the Needleman-Wunsch algorithm (http://www.ebi.ac.uk/Tools/psa/emboss_needle/nucleotide.html).

2.7 Transient expression in tobacco

Tobacco (*N. tabacum* cv Petit Havana) was grown in the glasshouse at 21°C for four weeks prior to transformation. 1.5µl expression vector was introduced into 50µl *A. tumefaciens* strain GV3101 (pMP90) by mixing them in liquid N_2 before incubating at 37^{o}C for 5min. 1ml LB is added to the mixture and incubate at 28^{o}C for 3 h at 200rpm. The transformed cells were harvested by centrifugation at 15700*g* for 30 s and resuspended in 100µl of LB media. The cells were plated on

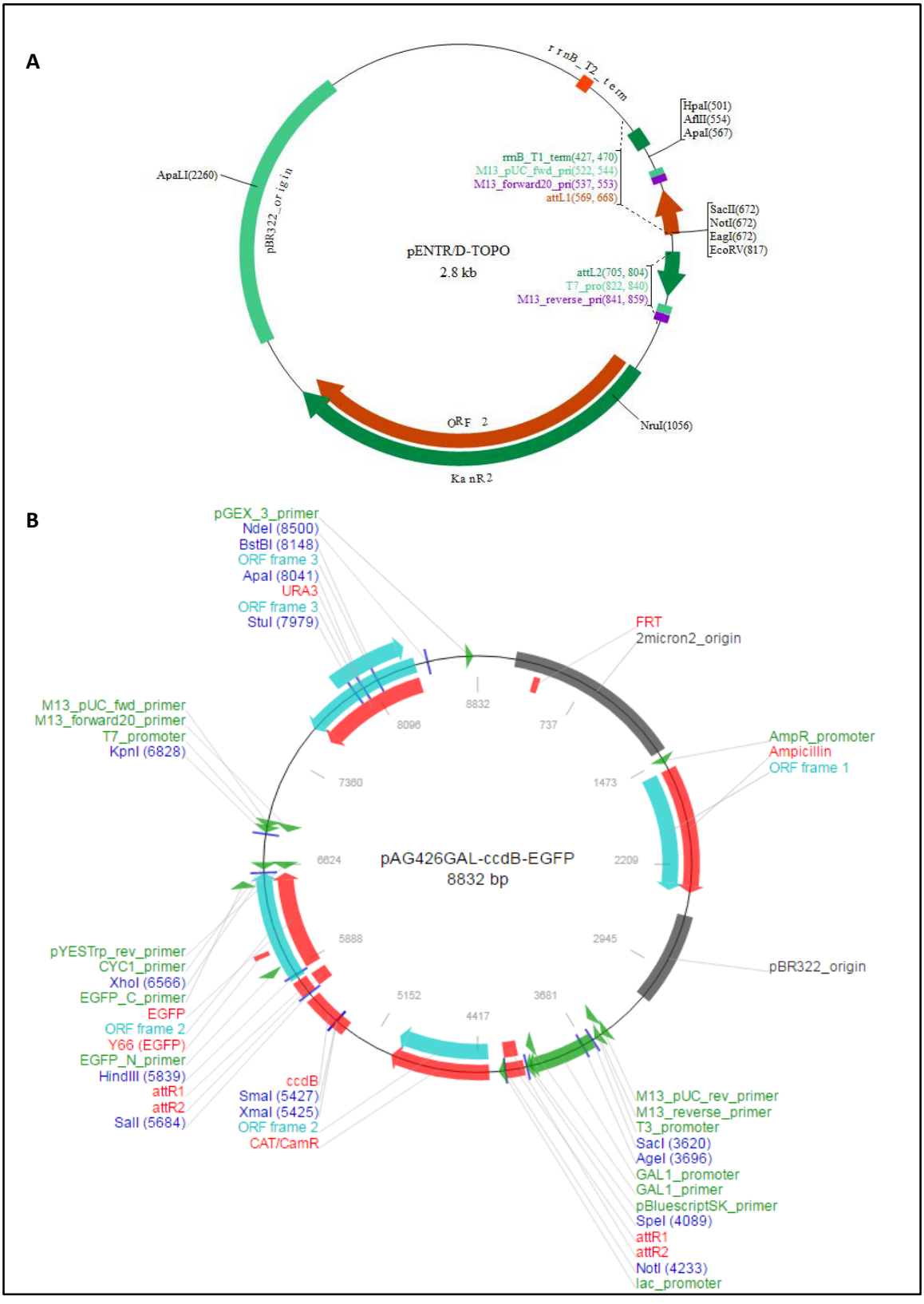

Figure 2.2 Vectors used in this study.

Vector map of pENTR/D-TOPO (A), *S. cerevisae* destination vectors pAG426GAL-ccdB-EGFP (B), *A. thaliana* destination vectors pMDC32 (C), and pMDC83 (D). Figures taken from Curtis and Grossniklaus (2003) and Alberti et al. (2007).

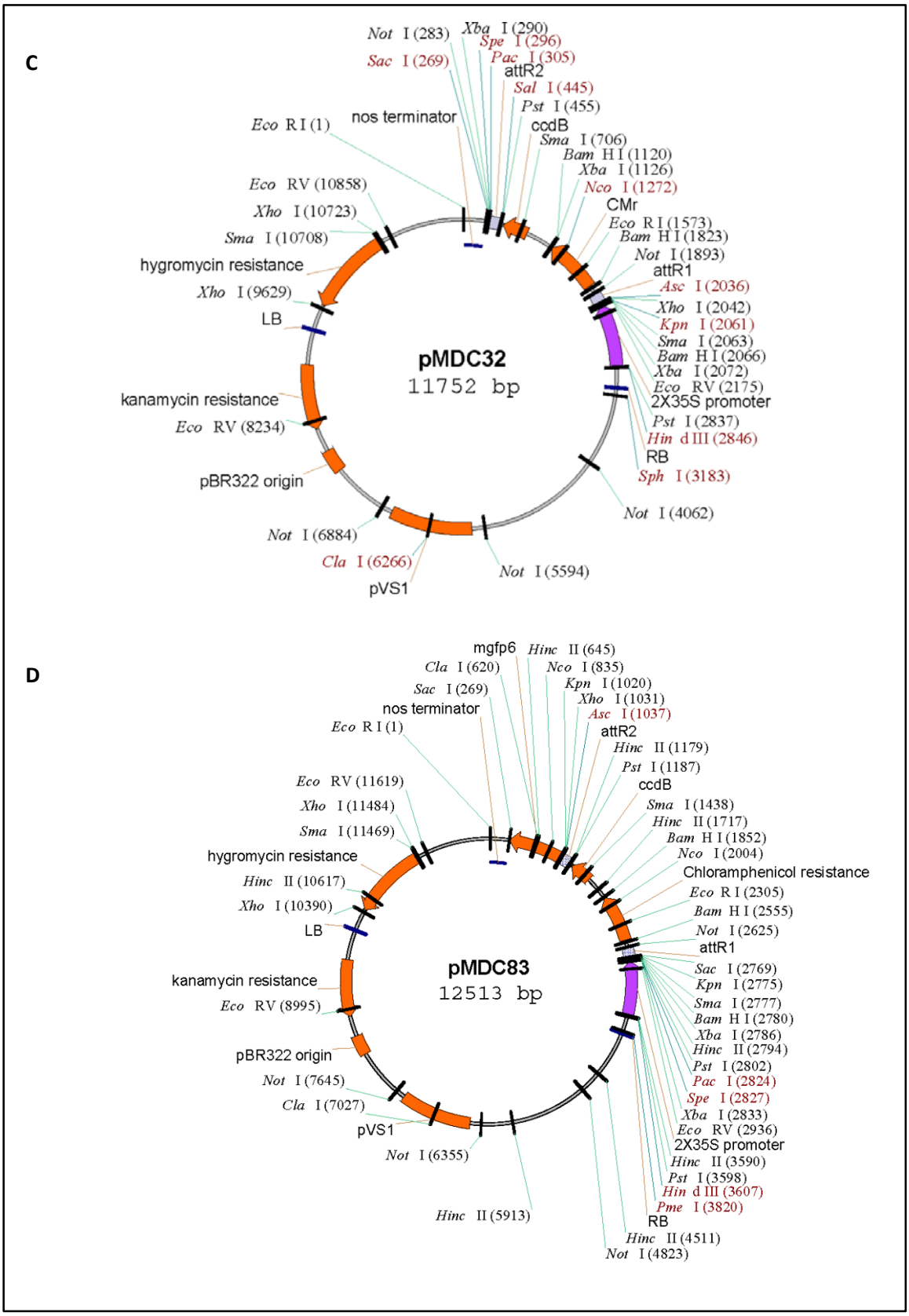

Figure 2.2 continued

25µM rifampicin (in methanol), 30µM gentamycin, and 25µM kanamycin. A colony PCR was used with gene-specific primers (Table 2.7) to determine positive colonies. A single positive colony was inoculated into 5ml LB media supplemented with previously mentioned antibiotics and the culture was grown overnight at 28^{o}C at 200rpm. The cells were harvested by centrifugation for 5 min at 3441*g*. The pellet was washed once with 1ml of infiltration medium (50mM Mes, 2mM $Na_3PO_4 \cdot 12H_2O$, 1mM acetosyringone, and 5 mg/ml D-Glucose) and then resuspended in 2ml of the same buffer. The mixture was left in the room temperature for 2 h before its OD_{600} was measured. The bacterial suspension OD_{600} was diluted to 0.5 by adding the infiltration buffer up to 3ml. For experiments requiring co-expression of two different constructs, the cells carrying two different constructs were mixed together with both cells had 0.5 OD_{600}.

A small hole was made on the lower epidermal surface of the leaf using a small needle before the bacterial suspension was inoculated using a 1-ml syringe without a needle by gentle pressure. The imaging of the leaf transformed area was done 48 h after the infiltration.

2.8 Confocal fluorescent microscopy

Plants were analysed by confocal laser scanning microscopy (Leica TCS SP8 Confocal, Germany) with GFP excitation, 514 nm and detection 520-555 nm. LTI6b-mOrange2 was detected using 561nm excitation and 560-565nm emission. Autofluorescence was detected using 633nm excitation and 650-700nm emission. Prior to imaging, *A. thaliana* T_3 seedlings were grown on 0.5 MS containing 1 % (w/v) sucrose and 0.8 % (w/v) agar for 7 days with or without 15µM Zn (as described in Section 2.2.1). Whole seedlings were placed on the slide in water and covered with a glass coverslip for imaging with a Leica TCS SP8 Confocal 63x 1.2 N.A glycerol immersion objectives.

The tobacco cells were imaged by preparing three weeks-old tobacco plants that had been transiently transformed for two days (as described in Section 2.7). A disk of transfected leaf was cut out. The disk was placed on the slide in water and covered with a glass coverslip for imaging using the Leica TCS SP8 Confocal 63x 1.2 N.A glycerol immersion objectives. LTI6b-mOrange2 in pB7FWG2 was used as a marker for the plasma membrane.

2.9 Bioinformatic analyses

To find barley bZIP sequences, the rice OsbZIP48 amino acid sequence was retrieved from the plant transcription factor database V2.0 (PlantTFDB) (http://planttfdb_v2.cbi.edu.cn/). Using the IPK BLAST server (Mayer et al., 2012) a search was conducted for related barley *bZIPs* in the

barley cultivar Barke, Bowman, and Morex, on the database assembly_WGSBarke/Bowman/Morex. The OsbZIP48 coding sequence (CDS) was aligned with the resulting contigs database to predict an open reading frame using Clustal Omega (http://www.ebi.ac.uk/Tools/msa/clustalo/). For every contig analysed, the resulting predicted barley *bZIP* was BLASTed against the database above to see if any additional *bZIPs* could be identified. Additionally, all predicted genes were BLASTed against all cDNA databases available in the IBSC (full-length cDNA, HC_genes_CD_Seq, and LC_genes_CD_Seq) to confirm their open reading frames.

The BLAST program at the International barley Sequencing Consortium database (Mayer et al., 2012) was used to identify P_{1B-2}-ATPase in barley. A preliminary HvHMA2/3 sequence (obtained prior to the start of this project) was used as a reference to obtain the complete sequence from the database. Meanwhile, the BLAST program at the International Wheat Genome Sequencing Consortium database (http://urgi.versailles.inra.fr/srs83/displayTool.do?toolName=BlastN) was used for finding the orthologs of HvHMA2 and HvHMA3 in wheat. The NCBI accession number of HvHMA2 and HvHMA3 are GU177852 and AK369525 respectively. Once all the genomic sequences of P_{1B-2}-ATPases were obtained, the open reading frame of each gene was predicted using Genemark (http://opal.biology.gatech.edu/GeneMark/; M. Borodovsky and A. Lukashin, unpublished data). The predicted CDS were aligned with their closest homolog cDNA sequences as a template (HvHMA2, HvHMA2/3 and HvHMA3) using ClustalO (Sievers et al., 2011). Also, a BLAST search using ESTs or cDNA databases was performed to confirm the CDS. EMBOSS Transeq programme (Rice et al., 2000) was used to determine translation of the coding sequences to protein sequences.

For phylogenetic analysis, MEGA7 was used to construct a Neighbour-Joining phylogenetic tree with 1000 replicates (http://www.megasoftware.net/). The multiple sequence alignments were made with the ClustalW module within MEGA7 using default parameters: gap opening penalty = 11; gap extension penalty = 1; protein weight matrix = BLOSUM with residue specific and hydrophilic penalties; gap separation distance = 5 and a 30 % delay divergent cutoff. This multiple alignment was used to identify completely conserved residues (Table 2.8). The sequences used to generate the trees are in Appendix 1 and Appendix 3. CDS were translated into protein sequences using the Translate tool from ExPASy Bioinformatics Resource Portal (http://web.expasy.org/translate/). All computational analyses carried out and databases used are summarised in Table 2.8. Typically, the sequences were entered into the programme/web server and the output was saved. If this option was unavailable, screenshots were taken instead.

Table 2.8 Tools used for bioinformatics analysis in this project

Analysis	Programme/database	Website	Reference(s)
Conserved domains	Pfam database	http://pfam.xfam.org	Bateman et al. (2004)
	PROSITE	http://prosite.expasy.org/	Hulo et al. (2006)
A. thaliana genome information	TAIR	http://www.arabidopsis.org/	Huala et al. (2001), Rhee et al. (2003), Swarbreck et al. (2008) and Lamesch et al. (2012)
Barley BLAST search	ViroBLAST	http://webblast.ipk-gatersleben.de/barley/viroblast.php	Deng et al. (2007)
Wheat BLAST search	ViroBLAST	https://urgi.versailles.inra.fr/blast/blast.php	Deng et al. (2007)
Rice genome information	Rice Genome Annotation Project	http://rice.plantbiology.msu.edu/	Ouyang et al. (2007)
Multiple sequence alignments	ClustalW and GeneDoc	http://www.clustal.org/	Thompson and Gibson (2002)
Phylogenetic analysis	MEGA7	http://www.megasoftware.net/	Kumar et al. (2016)
TM regions prediction	SOSUI	http://harrier.nagahama-i-bio.ac.jp/sosui/sosui_submit.html	Hirokawa et al. (1998) and Mitaku and Hirokawa (1999)
	TMHMM	http://www.cbs.dtu.dk/services/TMHMM/	Sonnhammer et al. (1998) and Krogh et al. (2001)
	TMPred	http://www.ch.embnet.org/software/TMPRED_form.html	Hofmann (1993)
	TOPCONS	http://topcons.cbr.su.se/	Bernsel et al. (2009)

2.10 Statistical analysis

Two-way ANOVA was used for statistical analysis, conducted using Minitab and Prism software, with the threshold for statistical significance difference taken at a 95% confidence interval. Tukey's HSD post-hoc test was performed to determine significant differences for all measurements except for gene expression level measurement, which used Fishers Least Significant Difference (LSD) instead. Values with the same letter are not significantly different ($P \leq 0.05$).

Chapter 3:

Identification and characterization of additional mutant alleles for *A. thaliana* bZIP transcription factors

3.1 Introduction

3.1.1 Reverse genetics and *A. thaliana*

Gene function can be investigated by utilizing reverse genetics. Generally, in this approach, a gene of unknown function can be disrupted and then the resulting phenotype examined. This contrasts with forward genetics that aims to find the genetic basis of a particular phenotype. T-DNA insertion mutants have been instrumental in revealing the physiological role of thousands of genes in *A.thaliana* and is becoming a useful tool in rice (Yi and An, 2013). *A.thaliana*, a member of the *Brassicaceae* (mustard) family, is an excellent genetic model, suitable for analyses because of its small size and rapid generation time; high fecundity and ability to self-fertilize; small genome (125 Mb) and ease of transformation (Koornneef and Meinke, 2010). There is a large collection of *A. thaliana* T-DNA mutants that are freely available through the *Arabidopsis* Biological Resource Centre (ABRC) and the Nottingham *Arabidopsis* Stock Centre (NASC). These mutants are convenient tools to elucidate gene function as shown by Assuncao et al. (2010) and Inaba et al. (2015) in their characterization of bZIP19 and bZIP23 TFs. Inserting a foreign element into a gene disrupts its translation and expression but can also act as a marker for identifying the point of insertion. Since *A.thaliana* has small introns and little intergenic material, T-DNA insertion usually disrupts gene function (Krysan et al, 1999). However, depending on the insert position it should be noted that presence of a T-DNA does not always result in a complete knockout; it is possible to still translate part of the sequence that may result in a functional truncated protein or a reduction in expression rather than a complete knockout (Krysan et al, 1999).

3.1.2 *A. thaliana* bZIP19 and bZIP23 are important for the Zn deficiency response

As discussed in the general introduction, particular transcription factors (TFs) are thought to play an important role in responding to Zn deficiency. Evidence in *A. thaliana* indicates that bZIP19 and bZIP23, TFs of the bZIP family (basic-region leucine zipper), are key players regulating this response (Assuncao et al., 2010). In *A. thaliana*, seventy-five bZIP TFs have been identified so far and they can be divided into ten groups based on sequence similarity and the presence of

certain motifs (Jakoby et al., 2002) (Figure 1.4). F-group bZIPs in *A.thaliana* consist of bZIP19, bZIP23 and also bZIP24 but the latter has been suggested to have a role in salt tolerance rather than in Zn responses (Yang et al., 2009a). bZIP19 was first identified using yeast one hybrid screening using the promoter of the Zn-deficiency regulated gene, *ZIP 4*, as bait (Assuncao et al., 2010). TFs bind to the promoter regions of responsive genes, resulting the up- or down-regulation of the gene by recruiting or blocking transcription machinery such as RNA polymerase (Orphanides et al., 1996). The specific mechanism by which *A.thaliana* bZIP19 and bZIP23 sense and respond to Zn is still far from clear, but Assuncao et al. (2013) proposed that they may be activated depending on the Zn status of the cell. They suggested a model whereby bZIP19 and bZIP23 would be activated under Zn deficiency when Zn would no longer be bound to their Cys/His motifs; this would allow them to enter the nucleus where they then bind to ZDREs in the promoters of Zn-responsive genes (Figure 1.3). The latter include the ZIPs (Zrt/Irt-like proteins) and *NAS* genes, which form part of the adaptation response to increase cellular Zn levels. The model proposed for bZIP19 and bZIP23 in the Zn-deficiency response is shown in Figure 1.3. The sequences of the *A.thaliana* F-group bZIPs highlighting the bZIP domain and the Cys/His motifs is shown in Figure 3.1 Assuncao et al. (2013).

A. thaliana has fifteen members of the ZIP family (Guerinot, 2000) and a subset (*ZIP1*, *3*, *4*, *5*, *9*, *10*, *12*, and *IRT3)* are regulated by bZIP19 and 23 (Assuncao et al., 2010). There is some specificity in the regulation of these ZIPs with bZIP19 predominantly regulating *ZIP9* expression and bZIP23 regulating *ZIP12* (Inaba et al., 2015). It should be noted that some of the Zn-transporting ZIPs have a broader metal specificity. For example, AtZIP1 has transport capability for both Zn and Mn, based on *S. cerevisiae* complementation and plant mutant analysis (Milner et al., 2013). Additionally, the expression of some ZIP transporters is influenced by other metal micronutrient levels. For example, AtZIP4 is down-regulated under Cu deficiency (Yamasaki et al., 2009, Wu et al., 2015b). Therefore it is important to understand the specificity of the responses influenced by the F-group bZIPs and this will be considered in this thesis.

Assuncao et al. (2010) isolated homozygous T-DNA insertion lines for *bZIP19* and *bZIP23* (*bzip19-1* and *bzip23-1* respectively), which did not show any Zn-sensitive phenotype when grown on full MS agar, but when grown on a Zn-deficient hydroponic system, *bzip19-1* was significantly stunted compared to the WT. The homozygous *bzip19-1 bzip23-1* double mutants were severely affected under Zn deficiency both on MS agar and in hydroponic culture (Assuncao et al., 2010). Significantly, in this double mutant, compared to WT there is a strong reduction in the expression of a subset of genes under Zn deficiency, many of which are known to play a role in Zn transport and homeostasis (Assuncao et al., 2010). When either *bZIP19* or *bZIP23* is expressed in the double mutant background under the 35S promoter, they complement the Zn-hypersensitive phenotype

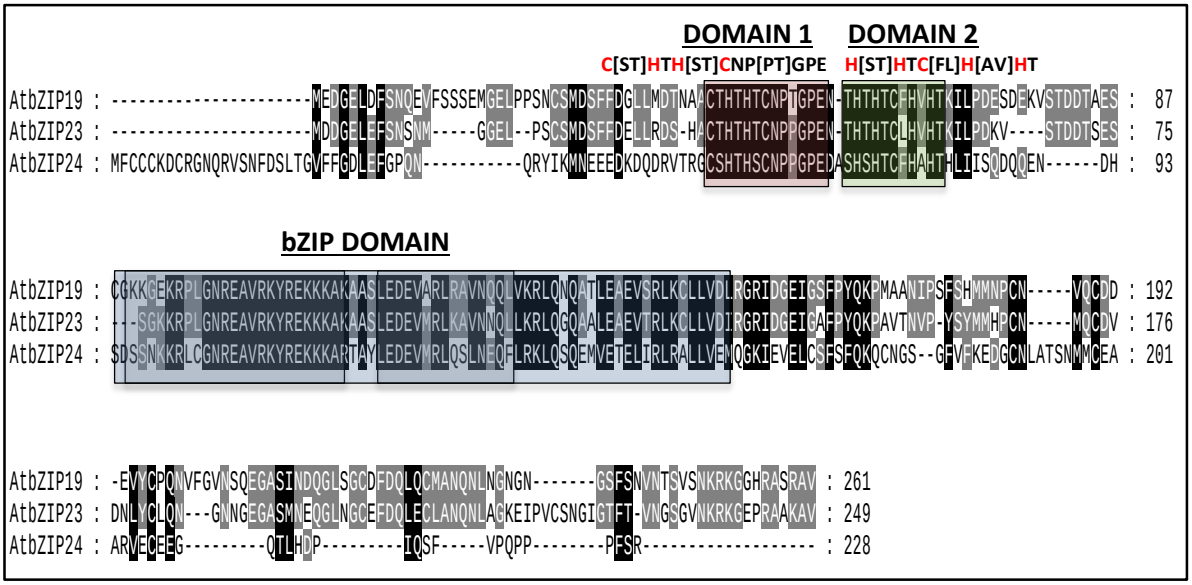

Figure 3.1 Amino acid multiple alignment of *A. thaliana* F-group bZIPs.

Sequences were aligned using the Clustal Omega algorithm (Sievers et al., 2011) and presented using GeneDoc (Nicholas and Nicholas Jr, 1997). For the sequences aligned here: black = conserved residues, and grey = conserved in two of the sequences. The bZIP domain and the two conserved Cys/His-rich domains (domain 1 and 2) are highlighted. Above the latter two are the sequence of the *A. thaliana* F-group bZIPs (Jakoby et al. 2002). The bZIP domain is boxed according to information given for AtbZIP19 at http://www.uniprot.org/ with the first box indicating the basic region and the second box indicating the leucine zipper region within the domain.

(Assuncao et al., 2010). During the course of this project, Inaba et al. (2015) isolated two alternative *bzip19* single mutants and an alternative *bzip23* single mutant. They used an alternative agar-based medium for generating Zn deficiency and found in this case that the *bzip19* mutants were inhibited in growth. The *bzip23* mutant was inhibited at both 0 Zn and at high Zn on this medium but there was a reduction in the expression of particular target genes (*ZIP12*) under Zn deficiency compared to WT.

3.1.3 Aims

The aim of this chapter was to further investigate the role of *A. thaliana* bZIP19 and bZIP23 in the Zn-deficiency response and provide a system to be used to test whether there was a conserved mechanism for F-group bZIPs in *H.vulgare*. Specific aims include:

1. To confirm the role of bZIP19 and bZIP23 in the Zn-deficiency response, by generating further mutant alleles.
2. To characterize these new mutants to provide further information about the role of bZIP19 and bZIP23. The reported *bzip19-1 bzip23-1* double mutant line has T-DNA inserts in the promoter regions (Assuncao et al. 2010); this study will investigate the effect of T-DNA inserts at other regions of *bZIP19* and *bZIP23* on the Zn deficiency response. A major aim of this thesis was to test conservation of function by expressing *H.vulgare* bZIPs in these mutants (see chapter 4). Because there can be problems with silencing in mutants when carrying out complementation experiments and, because this can be line dependent, it was considered prudent to attempt to isolate several insertion mutants at the same time for future transformation.
3. To investigate the specificity of the mutant response for Zn and to assess the influence of other micronutrients.

3.2 Results

3.2.1 Isolation of T-DNA insertion *bzip19 bzip23* double mutants

Assuncao et al. (2010) showed that the cross between *bzip19-1* (Salk line: N644252) and *bzip23-1* (Salk line: N656437) generates a *bzip19-1 bzip23-1* double mutant line which exhibits a Zn-hypersensitive phenotype. It shows markedly reduced growth on Zn-deficient agar media, but is unaffected, compared to WT under standard Zn conditions. They stated that neither *bzip19-1* nor *bzip23-1* mutants showed a difference from WT when grown on this media, although the *bzip19-1* mutant did show a detrimental response in hydroponic culture on low Zn. The T-DNA insertion sites for both *bzip19-1* and *bzip23-1* of this double mutant line are within the promoter region. Other potential *bzip19* and *bzip23* mutant lines are available from the European Arabidopsis Stock Centre (NASC) and they have different predicted T-DNA insertion sites than N644252 and N656437. Therefore, several different *bzip19* and *bzip23* single mutant lines were obtained and crossed to create different sets of *bzip19 bzip23* double mutants with different T-DNA insertion sites. During the latter period of this thesis work, Inaba et al. (2015) reported on two alternative mutant alleles for bZIP19 and bZIP23 but did not isolate double mutants. There was some confusion in this study on nomenclature as in certain places the original mutant alleles isolated by Assuncao et al. (2010) seem to have been renamed. We use the original mutant allele nomenclature here (Assuncao et al., 2010) and indicate later in the work how the mutant alleles isolated in this study compare to those of Inaba et al. (2015).

The general steps in isolating novel *bzip19 bzip23* double mutants are given in Figure 3.2. Searching with At4g35040 (*AtbZIP19*) and At2g16770 (*AtbZIP23*) identified Salk lines with the T-DNA inserts within the promoter and coding regions of these *bZIPs.* Figure 3.3 is useful to show the intron and exon positions in *AtbZIP19* and *AtbZIP23.* Based on the alignments, N657869, N506692, and N653060 seed lines were identified and obtained from the NASC (Table 3.1). N656437 line described in Assuncao et al. (2010) was also obtained but as the original N64452 was a retired line, N667534 was obtained instead; this had the same insertion site as N64452. To genotype the mutants by PCR, gene specific primers to detect the WT gene and a gene-specific primer together with a T-DNA primer were used to detect the presence of a T-DNA insert in the gene of interest (Figure 3.4).

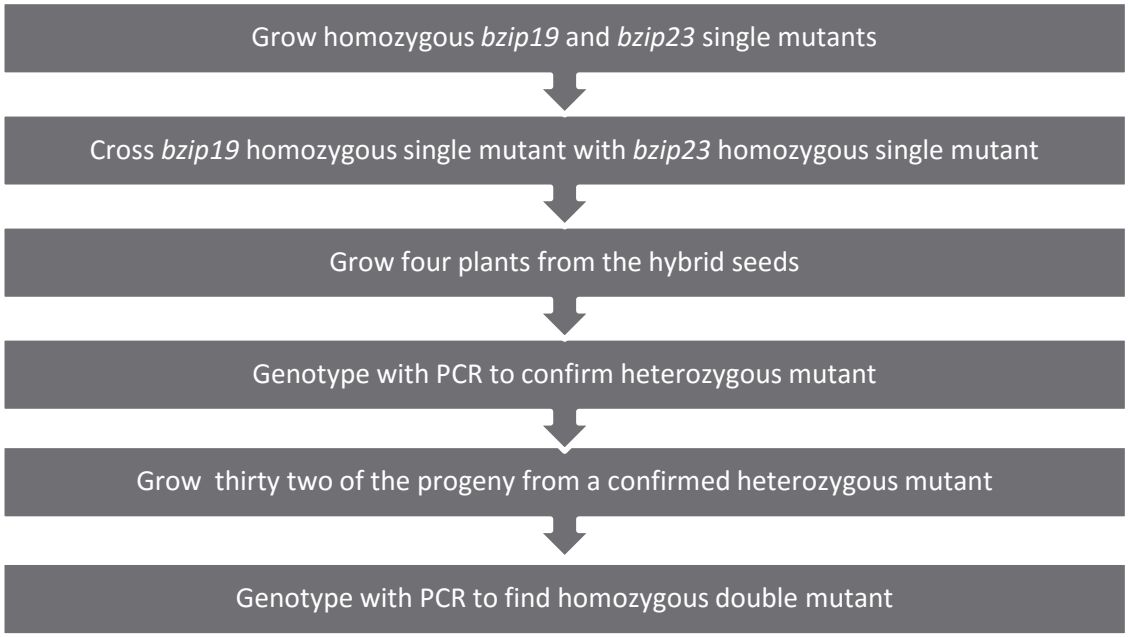

Figure 3.2 Steps in isolating *bzip19 bzip23* double mutants

Table 3.1 *bzip19* and *bzip23* mutant alleles used in three different studies

Line Number	**SALK Number**	**Segregation Status supplied**	**Gene**	**Assuncao et al. (2010) mutant name**	**Inaba et al. (2015) mutant name**	**Proposed mutant name by this study**
N667534	SALK_144252C	Homozygous	*bZIP19*	*bzip19-1*	*N/A*	*bzip19-1*
N657869	SALK_005336C	Homozygous	*bZIP19*	N/A	*bzip19-1*	*bzip19-4*
N506692	SALK_006692	Segregating	*bZIP19*	N/A	*bzip19-2*	*bzip19-2*
N583399	SALK_083399	Segregating	*bZIP19*	N/A	*bzip19-3*	N/A
N656437	SALK_045200C	Homozygous	*bZIP23*	*bzip23-1*	*bzip23-1, bzip23-2* (in different parts of paper)	*bzip23-1*
N653060	SALK_018248C	Homozygous	*bZIP23*	N/A	*bzip23-1, bzip23-2* (in different parts of paper)	*bzip23-2*

*the background of these lines is Col-8 / *N/A is not applicable, as mutant was not used

A: *AtbZIP19* genomic DNA sequence

AATTAAAATTTAGTTCAAGACCTACTTTAAAGCCTTTTACAAAAAAAGAAAAGAATTCTCTAAGTCGAAATCGT
TATCGTAGTACGTTCATGTCTTTTCTCCGGCCACCGAAACGATGCCATCTGTTTAGTGCGCCTTTATAATTCAAC
GACCCTTTGTACTTTTCCGATTCCTCTTTCTCTATAACTTCATCTCTCCCATTCTCTTCACTCTTCTCAAAAATTCG
ATCTTTAGGGTTTTTCTTTTATCCTCTTATCGCTAATCTGGAGCTCTATAGAGACTATAAAGGTA^TGTTTTTTTT
TCCTCAATTACAGGCTCGGATGCTCAAATTTTGTAAAAAATGACTATTTTCTATTGCTGAATTGCTCGAATTGTT
GTGAATTTAGGGTTTTTGATTGATTCGGGAGCTCGAGATTTGACTTCTTTTAGCTGATTCGGCAAGTTTGTATCT
AGAAAGGATCGATTGGTGAGGTCAATAGT^GGTTGGTGGGTTTTAGTAATGGAAGACGGTGAGCTTGATTTC
TCCAATCAGGAAGTGTTTTCGAGTTCGGAGATGGGTGAATTACCACCTAGCAATTGTTCGATGGATAGTTTCTT
TGATGGGCTTTTAATGGATACTAATGCTGCTTGTACCCACACTCACACCTGTAACCCCACTGGACCAGAGAACA
CTCATACTCACACGTGCTTCCATGTCCACACCAAGATTCTCCCGGATGAGAGCGATGAAAAAGTTTCTACTGAT
GATACAGCTGAGTCTTGTGGGAAGAAGGGTGAAAAGAGACCTTTGGGAAACCGGGAAGCGGTTAGAAAGTA
TAGAGAGAAGAAGAAGGCTAAAGCTGCTTCTTTGGAGGATGAGGTTGCAAGGCTTAGGGCGGTGAATCAGC
AGCTGGTGAAGAGGTTGCAAAATCAGGCTACCTTGGAAGCTGAGGTTTCGAGGCTTAAGTGTTTGCTTGTGG
ATTTGAGAGGAAGAATAGATGGAGAGATTGGATCTTTTCCTTATCAGAAACCTATGGCTGCAAATATTCCTTCT
TTCTCGCACATGATGAATCCTTGTAATGTACAATGTGATGATGAAGTTTATTGCCCTCAGAATGTGTTTGGAGT
GAATAGCCAAGAAGGTGCCTCGATCAATGACCAAG^GGTTAAGTGGTTGTGATTTTGATCAGCTACAATGCAT
GGCTAATCAGAACTTAAATGGAAATGGAAACGGATCATTCAGCAACGTCAATACATCTGTCTCGAATAAGAGA
AAAGGTGACACTTTTATTCTGTACCTTAGAGTTTTCTCTGTAAATCGTTCTGGTTTAGAACCGGAGGTTGTTTAC
TCACTCTGATTATTGGTCAACTCTTGCCTTAGTATGTCTTATAATGTGAAGCAAATTCGTGACGTTCTCATTTAG
TTTGCCTCATAGAATTTGTATGAACTCACTTATGTTTTTGACTCATCGCTTAGGTGGGCATCGTGCATCAAGAGC
AGTTTGAAGCATCATCAAGCTTGTACTATCTATTTCCACCAGCATAGATATTGTATTCCAAATAAGTTGTAGAGT
TCAGCTGCAGGATCAGCTTCGCTCAGGTTCCTTTGTATCCTCATTTTTGTTTTTTGTTTTCTGACTCTCTTTCCCTT
CCATTGTATTTCCTTGTTGAGCTTGACAAACTAGAAGGATGATATATTGTTAATACAACAAACTCAAATGTTCTG
TGTGTTCTTGCCATTTGTTTTCATACTTGAGCTGCTTCTTCTTAAGTTTATGTCGAAGAAGTTGATTG

UTR CDs ^ *bzip19*-1 ^ *bzip19-2* ^ *bzip19-4* bZIP19F2 bZIP19R2

Figure 3.3 The relevant sequence information for (A) *AtbZIP19* and (B) *AtbZIP23*.

The untranslated region (UTR) and coding sequence (CDs) are indicated by grey and yellow highlighted sequences, respectively. The intron is indicated by non-highlighted sequence. The primers for genotyping and gene knockout confirmation at RNA level are also indicated in the figure in red. The position of T-DNA insertion for bzip19 and bzip23 mutants used in this thesis are also shown.

B: *AtbZIP23* genomic DNA sequence

AATAGAATCTTCTGCAATTCGAAATTCCTTTTGGTACGTCCATGTCTTCTTTCCGCCATGGAAATAATGCCATCT
GTTAATCATCAATGTTCATTGCACCTCTTCATCTCTAGGGTTCCCATTTCTAATTCTCTCTTAAACCCTTCTCGCC
GTTTTCGCCCATAAGTTTCTCAATTCCCAAATTCGCAATCGTAATGGCGATTCTCCTCAAGCTTTCGTCTTGCTG
ATCCTTTAAAGGTACGATTTTTCTATTCAATTTAGTATCAGCCAATGATTAGTTATTGATAATTGGTTCTGAATC
GCTTGGATTGTGTTTTCACTCTGCAATTAGGTTGTT^GTTTGGTTTTTGATCACAAAGTCTCATACTTTTTGGTT
AAGATTCAATCAAAAGAGTCAAAGGTTACTTCTTTGTTACTGGGTTTTGAGTAATGGACGACGGTGAGCTTGA
GTTTTCGAATTCAAACATGGGTGGTGAATTACCTAGCTGTTCGATGGATTCGTTCTTCGATGAGCTTTTGAGAG
ATTCTCATGC^TTGTACTCATACTCACACTTGTAATCCTCCGGGACCAGAGAACACACATACTCACACATGTCTC
CATGTGCACACCAAGATTCTTCCTGACAAAGTTTCTACTGATGATACATCGGAATCTTCAGGGAAGAAGAGAC
CTTTAGGGAATAGAGAAGCGGTTAGAAAGTATAGGGAGAAGAAGAAGGCTAAAGCGGCTTCGTTGGAGGAT
GAGGTTATGAGGCTTAAGGCGGTTAATAATCAGCTGTTGAAGAGGTTGCAAGGTCAAGCTGCATTGGAAGCT
GAGGTTACTAGGCTCAAGTGTTTGCTTGTTGATATAAGAGGAAGAATTGATGGAGAGATTGGTGCGTTTCCTT
ATCAGAAACCTGCGGTTACAAACGTGCCTTACTCATACATGATGCATCCTTGCAATATGCAATGTGATGTTGAT
AACTTGTACTGCCTTCAAAATGGGAATAATGGAGAAGGTGCATCGATGAATGAGCAAGGGCTAAATGGTTGT
GAGTTTGATCAGCTAGAATGCTTGGCTAATCAGAATTTAGCTGGCAAGGAGATCCCTGTTTGTAGTAATGGAA
TTGGAACATTCACTGTCAATGGATCCGGCGTTAATAAGAGAAAAGGTGACATTCTAGTTCCTTTGGATCTCTTT
CCTAGAGGCTGTCCTTAATAGCTATATCTTTATACAGTTTTCATCGTAGTTACTTCCATATTGTCACTGTACTTAT
CCTGGAATTGTGTCATTTCTGAGGTTCCCTTGAACGTTTTTTGTTTAAACTTGTGGTTTGTGTATATTTTGTTTAT
GAACTCAAGGTTTTTGATCTTGCAACAGGTGAGCCTCGAGCAGCGAAAGCAGTTTGAAGTATCATCAATCATG
TGATACTATCAATCATTCACCCCATTTTCAAGTTGGTAGTTAATTTTCTTCCAATAAGTAGTAGAGTTCAACTGC
ATCACCAGCTTCCTTCAAGTCCATTTGTGCTATCATCAGGTTTTTAGTCTCTTTGCATTTCCTTGTTGAGCTCGTT
GAAGCTAGAAATAAGACTTGTTAATATTCAAATCGAGTTTGCTATTTGGTTTTGTACTTTAGTAGCTTCTTTTTT
TGTTGTGAAGTTCTTGTAGAAGAGATTGAATGTTGCATTTGGAAAAGTAAGTTATGGGAAGCCATCTCGACAA
TTAGTAACTTGGTTGTTTTCGACTT

UTR CDs ^ *bzip23-1* ^ *bzip23-2* bZIP23F2 bZIP23R2

Figure 3.3 continued

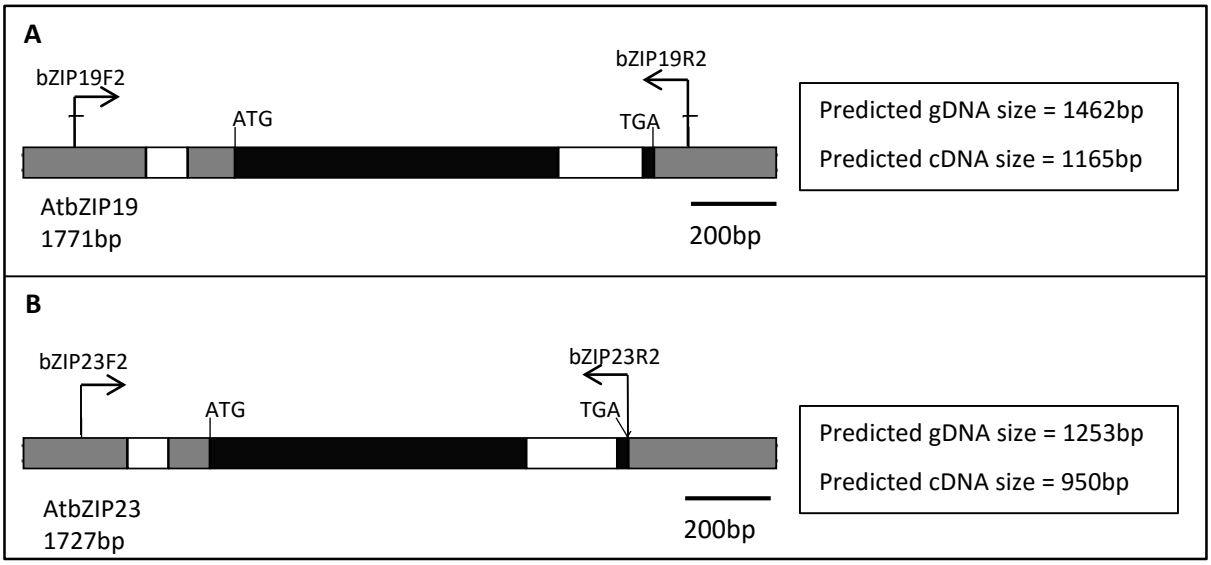

Figure 3.4 Schematic diagrams of *AtbZIP19* and *AtbZIP23* gene structure.

The binding site of (A) bZIP19F2 and bZIP19R2, and (B) bZIP23F2 and bZIP23R2 primers that were used for genotyping and knockout confirmation at RNA level of *bzip19* and *bzip23* mutants respectively are shown. The PCR product size of these two primer sets are shown next to the schematic diagrams. Black bars represent exons, white bars represent introns and grey bars represent UTRs.

The genotyping of the potential single mutants is shown in Figure 3.5. This procedure was carried out for ten plants for each line and representatives are shown. A WT PCR product for *bZIP19* can be detected by amplification with bZIP19F2 primer and bZIP19R2 primer; these were predicted to yield a 1462bp PCR product. Meanwhile to check the presence of a T-DNA insert, the T-DNA left border primer (LBa) and bZIP19R2 were used. In addition, a smaller PCR product amplified by LBb and bZIP19R2 primer were also used to check the presence of T-DNA insert. The amplification with these three sets of primers indicated that N667534, N506692 and N657869 lines were homozygous (Figure 3.5A showing representative plants). The two *bzip23* lines (N656437 and N653060) were also confirmed to be homozygous as no WT size products were amplified and the T-DNA fragments flanking *bZIP23* were amplified (Figure 3.5B). Table 3.2 shows the selected maternal plants, which are *bzip19* and their crossed partners, which are *bzip23*. Four progeny from the crossed plants were grown to obtain a heterozygous plant, confirmed by PCR. Thirty-two of the progeny (F2) from the heterozygous plant were grown and genotyped with PCR, until a homozygous plant was isolated.

Figure 3.6 shows the results confirming the cross to generate a heterozygote for each cross. As the maternal plant was a *bzip19* mutant, the plants were initially checked for a *bZIP23* insertion. Three sets of primers were used: (A) bZIP23F2 + bZIP23R2, (B) LBa +bZIP23R2 and (C) LBb+bZIP23R2. LBa and LBb were T-DNA insertion left-border primers. The plants at this stage were expected to produce a product with each set of primers detecting inserts in *bZIP23*, indicating that they were heterozygous double mutants. Progeny from all five crosses seemed to be heterozygous since all of them had a WT *bZIP23* band and the two T-DNA left border bands (Figure 3.6). The progeny from each of these crosses were then genotyped to detect a double homozygous mutant. An example PCR of the genotyping for the progeny from these crosses for the particular homozygote isolated is shown in Figure 3.7. The confirmed homozygous: homozygous *bzip19/bzip23* plants based on the final genotype screenings are indicated in Table 3.2. Also indicated in this table is the mutant allele name given to these mutants.

To determine the exact position of T-DNA within the mutants isolated in this study the products obtained with bZIP19R2/bZIP23R2 and the left-border LBa primer of confirmed homozygous: homozygous plants were extracted from the gel, purified, and sequenced. The position of the T-DNA insertion site for the different mutant lines is given in Table 3.3. The N667534 line was not sequenced here but Assuncao et al. (2010) claims that the T-DNA insert is 18bp upstream of the *bZIP19* start codon. Assuncao et al. (2010) also claim that for N656437, the T-DNA insertion is 91bp upstream of *bZIP23* start codon and the sequencing of bZIPR2+LBa PCR product has confirmed this here.

To confirm whether these unique *bzip19 bzip23* double mutants were knockout mutants, it was important to characterize these lines at the mRNA level. RNA from these double mutants

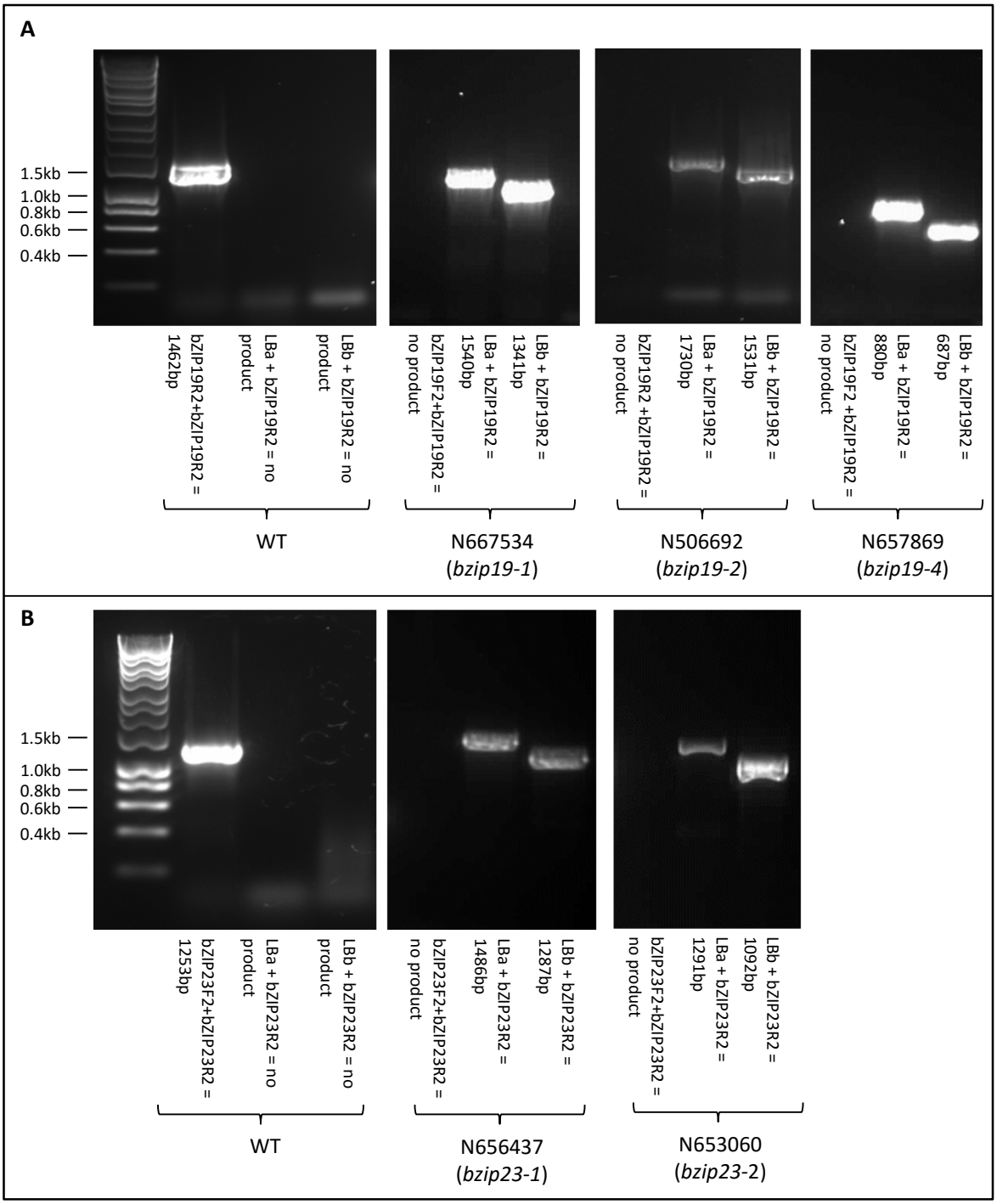

Figure 3.5 Genotyping potential *bzip19* and *bzip23* single mutant lines.

bzip19: N667534, N506692 and N657869 (A), and *bzip23*: N656437 and N653060 (B). DNA isolated from individual plants was amplified with three sets of primers (bZIP19/23F2+bZIP19/23R2, LBa+bZIP19/23R2, and LBb+bZIP19/23R2) for genotyping. Genomic DNA from Col-8 WT plants is also included in the reaction as a control to amplify a WT product. The molecular weight markers are shown next to the gel image and the predicted product size of each reaction is shown in below the gel image.

Table 3.2 Plant lines crossed to generate heterozygotes and the double *bzip19 bzip23* plants with their mutant allele designation.

***bzip19* (maternal)**	***bzip23***	**Heterozygote crossed plants**	**Double homozygous *bzip19 bzip23* mutants**	**Mutant allele name**
N506692#I (heterozygous)	N656437#F (homozygous)	N506692#I x N656437#F	N506692#IxN656437#F#2-3#24	*bzip19-2 bzip23-1*
N657869#F (homozygous)	N656437#F (homozygous)	N657869#F x N656437#F	N657869#FxN656437#F#1-1#8	*bzip19-4 bzip23-1*
N657869#I (homozygous)	N653060#G (homozygous)	N657869#I x N653060#G	N657869#IxN653060#G#1-3#22	*bzip19-4 bzip23-2*
N667534#A (homozygous)	N653060#G (homozygous)	N667534#A x N653060#G	N667534#AxN653060#G#1-1#19	*bzip19-1 bzip23-2*
N667534#J (homozygous)	N656437#C (homozygous)	N667534#J x N656437#C	N667534#JxN656437#C#2-4#5#7	*bzip19-1 bzip23-1*

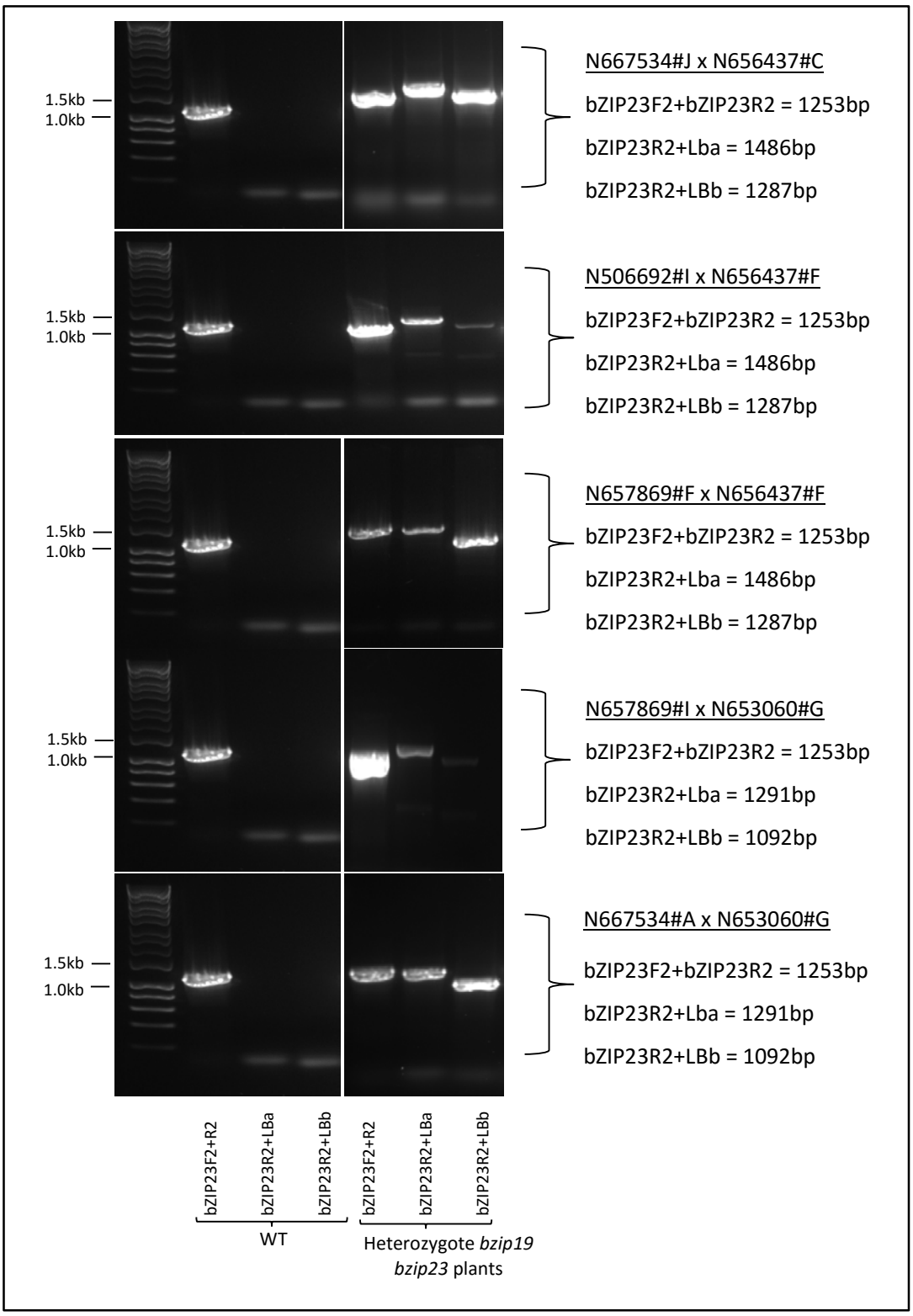

Figure 3.6 Genotyping the progeny from the crosses:

(a) N667534#JxN656437#C (b) N506692#IxN656437#F, (c) N657869#FxN656437#F, (d) N657869#IxN653060#G and (e) N667534A#AxN653060#G, amplified with three sets of primer to determine their genotype (indicated at the bottom and the side of the gel). In each genotyping with PCR, WT plants are included in the reaction as a control. The molecular weight marker and the predicted PCR product sizes are indicated next to the gel image.

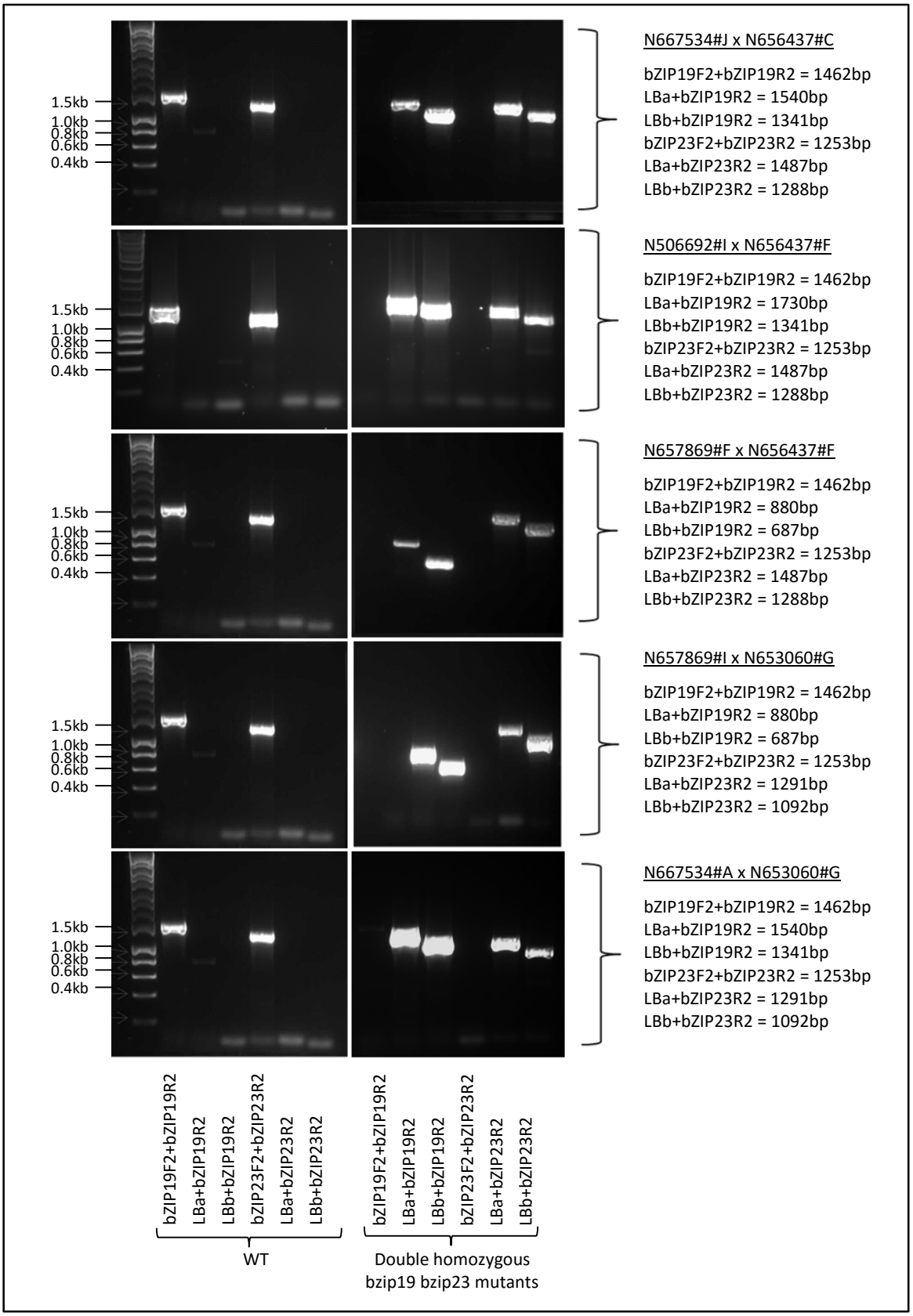

Figure 3.7 The screening of potential homozygous:homozygous *bzip19*/bzip23 F2 plants: N506692#I x N656437#F, N657869#F x N656437#F, N657869#I x N653060#G and N667534#A x N653060#G. A WT plant is also included in the reaction as a control. The molecular weight marker and the expected PCR product sizes are given next to the corresponding gel image.

Table 3.3 Sequencing analysis of the T-DNA insertion site for different mutant lines. (The T-DNA insertion site is indicated by '^').

Mutants	Alignment of the sequence obtained from sequencing with *bZIP19/bZIP23* genomic DNA or pBIN-ROK2 left-border sequence)
bzip19-2	Alignment with *bZIP19* gDNA *bzip19-2* 136 --------GG-^TGTTTTTTTTTCCTCAATTACAGGCTCGGATGCTCAAA 175 || ^||||||||||||||||||||||||||||||||||||||| bZIP19 280 ACTATAAAGGTATGTTTTTTTTTCCTCAATTACAGGCTCGGATGCTCAAA 329 Alignment with pBIN-ROK2 left-border sequence *bzip19-2* 103 GTCAATTTGTTTACACCACAATATATTGGCGGTGG^TGTTTTTTTTCCT- 151 |||||||||||||||||||||||||||||||||^ .|||| pBIN-ROK2 136 GTCAATTTGTTTACACCACAATATATTGGCGGTGG^---------ATCCTG 176 (T-DNA insertion is 207bp before the start codon.)
bzip19-4	Alignment with *bZIP19* gDNA *bzip19-4* 333 -----AAGTTGTCT-----------AAG^GGTTAAGTGGTTGTGATTTTG 365 |||.||.|| |||^||||||||||||||||||||| bZIP19(gDNA) 1113 CCAAGAAGGTGCCTCGATCAATGACCAAG^GGTTAAGTGGTTGTGATTTTG 1162 Alignment with pBIN-ROK2 left-border sequence *bzip19-4* 301 CAGTACATTAAAAACGTCCGCAATGTGTTATTAAGTTGTCTAAG^GGTTAA 350 |||||||||||||||||||||||||||||||||||||||||^.||.|| pBIN-ROK2 91 CAGTACATTAAAAACGTCCGCAATGTGTTATTAAGTTGTCTAAG^CGTCAA 140 (T-DNA insertion is 643bp or 640bp, if consider 'AAG' is a gene sequence, after the start codon.)
bzip23-1	Alignment with *bZIP23* gDNA *bzip23-1* 108 ---------TCAAT-----------TTGTT^GTTTGGTTTTTGATCACAAA 137 |||.| |||||^|||||||||||||||||| bZIP23 308 ATTGTGTTTTCACTCTGCAATTAGGTTGTT^GTTTGGTTTTTGATCACAAA 357 Alignment with pBIN-ROK2 left-border sequence *bzip23-1* 101 CTAAGCGTCAATTTGTT^GTTTGGTTTTTGATCACAAAGTCTCATACTTTT 150 |||||||||||||||||^ |||..|.|||||..|.||.|.| pBIN-ROK2 130 CTAAGCGTCAATTTGTT^-------TTTACACCACAATATATCCTGC---- 166 (T-DNA insertion is 91bp or 96bp, if consider 'TTGTT' is a gene sequence, before the start codon.)
bzip23-2	Alignment with *bZIP23* gDNA *bzip23-2* 325 -------------^TTGTACTCATACTCACACTTGTAATCCTCCGGGACC 360 ^||||||||||||||||||||||||||||||||||||| bZIP23 519 AGAGATTCTCATG^TTGTACTCATACTCACACTTGTAATCCTCCGGGACC 568 Alignment with pBIN-ROK2 left-border sequence combined 301 CTTATTAAGTTAGAGATTCTCATG^TTGTACTCATACTCACACTTGTA-AT 349 |||||||||||||||||||||||^ |.|.|| |||| .|| || pBIN-ROK2 118 CTTATTAAGTTAGAGATTCTCATG^------TTACAC-CACA---ATATAT 161 (T-DNA insertion is 104bp after the start codon.)

was extracted and cDNA generated. The *bZIP19* and *bZIP23* expression was tested by amplifying WT products (1165bp for bZIP19 and 950bp for bZIP23) (Figure 3.8). No WT products were produced in the potential double mutants. In the control WT cDNA, these products were clearly seen. Also, Figure 3.8 provides a schematic showing the mutant alleles isolated in this study.

3.2.2 *bzip19 bzip23* double mutants are adversely affected by Zn deficiency

All four newly generated *bzip19 bzip23* double mutants were grown alongside the WT and their corresponding *bzip19* and *bzip23* single mutants to provide a direct comparison on Zn-deficient media (0µM), and media containing standard (15µM) Zn. Here half MS-media was used whereas full MS was used previously in the study by Assuncao et al. (2010) with the *bzip19-1 bzip23-1* double mutant. This agarose plate assay shown in Figure 3.9 provides a basic comparison of the mutant phenotype. Figure 3.9A shows photographs of seedlings grown under both of these conditions and Figure 3.9B provides data on the fresh weight of whole plants, shoots, and roots. Analysis from the two-way ANOVA revealed that there is a significant interaction between genotype and Zn concentration on total fresh weight, shoot fresh weight, and root fresh weight as shown in Table 3.4.

Seedlings grown at 15µM Zn did not show a significant difference in total, shoot or root fresh weight per seedling between genotypes (Figure 3.9). When grown on 0µM Zn, all four *bzip19 bzip23* double mutants had a significantly lower total, shoot, and root fresh weight than WT and single mutant seedlings (Figure 3.9). All the *bzip19* single mutants also showed a significant reduction in total fresh weight, shoot fresh weight, and root fresh weight compared to WT seedlings under low Zn (Figure 3.9). Although in certain cases there were slight reductions in the mean fresh weight of *bzip23* mutants compared to WT, generally these were not consistently significant. Thus, the reductions seen in the *bzip19* mutants were more apparent than those observed in the *bzip23* single mutants.

3.2.3 *bzip19-4 bzip23-2* and its corresponding single mutants had similar phenotype to *bzip19-1 bzip23-1* and its respective single mutants

The *bzip19-4 bzip23-2* double mutants and their corresponding single mutants (*bzip19-4* and *bzip23-2*) were grown independently alongside the WT, *bzip19-1 bzip23-1* double mutants and their corresponding single mutants (*bzip19-1* and *bzip23-1)* to provide a direct comparison on Zn-deficient media, and media containing standard (15µM) Zn and to investigate the effect of different T-DNA insertion sites on the mutants phenotype. The media used here is 0.5MS, whereas Assuncao et al. (2010) used full MS and we used agarose instead of agar. Figure 3.10A

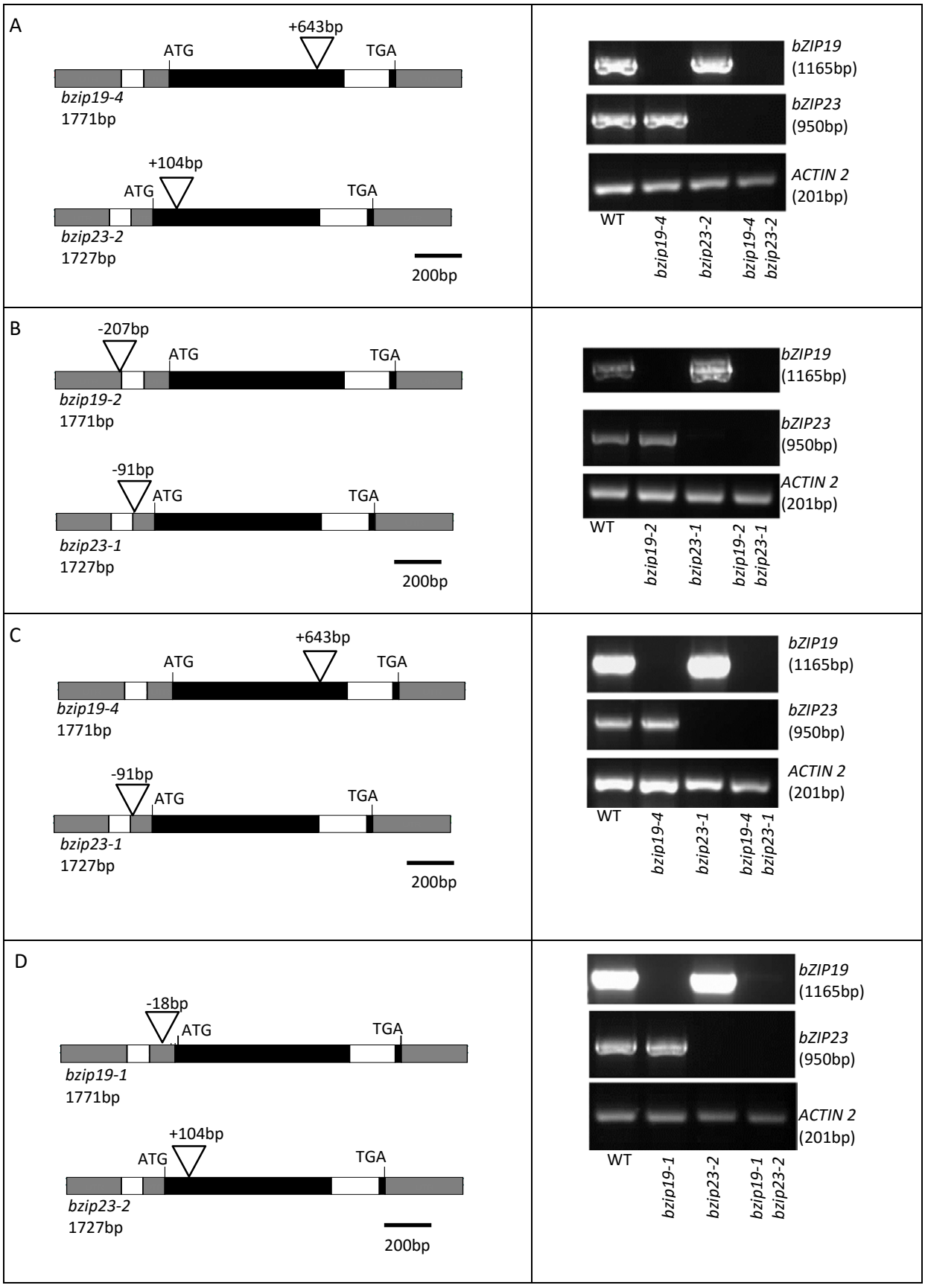
A
+643bp
ATG
TGA
bzip19-4
1771bp
+104bp
ATG
TGA
bzip23-2
1727bp
200bp
bZIP19
(1165bp)
bZIP23
(950bp)
ACTIN 2
(201bp)
WT
bzip19-4
bzip23-2
bzip19-4
bzip23-2
B
-207bp
ATG
TGA
bzip19-2
1771bp
-91bp
ATG
TGA
bzip23-1
1727bp
200bp
bZIP19
(1165bp)
bZIP23
(950bp)
ACTIN 2
(201bp)
WT
bzip19-2
bzip23-1
bzip19-2
bzip23-1
C
+643bp
ATG
TGA
bzip19-4
1771bp
-91bp
ATG
TGA
bzip23-1
1727bp
200bp
bZIP19
(1165bp)
bZIP23
(950bp)
ACTIN 2
(201bp)
WT
bzip19-4
bzip23-1
bzip19-4
bzip23-1
D
-18bp
ATG
TGA
bzip19-1
1771bp
+104bp
ATG
TGA
bzip23-2
1727bp
200bp
bZIP19
(1165bp)
bZIP23
(950bp)
ACTIN 2
(201bp)
WT
bzip19-1
bzip23-2
bzip19-1
bzip23-2

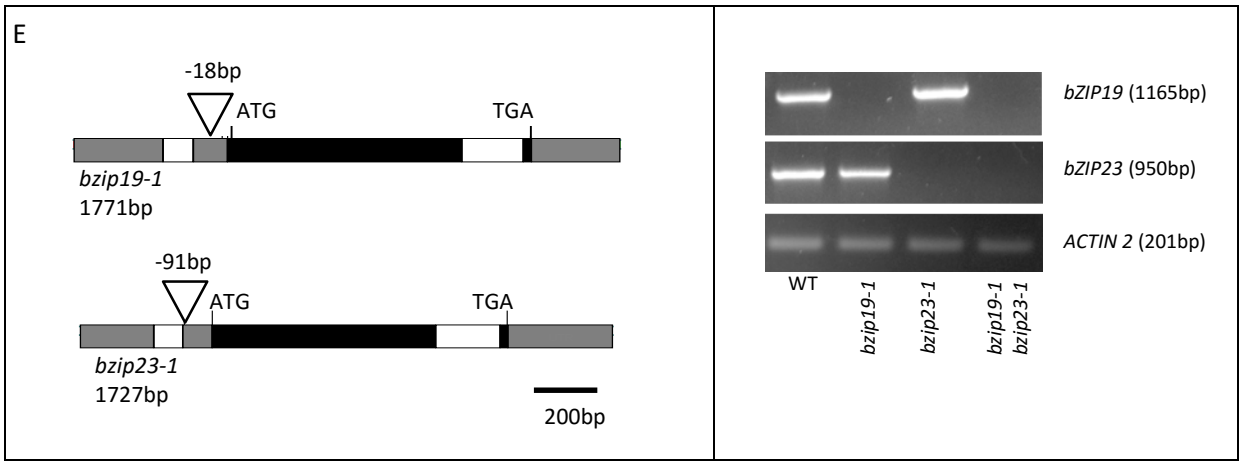

Figure 3.8 Confirmation of the double mutant alleles at the RNA level.

Left, Schematic drawings of the *bzip19* and *bzip23* mutant alleles (A) *bzip19-4 bzip23-2*, (B) *bzip19-2 bzip23-1*, (C) *bzip19-4 bzip23-1*, (D) *bzip19-1 bzip23-2*, and (e) *bzip19-1 bzip23-1*. Black bars represent exons, white bars represent introns and grey bars represent untranslated regions. A of ATG is taken as 0. T-DNA is represented by triangle. Right, corresponding RT-PCR (see Figure 3.2 for primers used and their binding site) showing lack of expression of bZIP19 and bZIP23 at the RNA level in the double mutants. *ACTIN2* is included as a control.

Table 3.4 Statistical analysis of two-way ANOVA for evaluating interaction between genotype and Zn concentration for experiment given in Figure 3.9

Measurement	***bzip19-2 bzip23-1***	***bzip19-4 bzip23-1***	***bzip19-4 bzip23-2***	***bzip19-1 bzip23-2***
Total fresh weight	$F_{3,30}$ = 31.88, P<0.0001	$F_{3,30}$ = 123.0, P<0.0001	$F_{3,30}$ = 44.47, P<0.0001	$F_{3,30}$ = 170.8, p<0.0001
Shoot fresh weight	$F_{3,30}$ = 29.26, P < 0.0001	$F_{3,30}$ = 83.54, P < 0.0001	$F_{3,30}$ = 62.56, P < 0.0001	$F_{3,30}$ = 165.4, P < 0.0001
Root fresh weight	$F_{3,30}$ = 20.30, P<0.0001	$F_{3,30}$ = 89.90, P < 0.0001	$F_{3,30}$ = 7.823, P = 0.0005	$F_{3,30}$ = 95.79, P < 0.0001

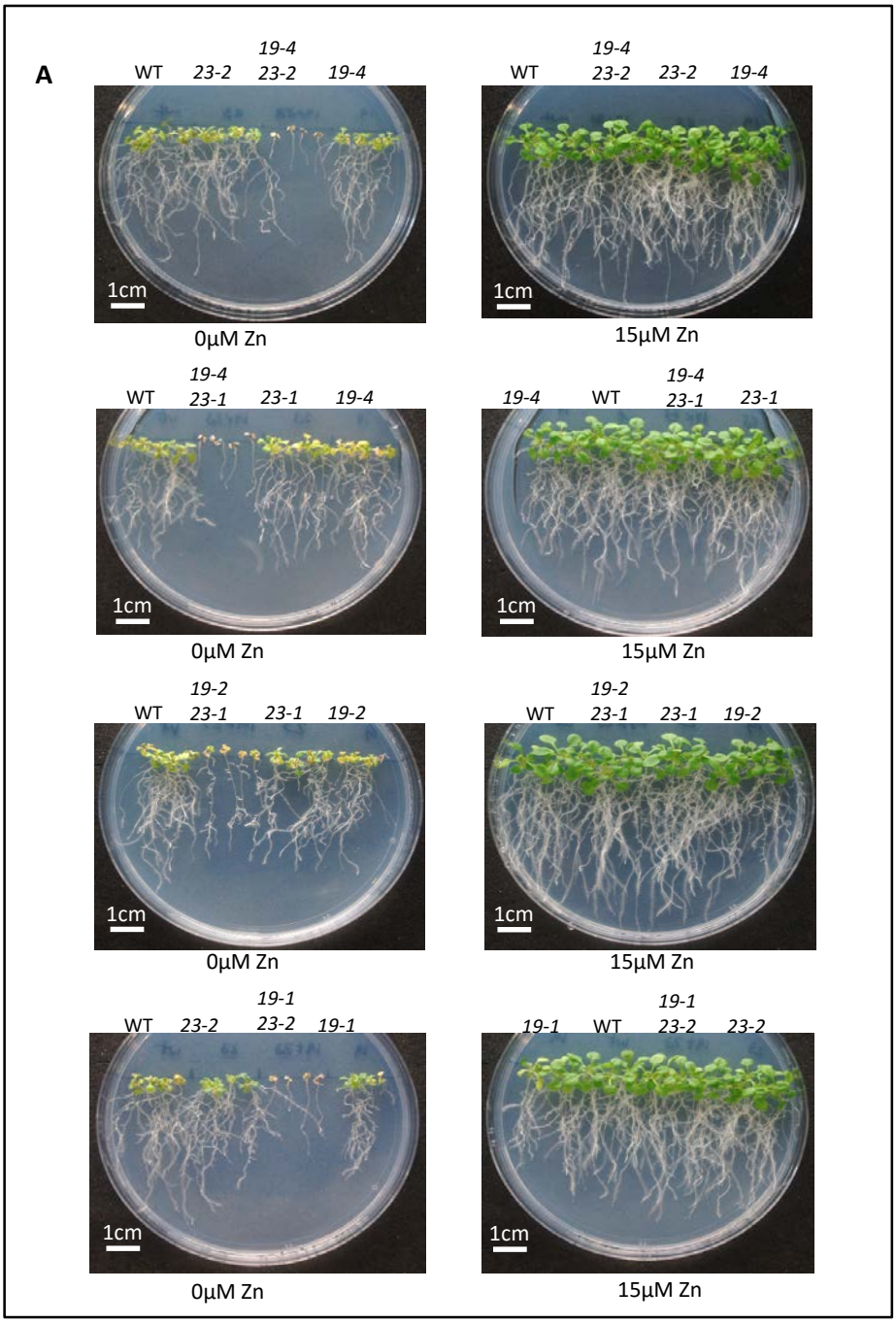

Figure 3.9 All four unique *bzip19 bzip23* double mutants show an adverse effect to Zn deficiency.

(A) WT, *bzip19, bzip23,* and *bzip19 bzip23* T-DNA insertion *A. thaliana* mutants grown on agarose 0.5 MS plates for 21 days with 0µMZn or 15µMZn**.** (B) For each growth condition, fresh weight measurements for total weight, shoot weight and root weight are shown. The means (+/- SEM) were based on six plates with four seedlings per line, per plate, each plate containing four plant lines. Means not sharing a letter are significantly different ($p \leq 0.05$); Tukey post-hoc test.

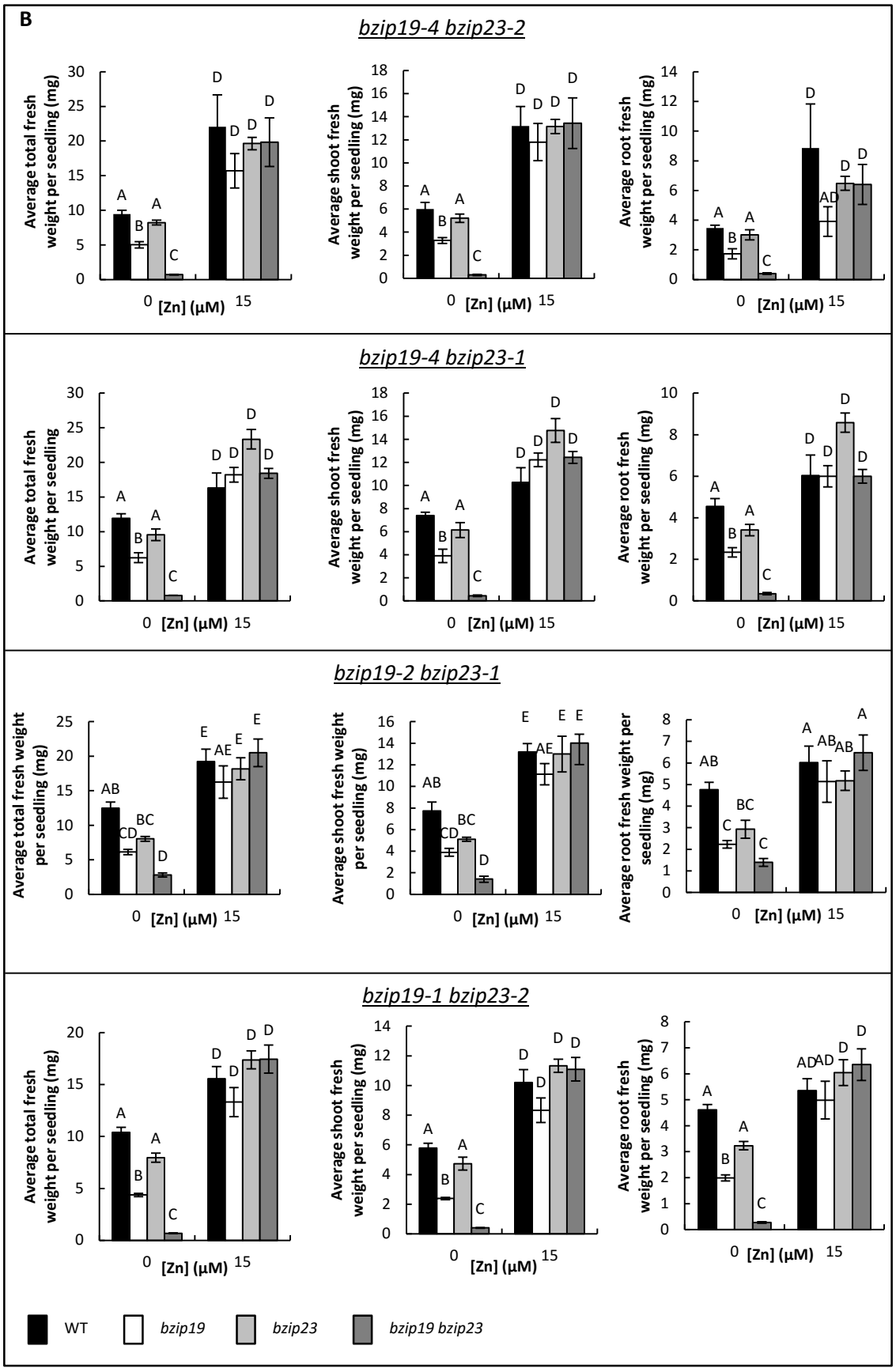

Figure 3.9 continued

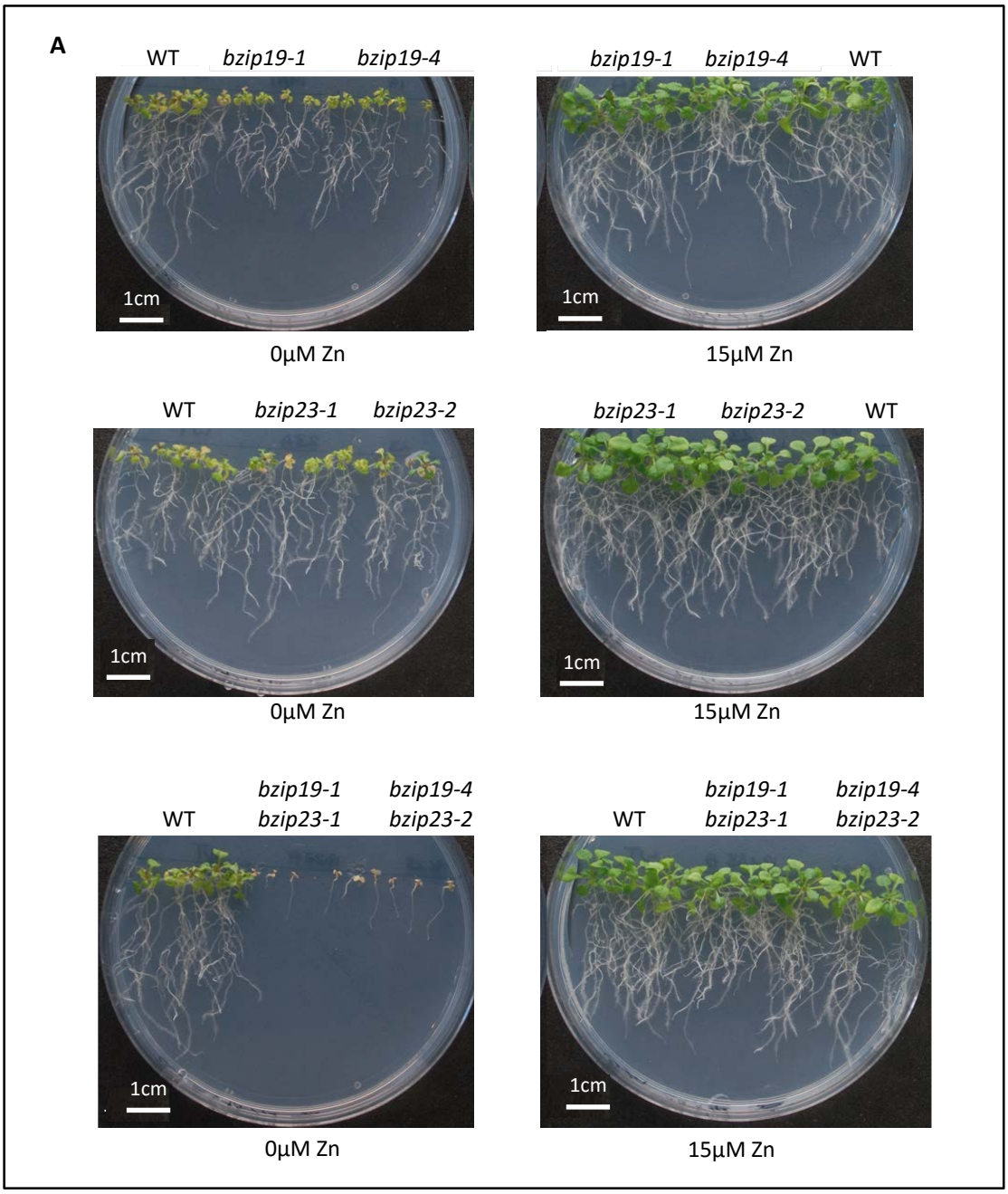

Figure 3.10 Direct comparison of single and double mutant bZIP alleles.

(A) *bzip19-4* and *bzip19-1, bzip23-2* and *bzip23-1, bzip19-4 bzip23-2 and bzip19-1 bzip23-1* were directly compared by growing on agarose 0.5 MS plates for 21 days with 0µM Zn or 15µM Zn. (B) For each growth condition, total fresh weight is shown. The means (+/- SEM) were based on six plates, with five seedlings per line, per plate, each plate containing three plant lines. Means not sharing a letter are significantly different ($p \leq 0.05$); Tukey post-hoc test.

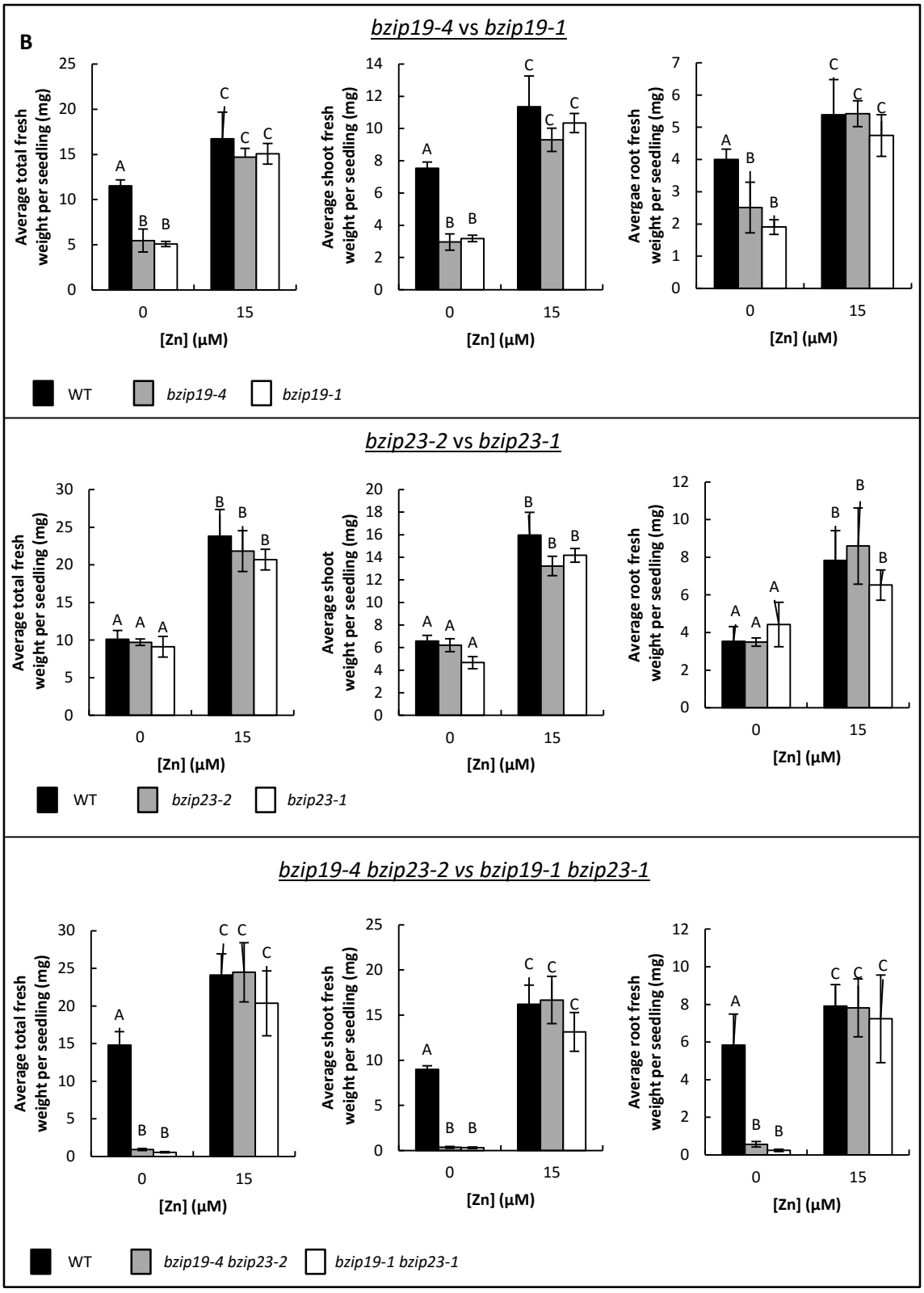

Figure 3.10 continued

shows photographs of seedlings and Figure 3.10B provides data on the fresh weight of whole plants, shoots, and roots. This showed that the corresponding mutants behaved similarly to each other when grown alongside. The double mutants and *bzip19* single mutants, but not the *bzip23* single mutants, showed a Zn-deficiency hypersensitivity.

3.2.4 Double *bzip19 bzip23* T-DNA insertion mutants are adversely affected by Zn deficiency when grown hydroponically

To compare the growth at a later stage, all four unique *bzip19 bzip23* double mutants were grown together with WT and their respective *bzip19* and *bzip23* single mutants on nutrient solution containing either standard (0.38µM) or 0µM Zn. The plants were grown for 40 days under short day conditions and various parameters were measured (Figure 3.11A to D). Overall, similar differences in growth responses were seen in the hydroponic system to those observed in the plate experiments. Analysis from the two-way ANOVA revealed that there was a significant interaction between genotype and Zn concentration on total weight, shoot weight, root weight, root length and rosette diameter as shown in Table 3.5.

At 0.38µM Zn there were no significant differences apparent between WT and the other genotypes (Figure 3.110B). At 0µM Zn, generally the *bzip23* single mutants were similar to WT for all parameters (Figure 3.11B to D). Generally, all *bzip19* mutants, apart from *bzip19-2,* were significantly lower for most parameters than WT seedlings (Figure 3.11B to D). The root-length response was variable amongst these mutants and there was not a consistent decrease compared to WT. The *bzip19-4* showed a contradictory result for root length; statistical analysis revealed no significant difference at 0µM Zn between *bzip19-4* and WT seedlings when grown together with *bzip19-4 bzip23-1* whereas the same *bzip19-4* mutant grown together with *bzip19-4 bzip23-2* showed a significant difference to the WT seedlings (Figure 3.11C). The fresh weight data however, indicated a significant decrease compared to WT in both situations. The *bzip19 bzip23* double mutants showed a marked Zn-deficiency hypersensitivity although perhaps the *bzip19-2 bzip23-1* mutant was not affected quite as strongly as the other double mutants when compared to WT.

3.2.5 Zn-concentration dependency of the *bzip19-4 bzip23-2* double mutant

It was important to determine the concentration of Zn that rescues the *bzip* double mutants as this has not been investigated previously and it reveals information about the sensitivity of the response. Previously for double mutants only 0 and 30µM Zn had been compared in plate-based assays on MS media (Assuncao et al. 2010). Using a range of Zn

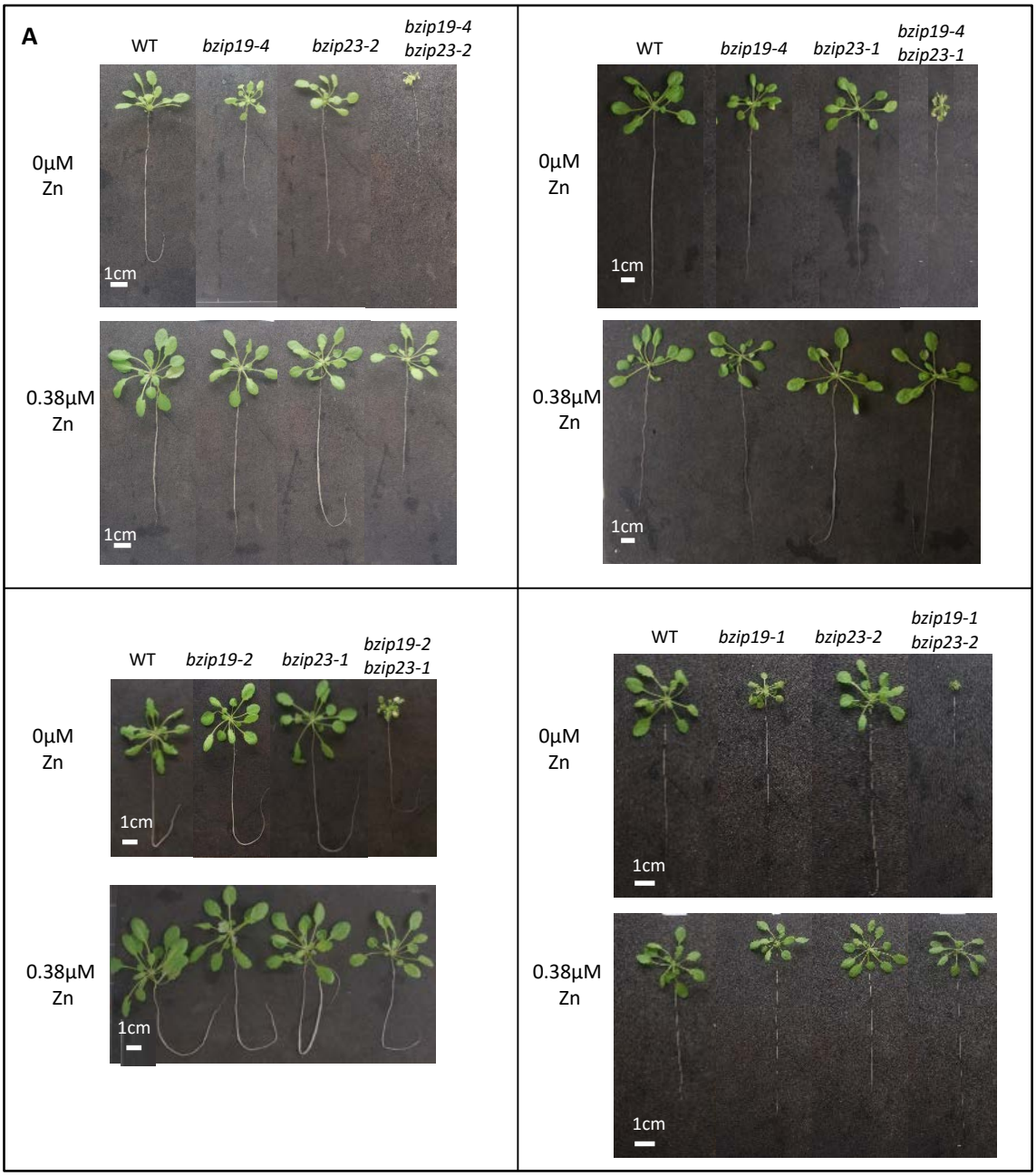

Figure 3.11 All four unique *bzip19 bzip23* double mutants show an adverse effect under Zn deficiency.

(A) WT, *bzip19, bzip23,* and *bzip19 bzip23* T-DNA insertion *A. thaliana* mutants grown on hydroponic culture for 40 days with 0µM Zn or 0.38µM Zn. Data shows mean of (B) total fresh weight and shoot fresh weight, (C) root fresh weight and root length, and (D) rosette diameter per seedling of different *bzip19* and *bzip23* mutants (singles and doubles). The data was based on 30 seedlings (+/- SEM) from two tubs and each tub containing four plant lines with fifteen seedlings per line. Means not sharing a letter are significantly different; Tukey post-hoc test.

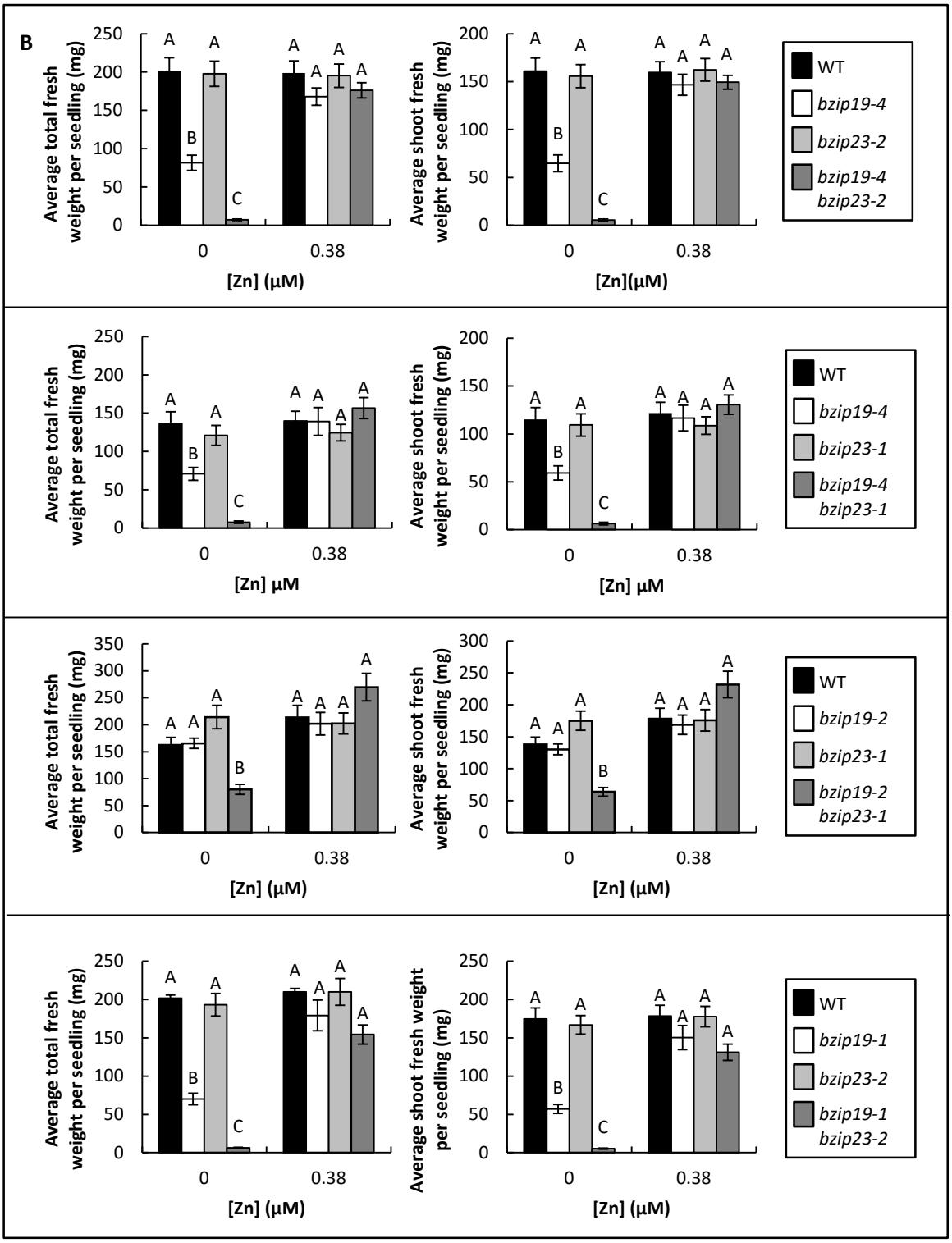

Figure 3.11 continued

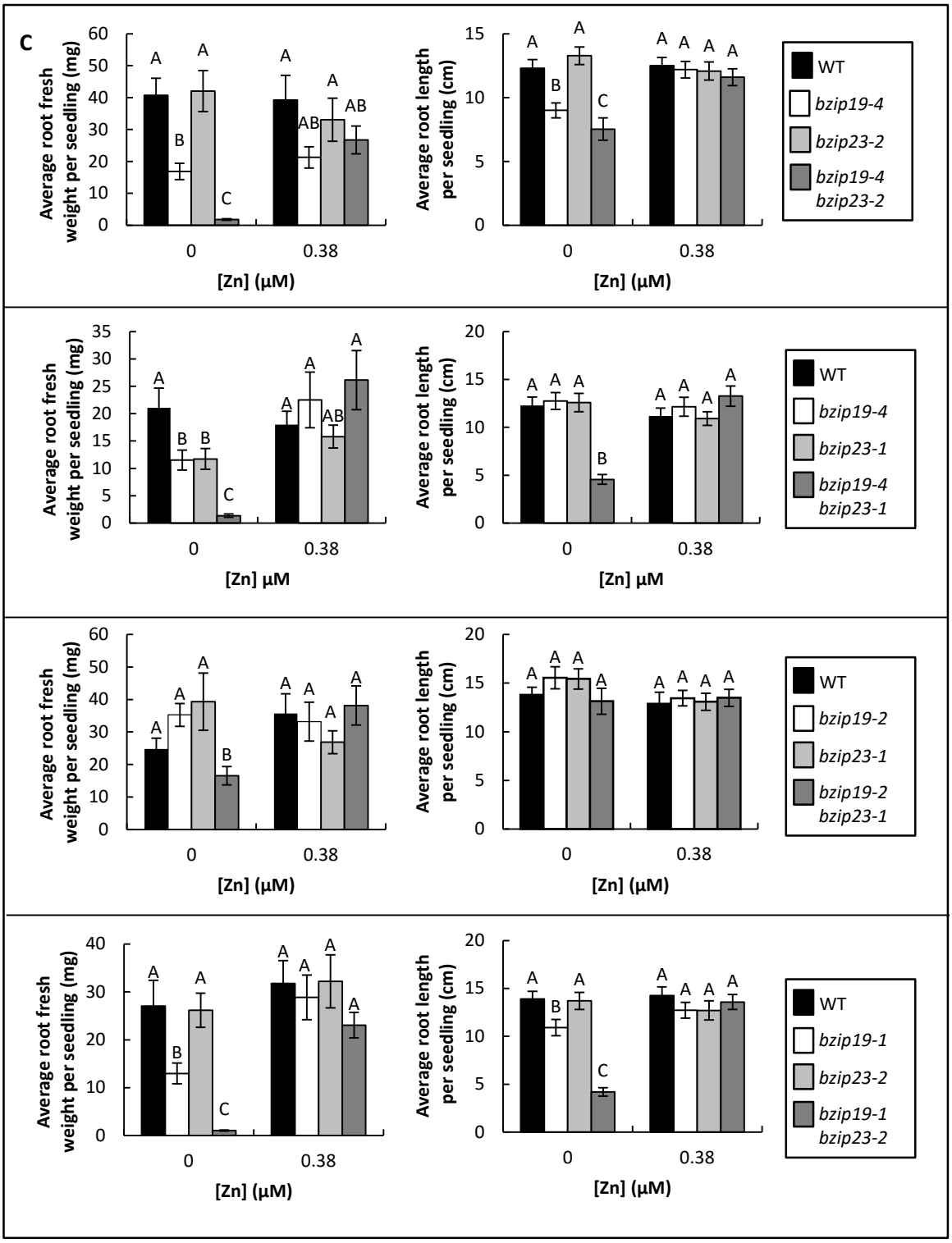

Figure 3.11 continued

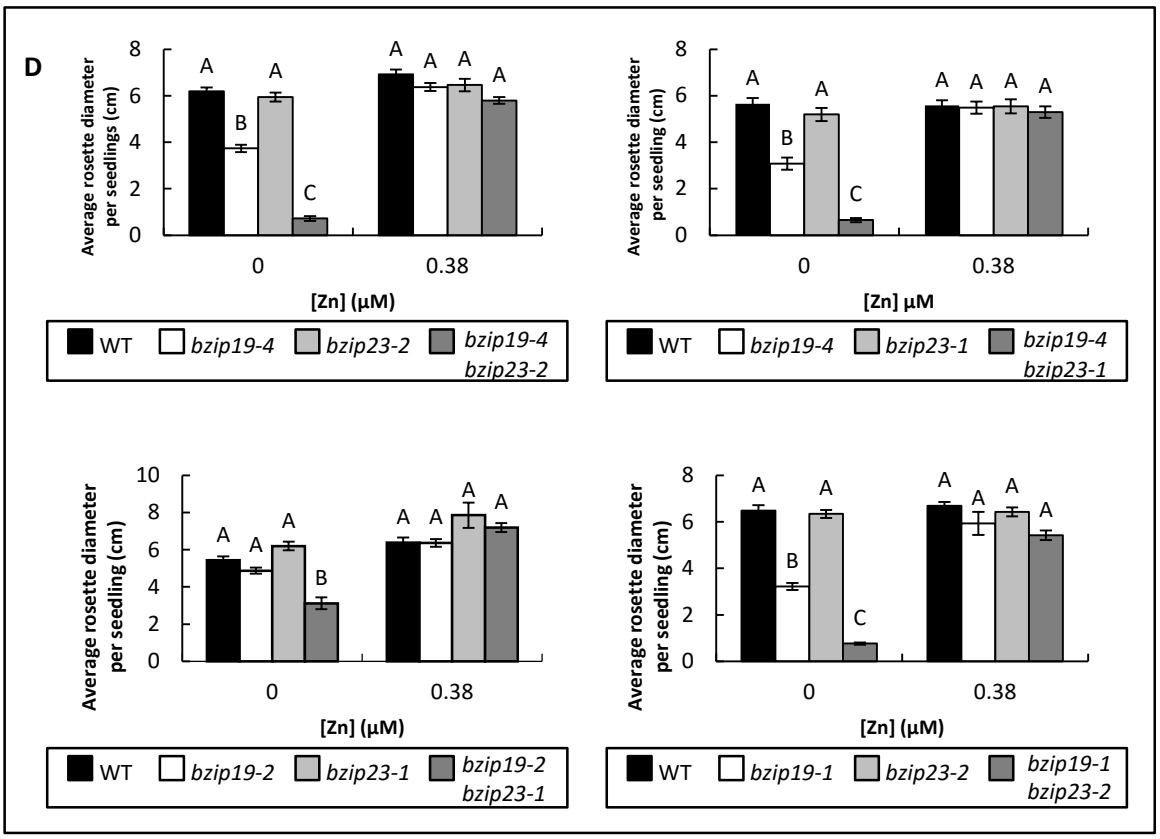

Figure 3.11 continued

Table 3.5 Statistical analysis of two-way ANOVA for evaluating interaction between genotype and Zn concentration for experiment given in Figure 3.11

Measurement	***bzip19-2 bzip23-1***	***bzip19-4 bzip23-1***	***bzip19-4 bzip23-2***	***bzip19-1 bzip23-2***
Total fresh weight	$F_{3, 114}$ = 17.42, P < 0.0001	$F_{3, 114}$ = 86.01, P < 0.0001	$F_{3, 114}$ = 139.0, P < 0.0001	$F_{3, 114}$ = 112.2, P < 0.0001
Shoot fresh weight	$F_{3, 114}$ = 19.49, P < 0.0001	$F_{3, 114}$ = 87.65, P < 0.0001	$F_{3, 114}$ = 137.8, P < 0.0001	$F_{3, 114}$ = 111.1, P < 0.0001
Root fresh weight	$F_{3, 114}$ = 4.716, P = 0.0039	$F_{3, 114}$ = 37.57, P < 0.0001	$F_{3, 114}$ = 33.66, P < 0.0001	$F_{3, 114}$ = 31.28, P < 0.0001
Root Length	$F_{3, 114}$ = 1.199, P = 0.3133	$F_{3, 114}$ = 27.58, P < 0.0001	$F_{3, 114}$ = 8.377, P < 0.0001	$F_{3, 114}$ = 30.27, P < 0.0001
Rosette diameter	$F_{3, 114}$ = 24.31, P < 0.0001	$F_{3, 114}$ = 93.48, P < 0.0001	$F_{3, 114}$ = 138.5, P < 0.0001	$F_{3, 114}$ = 223.0, P < 0.0001

concentrations, initially in the micromolar range (results not shown) but then in the nanomolar range we found that between 750nM and 1µM the *bzip19-4* single and *bzip19-4 bzip23-2* double mutants were restored to WT growth levels (Figure 3.12). Analysis from the two-way ANOVA revealed there is a significant interaction between genotype and Zn concentration on total weight ($F_{21, 171}$=4.79, P<0.05), shoot weight ($F_{21, 171}$=1.71, P<0.05) and root weight ($F_{21, 171}$=1.79, P<0.05). When grown on 1000nM Zn, the double mutants did not show any significant differences in total, shoot and root fresh weight compared to WT seedlings (Figure 3.12B).

3.2.6 Other micronutrient deficiencies (Mn, Cu and Fe) do not impact the response of the *bzip19-4 bzip23-2* double mutants compared to WT.

The specificity of the response was investigated, as previously *bzip* double mutants have not been shown under other micronutrient deficiency conditions and therefore it was important to test that this response was Zn-specific. The response of the mutants to Mn, Cu, and Fe deficiency were tested as some of the IRT/ZIPs have previously been shown to transport or be regulated by Mn and Fe (Vert et al., 2001, Vert et al., 2002, Wintz et al., 2003, Smeets et al., 2009, Milner et al., 2013). Results for the response of the mutants to Mn and Cu deficiency are shown in Figure 3.13 and Figure 3.14 respectively. WT, *bzip19-4* and *bzip23-2* single and *bzip19-4 bzip23-2* double mutants were grown on 0µM Zn media or 15µM Zn media in combination with 0µM Mn or 50µM Mn. For the Cu experiment, the same combination was used but with 0.05µM Cu as a standard Cu concentration, and 50µM Bathocuproine was added to chelate any residual Cu for Cu-deficient media. Fresh weight of seedlings was reduced at 15µM Zn 0µM Mn compared to control conditions (15µM Zn 50µM Mn) but in this case, the *bzip* mutants responded similarly to WT. In addition, there was no influence of Mn on the Zn-deficiency response observed in these mutants as they showed similar responses compared to WT in terms of fresh weight in the presence or absence of Mn. The same observation was obtained in the Cu concentration but seedlings grown on 0µM Zn 0µM Cu were significantly smaller than seedlings grown on 0µM Zn 0µM Cu (Figure 3.14). For Fe experiment, there was no significant effects on the response of the mutants compared to WT when grown under Fe deficiency or toxicity (Figure 3.15), thus the responses observed in these mutants is Zn specific.

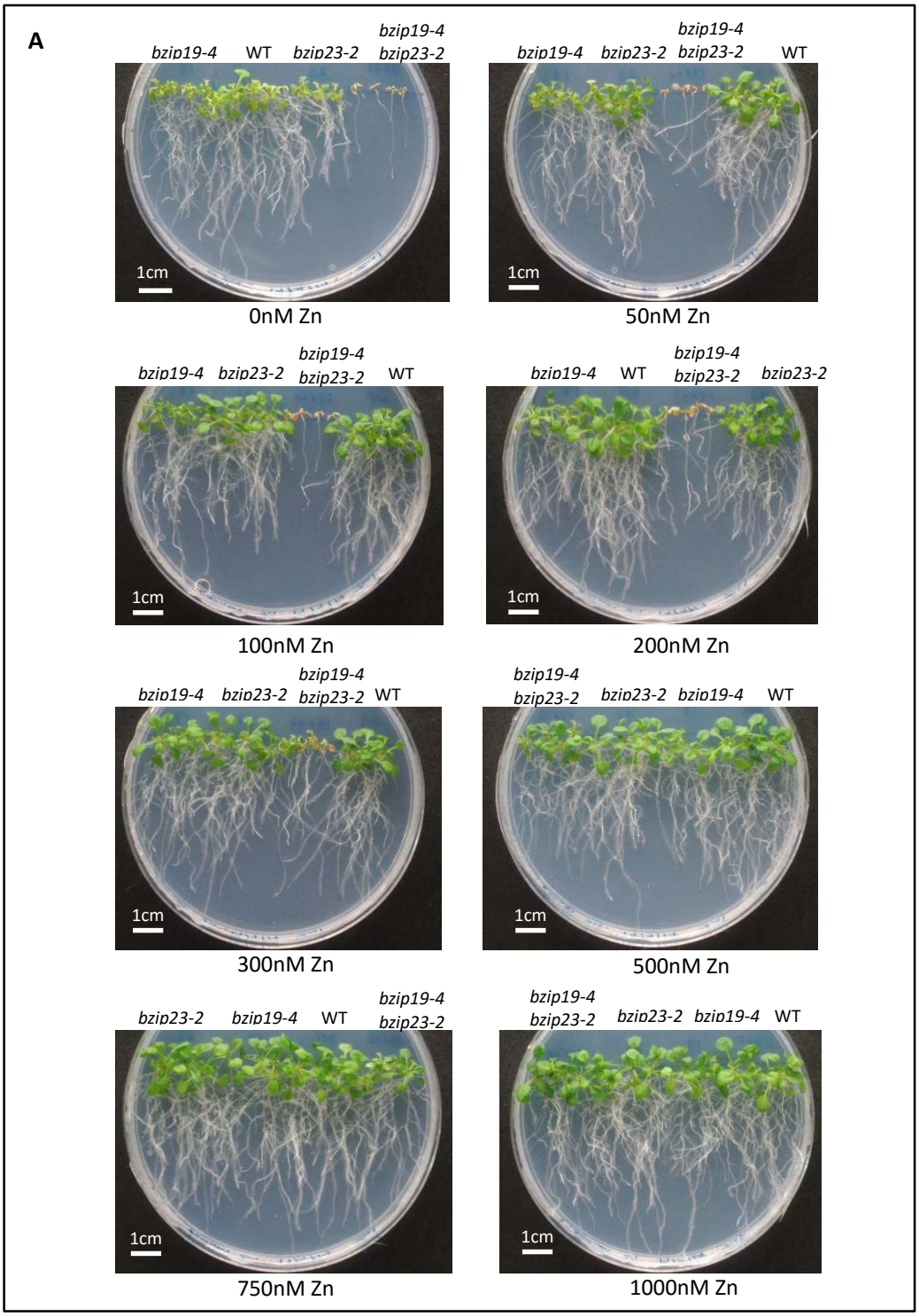

Figure 3.12 Zn-concentration dependency of the *bzip19-4 bzip23-2* double mutant.

The Zn-hypersensitive phenotype was rescued by nanomolar Zn. (A) The representative images of double *bzip19-4 bzip23-2* mutants grown alongside WT, *bzip19-4* and *bzip23-2* single mutants on 0.5 MS media containing a range of Zn concentrations for 19 days. (B) Comparison of mean total, shoot, and root fresh weight of the lines for a range of Zn concentrations. The data are based on the means from six plates (+/- SEM) with four seedlings per line, per plate, each plate containing three plant lines. *, p≤0.05 = significantly different to the mean of WT. #, p≤0.05 = significantly different to the mean of *bzip19-4* and *bzip23-2*.

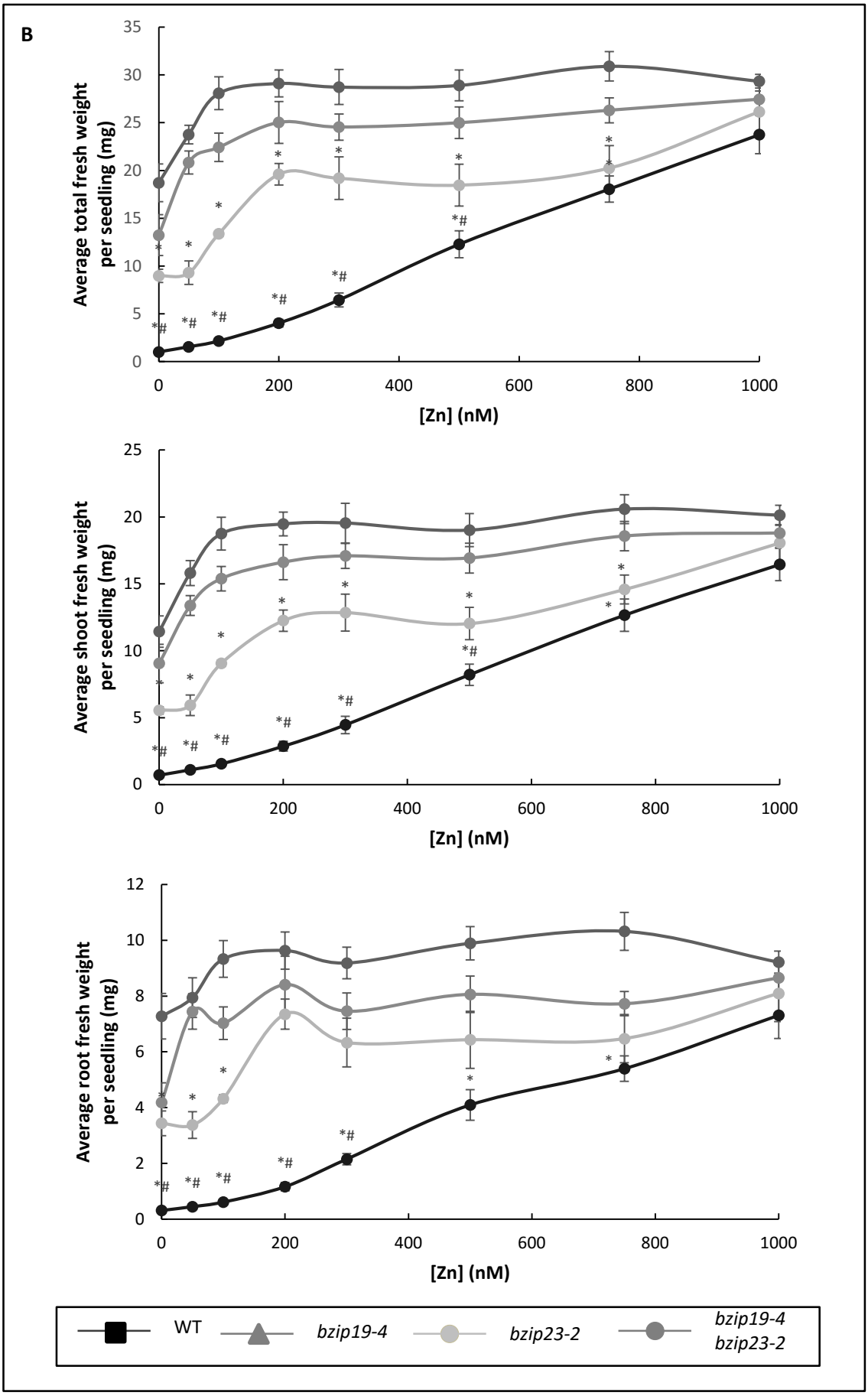

Figure 3.12 continued

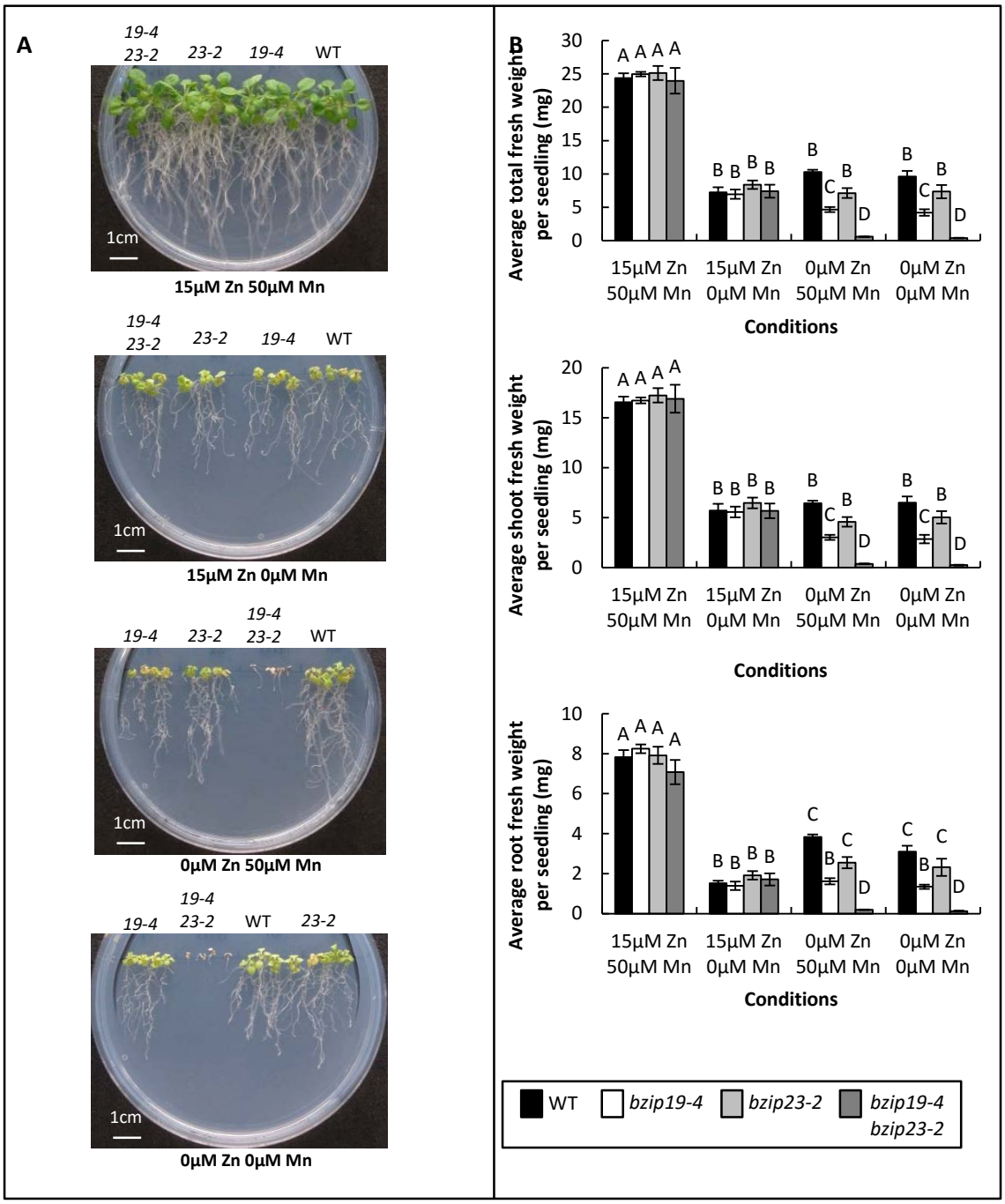

Figure 3.13 Mn deficiency does not affect the phenotype of Zn deficient seedlings.

(A) Double *bzip19-4 bzip23-2* mutants were grown together with WT, *bzip19-4,* and *bzip23-2* single mutants on 0.5 MS under a range of Zn and Mn concentrations for 21 days. (B) Total, shoot and root fresh weight is shown; the means (+/- SEM) were based on six plates, with four seedlings per line, per plate, each plate containing four plant lines. Means not sharing a letter are significantly different (p≤0.05); Tukey post-hoc test.

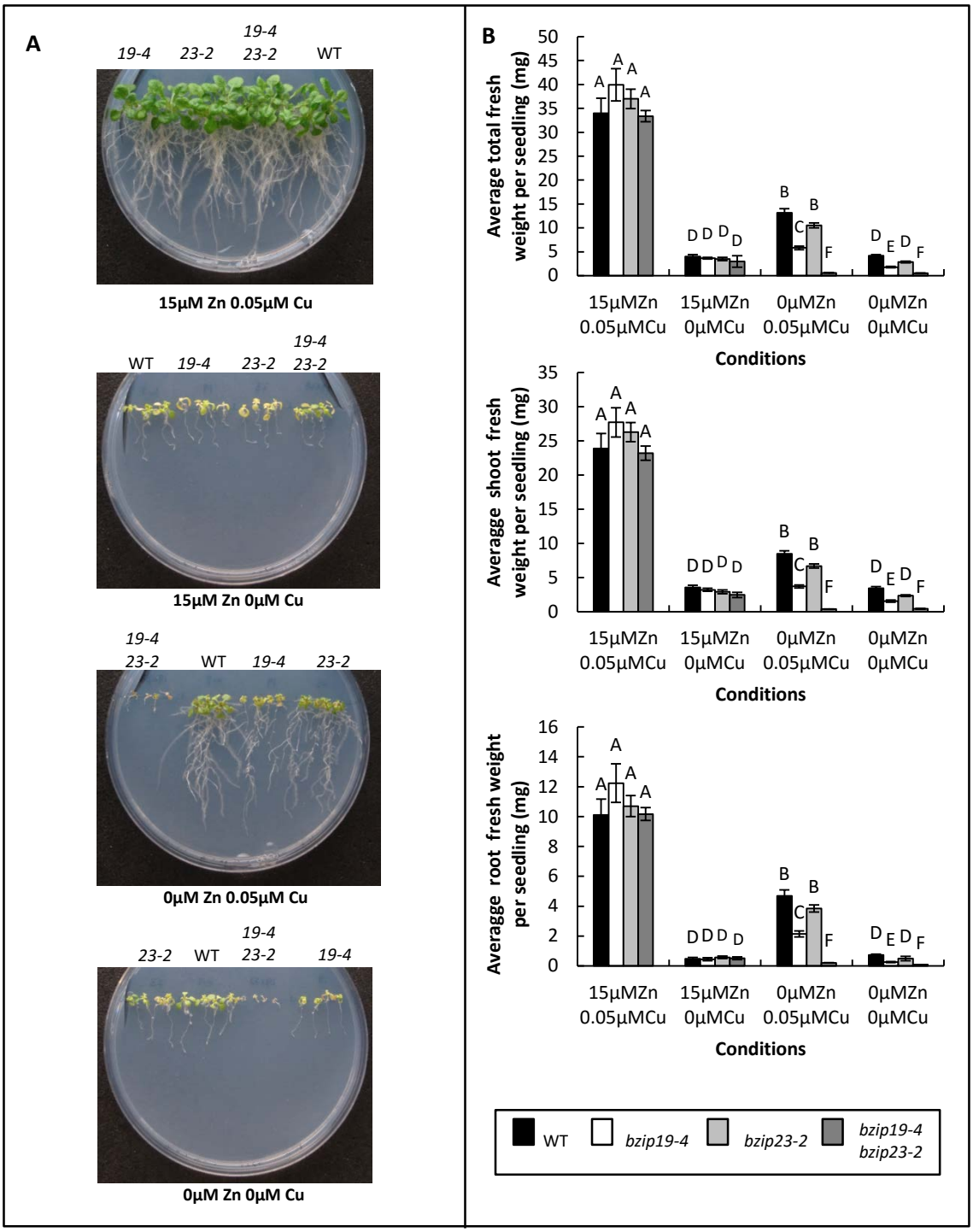

Figure 3.14 Cu deficiency does not specifically affect *bzip19, bzip23* and *bzip19 bzip23* mutants compared to WT.

(A) WT, *bzip19-4, bzip23-2* and *bzip19-4 bzip23*-2 mutants grown on 0.5 MS media under a range of Cu and Zn concentrations for 22 days. For the 0 Cu conditions, no Cu was added to the media and the Cu chelator, Bathocuproine (50µM) was present. (B)Total, shoot and root fresh weight is shown; the means (+/- SEM) were based on six plates, with four seedlings per line, per plate, each plate containing four plant lines. Means not sharing a letter are significantly different (p≤0.05); Tukey post-hoc test.

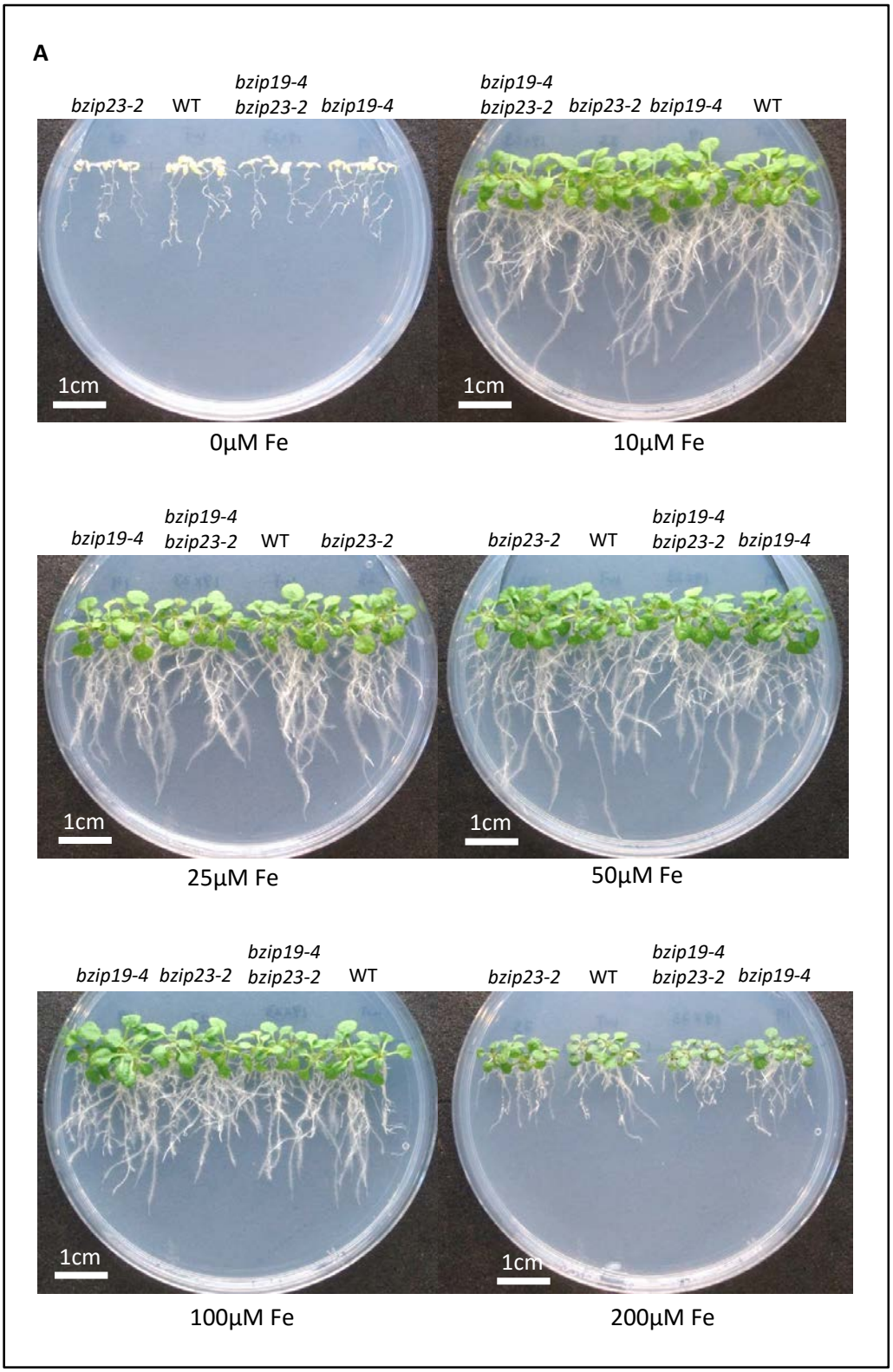

Figure 3.15 Increasing Fe concentrations does not affect *bzip19-2 bzip23-2* mutants.

(A) Double *bzip19-2 bzip23-2* mutants were grown together with WT, *bzip19-2,* and *bzip23-2* single mutants on 0.5 MS under a range of Fe concentrations for 21 days. (B) Total, shoot and root fresh weight is shown; the means (+/- SEM) were based on six plates, with four seedlings per line, per plate, each plate containing four plant lines. Means not sharing a letter are significantly different ($p \leq 0.05$); Tukey post-hoc test.

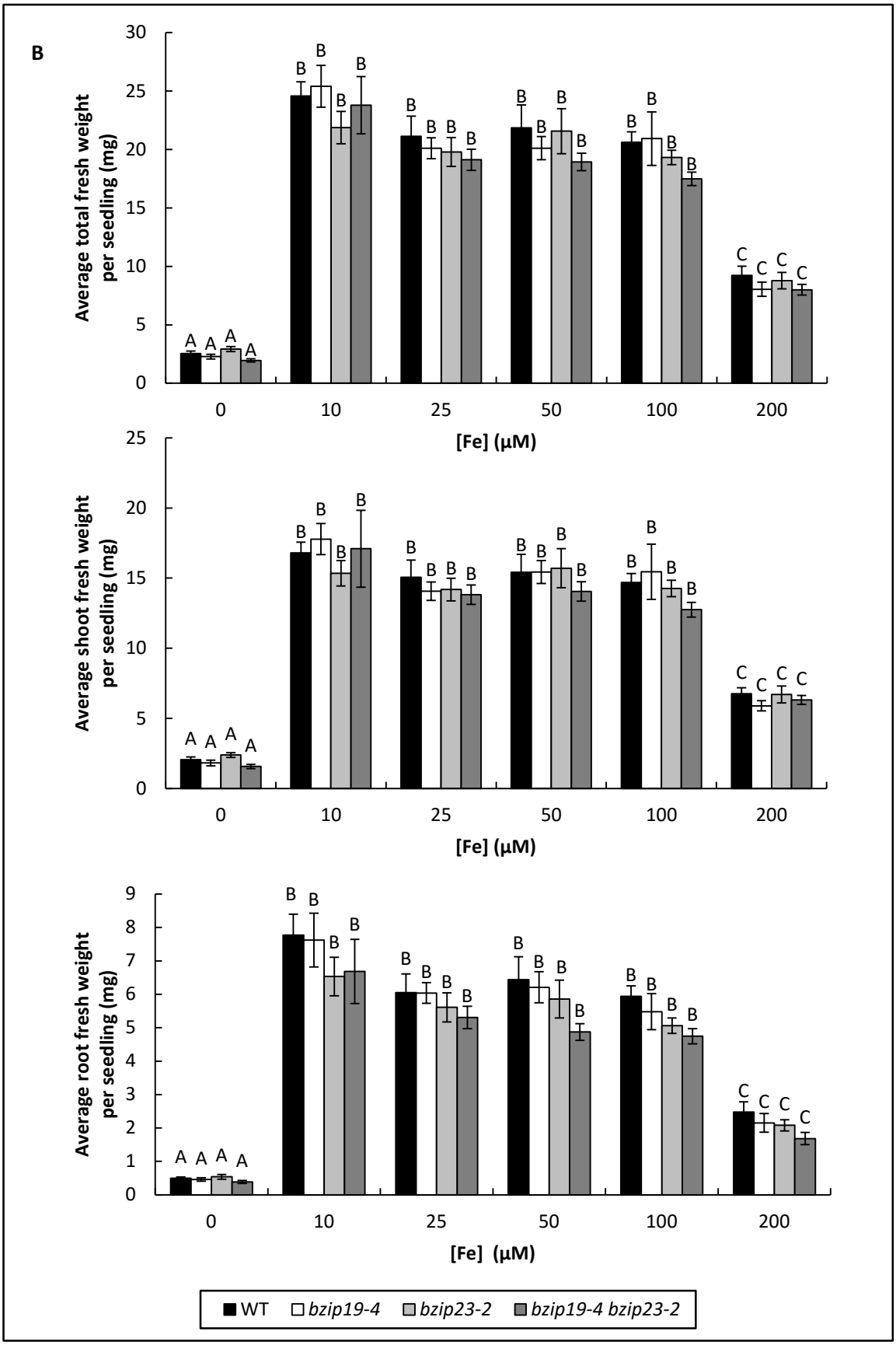

Figure 3.15 continued

3.3 Discussion

The T-DNA insertion *bzip19-1 bzip23-1* double mutant has been shown previously to be useful for studying Zn sensing in *A. thaliana*. It shows strong growth reduction when grown at low Zn supply but it is unaffected when grown in Zn-sufficient and Zn-excess conditions (Assuncao et al., 2010). The T-DNA insertion sites for the previously characterised *bzip19-1 bzip23-1* double mutant are in the promoter regions. Here the effects of T-DNA insertions at other positions were investigated. Four unique *bzip19 bzip23* double mutants having different combination of T-DNA insertion sites were isolated in this study. All the double mutants used in this study exhibited a Zn-hypersensitive phenotype even though there were differences in their T-DNA insert positions. The position of T-DNA in the *A. thaliana* genome can have different possible outcomes (Krysan et al., 1999). Usually, mutants with the T-DNA inserted in the coding region can disrupt the gene function completely and this kind of mutant is known as a knock-out mutant. If in the promoter or 5' UTR this can also lead to complete knock-out mutants or to knock-down mutants, where there is only reduced expression of the gene. Depending on the insert position, partial-length transcripts can be produced which in some cases may show the same or an altered function. The mutants used in this study did not produce any bZIP19 or bZIP23 full-length transcripts. They all appeared to be knock-out mutants although we cannot exclude the possibility for some of them that a functional truncated product was produced. Phenotypic observation and fresh weight analysis found that all four *bzip19 bzip23* double mutants showed extreme hypersensitivity to Zn-deficient conditions and grew normally in standard Zn conditions. This confirms a role for the TFs bZIP19 and bZIP23 in modulating the response of *A. thaliana* to Zn deficiency. The phenotype observed in the mutants is consistent with Zn deficiency associated symptoms found in plants. The observations include stunted growth, chlorosis and necrosis of the leaves. Zn deficiency is characteristically associated with stunted growth. This response is largely attributed to the disturbance of auxin biosynthesis (Henriques et al., 2012), as a result of increased oxidative stress (Brown et al., 1993). Auxin is required for cell elongation and plant growth (Fu and Harberd, 2003), but during periods of Zn deficiency, concentrations become depleted, thereby stunting growth (Skoog, 1940). The first physiological response to Zn deficiency is a reduction in shoot biomass (Cakmak et al., 1997) with effects generally more profound in shoots than roots (Lombnaes and Singh, 2003). Chlorosis and necrosis of the leaves observed in the mutants under Zn deficiency are the result of chlorophyll reduction (Wang et al., 2009). Zn deficiency disrupts the function of many enzymes, including CA (Salama et al., 2006), an enzyme required for photosynthesis. A loss of substrate for carboxylation as a result of Zn deficiency is therefore inhibitory to photosynthesis (Salama et al., 2006).

All *bzip19* single mutants also displayed some sensitivity to Zn deficiency but they were less severe than the response seen in the double mutant when grown on 0.5 MS agar media. In the study by Assuncao et al. (2010) the *bzip19-1* mutant did not exhibit Zn-deficient phenotypes on full MS-based Zn-deficient medium. However, in the current study when this mutant was grown alongside the *bzip19-4* single mutant on 0.5MS both were seen to be inhibited on 0 Zn. It was found here that when grown on the Zn-deficient hydroponic system, the *bzip19-2* single mutant did not seem to be significantly different to WT under Zn deficiency but the double mutant combination was strongly inhibited. The full-length transcript in *bzip19-2* single mutants was not detected, suggesting the gene appeared to be knocked out in this mutant although it is possible that there was a truncated product that could have some functional activity. Certainly, the *bzip19-2 bzip23-1* double mutant was significantly different from the WT but perhaps not as inhibited as the other *bzip19 bzip23* double mutants. Therefore, this mutant was not pursued and the focus was mainly on the *bzip19-4 bzip23-2* double mutant in further studies.

No significant differences were seen in the *bzip23* mutants in the plate assays and the hydroponic experiments conducted here (nor in the experimental conditions in Assuncao et al (2010). This suggests that there is functional redundancy and that bZIP19 can compensate for the lack of bZIP23. Assuncao et al. (2010) suggested that these two TFs act redundantly, indicated by the expression of *bZIP19* or *bZIP23* in the *bzip19 bzip23* double mutant under the control of CaMV35S promoter, showing they can complement the mutant phenotype. Members of the bZIP TF family are capable of forming both homodimers and heterodimers (Jakoby et al., 2002). However, the redundancy seen suggest that these particular TFs function predominantly as homodimers. This is consistent with predictive analyses that suggest that the bZIPs within plants tend to preferentially form homodimers rather than heterodimers (Deppmann et al., 2006). Inaba et al. (2015) have shown that bZIP23 regulates *ZIP12* expression and that loss of bZIP 19 has little effect on the expression of this gene. Therefore, it does seem that bZIP23 has some specific functions. Indeed on their MGRL media a a small but significant inhibition was observed in the *bzip23* mutants, but in that case they were inhibited at most Zn concentrations tested, and not just at 0 Zn. There were marked differences in the concentrations of a number of the minerals but relatively there was a notable increase in Na and also Cu in these experiments. The effect of Cu toxicity includes the inhibition of root growth and reduction of plant biomass (Lequeux et al., 2010) due to an increase of reactive oxygen species (ROS) (Smeets et al., 2009). High Na concentration can induce osmotic stress and ion toxicity to plants (Myouga et al., 2008). Membranes in the roots can be disrupted by osmotic stress and water absorption capacity in plants can be reduced in the early stage (Li et al., 2016). Subsequently, there would be ion-accumulation that can induce severe Na^+/K^+ imbalance and toxic effects (Ismail et al., 2014,

Deinlein et al., 2014, Zhang and Shi, 2013). Thus it is possible that other nutrients were affecting the response of the *bzip23* mutants in this case. It is clear however that both bZIP19 and bZIP23 function in the Zn deficiency response as the original double mutants and the further double mutants isolated here have a severe Zn-deficiency phenotype, and this is much stronger than the *bzip19* mutants.

Further characterisation of *bzip19-4 bzip23-2* conducted here showed that a very low Zn concentration (1µM Zn) can rescue the Zn-deficient phenotype, suggesting the response is highly sensitive. Also from studies here, it appeared that bZIP19 and bZIP23 are specific to the Zn-deficiency response. The *bzip19-4 bzip23-2* double mutant and its corresponding single mutants have similar responses to WT when other micronutrient deficiencies (Mn, Fe, and Cu) were imposed on them. These micronutrient deficiencies did not exacerbate the symptoms of deficiency in the mutant, nor did adequate micronutrients help to rescue the Zn-deficiency phenotype. The *bzip19-4 bzip23-2* double mutant described in this chapter shows a clear Zn-deficient phenotype and it will be used in the next chapter for barley bZIP functional analyses.

Chapter 4:

Exploring the role of barley bZIP transcription factors in the Zn-deficiency response mechanism

4.1 Introduction

4.1.1 Barley as a model organism for cereals

Unlike *A. thaliana*, the knowledge about Zn sensing in cereals remains largely unknown. As Zn deficiency is a serious problem in crops, it is important to know if the same Zn sensing model is operating. Barley is closely related to wheat and ranks fourth among cereals in farming acreage. It is grown widely (being more tolerant than wheat to difficult growing conditions), and is used for animal fodder, as a source of fermentable material for beer and certain distilled beverages, and as a component of various health foods. It has also shown promise in molecular farming for producing human therapeutic proteins or animal vaccines (Mrízová et al., 2014). As a diploid member of the grass family, it a natural model for the genetics and genomics of the Triticeae tribe, especially hexaploid wheat (Schulte et al., 2009). There are now excellent genetic resources for this economically important species (genome sequence information, efficient transformation methods, germplasm availability) which are revitalising gene discovery. This is leading to rapid progress in elucidating pathways involved in regulating growth and development and responses to abiotic stress.

4.1.2 The binary vector system for *A. thaliana* transformation

In the previous chapter, several *bzip19 bzip23* double mutants have been isolated. This chapter is focussed mainly on *bzip19-4 bzip23-2* double mutants here for expression of barley F-group bZIPs. The primary aim was to assess whether the mechanisms for responding to Zn deficiency in Arabidopsis were conserved in barley by using them for complementation tests. One way to introduce and express foreign DNA in *A. thaliana* is by using a Gateway-compatible *A. tumefaciens* binary vector system. *A. tumefaciens* is commonly used for plant transformation due its ability to transfer foreign genes into the nucleus of infected plant cells (Chilton et al., 1977). A plant transformation system known as the binary vector system has been developed and it allows propagation in *E. coli* and then transfer into *A. tumefaciens* and finally plants (Bevan, 1984). The two important components of the binary vector system are the binary plasmid and the *vir* helper

plasmid (Hoekema et al., 1983, Hellens et al., 2000). The binary plasmid contains T-DNA, which consists of a transgene as well as a plant selectable marker and both of them are flanked by left and right border (Joos et al., 1983, Pitzschke and Hirt, 2010). The *vir* helper plasmid harbours the *vir* genes that facilitate the transfer and the integration of the T-DNA into the plant genome (Chilton et al., 1977, Garfinkel and Nester, 1980, Ooms et al., 1980, Ooms et al., 1982).

pMDC32 and pMDC83 are binary destination vectors developed for gene functional analysis in plants (Curtis and Grossniklaus, 2003). Both of them have the Gateway cassette containing the recombination sites (Karimi et al., 2002) positioned adjacent to a dual 35S CaMV promoter (Figure 4.1). The CaMV35S promoter allows constitutive gene expression of the transgene (Odell et al., 1985). This system was a useful way to introduce barley F-group *bZIPs* into *bzip19 bzip23* double mutants. These two vectors utilise strict selection during the cloning and propagation stages due to the presence of a kanamycin resistance gene and *ccdB* gene. The *ccdB* gene, which encoding a toxic protein, is positioned within the recombination site of the vectors and is replaced once the gene of interest is integrated. Thus, unsuccessful recombination will negatively affect the growth of the host (*E. coli*). Further selection for positive constructs can be done with kanamycin treatment. These two destination vectors contain the hygromycin phosphotransferase (*hpt*) gene within the T-DNA borders, which allows for selection of positive transformed plants (Curtis and Grossniklaus, 2003). Figure 4.1 shows the T-DNA features of pMDC32 and pMDC83.

pMDC83 is slightly different to pMDC32 since it includes the *GFP* gene that permits C-terminal GFP tagging, making it suitable for localisation studies (Curtis and Grossniklaus, 2003). Both pMDC32 and pMDC83 have successfully been used for plant functional studies. For example, barley *HvHMA1* is a P_{1B}-ATPase gene encoding an efflux transporter of Zn and Cu from plastids (Mikkelsen et al., 2012). *HvHMA1* expression in *A. thaliana hma1-2* mutants under control of the 35S promoter partially rescued the mutant's phenotype under high light conditions (Mikkelsen et al., 2012). Menguer et al. (2013) used pMDC83 to express *O. sativa* metal tolerance protein 1 (*OsMTP1*) in the *A. thaliana* Zn-sensitive *mtp1-1* mutant. The Zn-sensitive phenotype of *mtp1-1* was rescued by *OsMTP1-GFP* and the tag also demonstrated that OsMTP1 was localised to the tonoplast (Menguer et al., 2013).

4.1.3 The regulation of the Zn homeostatic network in plants

Zn homeostasis in plants is thought to be controlled by a tightly regulated network of sensors monitoring the Zn status and signal transducers controlling the coordinated expression of proteins involved in Zn acquisition from the soil, mobilization between organs and tissues, and

sequestration within cellular compartments (Clemens, 2001). In *A. thaliana*, adaptation to Zn deficiency is controlled by two TFs known as bZIP19 and bZIP23. These two TFs, together with bZIP24, are in the F-group of bZIP TFs (Correa et al., 2008). bZIPs characteristically all contain a leucine zipper-dimerization motif and a highly conserved basic domain, which are capable of binding DNA in a sequence-specific manner. AtZIP4 is strongly induced under Zn deficiency and contains two copies of a specific Zn-deficiency response element (ZDRE) in its promoter. This sequence is thought to be important for transcriptional regulation via bZIP19 and bZIP23. Transcriptomics analyses, comparing Zn-deficiency enhanced transcripts in the *bzip19-1 bzip23-1* double mutant and WT, revealed a cohort of genes that showed differential regulation. These genes contained one or more copies of the 10-bp imperfect palindrome (ZDRE) in their promoter region (Assuncao et al., 2010). *ZIP* transporters and *NAS* genes were the main genes identified in this approach. A proteomics analysis using iTRAQ (isobaric Tags for Relative and Absolute Quantification) was recently implemented to identify proteins that showed bZIP19-dependent induction under Zn deficiency. ZIP proteins were again identified (AtZIP3 and AtZIP9) but also members of the defensin-like family of proteins. Although bZIP19 and bZIP23 TFs do have a clear involvement in the Zn-deficiency response in *A. thaliana*, little is known about the mechanisms existing in cereal crop species and a thorough understanding of Zn-sensing mechanisms in plants is still far from complete. However, studies have shown an increase in the expression of the ZIP transporter genes, *HvZIP3,* 5, 7, 8, 10 and 13 under Zn deficiency (Tiong et al, 2014; Tiong et al, 2015), suggesting a role in primary Zn uptake and root to shoot translocation (Figure 4.2).

4.1.4 Localisation of bZIPs

bZIP proteins from all groups contain a nuclear localization signal in their basic region (Jakoby et al., 2002). This is consistent with their roles as TFs that bind to the promoter of targeted genes in the nucleus. *A. thaliana* bZIP19 and bZIP23 have been reported to be localised in the nuclei as well as cytoplasm of *A. thaliana* roots expressing *P35S::AtbZIP19::gfp* or *P35S::AtbZIP23::gfp* grown on MS medium with normal Zn conditions (Inaba et al., 2015). However, the localisation of AtbZIP19 and AtbZIP23 under Zn-deficient conditions was not indicated. Assuncao et al. (2013) suggested a model whereby Cys/His motifs in AtbZIP19 and AtbZIP23 may be involved in localising these TFs to the nucleus in response to Zn deficiency. Glover-Cutter et al. (2014) showed that BdbZIP10/11, the orthologue of AtbZIP19 and AtbZIP23 in *B. distachyon*, was localised in the nucleus and its level there was enhanced in response to oxidative stress. Yang et al. (2009a) showed that salt stress enhanced the nuclear localisation of AtbZIP24.

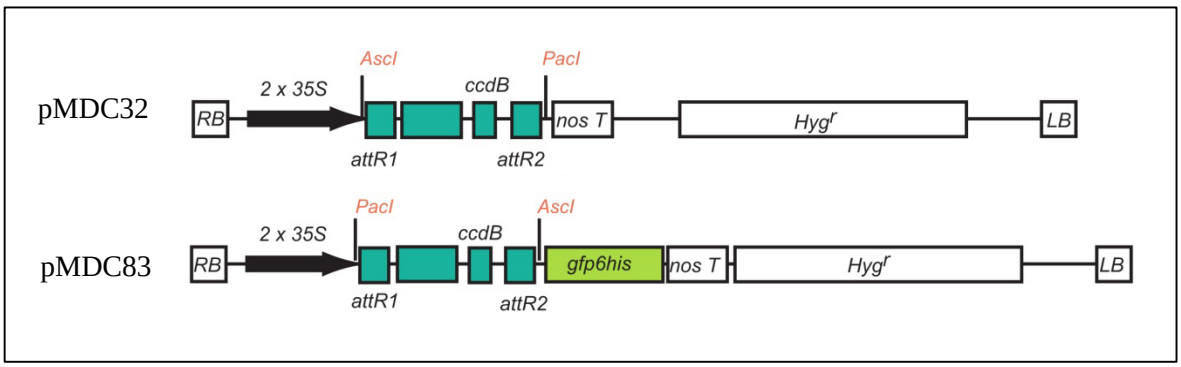

Figure 4.1 Schematics of the pMDC32 and pMDC83 Gateway-compatible *A. thaliana* destination vectors.

Both vectors contain recombination sites flanked by *AscI* and *PacI* recognition sites, hygromycin resistance genes (Hyg^r), LB = left border and RB = right border sequences, and a dual 35S promoter. pMDC83 harbours a C-terminal GFP-6His-tag. Figure is taken from Curtis and Grossniklaus (2003).

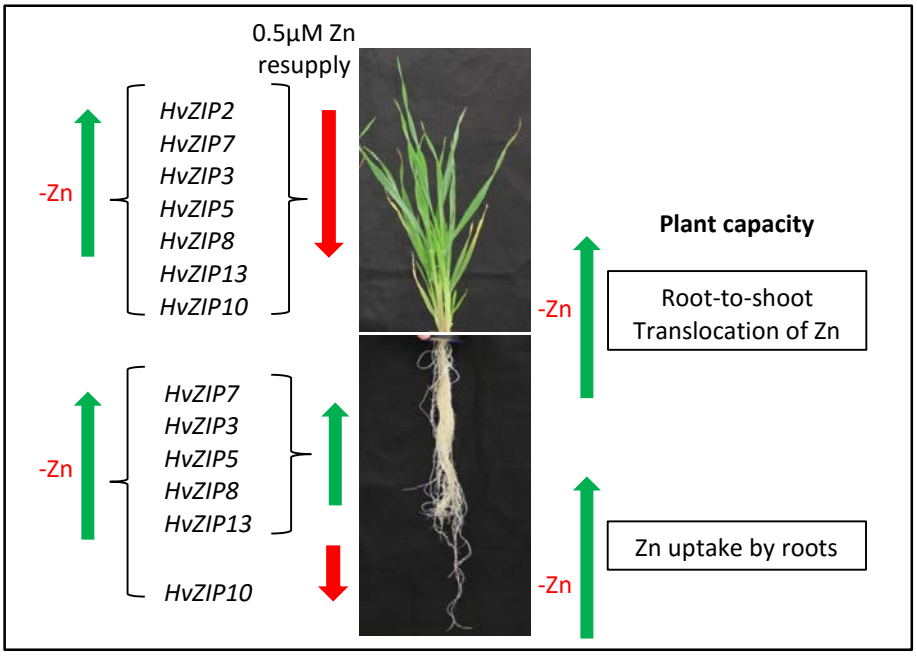

Figure 4.2 Six barley *ZIP* genes are up-regulated by Zn deficiency.

The diagram represents barley *ZIP* expression in response to Zn deficiency (-Zn) and resupply of Zn (+Zn) for 2 days. Increased and reduce gene expression level are indicated by green and red arrows respectively. The diagram is adapted from Tiong et al. (2015).

4.1.5 Aims

In this chapter, the aim was to extend what is known about the role of bZIPs in regulating Zn deficiency in *A. thaliana* and to provide information in barley to indicate whether the mechanisms for sensing and responding to Zn deficiency in cereals is conserved. Specific aims include:

1. To identify F-group bZIP orthologues in barley and conduct phylogenetic analyses to evaluate the evolutionary relationships between these proteins.
2. To identify similarities between the F-group bZIPs using multiple sequence alignments and to find conserved residues and identify a domain architecture.
3. Generate expression constructs containing the F-group *bZIP* coding sequences (CDSs), which will be used to generate transgenic *A. thaliana* lines.
4. To isolate several independent lines expressing barley F-group *bZIP* genes in *A. thaliana* WT and *bzip19-4 bzip23-2*.
5. To conduct plate-based metal tolerance assays with these lines to explore the conservation of function between *A. thaliana* and barley F-group bZIPs. This will reveal whether barley F-group bZIPs can complement the defects in *A. thaliana bzip19-4 bzip23-2* mutants.
6. To develop a hydroponic assay for barley for determining the response to Zn deficiency. The fresh weight measurement and the expression level measurement of known Zn-deficiency induced *ZIP* genes will be used to determine the suitability of this hydroponic assay.
7. To measure the change in expression level of barley *bZIPs* in response to Zn deficiency.
8. To examine the cellular localisation of HvbZIP56 by generating GFP-tagged expression constructs and producing transgenic *A. thaliana* lines. In addition, *HvbZIP56* with a GFP-tag will be transiently expressed in tobacco leaves for further confirmation of localisation.

4.2 Results

4.2.1 Finding F-group bZIPs in barley

A BLAST programme known as ViroBLAST (Deng et al., 2007), was used to search F-group bZIPs in barley. ViroBLAST can be found in the International Barley Sequencing Consortium (IBSC) website (http://webblast.ipk-gatersleben.de/barley/viroblast.php) where the following databases were used: assembly_WGSMorex/Bowman/Barke, HC_genes_CDS_Seq and LC_genes_CDS_Seq. The first database is the genomic assembly from Whole Genome Shotgun sequencing of Morex, Bowman, and Barke cultivar. The two latter databases are barley gene annotations derived from the Morex 55x WGS sequence and gene models were filtered for high-confidence (HC) and low-confidence (LC) predictions based on sequence homology to other angiosperm proteins (Mayer et al., 2012). In addition, the full-length cDNA (FLcDNA) database was also selected in the analyses consisting of 172,000 clones, which were constructed from a two-row malting barley cultivar (Haruna Nijo) under normal and stressed conditions (Matsumoto et al., 2011).

Initial searches with AtbZIP19 and AtbZIP23 at the start of this project were unsuccessful and therefore we searched with the F-group rice coding sequence (CDS) *OsbZIP48*/*53* (LOC_Os06g50310) and then with the bZIPs resulting from this search. *OsbZIP48*/*53* shows 45% and 47% percentage identity to *AtbZIP19* and *AtbZIP23*, respectively (Assunção et al., 2010). Seven barley F-group bZIPs were identified. Later during this project, Pourabed et al. (2015) published a study where they had searched with just the bZIP domain of a representative from each *A. thaliana* and rice subgroup and identified a total of eighty-nine barley bZIPs. From their phylogenetic analyses, they classified six of the eighty-nine as belonging to the F-group (HvbZIP55, HvbZIP56, HvbZIP57, HvbZIP58, HvbZIP61, and HvbZIP62). Five of predicted sequences in this study were identical to these and here, the same nomenclature has been adopted (HvbZIP55, HvbZIP56, HvbZIP57, HvbZIP58, and HvbZIP62). The two additional sequences that we identified have been named HvbZIP1 and HvbZIP10 following the nomenclature of Li et al. (2015). HvbZIP61, a sequence reportedly from Haruna Nijo, was not identified in our initial searches and it is seen to be more divergent than the other seven barley F-group sequences in phylogenetic analyses (Figure 4.3). When analysing this sequence further, it was seen to have less than 11% identity to the other barley F-group bZIPs and it was seen to be very similar to a sequence from *Acyrthosiphon pisum* (pea aphid), with 95% identity. Further examination showed that there was no orthologue of HvbZIP61 found in the wheat or rice genomes and it is the only sequence not found in an analysis of barley contigs. Therefore, it seems likely that when the original libraries were prepared in the study of Matsumoto et al. (2011), this sequence may have been aphid in

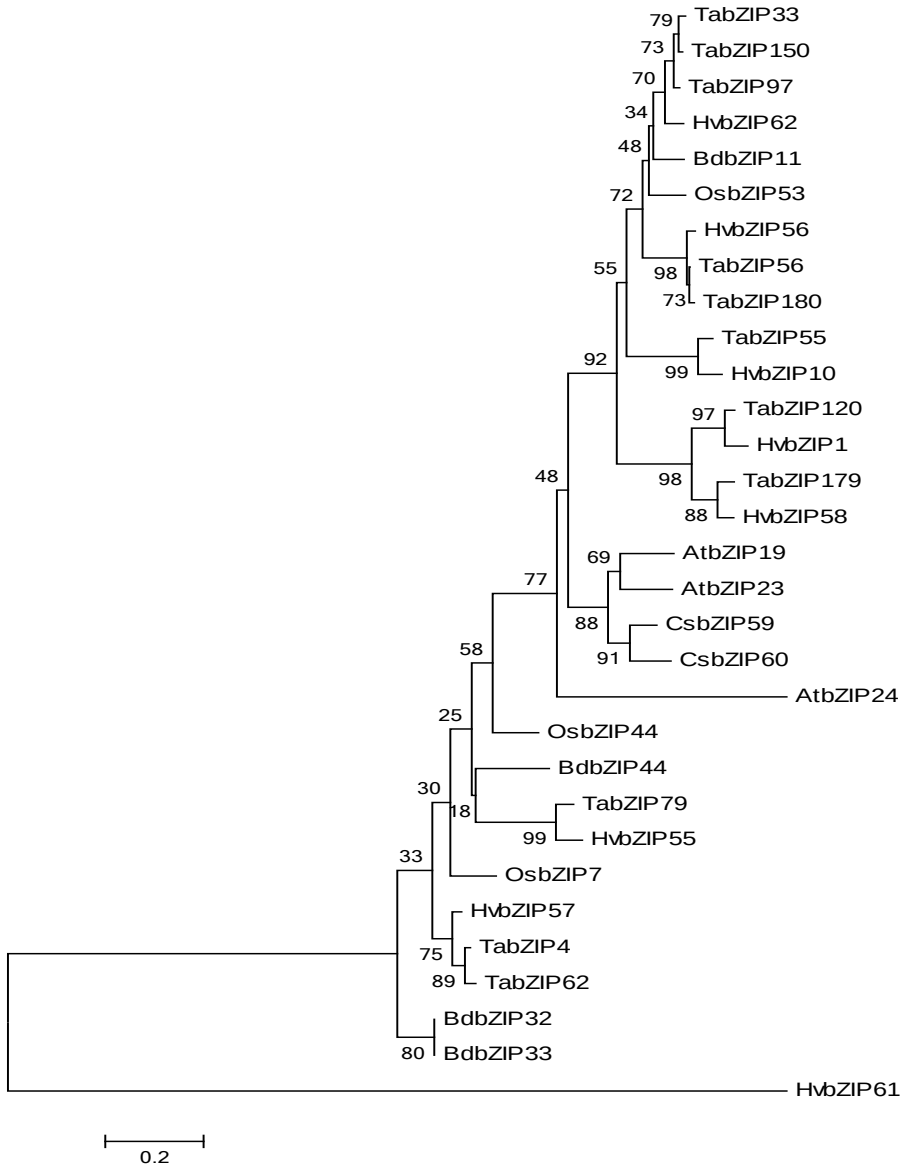

Figure 4.3 Phylogenetic analyses of F-group bZIP proteins from barley including HvbZIP61 and a range of other species.

The phylogenetic analyses shows a non-rooted, bootstrapped plot (1000 replicates) constructed using a multiple alignment of bZIPs from barley, wheat, *B. distachyon*, rice, *A. thaliana,* and cucumber. The tree was constructed using MEGA 7 (Kumar et al., 2016). The percentage of replicate trees in which the associated taxa clustered together in the bootstrap test (1000 replicates) are shown next to the branches (Felsenstein, 1985). The tree is drawn to scale, with branch lengths in the same units as those of the evolutionary distances used to infer the phylogenetic tree. The evolutionary distances were computed using the Poisson correction method (Zuckerkandl and Pauling, 1965) and are in the units of the number of amino acid substitutions per site. The analyses involved 31 amino acid sequences. All positions containing gaps and missing data were eliminated. There were a total of 93 positions in the final dataset. Accession numbers and identifier of the predicted proteins are listed in Appendix 1.

origin. Table 4.1 provides the sequence information for the seven F-group bZIPs identified here in barley.

Morex and Bowman cultivar databases provide most information for finding barley F-group members. However, there were several differences between the sequences in these two cultivars. *HvbZIP1*, *HvbZIP10*, *HvbZIP55*, *HvbZIP56*, and *HvbZIP57* CDSs were identical in both cultivars but not *HvbZIP58* and *HvbZIP62* CDS. *HvbZIP62* CDS in Bowman is nine base pairs longer than the one in Morex. *HvbZIP58* full-length CDS was only found in Haruna Nijo. Both Morex and Bowman searches provided only partial sequences for HvbZIP58, which covered both ends but not the middle part of the gene. There were several nucleotide differences and six additional nucleotides compared to the *HvbZIP58* in Haruna Nijo. Between Morex and Bowman sequences that covered *HvbZIP58*, there was one nucleotide difference.

4.2.2 Phylogenetic analyses of the F-group bZIPs

The seven barley F-group sequences (HvbZIP61 excluded) are shown in an unrooted phylogenetic tree (Figure 4.4) together with F-group bZIP protein sequences previously identified from rice, *B. distachyon*, wheat, *A. thaliana*, and cucumber (Assunção et al., 2010, Baloglu et al., 2014, Li et al., 2015, Liu and Chu, 2015, Pourabed et al., 2015). Li et al., (2015) presented ten F-group *TabZIPs* in their survey of wheat bZIPs. However, a closer examination indicated that some of these were homeologues of the same gene. These have been included in the tree presented here. Monocot and dicot representatives in this F-group clade of bZIPs indicate a conserved evolution and could indicate that there is conservation of function. The wheat F-group bZIPs are the most closely related sequences to each of the seven barley bZIPs. Previously, ninety-six *B. distachyon* bZIP (*BdbZIPs*) have been identified and three (BdbZIP11, BdbZIP32 and BdbZIP33) have been shown to group with *A. thaliana* F-group bZIPs (Liu and Chu, 2015). BdbZIP11 is referred to as BdbZIP10 by Glover-Cutter et al. (2014) and this has been implicated in oxidative stress and the Zn-deficiency responses in *B. distachyon*. HvbZIP62 and HvbZIP56 are most closely related to BdbZIP11 (76% and 65% identity respectively). The phylogenetic analysis would suggest that BdbZIP11, OsbZIP53 and HvbZIP1,10,55,56, and 62 share a common ancestor and it is interesting that there are more barley and wheat members of this cluster than the single members for rice and *B. distachyon*. It would suggest that barley and wheat have undergone gene duplication, which may have occurred prior to their evolution into distinct species. The other barley bZIPs, HvbZIP55 and HvbZIP57 cluster separately from these together with other wheat, rice and *B. distachyon* sequences. In this case, there seems to be the same number of *B. distachyon* and rice bZIPs and barley and wheat have not undergone such a degree of duplication.

Table 4.1 Sequence information for the barley F-group bZIP.

	Contigs	Position	NCBI cDNA accession No. (cultivar)	MIPs[1] cDNA accession No. (cultivar)	Amplification /Cloning	Molecular weight (Da)[2] of GP sequence
HvbZIP1	morex_contig_11993 (Full-length) bowman_contig_63503 (Full-length and identical to the Morex background) barke_contig_276336 (partial sequence)	Chromosome 7HL :33,218,969-33,219,416	Not found	MLOC_2245.1 (Morex)	Yes/Yes	19,857
HvbZIP10	morex_contig_1563657 (Full-length) bowman_contig_846659 (Full-length and identical to the Morex background) barke_contig_268371 ((Full-length but 3bp longer than found in Morex or Bowman)	Chromosome 7H: 536,391,693-536,392,374	Not found	MLOC_12585.1 (Morex)	Yes/Yes	24,329
HvbZIP55	morex_contig_136513 (Full-length) bowman_contig_63503 (Full-length and identical to the Morex background) barke_contig_282304 and 486135 (partial sequences)	Chromosome 3H: 461,941,056-461,941,698	AK354846.1 (Haruna Nijo)	MLOC_5655 (Morex)	Yes/Yes	23,011
HvbZIP56	morex_contig_38563 (Full-length) bowman_contig_1981097 (Full-length and identical to the Morex background) barke_contig_1785171 (partial sequence)	Chromosome 7H: 591,350,097-591,350,849	AK253086.1 (Haruna Nijo)	MLOC_53694.1 (Morex)	Yes/Yes	27,243
HvbZIP57	morex_contig_1565570 (Full-length) bowman_contig_1995766 (Full-length and identical to the Morex background)	Chromosome 1H: 35,678,456-35,679,076	AK371968.1 (Haruna Nijo)	MLOC_13410 (Morex)	Yes/Yes	23,972
HvbZIP58	morex_contig_236589 and 1591639 (partial sequences) bowman_contig_1978011 and 123086 (partial sequences)	Chromosome7HL: 38,634,376-38,634,982	AK354735.1 (Haruna Nijo)	Not found	Yes/Yes	21,819
HvbZIP61	Not found	Not found	AK361769.1 (Haruna Nijo)	Not found	No/No	35,779[3,4]
HvbZIP62	morex_contig_44880 (Full length) bowman_contig_849113 (Full-length but 9bp longer than found in Morex)	Chromosome 5H: 9,201,389-9,202,168	Not found	MLOC_60894.1 (Morex)	Yes/Yes	27,539

1. Accession from Low confidence data MIPS (Munich Information Center for Protein Sequences)
2. Expassy molecular weight predictor: http://web.expasy.org/compute_pi
3. Molecular weight predicted from the putative Haruna Nijo sequence.
4. HvbZIP61 shows 95% identity to sequence from *Acyrthosiphon pisum* (pea aphid) and therefore may not be a barley sequence

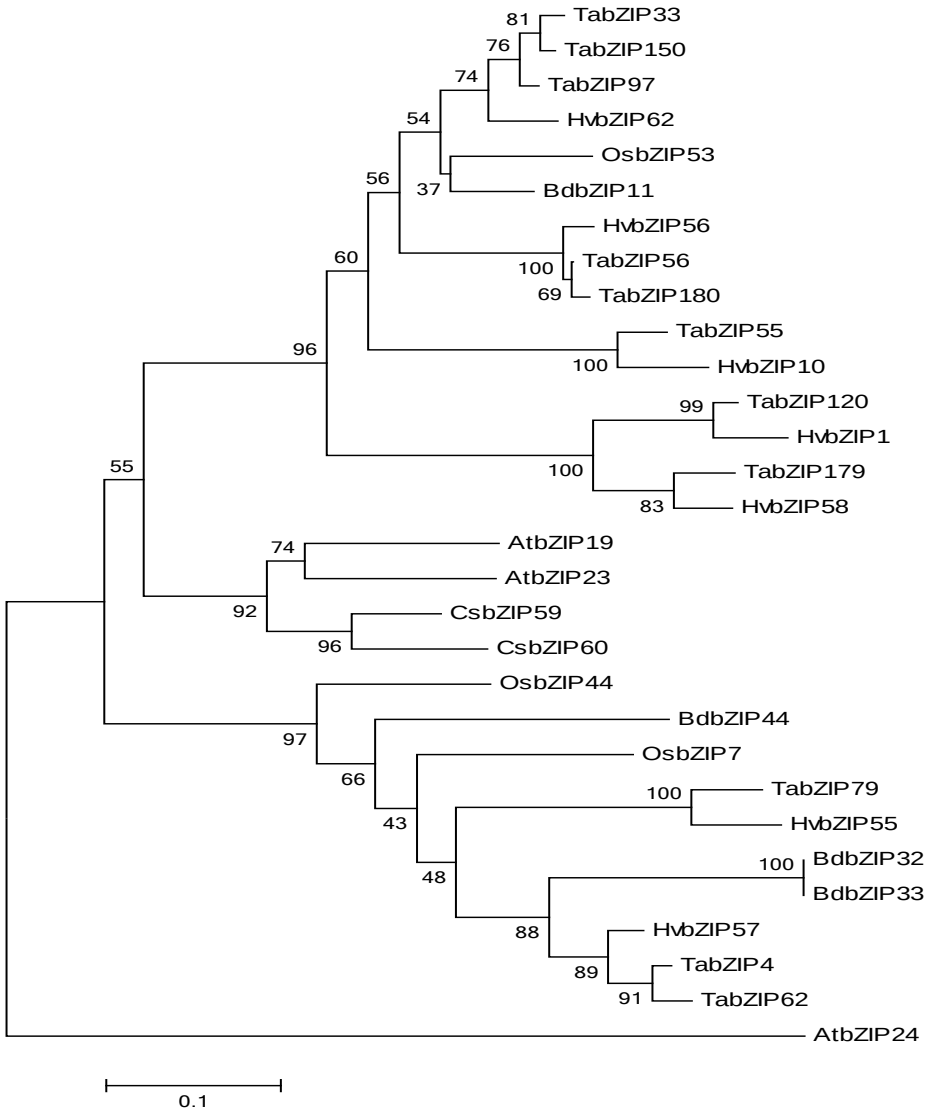

Figure 4.4 Phylogenetic analyses of F-group bZIP proteins from barley excluding HvbZIP61 and a range of other species.

The phylogenetic analyses shows a non-rooted, bootstrapped plot (1000 replicates) constructed using a multiple alignment of bZIPs from barley, wheat, *B. distachyon*, rice, *A. thaliana,* and cucumber. The tree was constructed using MEGA 7 (Kumar et al., 2016). The percentage of replicate trees in which the associated taxa clustered together in the bootstrap test (1000 replicates) are shown next to the branches (Felsenstein, 1985). The tree is drawn to scale, with branch lengths in the same units as those of the evolutionary distances used to infer the phylogenetic tree. The evolutionary distances were computed using the Poisson correction method (Zuckerkandl and Pauling, 1965) and are in the units of the number of amino acid substitutions per site. The analyses involved 30 amino acid sequences. All positions containing gaps and missing data were eliminated. There were a total of 91 positions in the final dataset. Accession numbers and identifier of the predicted proteins are listed in Appendix 1.

It was of interest to explore if there were functional differences in the members of these two broad clusters. Of note is that AtbZIP24 is the most divergent.

The seven barley F-group bZIPs and HvbZIP61 range in predicted molecular weight from 19.9 to 27.5 KDa (Table 4.1) and vary in their percentage identity (Table 4.2). HvbZIP56 and HvbZIP62 are closely related (65% Identity), and they show the highest identity to AtbZIP19 and AtbZIP23. HvbZIP58 and HvbZIP1 show high identity to each other (73% identity). When aligned together with *A. thaliana* F-group bZIPs, all the barley F-group bZIPs and HvbZIP61 have the bZIP domain like the *A. thaliana* bZIPs. This is highly conserved especially over the basic region, which is rich in positive residues lysine and arginine that function in DNA binding. The leucine-zipper region is downstream of this and is thought to function in dimerization with other bZIP proteins forming either homo or heterodimers (Jakobs et al., 2002). Cys/His-rich domains 1 and 2 are seen in all the barley bZIPs apart from HvbZIP10 and it is also not in HvbZIP61 (Figure 4.5). An alignment is also shown where HvbZIP61 is excluded as it is no longer considered a barley gene (Figure 4.6). For HvbZIP10 Morex, Bowman and Barke as well as Golden Promise all lack these Cys/His domains.

4.2.3 Cloning F-group *bZIP* genes from barley cv. Golden Promise

Using the sequence predictions, seven F-group bZIPs (*HvbZIP1*, *HvbZIP10*, *HvbZIP55*, *HvbZIP56*, *HvbZIP57*, *HvbZIP58* and *HvbZIP62*) were successfully amplified from cDNA prepared from the barley cultivar Golden Promise grown in Zn-deficient hydroponic assays for seven days (Figure 4.7). The primers to amplify barley *bZIPs* and their sizes are shown in Table 2.7. For some the size was not quite as predicted (e.g. HvbZIP56) however they were taken forward to the next stage. All amplified products were extracted and purified from the gel and introduced into the entry vector (pENTR/D-TOPO®) using TOPO cloning system which utilises DNA topoisomerase I to cleave the entry vector and ligate the PCR product. The bZIP entry clones were named pENTR/D *HvbZIP1*, pENTR/D *HvbZIP10*, pENTR/D *HvbZIP55*, pENTR/D *HvbZIP56*, pENTR/D *HvbZIP57*, pENTR/D *HvbZIP58*, and pENTR/D *HvbZIP62*. They were transformed into One Shot® TOP10 chemically competent *E. coli* cells and selected on kanamycin. Ten colonies were selected for each construct for colony PCR as the first stage of verification. Figure 4.8A shows an example of the colony PCR for pENTR *HvbZIP56*. The purified plasmids from selected colonies were analysed by restriction analyses to confirm that the *bZIPs* had inserted into the vector in the correct orientation. The restriction enzyme analyses and gel electrophoresis results indicated that the pENTR/D vectors contained *HvbZIP56* (Figure 4.8B) or the other F-group *bZIPs* correctly inserted

Table 4.2 Percentage identity for barley and *A. thaliana* F-group bZIPs.

Results obtained using EMBOSS Needle (McWilliam et al., 2013). Percentage identities are shown in top diagonal none-shaded, percentage similarities are shown in bottom diagonal. The barley sequences apart from HvbZIP61 used in the analyses are those cloned from Golden Promise in this study.

Sequence	AtbZIP19	AtbZIP23	AtbZIP24	HvbZIP1	HvbZIP10	HvbZIP55	HvbZIP56	HvbZIP57	HvbZIP58	HvbZIP61	HvbZIP62
AtbZIP19		69.5	28.4	33.0	34.9	33.6	43.3	38.6	34.4	8.3	41.4
AtbZIP23	80.3		32.6	33.0	38.3	35.6	41.5	39.9	36.6	9.4	44.7
AtbZIP24	45.2	44.1		28.2	25.1	27.5	30.7	28.2	33.8	10.8	29.4
HvbZIP1	44.3	43.3	43.1		42.9	33.1	45.8	33.7	72.9	9.7	42.4
HvbZIP10	48.1	52.9	36.9	49.3		31.4	56.4	28.7	36.3	9.3	50.5
HvbZIP55	46.6	47.0	41.6	41.8	41.7		36.5	50.2	36.2	10.1	30.6
HvbZIP56	58.5	52.9	45.1	52.7	65.6	53.6		39.9	45.1	7.5	65.1
HvbZIP57	47.4	49.6	41.8	43.4	39.8	58.0	48.2		36.1	8.8	39.3
HvbZIP58	44.0	49.1	47.1	79.3	43.6	46.9	51.9	41.7		9.5	42.5
HvbZIP61	16.2	15.4	18.5	15.1	13.8	15.4	13.8	15.9	13.3		9.7
HvbZIP62	55.9	59.5	43.2	48.8	57.8	39.7	71.7	49.6	49.3	13.3	

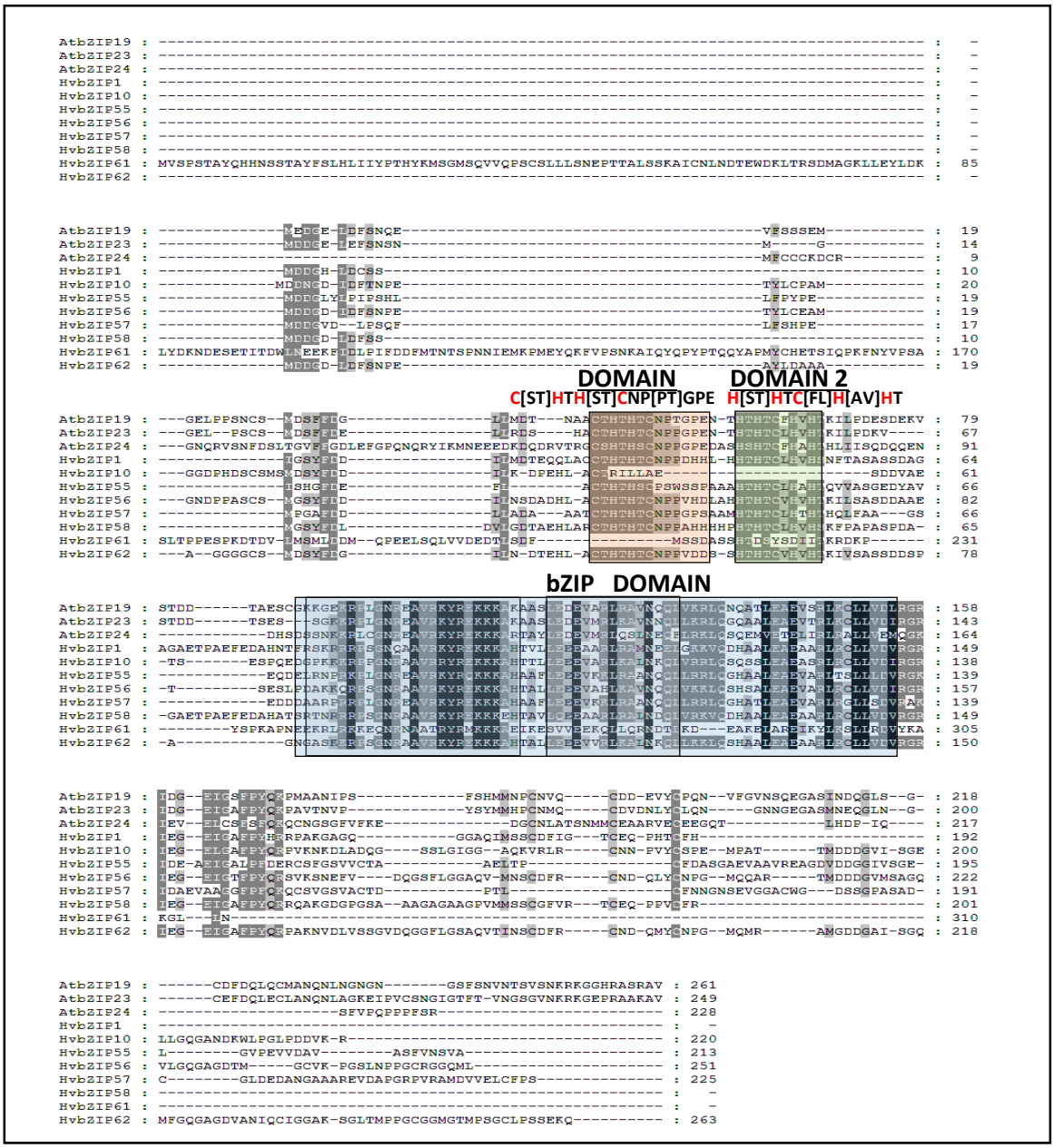

Figure 4.5 Amino acid multiple alignment of *A. thaliana* and barley F-group bZIPs including HvbZIP61.

The barley sequences apart from HvbZIP61 used in the analyses are those cloned from Golden Promise in this study. Sequences were aligned using the Clustal Omega algorithm (Sievers et al., 2011) and presented using GeneDoc (Nicholas and Nicholas Jr, 1997). For the sequences aligned here: black = conserved residues, dark grey = conserved in at least nine of the sequences, and light grey = conserved in at least seven of the sequences. The bZIP domain and the two conserved Cys/His-rich domains (domain 1 and 2) are highlighted. Above the latter two are the sequence of the *A. thaliana* F-group bZIPs (Jakoby et al. 2002). The bZIP domain is boxed according to information given for AtbZIP19 at http://www.uniprot.org/ with the first box indicating the basic region and the second box indicating the leucine zipper region within the domain.

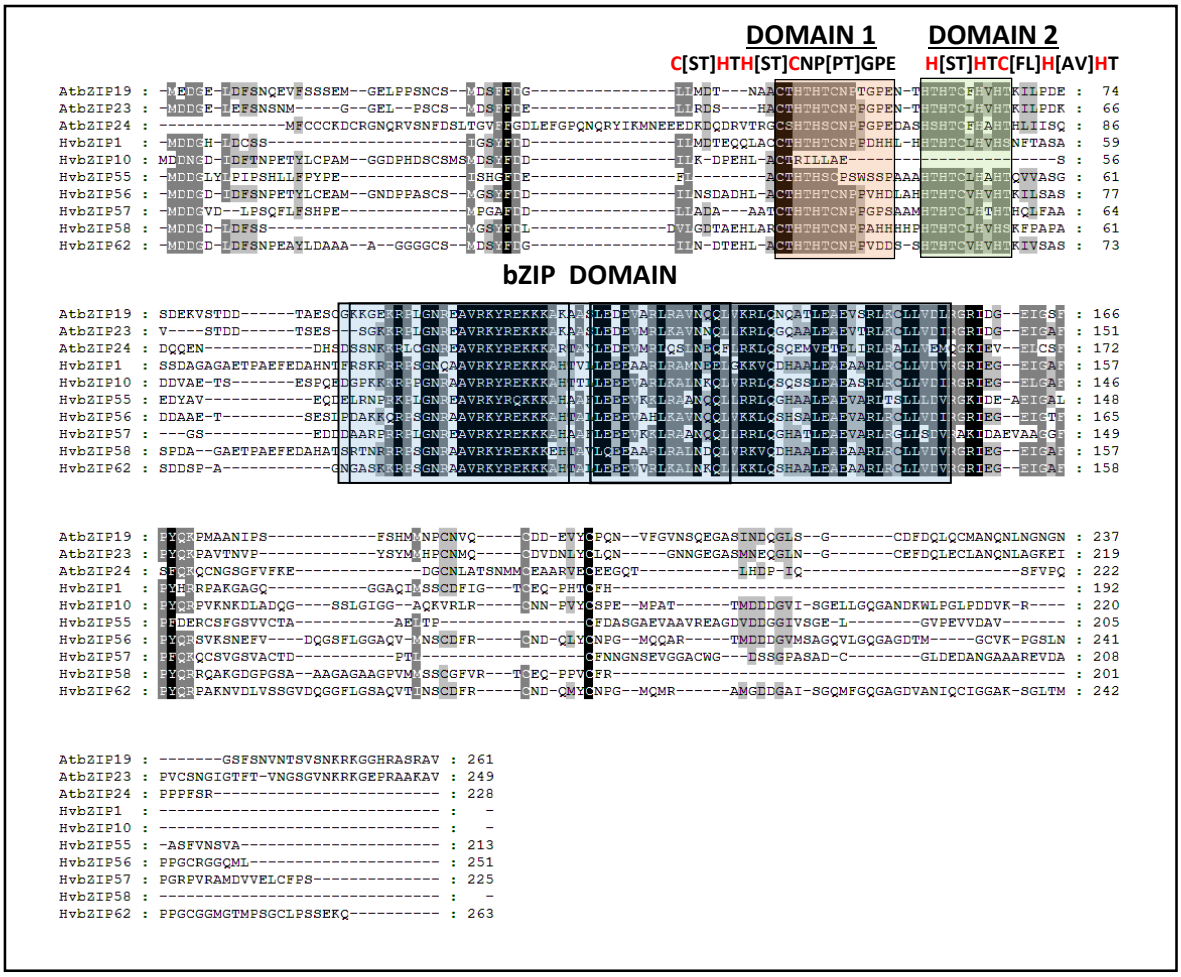

Figure 4.6 Amino acid multiple alignment of *A. thaliana* and barley F-group bZIPs excluding HvbZIP61.

The barley sequences apart from HvbZIP61 used in the analyses are those cloned from Golden Promise in this study. Sequences were aligned using the Clustal Omega algorithm (Sievers et al., 2011) and presented using GeneDoc (Nicholas and Nicholas Jr, 1997). For the sequences aligned here: black = conserved residues, dark grey = conserved in at least nine of the sequences, and light grey = conserved in at least seven of the sequences. The bZIP domain and the two conserved Cys/His-rich domains (domain 1 and 2) are highlighted. Above the latter two are the sequence of the *A. thaliana* F-group bZIPs (Jakoby et al. 2002). The bZIP domain is boxed according to information given for AtbZIP19 at http://www.uniprot.org/ with the first box indicating the basic region and the second box indicating the leucine zipper region within the domain.

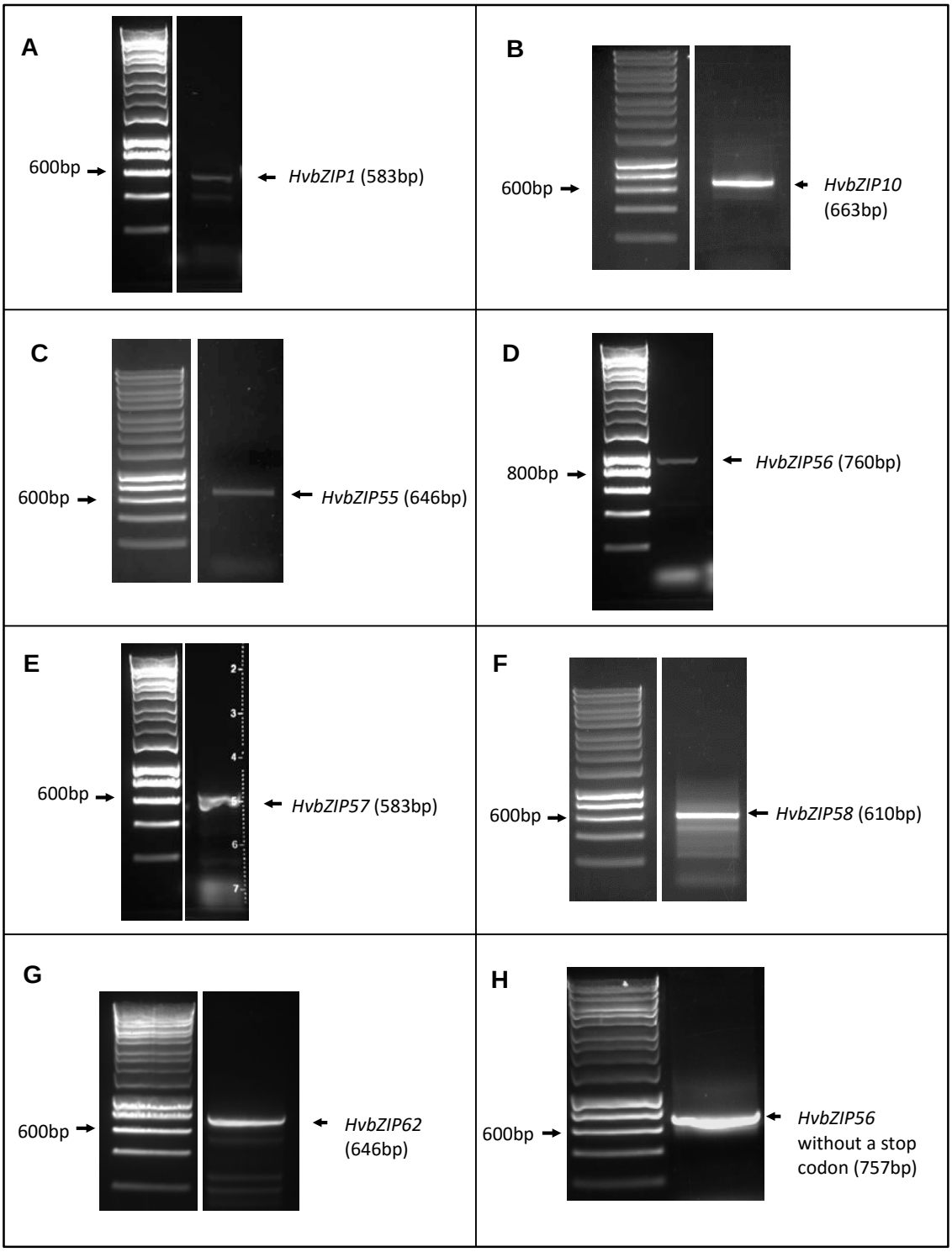

Figure 4.7 Seven F-group bZIP products amplified from barley cDNA with Pfu.

Predicted product sizes are indicated on right and predicted molecular marker sized indicated on left. Full-length coding sequence of *HvbZIP1* (A), *HvbZIP10* (B), *HvbZIP55* (C), *HvbZIP56* (D), *HvbZIP57* (E), *HvbZIP58* (F), and *HvbZIP62* (G) were amplified with using Pfu polymerase to produce a blunt end PCR product. *HvbZIP56* without the stop codon (H) was also amplified using primers HvbZIP56topo_F and HvbZIP56topo_NS.

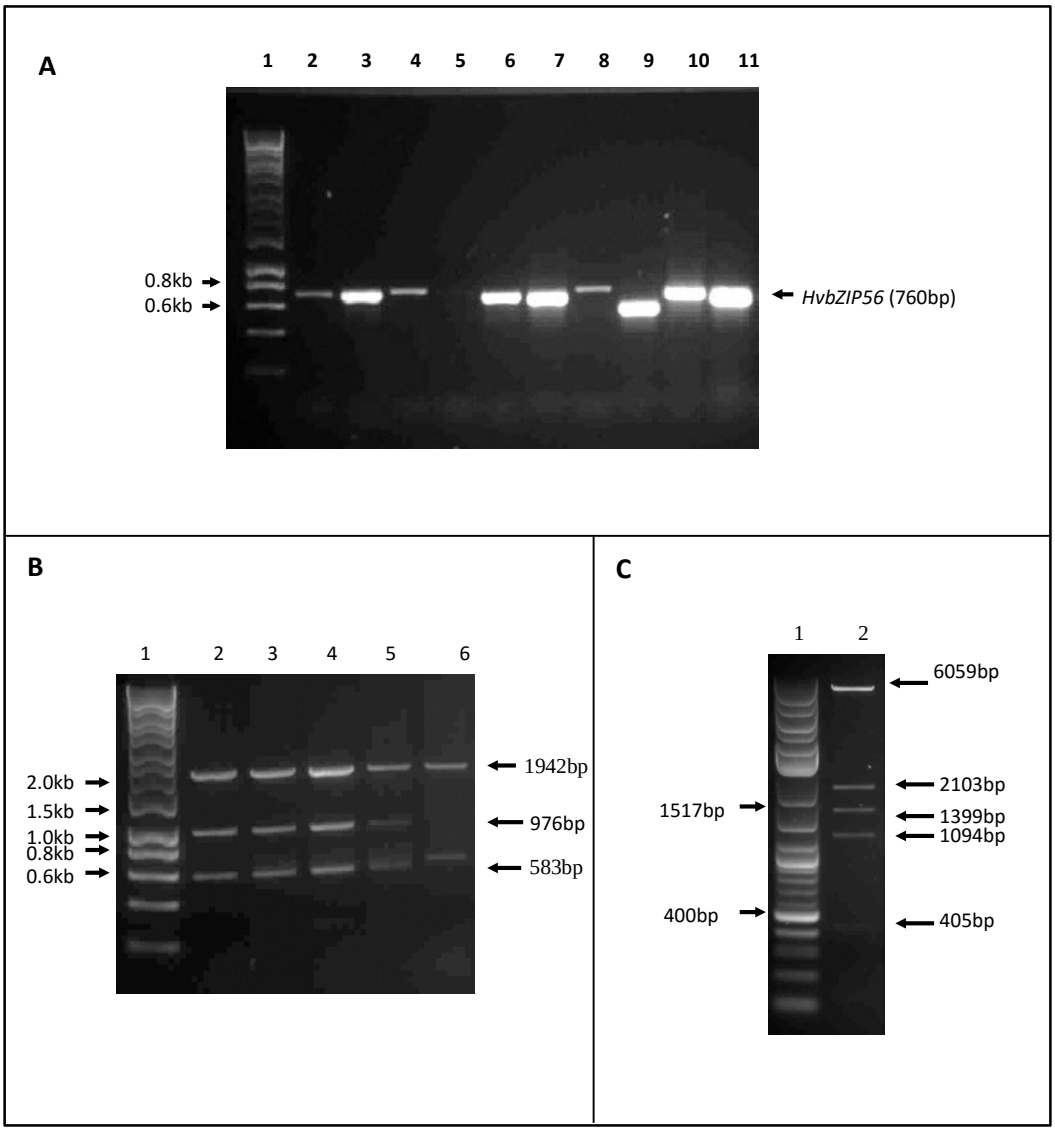

Figure 4.8 Cloning of *HvbZIP56* into entry vector pENTR and *A. thaliana* expression vector pMDC32.

(A) Colony PCR and gel electrophoresis to show the successful transformation of One Shot® TOP10 *E. coli* strains with the entry vectors pENTR/D-TOPO®. Ten colonies of TOP10 *E. coli* potentially carrying pENTR *HvbZIP56* (lane 2 – 11) were tested using primers HvbZIP56topo_F and HvbZIP56topo_S (Table 2.7). (B) Analyses of *HvbZIP56* cloned into TOPO pENTR/D Entry Vector ™ using restriction enzymes *PvuII*. Five clones were tested and shown on the gel (lane 2 -6). (C) Analyses of *HvbZIP56* in plant destination vector pMDC32. Digestion of pMDC32 *HvbZIP56* with enzymes *EcoRV* and *XhoI* (lane 2). Predicted product sizes are shown on the figure. Lane 1: molecular marker.

(Table 4.3). Restriction enzymes that can cut the entry clones in the gene and the entry vector backbone were used.

Since the barley *bZIP* entry clones contain 'att L' sites, all *bZIPs* can be efficiently transferred into *A. thaliana* destination vector, pMDC32 so that they can be expressed constitutively in *A. thaliana*. *HvbZIP56* without a stop codon was introduced into pMDC83, which can tag its C-terminus with EGFP. The expression clones containing the *HvbZIPs* were transformed into DH5α *E. coli* cells and selected on kanamycin. Colony PCR was performed on ten selected colonies of each *bZIP* using respective Topo primers amplifying the whole cDNA followed by a diagnostic restriction analyses to confirm the introduction of barley *bZIPs* into pMDC32 or pMDC83. Figure 4.8C shows an example of the restriction diagnostic analyses for pMDC32 *HvbZIP56*.

As a final verification, the expression vectors were sequenced with pMDC35S forward primer and pMDCnosR reverse primer. All barley F-group bZIP CDSs are listed in Appendix 2. The sequence analyses confirmed that all *bZIP* sequences corresponded to the Morex cultivar except for *HvbZIP58* and *HvbZIP62*. Both of them had an identical nucleotide sequence to the Bowman cultivar. The *HvbZIP58* clone had two different nucleotides compared to Morex cultivar (Figure 4.9A), which resulted in two amino acid changes (lysine-83 to asparagine-83 and histidine-113 to arginine-113) (Figure 4.9B). The *HvbZIP62* clone had nine additional nucleotides and six different nucleotides compared to the Morex sequence (Figure 4.10A), leading to three additional amino acids and two amino acid changes (Figure 4.10B). Sequence analyses also confirmed that these *bZIPs* were inserted correctly into the pMDC32 and pMDC83 destination vectors. Table 4.4 displays the expression vectors generated in this study. All seven barley F-group *bZIP*s were transformed into *A. thaliana* using *A. tumefaciens* transformation. The successful transformed *A. tumefaciens* colonies were screened by colony PCR using respective Topo primers that amplified the whole cDNA. Figure 4.11 shows an example of colony PCR and the predicted products for pMDC32 *HvbZIP56* in GV3850 *A. tumefaciens* strains. *A. tumefaciens* transformants containing pMDC32 *HvbZIP1*, pMDC32 *HvbZIP10,* pMDC32 *HvbZIP56*, pMDC32 *HvbZIP55*, pMDC32 *HvbZIP57,* pMDC32 *HvbZIP58*, pMDC32 *HvbZIP62*, and pMDC83 *HvbZIP56* were used to transform *A. thaliana* WT and *bzip19-4 bzip23-2*. Table 4.5 shows the *A. thaliana* transgenic lines generated in this thesis. Multiple lines were initially generated for each and at least four were taken forward to final homozygous T_3 independent lines that were 100% resistant to hygromycin. These lines were all confirmed to be around 75% resistant to hygromycin at T_2 stage.

The expression of barley F-group *bZIPs* in the T_3 plants was confirmed at the RNA level. RNA of these plants was extracted and cDNA was synthesised subsequently. RT-PCR results showing the expression of *HvbZIP56* in WT (Figure 4.12) and *bzip19-4 bzip23-2* mutant plants (Figure 4.13)

Table 4.3 The Gateway-compatible entry vectors constructed

Plasmid	**Description**
pENTR/D *HvbZIP1* with stop codon	CDS of *HvbZIP1*
pENTR/D *HvbZIP1b* with stop codon	CDS of *HvbZIP1b*
pENTR/D *HvbZIP10* with stop codon	CDS of *HvbZIP10*
pENTR/D *HvbZIP55* with stop codon	CDS of *HvbZIP55*
pENTR/D *HvbZIP56* with stop codon	CDS of *HvbZIP56*
pENTR/D *HvbZIP56* without stop codon	CDS of *HvbZIP56* that can be C-terminally tagged
pENTR/D *HvbZIP57* with stop codon	CDS of *HvbZIP57*
pENTR/D *HvbZIP58* with stop codon	CDS of *HvbZIP58*
pENTR/D *HvbZIP62* with stop codon	CDS of *HvbZIP62*

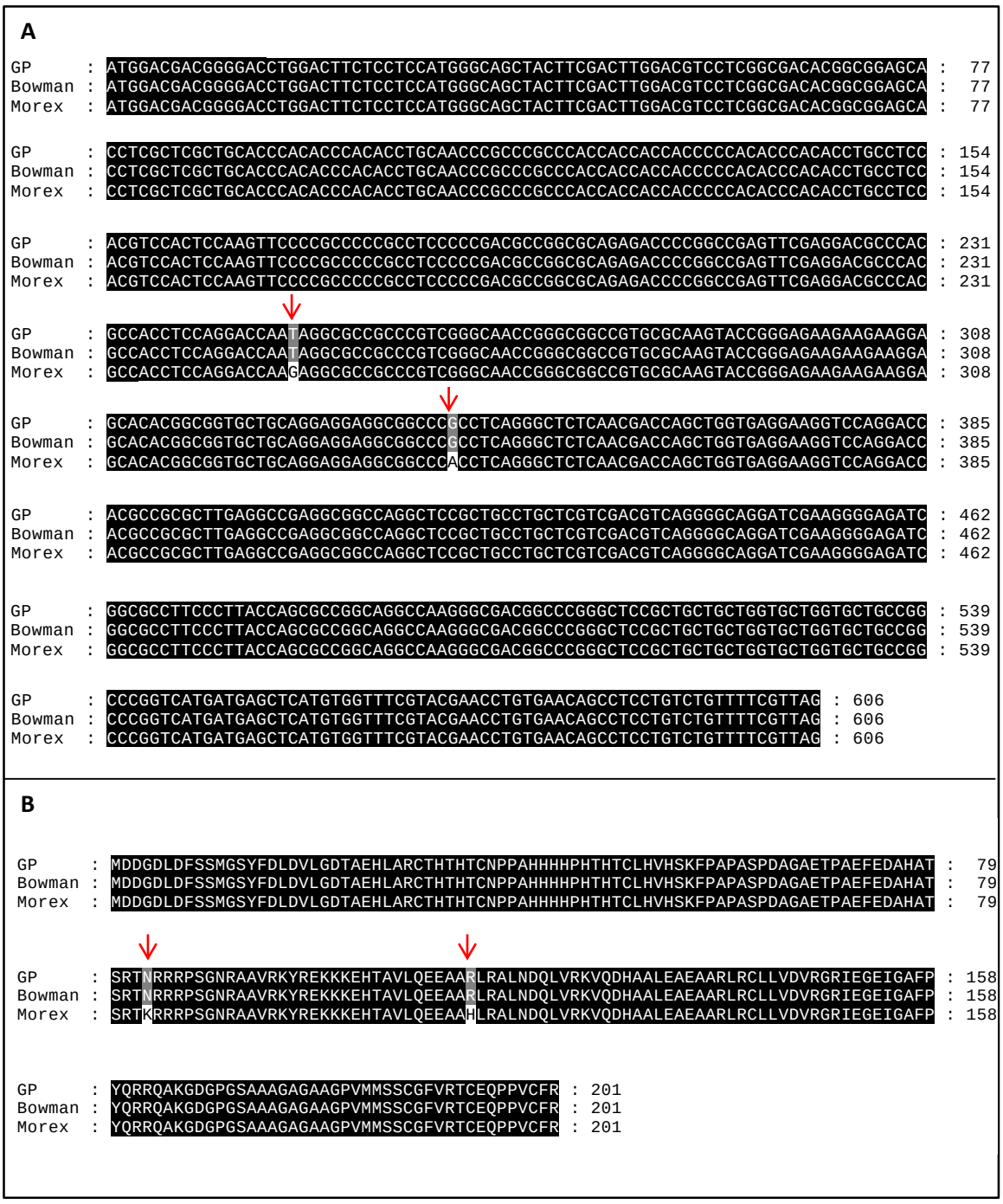

Figure 4.9 Multiple sequence alignment of HvZIP58 from different barley cultivars.

HvbZIP58 coding sequences (A) and amino acid sequences (B) from Golden Promise (GP), Bowman and Morex were aligned using the Clustal Omega algorithm (Sievers et al., 2011) and presented using GeneDoc (Nicholas and Nicholas Jr, 1997). For the sequences aligned here: black = conserved residues, grey = conserved in two of the sequences. The red arrow indicated the difference between sequences.

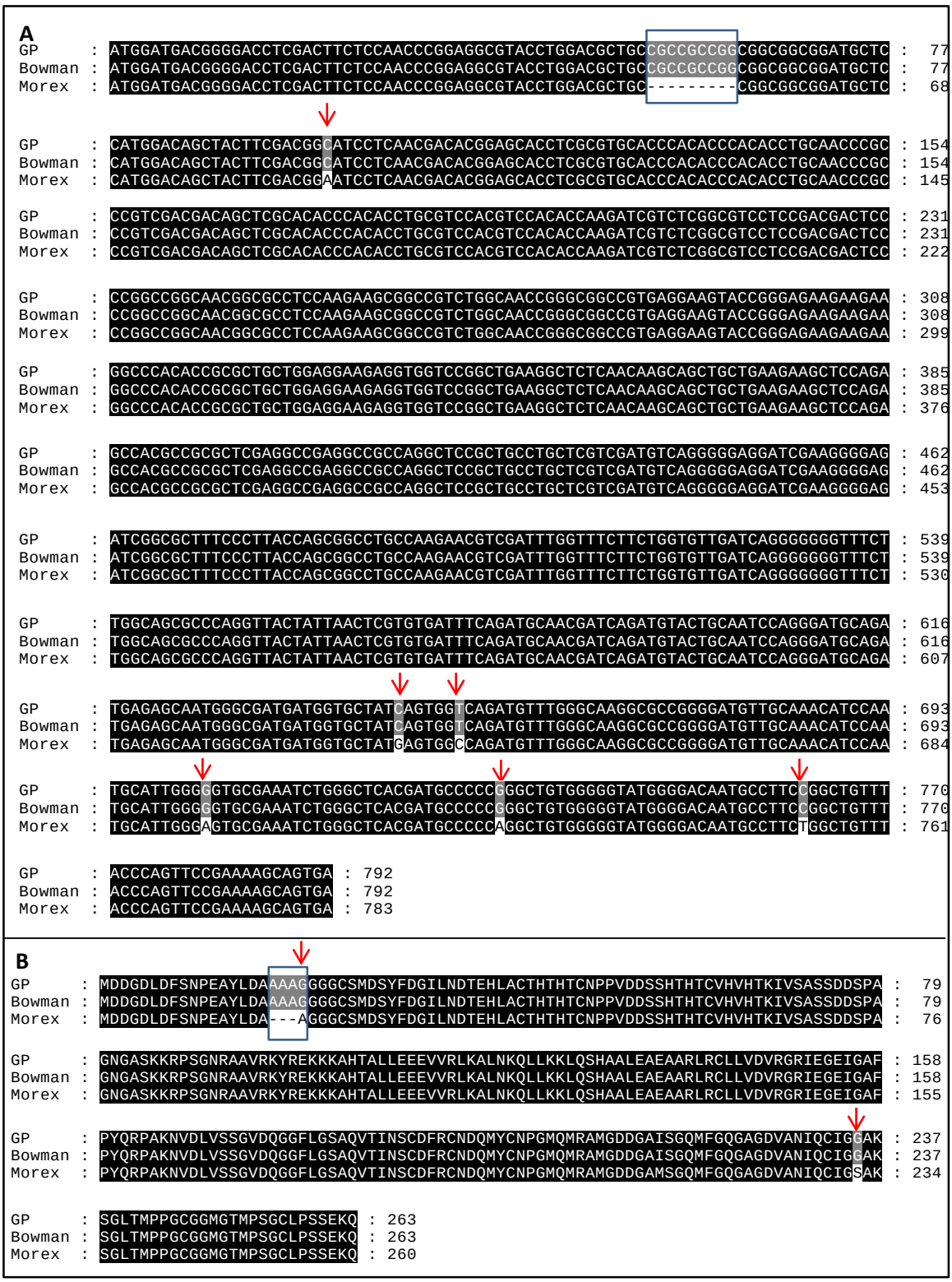

Figure 4.10 Multiple sequence alignment of HvbZIP62 from different barley cultivars.

HvbZIP62 coding sequences (A) and amino acid sequences (B) from Golden Promise (GP), Bowman and Morex were aligned using the Clustal Omega algorithm (Sievers et al., 2011) and presented using GeneDoc (Nicholas and Nicholas Jr, 1997). For the sequences aligned here: black = conserved residues, grey = conserved in two of the sequences. The red arrow indicated the difference between sequences and the blue box indicates the position of the additional sequence.

Table 4.4 The expression vectors generated for expressing *HvbZIP* genes in plants (*A. thaliana*) in this study

Plasmid	**Construct**
pMDC32 *HvbZIP1*	*P35S::HvbZIP1*
pMDC32 *HvbZIP1b*	*P35S::HvbZIP1b*
pEG100 *HvbZIP1b*	*P35S::HvbZIP1b*
pMDC32 *HvbZIP10*	*P35S::HvbZIP10*
pMDC32 *HvbZIP55*	*P35S::HvbZIP55*
pMDC32 *HvbZIP56*	*P35S::HvbZIP56*
pMDC32 *HvbZIP57*	*P35S::HvbZIP57*
pMDC32 *HvbZIP58*	*P35S::HvbZIP58*
pMDC32 *HvbZIP62*	*P35S::HvbZIP62*
pMDC83 *HvbZIP56*	*P35S::HvbZIP56::gfp*

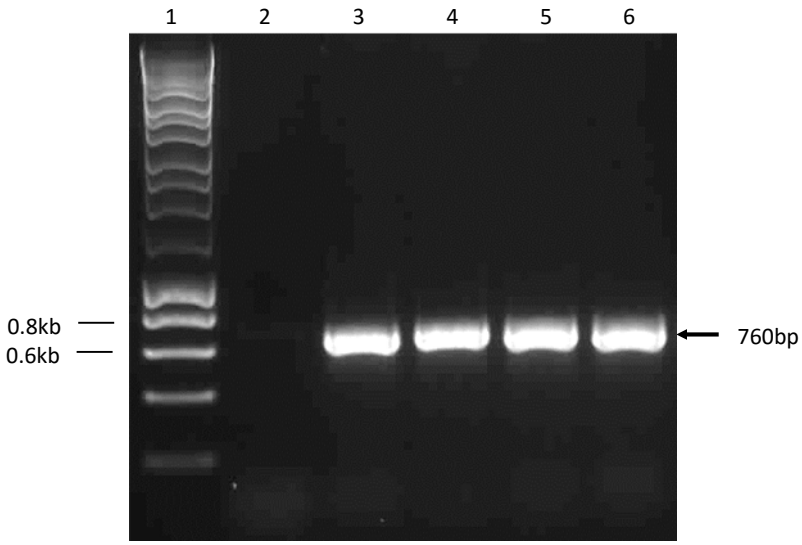

Figure 4.11 *A. tumefaciens* transformed with pMDC32 *HvbZIP56*.

Colony PCR and gel electrophoresis to show the successful transformation of *A. tumefaciens* GV3850 with the *A. thaliana* expression vectors pMDC32 *HvbZIP56*. Predicted product size is shown on the figure. Lane 1: molecular markers. Four out of five colonies of GV3850 pMDC32 *HvbZIP56* showing the predicted 760bp product (lane 2 to 6) using primers HvbZIP56topo_F and HvbZIP56topo_S (Table 2.7).

Table 4.5 The transgenic *A. thaliana* lines created for expressing *bZIP* genes. Each plasmid was transformed into WT and *bzip19-4 bzip23-2* plants.

The construct specifies the promoter the gene is expressed under and whether there are any fusions e.g. to a GFP reporter.

Plasmid	**Construct**	**Transformed into**	**# of T3 independent homozygous lines**
pMDC32 *HvbZIP1*	*P35S::HvbZIP1*	WT	3
pMDC32 *HvbZIP1*	*P35S::HvbZIP1*	*bzip19-4 bzip23-2*	4
pMDC32 *HvbZIP1b*	*P35S::HvbZIP1b*	WT	*
pMDC32 *HvbZIP1b*	*P35S::HvbZIP1b*	*bzip19-4 bzip23-2*	*
pEG100 *HvbZIP1b*	*P35S::HvbZIP1b*	WT	*
pEG100 *HvbZIP1b*	*P35S::HvbZIP1b*	*bzip19-4 bzip23-2*	*
pMDC32 *HvbZIP10*	*P35S::HvbZIP10*	WT	*
pMDC32 *HvbZIP10*	*P35S::HvbZIP10*	*bzip19-4 bzip23-2*	*
pMDC32 *HvbZIP55*	*P35S::HvbZIP55*	WT	*
pMDC32 *HvbZIP55*	*P35S::HvbZIP55*	*bzip19-4 bzip23-2*	*
pMDC32 *HvbZIP56*	*P35S::HvbZIP56*	WT	*
pMDC32 *HvbZIP56*	*P35S::HvbZIP56*	*bzip19-4 bzip23-2*	4
pMDC83 *HvbZIP56*	*P35S::HvbZIP56::gfp*	WT	*
pMDC83 *HvbZIP56*	*P35S::HvbZIP56::gfp*	*bzip19-4 bzip23-2*	4
pMDC32 *HvbZIP57*	*P35S::HvbZIP57*	WT	*
pMDC32 *HvbZIP57*	*P35S::HvbZIP57*	*bzip19-4 bzip23-2*	4
pMDC32 *HvbZIP58*	*P35S::HvbZIP58*	WT	*
pMDC32 *HvbZIP58*	*P35S::HvbZIP58*	*bzip19-4 bzip23-2*	*
pMDC32 *HvbZIP62*	*P35S::HvbZIP62*	WT	*
pMDC32 *HvbZIP62*	*P35S::HvbZIP62*	*bzip19-4 bzip23-2*	4

* indicates transgenic plants still undergoing isolation process.

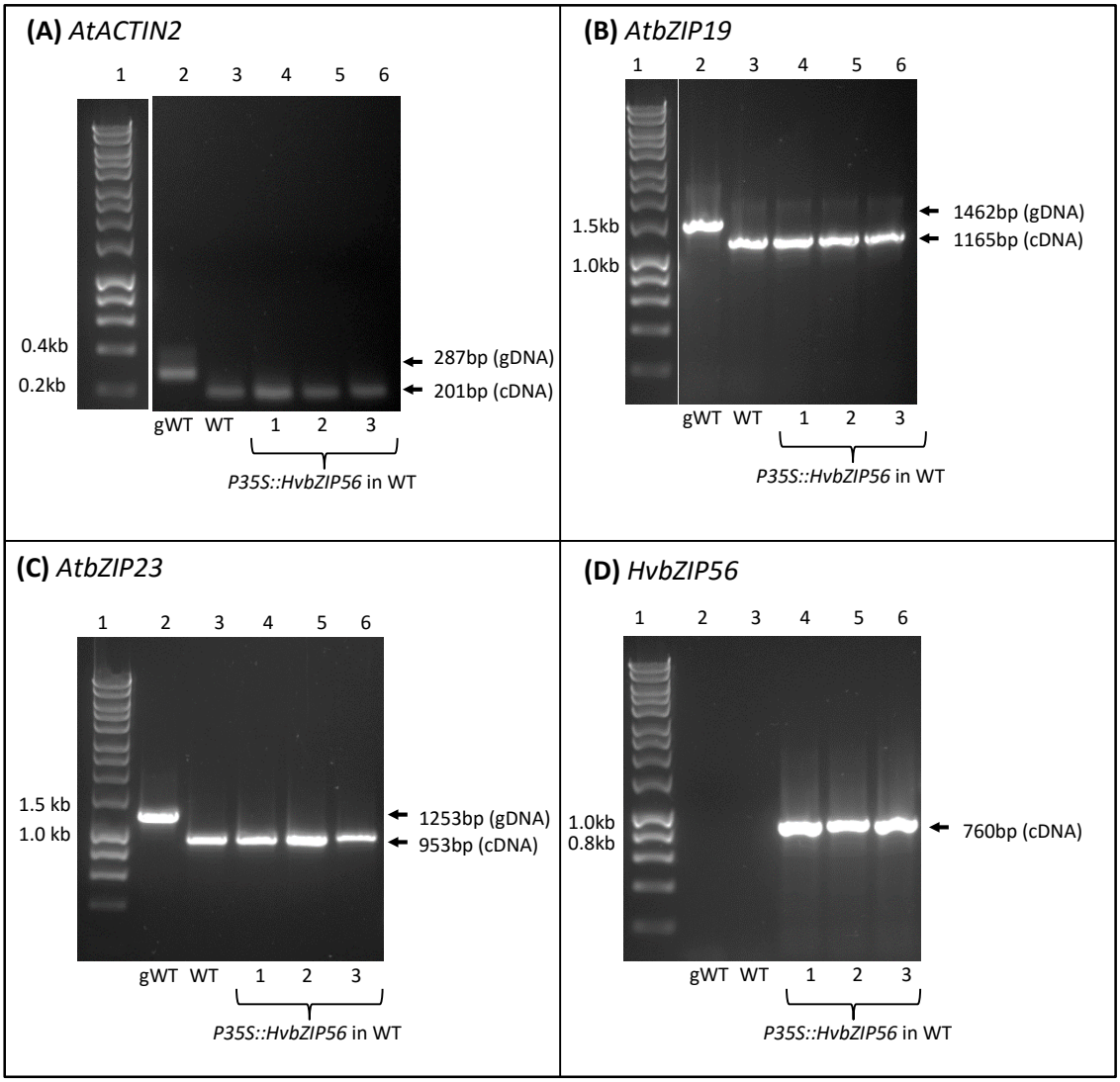

Figure 4.12 Expression of *HvbZIP56* in *A. thaliana* WT T_3 lines.

RT-PCR was carried out with appropriate primers for the genes indicated above the panels. The WT lines were transformed with pMDC32 *HvbZIP56*. Predicted product size is shown on figure. Lane 1: molecular markers, lane 2: Genomic DNA (gWT), lane 3 = cDNA (size from WT), lane 4-6 = cDNA form transformed lines. (A) Actin2 F and Actin2 R primers amplify a fragment of *AtACTIN2*. (B) *A. thaliana bZIP19* expression in using primers bZIP19F2 and bZIP19R2. (C) *A. thaliana bZIP23* expression using primers bZIP23F2 and bZIP23R2. (D) *HvbZIP56* expression using primers HvbZIP56topo_F and HvbZIP56topo_S. Primer sequences outlined in Table 2.7.

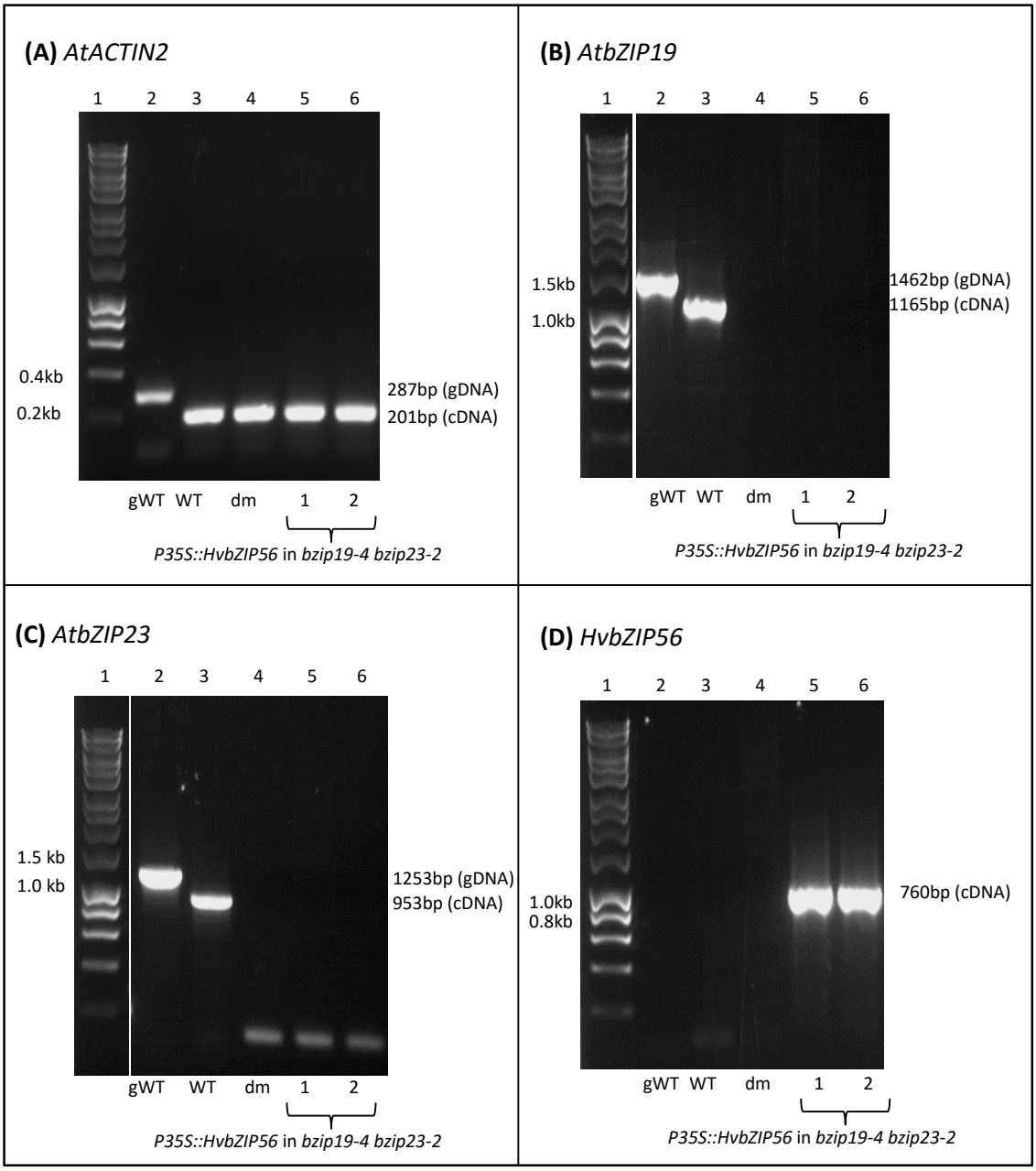

Figure 4.13 Expression of *HvbZIP56* in *A. thaliana bzip19-4 bzip23-2* T_3 lines.

RT-PCR was carried out with appropriate primers for the genes indicated above the panels. The *bzip19-4 bzip23-2* **d**ouble **m**utant (dm) lines were transformed with pMDC32 *HvbZIP56*. Predicted products shown on figure. Lane 1: molecular markers, lane 2: Genomic DNA (gWT), lane 3 = cDNA (size from WT), lane 4 = *bzip19-4 bzip23-2,* and lane 5-6 = cDNA from transformed lines. (A) Actin2 F and Actin2 R primers amplify a fragment of *AtACTIN2*. (B) *A. thaliana bZIP19* expression in using primers bZIP19F2 and bZIP19R2. (C) *A. thaliana bZIP23* expression using primers bZIP23F2 and bZIP23R2. (D) *HvbZIP56* expression using primers HvbZIP56topo_F and HvbZIP56topo_S. Primer sequences outlined in Table 2.7.

that had been transformed with pMDC32 *HvbZIP56* are shown as examples. The expression of HvbZIP62 in *bzip19-4 bzip23-2* mutant plants is also shown in Figure 4.14. All tested plants expressed *AtACTIN2* (ACTIN 2 = At3G18780) as indicated by the amplification of the predicted 201bp products (Figure 4.12A, Figure 4.13A and Figure 4.14A).These samples were free from genomic DNA contamination as indicated by the absence of the predicted product size of 287bp for genomic *AtACTIN2* (lane 2). All transformed and untransformed WT expressed full-length *AtbZIP19* and *AtbZIP23* as shown by the amplification of 1165bp predicted and 953bp product (Figure 4.12B and C). Meanwhile, two independent *bzip19-4 bzip23-2* transformed with pMDC32 *HvbZIP56* and pMDC32 *HvbZIP62* do not express *AtbZIP19* and *AtbZIP23* (Figure 4.13/Figure 4.14B and C respectively). The three independent WT and the two *bzip19-2 bzip23-2* lines transformed with pDMC32 *HvbZIP56* exhibit a full-length product, confirming the *HvbZIP56* expression, while the expression of *HvbZIP62* is confirmed at the RNA level in the two independent lines by the full-length product of 783bp. The expression of *HvbZIP1*, *HvbZIP57,* and *HvbZIP56:GFP* at the RNA level in *bzip19-4 bzip23-2* mutant plants were confirmed using the same method (results not shown). The product amplified with HvbZIP56topo_F and HvbZIP56topo_S seems to vary slightly in different amplifications (from the initial amplification through to expression in transgenic lines). The reason for this is not certain but the sequencing in the final clones indicated the correct product had been cloned.

4.2.4 Barley bZIP56, bZIP62, bZIP57 but not bZIP1 rescues the Zn-deficiency phenotype of *A. thaliana bzip19-4 bzip23-2*

The clear Zn-deficiency phenotype in *A. thaliana bzip19-4 bzip23-2* double mutants (Chapter 3) is a useful tool for investigating the function of barley F-group bZIPs. By using a functional complementation approach, a potential role of the barley F-group bZIPs in the Zn-deficiency response mechanism could be tested. To determine whether there is conservation of function between *A. thaliana* and barley bZIPs, HvbZIP56, HvbZIP62, HvbZIP57 and HvbZIP1 were tested to see whether they could complement the Zn-deficiency response of the *bzip19-4 bzip23-2* double mutant. At least four independent lines with the barley bZIPs expressed under the 35S promoter were isolated and they were shown to express the transgene (see Section 4.2.3). The *bzip19-4 bzip23-2* independent lines (T_3 generation) expressing respective barley *bZIPs* were grown alongside the WT and the *bzip19-4 bzip23-2* double mutants to provide a direct comparison on Zn-deficient media. Figure 4.15A shows photographs of seedlings grown under this condition and Figure 4.15B provides data on the fresh weight of whole plants, shoots, and roots.

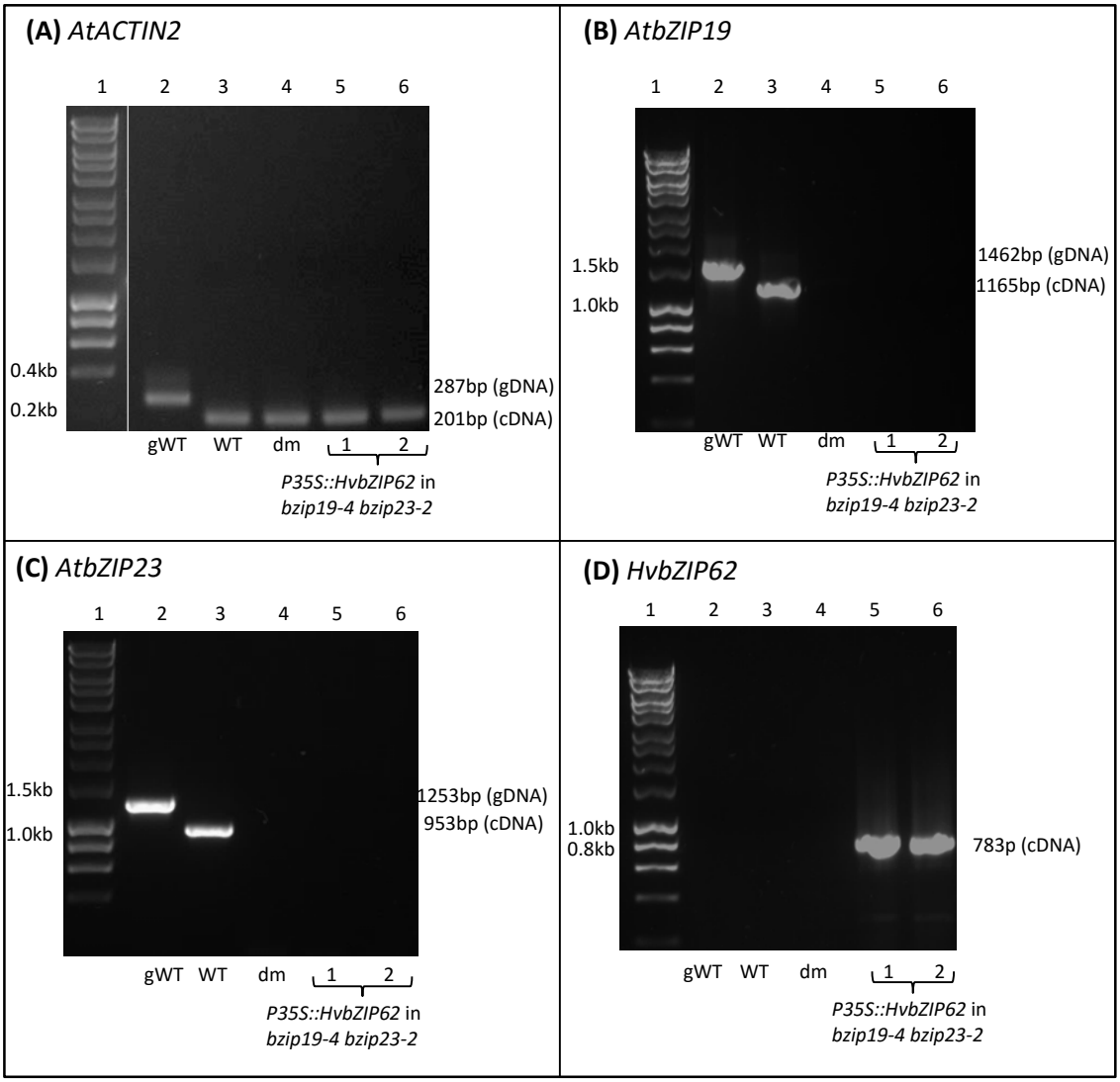

Figure 4.14 Expression of *HvbZIP62* in *A. thaliana bzip19-4 bzip23-2* T_3 lines.

RT-PCR was carried out with appropriate primers for the genes indicated above the panels. The *bzip19-4 bzip23-2* **d**ouble **m**utant (dm) lines were transformed with pMDC32 *HvbZIP62*. Predicted products shown on figure. Lane 1: molecular markers, lane 2: Genomic DNA (gWT), lane 3 = cDNA (size from WT), lane 4 = *bzip19-4 bzip23-2*, and lane 5-6 = cDNA from transformed lines. (A) Actin2 F and Actin2 R primers amplify a fragment of *AtACTIN2*. (B) *A. thaliana bZIP19* expression in using primers bZIP19F2 and bZIP19R2. (C) *A. thaliana bZIP23* expression using primers bZIP23F2 and bZIP23R2. (D) *HvbZIP62* expression using primers HvbZIP62topo_F and HvbZIP62topo_S. Primer sequences outlined in Table 2.7.

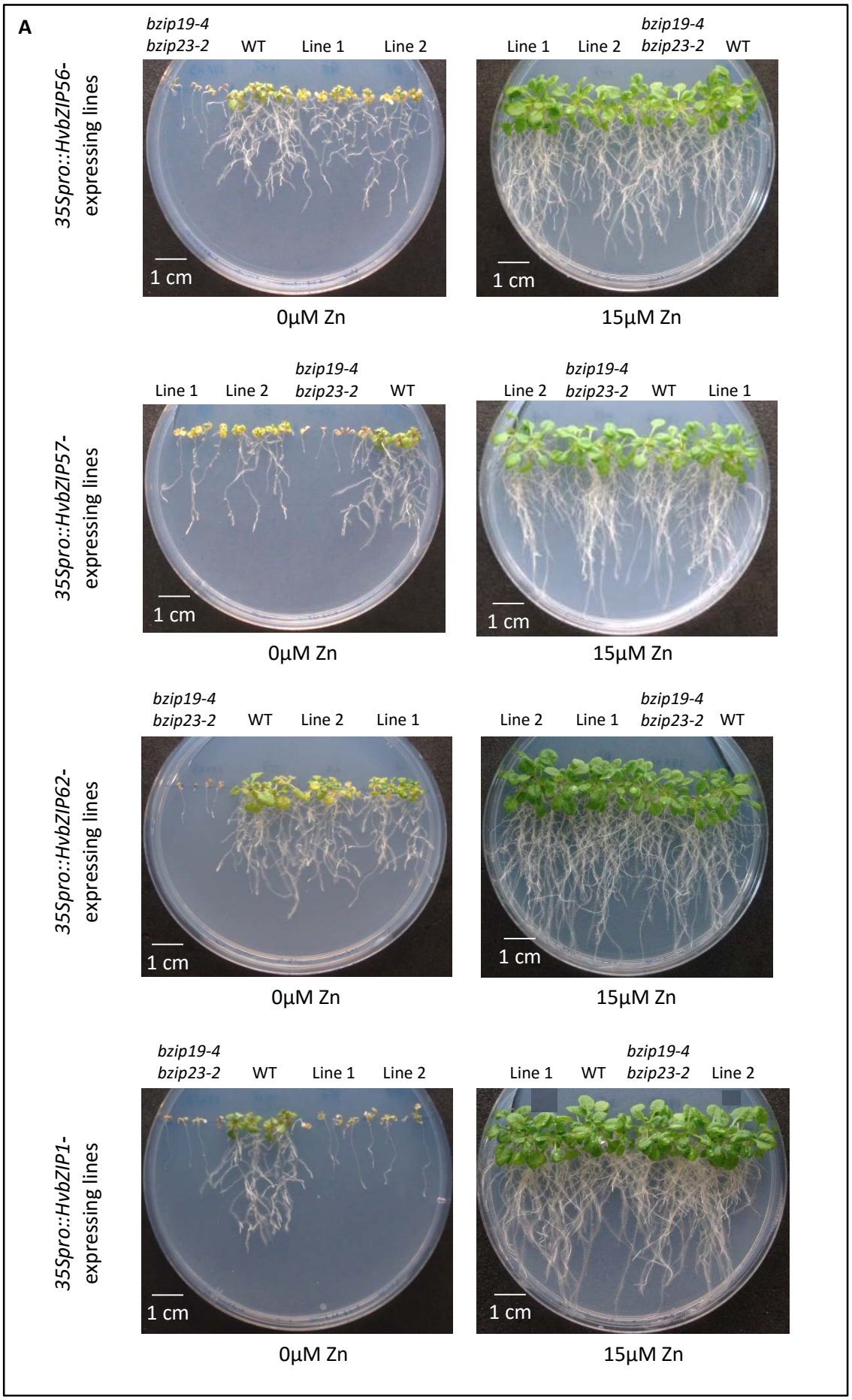
A
35Spro::HvbZIP56-expressing lines
bzip19-4 bzip23-2
WT
Line 1
Line 2
1 cm
0µM Zn
15µM Zn
35Spro::HvbZIP57-expressing lines
35Spro::HvbZIP62-expressing lines
35Spro::HvbZIP1-expressing lines

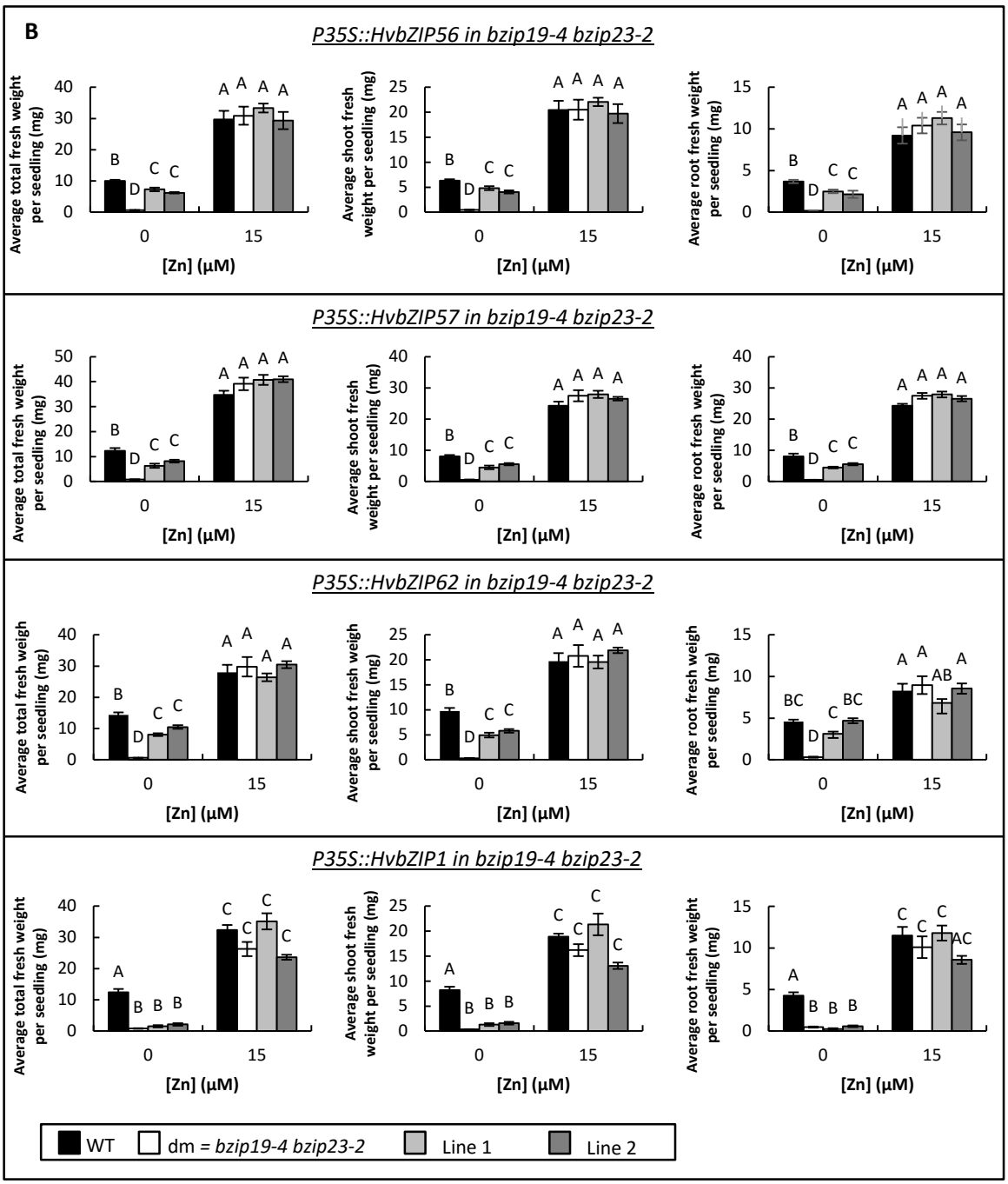

Figure 4.15 Expression of *HvbZIP56*, *HvbZIP57*, *HvbZIP62* but not *HvbZIP1* partially rescue Zn-deficiency phenotype of *A. thaliana bzip19-4 bzip23-2* double mutants.

(A) Representative images of WT and *bzip19-4 bzip23-2* mutants grown together with two independent *bzip19-4 bzip23-2* mutants expressing barley *bZIP*s for 21 days on 0.5 MS media with 0µM Zn. (B) Data shows the average total fresh weight, shoot fresh weight, and root fresh weight of four different barley *bZIPs* expressed in *bzip19-4 bzip23-2* double mutants: *HvbZIP56*, *HvbZIP57*, *HvbZIP62*, *HvbZIP1*. The data was based the means from six plates for each condition (+/- SEM) with four seedlings per line, per plate, each plate containing four plant lines. Means not sharing a letter are significantly different (p≤0.05); Tukey post-hoc test.

When grown under Zn-deficiency conditions (0Zn), HvbZIP56, HvbZIP62, and HvbZIP57 but not HvbZIP1 could partially restore the growth of the *A. thaliana bzip19-4 bzip23-2* double mutant, almost to WT levels (Figure 4.15). Although performance was markedly improved, they did not restore it completely. A comparison was made between *HvbZIP56*–expressing plants and the *bzip19-4* single mutant and growth was restored to this level (Figure 4.16).There was no significant difference at standard Zn (15µM) in the lines. The same partial rescue was also obtain when GFP-tagged *HvbZIP56* was expressed in *bzip19-4 bzip23-2* indicating that the GFP tag had no detrimental effect (Figure 4.17) and the plants would be useful for localisation studies (see later). Higher concentrations of Zn were tested to see if there was any effect of expressing *HvbZIP56*. The growth level of double mutants expressing *HvbZIP56* was similar at these higher concentrations to the double mutant, and all were similar to WT (Figure 4.18). Additionally, *HvbZIP56*-expressing WT *A. thaliana* lines were generated, but no increase in resistance to Zn deficiency was found, nor any effect at elevated Zn compared to WT controls (Figure 4.19).

4.2.5 Identifying HvbZIP1b

Since HvbZIP1 did not restore the Zn-hypersensitivity phenotype of the *bzip19-4 bzip23-2* double mutants, this was investigated further. Further sequence information had been released by this time and re-analysed. It was seen that there was another potential start site upstream. This added a potential extra 189bp or 63 amino acids (Figure 4.20) to the sequence.

RT-PCR was used with primers to the new start site and the end to determine whether HvbZIP1b was expressed. Figure 4.21A shows that this sequence could be amplified, demonstrating there is a transcript present in Golden Promise. This was cloned into pMDC32 and pEG100 (Figure 4.21B and C respectively) and *bZIP19-4 bzip23-2* double mutants. The reason for cloning into pEG100 was to allow *HvbZIP1b* to be expressed together with *HvbZIP56* in the *bzip19-4 bzip23-2* double mutants. pEG100 has a different selection allowing *HvbZIP1b*-expressing plants to be selected. bZIPs have been shown to be expressed as homodimers and heterodimers. It was of interest to test whether expression of *HvbZIP56* together with *HvbZIP1b* could fully complement the *bzip19-4 bzip23-2* double mutant fully. T_3 seed have recently been obtained for these but the analysis has not yet been carried out. At this point with further sequence information available, there have been no indications that any of the other F-group bZIPs contain additional regions.

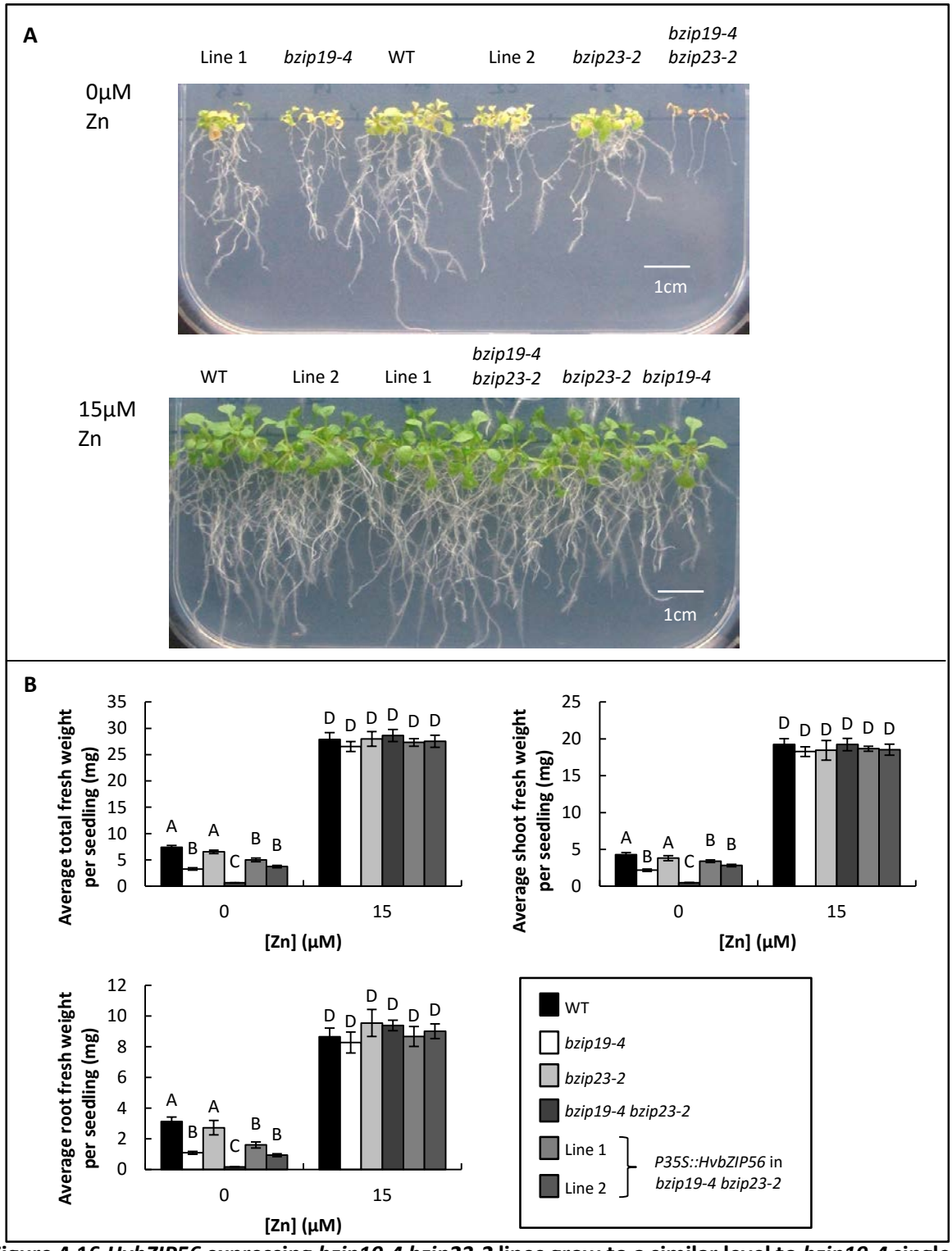

Figure 4.16 *HvbZIP56* expressing *bzip19-4 bzip23-2* lines grow to a similar level to *bzip19-4* single mutant under Zn deficiency.

WT, *bzip19-4, bzip23-2, bzip19-4 bzip23-2* mutants and transgenic lines grown on 0.5 MS media for 21 days with 0µMZn or 15µMZn. (A) Images of representative plates; (B) total, shoot and root fresh weight are shown for each construct. The means (+/- SEM) were based on six plates, with four seedlings per line, per plate, each plate containing four plant lines. Means not sharing a letter are significantly different ($p \leq 0.05$); Tukey post-hoc test.

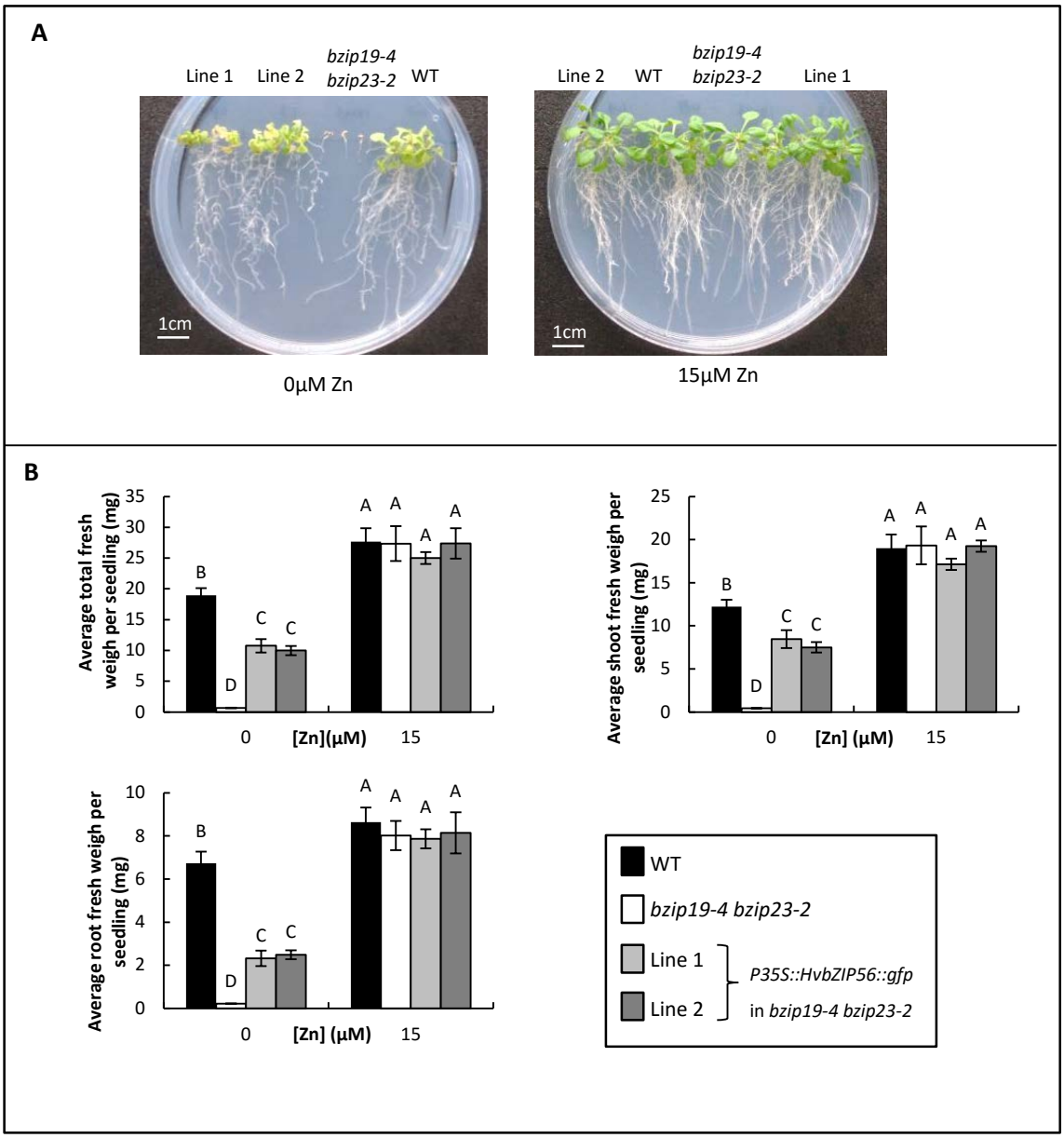

Figure 4.17 Expression of *HvbZIP56-GFP* partially rescue Zn-deficiency phenotype of *A. thaliana bzip19-4 bzip23-2* double mutants.

(A) Representative images of WT and *bzip19-4 bzip23-2* mutants grown together with two independent *bzip19-4 bzip23-2* mutants expressing barley *HvbZIP56-GFP* for 21 days on 0.5 MS media with 0µM Zn. (B) Data shows the average total fresh weight, shoot fresh weight, and root fresh weight of barley *HvbZIP56-GFP* expressed in *bzip19-4 bzip23-2* double mutants. The data was based the means from six plates for each condition (+/- SEM) with four seedlings per line, per plate, each plate containing four plant lines. Means not sharing a letter are significantly different ($p \leq 0.05$); Tukey post-hoc test.

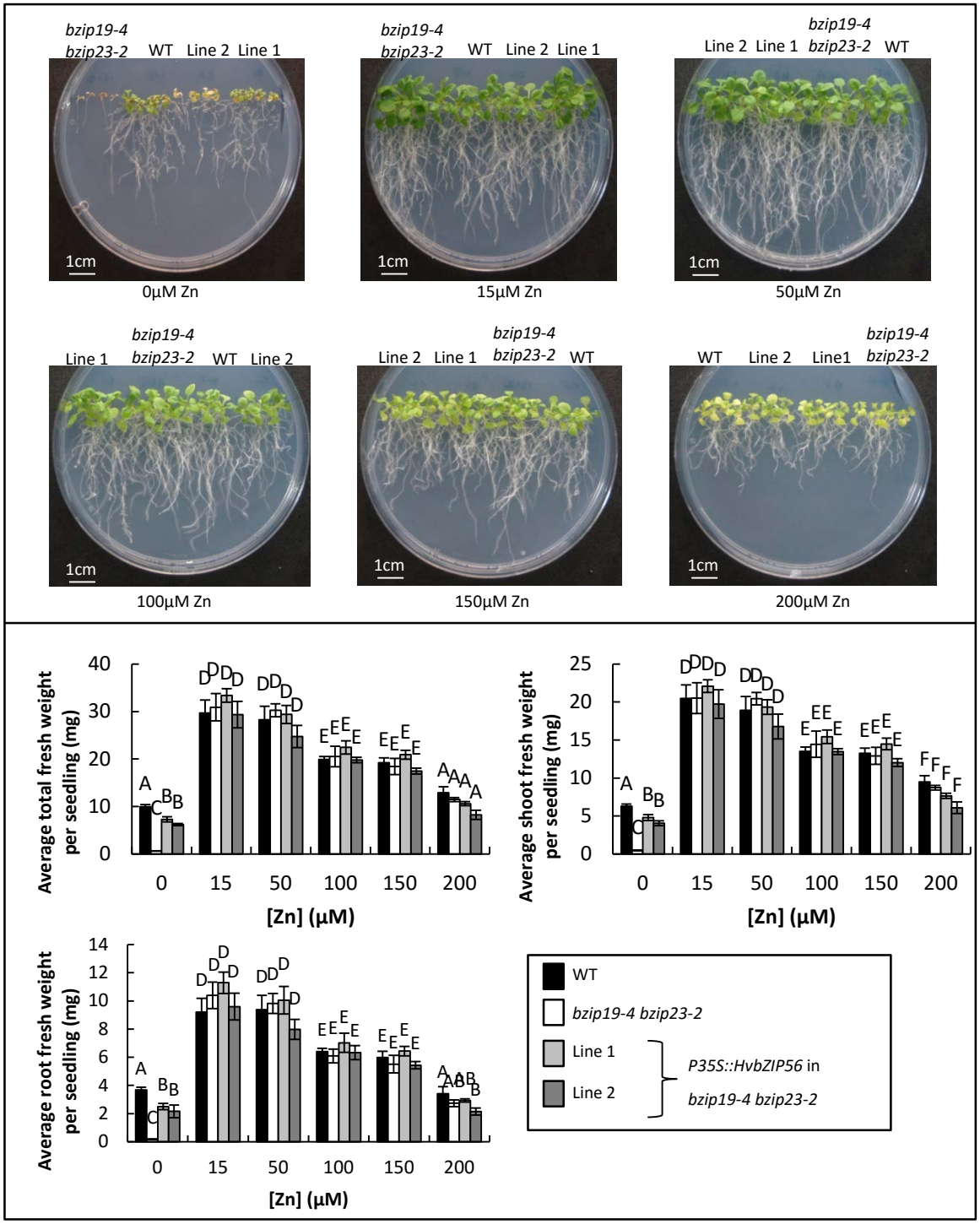

Figure 4.18 HvbZIP56 has little influence on the *A. thaliana bzip19-4 bzip23-2* mutant at elevated Zn.

WT, *bzip19-4 bzip23*-2 mutants and transgenic double mutant lines expressing *HvbZIP56* were grown on 0.5 MS media for 21 days with a range of Zn concentrations. Total, shoot and root fresh weight are shown. The data are based on means from six plates (+/- SEM) with four seedlings per line, per plate, each plate containing four plant lines. Means not sharing a letter are significantly different ($p \leq 0.05$); Tukey post-hoc test.

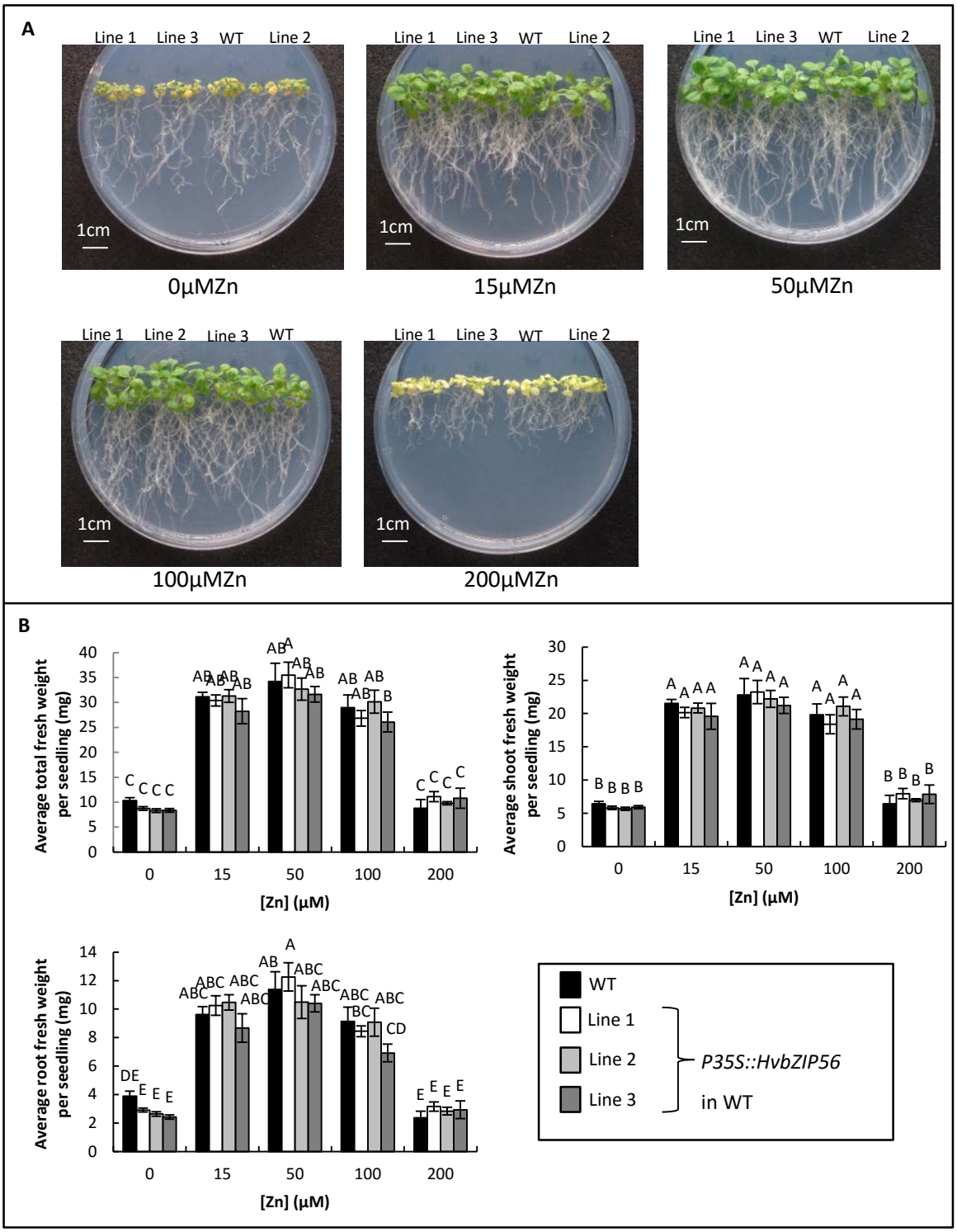

Figure 4.19 *HvbZIP56* expression in WT *A. thaliana* does not influence their response to Zn deficiency or Zn excess.

(A) Images of representative plates containing WT and *35Spro::HvbZIP56*-expressing lines grown on 0.5 MS media under a range of Zn concentrations. (B)Total, shoot and root fresh weight are shown; the means (+/- SEM) were based on six plates with four seedlings per line, per plate, each plate containing three plant lines. Means not sharing a letter are significantly different ($p \leq 0.05$); Tukey post-hoc test.

A

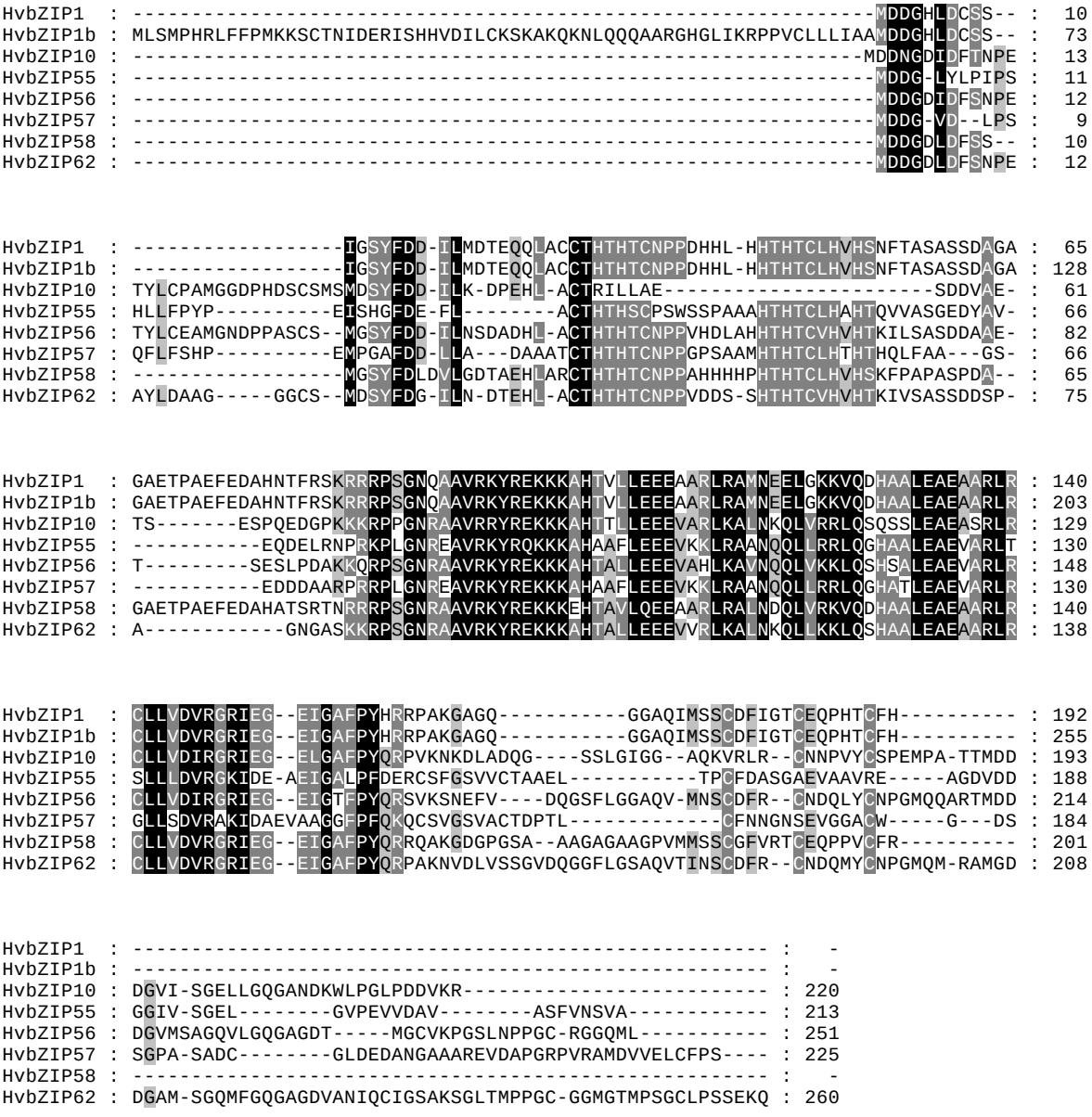

Figure 4.20 HvbZIP1b amino acid alignment with *A. thaliana* and barley F-group bZIPs.

(A) Alignment omitting *A. thaliana* F-group bZIPs; (B) Alignment including *A. thaliana* F-group bZIPs. Sequences were aligned using the Clustal Omega algorithm (Sievers et al., 2011) and presented using GeneDoc (Nicholas and Nicholas Jr, 1997). For the sequences aligned here: black = conserved residues, dark grey = conserved in at least seven of the sequences, and light grey = conserved in at least five of the sequences.

B

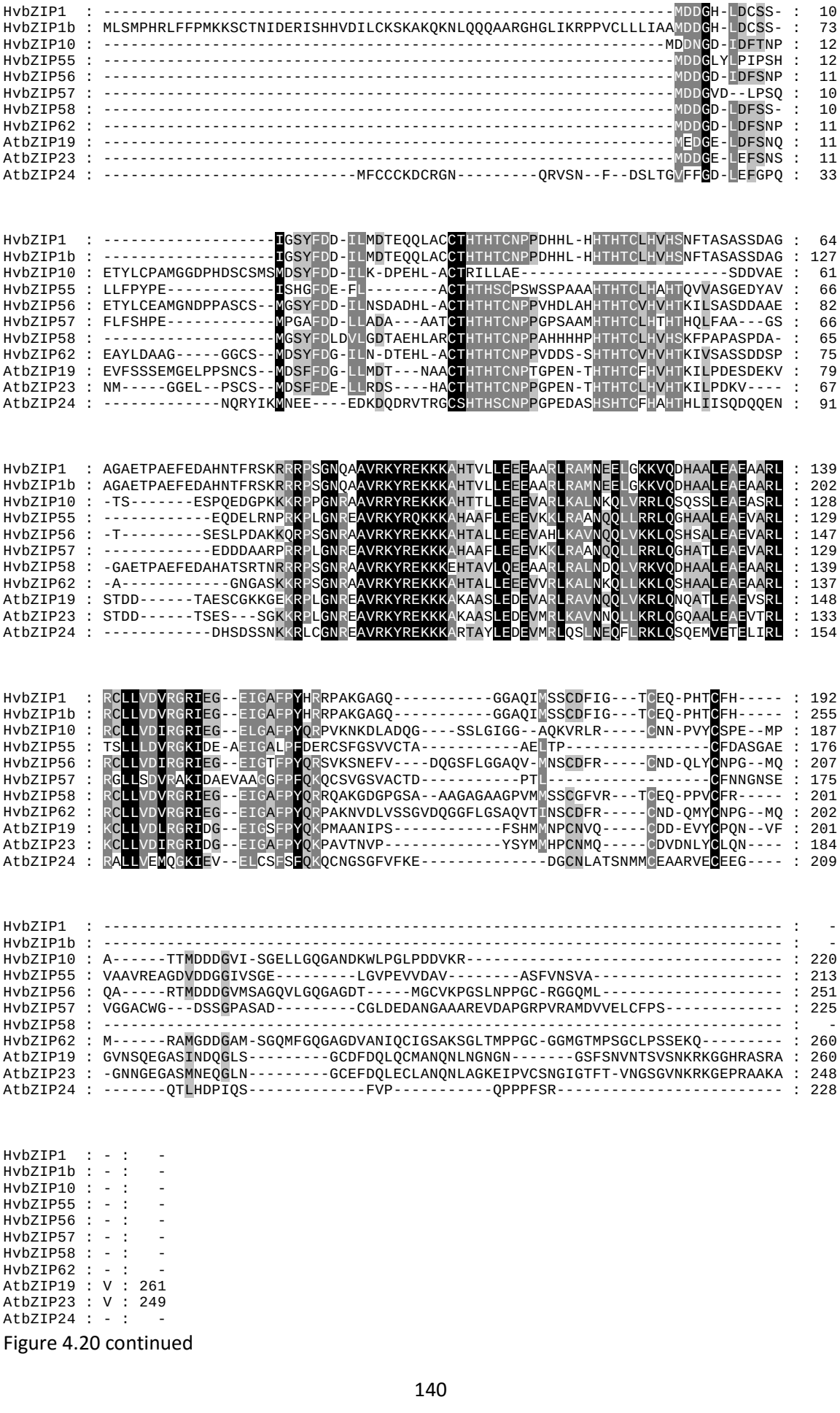

Figure 4.20 continued

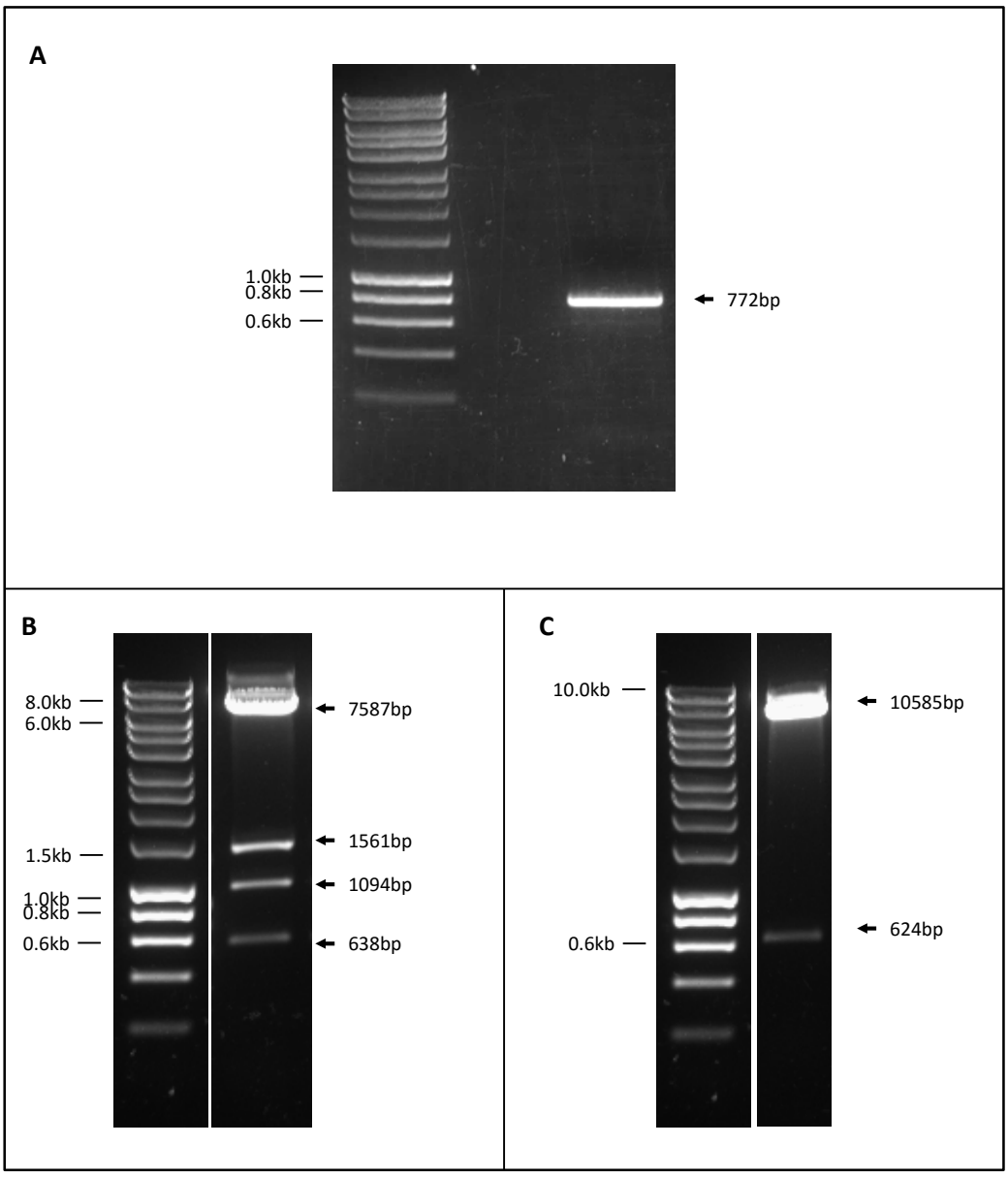

Figure 4.21 Cloning of *HvbZIP1b* into *A. thaliana* expression vectors.

(A) Full-length coding sequence of *HvbZIP1b* was amplified with HvbZIP1btopo_F and HvbZIP1btopo_S (Table 2.7) using Pfu polymerase to produce a blunt end PCR product. Both pMDC32 (B) and pEG100 (C) vectors were confirmed to carry *HvbZIP1b* using restriction enzymes *XhoI*. Predicted product sizes are indicated on right and predicted molecular marker sized indicated on left.

4.2.6 The expression of *HvbZIP56* rescues the *bzip19-4 bzip23-2* double mutant on high Cu and Fe at 1µM Zn supply

In Chapter 3, it was shown that on standard 0.5 MS, the micronutrients Cu, Fe, and Mn had no marked influence on the response of the *bzip19-4 bzip23-2* double mutants. As part of another study (Griffin and Williams, unpublished), it was seen that in hydroponic culture, elevated Cu did have a detrimental effect. In this hydroponics, the ratio of Zn to Cu was markedly different as Zn concentrations are much lower in that media. Therefore, in this mutant study, the Zn concentration was reduced to 1µM (a concentration that rescues the *bzip19-4 bzip23-2* double mutants [see Figure 3.12 in Chapter 3]) and the influence of Cu, Fe, and Mn were tested. Taking advantage of transgenic *bzip19-4 bzip23-2* double mutant lines expressing *HvbZIP56* that were generated here, the specificity of *HvbZIP56* was also tested by growing the lines together with *bzip19-4 bzip23-2* mutants on different Cu, Fe, and Mn concentrations on 0.5 MS media with 1µM Zn (Figure 4.22, Figure 4.23, and Figure 4.24 respectively). On this low Zn medium, the fresh weight of seedlings was significantly reduced starting at 10µM Cu (Figure 4.22) and at 100µM Fe (Figure 4.23) compared to WT, and the expression of *HvbZIP56* rescued the growth completely to the WT level. For Mn, the *bzip19-4 bzip23-2* double mutants and the transgenic lines had a similar response to the WT when grown under both Mn deficiency and toxicity (Figure 4.24), thus the response was specific to Cu and Fe only when supplied with 1µM Zn.

4.2.7 Localisation of HvbZIP56 in plant cells

Confocal microscopy was used to visualise the localisation of HvbZIP56 in *A. thaliana bzip19-4 bzip23-2* double mutants. As seen previously in Figure 4.16, the GFP-tagged construct behaved similarly to the non-tagged construct; HvbZIP56-GFP could partially rescue the Zn-deficiency phenotype of the *bzip19-4 bzip23-2* double mutants. Therefore, these plants were used to determine the cellular localisation of HvbZIP56. Figure 4.25 (cotyledons) and Figure 4.26 (roots) are representative images of the localisation results for HvbZIP56 from at least three independent seedlings (T_3 generation) grown on standard Zn (15µM) and 0µM Zn 0.5 MS media for seven days (Table 4.5). In these stable lines there was no marked difference in localisation when seedlings were grown with (as shown in Figure 4.25C and D, and Figure 4.26C and D) or without Zn (as shown in Figure 4.25A and B, and Figure 4.26A and B). In both cases, HvbZIP56-GFP was seen at the nucleus and cytoplasm of cotyledons (Figure 4.25) and roots of transgenic plants (Figure 4.26). Also, there was GFP emission seen in cytoplasmic strands supporting that HvbZIP56 was localised in cytoplasm (Figure 4.25C). A similar localisation was observed when *HvbZIP56-GFP* was transiently expressed in tobacco (*Nicotiana benthamiana*). As seen in Figure 4.27A, B, and C, HvbZIP56 was localised in the cytoplasm and nuclei. To determine that HvbZIP56 was not localised

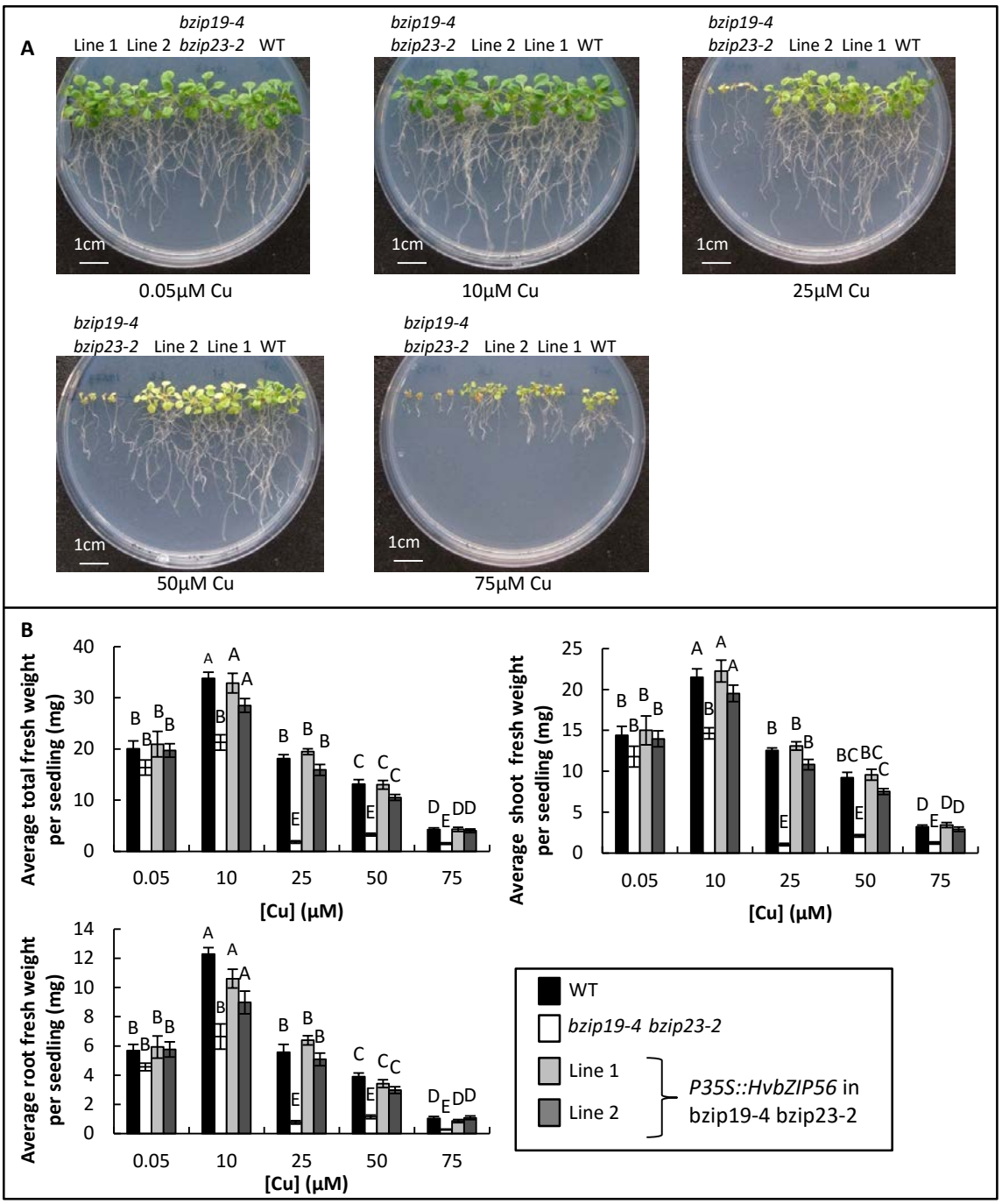

Figure 4.22 High Cu concentrations influence the response of *bzip19-4 bzip23-2* mutants when supplied with 1µM Zn and the expression of *HvbZIP56* in *bzip19-4 bzip23-2* mutants rescues the phenotype.

(A) WT, *bzip19-4 bzip23*-2 mutants and transgenic lines grown on 0.5 MS with 1µM Zn media for 21 days with a range of Cu concentrations. (B) Total, shoot and root fresh weight are shown. The data was based on means from six plates (+/- SEM) with four seedlings per line, per plate, each plate containing four plant lines. Means not sharing a letter are significantly different ($p \leq 0.05$); Tukey post-hoc test.

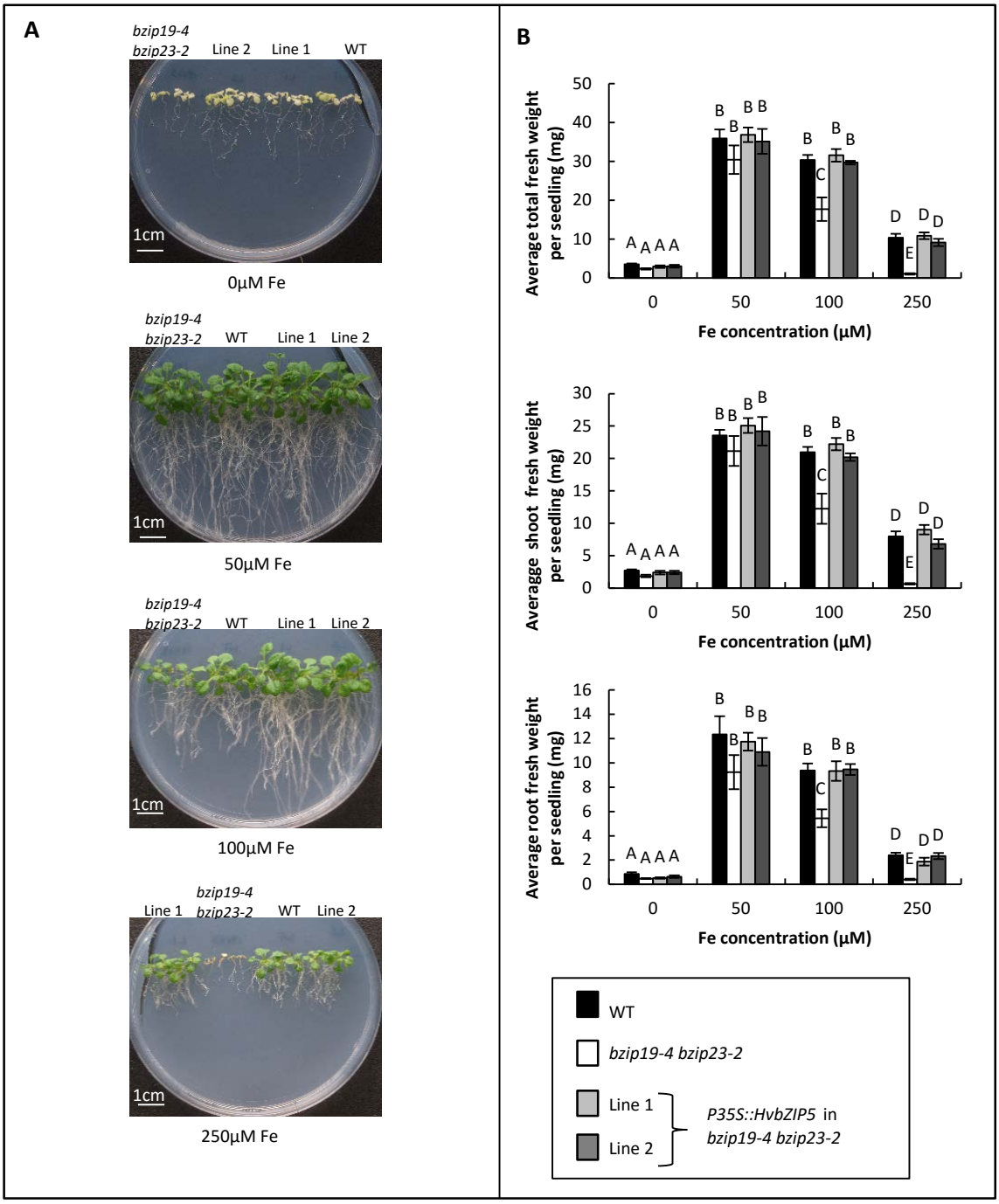

Figure 4.23 High Fe concentrations influence the response of *bzip19-4 bzip23-2* mutants when supplied with 1µM Zn and the expression of *HvbZIP56* in *bzip19-4 bzip23-2* mutants rescue the phenotype.

(A) Representative images of WT and *bzip19-4 bzip23-2* mutants grown together with two independent *P35S::HvbZIP56 in bzip19-4 bzip23-2* (line 1 and 2) on 0.5 MS media with 1µM Zn for 21 days with a range of Fe concentrations. (B) Total, shoot and root fresh weight are shown. The data was based on means from six plates (+/- SEM) with four seedlings per line, per plate, each plate containing four plant lines. Means not sharing a letter are significantly different (p≤0.05); Tukey post-hoc test.

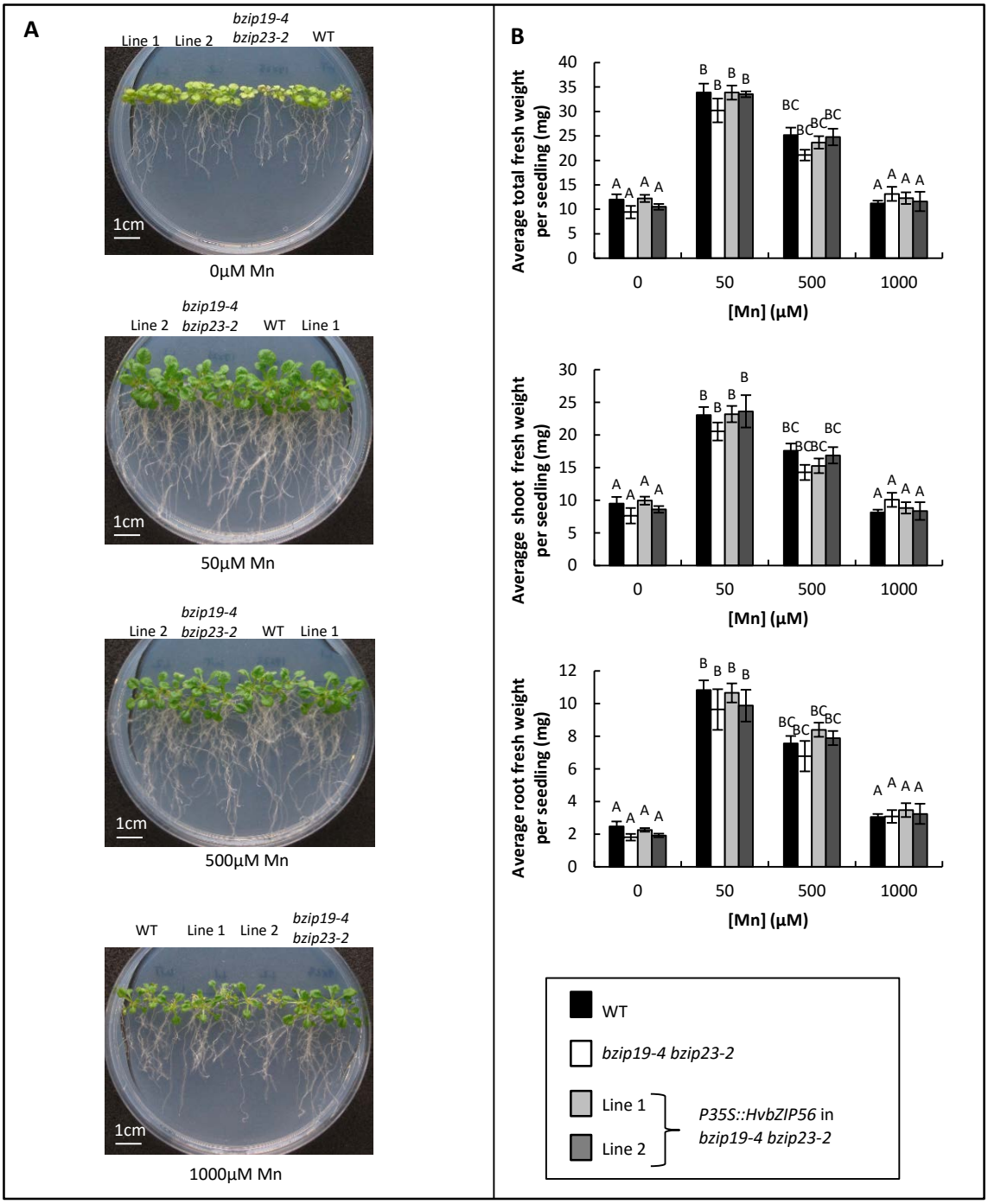

Figure 4.24 High Mn concentrations do not influence the response of *bzip19-4 bzip23-2* mutants when supplied with 1µM Zn and the expression of *HvbZIP56* in *bzip19-4 bzip23-2* mutants does not have any effect on the mutants.

(A) Representative images of WT and *bzip19-4 bzip23-2* mutants grown together with two independent *P35S::HvbZIP56 in bzip19-4 bzip23-2* (line 1 and 2) on 0.5 MS with 1µM Zn media for 21 days with a range of Mn concentrations. (B) Total, shoot and root fresh weight are shown. The data was based on means from six plates (+/- SEM) with four seedlings per line, per plate, each plate containing four plant lines. Means not sharing a letter are significantly different ($p \leq 0.05$); Tukey post-hoc test.

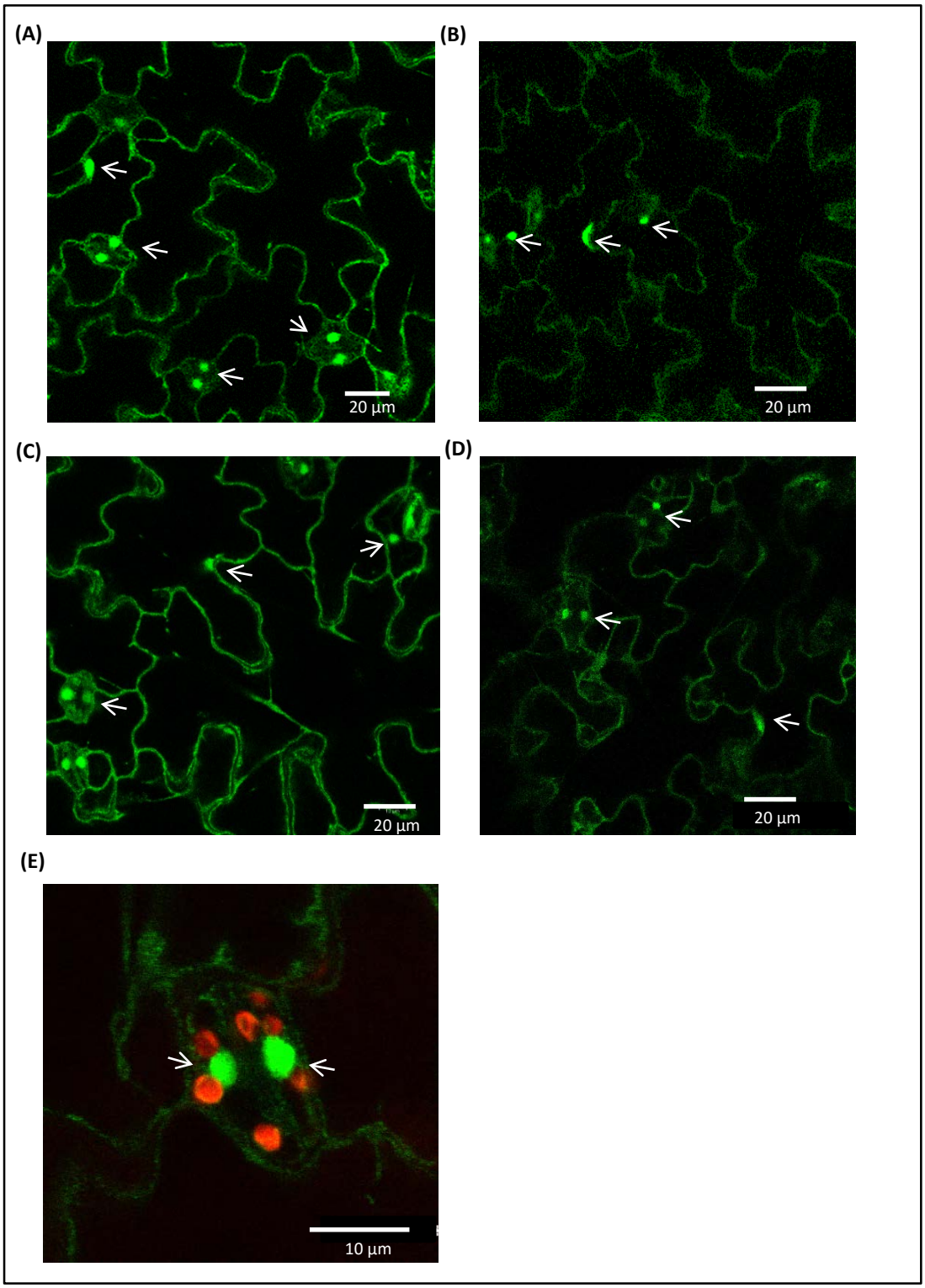

Figure 4.25 Subcellular localisation of bZIP56-GFP in cotyledons.

Confocal microscopy showing stable expression of *P35S::HvbZIP56::gfp* in the cotyledon of *A. thaliana bzip19-4 bzip23-2* mutant showing expression in cytoplasm and nuclei (white arrows). Image (A) and image (B) are from two independent seedlings grown under Zn-deficient treatment, while (image (C) and image (D) are from two independent seedlings grown under normal Zn conditions. At higher magnification the expression of *HvbZIP56* in the nucleus (green) of guard cells is seen with the chloroplast autofluorescence shown in red (E).

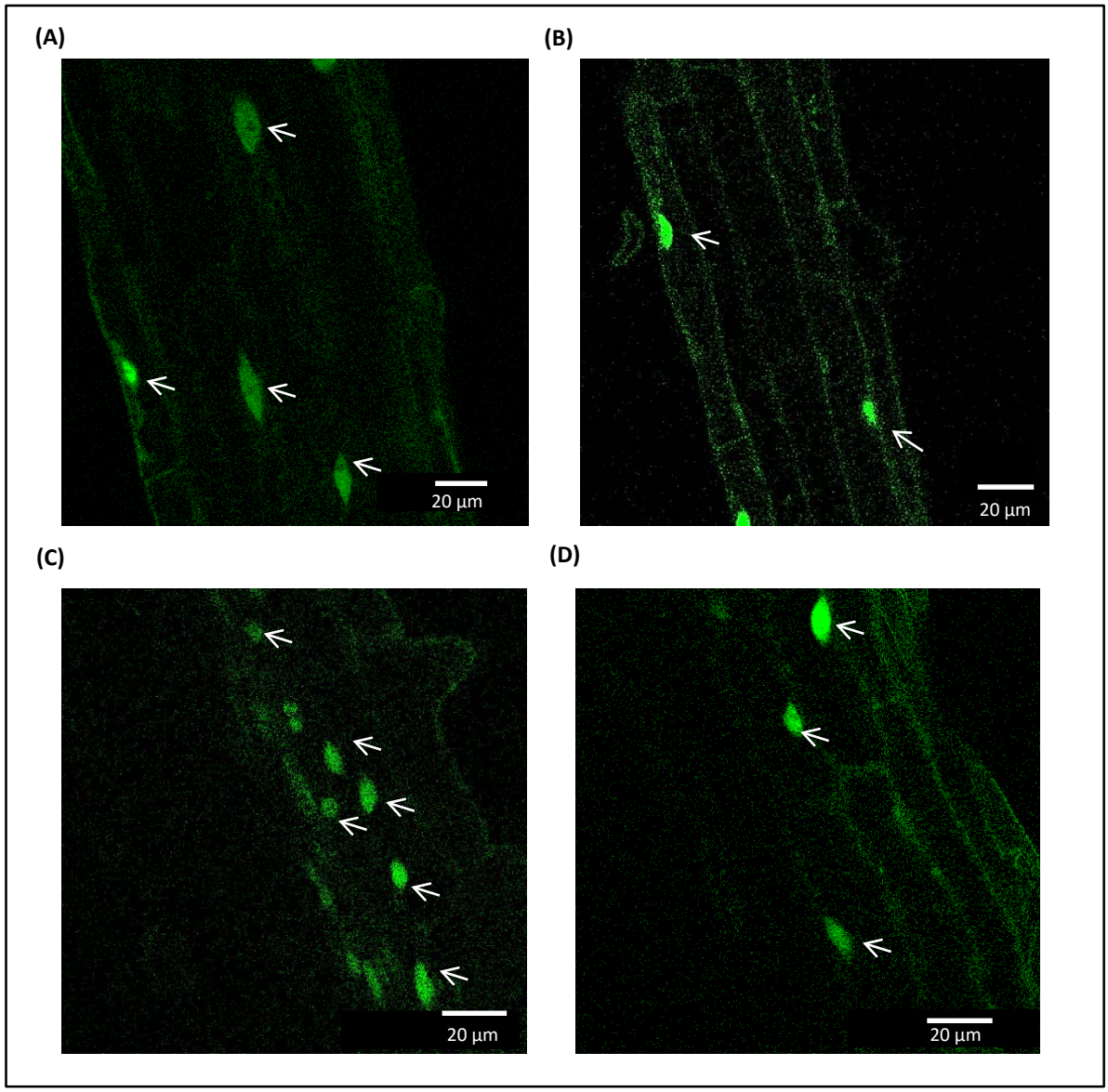

Figure 4.26 Subcellular localisation of bZIP56-GFP in roots.

Confocal microscopy showing stable expression of *P35S::HvbZIP56::gfp* in the root cells of *A. thaliana bzip19-4 bzip23-2* mutant showing expression in cytoplasm and nuclei (white arrows). The expression is seen in the nuclei and in the cytoplasm. Image (A) and image (B) are from two independent seedlings grown under Zn-deficient treatment, while image (C) and image (D) are from two independent seedlings grown under normal Zn conditions.

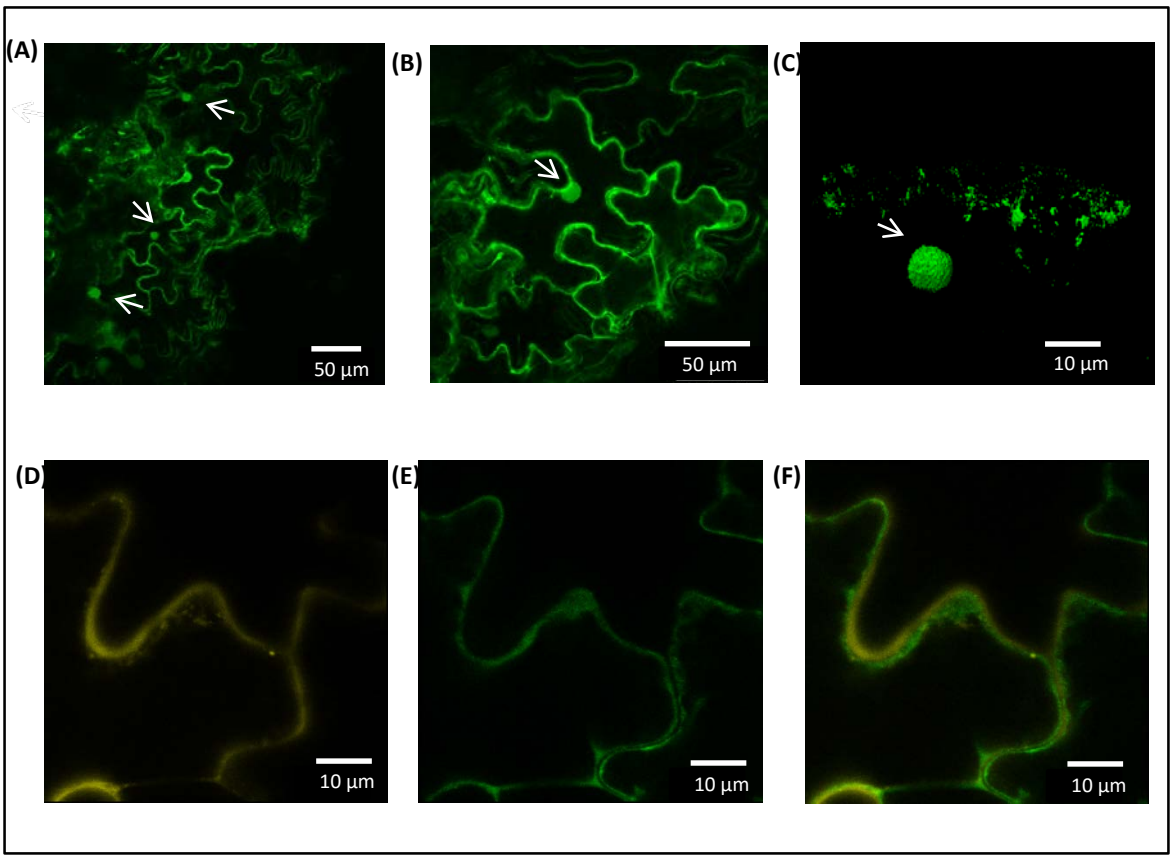

Figure 4.27 Localisation of HvbZIP56-GFP in tobacco.

Confocal images: Top panel: Transient expression of *P35S::HvbZIP56::gfp* in tobacco showing localisation in the cytoplasm and nucleus at increasing levels of magnification (A,B,C). Lower panel: localisation of 3*5Spro::HvbZIP56-GFP* (green) in cytoplasm (D) and *P35S::LTI6b-mOrange2* (orange) at the plasma membrane (E), the overlay showing LTI6b-mOrange2 is external to HvbZIP56-GFP (F).

in the plasma membrane, a transient expression in tobacco was carried out with LTI6b-mOrange2 (McGavin et al., 2012) in pB7FWG2, which is a marker for the plasma membrane. As shown in Figure 4.27 D, E, and F, the plasma membrane using could be distinguished LTI6b-mOrange2 and HvbZIP56 was localised adjacent to this.

4.2.8 Regulation of barley bZIPs

A key question is whether F-group bZIPs themselves are regulated by Zn deficiency. A number of deficient hydroponic culture media were tested to impose Zn deficiency and here the results using Lombnaes and Singh (2003) method is shown. Barley plants grown hydroponically were pre-treated with 8µM Zn for 7 days prior to the normal Zn treatment (8µM Zn) and Zn-deficient treatment (0µM Zn). Total fresh weight, shoot and root fresh weight were measured over time in addition to visual observation. Symptoms of Zn deficiency started to become apparent at seven days in terms of reduction in fresh weight of shoots (Figure 4.28). By fourteen days both shoot and root fresh weight were reduced and leaves showed chlorosis and withering at the tips.

Also, to establish that Zn deficiency was affecting gene expression of particular *ZIPs* as reported previously (Tiong et al., 2015), the response of *HvZIP5*, *HvZIP10*, *HvZIP13* and *HvZIP14* were measured using qRT-PCR. The qRT-PCR primers used in these reactions are listed in Table 2.7. Expression levels were quantified relative to the expression of the house-keeping gene, *HvRNABP* at day 0 of treatment. This gene is constitutively expressed by all cells and was invariably expressed over time and in response to Zn deficiency. This allowed for a comparison to assess how much the gene of interest differed in expression in comparison to the *HvRNABP* baseline, giving a fold increase or decrease. This calculated fold difference was used as the basis for comparing gene expression between conditions and over time. *HvZIP5*, *HvZIP10* and *HvZIP13* were generally markedly up-regulated under these conditions of Zn deficiency while *HvZIP14* was not up-regulated (Figure 4.29) and these results are consistent with those of Tiong et al. (2015) where a larger number of *ZIPs* were characterized.

Having established the correct conditions for generating Zn deficiency in barley, it was important to test whether barley F-group *bZIPs* were Zn-regulated. Initially, Assuncao et al. (2010) reported around two-fold up-regulation of *A. thaliana bZIP19* and *bZIP23* under Zn deficiency but later, they indicated that they were not significantly Zn-regulated (Assuncao et al., 2013). Of those investigated, *HvbZIP1* was the most markedly up-regulated by Zn deficiency showing a response both in roots and shoots (Figure 4.30). *HvbZIP58* was moderately up-regulated in roots and shoots whereas *HvbZIP57* was up-regulated by Zn deficiency only in roots. *HvbZIP56* and *HvbZIP62*

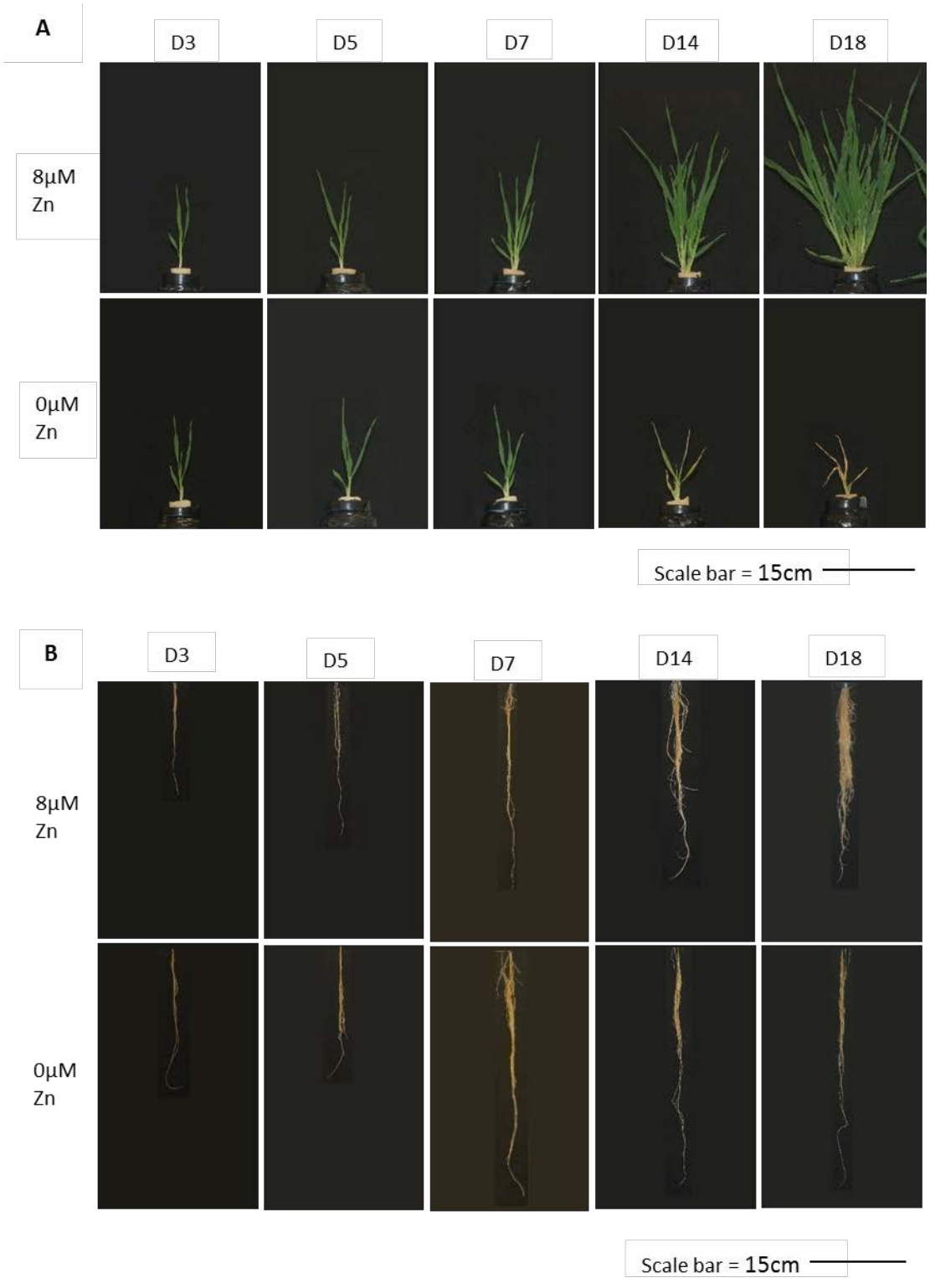

Figure 4.28 Barley displays deficiency symptoms when grown under Zn-deficient conditions.

Barley was grown on normal Zn (8µM Zn) for 7 days before they were treated with either 8µM Zn (+Zn) and 0µM Zn (-Zn) for 0, 7 and 14 days. Photographs of shoots (A) and roots (B) and mean fresh weight measurements per plant (+/- SEM) for total fresh weight, shoot weight and root weight (C). #, $p \leq 0.05$ = significantly different to the mean of Zn-treated plants (+/- SEM). *, $p \leq 0.05$ = significantly different to the mean of Day 0 plants (+/- SEM); Tukey post-hoc test

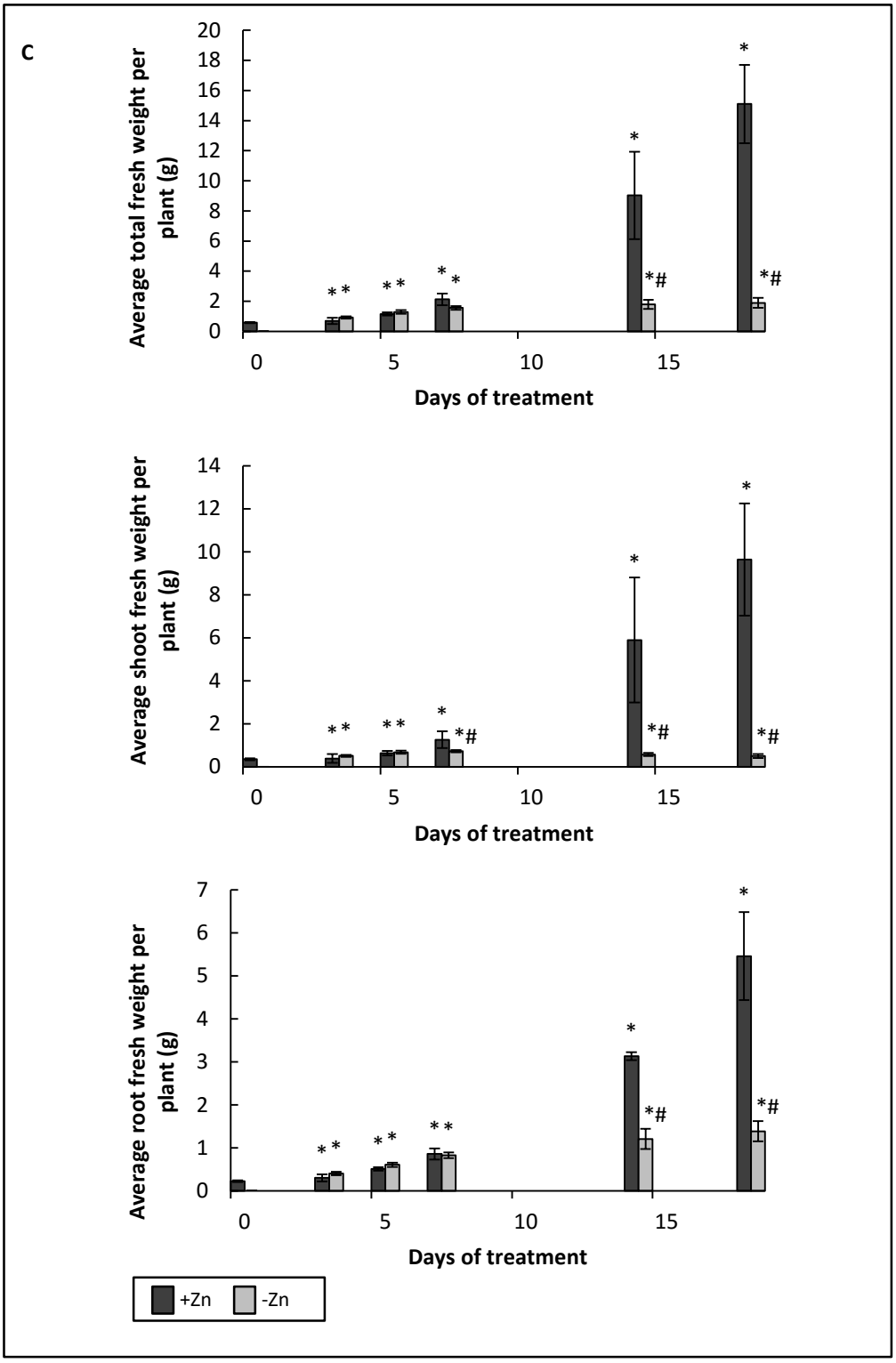

Figure 4.28 continued

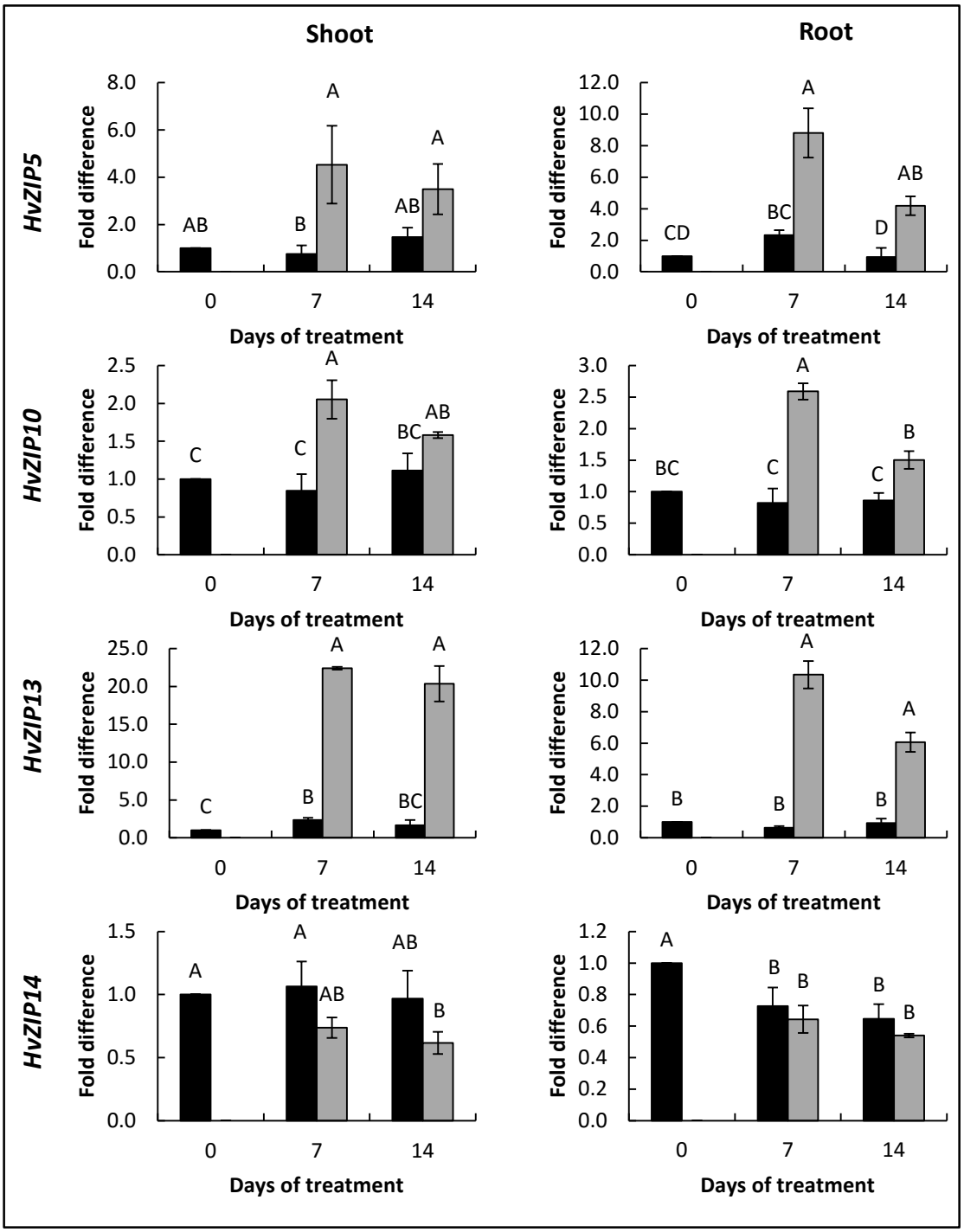

Figure 4.29 Regulation of *ZIPs* following imposition of Zn-deficiency conditions.

Real-time PCR determining gene expression of barley *ZIPs* in roots and shoots over time in response to Zn deficiency. The gene relative expression levels were calculated based on Pfaffl (2001) standardised by normalizing to *HvRNABP* (Mikkelsen et al., 2012) and analyzed using Opticon software. Expression levels were relative to expression at day 0 of the treatment,which was expressed as 1. All data are means (+/- SEM) of three biological replicates. Black bar and grey bar indicate gene expression level under 8µM Zn (+Zn) and 0µM Zn (-Zn) conditions respectively. Means not sharing a letter are significantly different (P≤0.05); Fisher's Least Significant Difference (LSD) post-hoc test.

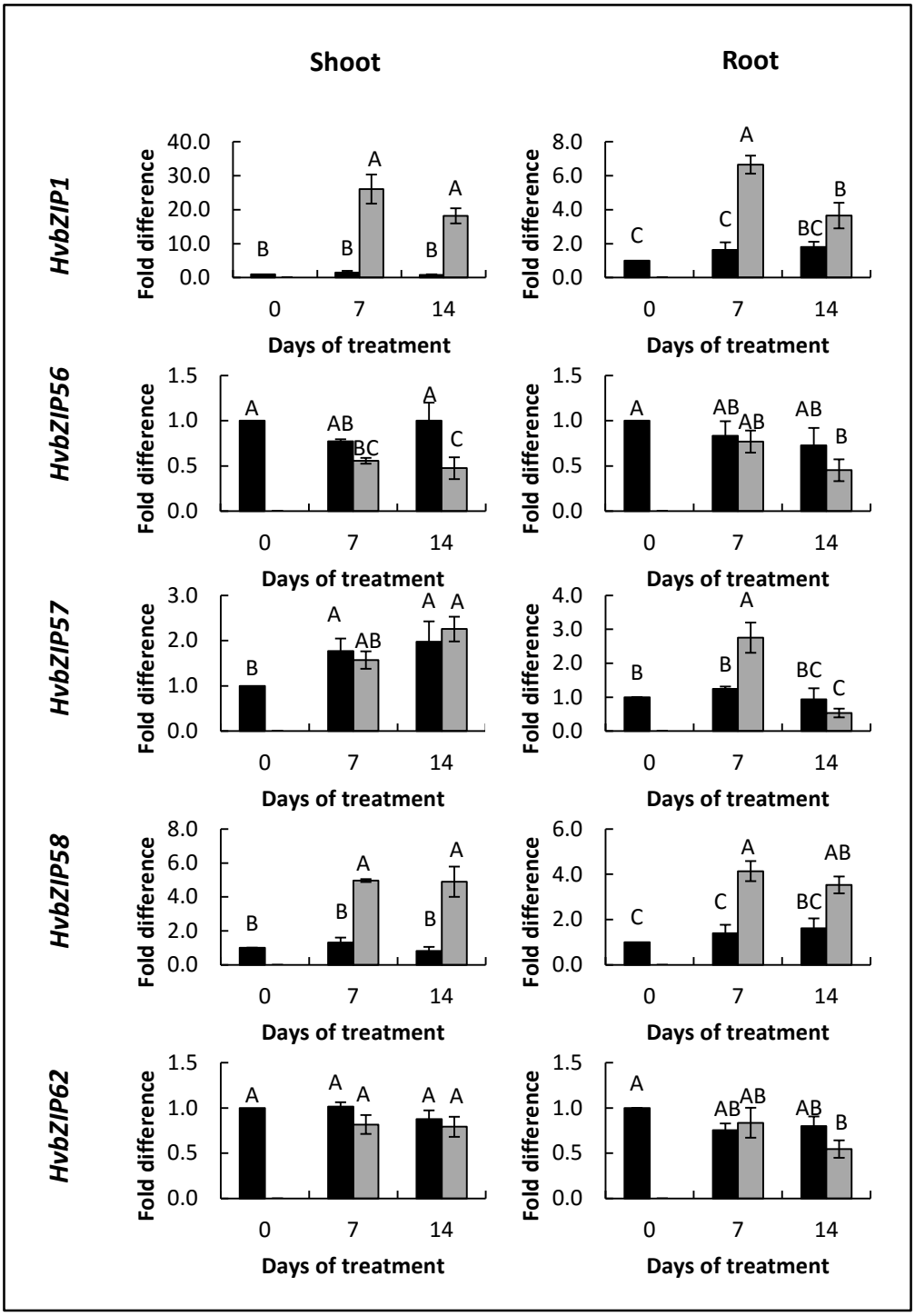

Figure 4.30 Real-time PCR to determine gene expression of barley *bZIPs* in roots and shoots of barley over time in response to Zn deficiency.

RNABP was used for normalization. All data are means (+/- SEM) of three biological replicates. Black bar and grey bar indicate gene expression level under 8µM Zn (+Zn) and 0µM Zn (-Zn) conditions respectively. The expression levels are relative to expression at day 0 of the treatment, which was expressed as 1. Means not sharing a letter are significantly different (P≤0.05); Fisher's Least Significant Difference (LSD) post-hoc test.

showed little up-regulation after seven days and in fact, *HvbZIP56* was down-regulated after fourteen days in the shoots. *HvbZIP56* and *HvbZIP62* were also tested over a shorter time period (three to five days) in case they were up-regulated genes but there was no marked effects on Zn deficiency over this short time period (Figure 4.31). The varying degree of up-regulation of the bZIPs in response to Zn may indicate distinct roles.

4.2.9 Expression level of barley F-group *bZIPs* in different tissues

Mayer et al. (2012) has produced data for barley gene expression levels, which can be accessed in the form of Fragments Per Kilobase of transcript per Million mapped reads (FPKM) values associated with the predicted genes. The data were generated based on Morex cultivar RNA-seq information (Mayer et al., 2012). Eight barley tissues are available in the database (Table 4.6). The expression of the barley F-group bZIPs in these tissues under normal Zn is shown in Figure 4.32.

HvbZIP62 has the highest expression in barley showing high expression particularly in the developing inflorescences (Figure 4.32). *HvbZIP56* shows highest expression in developing grain (five days after anthesis, three to five mm long caryopses) compared to other tissues (Figure 4.32). *HvbZIP55* and *HvbZIP58* show the lowest expression levels in all tissues compared to the other F-group *bZIPs* (Figure 4.32). *HvbZIP10* and *HvbZIP57* have their highest expression in root tissues (Figure 4.32). Some of the *bZIPs* are not expressed at all in certain tissues. For example, no expression is detected in young developing inflorescences (5mm) for *HvbZIP1* and *HvbZIP10*, while *HvbZIP58* is not expressed in developing inflorescences (1-1.5 cm) (Figure 4.32). In addition, *HvbZIP55* is only expressed in 4-day embryos and shoots (Figure 4.32).

4.2.10 Investigating the presence of ZDRE and other core motifs in promoters of barley *ZIPs* and *bZIPs*

Thirteen barley *ZIP* transporter genes have been identified to date and these have been characterized to differing extents (Table 4.7). In this study, bioinformatics was conducted to identify the promoter regions for these genes and then these were analysed to determine whether a similar ZDRE is seen in these genes as observed for some of the *A. thaliana* genes induced by Zn deficiency. We have listed sequences and their positions that are the same as the proposed ZDRE consensus sequence (RTGTCGACAY) and also indicated whether this is palindromic. Five barley *ZIPs* (*HvZIP3*, *HvZIP5*, *HvZIP7*, *HvZIP8*, *HvZIP10*) contain palindromic ZDRE motifs in their promoters (Table 4.7) and these have all been shown to be up-regulated under Zn deficiency (Tiong et al., 2015, this study). Apart from *HvZIP10*, which has not been tested, all of

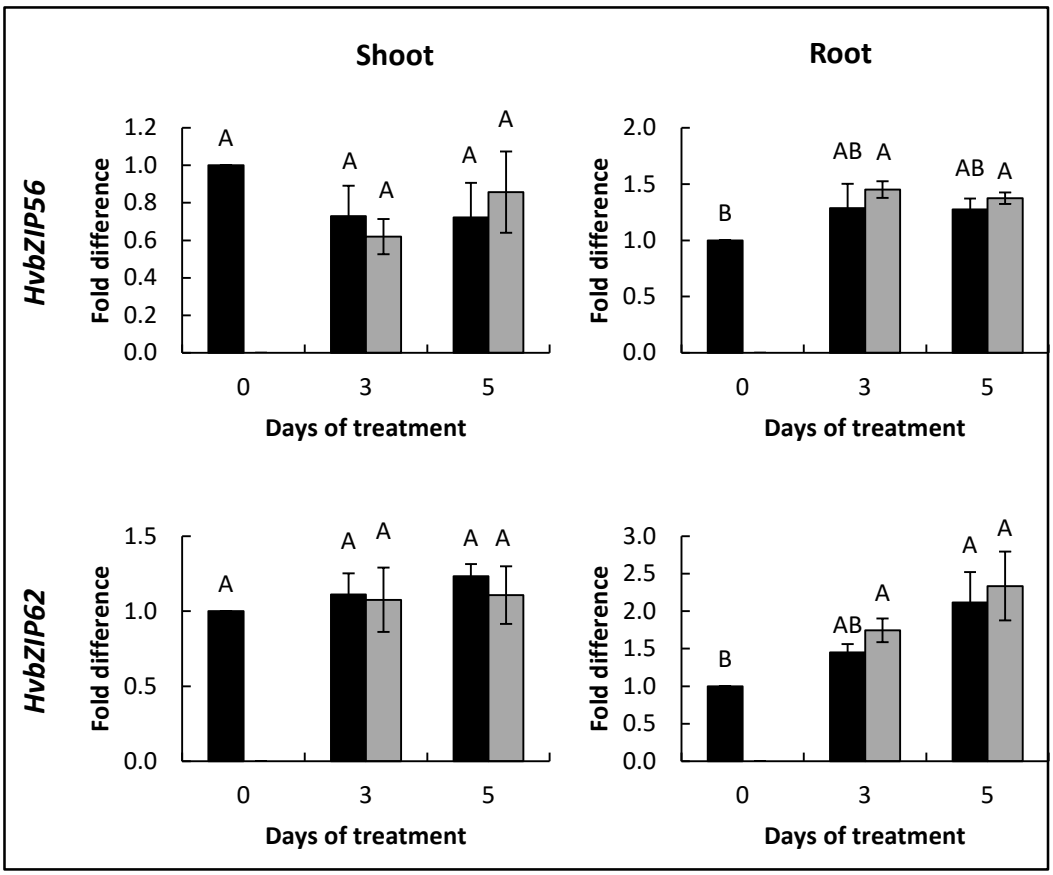

Figure 4.31 *HvbZIP56* and *HvbZIP62* show no marked changes in response to Zn deficiency measured over a shorter time period.

The fold difference (±SE) in gene expression of *HvbZIP56* and *HvbZIP62* in comparison to the control gene (*HvRNABP*) in shoots and roots at day 0, 3, and 5. All data are means (+/- SEM) of three biological replicates. Black bar and grey bar indicate gene expression level under 8µM Zn (+Zn) and 0µM Zn (-Zn) conditions respectively. The expression levels were expressed relative to expression at day 0 of the treatment, which was expressed as 1. Means not sharing a letter are significantly different (P≤0.05); Fisher's Least Significant Difference (LSD) post-hoc test.

Table 4.6 Eight barley tissues available for gene expression analyses. The data were extracted from the Morex barley RNA-seq database (Mayer et al., 2012).

Tissue abbreviation	Tissue description
EMB	4-day embryos dissected from germinating grains
ROO	Roots from the seedlings (10 cm shoot stage)
LEA	Shoots from the seedlings (10 cm shoot stage)
INF1	Young developing inflorescences (5mm)
INF2	Developing inflorescences (1-1.5 cm)
NOD	Developing tillers at six-leaf stage, 3rd internode
CAR5	Developing grain, bracts removed (5 DPA)
CAR15	Developing grain, bracts removed (15 DPA)

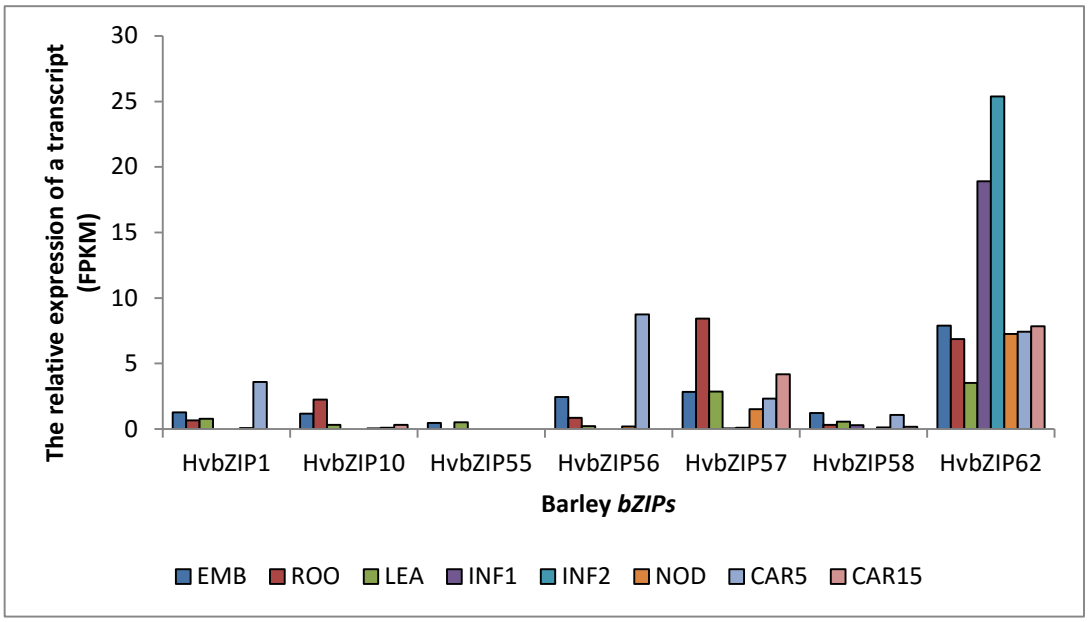

Figure 4.32 Expression pattern of barley F-group *bZIPs* in different tissues.

Expression levels were obtained from the RNA-seq database (Mayer et al., 2012). There are eight barley tissues available for the analyses (Table 4.6).

Table 4.7 ZDRE and the A-, T-, C-, G-box positions in barley *ZIP* (non-shaded) and *bZIP* (shaded) promoters.

Barley ZIP/bZIP	No. of potential ZDRE motifs	Closest ZDRE Sequence (5' to 3') RTGTCGACAY (Morex/Bowman)	Position (upstream from the start codon) ZDRE (closest sequence)	No. of A-, T-, C-, and G-box found in the promoter (position upstream from the start codon)
HvIRT1	1	CTGTCGCCAC	1186bp	1 A-box (76bp) 1 G-box (797bp)
HvZIP1	1	ATGTCTCGAG	295bp	1 A-box (89bp)
HvZIP2	1	CTGACGACAC	730bp	None
HvZIP3	2	GTGTCAACAC GTGTCGACAA*	546bp 1604bp	None
HvZIP5	2	GTGTCGACAC* GTGTCGACAC*	689bp 928bp	None
HvZIP6	2	GTTTCGACAC ATGTGCAAAG	186bp 311bp	None
HvZIP7	1	ATGTCGACAT*	672bp	1 C-box (410bp)
HvZIP8	1	GTGTCGACAC*	658bp	1 A-box (74bp) 1 G-box (735bp)
HvZIP10	1	GTGTCGACAC*	443bp	1 G-box (668bp)
HvZIP11	1	ATGTCGGCTT	165bp	None
HvZIP13	1	ATGTCGTCAC	243bp	1 G-box (622bp)
HvZIP14	2	AAGTCAACAA ATGTCTTGAC	187bp 1055bp	None
HvZIP16	1	ATGCCCACAC	496bp	None
HvbZIP1	1	ATGTCGACAT*	113bp	1 G-box (56bp)
HvbZIP10	1	ATGACGACAT	397bp	1 A-box (943bp)
HvbZIP55	1	TGTCTAGACA	1022bp	None
HvbZIP56	1	ATGTCATCGA	988bp	None
HvbZIP57	1	TGTCGTCCGA	131bp	1 G-box (274bp)
HvbZIP58	1	ATGTCGACAC*	106bp	1 G-box (58bp)
HvbZIP61	N/A	N/A	No promoter sequence was found	N/A
HvbZIP62	1	ATGCCCACAT	749bp	None

* = ZDRE motif palindromic

these have been shown to transport Zn when expressed in *S. cerevisiae* (Table 4.7). This is consistent with the model proposed for Zn sensing and response under Zn deficiency whereby the binding of bZIPs to ZDRE motifs in *ZIP* promoters under Zn deficiency is proposed to lead to enhance expression. *HvZIP1*, *HvZIP2*, *HvZIP6*, *HvZIP11*, *HvZIP13*, *HvZIP14*, *HvZIP16*, and *HvIRT1* do not have this motif (the closest sequence is listed) and apart from *HvZIP13*, these *ZIPs* have not been shown to have a clear role under Zn deficiency. The exact function of some of these has not yet been clarified and indeed some may transport other metals. Incidentally, Assuncao et al. (2010) mutated the core sequence of 'TCGA' to 'TAGA' and in this case, there was no shift in the EMSA assay. None of barley ZIPs and bZIPs correspond to the mutated version.

ZDRE domains in the barley *bZIPs* were also investigated. Interestingly the only ones with a completely conserved ZDRE domain where promoter information was available were *HvbZIP1* and *HvbZIP58*. As shown previously these two *bZIPs* showed marked up-regulation under Zn deficiency in both root and shoot tissue (Figure 4.30). *HvbZIP57*, which showed a moderate amount of up-regulation but only in roots, did not possess a ZDRE domain in its promoter (Figure 4.30).

In addition to ZDRE domains, the presence of A-box (TACGTA), T-box (AACGTT), C-box (GACGTC), and G-box (CACGTG) were also investigated as these motifs contains an ACGT core motif where bZIP TFs can bind (Izawa et al., 1993, Assuncao et al., 2010). As shown in Table 4.7, all barley ZIPs except *HvZIP3*, *HvZIP5*, *HvZIP6*, *HvZIP11*, *HvZIP14*, *HvZIP16* contain at least one of the motifs in their promoter. This group of ZIPs was a mixture of both Zn-deficiency induced and non-induced ZIPs. Interestingly, the investigation of these motifs in the promoter of *bZIPs* showed a particular pattern. All Zn-deficiency induced *bZIPs* investigated here (*HvbZIP1*, *HvbZIP57*, and *HvbZIP58*) and also *HvbZIP10*, whose expression level was also markedly up-regulated by Zn deficiency (Griffin and Williams, unpublished) contain one of these motifs in their promoter (Table 4.7). The significance of this is yet to be determined but could indicate that particular bZIPs are up-regulated via other F-group bZIPs.

4.2.11 Investigating the presence of ZDRE and other core motifs in promoters of barley *Asparagine synthetases* (*ASNs*)

BdBZIP10 is the orthologue of *A. thaliana* bZIP19 and bZIP23 in *B. distachyon* and it has shown to bind to the promoter of BdZIP4 and BdASN1 (Glover-Cutter et al., 2014). The promoter of *BdASN1* does not contain a ZDRE like *BdbZIP4* but it has one A-box and two G-boxes (Glover-Cutter et al., 2014). In this study, bioinformatics was conducted to identify the orthologues of *BdASN1* in barley and their promoter regions for these genes. Then these were analysed to

determine whether similar motifs found in the promoter of *BdASN1* were present. Five orthologues of *BdASN1* were identifed in barley through BLAST search with *BdASN1* CDS (Table 4.8). The percent identity of barley ASNs compared to BdASN1 ranged from 65% to 68% (Table 4.8). The closest to BdASN1 is HvASN5 with 68% percentage identity (Table 4.8). None of the barley *ASNs* has a ZDRE except *HvASN1* (Table 4.8). The ZDRE sequence is identical to the consensus and thus, it is fully conserved. Others have at least one A-box or G-box in their promoter except *HvASN4* (Table 4.8). The search for ZDRE and other motifs cannot be performed for *HvASN4* due to its promoter sequence not being available in the databases.

Table 4.8 ZDRE and the A-, T-, C-, G-box positions in barley *ASNs* promoters.

Gene	Accession No	Percentage identity compared to BdASN1	ZDRE (position before start codon)	A,T,C,G-box (position before start codon)
HvASN1	AK359770	66.2%	ATGTCGACAC (529bp)	2 A-box (373bp and 482bp)
HvASN2	AK357350	67.8%	None	1 A-box (86bp), 1 G-box (344bp)
HvASN3	AK353762	66.2%	None	None
HvASN4	AK363899	65.1%	N/A	N/A
HvASN5	AK361923	68.5%	None	1 G-box (203bp)

4.3 Discussion

4.3.1 Seven F-group bZIPs were identified in barley using bioinformatics analyses and shown to be expressed

Seven related F-group bZIPs were found from the bioinformatics analyses (HvbZIP1, HvbZIP10, HvbZIP55, HvbZIP56, HvbZIP57, HvbZIP58, and HvbZIP62) and these were all found to be expressed in barley Golden Promise cultivar. However, *HvbZIP58* and *HvbZIP62* had slightly different coding sequences in two cultivars, which resulted in amino acid changes and additions. These *bZIPs* that had been cloned from Golden Promise had identical sequences to the Bowman cultivar sequences, suggesting Golden Promise and Bowman may be more closely related. Golden Promise originated from the Maythorpe cultivar, which had been mutated with gamma ray, making this cultivar dwarf (Sigurbjorsson and Micke, 1969). Other Golden Promise phenotypes include a compact inflorescence and early flowering and these characteristics of Golden Promise have been attributed to a single recessive mutation known as *Gpert* (Thomas et al., 1984). The barley F-group showed higher than 30% identity to each other with some members showing up to 73% identity. HvbZIP61 was less related to the other barley F-group bZIPs with less than 11% identity (Table 4.2). Pourabed et al. (2015) included it as a barley F-group member as it was found to be most closely related to this group phylogenetically, however our analyses suggests that this may instead be an aphid sequence. HvbZIP61 cDNA sequence is mentioned in both Li et al. (2015) and Pourabed et al. (2015) studies but it is originally from Haruna Nijo cultivar cDNA libraries generated by Matsumoto et al. (2011). HvbZIP61 cDNA clone was generated from the flag leaf at the vegetative stage, which could have been infected with aphids, thus contaminating the samples. Aphid infestation in barley is a widespread problem around the world and it can transmit Barley yellow dwarf viruses, leading to diseases, which can reduce barley production and quality (Miller and Rasochova, 1997, Gao et al., 2014).

HvbZIP56 and HvbZIP62 were most closely related to *A. thaliana* bZIP19 and bZIP23. Phylogenetic analyses of the bZIP family indicates that most bZIP groups contain monocot and dicot members suggesting that diversification of bZIPs occurred before the divergence of monocots and dicots (Pourabed et al., 2015, Liu and Chu, 2015); our analyses for the F-group would concur with this. While the seven barley bZIPs fall clearly into the F-group, *A. thaliana* contains only three, indicating that gene duplication and further diversification occurred subsequent to the dicot/monocot split. This study was carried out to define the role of these F-group bZIP TFs in cereals more clearly and to test whether there was a link with the Zn-deficiency response mechanism.

4.3.2 Functional complementation as a tool for demonstrating a role for bZIPs in Zn deficiency

The availability of genetic resources in barley is not as great as in *A. thaliana* and therefore in this study, a heterologous complementation approach was used involving the use of *bzip19-4 bzip23-2* double mutants, which had been shown to be extremely hypersensitive to Zn-deficient conditions (see Chapter 3). Here the evidence is provided to indicate that barley bZIP TFs, HvbZIP56, HvbZIP57, and HvbZIP62 can function in the Zn deficiency response by demonstrating their ability to partially complement the *A. thaliana bzip19-4 bzip23-2* double mutant when grown on low Zn.

Assuncao et al. (2013) make the point that either AtbZIP19 or AtbZIP23 expression (under the 35S promoter) in the double mutant background (*bzip19-1 bzip23-1*) completely complements the Zn-hypersensitive phenotype suggesting that bZIP19 and bZIP23 are redundant and thus function as homodimers. Here *HvZIP56*, *HvbZIP57*, and *HvbZIP62* are also expressed under the 35S promoter but they do not fully complement the double mutants. This suggests that perhaps there are some functions of the *A. thaliana* bZIPs that cannot be performed (as efficiently) by the barley bZIPs. Having an expanded number of bZIPs, it may be the case that barley bZIPs function more efficiently as heterodimers to regulate certain genes and so it may be useful in future to test whether expressing two barley *bZIPs* together fully rescues the mutant. These lines expressing *HvbZIP56* in this study were used to determine the effect on gene expression. *A. thaliana ZIP9* and *ZIP12* have been shown previously to be up-regulated by Zn deficiency (Inaba et al., 2015) and the expression of *HvbZIP56* in the *bzip19-4 bzip23-2* double mutants resulted in the up-regulation of *A. thaliana ZIP4, ZIP9 and ZIP12* (Griffin and Williams, unpublished). This indicates that the response to Zn deficiency by regulating the expression of *ZIPs* is conserved across species. The lack of full complementation may indicate that although gene expression of these key ZIPs can be achieved, the differences in structure may mean that they are not quite as efficient at inducing the range of target genes as the native F-group bZIPs.

HvbZIP1, on the other hand, does not complement the double mutants at all, suggesting it may not be involved in Zn-deficiency responses. It is possible that this did not rescue due to it missing some N-terminal sequence. Later in the project, more sequences was released. HvbZIP1 was re-analysed and additional N-terminal sequence was identified. The longer transcript could be amplified and therefore *HvbZIP1b* was cloned and expressed in the *bzip19-4 bzip23-2* double mutants to determine whether this complements the *A. thaliana bzip19-4 bzip23-2* double mutants. The plants have only just become available and have not been analysed in this project. Here we have only tested HvbZIP1, HvbZIP56, HvbZIP57, and HvbZIP62 but in future, it will be

important to test the other barley bZIPs to determine whether they all play a role in Zn deficiency or whether there is functional diversity within this group. The involvement in oxidative stress responses has been shown for an F-group bZIP in *B. distachyon*, BdbZIP10/11, as its overexpression leads to increased oxidative stress resistance and cell viability (Glover-Cutter et al., 2014). In *A. thaliana*, the third F-group member, bZIP24 has been implicated in resistance to salt stress and it is therefore possible that some of the barley F-group bZIPs have broader roles. This assumption could be true but all seven barley F-group bZIPs are more related to AtbZIP19 and AtbZIP23 than AtbZIP24 phylogenetically, indicating their roles may be less related to AtbZIP24.

4.3.3 The presence of ZDRE motifs supports a conserved mechanism for responding to Zn deficiency although they are unlikely to be the sole determinant.

In addition to *A. thaliana*, conserved ZDRE domains have now been found in *ZIP4* orthologues from four other species of Brassicaceae (*Arabidopsis lyrata*, *Arabidopsis halleri*, and *Cochlearia pyrenaica*, and *Noccaea caerulescens*), even though other regions of the promoters showed low sequence conservation (Assunção et al., 2010, Lin et al., 2016). Two ZDRE domains were found and at least for *A. thaliana* and *N. caerulescens*, these ZDRE domains to seem to play important roles in the response of AtZIP4/NcZNT1 to Zn deficiency. For all five species, they are located within 250bp of the predicted ATG start codon of the gene and all with similar distance between both ZDREs. If the mechanism for responding to Zn deficiency is conserved in cereals, the ZIPs that are up-regulated by Zn deficiency may be expected to contain a ZDRE domain. In this study, *HvZIP5*, *HvZIP10,* and *HvZIP13* are up-regulated by Zn deficiency whereas ZIP14 is not. This is in agreement with Tiong et al. (2015) who analysed thirteen *HvZIP* genes and found that six of the thirteen *HvZIP* genes analysed were strongly induced by Zn deficiency (*HvZIP3*, *HvZIP5*, *HvZIP7*, *HvZIP8*, *HvZIP10* and *HvZIP13*) whereas the remaining seven (*HvIRT1*, *HvZIP1*, *HvZIP2*, *HvZIP6*, *HvZIP11*, *HvZIP14* and *HvZIP16*) were not. Our analyses of the promoter regions shows that only the genes that were enhanced by Zn deficiency contained a palindromic ZDRE domain.

The only exception to this is *HvZIP13*. It did contain a motif that was only 1bp different but it was not palindromic and so it remains to be tested whether this motif is important in responding to Zn deficiency or whether *HvZIP13* is regulated by an alternative mechanism. However, the definition of ZDRE could be less rigid to that claimed by Assuncao et al. (2010) where the core sequence (TCGA) of the 10bp-palindrome must be identical. At*ZIP9* was up-regulated by Zn deficiency and its promoter contained a ZDRE with 1bp mismatch in its potential ZDRE (Inaba et al., 2015). Therefore, the definition of ZDRE might not be as strict as claimed by Assuncao et al. (2010) or the ZDRE itself is not a crucial component in the mechanism of F-group

bZIPs. Jain et al. (2013) supported a role for the ZDRE domain as being pivotal in *A. thaliana* ZIPs in responding to Zn deficiency but because in their experiments AtZIP2 was responsive to Zn deficiency, they suggested it may not be the only determinant for Zn-deficiency responsiveness. Studies in our lab indicate that *AtZIP2* is not up-regulated by Zn deficiency as seen for *AtZIP9* and *AtZIP12* (Griffin and Williams, unpublished) and so is still consistent with the ZDRE, perhaps in a less rigid form being important in this process. Overall, the results in barley demonstrating the presence of a ZDRE domain in the promoters of genes strongly induced by Zn deficiency would suggest a conserved mechanism in responding to Zn deficiency.

HvZIP13 is most closely related to BdZIP13, which was named BdZIP3 in the study by Glover-Cutter et al. (2015). Overexpression of *BdbZIP10* in *B. distachyon* targets this *ZIP* transporter but not *BdZIP5* (Glover-Cutter nomenclature). The latter is most closely related to HvZIP5 and HvZIP8. BdZIP13, HvZIP13, HvZIP5 and HvZIP8 are all in the same clade as *A. thaliana AtZIP12* which is proposed to be up-regulated by AtbZIP23 (Inaba et al, 2015) whereas AtZIP9 and AtZIP4 are in a different clade. There are several F-group bZIPs in barley, which seem to have a role in Zn deficiency as shown earlier; therefore in *B. distachyon* there could be other BdbZIPs potentially responsible for regulating BdZIP5. BdbZIP10 may have other broader functions related to oxidative stress and this will be interesting to explore with the barley F-group bZIPs. Nevertheless certainly the evidence we present for HvbZIP56, HvbZIP57 and HvbZIP62 in complementing the Zn-deficiency phenotype of the *A. thaliana bzip19-4 bzip23-2* mutant would support an important role in responding to deficits in this micronutrient.

Other than the ZDRE, DNA elements containing an ACGT core motif such as A-, T-, C-, and G-box are also thought to be the binding site of the basic region of plant bZIPs (Izawa et al., 1993, Assuncao et al., 2010). In this study, various *ZIP* membrane transporters had these DNA elements in their promoter regardless of their responsiveness to Zn deficiency. This suggests that these DNA elements might not be directly significant for controlling *ZIP* expression during Zn deficiency. However, the significance of these DNA elements in Zn deficiency responses should not be disregarded until the complete mechanisms understood. *B. distachyon ASN1* is one of the F-group bZIP targeted gene that has been shown to have A-box and G-box, and its expression level is enhanced by oxidative stress (Glover-Cutter et al., 2014). The expression level of its homologue in *A. thaliana* has been shown to be up-regulated by both Zn deficiency (van de Mortel et al., 2006) and oxidative stress (Abercrombie et al., 2008). In this study, five *BdASN1* orthologues in barley have been identified and some of them have A-box and G-box in their promoters. One ZDRE was also found in the promoter of *HvASN1*. Avila-Ospina et al. (2015) has reported that these barley ASNs can be grouped into the dark-induced *ASNs*, which are *HvASN1*, *HvASN4*, and *HvASN5*, and dark-repressed, which is *HvASN3*. The expression level of *HvASN2* under these conditions was not

measured as no specific primers could be found for this gene (Avila-Ospina et al., 2015). This finding could indicate that barley F-group bZIPs might have broader roles. Future works could involve testing the expression levels of these barley *ASNs* under Zn-deficiency. Interestingly, the four barley *bZIPs* markedly up-regulated by Zn deficiency (*HvbZIP1*, *HvbZIP10*, *HvbZIP57*, and *HvbZIP58*) had one of these elements in their promoters. The Zn-deficiency response might be more complex than initially thought as other bZIPs might bind to the promoters of these four *bZIPs* promoter so that they can be activated or deactivated. This could be tested via EMSAs and chromatin immunoprecipitation (ChIP) assays in the future.

4.3.4 Regulation of F-group bZIPs

In *A. thaliana*, *AtbZIP19* and *AtbZIP23* were initially reported as being about two-fold up-regulated under Zn deficiency whereas *AtbZIP24*, another F-group member, was unaffected by Zn status (Assuncao et al. 2010). In a later review, the same group suggest that in a detailed analyses *AtbZIP19* and *AtbZIP23,* expression levels are not significantly affected under Zn deficiency (Assuncao et al. 2013). They hypothesized that a Cys/His-motif in the N-terminal region of the basic domain may function as a Zn-sensor and postulated a model whereby this region acts in a post-translational regulation mechanism. Under normal Zn supply, it was suggested that Zn would be bound to this motif and in this conformation, the TF would be non-functional. But when released from this motif under Zn deficiency they would become active and would target the ZIP transporters in the nucleus. All three *A. thaliana* F-group bZIPs have two Cys/His-rich domains (Assuncao, 2010), but only AtbZIP19 and AtbZIP23 are believed to play a direct regulatory role in the Zn homeostatic network (Assuncao, 2010). All barley F-group bZIPs contain these domains apart from HvbZIP10. This has now been successfully cloned here and transformed into *A. thaliana*. These plants are not at the analysis stage but when they are, it will be interesting to determine whether the lack of this domain has any effect on functional complementation, which may indicate the significance of these domains.

Concerning transcriptional regulation, Inaba et al. (2015) claimed that *AtbZIP19* and *AtbZIP23* do not respond to Zn deficiency but did in fact show slight up-regulation of *AtbZIP19* under these conditions compared to basal conditions. In barley, under Zn deficiency *HvbZIP1* was markedly up-regulated in roots and shoots. Meanwhile, *HvbZIP57* and *HvbZIP5* showed up-regulation in shoot and root tissue respectively; little induction was observed for *HvbZIP56* and *HvbZIP62*. Overall, it would seem that transcriptional regulation of the bZIPs themselves may not be a major feature in the mechanistic response in barley to Zn as HvbZIP56, while not showing a marked transcriptional response can rescue the Zn-deficiency hypersensitivity response of the *bzip19-4 bzip23-1* mutant. Although it should be noted that there it was expressed under the 35S

promoter. So, the mechanism whereby these TFs sense Zn deficiency is still to be determined. Targeting to the nucleus as part of the mechanism for activation of F-group *bZIPs* has been supported for other *bZIPs*. For example, BdbZIP10/11 showed enhanced levels in the nucleus following exposure to oxidative stress and this was suggested to be due to post-translational modifications enhancing stability or directing subcellular localization (Glover-Cuttter et al. 2015). Yang et al. (2009a) also found that AtbZIP24 was targeted preferentially to the nucleus in response to salt stress. This study with HvbZIP56 and the study with AtbZIP19 and AtbZIP23 (Inaba et al. 2015) indicates that these F-group bZIPs are in the nucleus as well as cytoplasm during normal Zn conditions; while this is consistent with them acting as TFs to up-regulate *ZIP* transporter genes, targeting to the nucleus solely under Zn deficiency cannot explain the mechanism for Zn responsiveness.

F-group *bZIPs* expression under normal Zn conditions in various barley tissues were analysed in the dataset produced by Mayer et al. (2012), which is based on RNA-seq. The expression pattern of each F-group *bZIP* differed, suggesting they might play slightly different roles. All were expressed in root tissue and this is consistent with a mechanism to induce *ZIP* genes to take up more Zn into the cells in the roots. There is variable expression in other tissues depending on the bZIP in question. The developing inflorescence is notable for highest expression of *HvbZIP62*. Here they could be important for transferring Zn to the flowers and fruit (Kirchoff and Claßen-Bockhoff, 2013). Perhaps the expression of *HvbZIP62* is high in this tissue even at the normal Zn conditions so that Zn mobilisation to crucial sink tissues is not disrupted. The other notable tissue with high expression of F-group *bZIPs* is the early developing grain. NA is a Zn-ligand that is involved in accumulation of Zn in the grains and it is synthesized by NAS (Clemens et al., 2013), which is one the F-group bZIPs targeted genes in *A . thaliana* (Assuncao et al., 2010). The high expression of *HvbZIP56* in the developing grains compared to other tissues could be for maintaining the optimum level of NA, which is crucial for assisting Zn loading in the grains. It will be interesting in the future to determine the expression pattern for barley F-group *bZIPs* in different tissues under Zn-deficient conditions especially for ones that are transcriptionally regulated.

4.3.5 Micronutrient effects at low Zn

Results in hydroponics (Griffin and Williams, unpublished) showing an inhibiting effect of elevated Cu led us to investigate in more detail the effect of other micronutrients when the Zn levels were kept relatively low. AtbZIP19 and AtbZIP23 have been demonstrated to be involved in Zn-specific response (see Chapter 3). However, when Zn was reduced to 1µM in the medium, Cu and Fe but not Mn inhibited *bzip19-4 bzip23-2* double mutants growth. This could be due to the

broad specificity of some of the ZIP transporters that could transport Cu and Fe as well as Zn. We hypothesise that an excess of Cu or Fe is able to outcompete Zn for ZIP binding and transport, leading to an uptake of these ions rather than Zn into the cell. This could induce conditions of Zn deficiency for the cell, which could respond by inducing up-regulation of *ZIPs* by AtbZIP19 and AtbZIP23. These ZIPs can then increase Zn uptake into the cell. This would affect the *bzip19-4 bzip23-2* double mutant because there are no bZIPs to detect the low intracellular Zn, so no extra ZIPs are transcribed, resulting in no extra Zn ions in the cell. The expression of *HvbZIP56* in *bzip19-4 bzip23-2* double mutants rescued this Cu and Fe hypersensitivity response which is consistent with their ability in this system to up-regulate *A. thaliana ZIPs.*

Indeed, studies have shown that some *A. thaliana* Zn-transporting ZIPs have the ability to transport Cu and Fe as well Zn. For example, AtZIP2 and AtZIP4 have previously been demonstrated to transport Cu as they can complement the *S. cerevisiae ctr1* mutant that is defective in high-affinity Cu uptake (Wintz et al., 2003); this result was not reproduced for AtZIP2 in a more recent study, which instead indicated AtZIP2 functions in Zn and Mn transport (Milner et al., 2013). Meanwhile, both *A. thaliana* AtIRT1 and AtIRT2 have the ability to complement the *fet3*Δ*fet4*Δ yeast strain defective in both high- and low-affinity Fe acquisition suggesting their roles in Fe transport (Eide et al., 1996, Vert et al., 2002). Toxic Mn levels did not affect *bzip19-4 bzip23-2* double mutants, would suggest that Mn is not a major competitor for the Zn influx mechanism. Alternatively, the results could be explained by a possible increase in oxidative stress in the *bzip19-4 bzip23-2* double mutant when the Cu/Fe:Zn ratio is high and lack of bZIPs means that the seedlings cannot respond appropriately. The fact that HvbZIP56 can rescue this hypersensitivity again indicates that there is conservation of function between *A. thaliana* and barley bZIPs. Further work is necessary to clarify these results and could include determining the concentration of various ions in the tissues and also response of oxidative-stress markers.

Overall, the results in this chapter indicate that that particular member of the barley F-group bZIPs can function in the Zn-deficiency response. The presence of ZDRE in the promoter of some barley ZIP transporters and the up-regulation of these particular ZIP transporters under Zn deficiency suggests a conserved mechanism in responding to Zn deficiency. Therefore, these F-group bZIPs could represent novel targets for improving nutrient efficiency in crops. However, the lack of improved efficiency in WT plants expressing barley bZIPs subjected to Zn deficiency may indicate further regulatory processes are in play.

Chapter 5:

Functional Analyses of the barley P_{1B-2}-ATPase, HvHMA3

5.1 Introduction

Zn and Cd transport in plants involves several membrane transporters, with P_{1B}-ATPases having important roles. The P_{1B}-ATPase family can be classed into seven major groups based on phylogenetic analysis and substrate specificities (Smith et al., 2014). In *A. thaliana*, sub-group 2, P_{1B-2}-ATPases, have been implicated in Zn and Cd transport. Information about transport specificity and physiological role has been investigated using heterologous expression in yeast (Mills et al., 2010, Migocka et al., 2015) and also using T-DNA insertional mutants (Hussain et al., 2004; Morel et al. 2009). Based on *A. thaliana hma2 hma4* double mutant characterisation, AtHMA2 and AtHMA4 have been suggested to play key roles in the translocation of Zn as well as Cd from root to shoot (Hussain et al., 2004, Mills et al., 2010). AtHMA3, another member of *A. thaliana* P_{1B-2}-ATPases, also transports Zn and Cd and is proposed to have a role in Zn and Cd detoxification by sequestering excess levels in the vacuole (Morel et al., 2009).

Understanding the transport of Zn and detoxification of Cd in barley and wheat is crucial, as they are major food sources for humans and animals. P_{1B-2}-ATPases have also been studied in monocots and again there is evidence for a role in Zn and Cd transport. In rice, OsHMA2 mediates Zn and Cd transport from root to shoot (Sato-Nagasawa et al., 2012). The orthologue of *A. thaliana* AtHMA3 in rice, OsHMA3, has been proposed to be a vacuolar Cd transporter in roots, reducing cytoplasmic Cd levels and consequently transport of Cd to the shoot (Miyadate et al., 2011, Ueno et al., 2011). TaHMA2 from wheat is also involved in Zn and Cd transport. When it was overexpressed in rice it increased root to shoot Zn and Cd translocation (Tan et al., 2013). The over-expression of TaHMA2 improved tolerance to moderate Zn stress and Zn deficiency, but resistance to Cd and Zn decreased under high levels of the respective metals (Tan et al. 2013). HvHMA2, a barley P_{1B-2}-ATPase, functions in Zn and Cd transport demonstrated using heterologous expression in *S. cerevisiae* and by complementing the Zn-dependent phenotype of Arabidopsis *hma2 hma4* double mutants (Mills et al., 2012). HvHMA2 confers Zn resistance to the Zn-sensitive mutant, *zrc1 cot1* and confers Cd sensitivity to WT yeast (Mills et al., 2012). Expression of GFP-tagged P_{1B-2}-ATPases has provided information on their localisation in plant cells: OsHMA2-GFP localises to the plasma membrane in onion epidermal cells (Yamaji et al.,

2013) and GFP-HvHMA2 localises to the plasma membrane and possibly chloroplast membrane when expressed in *A. thaliana* (Mills et al., 2012).

In contrast to HvHMA2, there is little information about HvHMA3, another P_{1B-2}-ATPase. Phylogenetic analyses shows that HvHMA3 is closely related to OsHMA3 (Zorrig et al., 2011, Mills et al., 2012), a vacuolar Cd transporter (Miyadate et al. (2011). Interestingly, OsHMA3 was identified as the recessive allele in the high Cd accumulation *Indica* rice cultivars. This loss-of-function *OsHMA3* allele had a mutation at the 80th amino acid (Ueno et al., 2010) and this resulted in plants with enhanced root-to-shoot Cd transport, due to the inability of OsHMA3 to sequester Cd into root vacuoles (Ueno et al., 2010, Miyadate et al., 2011). Recently, another loss-of-function *OsHMA3* allele has been identified in particular cultivars of *Japonica* rice that had unusually high shoot Cd levels; in this case, the mutation responsible is in the 380th amino acid (Yan et al., 2016). This type of allelic variation was also found in *A. thaliana* where the loss-of-function *AtHMA3* allele was found among natural *A. thaliana* accessions with high Cd accumulation in leaves (Chao et al., 2012).

As discussed in the general introduction, *A. thaliana* T-DNA insertion mutants are powerful tools for characterising genes of interest. Complementation of mutant phenotypes can suggest a similar function for the unknown gene (Mills et al., 2012, Menguer et al., 2013). The *A. thaliana hma3-1* mutant may be a useful mutant for characterizing HvHMA3. The T-DNA is inserted in the first exon, and no *AtHMA3* transcript was found in this mutant (Hussain et al., 2004). This mutant exhibited impaired Zn and Cd tolerance compared to WT, a phenotype observed by measuring root length with a range of metals (Morel et al., 2009). AtHMA3 is localised to the tonoplast and is thought to be involved in sequestering these metals into the vacuole. AtMTP1 is another vacuolar Zn transporter, but from the CDF family. It is involved in sequestration of excess Zn from the cytoplasm into vacuoles to maintain Zn homeostasis (Kobae et al., 2004, Desbrosses-Fonrouge et al., 2005, Tanaka et al., 2013). A T-DNA insertion knockout mutant of MTP1 in the Wassilewskija (Ws) ecotype of *A. thaliana, mtp1-1,* has been shown to exhibit a Zn-sensitive phenotype (Kobae et al., 2004). The insertion site of the T-DNA is toward the end of the coding region of *AtMTP1* (Kobae et al., 2004). It should be mentioned that in the Ws ecotype, AtHMA3 is considered to be functional whereas in Columbia (Col) it is considered none-functional due to a polymorphism found in an exon of AtHMA3 leading to a premature stop codon (Hussain et al., 2004, Chao et al., 2012).

5.1.1 Aims

A number of aims have been set out to further investigate P_{1B-2}-ATPases in cereals, especially barley HvHMA3, which is yet to be characterised.

1. To do *in silico* analyses of P_{1B-2}-ATPases in barley and wheat so that it can provide a preliminary understanding about their structure and function. These analyses can be done by:
    a. Identifying P_{1B-2}-ATPases orthologues in barley and wheat
    b. Identifying similarities between the P_{1B-2}-ATPases using multiple sequence alignments to find conserve residues
    c. Analysing HvHMA3 polymorphisms and their relation to rice OsHMA3 polymorphisms
    d. Conducting phylogenetic analyses on the P_{1B-2}-ATPases to evaluate the evolutionary relationship between these proteins.
2. AtHMA3 and AtMTP1 are vacuolar proteins. Single mutants have been characterized previously for both, but it was of interest here to determine the effect of knocking out both genes under Zn and Cd stress.
3. To clone full-length coding region of *HvHMA3* and generate *A. thaliana* and *S. cerevisiae* expression vectors.
4. To conduct complementation experiments to determine whether HvHMA3 can rescue the metal-dependent phenotypes of *A. thaliana* mutants.
5. To carry out heterologous expression of *HvHMA3* and *HvHMA3-GFP* in WT *S. cerevisiae* and two different *S. cerevisiae* mutants: Zn-hypersensitive *zrc1 cot1* and Cd-hypersensitive *ycf1* for investigating the substrate specificity of *HvHMA3*.

5.2 Results

5.2.1 Identifying P_{1B-2}-ATPases in barley and wheat

HvHMA2 and HvHMA3 are barley P_{1B-2}-ATPases and to date only HvHMA2 has been characterized (Mills et al., 2012). Searching for related sequences in barley, HvHMA3 was identified and also a further preliminary sequence that had slightly higher homology to HvHMA2 than HvHMA3; because of that, this was called HvHMA2/3. The preliminary HvHMA2/3 sequence was used as a query sequence in the International Barley Sequencing Consortium databases (http://webblast.ipk-gatersleben.de/barley/viroblast.php) to find its complete sequence. This information became available later in the project when further sequence information was released. Results indicated that a contig from Bowman cultivar had the highest similarity to the HvHMA2/3 preliminary sequence (Table 5.1). Following detailed sequence analysis, a predicted open reading frame for HvHMA2/3 was obtained. *HvHMA2*, *HvHMA2/3* and *HvHMA3* coding sequences (CDs) were used as query sequences in the Wheat Portal of Unitè de Recherches en Gènomique Info (URGI) to search for wheat orthologues. URGI is a resource for databases and tools to study genetics and genomics of wheat (https://urgi.versailles.inra.fr/blast/blast.php). Unlike barley, wheat is hexaploid (AABBDD) and its genome is yet to be fully sequenced and annotated. Using this method, contigs from chromosome 7AL, 7BL and 7DL matched the full-length CDs of *HvHMA2*, while full-length HvHMA3 orthologues were found in contigs from chromosome 5AL, 5BL and 5DL. Using these contig sequences, a predicted CDs of wheat *HMA2* homeologues (*TaHMA2 7AL/7BL/7DL*) and *HMA3* (*TaHMA3 5AL/5BL/5DL*) were obtained and translated for the protein sequences. None of HvHMA2/3 orthologues in wheat were full-length CDs. The BLAST searches in the URGI databases using *HvHMA2/3* CDs as query sequences found partial sequences of the *HvHMA2/3* orthologues in chromosome 7 (AL, BL, and DL), which was the same chromosome as for *TaHMA2* homeologues.

5.2.2 Percentage identity of P_{1B-2}-ATPases

The protein sequences of P_{1B-2}-ATPases of *A. thaliana*, rice, barley and wheat were aligned using Clustal Omega (Sievers et al., 2011) (Table 5.2). The percentage identities between different sequences are shown in Table 5.2. The protein sequence alignment results show that regions of conservation exist throughout the P_{1B-2}-ATPases sequences, at the amino acid level and that the degree of identity is high (Figure 5.1). Based on Table 5.2, all tested P_{1B-2}-ATPases had percentage identity ranging from 34.5 % to 92.7 %. TaHMA2 7DL and TaHMA3 5BL were highly identical to their orthologues in barley (92.7 % and 91.7 % respectively). The newly found P_{1B-2}-ATPase in barley, HvHMA2/3 showed slightly higher identity to HvHMA2 (69.1 %) than HvHMA3 (50.5 %).

Table 5.1 Barley and wheat P_{1B-2}-ATPases identified from bioinformatics analyses

Gene	Contigs	Position	NCBI cDNA accession No. (cultivar)	MIPs[1] cDNA accession No. (cultivar)
HvHMA2	- morex_contig_9469 (Full-length) - bowman_contig_1558472 (Full-length and identical to the Morex background) - barke_contig_400996 (partial sequence)	Chromosome 7: 534395957-534401815	AK363365.1 (Haruna Nijo)/ GU177852.1 (Golden Promise)	MLOC_10131 (Morex)
HvHMA2/3	- morex_contig_37799 (Full-length) - bowman_contig_61576 (Full-length and identical to the Morex background) - No Barke sequence was found	Chromosome 7: 537100055-537106018	Not found	MLOC_52795.2 (Morex)
HvHMA3	- morex_contig_1582352 (Full-length) - bowman_contig_1988581 (Full-length and identical to the Morex background) - barke_contig_12746 and 9670 (partial sequences)	Chromosome 5: 497460007-497463394	AK369525 (Haruna Nijo)	MLOC_18862 (Morex)
TaHMA2 (Chr7AL)	- scaffold_556712	Chromosome7AL: 90458-108176	Not available	Not available
TaHMA2 (Chr7BL)	- scaffold_579416	Chromosome 7BL: 14127-24069	Not available	Not available
TaHMA2 (Chr7DL)	- scaffold_602651	Chromosome 7DL: 105511-113285	Not available	Not available
TaHMA2/3 (Chr7AL)	- scaffold_557470	Chromosome 7AL: 61467- 62752	Not available	Not available
TaHMA2/3 (Chr7BL)	- scaffold_577252	Chromosome 7BL: 118443-123897	Not available	Not available
TaHMA2/3 (Chr7DL)	- scaffold_603863	Chromosome 7DL: 43,200-49,689	Not available	Not available
TaHMA3 (Chr5AL)	- scaffold_375473	Chromosome 5AL: 29654-33170	Not available	Not available
TaHMA3 (Chr5BL)	- scaffold_404346	Chromosome 5BL: 222727-226166	Not available	Not available
TaHMA3 (Chr7DL)	- scaffold_435190	Chromosome 5DL: 5098-8725	Not available	Not available

Table 5.2 Percentage identity/similarity of *A. thaliana*, rice, barley and wheat P_{1B-2}-ATPase protein sequences.

The TaHMA2/3 homeologues are not included since they are only partial sequences. Results obtained using the Clustal Needle (Li et al., 2015). See Appendix for the protein accession numbers.

Sequence	AtHMA4	AtHMA2	AtHMA3	HvHMA2	HvHMA2/3	HvHMA3	OsHMA2	OsHMA3	TaHMA2 7DL	TaHMA3 5BL
AtHMA4		58.2%	44.8%	41.5%	41.3%	34.5%	43.0%	36.8%	41.5%	34.1%
AtHMA2	67.5%		55.4%	49.3%	48.2%	43.5%	47.2%	42.6%	48.0%	41.8%
AtHMA3	54.4%	65.8%		39.8%	41.7%	47.6%	39.0%	38.3%	40.8%	46.6%
HvHMA2	56.1%	61.8%	52.5%		69.1%	48.7%	70.8%	48.7%	92.7%	48.9%
HvHMA2/3	56.0%	63.7%	55.2%	76.8%		50.5%	65.0%	50.5%	69.4%	50.1%
HvHMA3	47.7%	58.3%	64.2%	59.2%	59.8%		45.2%	62.8%	48.4%	91.7%
OsHMA2	55.7%	60.0%	50.4%	78.7%	72.7%	54.7%		45.4%	71.4%	43.2%
OsHMA3	50.6%	57.8%	51.3%	60.8%	61.9%	69.5%	57.0%		46.9%	62.4%
TaHMA2 7DL	56.3%	60.6%	54.0%	95.3%	76.6%	58.5%	79.2%	58.5%		48.1%
TaHMA3 5BL	46.6%	55.3%	63.2%	59.6%	59.9%	94.3%	53.1%	68.7%	58.7%	

Top diagonal none-shaded = percent identity. Bottom diagonal = percent similarity

5.2.3 Membrane topology of P_{1B-2}-ATPases

The predicted presence and number of TMs were determined using the SOSUI 1.11 online server (http://harrier.nagahama-i-bio.ac.jp/sosui/sosui_submit.html) (Hirokawa et al., 1998), the TMHMM 2.0 online server (http://www.cbs.dtu.dk/services/TMHMM/) (Krogh et al., 2001), the TMpred online server (http://www.ch.embnet.org/software/TMPRED_form.html) (Hofmann and Stoffel, 1993), and the TOPCONS online server (http://topcons.net/) (Bernsel et al., 2009). These programmes analysed the hydrophobicity of each residue to predict membrane-spanning regions of HvHMA2/3 and HvHMA3 (Table 5.3). There are some differences with the predictions obtained from different programmes but typically they range from five to eight TMs. All programmes predict that the N-termini are cytoplasmic.

The alignments of HvHMA2/3 and HvHMA3 protein sequence with several P_{1B-2}-ATPases showed that HvHMA2/3 and HvHMA3 contain motifs found in all P-types (Figure 5.1). In the phosphorylation domain, these conserved P-types motif were found in both proteins: (A) the **D**$_{411}$KTGT motif (position of **D** for HvHMA3 is 413), that contains the phosphorylated aspartate; (B) the **G**$_{590}$DGxNDxP motif (position of **G** for HvHMA3 is 614), that contains D residues that might bind Mg (Toyoshima, 2009); **P**$_{569}$xxK motif (position of **P** for HvHMA3 is 593), that contains the K residue that may interact with the oxygen of the phosphate transferred from ATP (Jorgensen et al., 2003). There is a region in P-ATPases that functions as the 'actuator' of the gating mechanism that regulates substrate binding and release (Williams and Mills, 2005). The conserved TGE motif in the actuator region was found in both HvHMA2/3 and HvHMA3. HvHMA2/3 and HvHMA3 also have motifs characteristic of P_{1B}-ATPases (Williams and Mills, 2005) including the **H**$_{433}$P locus (position of **H** for HvHMA3 is 453) in the predicted large cytoplasmic loop (present in most P_{1B}-ATPases but not in other P-types). P_{1B}-ATPases usually have putative heavy Metal-Binding Domains (MBDs) in the N or C termini and the CPx/SPC motif in TM6 (Mills et al., 2005, Mills et al., 2010). HvHMA2/3 and HvHMA3 contain the **C**PC motif in the predicted TM6 (**C**$_{347}$ and **C**$_{369}$ for HvHMA2/3 and HvHMA3 respectively). A "heavy-metal-associated domain" in both HvHMA2/3 and HvHMA3 N-termini is recognised by the PROSITE databases (http://prosite.expasy.org/). Within this domain, the motif GxCCxxE occurs in all the plant P_{1B-2} sub-class (Figure 5.1). P_{1B}-ATPases can be divided into subsets 1-7 depending on the potential cation coordinating residues present in the sixth, seventh and eight TMs (Williams and Mills, 2005, Arguello et al., 2007). For the P_{1B-2} subclass, these are TM6: CPCx_4SxP; TM7: Nx_7K; TM8: DxG. Numbered for HvHMA2/3 they are: C_{347}, P_{348}, C_{349}, S_{354} and P_{356} in TM6, N_{649} and K_{657} in TM7, and G_{680} in TM8 (Figure 5.1). The amino acid positions for HvHMA3 are as follows: C_{369}, P_{370}, C_{371}, S_{376} and P_{378} in TM6, N_{673} and K_{681} in TM7, and $_{G702}$ in TM8 (Figure 5.1). The P_{1B-2}-ATPases are suggested to have eight

Table 5.3 The number of HvHMA2/3 and HvHMA3 TMs obtained from different programmes.

Programme	Number of predicted TMs	
	HvHMA2/3	HvHMA3
SOSUI	8	8
TMHMM 2.0	6	5
TMpred	7	7
TOPCONS	8	8

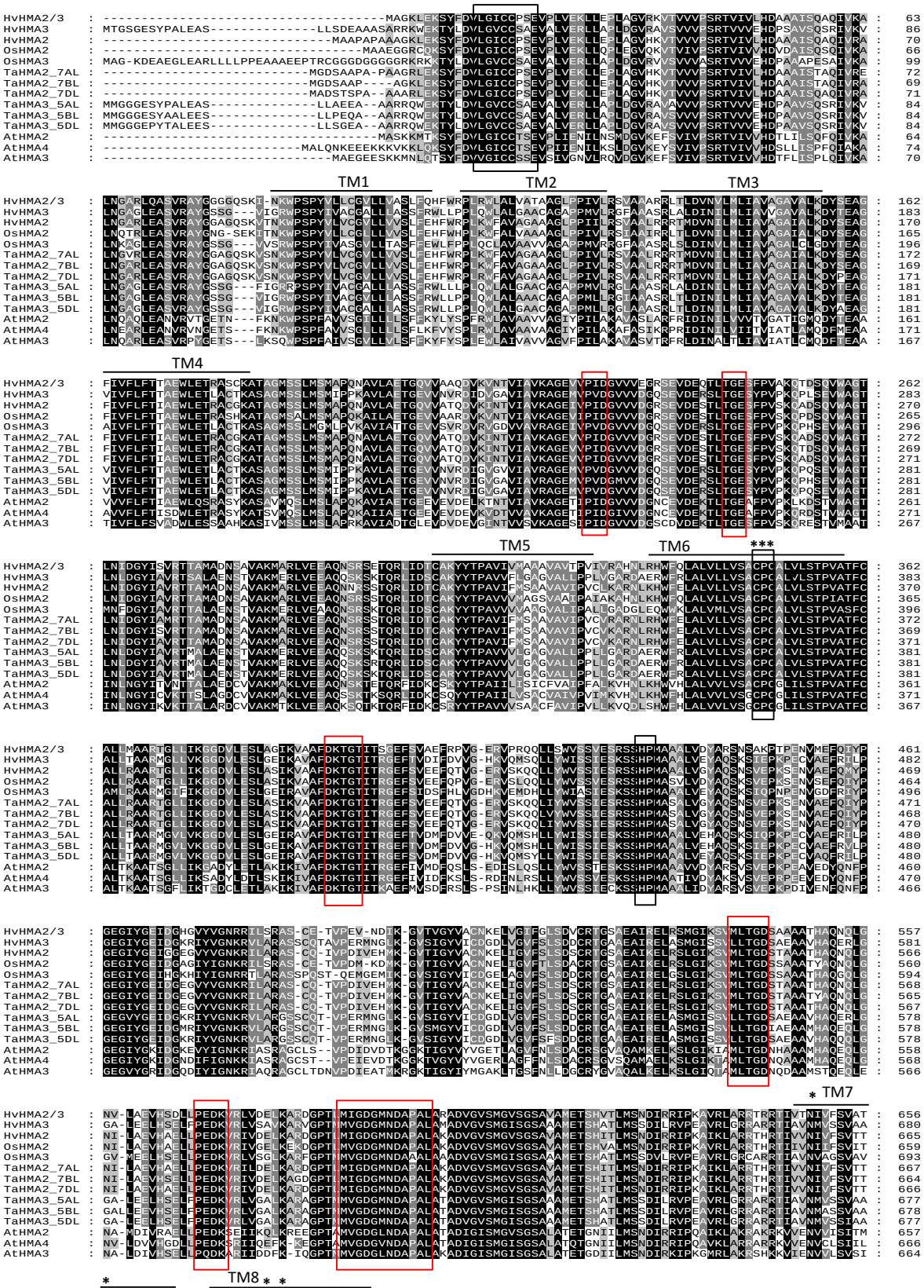
TM1
TM2
TM3
TM4
TM5
TM6
***
TM7
*
TM8
* *

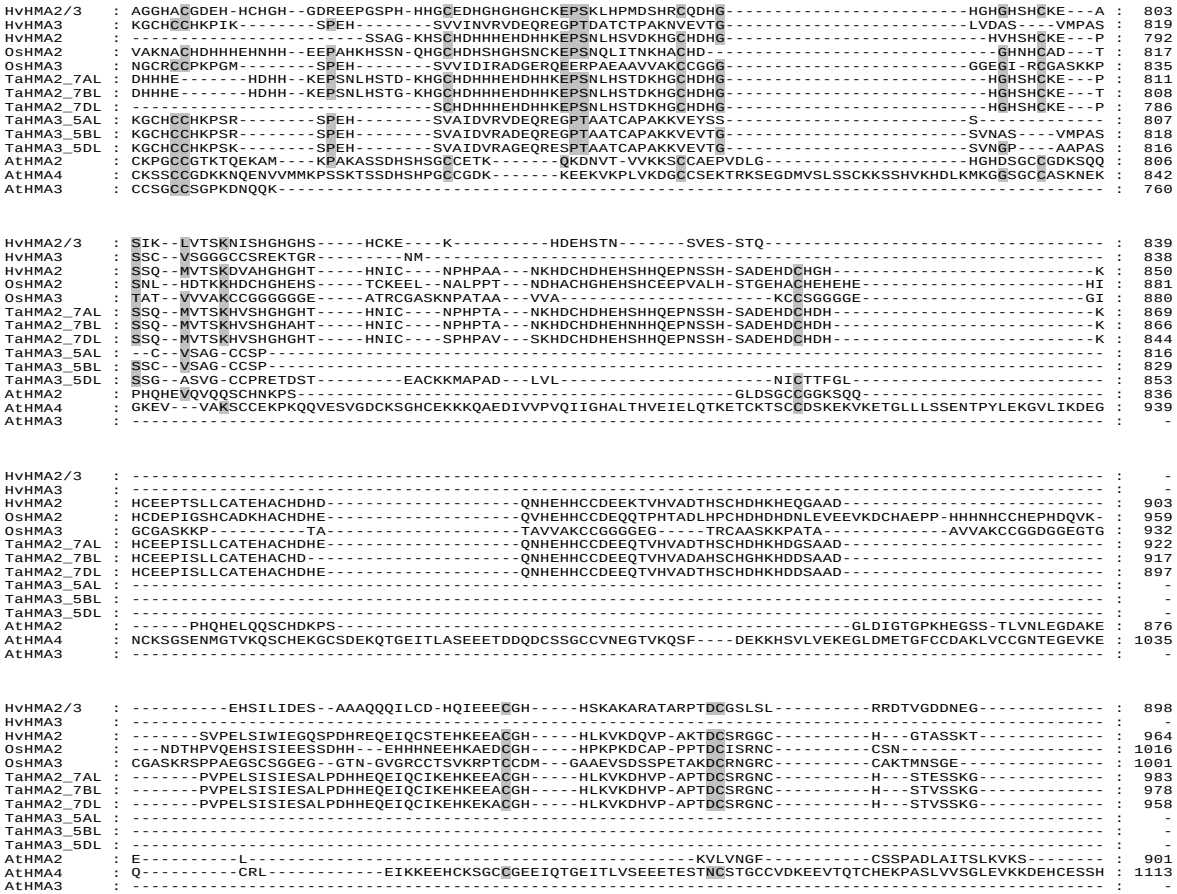

Figure 5.1 Alignment of HvHMA3 with barley, wheat, rice and *A. thaliana* P_{1B-2}-ATPases showing the predicted TMs.

The predicted TMs for HvHMA3 are indicated as predicted by SOSUI prediction programme. Sequences were aligned using the Clustal Omega algorithm (Sievers et al., 2011) and presented using GeneDoc (Nicholas and Nicholas Jr, 1997). For the sequence aligned here: black = conserved residues, dark grey = 8 – 9 of 10 proteins, light grey = conserved in 6 – 7 of organisms. Red boxes indicate motifs conserved in P-type ATPases, black boxes indicate motifs in P_{1B}-ATPases subgroup, and asterisks indicate residues conserved in P_{1B-2}-ATPases that may co-ordinate the metal ion during transmembrane transport and contribute to ion specificity. TaHMA2/3 homeologues are not included in the alignment, as they do not have a complete sequence.

TM domains based on alignments and prediction programs (Figure 5.2) HvHMA2/3 predicted topology seems more similar to HvHMA2 than HvHMA3 (Figure 5.2). The predicted C-terminus of HvHMA3 is shorter than its orthologue in rice (Figure 5.2).

5.2.4 Polymorphism in the coding region of HvHMA3

In rice, two non-functional alleles of the HvHMA3 orthologues, OsHMA3, have been identified in several high Cd-accumulation cultivars (Ueno et al., 2010, Yan et al., 2016). The first non-functional allele was found in the *Indica* cultivars in the coding region leading to a mutation in 80th amino acid residue from Arg to His (Ueno et al., 2010). This allele was not present in any of the *Japonica* cultivars but another non-functional OsHMA3 allele was found in this type of rice where a single nucleotide polymorphism (SNP) in the coding region caused a mutation in 380th amino acid residue from Ser to Arg (Yan et al., 2016). The bioinformatics analyses was done to determine if HvHMA3 from Haruna Nijo, Bowman and Morex cultivars have the same non-functional alleles. HvHMA3 from different cultivars were aligned with OsHMA3 from low and high Cd-accumulation cultivars of the *Indica* and the *Japonica* rice and it reveals that the rice OsHMA3 non-functional alleles are not found in any barley cultivars (Figure 5.3). However, the comparison between the three barley demonstrates that there were two SNPs that lead to changes in amino acids detected at the 84th and 668th position. Val (Haruna Nijo) changed to Gly (Bowman/Morex) at 84th amino acids, while Arg (Haruna Nijo) changed to Cys (Bowman/Morex) at 668th amino acid (Figure 5.3). These two amino acids from Haruna Nijo but not Bowman and Morex were conserved in all rice cultivars (Figure 5.3). Prediction with SOSUI programme showed the position of the two rice HMA3 alleles and also the position of the two polymorphisms detected in HvHMA3 Haruna Nijo (Figure 5.4).

5.2.5 Phylogenetic analyses of P_{1B}-ATPases

In order to perform phylogenetic analyses of the P_{1B}-ATPases family, a complete set of protein sequences was established (see Appendix). *B. distachyon* sequences were retrieved from Aramemnon (http://aramemnon.uni-koeln.de/) using barley P_{1B}-ATPase as query sequences. Sequences of *A. thaliana*, rice and barley were obtained from Mills et al. (2012). Section 5.2.1 describes the sequence of HvHMA2/3, and wheat P_{1B-2}-ATPases. A phylogenetic analysis was conducted for P_{1B}-ATPases from the 45 collected P_{1B}-ATPase proteins for which completed sequence were available except for TaHMA2/3 homeologue protein sequences, which were partial. The phylogenetic analyses revealed that there are three subgroups: P_{1B-1}, P_{1B-2} and P_{1B-4}. (Figure 5.5). All the orthologues of AtHMA5, AtHMA6, AtHMA7 and AtHMA8 that were identified

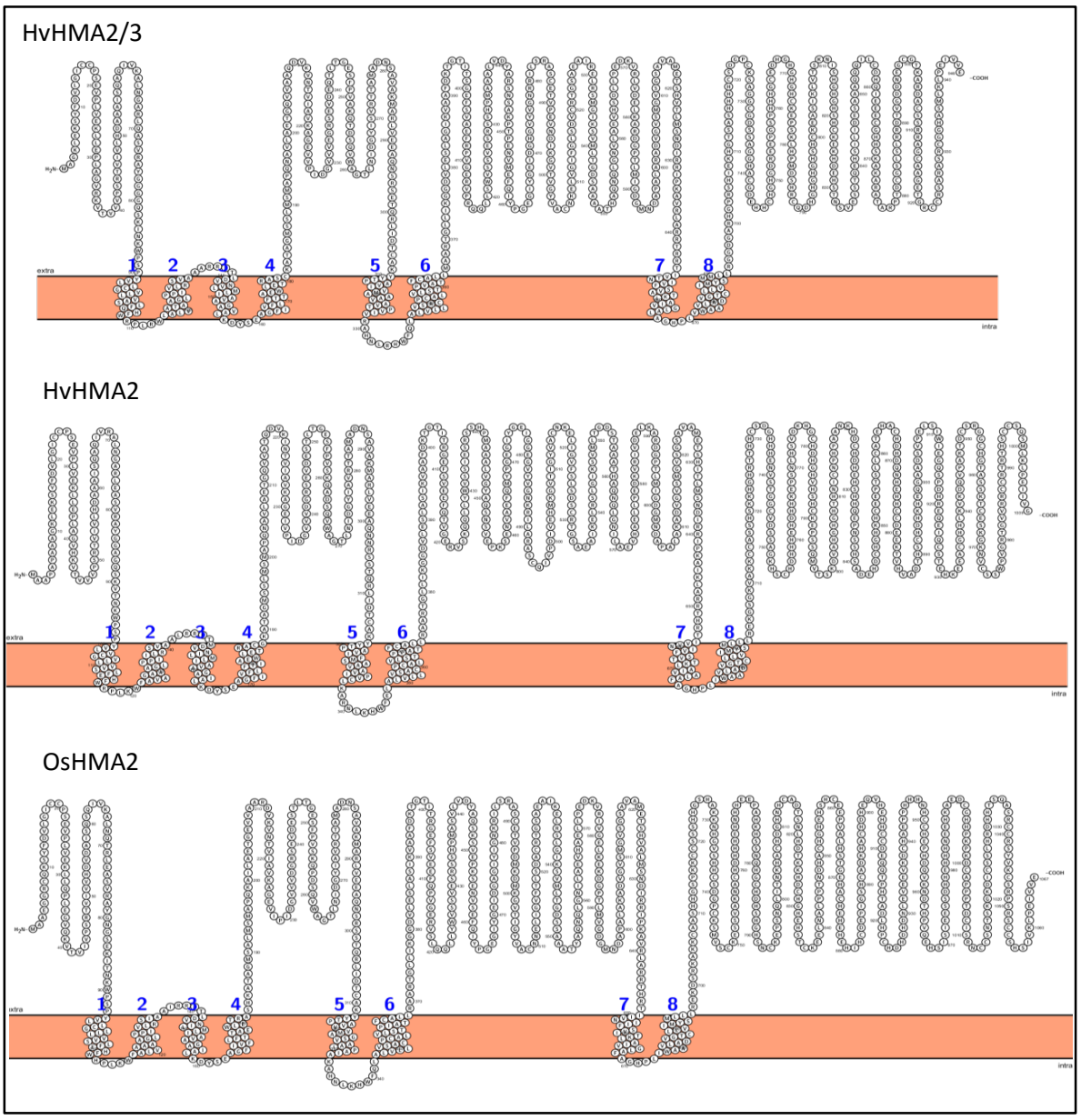

Figure 5.2 The predicted membrane protein topology of P_{1B-2}-ATPases in barley and rice.

Membrane protein topology diagrams showing 2D structure of the HvHMA2/3, HvHMA2, OsHMA2, HvHMA3, and OsHMA3 based on consensus topology prediction using SOSUI (http://harrier.nagahama-i-bio.ac.jp/sosui/sosui_submit.html). Diagrams drawn using Protter (http://wlab.ethz.ch/protter/#).

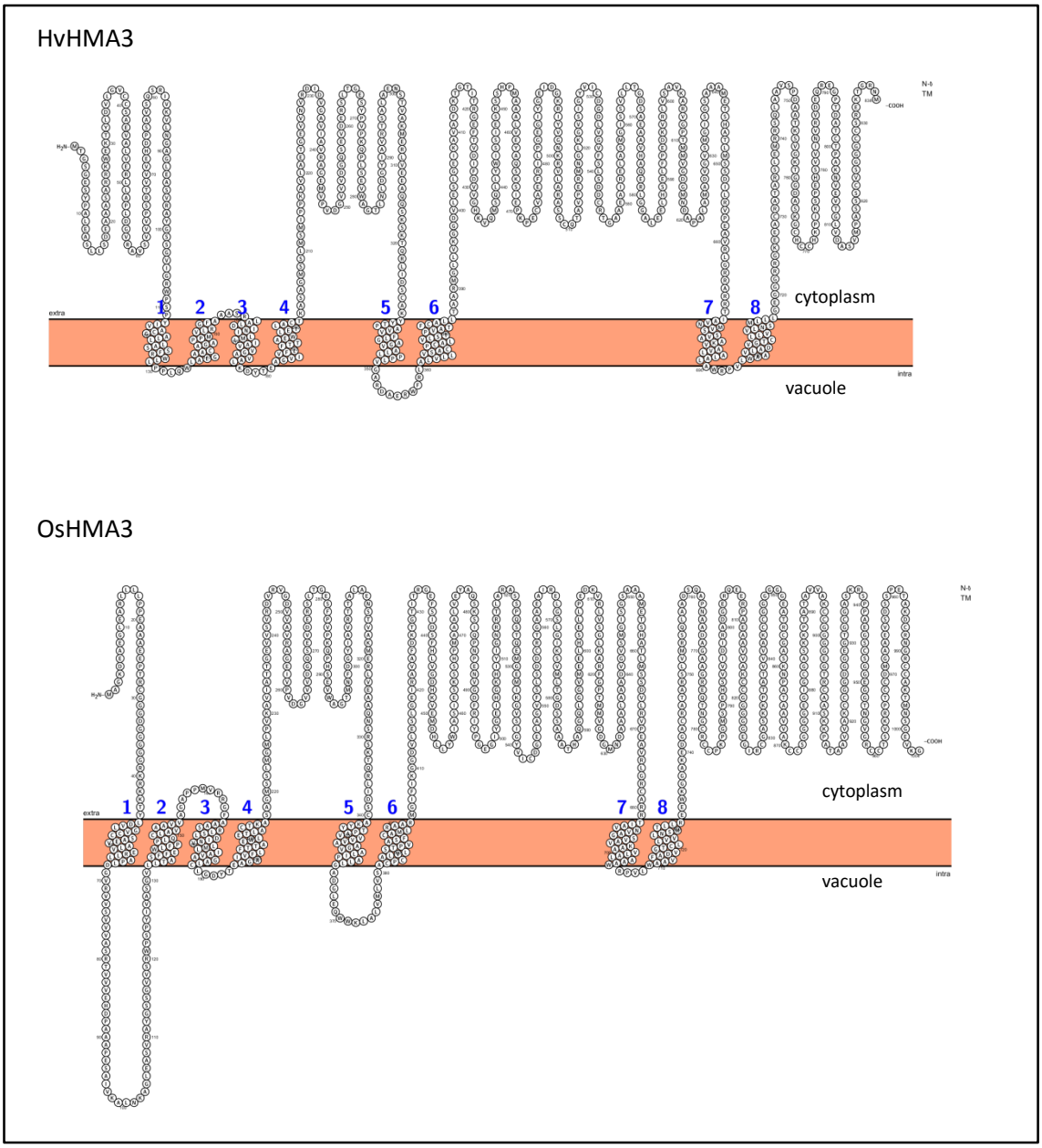

Figure 5.2 continued

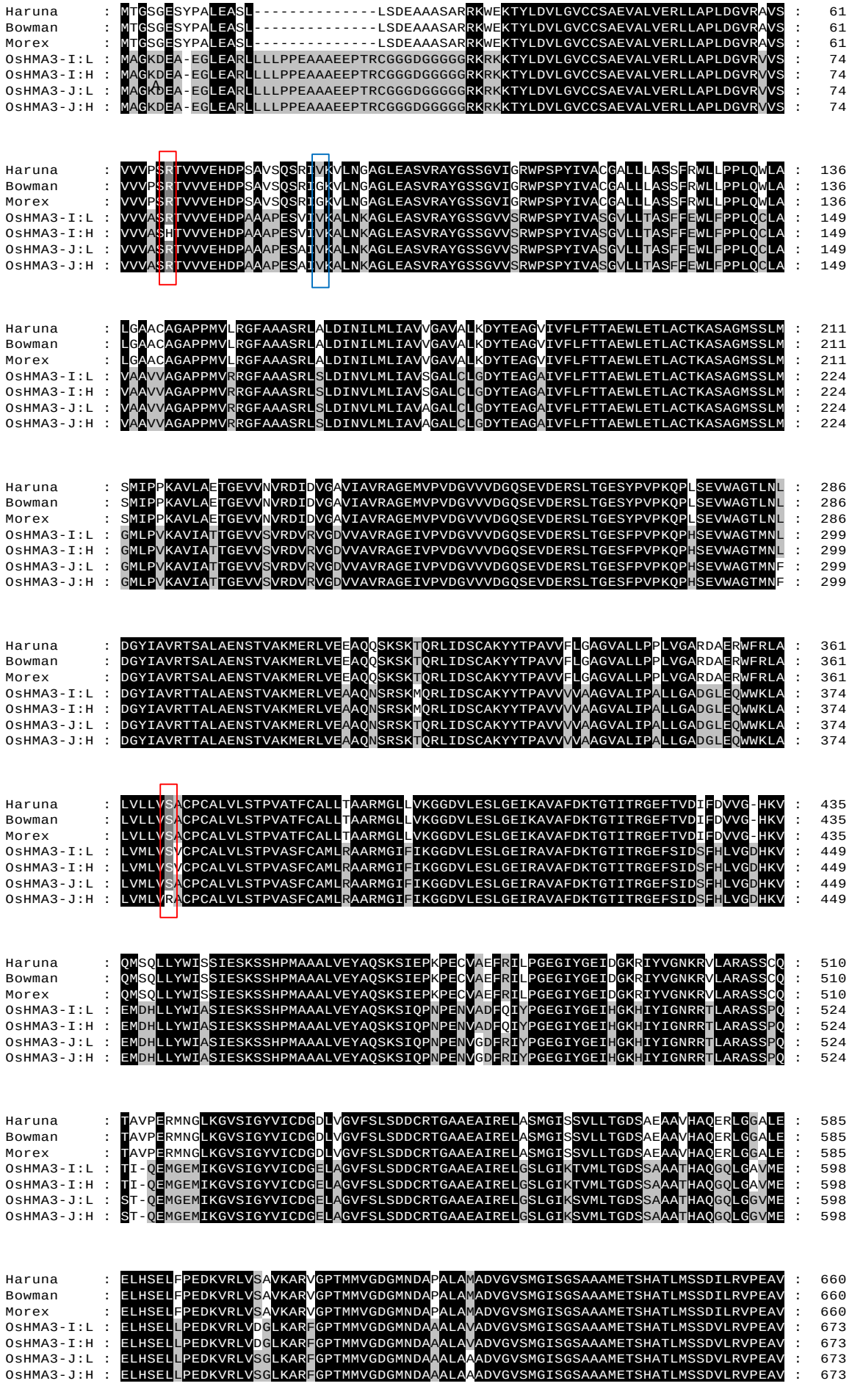
Haruna : MTGSGESYPALEASL--------------LSDEAAASARRKWEKTYLDVLGVCCSAEVALVERLLAPLDGVRAVS : 61
Bowman : MTGSGESYPALEASL--------------LSDEAAASARRKWEKTYLDVLGVCCSAEVALVERLLAPLDGVRAVS : 61
Morex : MTGSGESYPALEASL--------------LSDEAAASARRKWEKTYLDVLGVCCSAEVALVERLLAPLDGVRAVS : 61
OsHMA3-I:L : MAGKDEA-EGLEARLLLLPPEAAAEEPTRCGGGDGGGGGRKRKKTYLDVLGVCCSAEVALVERLLAPLDGVRVVS : 74
OsHMA3-I:H : MAGKDEA-EGLEARLLLLPPEAAAEEPTRCGGGDGGGGGRKRKKTYLDVLGVCCSAEVALVERLLAPLDGVRVVS : 74
OsHMA3-J:L : MAGKDEA-EGLEARLLLLPPEAAAEEPTRCGGGDGGGGGRKRKKTYLDVLGVCCSAEVALVERLLAPLDGVRVVS : 74
OsHMA3-J:H : MAGKDEA-EGLEARLLLLPPEAAAEEPTRCGGGDGGGGGRKRKKTYLDVLGVCCSAEVALVERLLAPLDGVRVVS : 74
Haruna : VVVPSRTVVVEHDPSAVSQSRIVKVLNGAGLEASVRAYGSSGVIGRWPSPYIVACGALLLASSFRWLLPPLQWLA : 136
Bowman : VVVPSRTVVVEHDPSAVSQSRIGKVLNGAGLEASVRAYGSSGVIGRWPSPYIVACGALLLASSFRWLLPPLQWLA : 136
Morex : VVVPSRTVVVEHDPSAVSQSRIGKVLNGAGLEASVRAYGSSGVIGRWPSPYIVACGALLLASSFRWLLPPLQWLA : 136
OsHMA3-I:L : VVVASRTVVVEHDPAAAPESVIVKALNKAGLEASVRAYGSSGVVSRWPSPYIVASGVLLTASFFEWLFPPLQCLA : 149
OsHMA3-I:H : VVVASHTVVVEHDPAAAPESVIVKALNKAGLEASVRAYGSSGVVSRWPSPYIVASGVLLTASFFEWLFPPLQCLA : 149
OsHMA3-J:L : VVVASRTVVVEHDPAAAPESAIVKALNKAGLEASVRAYGSSGVVSRWPSPYIVASGVLLTASFFEWLFPPLQCLA : 149
OsHMA3-J:H : VVVASRTVVVEHDPAAAPESAIVKALNKAGLEASVRAYGSSGVVSRWPSPYIVASGVLLTASFFEWLFPPLQCLA : 149
Haruna : LGAACAGAPPMVLRGFAAASRLALDINILMLIAVVGAVALKDYTEAGVIVFLFTTAEWLETLACTKASAGMSSLM : 211
Bowman : LGAACAGAPPMVLRGFAAASRLALDINILMLIAVVGAVALKDYTEAGVIVFLFTTAEWLETLACTKASAGMSSLM : 211
Morex : LGAACAGAPPMVLRGFAAASRLALDINILMLIAVVGAVALKDYTEAGVIVFLFTTAEWLETLACTKASAGMSSLM : 211
OsHMA3-I:L : VAAVVAGAPPMVRRGFAAASRLSLDINVLMLIAVSGALCLGDYTEAGAIVFLFTTAEWLETLACTKASAGMSSLM : 224
OsHMA3-I:H : VAAVVAGAPPMVRRGFAAASRLSLDINVLMLIAVSGALCLGDYTEAGAIVFLFTTAEWLETLACTKASAGMSSLM : 224
OsHMA3-J:L : VAAVVAGAPPMVRRGFAAASRLSLDINVLMLIAVAGALCLGDYTEAGAIVFLFTTAEWLETLACTKASAGMSSLM : 224
OsHMA3-J:H : VAAVVAGAPPMVRRGFAAASRLSLDINVLMLIAVAGALCLGDYTEAGAIVFLFTTAEWLETLACTKASAGMSSLM : 224
Haruna : SMIPPKAVLAETGEVVNVRDIDVGAVIAVRAGEMVPVDGVVVDGQSEVDERSLTGESYPVPKQPLSEVWAGTLNL : 286
Bowman : SMIPPKAVLAETGEVVNVRDIDVGAVIAVRAGEMVPVDGVVVDGQSEVDERSLTGESYPVPKQPLSEVWAGTLNL : 286
Morex : SMIPPKAVLAETGEVVNVRDIDVGAVIAVRAGEMVPVDGVVVDGQSEVDERSLTGESYPVPKQPLSEVWAGTLNL : 286
OsHMA3-I:L : GMLPVKAVIATTGEVVSVRDVRVGDVVAVRAGEIVPVDGVVVDGQSEVDERSLTGESFPVPKQPHSEVWAGTMNL : 299
OsHMA3-I:H : GMLPVKAVIATTGEVVSVRDVRVGDVVAVRAGEIVPVDGVVVDGQSEVDERSLTGESFPVPKQPHSEVWAGTMNL : 299
OsHMA3-J:L : GMLPVKAVIATTGEVVSVRDVRVGDVVAVRAGEIVPVDGVVVDGQSEVDERSLTGESFPVPKQPHSEVWAGTMNF : 299
OsHMA3-J:H : GMLPVKAVIATTGEVVSVRDVRVGDVVAVRAGEIVPVDGVVVDGQSEVDERSLTGESFPVPKQPHSEVWAGTMNF : 299
Haruna : DGYIAVRTSALAENSTVAKMERLVEEAQQSKSKTQRLIDSCAKYYTPAVVFLGAGVALLPPLVGARDAERWFRLA : 361
Bowman : DGYIAVRTSALAENSTVAKMERLVEEAQQSKSKTQRLIDSCAKYYTPAVVFLGAGVALLPPLVGARDAERWFRLA : 361
Morex : DGYIAVRTSALAENSTVAKMERLVEEAQQSKSKTQRLIDSCAKYYTPAVVFLGAGVALLPPLVGARDAERWFRLA : 361
OsHMA3-I:L : DGYIAVRTTALAENSTVAKMERLVEAAQNSRSKMQRLIDSCAKYYTPAVVVVAAGVALIPALLGADGLEQWWKLA : 374
OsHMA3-I:H : DGYIAVRTTALAENSTVAKMERLVEAAQNSRSKMQRLIDSCAKYYTPAVVVVAAGVALIPALLGADGLEQWWKLA : 374
OsHMA3-J:L : DGYIAVRTTALAENSTVAKMERLVEAAQNSRSKTQRLIDSCAKYYTPAVVVVAAGVALIPALLGADGLEQWWKLA : 374
OsHMA3-J:H : DGYIAVRTTALAENSTVAKMERLVEAAQNSRSKTQRLIDSCAKYYTPAVVVVAAGVALIPALLGADGLEQWWKLA : 374
Haruna : LVLLVSACPCALVLSTPVATFCALLTAARMGLLVKGGDVLESLGEIKAVAFDKTGTITRGEFTVDIFDVVG-HKV : 435
Bowman : LVLLVSACPCALVLSTPVATFCALLTAARMGLLVKGGDVLESLGEIKAVAFDKTGTITRGEFTVDIFDVVG-HKV : 435
Morex : LVLLVSACPCALVLSTPVATFCALLTAARMGLLVKGGDVLESLGEIKAVAFDKTGTITRGEFTVDIFDVVG-HKV : 435
OsHMA3-I:L : LVMLVSVCPCALVLSTPVASFCAMLRAARMGIFIKGGDVLESLGEIRAVAFDKTGTITRGEFSIDSFHLVGDHKV : 449
OsHMA3-I:H : LVMLVSVCPCALVLSTPVASFCAMLRAARMGIFIKGGDVLESLGEIRAVAFDKTGTITRGEFSIDSFHLVGDHKV : 449
OsHMA3-J:L : LVMLVSACPCALVLSTPVASFCAMLRAARMGIFIKGGDVLESLGEIRAVAFDKTGTITRGEFSIDSFHLVGDHKV : 449
OsHMA3-J:H : LVMLVRACPCALVLSTPVASFCAMLRAARMGIFIKGGDVLESLGEIRAVAFDKTGTITRGEFSIDSFHLVGDHKV : 449
Haruna : QMSQLLYWISSIESKSSHPMAAALVEYAQSKSIEPKPECVAEFRILPGEGIYGEIDGKRIYVGNKRVLARASSCQ : 510
Bowman : QMSQLLYWISSIESKSSHPMAAALVEYAQSKSIEPKPECVAEFRILPGEGIYGEIDGKRIYVGNKRVLARASSCQ : 510
Morex : QMSQLLYWISSIESKSSHPMAAALVEYAQSKSIEPKPECVAEFRILPGEGIYGEIDGKRIYVGNKRVLARASSCQ : 510
OsHMA3-I:L : EMDHLLYWIASIESKSSHPMAAALVEYAQSKSIQPNPENVADFQIYPGEGIYGEIHGKHIYIGNRRTLARASSPQ : 524
OsHMA3-I:H : EMDHLLYWIASIESKSSHPMAAALVEYAQSKSIQPNPENVADFQIYPGEGIYGEIHGKHIYIGNRRTLARASSPQ : 524
OsHMA3-J:L : EMDHLLYWIASIESKSSHPMAAALVEYAQSKSIQPNPENVGDFRIYPGEGIYGEIHGKHIYIGNRRTLARASSPQ : 524
OsHMA3-J:H : EMDHLLYWIASIESKSSHPMAAALVEYAQSKSIQPNPENVGDFRIYPGEGIYGEIHGKHIYIGNRRTLARASSPQ : 524
Haruna : TAVPERMNGLKGVSIGYVICDGDLVGVFSLSDDCRTGAAEAIRELASMGISSVLLTGDSAEAAVHAQERLGGALE : 585
Bowman : TAVPERMNGLKGVSIGYVICDGDLVGVFSLSDDCRTGAAEAIRELASMGISSVLLTGDSAEAAVHAQERLGGALE : 585
Morex : TAVPERMNGLKGVSIGYVICDGDLVGVFSLSDDCRTGAAEAIRELASMGISSVLLTGDSAEAAVHAQERLGGALE : 585
OsHMA3-I:L : TI-QEMGEMIKGVSIGYVICDGELAGVFSLSDDCRTGAAEAIRELGSLGIKTVMLTGDSSAAATHAQGQLGAVME : 598
OsHMA3-I:H : TI-QEMGEMIKGVSIGYVICDGELAGVFSLSDDCRTGAAEAIRELGSLGIKTVMLTGDSSAAATHAQGQLGAVME : 598
OsHMA3-J:L : ST-QEMGEMIKGVSIGYVICDGELAGVFSLSDDCRTGAAEAIRELGSLGIKSVMLTGDSSAAATHAQGQLGGVME : 598
OsHMA3-J:H : ST-QEMGEMIKGVSIGYVICDGELAGVFSLSDDCRTGAAEAIRELGSLGIKSVMLTGDSSAAATHAQGQLGGVME : 598
Haruna : ELHSELFPEDKVRLVSAVKARVGPTMMVGDGMNDAPALAMADVGVSMGISGSAAAMETSHATLMSSDILRVPEAV : 660
Bowman : ELHSELFPEDKVRLVSAVKARVGPTMMVGDGMNDAPALAMADVGVSMGISGSAAAMETSHATLMSSDILRVPEAV : 660
Morex : ELHSELFPEDKVRLVSAVKARVGPTMMVGDGMNDAPALAMADVGVSMGISGSAAAMETSHATLMSSDILRVPEAV : 660
OsHMA3-I:L : ELHSELLPEDKVRLVDGLKARFGPTMMVGDGMNDAAALAVADVGVSMGISGSAAAMETSHATLMSSDVLRVPEAV : 673
OsHMA3-I:H : ELHSELLPEDKVRLVDGLKARFGPTMMVGDGMNDAAALAVADVGVSMGISGSAAAMETSHATLMSSDVLRVPEAV : 673
OsHMA3-J:L : ELHSELLPEDKVRLVSGLKARFGPTMMVGDGMNDAAALAAADVGVSMGISGSAAAMETSHATLMSSDVLRVPEAV : 673
OsHMA3-J:H : ELHSELLPEDKVRLVSGLKARFGPTMMVGDGMNDAAALAAADVGVSMGISGSAAAMETSHATLMSSDVLRVPEAV : 673

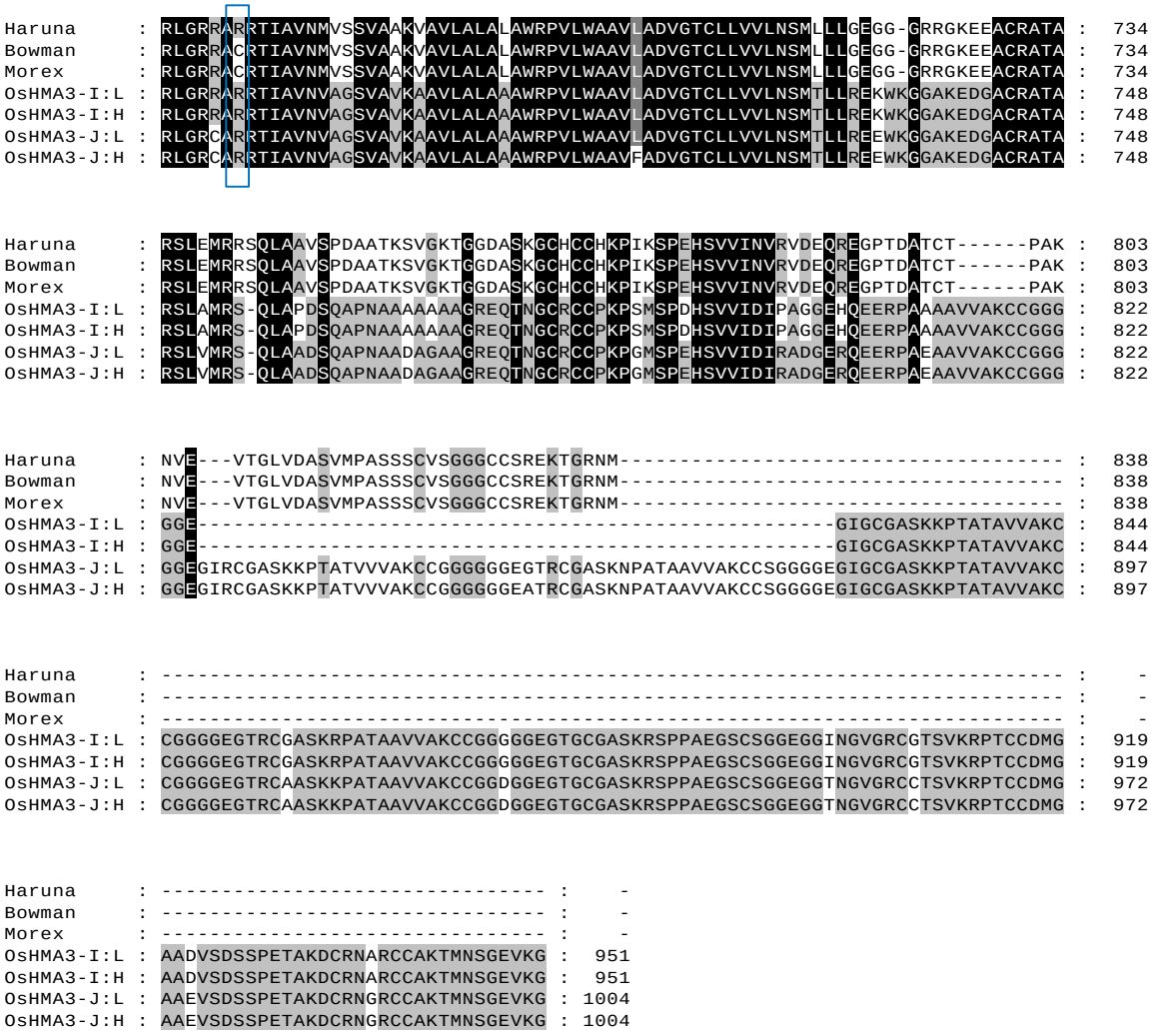

Figure 5.3 Alignment of HMA3 amino acid sequences from different barley and rice cultivars. HvHMA3 from Haruna Nijo (HvHMA3-H), Bowman (HvHMA3-B), and Morex (HvHMA3-M) with OsHMA3 from low Cd accumulation *Indica* cultivar (OsHMA3-I:L), high Cd accumulation Indica cultivar (OsHMA3-I:H), low Cd accumulation *Japonica* (OsHMA3-J:L), and high Cd accumulation *Japonica* cultivar (OsHMA3-J:H) were aligned using the Clustal Omega algorithm (Sievers et al., 2011) and presented using GeneDoc (Nicholas and Nicholas Jr, 1997). For the sequence aligned here: black = conserved residues, dark grey = 6 of 7 proteins, light grey = conserved 5 of 7 proteins. Red box indicates the position of non-functional OsHMA3 alleles and blue box indicates HvHMA3 residues differing in Haruna Nijo, Bowman, and Morex.

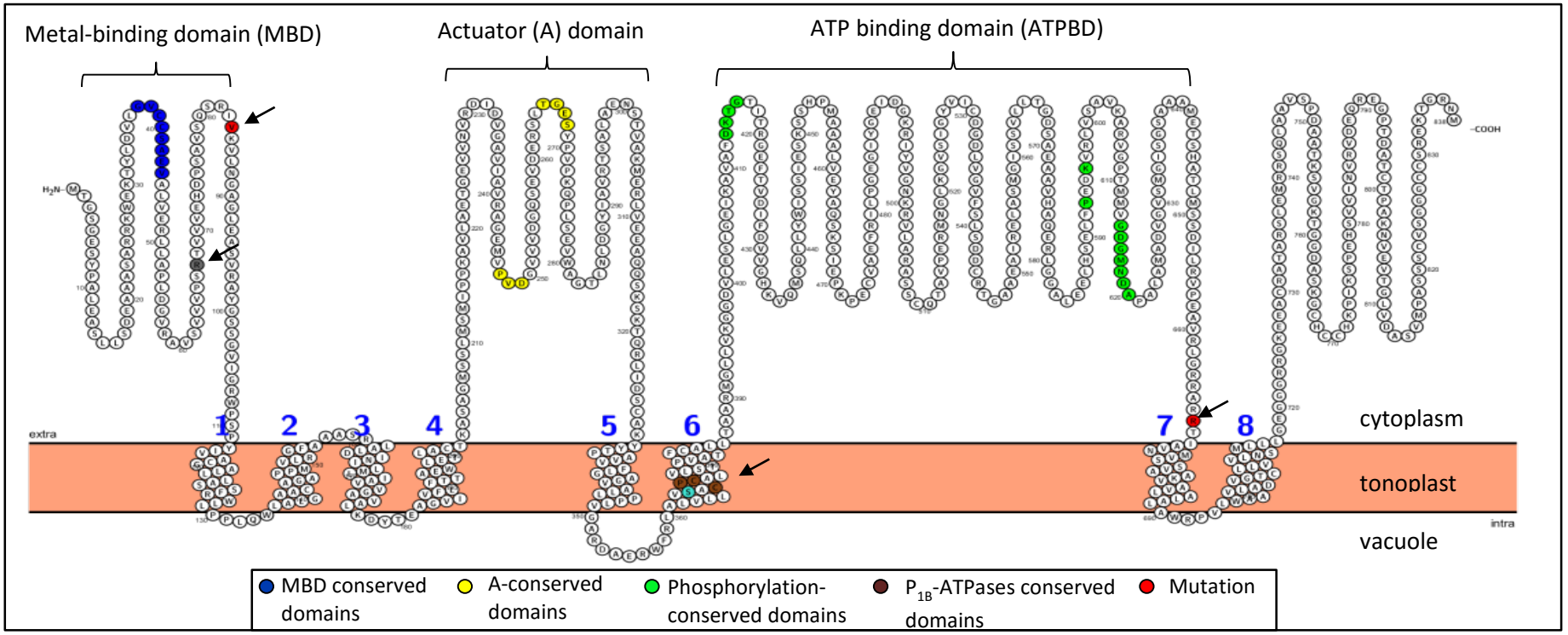

Figure 5.4 The predicted membrane protein topology of the Haruna Nijo HvHMA3 used in this study.

Membrane protein topology diagrams showing 2D structure of the HvHMA3 based on consensus topology prediction using SOSUI (http://harrier.nagahama-i-bio.ac.jp/sosui/sosui_submit.html). Diagrams drawn using Protter (http://wlab.ethz.ch/protter/#). Highlighted residues are predicted to be conserved metal binding domain (blue), conserved actuator domains (yellow), conserved phosphorylation domains (green), conserved P_{1B}-ATPases domain (TM-6; pink) or conserved in the third TM region (TM-3; pink). The mutated amino acids are in red and indicated by an arrow.

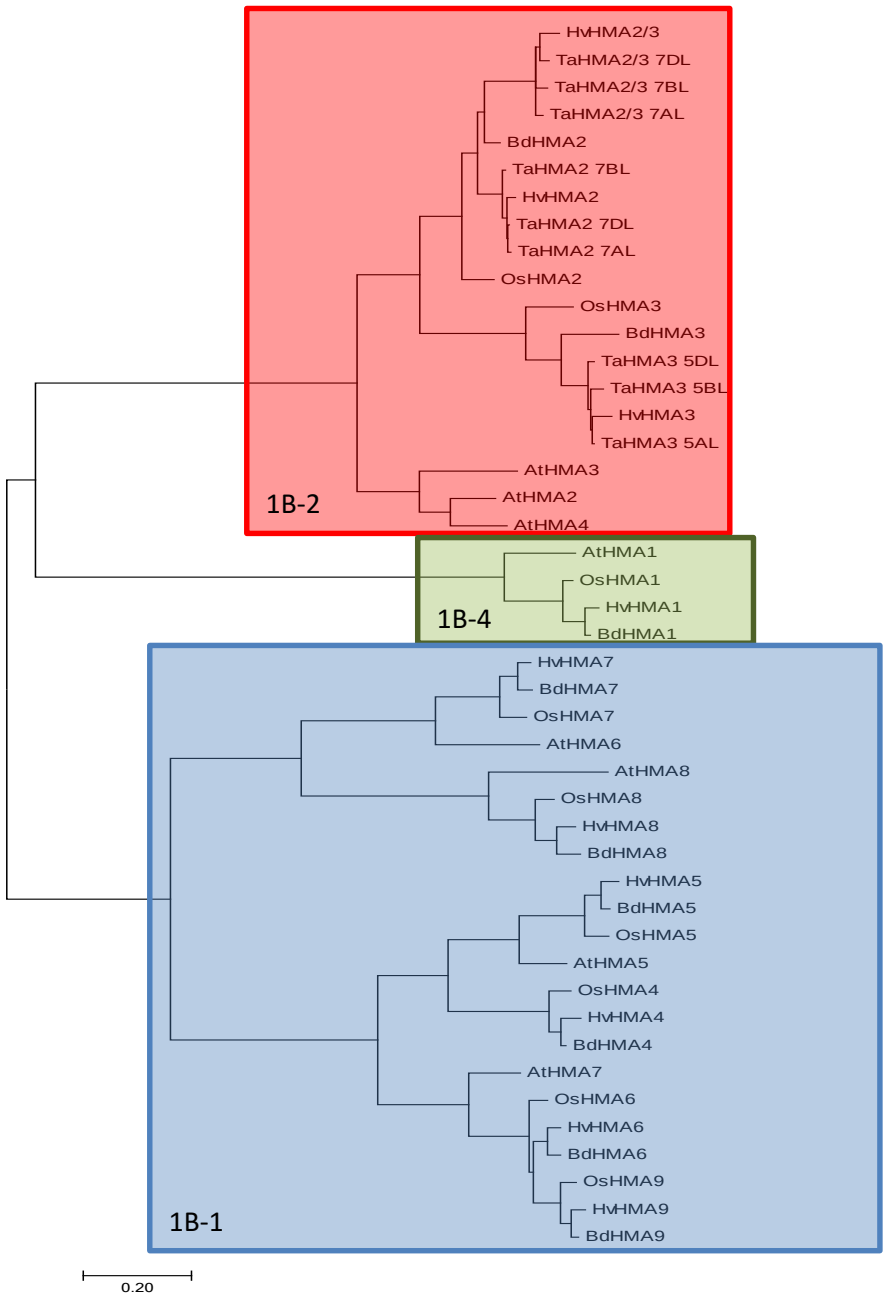

Figure 5.5 Phylogenetic analyses of P_{1B}-ATPases from a range of plant species.

The phylogenetic analyses shows a non-rooted, bootstrapped plot (1000 replicates) constructed using a multiple alignment of P_{1B}-ATPases identified in this study and also taken from Mills et al. (2012). The tree was constructed using MEGA 7 (Kumar et al., 2016). The tree is drawn to scale, with branch lengths in the same units as those of the evolutionary distances used to infer the phylogenetic tree. The evolutionary distances were computed using the Poisson correction method (Zuckerkandl and Pauling 1965) and are in the units of the number of amino acid substitutions per site.The P_{1B}-ATPases here fall into 1B-1 (purple box), 1B-2 (red box) and 1B-4 (green box) subgroups. Accession numbers and identifier of the predicted proteins are listed in Appendix 3.

in Poaceae species constituted a first subgroup, P_{1B-1}. The P_{1B-2} constituted the orthologues of AtHMA2, AtHMA3 and AtHMA4. The P_{1B-4} subgroup could be capable of transporting one or more of the group – Zn, Co and Cu based on genetic and functional studies of the *A. thaliana* and barley P_{1B}-ATPases. AtHMA1 and its orthologues in Poaceae species constituted a P_{1B-4} subgroup. Based on genetic and functional studies of the *A. thaliana* P_{1B}-ATPases, the membrane transporter proteins in P_{1B-1} subgroup are predicted to be capable of transporting Cu and potentially Ag, whereas the membrane transporter proteins in P_{1B-2} subgroup could transport Zn, Cd and Pb.

Another phylogenetic analysis was also performed on the second subgroup, P_{1B-2}, but also includes P_{1B-2}-ATPases from Brassicaceae and other dicotyledons taken from Zorrig et al. (2011)). Based on the P_{1B-2}-ATPase phylogenetic tree, there are three main groups: Brassicaceae, other dicotyledons, and Poaceae (Figure 5.6). Within Poaceae group, two separate clades grouping orthologues of OsHMA2 in one and orthologues of OsHMA3 in the other (Figure 5.6). TaHMA2/3 homeologues and HvHMA2/3 are closer phylogenetically to TaHMA2 homeologues and HvHMA2 than to TaHMA3 homeologues and HvHMA3 (Figure 5.6).

5.2.6 Isolation of T-DNA insertion *hma3 mtp1* double mutants

A. thaliana MTP1 is involved in Zn detoxification by sequestering excess Zn into the vacuole. The *mtp1-1* mutant is sensitive to Zn, compared to WT (Kobae et al., 2004, Menguer et al., 2013). AtHMA3 is also suggested to have a role in vacuolar Zn detoxification. The T-DNA insertion mutant known as *hma3-1* was found to be sensitive to Zn and Cd compared to WT (Morel et al., 2009). In this project, the effect of disrupting both AtMTP1 and AtHMA3 in *A. thaliana* on Zn and Cd was investigated to learn more about their relative role in heavy metal tolerance. To do this, single mutants were crossed to generate a *mtp1-1 hma3-2* double mutant. The *mtp1-1* mutant has been described previously (Kobae et al., 2004) and it was already available in the lab. The *hma3-1* mutant has been isolated by Hussain et al. (2004) and characterised previously by Morel et al. (2009). Here we isolated a novel mutant allele, *hma3-2* and also used the *hma3-1* mutant.

The AtHMA3 AGI code (AT4G30120.1) was used to search the Arabidopsis Information Resource (TAIR) website (http://www.arabidopsis.org/) and used to find available *AtHMA3* T-DNA insertion mutant lines in the T-DNA database website (http://signal.salk.edu/cgi-bin/tdnaexpress). There were thirteen available T-DNA insertion lines for *AtHMA3* but the *hma3-1* (N799967) and the FLAG_542C11 line (*hma3-2*) were chosen because the background of this line was Wassilewskija (Ws), which was same as for the *mtp1-1* mutant. The T-DNA insertion site was predicted by aligning FLAG_542C11 sequence with the AtHMA3 genomic and coding sequence and found to lie just after the second exon. AtHMA3F primer and AtHMA3R primer were

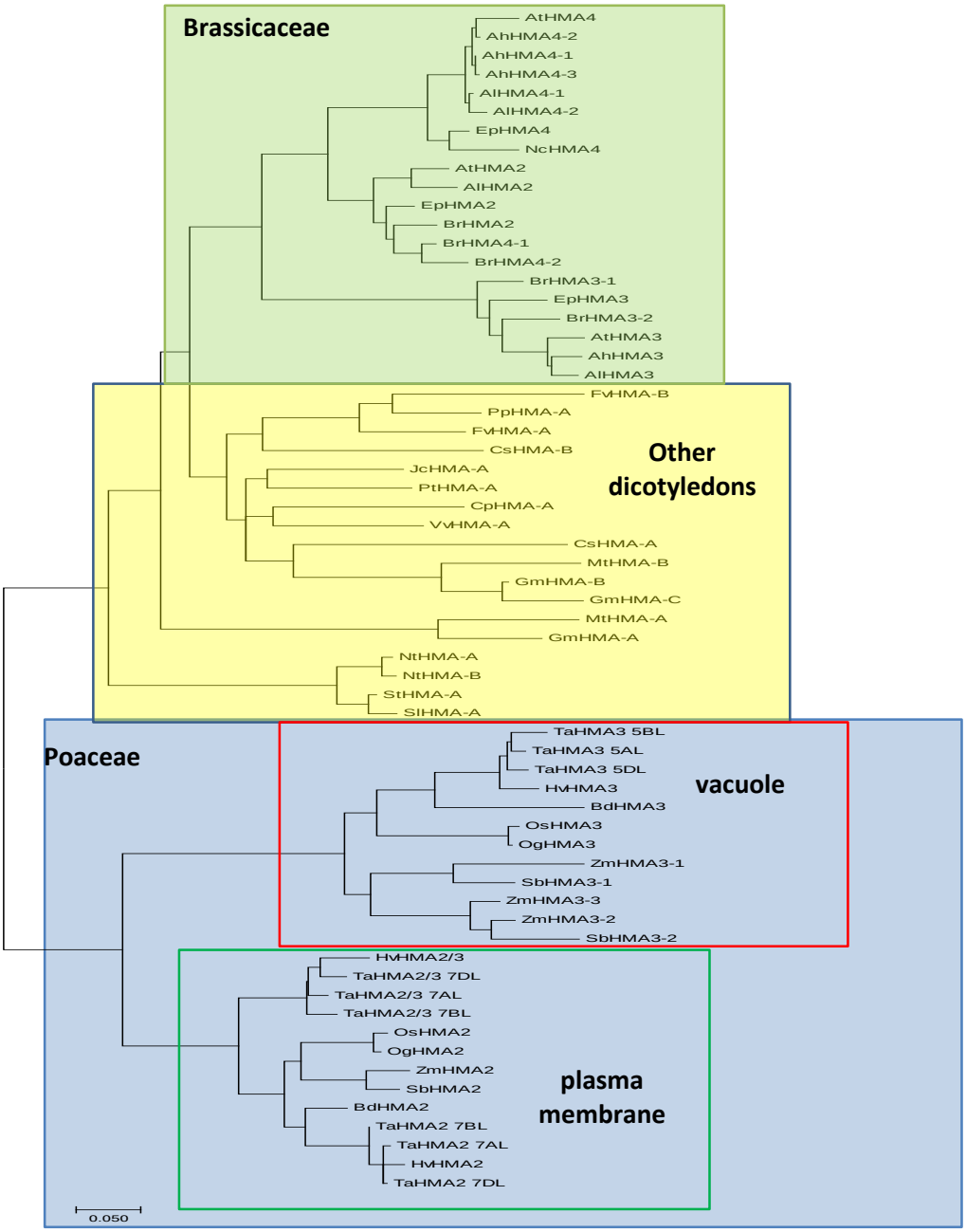

Figure 5.6 Phylogenetic analyses of the P_{1B-2}-ATPases family.

The phylogenetic analyses shows a non-rooted, bootstrapped plot (1000 replicates) constructed using a multiple alignment of P_{1B-2}-ATPases taken from Zorrig et al. (2011), Mills et al. (2012) and this study. The tree was constructed using MEGA 7 (Kumar et al., 2016). The tree is drawn to scale, with branch lengths in the same units as those of the evolutionary distances used to infer the phylogenetic tree. The evolutionary distances were computed using the Poisson correction method (Zuckerkandl and Pauling 1965) and are in the units of the number of amino acid substitutions per site. The P_{1B-2}-ATPases here were fall into Brassicaceae (green box), Poaceae (blue box) and other cotyledons (yellow box) groups. The Poaceae P_{1B-2}-ATPases can be further divided into two subgroups: localised in vacuole (red) and plasma membrane (green). Accession numbers and identifier of the predicted proteins are listed in Appendix 3.

specifically designed based on the alignment to amplify a PCR product that spanned the *hma3-1* and *hma3-2* predicted insertion site. Seed stock of *hma3-1* was obtained from the European Arabidopsis Stock Centre (NASC) while seed stock of *hma3-2* the Versailles Arabidopsis Stock Centre (INRA). The *hma3-1* was homozygous, while *hma3-2* was a segregating mutant population meaning homozygous seed had to be obtained from the progeny of this mutant.

The genotyping of the potential single mutants is shown in Figure 5.7. This procedure was carried out for ten plants for each line and representative are shown. A WT PCR product for *AtHMA3* can be detected by amplification by AtHMA3F primer and AtHMA3R primer; these were predicted to yield a 986bp PCR product. Meanwhile to check the presence of a T-DNA insert, AtHMA3F and the T-DNA left border primer were used (JL202 for *hma3-1* and LBT-DNA for *hma3-2*). The amplification with these two sets of primers indicated that both mutants were homozygous (Figure 5.7).

Two sets of *mtp1 hma3* double mutants were generated (*hma3-1 mtp1-1* and *mtp1-1 hma3-2*). Four progeny from the crossed plants were grown to obtain a heterozygous plant, confirmed by PCR. Figure 5.8 shows the results confirming the cross to generate a heterozygote for each cross. As the maternal plant for the first set of double mutant was a *hma3-1* mutant, the plants were initially checked for a *mtp1-1* insertion. Three sets of primers were used: (A) AtMTP1F + AtMTP1R, (B) AtMTP1 + LBT-DNA and (C) AtMTP1F (Kobae) + LBT-DNA. LBT-DNA was a T-DNA insertion left-border primer. For the second set of double mutant, its maternal plant was *mtp1-1*. So, the plants were initially checked for *hma3-1* insertion. Three sets of primers were used: (A) AtHMA3F + AtHMA3R, (B) AtHMA3F + LBT-DNA and (C) AtHMA3F + Flag TDNA fLB. LBT-DNA and Flag TDNA fLB were T-DNA insertion left-border primers. The plants at this stage were expected to produce a product with each set of primers detecting inserts in *AtMTP1* for *hma3-1 mtp1-1 or* in *AtHMA3* for *mtp1-1 hma3-2*, indicating that they were heterozygous double mutants. Progeny from both crosses seemed to be heterozygous since all of them had WT bands and the two T-DNA left border bands (Figure 5.8). Thirty-two of the progeny (F2) from the heterozygous plant were grown and genotyped with PCR, until a homozygous plant was isolated. An example PCR of the genotyping for the progeny from these crosses for the particular homozygote isolated is shown in Figure 5.9. Genotyping was carried out on three separate individual genomic preparations to confirm that the plant was a double mutant.

To determine the exact position of T-DNA within *hma3-2* mutants isolated in this study, the product obtained with AtHMA3F and LBT-DNA (Kobae) primers of confirmed homozygous: homozygous plants were extracted from the gel, purified, and sequenced. Meanwhile, the *hma3-1* line and the *mtp1-1* line were not yet sequenced but Hussain et al. (2004) claims that the T-DNA

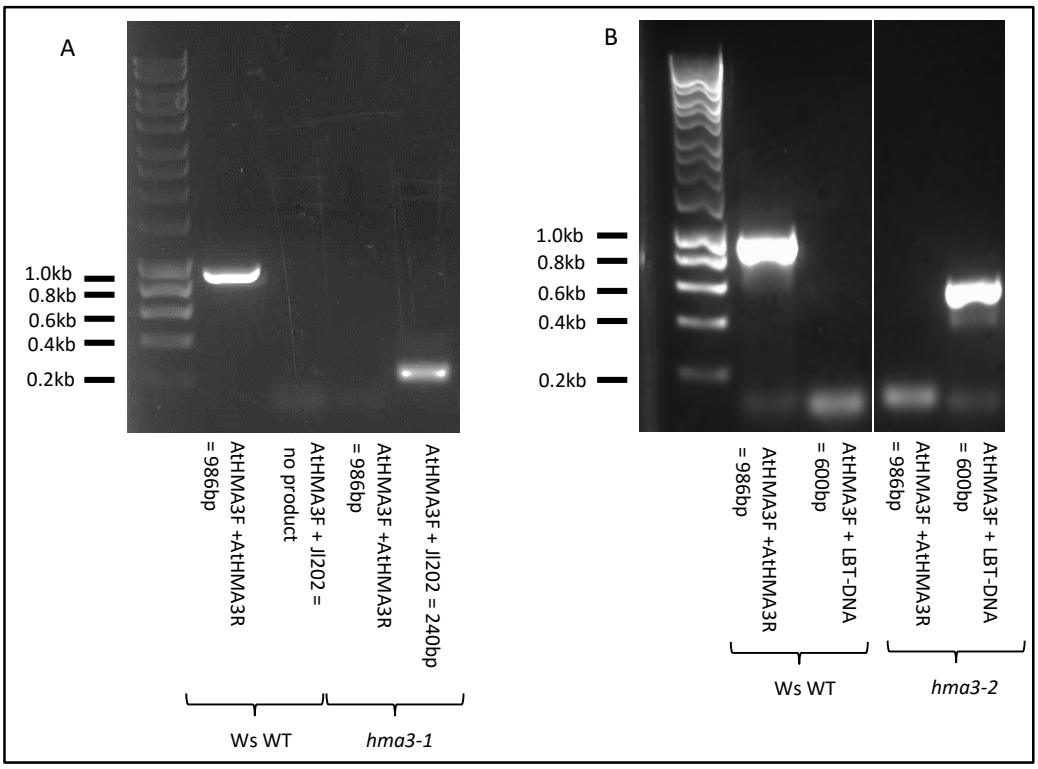

Figure 5.7 Genotyping potential *hma3-1* (A) and *hma3-2* (B) mutant lines.

DNA isolated from individual plants was amplified with a few sets of primers (AtHMA3F+AtHMA3R for both *hma3-1* and *hma3-2*, AtHMA3F+JL202 for *hma3-1* only, and AtHMA3F+LBT-DNA for *hma3-2* only) for genotyping. Genomic DNA from Ws WT plants was also included in the reaction as a control to amplify a WT product. The molecular weight markers are shown next to the gel image and the product size of each reaction is shown in below the gel image.

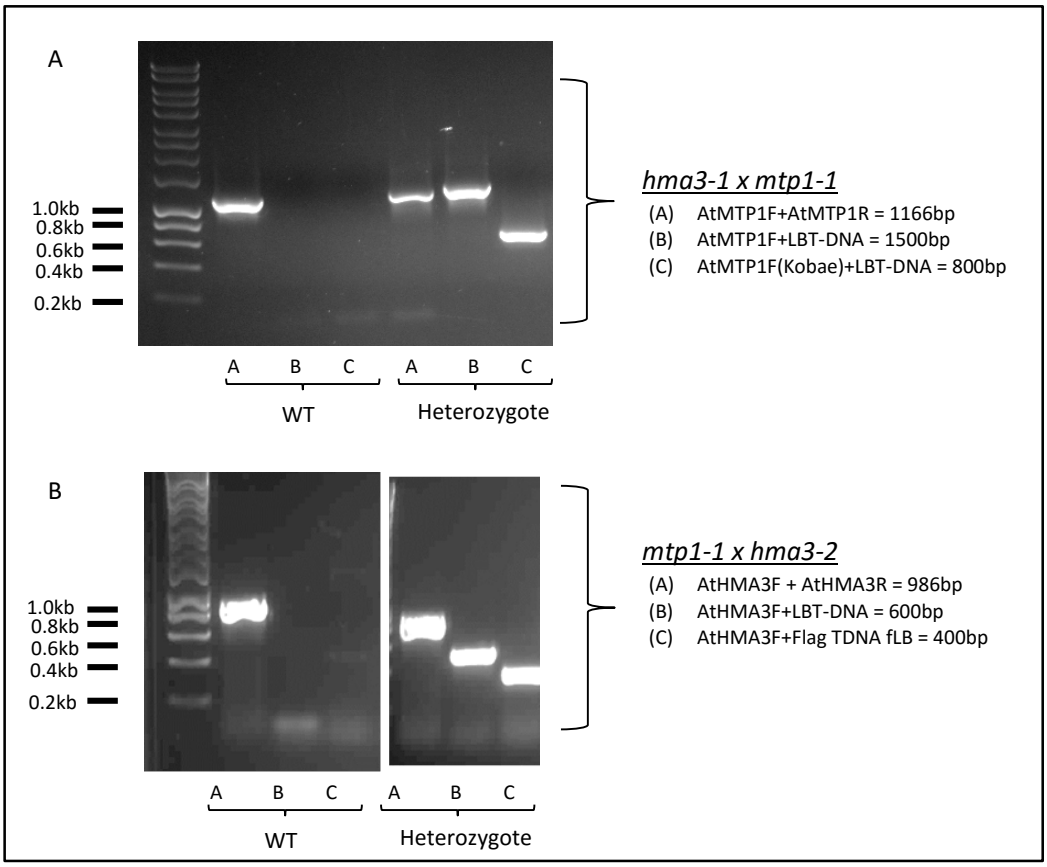

Figure 5.8 Genotyping crossed progenies: *hma3-1 x mtp1-1* (A), and *mtp1-1 x hma3-1* amplified with three sets of primer to determine their genotype.

In each genotyping with PCR, WT plants are included in the reaction as a control. The molecular weight marker and the expected PCR products sizes are indicated next to the gel image.

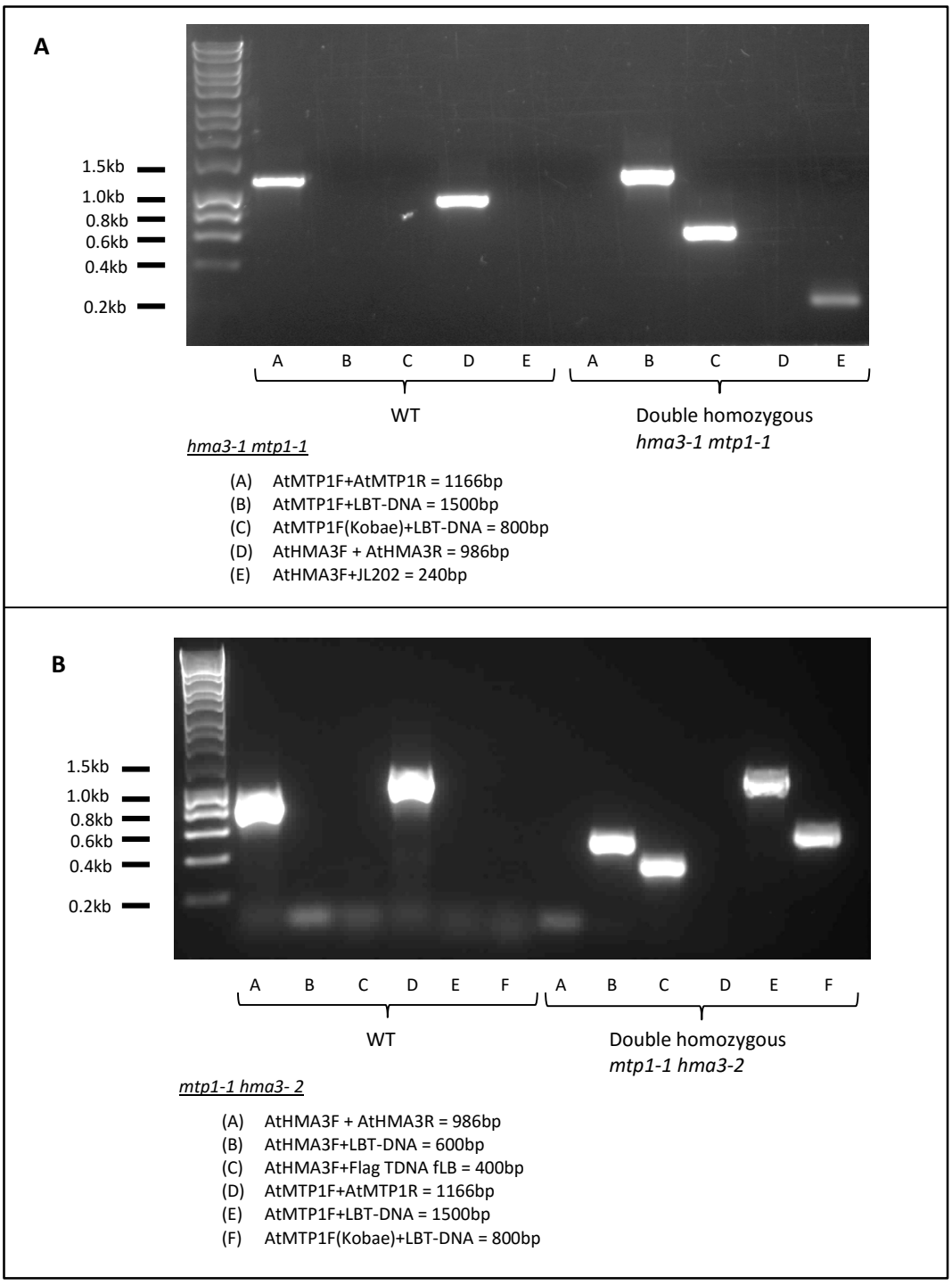

Figure 5.9 The screening of potential homozygous: homozygous *hma3-1 mtp1-1* (A) and *mtp1-1 hma3-2* (B) F2 plants.

A WT plant is also included in the reaction as a control. The molecular weight marker and the expected PCR product sizes are mentioned next to the corresponding gel image.

insert is 139bp from the start codon of the *AtHMA3* and for *mtp1-1*, the T-DNA insert is 1035bp from the start codon of AtMTP1 (Kobae et al., 2004). Based on the sequencing analyses, the T-DNA insert site for *hma3-2* was 387bp from the start codon (Figure 5.10).

To confirm whether these unique double mutants were knockout mutants, it was important to characterise these lines at the mRNA level. RNA from these double mutants were extracted and cDNA generated. The *AtHMA3* and *AtMTP1* expression was tested by amplifying WT products (567bp of *AtHMA3* and 1166bp of *AtMTP1*) (Figure 5.11). No products were produced in the mutants. In the control WT DNA, these products were clearly seen. Also, Figure 5.11 provides a schematic showing the mutant alleles isolated in this study.

5.2.7 Single *mtp1-1*, double *mtp1-1 hma3-2* and double *hma3-2 mtp1-1 A. thaliana* mutants are sensitive to Zn toxicity using a plate assay

The newly generated *hma3 mtp1* double mutants were grown alongside the WT and their corresponding *hma3* and *mtp1* single mutants, to provide a direct comparison on a range of increasing Zn media. This agarose plate assay provides a basic comparison of the mutant phenotypes. Figure 5.12A shows photographs of seedlings grown under these conditions and Figure 5.12B provides data on the fresh weight of whole plants, shoots, and roots. Analyses from the two-way ANOVA revealed there is a significant interaction between genotype and Zn concentration on total weight ($F_{15,72} = 9.922$, $p<0.0001$), shoot weight ($F_{15,72} = 9.362$, $p<0.0001$) and root weight ($F_{15,72} = 4.839$, $p<0.0001$).

In both set of experiments, seedlings grown at 0µM Zn had some yellow colouration of the leaves, shorter roots and less lateral root formation compared to other seedlings grown on higher Zn concentrations (Figure 5.12A). However, there was no observable phenotypic difference between the genotypes, showing no significant difference in total, shoot or root fresh weight per seedling (Figure 5.12B). When grown on 15µM Zn, the seedlings were healthy with no significant difference between them (Figure 5.12B). The Zn toxicity effect on the seedlings started to show when grown on 50µM Zn. All *hma3 mtp1* double mutants and *mtp1-1* single mutants had a significantly lower total, shoot, and root fresh weight than WT and *hma3* single mutant seedlings (Figure 5.12). When grown on 250µM Zn, both *hma3-1* and *hma3-2* showed a significant increase in total fresh weight, shoot fresh weight and root fresh weight compared to WT seedlings (Figure 5.12).

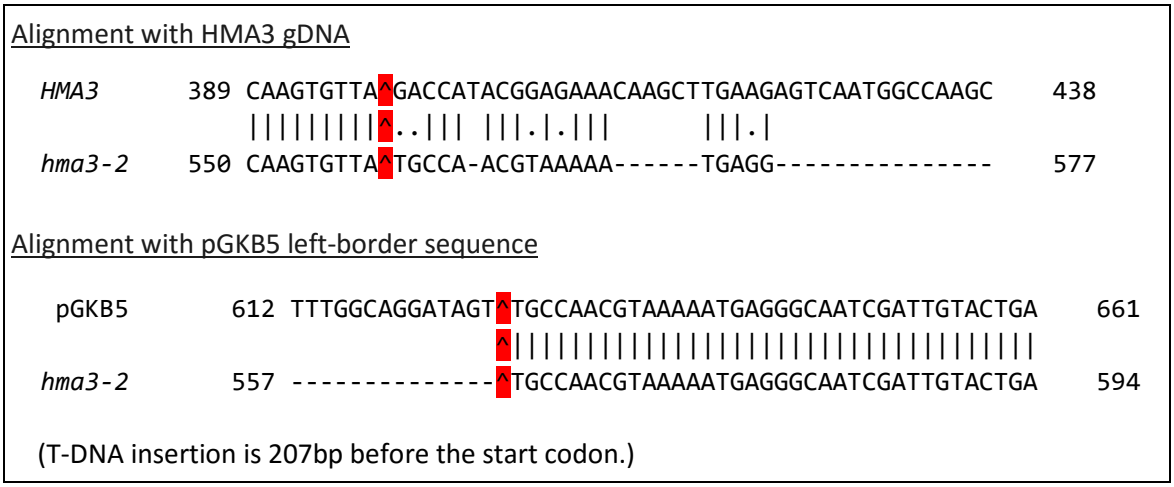

Figure 5.10 Sequencing analyses of the T-DNA insertion site for *hma3-2* mutant line.

The T-DNA insertion site is indicated by '^'. Sequences were aligned using the EMBOSS Needle (Li et al., 2015).

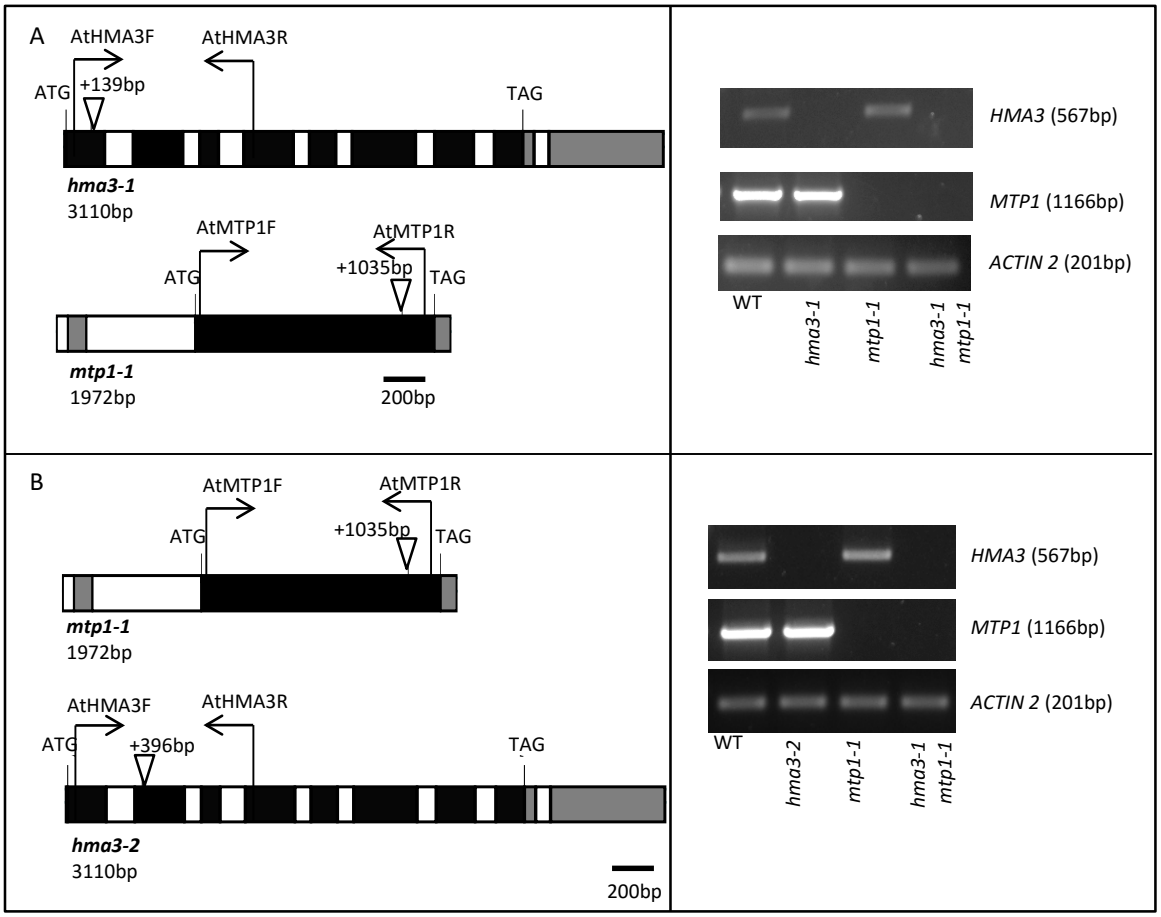

Figure 5.11 Mutant alleles for *HMA3* and *MTP1*.

Left, Schematic drawings showing the position of the inserts for mutant alleles: (A) *hma3-1 mtp1-1* and (B) *mtp1-1 hma3-2*. Black bars represent exons, white bars represent introns and grey bars represent untranslated regions. A of ATG is taken as 0. T-DNA is represented by triangle. The primers used in the reactions are also shown on the figures. Right, corresponding gel image showing the expression of *HMA3* and *MTP1* at RNA level in the different mutant lines, with *ACTIN2* as a control.

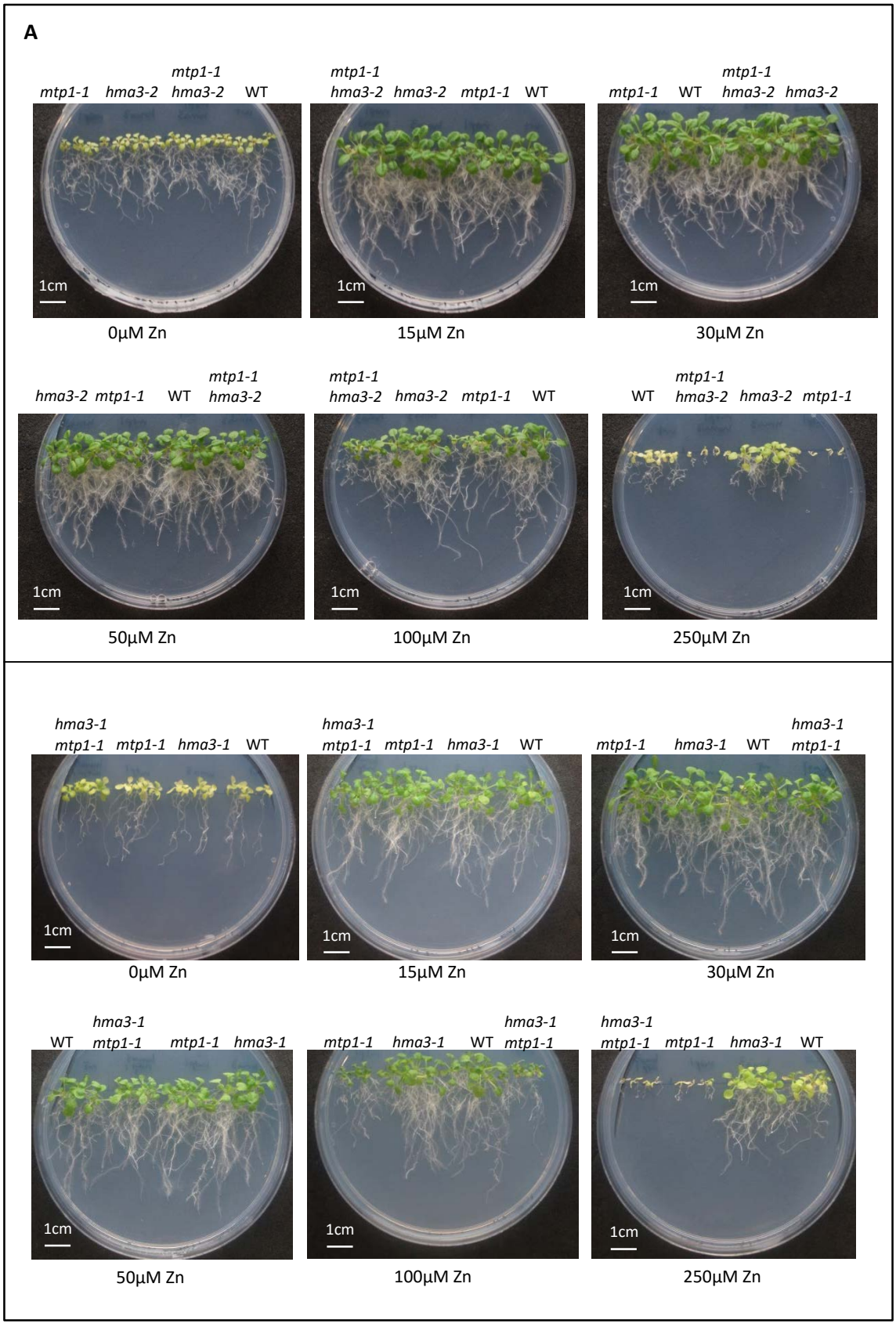
A
mtp1-1
mtp1-1 hma3-2 hma3-2 WT
1cm
0μM Zn
mtp1-1
hma3-2 hma3-2 mtp1-1 WT
1cm
15μM Zn
mtp1-1
mtp1-1 WT hma3-2 hma3-2
1cm
30μM Zn
hma3-2 mtp1-1 WT mtp1-1
hma3-2
1cm
50μM Zn
mtp1-1
hma3-2 hma3-2 mtp1-1 WT
1cm
100μM Zn
mtp1-1
WT hma3-2 hma3-2 mtp1-1
1cm
250μM Zn
hma3-1
mtp1-1 mtp1-1 hma3-1 WT
1cm
0μM Zn
hma3-1
mtp1-1 mtp1-1 hma3-1 WT
1cm
15μM Zn
mtp1-1 hma3-1 WT hma3-1
mtp1-1
1cm
30μM Zn
hma3-1
WT mtp1-1 mtp1-1 hma3-1
1cm
50μM Zn
mtp1-1 hma3-1 WT hma3-1
mtp1-1
1cm
100μM Zn
hma3-1
mtp1-1 mtp1-1 hma3-1 WT
1cm
250μM Zn

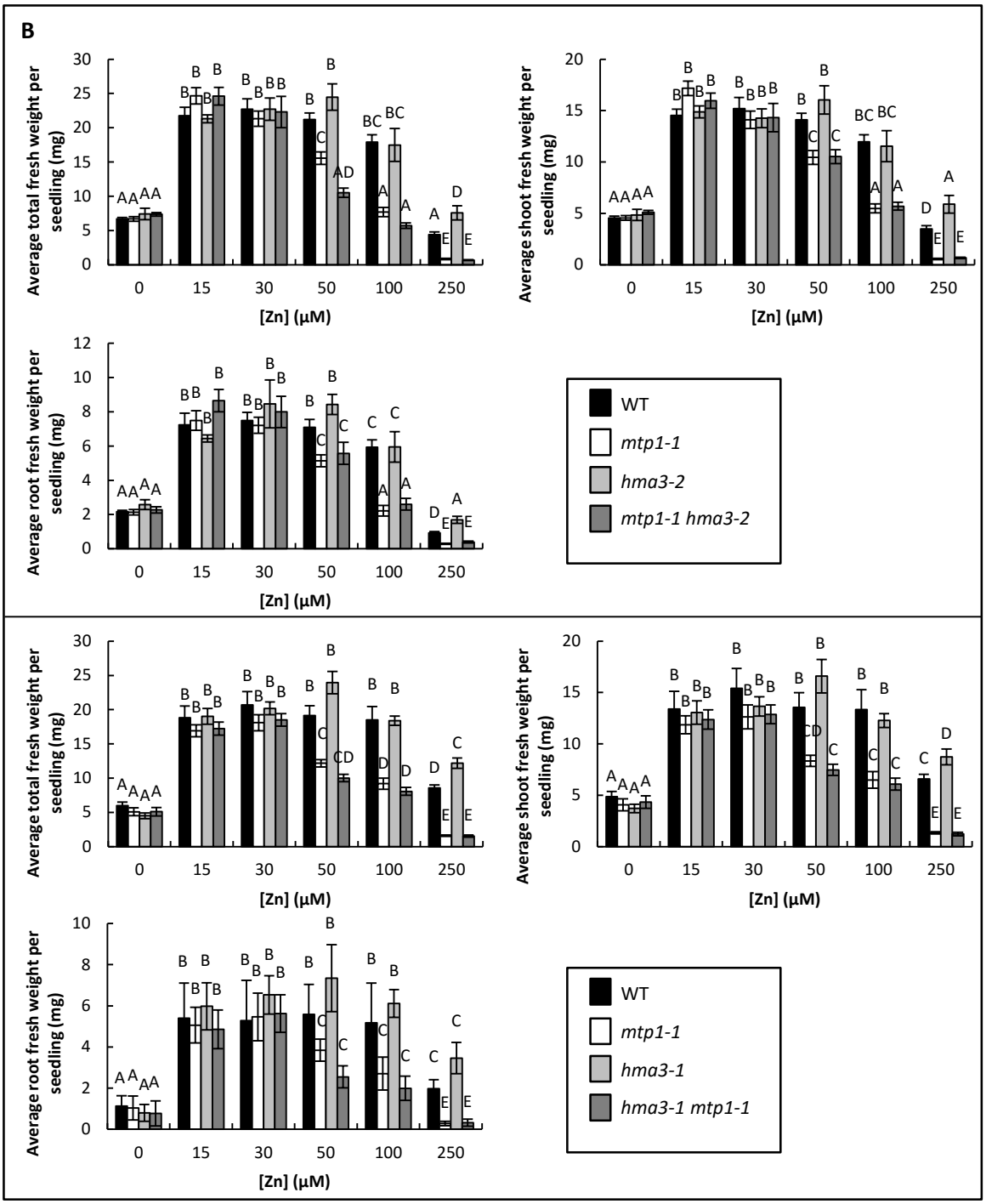

Figure 5.12 The two unique *hma3 mtp1* double mutants and *mtp1-1* single mutants but not *hma3* single mutants show an adverse effect to Zn toxicity.

(A) Representative images of two unique *hma3 mtp1* double mutants grown together with WT and their respective *hma3* and *mtp1-1* single mutants on 0.5 MS media under a range of Zn concentrations for 22 days**.** (B) Data shows the average total fresh weight, shoot fresh weight, and root fresh weight of two different *hma3* and *mtp1-1* mutants (singles and doubles) The data was based on six plates (+S.E) with four seedlings per line, per plate, each plate containing four plant lines. Means not sharing a letter are significantly different ($P \leq 0.05$); Tukey post-hoc test.

5.2.8 Single *mtp1-1* and double *mtp1-1 hma3-2 A. thaliana* mutants are sensitive to Zn toxicity using a hydroponic system

To compare the growth at a later stage, *mtp1-1 hma3-2* double mutants were grown together with WT and its respective *mtp1-1* and *hma3-2* single mutants on nutrient solution containing standard (0.38µM) and 20µM, 40µM, and 80µM Zn. The plants were grown for 40 days under short day conditions and various parameters were measured (Figure 5.13B). Overall, similar differences in growth responses were seen in the hydroponic system to those observed in the plate experiments. Analyses from the two-way ANOVA revealed that there was a significant interaction between genotype and Zn concentration on total weight ($F_{9,228}$=116.7, P<0.0001), shoot weight ($F_{9,228}$=121.7, P<0.0001), root weight ($F_{9,228}$=43.5, P<0.0001), root length ($F_{9,228}$=51.79, P<0.0001) and rosette diameter ($F_{9,228}$=75.19, P<0.0001).

At 0.38µM, Zn and 20µM Zn there were no visible differences apparent between WT and the other genotypes (Figure 5.13B). However, at 40µM Zn, *mtp1-1* and *mtp1-1 hma3-2* mutants were significantly reduced in all parameters measured compared to the WT and *hma3-2* (Figure 5.13B). At 80µM Zn, both *mtp1-1* and *mtp1-1 hma3-2* mutants had a severe reduction in all parameters relative to the other genotypes (Figure 5.13B). Interestingly, *mtp1-1* was generally smaller than *mtp1-1 hma3-2* but they were not significantly different in total, shoot, and root fresh weight (Figure 5.13B). It should be noted that *hma3-2* showed a similar response to WT at all Zn concentrations.

5.2.9 Response of *hma3-2* and *mtp1-1* mutants to Cd

Double *mtp1-1 hma3-2* mutants were grown together with WT and its respective *mtp1-1* and *hma3-2* single mutants to provide a direct comparison on toxic Cd media (20µM, 40µM, and 80µM) and media containing standard Cd (0µM). Figure 5.14A shows photographs of seedlings grown under both of these conditions and Figure 5.14B provides data on the fresh weight of whole plants, shoots, and roots. The results from two-way ANOVA showed there was a significant interaction between Cd concentration and genotype on total fresh weight ($F_{6,45}$ = 2.375, p = 0.0127), shoot weight ($F_{6,45}$= 67.95, p = 0.0445) and root weight ($F_{3,30}$ = 2.707, p = 0.0629). Seedlings grown at 0µM Cd grew well with large green leaves and an elaborate root system (Figure 5.14A). Seedlings grown at 20µM Cd displayed very poor growth. Seedlings had smaller yellower leaves and less root growth relative to the seedlings grown without Cd. However, there were no significant differences in fresh weight measurements between the genotypes (Figure 5.14B). At 40µM Cd, all seedlings failed to produce a root system. After 27 days growing on this concentration, seedlings only produced two small brown leaves that were smaller

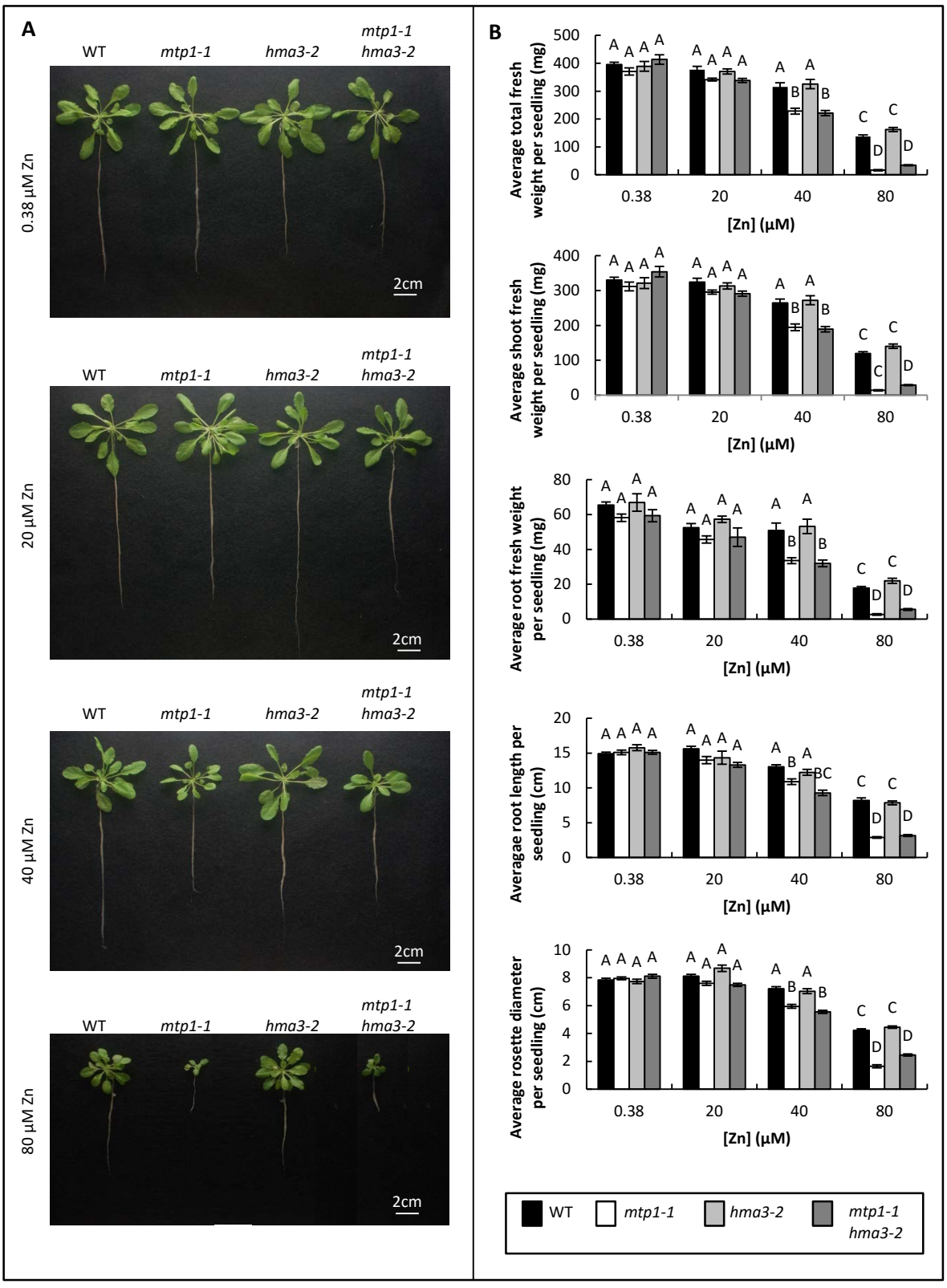

Figure 5.13 Zn toxicity phenotype of the *mtp1-1 hma3-2* double mutants in hydroponic assays.
(A) WT, *mtp1-1*, *hma3-2*, *mtp1-1 hma3-2* T-DNA insertion *A. thaliana* mutants grown on hydroponic culture for 40 days with a range of Zn concentrations. (B) Total, shoot, and root fresh weight, root length, and rosette diameter are shown; the means (+/- SEM) were based on 30 plants. Means not sharing a letter are significantly different (P≤0.05); Tukey post-hoc test.

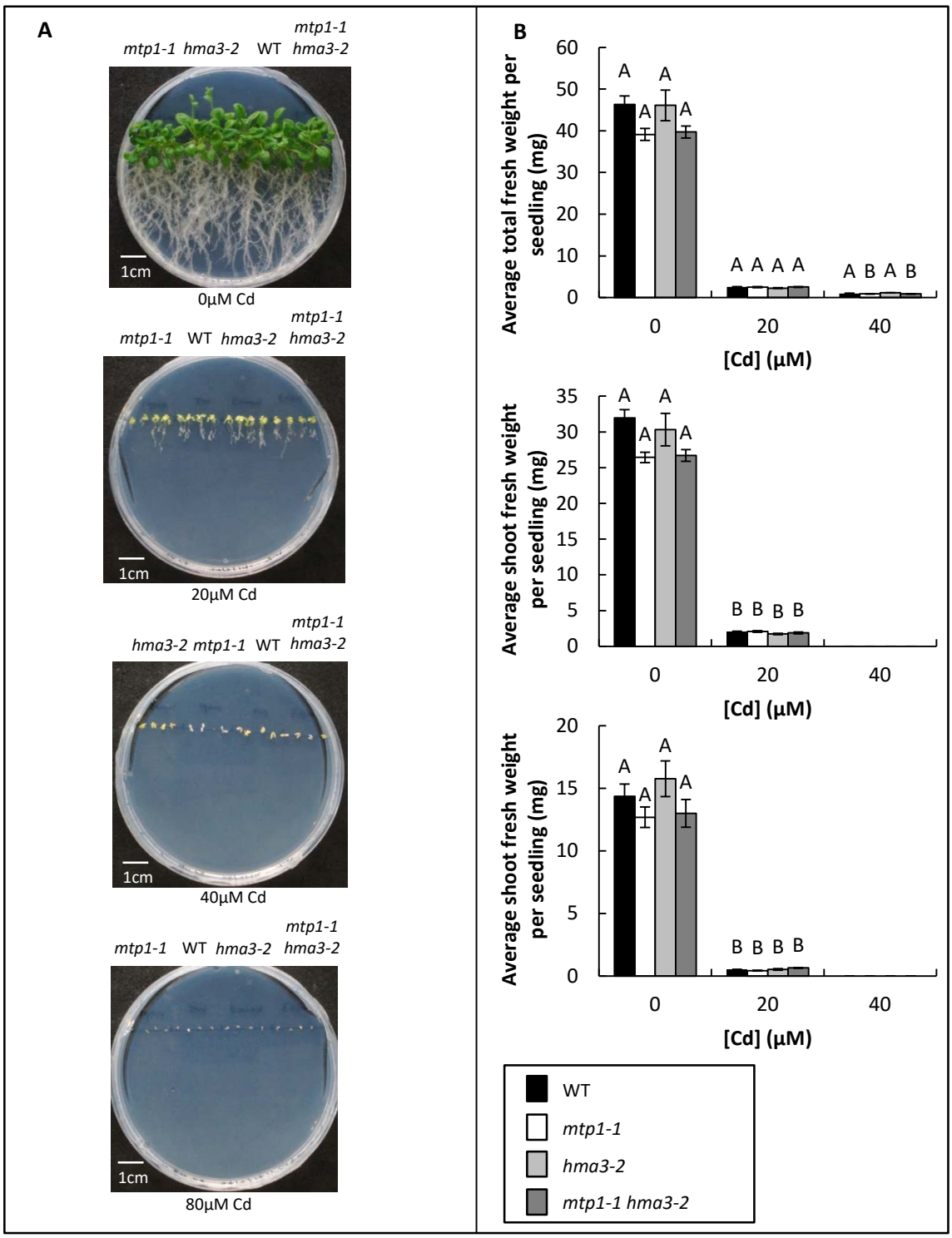

Figure 5.14 Cd toxicity does not specifically affect *mtp1-1*, *hma3-2* and *mtp1-1 hma3-2* mutants compared to WT.

(A) WT, *mtp1-1, hma3-2* and *mtp1-1 hma3*-2 mutants grown on 0.5 MS media under a range of Cd concentrations for 27 days. (B)Total, shoot and root fresh weight is shown; the means (+/- SEM) were based on six plates, with four seedlings per line, per plate, each plate containing four plant lines. Means not sharing a letter are significantly different ($p \leq 0.05$); Tukey post-hoc test.

than the leaves of seedlings grown on 20µM Cd (Figure 5.14A). There was no significant different between genotypes (Figure 5.14B). All seedlings germinated but failed to survive when grown at 80µM and no fresh weight measurements were taken (Figure 5.14A).

5.2.10 Cloning *HvHMA3* gene into *A. thaliana* and *S. cerevisiae* destination vectors

To characterise HvHMA3, it was cloned into *A. thaliana* and *S. cerevisiae* expression vectors. Gateway cloning technology (Katzen, 2007) was used for this. It was not possible to amplify full-length cDNA from Golden Promise for *HvHMA3* and therefore an *HvHMA3* cDNA clone was obtained from Dr. Takashi Matsumoto (Japan) (Matsumoto et al., 2011). This had been generated in a strategy to produce a library of full-length barley cDNAs. This library consisted of 172000 clones constructed from a two-row malting barley cultivar, Haruno Nijo, grown under normal and stressed conditions. A cDNA clone was not available for HvHMA2/3 and only partial sequences could be amplified (results not shown). pFLCIII *HvHMA3*, was used as the template to amplify *HvHMA3*. The full-length *HvHMA3* was amplified using Pfu with HvHMA3TopoF2 and HvHMA3WithStop primers. *HvHMA3* without the stop codon was also amplified with HvHMA3NoStop primer so that it could be tagged with EGFP.

As seen in Figure 5.15A and Figure 5.15B, a product around 2.5kb was produced for *HvHMA3withStop* and *HvHMA3NoStop* respectively, extracted from the gel and used in TOPO cloning. Ten colonies of transformed TOP10 *E. coli* were selected for each construct for colony PCR and colony 3, 5, 6, and 8 of pENTR *HvHMA3withStop* and colony 1, 3, 6, 8, and 10 may contain *HvHMA3NoStop* (Figure 5.15C). Restriction digests were carried out to confirm correct insert orientation with *EcoRV* and *PvuI* (Figure 5.16). *HvHMA3* with the stop codon was introduced into both *A. thaliana* expression vector pMDC32 and *S. cerevisiae* expression vector pAG426GAL-*ccdB*-EGFP. Meanwhile, the entry clone of *HvHMA3* without the stop codon was used to introduce *HvHMA3* into both *A. thaliana* expression vector pMDC83 and pAG426GAL-ccdB-EGFP so that it can be tagged with EGFP at its C-terminus for the localization study. All four expression clones containing *HvHMA3* were transformed with DH5α *E. coli* cells and selection on kanamycin for pMDC32/83 *HvHMA3* and ampicillin for pAG426GAL-*HvHMA3*::*EGFP*. Colony PCR was performed on ten selected colonies of each *HvHMA3* constructs using respective Topo primers amplifying the whole *HvHMA3* followed by the diagnostic restriction analyses to confirm the introduction of *HvHMA3* into the expression vectors in the correct orientation. Figure 5.17A shows an example of the restriction diagnostic analyses for pMDC32 *HvHMA3*. As a final verification, the expression vectors were sequenced. All constructs had identical HvHMA3 sequence to HvHMA3 CDs from pFLCIII *HvHMA3* (Haruna Nijo cultivar). Table 5.4 displays the *A. thaliana* and *S. cerevisiae* expression vectors generated in this study.

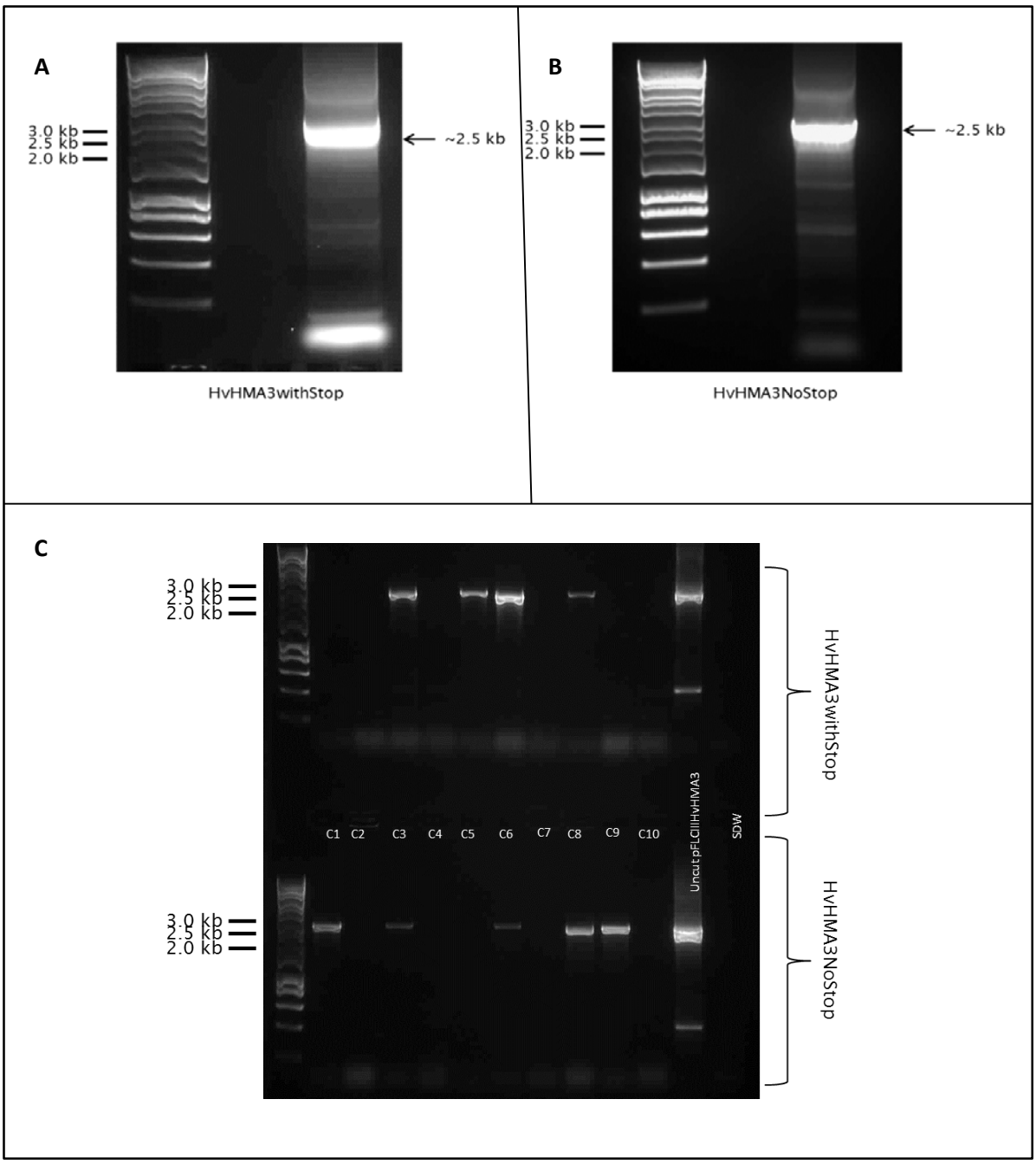

Figure 5.15 Cloning of *HvHMA3* into the entry vector, pENTR.

HvHMA3 with stop codon amplified using HvHMA3TopoF2 and HvHMA3WithStop primers (A), while *HvHMA3* without the stop codon amplified using HvHMA3TopoF2 and HvHMA3NoStop (B). Colony PCR and gel electrophoresis to show the successful transformation of TOP10 *E. coli* cells with the entry vectors pENTR *HvHMA3withStop* and pENTR *HvHMA3NoStop* using HvHMA3TopoF2 and HvHMA3NoStop primers (C).Primer sequences outlined in Table 2.7.

Table 5.4 The expression vectors generated for expressing *HvHMA3 gene* in *A. thaliana* and *C. cerevisiae* in this study

Plasmid	Construct	Primers used for sequencing
pMDC32 *HvHMA3*	*P35S::HvHMA3*	pDM35S, MDCnosR, HvHMA3F and HvHMA3R
pMDC83 *HvHMA3*	*P35S::HvHMA3::gfp*	pDM35S, GFPR, HvHMA3F and HvHMA3R
pAG426GAL-*HvHMA3*	*PGAL::HvHMA3*	M13F, M13R, HvHMA3F and HvHMA3R
pAG426GAL-*HvHMA3::EGFP*	*PGAL::HvHMA3::gfp*	M13F, M13R, HvHMA3F and HvHMA3R

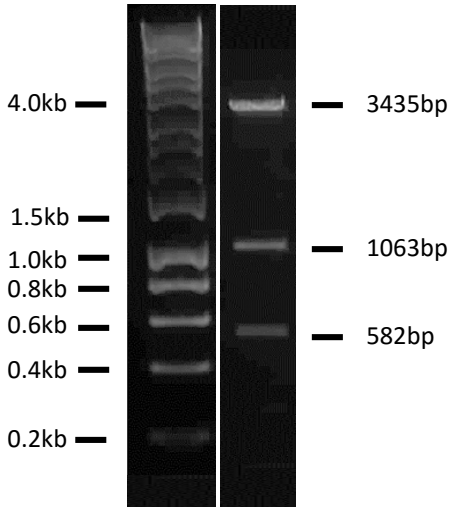

Figure 5.16 Diagnostic restriction analysis of the pENTR *HvHMA3withstop* entry vector.
Restriction digest analyses of pENTR *HvHMA3withStop* using *PvuI* and *EcoRV* restriction enzymes showed that it matched the predicted restriction digest profile. Predicted product sizes are indicated on right of the gel and predicted molecular marker size indicated on left of the gel.

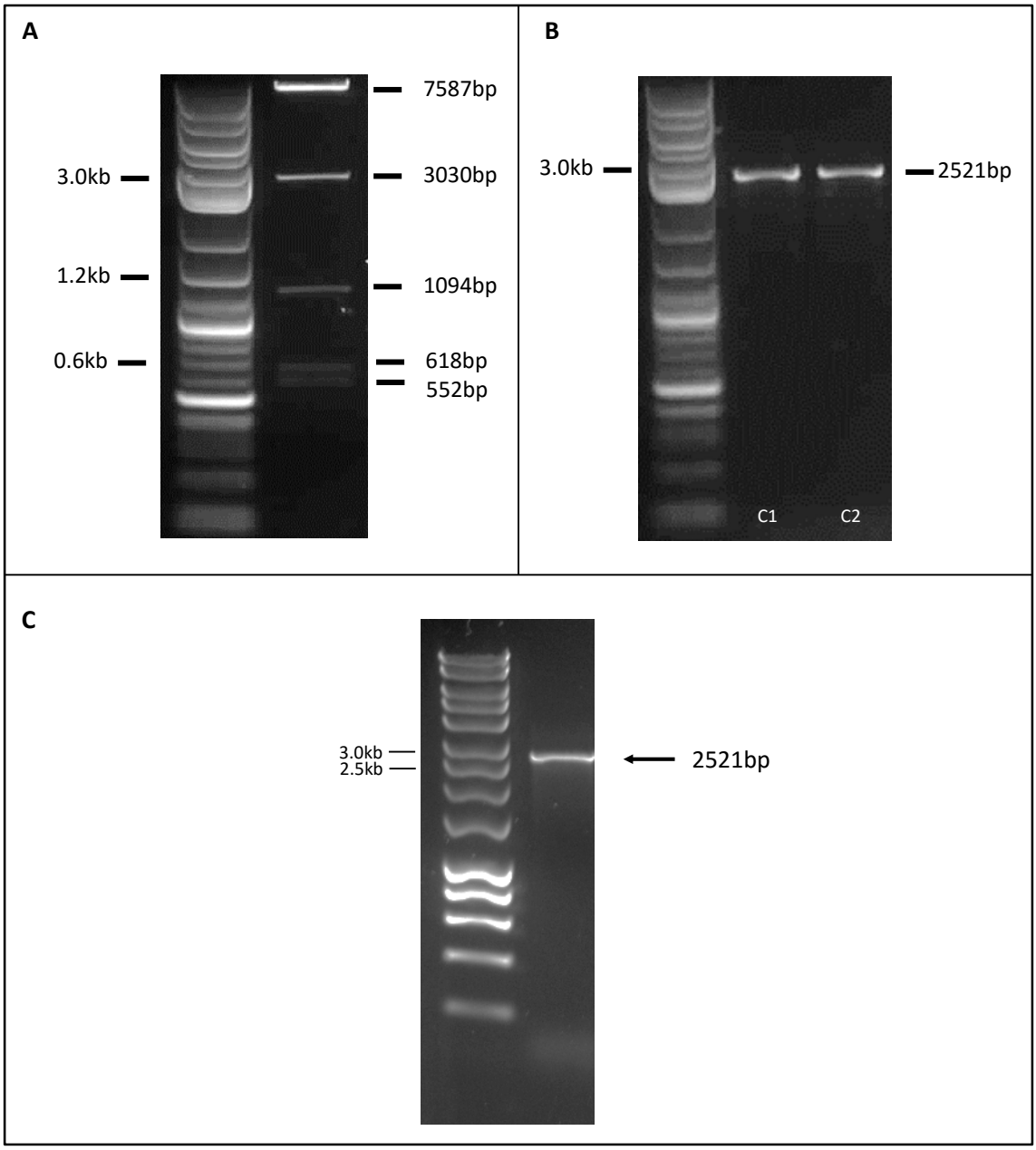

Figure 5.17 Cloning of *HvHMA3* into *A. thaliana* expression vector pMDC32 and *S. cerevisiae* expression vector pAG426GAL-ccdB-GFP.

Restriction digest analyses of pMDC32 *HvHMA3withStop* using *XhoI* restriction enzymes showed that it matched the predicted restriction digest profile (A). Colony PCR and gel electrophoresis to show two successful transformed colonies (C1 and C2) of *A. tumefaciens* GV3850 with the *A. thaliana* expression vectors pMDC32 *HvHMA3* (B). Colony PCR to show presence of the transformed plasmid, pAG426GAL-*HvHMA3::EGFP* in WT (BY4741) *S. cerevisiae* strain (C). Predicted product sizes are indicated on right of the gel and predicted molecular marker size indicated on left of the gel.

5.2.11 Expressing *HvHMA3* gene in *A. thaliana* and *S. cerevisiae* for functional analyses

The pMDC32 *HvHMA3* and the pMDC83 *HvHMA3* were transformed into *A. tumefaciens* for subsequent *A. thaliana* transformation. A few colonies were selected and analysed using colony PCR to identify successful transformants. The primer sets used contained sequences that would anneal to the full-length of the *HvHMA3* gene. Gel electrophoresis results indicate that the predicted products produced from colony PCR. Figure 5.17B shows an example of colony PCR and the predicted products for pMDC32 *HvHMA3* in GV3850. Table 5.5 shows the transgenic lines generated for this chapter. Only *mtp1-1* was transformed as it showed a clear Zn-dependent phenotype. Three to four final independent lines that were 100% resistant to hygromycin were identified for each plasmid.

The expression of *HvHMA3* in the T_3 plants was confirmed at the RNA level. RNA of these plants was extracted and cDNA was synthesised subsequently. PCR results showing the RNA transcript expression of *HvHMA3* in *mtp1-1* mutant plants (Figure 5.18) that had been transformed with pMDC32 *HvHMA3* are shown as an example. The RNA was of good quality as there was no genomic DNA contamination. This was shown by the primers amplifying *AtACTIN2*. All tested plants expressed *AtACTIN2* at the RNA level as indicated by the amplification of the predicted 201bp products (Figure 5.18A).These samples were free from genomic DNA contamination as indicated by the absence of the predicted product size of 287bp for genomic *AtACTIN2* (lane 2). All WT samples (genomic DNA and cDNA) expressed *AtMTP1* as shown by the amplification of 1166bp predicted (Figure 5.18B). Meanwhile, four independent *mtp1-1* transformed with pMDC32 *HvHMA3* do not express *AtMTP1* (Figure 5.18B lane 5 – 8). The four *mtp1-1* independent lines transformed with pDMC32 *HvHMA3* exhibit the full-length predicted product of 2521bp, confirming *HvHMA3* expression.

For the *S. cerevisiae* expression vectors carrying HvHMA3, they were transformed into three different *S. cerevisiae* strains: BY4741 (WT), *zrc1 cot1* (Zn-sensitive) and *ycf1* (Cd-sensitive). All transformed *S. cerevisiae* colonies grew on SC glucose minus uracil agar. Table 5.6 displays the transgenic *S. cerevisiae* lines generated in this way. Colony PCR of transformed *S. cerevisiae* colonies were performed with HvHMA3TopoF2 and HvHMA3WithStop producing 2521bp. Figure 5.17C shows an example of colony PCR for identifying pAG426GAL-*HvHMA3::EGFP* transformed into BY4741.

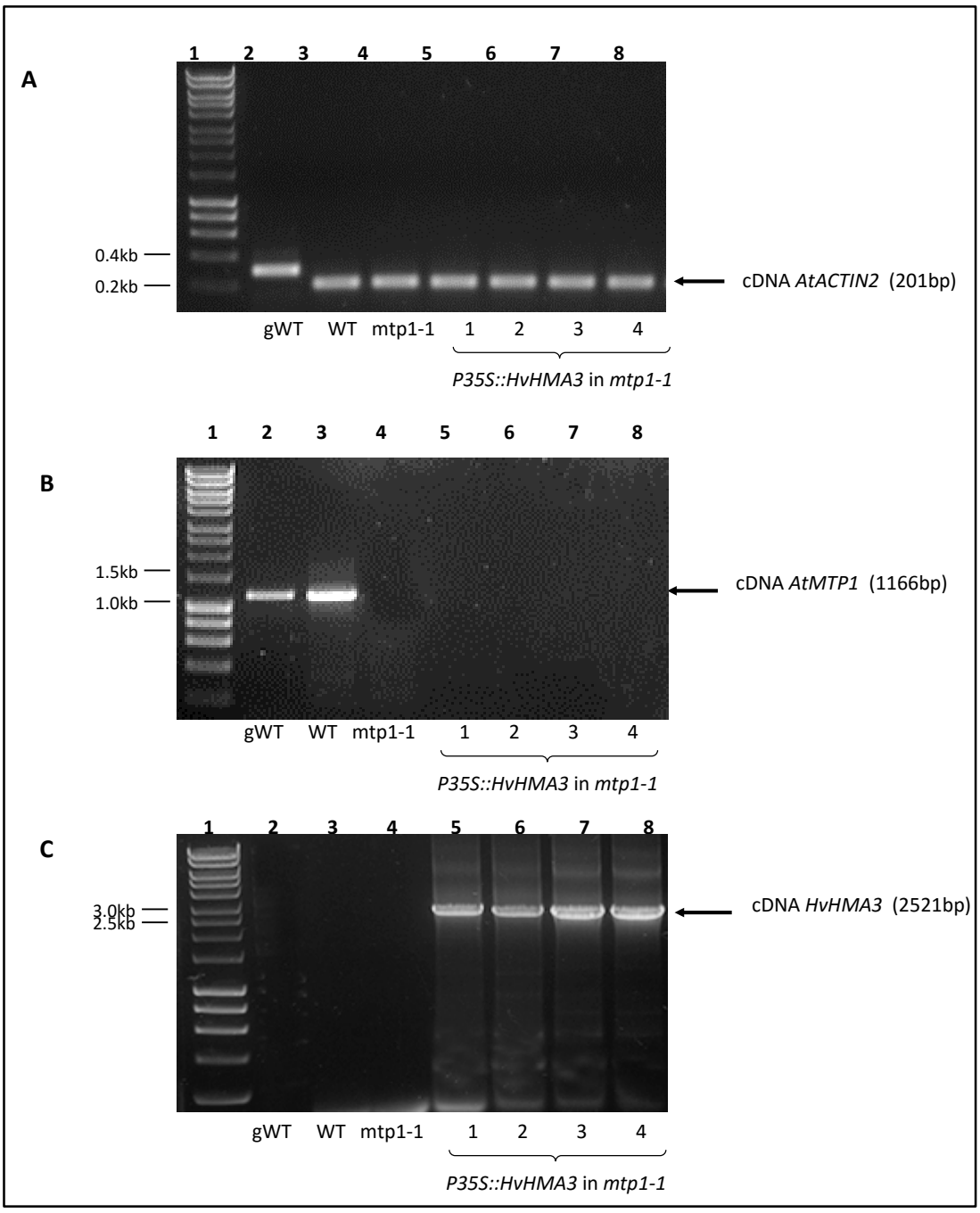

Figure 5.18 Expression of *HvHMA3* in *A. thaliana mtp1-1* T_3 lines.

PCR and gel electrophoresis using cDNA synthesised from RNA to show the genotypes of *mtp1-1* lines (1 – 4) transformed with pMDC32 *HvHMA3* (**A** – **C**). Predicted products shown on figure, Lane 1: molecular markers. **A**. Actin2 F and Actin2 R primers amplify a fragment of At *ACTIN2*, which shows consistent level of expression in all plant lines. **B**. *A. thaliana MTP1* expression is present only in the WT plant line using primers AtMTP1_F and AtMTP1_R (lane 2 and 3). Lane 4: *mtp1-1*. **D**. *HvHMA3* expression in four *mtp1-1* mutant lines transformed with pMDC32 *HVHMA3* using primers HvHMA3TopoF2 and HvHMA3WithStop (lanes 5 – 8). Primer sequences outlined in Table 2.7.

Table 5.5 The transgenic *A. thaliana* lines created for expressing *HvHMA3* gene.

Each plasmid was transformed into WT and *mtp1-1* plants. The construct specifies the promoter the gene is expressed under and whether there are any fusions e.g. to a GFP reporter.

Plasmid	**Construct**	**Transformed into**	**# of independent T3 homozygous lines**
pMDC32HvHMA3	*P35S::HvHMA3*	WT	3
pMDC32HvHMA3	*P35S::HvHMA3*	*mtp1-1*	4
pMDC83HvHMA3	*P35S::HvHMA3::gfp*	WT	*
pMDC83HvHMA3	*P35S::HvHMA3::gfp*	*mtp1-1*	*

* indicates transgenic plants still undergoing isolation process.

Table 5.6 Transgenic *S. cerevisiae* strains generated. *S. cerevisiae* strains transformed with yeast expression constructs (Table 5.3).

= number of independent transformants used in subsequent experiments.

#	**Strains**	**Genotype**
3	BY4741	[pAG426GAL-*HvHMA3withstop::egfp*] *MAT a*; *his3*-Δ 1; *leu2*-Δ 0; *met15*-Δ 0; *ura3*-Δ 0
2	*Ycf1*	[pAG426GAL-*HvHMA3withstop::egfp*] *MAT*α *ura3-52 his6 leu2-3,-112 his3-Δ200 trp1-901 lys2-801 suc2-Δ, ycf1::hisG*
2	*zrc1*-Δ *cot1*-Δ	[pAG426GAL-*HvHMA3withstop::egfp*] *MAT a*; *his3*-Δ 1; *leu2*-Δ 0; *met15*-Δ 0; *ura3*-Δ 0; *zrc1*::natMX *cot1*::*kanMX4*
3	BY4741	[pAG426GAL-*HvHMA3Nostop::egfp*] *MAT a*; *his3*-Δ 1; *leu2*-Δ 0; *met15*-Δ 0; *ura3*-Δ 0
4	*Ycf1*	[pAG426GAL-*HvHMA3Nostop::egfp*] *MAT*α *ura3-52 his6 leu2-3,-112 his3-Δ200 trp1-901 lys2-801 suc2-Δ, ycf1::hisG*
4	*zrc1*-Δ *cot1*-Δ	[pAG426GAL-*HvHMA3Nostop::egfp*] *MAT a*; *his3*-Δ 1; *leu2*-Δ 0; *met15*-Δ 0; *ura3*-Δ 0; *zrc1*::natMX *cot1*::*kanMX4*
4	BY4741	[pAG426GAL-ccdB-EGFP] *MAT a*; *his3*-Δ 1; *leu2*-Δ 0; *met15*-Δ 0; *ura3*-Δ 0
3	*Ycf1*	[pAG426GAL-ccdB-EGFP] *MAT*α *ura3-52 his6 leu2-3,-112 his3-Δ200 trp1-901 lys2-801 suc2-Δ, ycf1::hisG*
3	*zrc1*-Δ *cot1*-Δ	[pAG426GAL-ccdB-EGFP] *MAT a*; *his3*-Δ 1; *leu2*-Δ 0; *met15*-Δ 0; *ura3*-Δ 0; *zrc1*::natMX *cot1*::*kanMX4*

5.2.12 HvHMA3 rescues the Zn-dependent phenotype of the *A. thaliana mtp1-1* mutant

There was no a clear phenotype of *hma3* single mutants when grown on toxic Zn concentrations. However, the clear Zn-toxicity phenotype in *A. thaliana mtp1-1* single mutants is a useful tool for investigating the function of HvHMA3. At least four independent lines with *HvHMA3* expressed in *mtp1-1* under the 35S promoter were isolated and they were shown to express the transgene (see Section 5.2.11). Two *mtp1-1* independent lines (T_3 generation) expressing HvHMA3 were grown alongside the WT and the *mtp1-1* single mutants to provide a direct comparison on toxic Zn media. The lines were also grown on Zn-deficient media to test the ability of HvHMA3 under Zn-deficiency. Figure 5.19A shows photographs of seedlings grown under this condition and Figure 5.19B provide data on the fresh weight of whole plants, shoots, and roots.

When grown under Zn toxicity conditions, HvHMA3 could restore completely the growth of the *A. thaliana mtp1-1* single mutants to the WT level up to 150 µM Zn (Figure 5.19). However, at 200µM Zn, HvHMA3 could only partially restore the growth of the *A. thaliana mtp1-1* single mutant, almost to WT levels (Figure 5.19). Zn-deficiency was also tested to see if there was any effect of expressing *HvHMA3*, but as see in Figure 5.19, the growth level of *mtp1*-1 single mutants expressing *HvHMA3* was similar at this Zn-deficient condition to the *mtp1-1* mutant.

5.2.13 Functional analyses of HvHMA3 in *S. cerevisiae*

An *S. cerevisiae* growth assay was set up to test the heterologous expression of *HvHMA3* and *HvHMA3::EGFP* on Zn toxicity. Figure 5.20A shows the comparison of BY4741 (WT) expressing the empty vector (pAG426GAL-ccdB-EGFP) and *zrc1 cot1* expressing *HvHMA3*, *HvHMA3::EGFP* or the empty vector grown together on solid SC-ura media containing a range of Zn concentrations. These strains were also grown on solid SC-ura media containing glucose to see if there was any difference in growth. The results do not display any difference between BY4741 and *zrc1 cot1* strains (Figure 5.20A). Galactose was used as the carbon source instead of glucose to induce the expression of *HvHMA3* and *HvHMA3::EGFP* (Figure 5.20A). At 0mM Zn, no differences in growth was seen between BY4741 transformed with the empty vector and *zrc1 cot1* transformed with the empty vector, pAG426GAL- *HvHMA3*, or pAG426GAL- *HvHMA3::EGFP* (Figure 5.20A). As the Zn concentration increased, the BY4741 expressing empty vector grew very well even at the lowest dilution. However, the growth of *zrc1 cot1* strain deteriorated as the Zn concentrations increased (Figure 5.20A). The strain was completely inhibited on 0.3mM Zn. The same observation was obtained for *zrc1 cot1* expressing *HvHMA3* and *HvHMA3::EGFP* (Figure 5.20A).

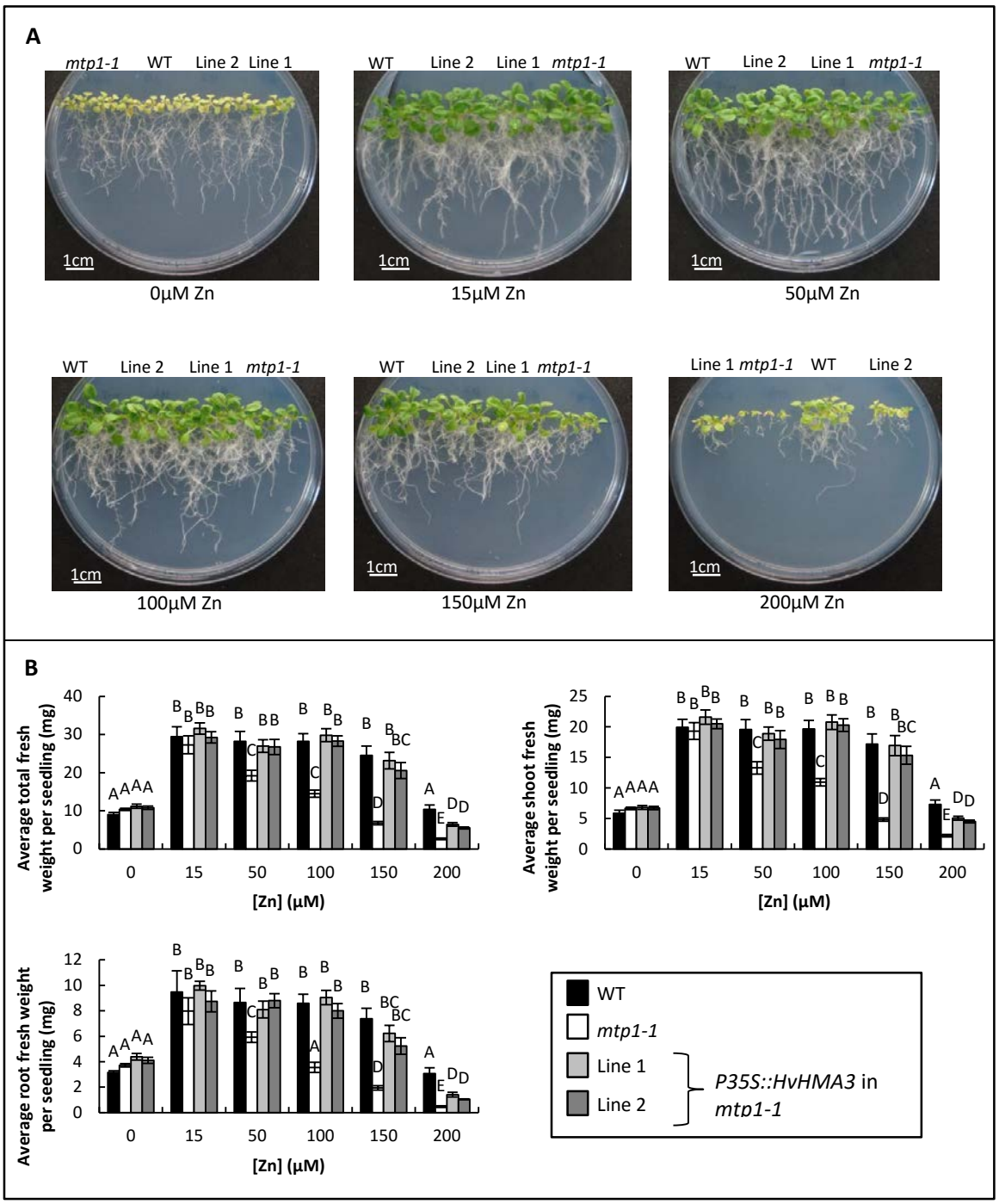

Figure 5.19 HvHMA3 rescues the Zn-toxicity phenotype of the *A. thaliana mtp1-1* single mutant up to 150µM Zn.

HvHMA3 was expressed under 35S promoter in *mtp1-1* single mutant (A) Representative images of WT and *mtp1-1* mutants grown together with two independent *mtp1-1* mutants expressing HvHMA3 for 21 days on a range of Zn concentrations (0µM, 15µM, 50µM, 100µM, 150µM, and 200µM) 0.5 MS media. (B) Total, shoot and root fresh weight is shown; the means (+/- SEM) were based on six plates, with four seedlings per line, per plate, each plate containing four plant lines. Means not sharing a letter are significantly different (p≤0.05); Tukey post-hoc test.

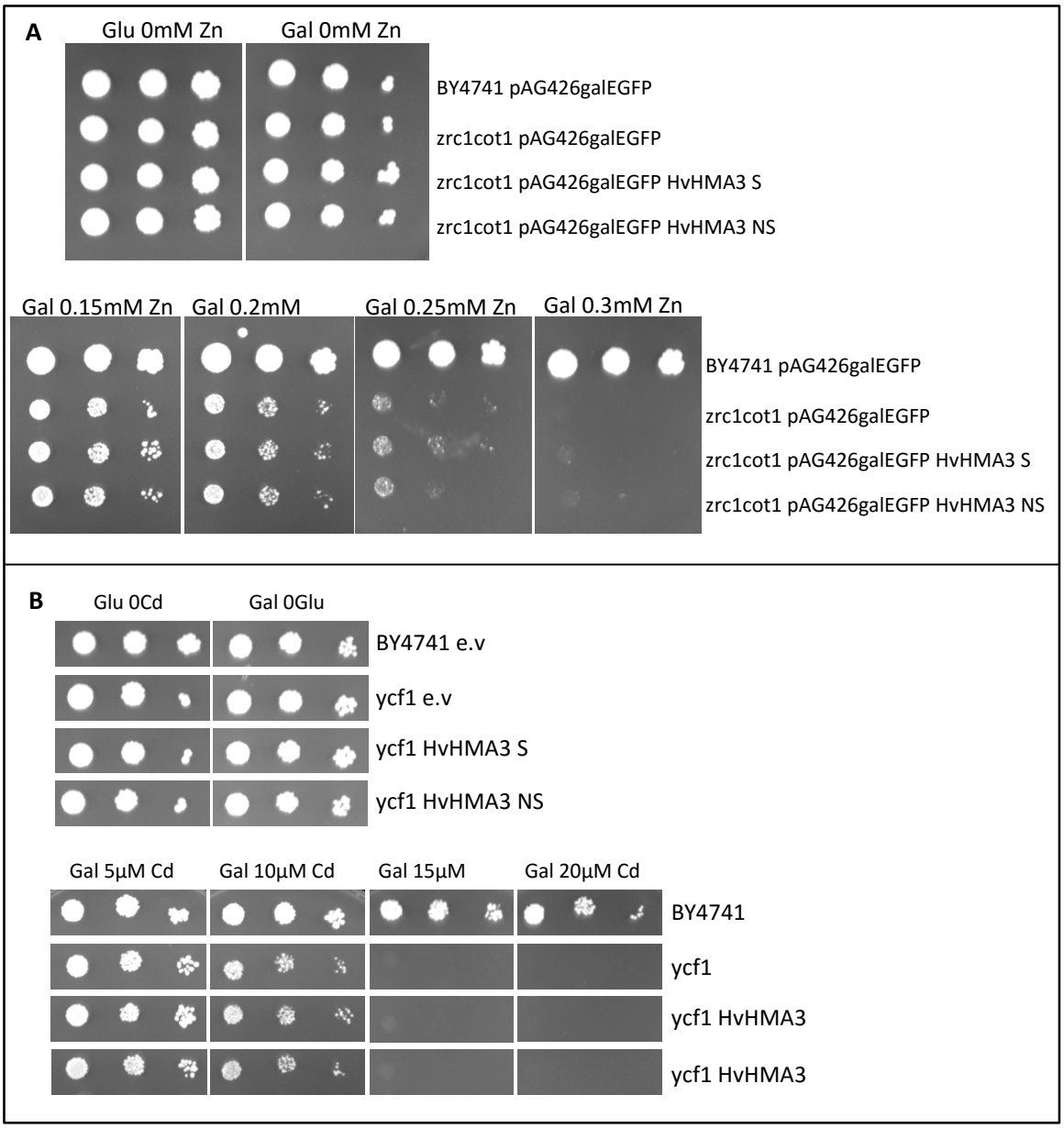

Figure 5.20 *HvHMA3* expression under a Gal-inducible promoter in *S. cerevisiae*.

HvHMA3 was expressed in Zn/Co-sensitive *zrc1 cot1* mutant (A) and Cd-sensitive *ycf1* mutant (B). Dilution series of WT transformed with the empty vector (EV; pAG426GAL-ccdB-EGFP) and the *S. cerevisiae* mutant strains transformed with the empty vector (EV; pAG426GAL-ccdB-EGFP), pAG426GAL-*HvHMA3withstop::EGFP* (*S*) or pAG426GAL-*HvHMA3nostop::EGFP* (*NS*) grown for 5 days. Photographs show undiluted, 1/10 and 1/100 dilutions of aliquots on agar containing either glucose (Glu) or galactose (Gal) as the carbon source, and varying concentrations of $ZnSO_4$ as indicated.

An independent growth assay was also set up to test the effect of *HvHMA3* expression in *S. cerevisiae* on toxic Cd. Figure 5.20B shows the comparison of BY4741 expressing the empty vector (pAG426GAL-ccdB-EGFP) and Cd-sensitive *S. cerevisiae* mutant, *ycf1* expressing *HvHMA3*, *HvHMA3::EGFP* or the empty vector grown together on solid SC-ura media containing a range of Cd concentrations. All *S. cerevisiae* strains had similar growth when grown on 0µM Cd supplied with glucose (Figure 5.20B). The induction of *HvHMA3* and *HvHMA3::EGFP* by galactose in all *S. cerevisiae* strains showed similar growth at 0µM Cd (Figure 5.20B). Also, all *S. cerevisiae* strains had similar growth at 5µM but they were less healthy compared to the same yeast strains grown on 0µM Cd (Figure 5.20B). At 10µM Cd, BY4741 expressing the empty vector grew better to other *ycf1* expressing *HvHMA3*, *HvHMA3::EGFP* or the empty vector. The expression of *HvHMA3* or *HvHMA3::EGFP* did not rescue *ycf1* mutant to the WT level at higher Cd concentrations (15µM or 20µM Cd) (Figure 5.20B).

5.2.14 Expression level of barley *P_{1B-2}-ATPases* in different tissues

Using the same database mentioned in Section 4.2.9, the expression pattern of P_{1B-2}-ATPases in different barley tissues was determined. Eight barley tissues are available in the database (Table 4.6). The expression of the barley P_{1B-2}-ATPases in these tissues under normal Zn is shown in Figure 5.21.

HvHMA2 has the highest expression in barley showing high expression particularly in the root and the early developing grain tissues (five days after anthesis, three to five mm long caryopses) (Figure 5.21). Both HvHMA2/3 and HvHMA3 shows similar low expression levels (Figure 5.21). HvHMA2/3 is highly expressed in root, developing tiller, and developing grain (fifteen days after anthesis, 10 mm long caryopses) tissues (Figure 5.21). Meanwhile, the most notable expression for HvHMA3 is in the root tissues (Figure 5.21).

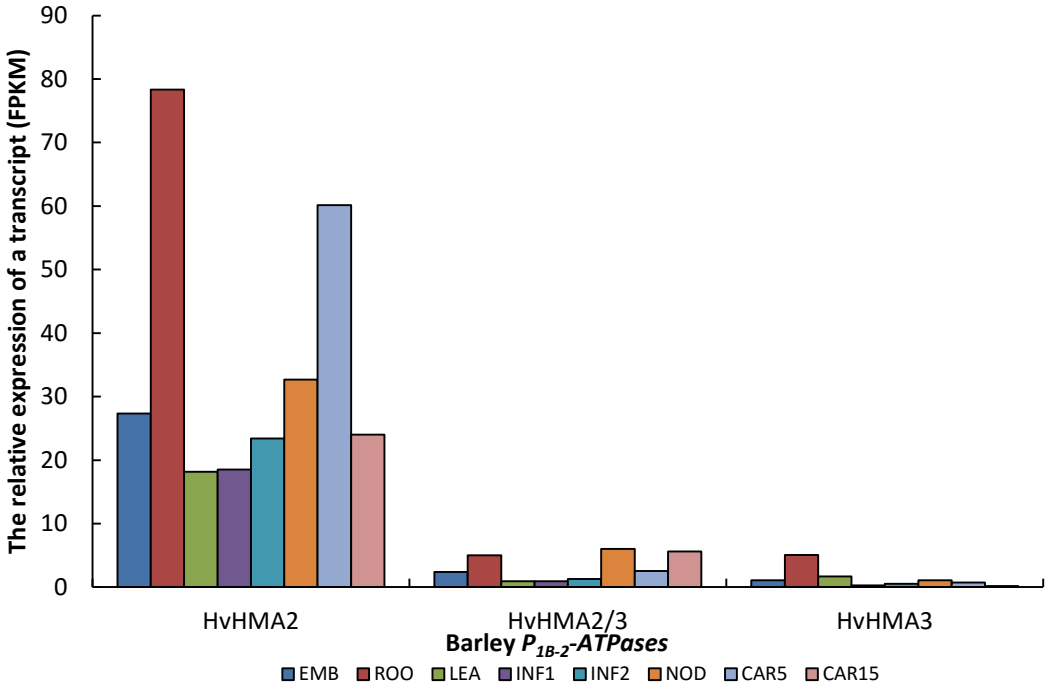

Figure 5.21 Expression pattern of barley *P_{1B-2}-ATPases* in different tissues.

Expression levels were obtained from the RNA-seq database (Mayer et al., 2012). There are eight barley tissues available for the analyses (Table 4.6).

5.3 Discussion

5.3.1 Sequence analyses of HvHMA3 and other members of barley and wheat P_{1B-2}-ATPases

Previous studies have identified that barley has two P_{1B-2}-ATPases, HvHMA2 and HvHMA3 (Mills et al., 2012) although only HvHMA2 was functionally characterized previously. This work has identified a third member of this subgroup, HvHMA2/3. It has also identified wheat orthologues of these barley genes. Homeologues for each of the wheat genes have been identified, although for TaHMA2/3, the sequence information is incomplete. For wheat P_{1B-2}-ATPases, only TaHMA2 has previously been functionally characterised (Tan et al., 2013).

HvHMA3 orthologues appear to be highly conserved in Poaceae and they all contain the residues that put them into the P_{1B-2} subgroup (Argüello, 2003). The N-terminal region of P_{1B-2}-ATPases is thought to be crucial for function (Verret et al., 2005). HvHMA3 and its orthologues in wheat, rice, and *B. distachyon* contain the GxCCxxE motif that appears to be conserved in the N-termini of all plant P_{1B-2}-ATPases, which may bind and also regulate metal transport (Verret et al., 2005, Wong et al., 2009, Xiang et al., 2015, Laurent et al., 2016). This region in AtHMA4 is crucial to its role as a Zn and Cd transporter; the mutation of either of the cysteine residues in AtHMA4 abolished its ability to complement the Zn hypersensitivity of *zrc1* and the Cd hypersensitivity of the *ycf1* mutant *S. cerevisiae* strains (Verret et al., 2005). Zn and Cd bind to CCxxE motif with greater affinity than other metals and the importance of this motif in AtHMA2 has been shown in the study where the mutation of these residues alters the metal-binding affinity of the N-terminal domain and reduces the ATPase activity but not the metal dependence of the membrane transporter (Eren et al., 2007). The deletion of the N-terminal region of HvHMA2 resulted in the elimination of Cd sensitivity conferred to WT *S. cerevisiae* and Zn resistance conferred to the *zrc1 cot1* mutant (Mills et al., 2012).

The C-terminal region of P_{1B-2}-ATPases have been shown to be crucial to certain P_{1B-2}-ATPases such as AtHMA4 as this region may function as an autoregulatory domain (Mills et al., 2005, Baekgaard et al., 2010). The deletion of C-terminus of AtHMA4 suppressed its rescue of *hma2 hma4* mutant (Mills et al., 2010). In addition, the expression of full-length *AtHMA4* in tobacco was required for enhanced transfer of Zn from root to shoot as the expression of the *AtHMA4* lacking C-terminal region caused the Zn concentration to be increased in the roots but decreased in the shoots (Siemianowski et al., 2011). The expression of *AtHMA4* C-terminal region alone in WT *S. cerevisiae* caused it to have a strong Cd resistance indicating a role in metal binding (Mills et al., 2010). In contrast to AtHMA4, the C-terminal domain of AtHMA2 is not essential for

function in planta as deleting it does not significantly affect its ability to restore growth of the *hma2 hma4* mutant (Wong et al., 2009). The rice OsHMA2 C-terminus, however, is crucial to its function as deletion of this region reduces its ability to translocate Zn and Cd from root to shoot (Sato-Nagasawa et al., 2012). In contrast, the C-terminal region in barley HvMA2 had little effect on *S. cerevisiae* metal tolerance (Mills et al., 2012).

The sequence comparison between HvHMA2/3 and HvHMA3 and several P_{1B-2}-ATPases has identified invariant residues and key putative metal coordination residues in TM6, TM7 and TM8 that are conserved in P_{1B-2}-ATPases. Some of these residues have been tested in *A. thaliana*. For example, the mutation of AtHMA4 CPC motif to GPC caused the loss of Cd and Zn resistance conferred on *S. cerevisiae* (Mills et al., 2005). In addition, mutating CPC to SPC in AtHMA4 abolished its ability to rescue *ycf1* mutant on elevated Cd and the *zrc1* mutant on high Zn (Verret et al., 2005). HvHMA2 key residues have also been investigated. The mutation of proline, which was the part of the CPC motif, decreased the Cd sensitivity when expressed in WT *S. cerevisiae* and the same observation was made when key residues in TMs 6 and 7 mutation were expressed in WT *S. cerevisiae* (Mills et al., 2012). In addition, all mutations reduced Zn resistance conferred by HvHMA2 to *zrc1 cot1* (Mills et al., 2012). These studies suggest that these residues are important and future works will test these residues in HvHMA2/3 and HvHMA3.The homeologues of P_{1B-2}-ATPases in wheat are highly similar to the barley P_{1B-2}-ATPases. As indicated in the phylogenetic tree (Figure 5.4), barley P_{1B-2}-ATPases and wheat P_{1B-2}-ATPases seem closely related. In addition, the percentage identity between barley P_{1B-2}-ATPases and their homeologues in wheat are very high. Because of that, barley and wheat P_{1B-2}-ATPases might share the same function.

Group 2 of P_{1B-2}-ATPases can be divided into two subgroups. HvHMA2, HvHMA2/3, TaHMA2 7AL, TaHMA2 7BL, TaHMA2 7DL, TaHMA2/3 7AL, TaHMA2/3 7BL, and TaHMA2/3 7DL are closely related to OsHMA2. Since closely related P_{1B}-ATPases may share a common function, we may expect those barley and wheat P_{1B-2}-ATPases to have the same substrate specificity as rice OsHMA2 and barley HvHMA2. OsHMA2 functions in Cd and Zn transport at the plasma membrane (Sato-Nagasawa et al., 2012). In addition, HvHMA2 has been shown to transport Zn and Cd and may play a similar role to AtHMA2 and AtHMA4 in *A. thaliana* in transferring these ions from roots to shoots (Mills et al., 2012). Meanwhile, predictions from phylogenetic analyses may suggest HvHMA3, TaHMA3 Chr5BL, TaHMA3 Chr5DL and TaHMA3 Chr5AL could have roles as vacuolar Cd pumps in roots as has been shown in OsHMA3 (Miyadate et al., 2011). The same pattern is seen in *A. thaliana* P_{1B-2}-ATPases. AtHMA2 and AtHMA4 are closely related to each other and they have been shown to be Zn/Cd pumps at the plasma membrane of root pericycle cells (Mills et al., 2005, Mills et al., 2003, Eren et al., 2006, Verret et al., 2004, Hussain et al., 2004). On the other hand,

AtHMA3 is slightly different than those two proteins and it has been suggested to function as a Zn and Cd vacuolar pump (Morel et al., 2009). Based on these observations, it is hypothesized that HvHMA3 functions in vacuolar Zn and Cd sequestration. However, it might be risky to directly transfer the knowledge acquired through the study of P_{1B}-ATPases in one plant species to P_{1B}-ATPases from other species, as no strict orthology relationship links the Brassicaceae P_{1B}-ATPases to the Poaceae ones (Zorrig et al., 2011). Therefore, there is a need to do *in vivo* functional analyses of HvHMA2/3 and HvHMA3 in addition to the *in silico* analyses.

The three barley *P_{1B-2}-ATPases* expression on normal Zn conditions in various barley tissues were analysed in the dataset produced by Mayer et al. (2012), which is based on RNA-seq. The expression pattern of *P_{1B-2}-ATPases* differed, suggesting they might play slightly different roles. The root tissues and the developing inflorescence are notable for highest expression of *HvHMA2*, which consistent with its role in transporting Zn from roots to other sink tissues. The expression levels of *HvHMA2* in other tissues are also higher than *HvHMA2/3* and *HvHMA3* suggesting its crucial role in Zn mobilisation in barley even at normal Zn conditions so that it is not disrupted. The low expression levels of *HvHMA2/3* and *HvHMA3* could be that both of the genes are inducible upon stresses. The orthologue of *HvHMA3* in rice, OsHMA3, has been shown to be induced in root tissues by Cd treatment (Ueno et al., 2010, Miyadate et al., 2011). Perhaps, *HvHMA3* could have the same response upon Cd-toxicity. HvHMA3 transcripts were reported to be slightly induced in roots under Cd treatment (Kaznina et al., 2014) but examining the primers chosen for this analysis indicated that they would be more likely to bind to *HvHMA1* than *HvHMA3*. Even though *HvHMA2/3* shows very low expression compared to *HvHMA2*, there are three notable tissues where it is highly expressed. These tissues are root, developing tiller, and developing grain, which suggesting *HvHMA2/3* could be involved in mobilizing Zn from root to sink tissues likes *HvHMA2*. The root tissue is the most notable for highest expression of *HvHMA3*. Here, *HvHMA3* could be important for sequestration of excess Zn and Cd. It will be interesting in the future to determine the expression pattern for barley *P_{1B-2}-ATPases* in different tissues under Zn/Cd stress conditions.

5.3.2 The effect of knocking out both *AtMTP1* and *AtHMA3* on Zn and Cd sensitivity in *A. thaliana*

Arabidopsis Ws background was chosen instead of Col-0 background for the HvHMA3 functional analyses because AtHMA3 is non-functional in Col-0 due to a base pair deletion inducing a stop codon, producing a truncated protein that is lacking the essential large cytosolic loop and the seventh and eight transmembrane helices (Hussain et al., 2004, Chao et al., 2012). Two unique *hma3 mtp1* double mutants were isolated in this study. Previous works indicates that

AtMTP1 and AtHMA3 are expressed on the tonoplast (Kobae et al., 2004, Morel et al., 2009) but it is not clear whether AtMTP1 and AtHMA3 function in the same vacuoles. Double mutants were generated to see if there was any additive effect on Zn toxicity or Cd toxicity. The generated double mutants could also provide a good system to investigate the biochemical and physiological characteristics of Zn and Cd toxicity and adaptive mechanism to Zn stress in plants expressing *HvHMA3*. Instead of generating an additive effect, *mtp1-1 hma3-2* mutants showed a different response. Based on the agarose plate assays and hydroponic system, the *mtp1-1* mutant but not *hma3-2* or *hma3-2* was shown to be susceptible to high Zn. This is in contrast to what has been reported previously for *hma3-1* (Morel et al., 2009). The difference may be explained by the type of media used to test the mutants. In our study, we used 0.5 MS media while Morel et al. (2009) used a media with a different nutrient composition. In their media, *hma3-1* roots showed a small but significant reduction in length compared to the WT (Morel et al., 2009) but here both *hma3* mutants responded slightly better than the WT seedlings in the agarose plate assays. *hma3 mtp1* double mutants showed a similar sensitivity to high Zn as *mtp1-1* mutants. *hma3-1* mutants has T-DNA insertion in the first exon (Hussain et al., 2004), while *hma3-2* mutant T-DNA insertion site is in the second exon. The difference between the T-DNA insertion site does not affect the phenotype as both mutants had similar effects on both Zn toxicity and Cd. Both disrupt the *HMA3* CDs and can be considered as knockouts. The phenotype of both *hma3-1* and *hma3-2* was also tested on growth media used by Morel et al. (2009) but the mutants including the WT plants did not grow very well and no conclusion could be made. This requires further repetition. Therefore, it is not yet determined if the *hma3-1* mutants behave the same way as claimed by Morel et al. (2009).

5.3.3 Functional analyses of HvHMA3

In this study, a heterologous complementation approach was used involving the use of *mtp1-1* single mutants, which had been shown to be extremely hypersensitive to high Zn concentrations in this study and other previous studies (Kobae et al., 2004, Kawachi et al., 2009, Menguer et al., 2013). *A. thaliana hma3-1* or *hma3-2* single mutants were not used as neither had a clear Zn-toxicity phenotype. Here the evidence is provided to indicate that HvHMA3 can function in the Zn-toxicity response by demonstrating its ability to complement the *A. thaliana mtp1-1* single mutant at elevated Zn levels; although it did not rescue at the highest concentrations tested. This suggests that HvHMA3 can transport Zn to some extent. AtMTP1 seems to make plants more resistance to higher Zn toxicity compared to HvHMA3. Kobae et al. (2004) have demonstrated that *AtMTP1* expression under the 35S promoter in *mtp1-1* single mutant completely complements the Zn-hypersensitive phenotype when grown on high Zn

concentrations as high as 400µM Zn on full MS medium. *HvHMA3* was expressed under the same promoter (35S) but did not fully complement the *mtp1-1* mutant at 200µM Zn, suggesting perhaps there are some functions of the *A. thaliana* MTP1 that cannot be performed as efficiently by the barley HMA3.

Cd did not specifically affect the *mtp1-1, hma3-1*, *hma3-2*, *mtp1-1 hma3-2* or *hma3-1 mtp1-1* and they responded similarly to WT. The concentration range could be reduced in future experiments, as at the concentrations used here, there was severe inhibition of all genotypes. *HvHMA3* was expressed in *S. cerevisiae* to investigate its properties further. When heterologously expressed under the galactose promoter, *HvHMA3* did not complement the Cd-sensitive *S. cerevisiae* mutant Δ*ycf1,* suggesting that HvHMA3 might not transport Cd. The colony PCR of Δ*ycf1* mutant expressing *HvHMA3* indicates that the full-length *HvHMA3* was expressed in the mutants. Previously, *AtHMA3* restored the Cd hypersensitivity of Δ*ycf1* while for OsHMA3, the results depended on the sequence used. *Indica* rice cultivars such as Anjana Dhan, Cho-Ko-Koku and Jarjan had a mutation at the 80th amino acid residue from Arg to His in their *OsHMA3* coding regions and its heterologous expression in *S. cerevisiae* did not confer Cd resistance to Δ*ycf1* (Ueno et al., 2010). Another *OsHMA3* allele was also found in *Japonica* cultivars with high Cd accumulation. This *OsHMA3* allele had a mutation at the 380th amino acid and it could not complement Cd-sensitive *S. cerevisiae* (Yan et al., 2016). The allelic variation among rice can determine the ability of OsHMA3 to function properly. When compared to OsHMA3 from different rice cultivars, the two non-functional *OsHMA3* alleles are not conserved in *HvHMA3* from all cultivars suggesting that barley HvHMA3 from the three cultivars could be functional. However, the comparisons of HvHMA3 between the three cultivars revealed that HvHMA3 from Haruna Nijo (cloned in this study) had two amino acid differences compared to HvHMA3 from Morex and Bowman. Compared to HvHMA3 from Bowman/Morex, Haruna Nijo HvHMA3 has two single amino acid mutations at the 84th position with Gly being substituted by Val, and at the 668th position with Cys being substituted by Arg. In the first amino acid change, both Gly and Val residues are nonpolar, while in the second amino acid change, the polar Cys residue is replaced by positively charged Arg residue in Haruna Nijo. The second amino acid change could possibly change the charge characteristics of the transporter proteins as positively charged Arg (within the physiological pH range) could repel Cd from entering the vacuole. Like rice, Cd accumulation in barley is genetically controlled (Wu et al., 2015). Based on 100 barley cultivars, a large genotypic difference in Cd accumulation was found and the position of HvHMA3 is close to the QTL that are responsible for the Cd translocation and accumulation in shoots and grains (Wu et al., 2015). Unlike high Cd accumulation cultivars found in rice, there was no significant difference in Cd concentration in barley roots between cultivars with different genotypes (Wu et al., 2015).

Further analyses of *HvHMA3* allelic variation is required in the future to determine if the two amino acid changes are important for HvHMA3 function. However, it should be noted that these two residues were conserved between Haruna Nijo and all rice varieties.

Heterologous expression of *HvHMA3* did not confer resistance to high Zn in Zn-sensitive *S. cerevisiae zrc1 cot1* mutant strains, indicating that HvHMA3 did not have the ability to transport Zn. The expression of *HvHMA3* orthologues in rice, *OsHMA3*, in *S. cerevisiae* also showed the same result (Ueno et al., 2010). HvHMA3 has the highest percent identity to OsHMA3 (62.8% percent identity). Other HvHMA3 orthologue such as *A. thaliana* AtHMA3 also were not able to complement the Zn-sensitive *S. cerevisiae zrc1* mutants (Morel et al., 2009). On the other hand, a less similar HvHMA3 orthologue in *A. halleri* has shown transport activity for Zn but not Cd (Becher et al., 2004). The potential Zn transport activity of HvHMA3 was shown in plants by its ability to rescue the Zn-hypersensitivity of *A. thaliana mtp1-1*. The rescue by the *HvHMA3* expression could have been by an alternative route as there was no direct Zn transport measurement to confirm that the rescue was due to Zn transport. Future works on HvHMA3 should include a localisation study and further mutant analyses to elucidate the actual function of HvHMA3. The *P35S::HvHMA3::gfp* and *PGAL::HvHMA3::gfp* constructs that have been generated in this study could be used for localisation studies in *A. thaliana* and *S. cerevisiae* respectively. Certainly, it may be interesting to mutate the two different residues in Bowman/Morex and Haruna Nijo to determine if they have any functional significance.

Chapter 6: General Discussion

6.1 Resolving Zn homeostatic mechanisms in plants

Plants have homeostatic mechanisms allowing them to survive under fluctuating conditions of nutrient supply. Some species and varieties tolerate micronutrient deficiency or excess better than others, and the underlying processes are complex. Clarifying the mechanisms involved in micronutrient sensing and signalling will be important in developing strategies for sustainable agriculture as crops that adapt better to a wider range of nutrient-stress conditions would have clear benefits. The heavy metal micronutrient Zn is the main focus of this thesis. Zn deficiency in crops is not only important because of the detrimental effects on yield but also because it leads to poor crop quality and reduced nutritional value (Sinclair and Krämer, 2012). It can even result in an increased susceptibility to pathogens (Poschenrieder et al., 2006, Helfenstein et al., 2015). Zn has numerous functions in plants and thus is essential for growth and development, but in excess leads to toxicity. Zn homeostasis is thus paramount and encompasses a tightly regulated network which involves: sensing mechanisms that monitor the Zn levels; acquisition from the soil; Zn binding to low molecular weight ligands such as nicotianamine; transfer to the xylem; translocation from root to shoot; remobilization during senescence; transfer into the phloem for transport to the seed/grain, and metabolism and storage in different regions of the seed/grain. Vacuolar sequestration is also an important process in regulating Zn concentrations within the cell and is particularly significant under elevated Zn. This together with allocation to other organelles where Zn is required for essential processes is important in controlling cellular levels. Competition with closely related heavy metals such as Cd is an issue and has received interest because of implications for biofortification and also because of relevance to phytoremediation strategies. Cross-talk with other homeostatic machinery for essential micro and macro nutrients adds another level of complexity and therefore Zn stress (deficiency or excess) cannot be considered in isolation.

Previously, the functional significance of F-group bZIP TFs in cereals was unknown; this thesis has addressed this, providing insight into this group in barley, an economically important crop. The seven members of this group (HvbZIP1, 10, 55, 56, 57, 58 and 62) have been cloned and some members functionally characterized. As well as providing a more comprehensive understanding of the adaptation to Zn deficiency in cereals, this thesis has also explored the role of P_{1B-2}-ATPases in Zn homeostasis. Here this new information from Chapters 3, 4 and 5 is discussed in relation to what is known in plants concerning the mechanisms controlling Zn levels;

areas that would benefit from further research will be highlighted and approaches that could be used suggested.

6.2 The role of bZIP transcription factors in the Zn-deficiency sensing mechanism

6.2.1 Are F-group bZIPs the primary sensors for Zn deficiency?

Transcription factors that respond to Zn levels to regulate gene expression have been identified in a range of different organisms including *S. cerevisiae* (*ZAP1*), *Schizosaccharomyces pombe* (*Loz1*), animals (*MTF-1*) and bacteria (ZntR and Zur) (Westin and Schaffner, 1988, Zhao and Eide, 1997, Corkins et al., 2013, Lin et al., 2014). Some act as repressors while others are activators of gene transcription. In *A. thaliana*, bZIP19 and bZIP23 are proposed to activate the transcription of a range of target genes including ZIP transporters under Zn deficiency (Assuncao et al., 2100; Inaba et al., 2015). Here a role in Zn-deficiency responses for AtbZIP19 and AtbZIP23 was confirmed by demonstrating the Zn-hypersensitivity in four novel double mutant alleles (Chapter 3), similar to that reported previously for *bzip19-1 bzip23-1* (Assuncao et al., 2010). With a primary aim to investigate the role of F-group bZIPs in cereals, this study has identified and cloned seven F-group bZIPs from barley (Chapter 4). The partial rescue of the Zn-deficiency phenotype of the *A. thaliana bzip19-1bzip23-2* double mutant indicates that at least three of them (HvbZIP56, HvbZIP57 and HvbZIP62) function in a similar way to AtbZIP19 and AtbZIP23 (Chapter 4). The *HvbZIP56*-expressing double mutants generated here have been used to show that this rescue is correlated with an up-regulation of ZIP transporters; *AtZIP4*, *AtZIP9* and *AtZIP12* up-regulation was restored by expressing *HvbZIP56* (Griffin, Nazri and Williams, unpublished).

In order to respond appropriately to the deficient environment, bZIP TFs must be able in some way to 'sense' the low Zn conditions and activate, although the mechanisms underlying this remain largely unknown. Clearly, AtbZIP19 and AtbZIP23 play important roles during Zn deficiency, although we cannot rule out broader responses in relation to oxidative stress. However, the question is whether there is a higher order of regulation? Are these the primary sensors of Zn deficiency or are there upstream signalling events? Figure 6.1 is taken from Claus and Chavarría-Krauser (2012) who sought to develop models of influx homeostasis in plant root cells; adaptation of influx-transporter expression was proposed as the major regulatory component. They considered three phases: sensing (Zn status is measured), transduction (decisions taken) and reaction (changes in cytosolic Zn concentrations occur). They discussed the validity of three models: Activator only, Activator with dimerization, Activator-Inhibitor model. In the model, activators are the TFs that can dimerize and the inhibitors either inhibit activators or

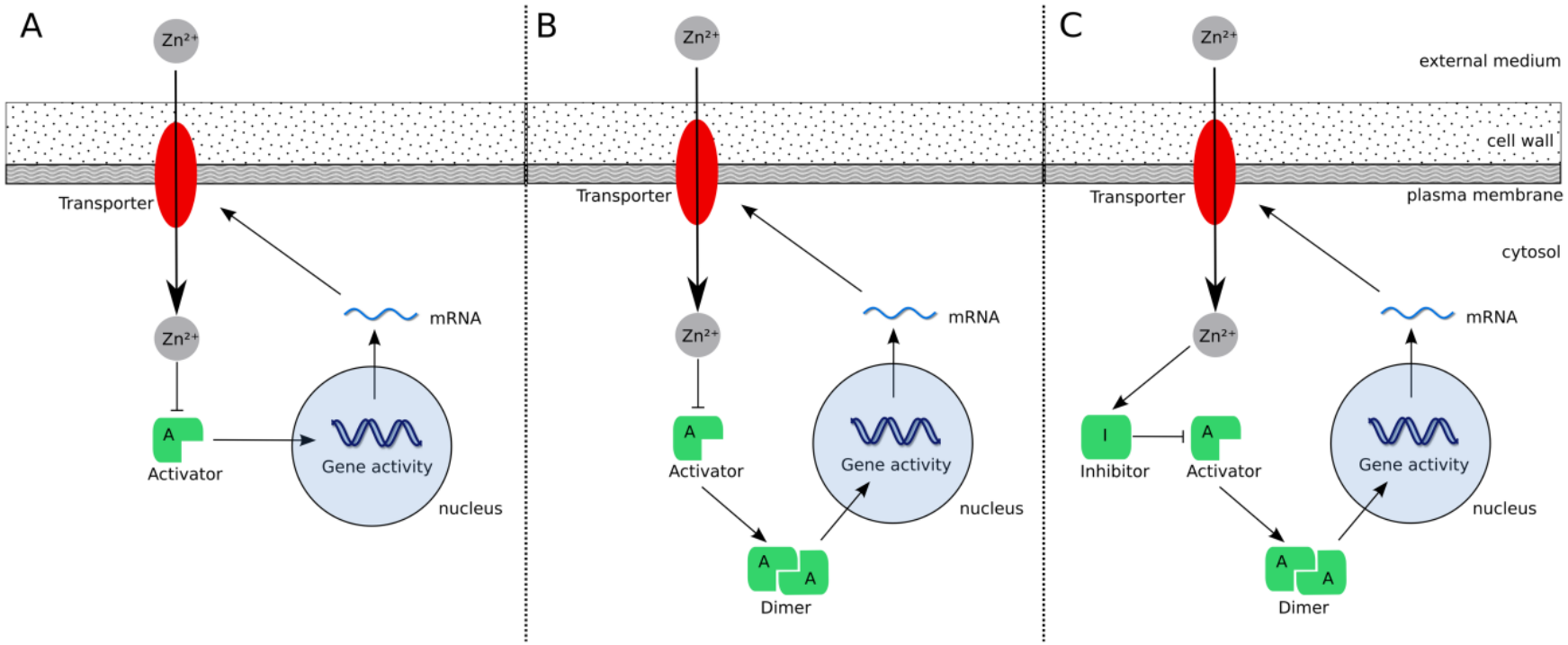

Figure 6.1 Three models of Zn uptake regulation in plant roots.

A, Activator only, B, Activator with dimerization, C, Activator-Inhibitor model [taken from Claus and Chavarria-Krauser (2012)].

directly repress gene activity. For this third model, they assumed that the activator and inhibitor can interact while they are not bound to the DNA and that the pairs cannot activate the gene and only the inhibitor senses the internal Zn. This model was favoured as it was considered to give better homeostatic control. As yet there is no evidence for this "inhibitor" and this may not be required for the mechanism proposed by Assuncao et al. (2013), discussed next.

Zn forms polyhedral coordination complexes with a variety of ligands, notably His and Cys (Dudev and Lim, 2000, Lu et al., 2009). The F-cohort of bZIP TFs cluster together phylogenetically and are also grouped based on the presence of two Cys/His-rich domains, suggested to function as a Zn sensor involved in reversible Zn binding (Assuncao et al., 2013). It is hypothesised that these TFs can sense the relative environment by binding of free cytosolic Zn to the Cys/His-rich residues (Assuncao et al., 2013). In this way, when Zn is bound, the TF is rendered inactive and has no transcriptional effect. The opposite is seen when cytosolic levels of Zn are low, allowing for translocation to the nucleus and binding of AtbZIP19/23 to their target ZIP genes. It is suggested that Zn binding causes a conformational change to the protein structure, thereby preventing its translocation to the nucleus or interaction with the DNA (Assuncao et al., 2013). All F-group barley bZIP TFs except HvbZIP10 have these two conserved Cys/His-rich domains (Chapter 4) and may therefore be activated by low Zn and target ZIP genes to enhance Zn uptake and overcome the deficit. The question of whether these motifs are key to the Zn-sensing mechanism remains to be tested rigorously. For instance, these two Cys/His domains are found in AtbZIP24, a regulator of salt stress in *A. thaliana*. The role of AtbZIP24 in the Zn-deficiency response has not been investigated and this is an important task for the future. HvbZIP1 possesses both domains and these are almost identical to those found in HvbZIP56; unlike the latter, it did not rescue the Zn hypersensitivity of the *bip19-4 bzip23-2* mutant, suggesting that these motifs are not the only determinants in Zn-responsiveness. However, there were other structural differences in HvbZIP1 such as a much shorter region C-terminal to the bZIP domain and the potential lack of N-terminal sequence, which affected its ability to rescue. HvbZIP1b that has now been cloned with this additional sequence and experiments in the future will test whether it will rescue the Zn hypersensitivity of the *bip19-4 bzip23-2* mutant. HvbZIP10, which has only one of the two Cys/His motifs, has also been cloned and expressed in *A. thaliana* double mutants. Unfortunately, the plants are not yet at the stage for testing, but this will be a priority as it could indicate whether two domains are necessary. In relation to the proposed mechanisms, it is essential that experiments are performed to directly determine whether these domains in F-groups do indeed bind Zn. This could be done by purifying the N-terminal region or even the entire bZIP and carrying out dithizone binding which detects Zn. Zn-binding capacity can also be measured using size exclusion chromatography-inductively coupled plasma mass spectrometry (SEC-ICP-MS). Both

of these techniques have been used for showing that the C-terminus of AtHMA4 binds Zn (Baekgaard et al., 2010). This information, combined with mutational analyses of these domains and complementation tests, should help clarify the role of the Cys/His domains.

There are also other considerations in relation to this mechanism. In order for the bZIP TF to sense that there is sufficient Zn in the environment, there must be a high enough level of Zn within the cytosol to bind to the reservoir of bZIP TFs and subsequently inactivate them. To avoid toxic levels of heavy metals within the cytosol, they are sequestered in organelles such as the vacuole (Clemens, 2001). Therefore, perhaps other intermediary ligands are involved to coordinate this (Assuncao et al., 2013). Additionally, bound Zn needs to be readily released from the TFs during times of deficiency (Assuncao et al., 2013), allowing the bZIPs to firstly become functionally active and to additionally provide Zn to other proteins that require it. It is important to note also that in this study, targeting to the nucleus of HvbZIP56 did not appear to be enhanced by Zn deficiency and this bZIP was found in the nucleus when Zn was present (Chapter 4). This may indicate that targeting to the nucleus can occur whether Zn is bound or not and hence is not fundamental to the mechanism, but activation of downstream genes only occurs by the unbound form. In yeast, the Zap1-regulated genes have been divided into two classes: those induced under mild Zn deficiency, which are proposed as first-line defense genes, acting to increase Zn uptake and mobilising intracellular pools and second-line defense genes responding to severe Zn limitation and functioning to allow adaptation (Wu et al., 2008). Detailed transcriptomics and proteomic studies in the future on barley with non-functional or down-regulated bZIPs would be useful in identifying targets for particular bZIPs and indicate whether there are different classes in relation to the extent of deficiency.

6.2.2 Interaction with the ZDRE

The family of bZIP TFs are characteristically known to bind to cis elements upstream of the target gene to induce transcription (Fujii et al., 2000). Each cis element usually has a specific palindrome sequence, which targets it to specific bZIP TFs (Fujii et al., 2000, Pourabed et al., 2015). In this way, genes are specifically and tightly up-regulated to bring about an appropriate response to the environment. Studies in *A. thaliana* have identified a conserved cis element within the promoter region of Zn-responsive genes, including many from the ZIP family (Assuncao et al., 2010). This region, the Zn-deficiency-response element (ZDRE), was first described as having a sequence of RTGTCGACAY (Assuncao et al., 2010). This sequence is unique from other bZIP binding regions (G-box, A-box) (Assuncao et al., 2010) and therefore proposed to be specific to Zn homeostasis. Lin et al. (2016) have carried out an elegant promoter-GUS analysis for AtZIP4 and *N. caerulescens* ZIP transporter NcZNT1; deletion of the two ZDRE domains in their respective

promoters had a marked effect on up-regulation by Zn deficiency, abolishing it almost completely. Screens of *AtZIP* gene promoter sequences have shown the ZDRE cis element to be present across nine ZIP members in the *A. thaliana* genome (Assuncao et al., 2010). These genes exhibit differential induction patterns from the WT in *bzip19-1 bzip23-1* mutants, in response to Zn deficiency (Assuncao et al., 2010). Evidence such as this suggests that this region is required for AtbZIP19/23 binding and therefore up-regulation of gene expression in the primary response to deficiency. *AtZIP* genes, which are not reported to be directly induced at the transcriptional level by Zn deficiency such as AtZIP2, do not possess the ZDRE palindrome (Assuncao et al., 2010). It is therefore expected that AtbZIP19/23 will not bind to their promoters. There are some conflicting reports that *AtZIP2* does show an increase in response to Zn deficiency (Jain et al., 2013) but in our lab this gene was not induced under low-Zn conditions (Griffin, Nazri and Williams, unpublished) and thus is consistent with the ZDRE domain being important. Jain et al. (2013) also noted that *AtZIP10,* although having a single ZDRE domain (which we have confirmed together with an additional less conserved potential element) was not up-regulated in response to Zn deficiency (although they did not show the data). It could be argued that other regulatory mechanisms are involved, independent of the bZIP and ZDRE interaction. However, it is important to measure responses to Zn deficiency over a time course, as there is a difference in the timing of up-regulation and the extent for some *ZIPs*, so drawing conclusions on a single time point can be misleading. These differences could relate to the particular tissue localisation of the ZIP and bZIP in question and when Zn-deficiency is first sensed, or it could indicate that there are differences in the sensitivity of different bZIPs, which could then lead to distinct subsets of genes regulated in certain tissues and cells. Results indicate that bZIPs do indeed show overall differences in their expression levels in particular tissues and in their tissue distribution, although these measurements are under Zn sufficiency (Chapter 4). Some such as *HvbZIP62* are highly expressed in most tissues while others are found more discretely.

Research here indicates that the ZDRE is found in certain barley *ZIP* promoters suggesting that this element is conserved across species. On the whole, like *A. thaliana*, only Zn-deficiency-induced *ZIPs* contain ZDRE in their promoters. The ZDRE domain in *HvbZIP13* was 1bp different and not palindromic but it was induced by Zn deficiency; therefore either the criteria for recognition by bZIPs is not as stringent as initially predicted or there are other mechanisms leading to up-regulation in this case.

Interestingly, two F-group bZIP TFs, *HvbZIP1* and *HvbZIP58*, have ZDREs in their promoter and they were strongly induced by Zn deficiency. These two TFs might therefore be controlled by other elements, possibly other bZIPs that bind to the ZDRE to become functionally active. However, this is unlikely to be the reason why the expression of *HvbZIP1* failed to rescue the Zn-

sensitive phenotype of *bzip19-4 bzip23-2* double mutants as in this case it was expressed under the 35S promoter and would have been constitutively expressed. We are still exploring the possibility that the extra N-terminal region of HvbZIP1 that was found in sequence analysis carried out later in this project is vital for its function. Further promoter analyses of F-group *bZIP* TFs also found that *HvbZIP1* and *HvbZIP58*, together with *HvbZIP10* and H*vbZIP57* contain one A-box or G-box in their promoter. All of these *bZIPs* are induced by Zn deficiency (*HvbZIP57* in the roots). As mentioned earlier, these two cis-elements are thought to be the binding site for bZIP TFs. Therefore, there could be a more complex regulatory system operating in barley, with F-group bZIPs regulating each other and possible other regulatory mechanisms involved. More detailed analyses is required to investigate this in the future. EMSAs are a useful technique for showing that barley F-group bZIPs interact with ZDRE domains (indicated by gel retardation) and this could be a starting point. ChIP could be performed which is powerful because it allows the identification of protein-DNA interactions that occur *in vivo*. Moreover, it could be used to evaluate whether cereal bZIP/ZIP promoter interactions are increased under Zn deficiency. A transgenic approach is necessary for this and it could be achieved by expressing the GFP-tagged HvbZIP56 in barley. This would be expected to be found at the site of transcription of its targets (ZIPs), and for this to be enhanced under Zn deficiency. Chromatin from *HvbZIP56-GFP* expressing barley could be isolated following growth under Zn replete and Zn-deficiency conditions. By immunoprecipitating HvbZIP56-GFP with an anti-GFP antibody, genomic DNA fragments that coimmunoprecipitate under each condition could be quantified using qPCR by screening along the barley ZIP or indeed bZIP promoters; we may expect there to be an enrichment in the target ZIP promoter regions and particularly the ZDRE motifs. As we have full genomic sequence information now for the barley ZIP genes, it will be straightforward to design suitable primers for this analysis. To capture novel targets, ChIP-seq could be conducted, which uses high-throughput DNA sequencing.

6.2.3 Further Post-translational regulation of bZIPs

The complete Zn-sensing model in plants is still not completely clear. Further post-translational regulation might play some role in this complex adaptation to Zn deficiency in plants. Partial rather than full rescue of the *bzip19-4 bzip23-2* double mutant by HvbZIP56/57/62 could indicate that perhaps barley bZIP homodimers are not as effective and that heterodimerization should be investigated. The orthologues of F-group bZIP in *A. thaliana*, AtbZIP19 and AtbZIP23, are suggested to form homodimers. The overexpression of either *AtbZIP19* or *AtbZIP23* in *bzip19-1 bzip23-1* double mutants completely complements the Zn-hypersensitive phenotype suggesting that AtbZIP19 and AtbZIP23 are redundant and thus function as homodimers. Barley HvbZIP56, HvbZIP57 and HvbZIP62, on the other hand, might form heterodimer between different groups of

bZIPs. This type of interaction is seen between members of C-group and S-group. The heterodimer formation between AtbZIP10 (C-group) and AtbZIP53 (S-group) is required for the binding to the promoter region of the proline dehydrogenase (*ProDH*) gene and subsequently activating its expression synergistically during the hypo-osmolarity response (Weltmeier et al., 2006, Satoh et al., 2004). Thus, future studies are required to determine if the expression of more than one barley *bZIPs* in *bzip19-4 bzip23-2* could fully rescue the mutant phenotype. Plants expressing *HvbZIP56* and *HvbZIP1b* have been generated and are awaiting further study.

bZIP TFs can also be post-translationally modified by phosphorylation. The transcriptional activity and stability of A-group and H-group have been shown to be regulated by phosphorylation inside the nucleus. The rice basic domain/Leu zipper factor, TRAB1 is a member of group A-bZIP in rice that is involved in the ABA stress response and it is phosphorylated prior to the induction of ABA-responsive genes facilitated by a group of kinases (Kagaya et al., 2002). SnRK2 kinases have been identified in rice to directly phosphorylate TRAB1 TF in response to ABA and induce ABRE-controlled reporter gene expression in an ABA-dependent mode (Kobayashi et al., 2005). Phosphorylation can also modulate bZIP activity by intracellular partitioning due to the introduction of negative charge, which subsequently inducing allosteric changes in the protein and alters its repulsive and attractive forces (Schutze et al., 2008). The parsley C-group CPRF2 and the parsley G-group bZIP GBF2 are modulated by light-dependent phosphorylation so that they can be translocated from the cytosol to the nucleus (Harter et al., 1994, Kircher et al., 1999) .

Interaction with other proteins could also alter F-group bZIP activity. C-group, D-group and A-group bZIPs have been shown to form specific complexes with non-bZIP proteins in the cytoplasm or the nucleus. *A. thaliana* D-group bZIPs are involved in pathogen defence system. Under pathogen attack, members of *A. thaliana* D-group are activated by physical interaction with the non-expressor-of-pathogenesis-related-genes-1 protein (NPR1, synonym NIM1) (Pieterse and Van Loon, 2004, Dong, 2004), thereby activating pathogenesis-related (PR) genes. The *A. thaliana* A-group member AtbZIP27 which mediates antagonistic regulation of flowering requires interaction with flowering locus T (FT) and terminal flower 1 (TFL1), and it recruits these floral regulators to promoters of floral identity genes (e.g. APETALA1 [AP1]) to regulate flowering (Abe et al., 2005, Wigge et al., 2005).

6.3 Downstream targets of F-group bZIPs

6.3.1 Zn-regulated genes

It is important for plants to maintain homeostatic levels of Zn within the cell cytosol to avoid the adverse effects of deficiency or toxicity. The ZIPs are thought to be primarily responsible for Zn uptake in the roots as well as translocation and sequestration throughout the whole plant (Guerinot, 2000). This family of transporters has the capacity for transporting a number of cations including Zn and are present throughout the Eukaryotic kingdom (Guerinot, 2000, Pedas and Husted, 2009, Milner et al., 2013). Much of what is known about the ZIP family of membrane transporters has been identified using the model organism *A. thaliana*, with evidence now emerging of their function in monocot species including barley (Tiong et al., 2014).

To date, fifteen members of the ZIP family have been identified in the *A. thaliana* genome (AtZIP1-12/AtIRT1-3) (Ricachenevsky et al., 2015), many of which are associated with Zn homeostasis. There is now good evidence for a number of these being up-regulated by Zn deficiency and this mediated by F-group bZIP TFs. The induction of *ZIP* gene expression is likely to be an adaptive response, increasing the number of membrane transporters and therefore relative Zn uptake to restore intracellular concentrations (Assuncao et al., 2010). Interestingly, not all of these *ZIP* transporters have been reported to be up-regulated in Zn deficient conditions. Also we are not certain about mechanisms for down-regulating the ZIPs under Zn excess, which is important in avoiding hyper-accumulation.

ZIP transporters have been observed to be differentially expressed both temporally and spatially in *A. thaliana* in response to Zn deficiency, suggesting they may have different contributions to maintaining homeostasis (Assuncao et al., 2013). The *A. thaliana* genes *AtZIP1*/*2*/*3*/*5*/*6* have all been reported to have a higher expression in root tissues in comparison to shoots (Milner et al., 2013) in response to Zn deficiency, while AtZIP7/*11* have been reported to be induced more in shoots than roots (Milner et al., 2013). This evidence suggests that different ZIPs may have distinct roles in uptake and mobilisation in plants. However in contrast, other studies have shown significantly greater expression of AtZIP*2*/*3*/*4*/*5*/*9*/*12* in *A. thaliana* shoots in comparison to roots (Jain et al., 2013). Inconsistencies in findings may be attributable to the different protocols used in different studies; variations in Zn concentrations and/or treatment durations are often reported as well as the technique used to quantify gene expression. As a result, there is still poor knowledge of the role of ZIP transporters at the individual level and in many circumstances, means their true physiological role is unknown (Ricachenevsky et al., 2015).

To date, thirteen ZIP transporters have been identified in the barley genome, HvIRT1, HvZIP1, HvZIP2, HvZIP3, HvZIP5, HvZIP6, HvZIP7, HvZIP8, HvZIP10, HvZIP11, HvZIP13, HvZIP14, and HvZIP16 (Tiong et al, 2015). Of these, six members (*HvZIP3/5/7/8/10/13*) have been reported to be directly induced in response to Zn deficiency (Tiong et al., 2014, Tiong et al., 2015, Jain et al., 2013). Yeast complementation studies have been equally important for the elucidation of ZIP transporters in barley and have so far shown the ability of HvZIP3/5/8 to restore the WT phenotype of *zrt1 zrt2* yeast mutants (Pedas et al., 2009). In the present study, *HvZIP5*/*10*/*13* expression was induced in barley shoot tissues in response to Zn deficiency. Previous studies have also reported increased *HvZIP5* expression in response to low Zn, but have interestingly shown expression to be significantly higher in the roots than shoots (Pedas et al., 2009). This early data suggested that HvZIP5 was primarily involved in Zn uptake at the roots and therefore involved in apoplastic and soil retrieval (Pedas et al., 2009). However, in light of this new evidence, the induced expression in shoot tissues may also suggest a functional role of HvZIP5 in root to shoot translocation in barley. Localisation studies may prove useful in elucidating this further, confirming whether it is present in the vasculature. Future research should focus on determining cell-specific Zn concentrations in relation to ZIPs and the use of marker technology to localise more transporters to specific membranes to appreciate fully their individual contributions to Zn homeostasis and to understand the Zn-deficiency response more comprehensively.

Bioinformatics has shown that there are ZDRE domains in the promoters of other barley genes including members of the Nicotianamine Synthase family (Griffin and Williams, unpublished) and oxidative stress reporters (see below). Additionally, in the plants generated during this project it has been shown that expression of *HvbZIP56* is able to up regulate *AtNAS4* in the *bzip19 bzip23* double mutant under Zn deficiency (Griffin, Nazri and Williams, unpublished) suggesting that the mechanism for up-regulating other genes involved in adapting to Zn-deficiency is conserved between *A. thaliana* and barley.

6.3.2 Broader roles for F-group bZIPs (oxidative stress response)

Zn is not redox active and as such does not directly donate or accept electrons (Eide, 2011) but there is a correlation between Zn deficiency and oxidative stress with low Zn increasing the production of reactive oxygen species (Günther et al., 2012, Glover-Cutter et al., 2014). Oxidative stress in cells as a result of low Zn could be due to: a reduction in activity of enzymes such as Cu/Zn superoxide dismutase; an increased binding of the redox active Cu and Fe metal ions because of low competing Zn; reduced Zn binding and hence protection of sulfhydryl groups in proteins. To reduce oxidative stress as a result of Zn deficiency, homeostatic mechanisms are very important to combat fluctuating levels. Yeast seems to have “proactive” rather than just

"reactive" mechanisms in place. That is the oxidative-stress resistance mechanisms are instigated through the Zn-responsive transcriptional activator ZAP1, which induces expression of antioxidant enzymes such as catalase as well as the ZIP family members.

Recently, Glover-Cutter et al. (2014) reported that the overexpression of *B. distachyon bZIP10*, a bZIP TF in *B. distachyon* that is highly homologous to AtbZIP19 and AtbZIP23, activates a protective transcriptional response that results in enhanced oxidative stress resistance and increased viability. They reported direct activation by BdbZIP10 of stress recovery factors, such as BdASN1, through binding to Box A and Box G elements (common bZIP DNA-binding motifs). The question is whether this is a general property of F-group bZIP TFs. Future work could investigate this as we have generated plant lines that could test aspects of this. We know that *AtASN1* is induced under oxidative stress (Abercrombie et al., 2008) and we have a system in place to investigate whether this gene is regulated by AtbZIP19 and AtbZIP23 or indeed by HvbZIP56. Comparisons of gene expression in *A. thaliana* WT, double mutants and *HvbZIP56*-expressing lines (both WT and *bzip19-4 bzip23* are available to us) will clarify whether this gene, and perhaps other oxidative stress reporters, is under the control of these TFs. Indeed, as we have other barley *bZIPs* expressed in the *A. thaliana* lines, we can explore their role in regulating not only *AtASN1* but also homologues of some of the oxidative stress reporter genes purported to be activated by BdbZIP10 (eg. CSD, superoxide dismutase; manganese superoxide disumutase1 and glutathione peroxidase. This could be supported by determining whether these genes are regulated in barley under Zn-deficiency as observed for *B. distachyon*. It should be noted, that in analysing these genes, a completely conserved ZDRE was found in *HvASN1* but not the other *HvASN* genes and so it would be informative to test the response of each of these genes to oxidative stress and Zn deficiency to determine whether a correlation exists.

Cu is reported to induce oxidative stress in plants and was one of the treatments used in Glover-Cutter et al. (2014) to generate this (Gaetke and Chow, 2003). When grown on toxic Cu with basal Zn supply, the *bzip19-4 bzip23-2* double mutants have a similar phenotype to the WT plants, suggesting that AtbZIP19 and AtbZIP23 might not be directly involved in oxidative stress (Chapter 3). On the other hand, the *bzip19-4 bzip23-2* double mutants were significantly stunted on Cu when the lowest Zn concentration that can rescue the mutants was used (Chapter 4). This could suggest a role for these genes in oxidative stress responses. Conversely, it could be argued that this inhibition of growth is still directly connected with Zn deficiency due to competition for uptake between Zn and Cu. Cu transport by the ZIPs has been reported (Wintz et al., 2003) and therefore increased external Cu could inhibit Zn uptake and lead to Zn deficiency in cells. The *bzip19-4 bzip23-2* mutants would therefore not be able to respond leading to reduced growth. A

competition effect does seem to operate in barley where exposure of roots to Zn deficiency resulted in a higher content of Cu and Fe but not Mn (Tiong et al., 2015).

A more direct way to explore the role of barley bZIPs in the Zn-deficiency response and more widely in oxidative stress resistance would be to generate knockout plants in barley for the bZIPs either alone or in combination. The advances in gene editing technology in crops make this a realistic goal for the future. If some are confirmed as having a role solely in Zn-deficiency or more widely as cross-functional stress TFs, they could be invaluable for future biotechnological or breeding strategies.

6.4 Other responses to Zn stress

6.4.1 The role of miRNA

Zn-deficiency regulation is intricate and other mechanisms should be considered together with the genes studied here in order to provide a full-picture of Zn homeostasis. It will be important to determine how miRNAs are involved and determine whether these are important in barley in regulating Zn-deficiency adaptation as has been observed in *S. bicolor* (Li et al., 2013). Certainly there could be a connection as in *S. bicolor*, several miRNAs were up-regulated in response to Zn deficiency and ZDRE motifs (allowing two mismatches outside the core sequence of the ZDRE) were reported to occur in the promoters of some of them: *miR166a*, *miR166b*, *miR166d*, *miR166k*, *miR168*, *miR398*, and *miR399c*. *mi398* targets CSD and could be involved in a mechanism to prioritise Zn delivery to carbonic anhydrase, therefore modulating responses to micronutrient deficiency (Li et al., 2013). *miR399c* up-regulation under Zn deficiency could target PHO2, which negatively regulates phosphate transporters leading to increased Pi accumulation (Li et al., 2013).

6.4.2 Micronutrient and macronutrient imbalances and cross talk

Zn stress is also associated with the imbalance of other micronutrients in the plant. While ionomic analyses was not performed in the current study, previous evidence has reported elevated levels of Cu and Fe in barley roots grown in Zn-deficient conditions (Pedler et al., 2000, Lombnes and Singh, 2003). It has been suggested that this may be the result of the concentration gradient across the plasma membrane or alternatively, by restricted translocation (Lombnaes, 2003). Additionally, studies have shown the hyper-accumulation of macronutrients as a result of Zn deficiency. Elevated levels of P are often associated with Zn starvation (Huang et al., 2000, Lombnes and Singh, 2003) as well as K and S (Jain et al., 2013). In term of Zn toxicity, it can cause

Fe and Cu level in plants to be reduced but it does not change the level of P and S (Jain et al., 2013). The effects of these imbalances may not be accounted for in the nutrient solutions used in the present study, therefore it is plausible that the Zn-deficient grown barley may have additionally suffered from altered levels of other heavy metals.

Differences observed in micronutrients and macronutrient levels as a result of Zn stress may be attributable to the cross talk of Zn with other homeostatic networks. Zn deficiency has been associated with the up-regulation and down-regulation of genes involved in several other homeostatic pathways, suggesting a molecular interaction. Studies have reported the attenuation and induction of Fe-related genes in *A. thaliana* root and shoots (Jain et al., 2013) during both Zn deficient and Zn-toxicity conditions. Other genes involved in S and K redistribution and uptake have also been reported to be directly suppressed by Zn deficiency (Jain et al., 2013). The effect on Pi-related genes is discussed previously.

6.5 The vacuole is a crucial compartment for Zn and Cd homeostasis

The vacuole is an essential organelle in plant cells. It can provide a firm structure to cells by using water to develop hydrostatic pressure (Marty, 1999). Other functions include storing nutrients and non-nutrients, and breaking down complex molecules (Marty, 1999). Certainly in relation to heavy metals, the vacuole represents a compartment where they can be stored when in excess and released during times of deficiency (Hall and Williams, 2003). The non-essential heavy metal Cd can be very toxic to plant cells, and plants respond to this stress by transporting the toxic heavy metal into the vacuole.

Zn concentration must be tightly controlled in the cytosol and any excess Zn can be stored in the vacuole and can be exported from there into the cytosol when required. Many membrane transporters are localised at the vacuolar membrane that have various functions and some of these have been implicated in Zn transport. For example, in barley HvMTP1, a member of the CDF family has been localised to the tonoplast and suggested to have a functional role in detoxification and vacuolar sequestration (Podar et al., 2012). This thesis has focussed on members of the P_{1B-2}-ATPase heavy metal transporters in barley and has used *A. thaliana* mutants and heterologous expression in yeast to determine a contribution to heavy metal homeostasis (Chapter 5). This has shown that HvHMA3 could be involved in Zn detoxification as it rescues the *A. thaliana mtp1-1* Zn-toxicity phenotype and although its localisation is not yet confirmed, it has high homology to rice P_{1B-2}-ATPases that localises to the tonoplast (Miyadate et al., 2011). The *mtp1* mutant was used for these experiments as a Zn-toxicity phenotype could not be confirmed for *A. thaliana hma3* mutants and further work is required on this. Figure 6.2 shows the proposed

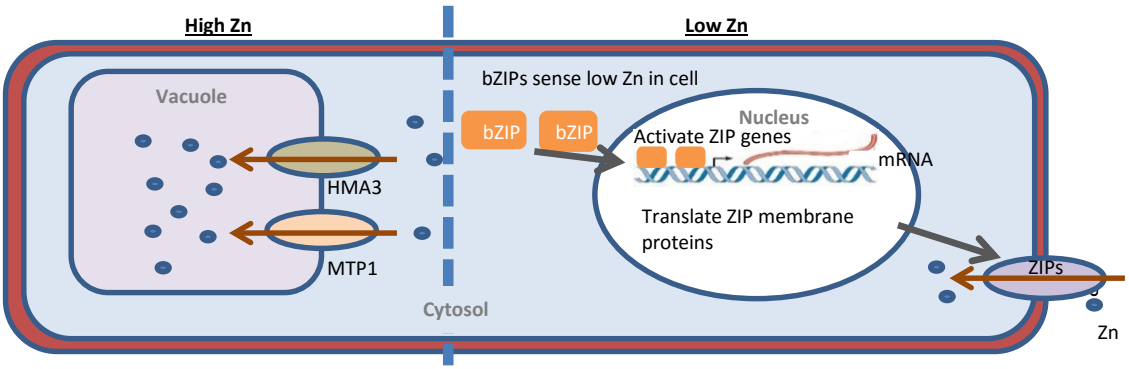

Figure 6.2 Zn homeostasis model in barley

Diagram to illustrate the potential model for maintaining optimum Zn level in barley cells. High Zn (left)-excess Zn is sequestered in the vacuole by HvMTP1 (Podar et al., 2012) and HvHMA3. Low Zn (right)- F-group bZIP TFs sense low Zn and trigger the transcription of Zn membrane transporters (*HvZIPs*), which increase Zn uptake into cells.

model for the role of HvHMA3 and HvMTP1 for Zn detoxification but as yet we cannot be sure that these transporters are expressed on the same vacuoles within a cell or expressed in the same tissues or under the same conditions.

The role of HvHMA3 in Cd detoxification is still unclear. The orthologues of HvHMA3 in various plants are shown to transport Cd such as rice OsHMA3 (Ueno et al., 2010, Miyadate et al., 2011); therefore, this gene could be important, like OsHMA3, in determining the level of Cd reaching the shoot. It will be interesting to determine in the future if HvHMA3 contributes to the large differences in Cd shoot and grain accumulation seen in barley cultivars (Wu et al., 2015a).

6.6 Potential for agriculture and human nutrition

Micronutrient malnutrition is a major health issue with more than half of the world population affected (Gibson et al., 2006). This is a particular issue in developing countries where there can be a reliance on staple foods, which are low in micronutrients such as cereal grains. As the estimates of world population are considered to be over nine billion by 2050 (DESA, 2015), sustainable agricultural practices are vital in meeting global demands for food, both in terms of quantity and quality.

Enhancing the micronutrient content in staple food crops using a variety of biofortification strategies is considered an important goal for food security. Understanding the mechanisms controlling Zn uptake and partitioning throughout the plant is vital in designing genetic biofortification schemes. The intricate controls over Zn sensing, uptake and translocation are starting to be appreciated in crop plants and future targets for manipulation are being identified. The benefit of manipulating bZIP levels is that they can control a more complex regulatory network of genes involved in Zn deficiency and so could be better targets for manipulation than those downstream. Interestingly, no marked effects of expressing barley *HvbZIP56* in WT *A. thaliana* were observed in this thesis but only preliminary tests were carried out. No effects were observed on response to Zn deficiency or Zn excess in terms of fresh weight measurements on plate assays but other parameters were not determined such as metal content or seed production when grown on low Zn soils. Also it is possible that other bZIPs could have more of a beneficial influence either expressed alone or in combination. It will also be important to test the effects of over-expressing these genes in barley. As *BdbZIP10* over-expression has been shown to improve resistance to oxidative stress in *B. distachyon*, it is possible that bZIP-expressing barley will be resistant to a wider range of stress conditions. In addition, it may be useful to have a more targeted expression of bZIPs to achieve higher Zn levels in the grain by employing grain-specific promoters to drive expression.

The manipulation of the bZIPs could have further benefits. Cu contamination of soils through the use of pesticides is an increasing problem for agriculture throughout the world. If Cu does compete effectively with Zn then Zn-deficiency could still occur in apparently Zn-sufficient soils. Altering particular bZIPs may improve this, but this would depend on which ZIPs were up-regulated and their relative affinities for Cu and Zn. Further work on the Cu/Zn interaction is required to develop the best strategies for improving yield and quality of crops.

For the mechanisms of Zn homeostasis to be fully characterised, it is important to understand the mechanisms of cross-communication between the different homeostatic pathways. This may prove to be very important when it comes to genetic engineering strategies, as manipulating the Zn regulatory pathways may have adverse effects on the distributions and concentrations of other essential micronutrients in the plant system.

Manipulation of HMA3 membrane transporters could be useful in generating Cd-free grains in temperate cereals. The importance of these transporters are shown in rice where it is the key gene in influencing Cd accumulation (Ueno et al., 2010, Miyadate et al., 2011). As OsHMA3 could also retain Zn in the roots, it is possible that the manipulation of OsHMA3 could also affect Zn concentrations in other part of plants. However, it has been shown that OsHMA3-overexpressing plants have optimum Zn concentrations in the shoot even though the Zn concentration in the roots is high (Sasaki et al., 2014). In OsHMA3 overexpressing plants, the *ZIPs* were seen to be up-regulated (Sasaki et al., 2014). Therefore, it is possible that the ZIP transporters compensate for the lack of Zn by taking up more Zn into the cells. Allelic variation of HvHMA3 should be explored in terms of identifying the most promising HvHMA3 structures for Cd transport.

Additionally, vast areas of land are unfit for agriculture because of heavy metal contamination. Identifying the mechanisms of Zn homeostasis could provide opportunities to engineer plant species suitable for remediating land for agricultural use. Phytoremediation is a technique currently employed today but largely impaired by the lack of suitable traits in the plant species available. By understanding the mechanisms of Zn uptake, sequestration and tolerance, it may be possible to engineer plants that are more efficient in these processes to enhance their use commercially. Understanding the mechanisms of Zn homeostasis in plants will inevitably have other beneficial future applications as our scientific knowledge continues to advance.

6.7 Conclusion

Zn-homeostatic mechanisms are vital in plants allowing them to cope with varying Zn supply. This study represents a significant step forward in understanding the mechanisms controlling Zn responses in cereal crops, and will aid in developing strategies for crop

improvement. New evidence has allowed for putative models of Zn homeostasis to be discussed, linking the activation of bZIP TFs with the up-regulation of target *ZIP* genes. Studies have so far identified many bZIP and ZIP orthologues across multiple species (Assuncao et al., 2010), suggesting the mechanism of Zn homeostasis may be shared across the plant kingdom. While the full picture is still incomplete, a good foundation has been laid into understanding the mechanisms underlying Zn homeostasis in plants. Future research will prove fundamental to accepting the role of F-group bZIPs as regulator of *ZIP* gene expression and may further contribute to the uncovering of Zn homeostasis in plants.

Reference

Abdel-Ghany, S.E., Muller-Moule, P., Niyogi, K.K., Pilon, M. and Shikanai, T. (2005) Two P-type ATPases are required for copper delivery in *Arabidopsis thaliana* chloroplasts. *Plant Cell,* 17, 1233–1251.

Abe, M., Kobayashi, Y., Yamamoto, S., Daimon, Y., Yamaguchi, A., Ikeda, Y., Ichinoki, H., Notaguchi, M., Goto, K. and Araki, T. (2005) FD, a bZIP protein mediating signals from the floral pathway integrator FT at the shoot apex. *Science,* 309 (5737), 1052-1056.

Abe, T., Taguchi-Shiobara, F., Kojima, Y., Ebitani, T., Kuramata, M., Yamamoto, T., Yano, M. and Ishikawa, S. (2011) Detection of a QTL for accumulating Cd in rice that enables efficient Cd phytoextraction from soil. *Breeding science,* 61 (1), 43-51.

Abercrombie, J.M., Halfhill, M.D., Ranjan, P., Rao, M.R., Saxton, A.M., Yuan, J.S. and Stewart, C.N. (2008) Transcriptional responses of *Arabidopsis thaliana* plants to As (V) stress. *BMC Plant Biology*, *8*(1), p.1.

Abourached, C., Catal, T. and Liu, H. (2014) Efficacy of single-chamber microbial fuel cells for removal of cadmium and zinc with simultaneous electricity production. *Water Research,* 51, 228-233.

Ahmad, I., Akhtar, M.J., Zahir, Z.A. and Jamil, A. (2012) Effect of cadmium on seed germination and seedling growth of four wheat (*Triticum aestivum* L.) cultivars. *Pakistan Journal of Botany,* 44 (5), 1569-1574.

Alberti, S., Gitler, A.D. and Lindquist, S. (2007) A suite of Gateway® cloning vectors for high-throughput genetic analysis in *Saccharomyces cerevisiae*. *Yeast,* 24 (10), 913-919.

Allen, H.E., Mcgrath, S., Mclaughlin, M., Peijnenburg, W., Sauvé, S. and Lee, C. (2001) *Bioavailability of metals in terrestrial ecosystems: importance of partitioning for bioavailability to invertebrates, microbes, and plants*. Society of Environmental Toxicology and Chemistry.

Alloway, B.J. (2004) *Zinc in soils and crop nutrition*. Brussels, Belgium: International Zinc Association.

Alloway, B.J. (2008) Micronutrients and Crop Production: An Introduction IN: Alloway, B.J. (ed.) *Micronutrient Deficiencies in Global Crop Production*. Dordrecht: Springer Netherlands, 1-39.

Alonso, J.M., Stepanova, A.N., Leisse, T.J., Kim, C.J., Chen, H., Shinn, P., Stevenson, D.K., Zimmerman, J., Barajas, P., Cheuk, R., Gadrinab, C., Heller, C., Jeske, A., Koesema, E., Meyers, C.C., Parker, H., Prednis, L., Ansari, Y., Choy, N., Deen, H., Geralt, M., Hazari, N., Hom, E., Karnes, M., Mulholland, C., Ndubaku, R., Schmidt, I., Guzman, P., Aguilar-Henonin, L., Schmid, M., Weigel, D., Carter, D.E., Marchand, T., Risseeuw, E., Brogden, D., Zeko, A., Crosby, W.L., Berry, C.C. and Ecker, J.R. (2003) Genome-wide insertional mutagenesis of *Arabidopsis thaliana*. *Science,* 301 (5633), 653-657.

Altschul, S.F., Madden, T.L., Schäffer, A.A., Zhang, J., Zhang, Z., Miller, W. and Lipman, D.J. (1997) Gapped BLAST and PSI-BLAST: a new generation of protein database search programs. *Nucleic Acids Research,* 25 (17), 3389-3402.

Andreini, C., Banci, L., Bertini, I. and Rosato, A. (2006) Counting the zinc-proteins encoded in the human genome. *Journal of Proteome Research,* 5 (1), 196-201.

Ang, L.H., Chattopadhyay, S., Wei, N., Oyama, T., Okada, K., Batschauer, A. and Deng, X.W. (1998) Molecular interaction between COP1 and HY5 defines a regulatory switch for light control of Arabidopsis development. *Molecular Cell,* 1 (2), 213-222.

Arasimowicz-Jelonek, M., Floryszak-Wieczorek, J. and Gwozdz, E.A. (2011) The message of nitric oxide in cadmium challenged plants. *Plant Science,* 181 (5), 612-620.

Argüello, J.M. (2003) Identification of ion-selectivity determinants in heavy-metal transport P1B-ATPases. *The Journal of Membrane Biology,* 195, 93-108.

Arguello, J.M., Eren, E. and Gonzalez-Guerrero, M. (2007) The structure and function of heavy metal transport P1B-ATPases. *Biometals,* 20 (3-4), 233-248.

Arrivault, S., Senger, T. and Kramer, U. (2006) The Arabidopsis metal tolerance protein AtMTP3 maintains metal homeostasis by mediating Zn exclusion from the shoot under Fe deficiency and Zn oversupply. *The Plant Journal,* 46 (5), 861-879.

Assuncao, A.G., Herrero, E., Lin, Y.F., Huettel, B., Talukdar, S., Smaczniak, C., Immink, R.G., Van Eldik, M., Fiers, M., Schat, H. and Aarts, M.G. (2010) *Arabidopsis thaliana* transcription factors bZIP19 and bZIP23 regulate the adaptation to zinc deficiency. *Proceedings of the National Academy of Sciences,* 107 (22), 10296-10301.

Assuncao, A.G., Persson, D.P., Husted, S., Schjorring, J.K., Alexander, R.D. and Aarts, M.G. (2013) Model of how plants sense zinc deficiency. *Metallomics,* 5 (9), 1110-1116.

Astolfi, S., Zuchi, S., Neumann, G., Cesco, S., Di Toppi, L.S. and Pinton, R. (2012) Response of barley plants to Fe deficiency and Cd contamination as affected by S starvation. *Journal of Experimental Botany,* 63 (3), 1241-1250.

Auld, D.S. (2001) Zinc coordination sphere in biochemical zinc sites. *Biometals,* 14, 271-313.

Avila-Ospina, L., Marmagne, A., Talbotec, J., Krupinska, K. and Masclaux-Daubresse, C. (2015) The identification of new cytosolic glutamine synthetase and asparagine synthetase genes in barley (*Hordeum vulgare* L.), and their expression during leaf senescence. *Journal of Experimental Botany*, erv003.

Axelsen, K.B. and Palmgren, M.G. (1998) Evolution of substrate specificities in the P-type ATPase superfamily. *Journal of Molecular Evolution,* 461, 84–101.

Azpiroz-Leehan, R. and Feldmann, K.A. (1997) T-DNA insertion mutagenesis in Arabidopsis: going back and forth. *Trends in Genetics,* 13 (4), 152-156.

Baekgaard, L., Mikkelsen, M.D., Sorensen, D.M., Hegelund, J.N., Persson, D.P., Mills, R.F., Yang, Z., Husted, S., Andersen, J.P., Buch-Pedersen, M.J., Schjoerring, J.K., Williams, L.E. and Palmgren, M.G. (2010a) A combined zinc/cadmium sensor and zinc/cadmium export regulator in a heavy metal pump. *Journal of Biological Chemistry,* 285 (41), 31243-31252.

Baekgaard, L., Mikkelsen, M.D., Sørensen, D.M., Hegelund, J.N., Persson, D.P., Mills, R.F., Yang, Z., Husted, S., Andersen, J.P., Buch-Pedersen, M.J., Schjoerring, J.K., Williams, L.E. and

Palmgren, M.G. (2010b) A combined zinc/cadmium sensor and zinc/cadmium export regulator in a heavy metal pump. *Journal of Biological Chemistry,* 285 (41), 31243-31252 .

Baldauf, S.L. (2003) Phylogeny for the faint of heart: a tutorial. *Trends in Genetics,* 19 (6), 345-351.

Baloglu, M.C., Eldem, V., Hajyzadeh, M. and Unver, T. (2014) Genome-wide analysis of the bZIP transcription factors in cucumber. *PLoS One,* 9(4), P.e96014

Balzergue, S., Dubreucq, B., Chauvin, S., Le-Clainche, I., Le Boulaire, F., De Rose, R., Samson, F., Biaudet, V., Lecharny, A., Cruaud, C., Weissenbach, J., Caboche, M. and Lepiniec, L. (2001) Improved PCR-walking for large-scale isolation of plant T-DNA borders. *Biotechniques,* 30 (3), 496-498, 502, 504.

Barabaschi, D., Tondelli, A., Desiderio, F., Volante, A., Vaccino, P., Valè, G. and Cattivelli, L. (2016) Next generation breeding. *Plant Science,* 242, 3-13.

Barabasz, A., Wilkowska, A., Tracz, K., Ruszczynska, A., Bulska, E., Mills, R.F., Williams, L.E. and Antosiewicz, D.M. (2013) Expression of HvHMA2 in tobacco modifies Zn-Fe-Cd homeostasis. *Journal of Plant Physiology,* 170 (13), 1176-1186.

Barrameda-Medina, Y., Montesinos-Pereira, D., Romero, L., Blasco, B. and Ruiz, J.M. (2014) Role of GSH homeostasis under Zn toxicity in plants with different Zn tolerance. *Plant Science,* 227, 110-121.

Barrow, N.J. (1993) *Mechanisms of reaction of zinc with soil and soil components*. Dordrecht, The Netherlands: Kluwer Academic Publishers.

Bashir, K., Ishimaru, Y. and Nishizawa, N.K. (2012) Molecular mechanisms of zinc uptake and translocation in rice. *Plant and soil,* 361 (1-2), 189-201.

Bashir, K., Takahashi, R., Nakanishi, H. and Nishizawa, N.K. (2013) The road to micronutrient biofortification of rice: progress and prospects. *Frontiers in Plant Science,* 4, 15.

Bateman, A., Coin, L., Durbin, R., Finn, R.D., Hollich, V., Griffiths-Jones, S., Khanna, A., Marshall, M., Moxon, S., Sonnhammer, E.L.L., Studholme, D.J., Yeats, C. and Eddy, S.R. (2004) The Pfam protein families database. *Nucleic Acids Research,* 32 (suppl 1), D138-D141.

Baxter, I., Tchieu, J., Sussman, M.R., Boutry, M., Palmgren, M.G., Gribskov, M., Harper, J.F. and Axelsen, K.B. (2003) Genomic comparison of P-type ATPase ion pumps in Arabidopsis and rice. *Plant Physiology* 132, 618–628.

Baxter, I.R., Vitek, O., Lahner, B., Muthukumar, B., Borghi, M., Morrissey, J., Guerinot, M.L. and Salt, D.E. (2008) The leaf ionome as a multivariable system to detect a plant's physiological status. *Proceedings of the National Academy of Sciences,* 105 (33), 12081-12086.

Beauclair, L., Yu, A. and Bouche, N. (2010) microRNA-directed cleavage and translational repression of the copper chaperone for superoxide dismutase mRNA in Arabidopsis. *The Plant Journal,* 62 (3), 454-462.

Becher, M., Talke, I.N., Krall, L. and Kramer, U. (2004a) Cross-species microarray transcript profiling reveals high constitutive expression of metal homeostasis genes in shoots of the zinc hyperaccumulator Arabidopsis halleri. *The Plant Journal,* 37 (2), 251-268.

Becher, M., Talke, I.N., Krall, L. and Krämer, U. (2004b) Cross-species microarray transcript profiling reveals high constitutive expression of metal homeostasis genes in shoots of the zinc hyperaccumulator Arabidopsis halleri. *The The Plant Journal,* 37 (2), 251-268.

Berg, J.M. and Shi, Y. (1996) The galvanization of biology: a growing appreciation for the roles of zinc. *Science,* 271 (5252), 1081-1085.

Bernsel, A., Viklund, H., Hennerdal, A. and Elofsson, A. (2009a) TOPCONS: consensus prediction of membrane protein topology. *Nucleic Acids Research,* 37 (Web Server issue), W465-468.

Bernsel, A., Viklund, H., Hennerdal, A. and Elofsson, A. (2009b) TOPCONS: consensus prediction of membrane protein topology. *Nucleic Acids Research*, gkp363.

Besemer, J. and Borodovsky, M. (2005) GeneMark: web software for gene finding in prokaryotes, eukaryotes and viruses. *Nucleic Acids Research,* 33 (suppl 2), W451-W454.

Bevan, M. (1984) Binary Agrobacterium vectors for plant transformation. *Nucleic Acids Research,* 12 (22), 8711-8721.

Bevan, M., Bancroft, I., Mewes, H.-W., Martienssen, R. and Mccombie, R. (1999) Clearing a path through the jungle: progress in Arabidopsis genomics. *BioEssays,* 21 (2), 110-120.

Beyer, W.N., Green, C.E., Beyer, M. and Chaney, R.L. (2013) Phytotoxicity of zinc and manganese to seedlings grown in soil contaminated by zinc smelting. *Environmental Pollution,* 179, 167-176.

Bhatnagar, S. and Taneja, S. (2001) Zinc and cognitive development. *British Journal of Nutrition,* 85 Suppl 2, S139-145.

Blaudez, D., Kohler, A., Martin, F., Sanders, D. and Chalot, M. (2003) Poplar metal tolerance protein 1 confers zinc tolerance and is an oligomeric vacuolar zinc transporter with an essential leucine zipper motif. *Plant Cell,* 15 (12), 2911-2928.

Blindauer, C.A. (2015) Advances in the molecular understanding of biological zinc transport. *Chemical Communication,* 51 (22), 4544-4563.

Bolan, N.S., Makino, T., Kunhikrishnan, A., Kim, P.-J., Ishikawa, S., Murakami, M., Naidu, R. and Kirkham, M.B. (2013) Chapter Four - Cadmium Contamination and Its Risk Management in Rice Ecosystems IN: Donald, L.S. (ed.) *Advances in Agronomy*. Academic Press, 183-273.

Boratyn, G.M., Camacho, C., Cooper, P.S., Coulouris, G., Fong, A., Ma, N., Madden, T.L., Matten, W.T., Mcginnis, S.D. and Merezhuk, Y. (2013) BLAST: a more efficient report with usability improvements. *Nucleic Acids Research,* 41 (W1), W29-W33.

Bose, J., Pottosin, Ii, Shabala, S.S., Palmgren, M.G. and Shabala, S. (2011) Calcium efflux systems in stress signaling and adaptation in plants. *Frontiers in Plant Science,* 2, 85.

Brenchley, R., Spannagl, M., Pfeifer, M., Barker, G.L.A., D/'Amore, R., Allen, A.M., Mckenzie, N., Kramer, M., Kerhornou, A., Bolser, D., Kay, S., Waite, D., Trick, M., Bancroft, I., Gu, Y., Huo, N., Luo, M.-C., Sehgal, S., Gill, B., Kianian, S., Anderson, O., Kersey, P., Dvorak, J., Mccombie, W.R., Hall, A., Mayer, K.F.X., Edwards, K.J., Bevan, M.W. and Hall, N. (2012) Analysis of the bread wheat genome using whole-genome shotgun sequencing. *Nature,* 491 (7426), 705-710.

Brnić, M., Wegmüller, R., Melse-Boonstra, A., Stomph, T., Zeder, C., Tay, F.M. and Hurrell, R.F. (2016) Zinc Absorption by Adults Is Similar from Intrinsically Labeled Zinc-Biofortified Rice and from Rice Fortified with Labeled Zinc Sulfate. *The Journal of nutrition,* 146 (1), 76-80.

Broadley, M.R., White, P.J., Hammond, J.P., Zelko, I. and Lux, A. (2007) Zinc in plants. *New Phytologist,* 173 (4), 677-702.

Brown, P.H., Cakmak, I. and Zhang, Q. (1993a) *Form and fucntion of zinc in plants* Dordrecht, The Nehtherlands: Kluwer Academic Publishers.

Brown, P.H., Cakmak, I. and Zhang, Q. (1993b) Form and Function of Zinc Plants IN: Robson, A.D. (ed.) *Zinc in Soils and Plants: Proceedings of the International Symposium on 'Zinc in Soils and Plants' held at The University of Western Australia, 27–28 September, 1993*. Dordrecht: Springer Netherlands, 93-106.

Brümmer, G.W., Gerth, J. and Tiller, K.G. (1988) Reaction kinetics of the adsorption and desorption of nickel, zinc and cadmium by geothite. *Journal of Soil Sciences,* 39, 37-52.

Burge, C. and Karlin, S. (1997) Prediction of complete gene structures in human genomic DNA. *Journal of Molecular Biology,* 268 (1), 78-94.

Burkhead, J.L., Reynolds, K.A., Abdel-Ghany, S.E., Cohu, C.M. and Pilon, M. (2009) Copper homeostasis. *The New Phytologist,* 182 (4), 799-816.

Cailliatte, R., Lapeyre, B., Briat, J.F., Mari, S. and Curie, C. (2009) The NRAMP6 metal transporter contributes to cadmium toxicity. *Biochemical Journal,* 422 (2), 217-228.

Cailliatte, R., Schikora, A., Briat, J.-F., Mari, S. and Curie, C. (2010) High-affinity manganese uptake by the metal transporter NRAMP1 is essential for Arabidopsis growth in low manganese conditions. *The Plant Cell,* 22 (3), 904-917.

Cakmak, I. (1997) Concentration of zinc and activity of copper/zinc superoxide dismutase in leaves of rye and wheat cultivars differing in sensitivity to zinc deficiency. *Plant Physiol,* 151, 91-95.

Cakmak, I. (2000) Possible roles of zinc in protecting plant cells from damage by reactive oxygen species. *The New Phytologist* 146, 185-205.

Cakmak, I. (2008) Enrichment of cereal grains with zinc: Agronomic or genetic biofortification? *Plant and Soil,* 302 (1), 1-17.

Cakmak, I., Ekiz, H., Yilmaz, A., Torun, B., Köleli, N., Gültekin, I., Alkan, A. and Eker, S. (1997) Differential response of rye, triticale, bread and durum wheats to zinc deficiency in calcareous soils. *Plant and Soil,* 188 (1), 1-10.

Cakmak, I., Sari, N., Marschner, H., Ekiz, H., Kalaycy, M., Yilmaz, A. and Braun, H.J. (1996) *Plant and Soil,* 180, 183.

Cappa, J.J. and Pilon-Smits, E.A. (2014) Evolutionary aspects of elemental hyperaccumulation. *Planta,* 239 (2), 267-275.

Caulfield, L.E., De Onis, M., Blossner, M. and Black, R.E. (2004) Undernutrition as an underlying cause of child deaths associated with diarrhea, pneumonia, malaria, and measles. *The American journal of Clinical Nutrition,* 80 (1), 193-198.

Cellier, M., Prive, G., Belouchi, A., Kwan, T., Rodrigues, V., Chia, W. and Gros, P. (1995) Nramp defines a family of membrane proteins. *Proceedings of the National Academy of Sciences,* 92 (22), 10089-10093.

Center, C.C. (2008). Copenhagen Consensus 2008.

Chaney, R.L. (1993) Zinc Phytotoxicity IN: Robson, A.D. (ed.) *Zinc in Soils and Plants: Proceedings of the International Symposium on 'Zinc in Soils and Plants' held at The University of Western Australia, 27–28 September, 1993*. Dordrecht: Springer Netherlands, 135-150.

Chanfreau, G.F. (2013) Zinc'ing down RNA polymerase I. *Transcription,* 4 (5), 217-220.

Chao, D.Y., Silva, A., Baxter, I., Huang, Y.S., Nordborg, M., Danku, J., Lahner, B., Yakubova, E. and Salt, D.E. (2012) Genome-wide association studies identify heavy metal ATPase3 as the primary determinant of natural variation in leaf cadmium in *Arabidopsis thaliana*. *PLoS Genetics,* 8 (9), e1002923.

Chasapis, C.T., Loutsidou, A.C., Spiliopoulou, C.A. and Stefanidou, M.E. (2012) Zinc and human health: an update. *Archives Toxicology,* 86 (4), 521-534.

Chen, C., Zhou, Q. and Cai, Z. (2014) Effect of soil HHCB on cadmium accumulation and phytotoxicity in wheat seedlings. *Ecotoxicology,* 23 (10), 1996-2004.

Chen, H., Chen, W., Zhou, J., He, H., Chen, L., Chen, H. and Deng, X.W. (2012) Basic leucine zipper transcription factor OsbZIP16 positively regulates drought resistance in rice. *Plant Science,* 193-194, 8-17.

Chen, Y.C. and Huerta, A.J. (1997) Effects of sulfur nutrition on photosynthesis in cadmium-treated barley seedlings. *Journal of Plant Nutrition,* 20 (7-8), 845-856.

Chilton, M.D., Drummond, M.H., Merio, D.J., Sciaky, D., Montoya, A.L., Gordon, M.P. and Nester, E.W. (1977) Stable incorporation of plasmid DNA into higher plant cells: the molecular basis of crown gall tumorigenesis. *Cell,* 11 (2), 263-271.

Chmielowska-Bak, J., Lefevre, I., Lutts, S. and Deckert, J. (2013) Short term signaling responses in roots of young soybean seedlings exposed to cadmium stress. *Journal of Plant Physiology,* 170 (18), 1585-1594.

Choi, H.-I., Hong, J.-H., Ha, J.-O., Kang, J.-Y. and Kim, S.Y. (2000) ABFs, a Family of ABA-responsive Element Binding Factors. *Journal of Biological Chemistry,* 275 (3), 1723-1730.

Choulet, F., Alberti, A., Theil, S., Glover, N., Barbe, V., Daron, J., Pingault, L., Sourdille, P., Couloux, A., Paux, E., Leroy, P., Mangenot, S., Guilhot, N., Le Gouis, J., Balfourier, F., Alaux, M., Jamilloux, V., Poulain, J., Durand, C., Bellec, A., Gaspin, C., Safar, J., Dolezel, J., Rogers, J., Vandepoele, K., Aury, J.-M., Mayer, K., Berges, H., Quesneville, H., Wincker, P. and Feuillet, C. (2014) Structural and functional partitioning of bread wheat chromosome 3B. *Science,* 345 (6194).

Ci, D., Jiang, D., Wollenweber, B., Dai, T., Jing, Q. and Cao, W. (2010) Cadmium stress in wheat seedlings: growth, cadmium accumulation and photosynthesis. *Acta Physiologiae Plantarum,* 32 (2), 365-373.

Claus, J. and Chavarria-Krauser, A. (2012) Modeling regulation of zinc uptake via ZIP transporters in yeast and plant roots. *PLoS One,* 7 (6), e37193.

Clemens, S. (2001) Molecular mechanisms of plant metal tolerance and homeostasis. *Planta,* 212 (4), 475-486.

Clemens, S., Deinlein, U., Ahmadi, H., Horeth, S. and Uraguchi, S. (2013) Nicotianamine is a major player in plant Zn homeostasis. *Biometals,* 26 (4), 623-632.

Clough, S.J. and Bent, A.F. (1998) Floral dip: a simplified method for *Agrobacterium*-mediated transformation of *Arabidopsis thaliana*. *The The Plant Journal,* 16 (6), 735-743.

Cobbett, C. and Goldsbrough, P. (2002) Phytochelatins and metallothioneins: roles in heavy metal detoxification and homeostasis. *Annual Review of Plant Biology,* 53 (1), 159–182.

Cohu, C.M. and Pilon, M. (2010) Cell biology of copper IN: Rüdiger, H. and Mendel, R.-R. (eds.) *Cell Biology of Metals and Nutrients Plant Cell Monographs*. Heidelberg: Springer, 55–74.

Colangelo, E.P. and Guerinot, M.L. (2006) Put the metal to the petal: metal uptake and transport throughout plants. *Current Opinion in Plant Biology,* 9 (3), 322-330.

Colcombet, J. and Hirt, H. (2008) Arabidopsis MAPKs: a complex signalling network involved in multiple biological processes. *Biochemical Journal,* 413 (2), 217-226.

Corkins, M.E., May, M., Ehrensberger, K.M., Hu, Y.-M., Liu, Y.-H., Bloor, S.D., Jenkins, B., Runge, K.W. and Bird, A.J. (2013) Zinc finger protein Loz1 is required for zinc-responsive regulation of gene expression in fission yeast. *Proceedings of the National Academy of Sciences,* 110 (38), 15371-15376.

Cornu, J.Y., Deinlein, U., Höreth, S., Braun, M., Schmidt, H., Weber, M., Persson, D.P., Husted, S., Schjoerring, J.K. and Clemens, S. (2015) Contrasting effects of nicotianamine synthase knockdown on zinc and nickel tolerance and accumulation in the zinc/cadmium hyperaccumulator Arabidopsis halleri. *The New Phytologist,* 206 (2), 738-750.

Correa, L.G., Riano-Pachon, D.M., Schrago, C.G., Dos Santos, R.V., Mueller-Roeber, B. and Vincentz, M. (2008) The role of bZIP transcription factors in green plant evolution: adaptive features emerging from four founder genes. *PLoS One,* 3 (8), e2944.

Curie, C., Alonso, J.M., Marie, L., Ecker, J.R. and Briat, J.-F. (2000) Involvement of NRAMP1 from *Arabidopsis thaliana* in iron transport. *Biochemical Journal,* 347 (3), 749-755.

Curie, C., Cassin, G., Couch, D., Divol, F., Higuchi, K., Le Jean, M., Misson, J., Schikora, A., Czernic, P. and Mari, S. (2009) Metal movement within the plant: contribution of nicotianamine and yellow stripe 1-like transporters. *Annals of Botany,* 103 (1), 1-11.

Curtis, M.D. and Grossniklaus, U. (2003) A Gateway Cloning Vector Set for High-Throughput Functional Analysis of Genes in Planta. *Plant Physiology,* 133 (2), 462-469.

Da Cunha, K.P.V., Do Nascimento, C.W.A., De Mendonça Pimentel, R.M. and Ferreira, C.P. (2008) Cellular localization of cadmium and structural changes in maize plants grown on a cadmium contaminated soil with and without liming. *Journal of Hazardous Materials,* 160 (1), 228-234.

Daghan, H., Arslan, M., Uygur, V. and Koleli, N. (2013) Transformation of Tobacco with ScMTII Gene-Enhanced Cadmium and Zinc Accumulation. *CLEAN – Soil, Air, Water,* 41 (5), 503-509.

Dai, X.P., Feng, L., Ma, X.W. and Zhang, Y.M. (2012) Concentration level of heavy metals in wheat grains and the health risk assessment to local inhabitants from Baiyin, Gansu, China *Advanced Materials Research*. Trans Tech Publication, 951-956.

Dauthieu, M., Denaix, L., Nguyen, C., Panfili, F., Perrot, F. and Potin-Gautier, M. (2009) Cadmium uptake and distribution in *Arabidopsis thaliana* exposed to low chronic concentrations depends on plant growth. *Plant and Soil,* 322 (1-2), 239-249.

Deinlein, U., Stephan, A.B., Horie, T., Luo, W., Xu, G. and Schroeder, J.I. (2014) Plant salt-tolerance mechanisms. *Trends Plant Science,* 19 (6), 371-379.

Deinlein, U., Weber, M., Schmidt, H., Rensch, S., Trampczynska, A., Hansen, T.H., Husted, S., Schjoerring, J.K., Talke, I.N., Kramer, U. and Clemens, S. (2012) Elevated nicotianamine levels in Arabidopsis halleri roots play a key role in zinc hyperaccumulation. *Plant Cell,* 24 (2), 708-723.

Delhaize, E., Gruber, B.D., Pittman, J.K., White, R.G., Leung, H., Miao, Y., Jiang, L., Ryan, P.R. and Richardson, A.E. (2007) A role for the AtMTP11 gene of Arabidopsis in manganese transport and tolerance. *The Plant Journal,* 51 (2), 198-210.

Deng, F.L., Yamaji, N., Xia, J.X. and Ma, J.F. (2013) A Member of the Heavy Metal P-Type ATPase OsHMA5 Is Involved in Xylem Loading of Copper in Rice. *Plant Physiology,* 163 (3), 1353-1362.

Deng, W., Nickle, D.C., Learn, G.H., Maust, B. and Mullins, J.I. (2007) ViroBLAST: a stand-alone BLAST web server for flexible queries of multiple databases and user's datasets. *Bioinformatics,* 23 (17), 2334-2336.

Deppmann, C.D., Alvania, R.S. and Taparowsky, E.J. (2006) Cross-species annotation of basic leucine zipper factor interactions: Insight into the evolution of closed interaction networks. *Molecular Biology and Evolution,* 23 (8), 1480-1492.

Desa, U. (2015) *World population prospects: the 2015 revision, key findings and advance tables*.

Desbrosses-Fonrouge, A., Voight, K., Schroder, A., Arrivault, S., Thomine, S. and U., K. (2005) *Arabidopsis thaliana* MTP1 is a Zn transporter in the vacuolar membrane which mediates Zn detoxification and drives leaf Zn accumulation. *FEBS Letter,* 579 (19), 4165-4174.

Despres, C., Delong, C., Glaze, S., Liu, E. and Fobert, P.R. (2000) The Arabidopsis NPR1/NIM1 protein enhances the DNA binding activity of a subgroup of the TGA family of bZIP transcription factors. *Plant Cell,* 12 (2), 279-290.

Didonato Jr., R.J., Roberts, L.A., Sanderson, T., Bosler Eisley, R. and Walker, E.L. (2004) Arabidopsis Yellow Stripe-Like2 (YSL2): a metal-regulated gene encoding a plasma membrane transporter of nicotianamine-metal complexes. *The Plant Journal,* 39 (3), 403-414.

Ding, Y., Chen, Z. and Zhu, C. (2011) Microarray-based analysis of cadmium-responsive microRNAs in rice (*Oryza sativa*). *Journal of Experimental Botany,* 62 (10), 3563-3573.

Dong, X. (2004) NPR1, all things considered. *Current Opinion in Plant Biology,* 7 (5), 547-552.

Dowling, D.N. and Doty, S.L. (2009) Improving phytoremediation through biotechnology. *Current Opinion in Biotechnology,* 20 (2), 204-206.

Dreyer, I., Horeau, C., Lemaillet, G., Zimmermann, S., Bush, D.R., Rodríguez-Navarro, A., Schachtman, D.P., Spalding, E.P., Sentenac, H. and Gaber, R.F. (1999) Identification and characterization of plant transporters. *Journal of Experimental Botany,* 50 (Special Issue), 1073-1087.

Duby, G. and Boutry, M. (2009) The plant plasma membrane proton pump ATPase: a highly regulated P-type ATPase with multiple physiological roles. *Pflügers Archiv - European Journal of Physiology,* 457 (3), 645-655.

Dudev, T. and Lim, C. (2000) Tetrahedral vs octahedral zinc complexes with ligands of biological interest: A DFT/CDM study. *Journal of the American Chemical Society,* 122 (45), 11146-11153.

Durmaz, E., Coruh, C., Dinler, G., Grusak, M.A., Peleg, Z., Saranga, Y., Fahima, T., Yazici, A., Ozturk, L. and Cakmak, I. (2011) Expression and cellular localization of ZIP1 transporter under zinc deficiency in wild emmer wheat. *Plant Molecular Biology Reporter,* 29 (3), 582-596.

Eckhardt, U., Marques, A.M. and Buckhout, T.J. (2001) Two iron-regulated cation transporters from tomato complement metal uptake-deficient yeast mutants. *Plant Molecular Biology,* 45 (4), 437-448.

Eide, D., Broderius, M., Fett, J. and Guerinot, M.L. (1996) A novel iron-regulated metal transporter from plants identified by functional expression in yeast. *Proceedings of the National Academy of Sciences,* 93, 5624–5628.

Eide, D.J. (2006) Zinc transporters and the cellular trafficking of zinc. *Biochimica et Biophysica Acta (BBA)-Molecular Cell Research,* 1763 (7), 711-722.

Eide, D.J. (2011) The oxidative stress of zinc deficiency. *Metallomics,* 3 (11), 1124-1129.

Ekmekci, Y., Tanyolac, D. and Ayhan, B. (2008) Effects of cadmium on antioxidant enzyme and photosynthetic activities in leaves of two maize cultivars. *Journal of Plant Physiology,* 165 (6), 600-611.

Englbrecht, C.C., Schoof, H. and Bohm, S. (2004) Conservation, diversification and expansion of C2H2 zinc finger proteins in the *Arabidopsis thaliana* genome. *BMC Genomics,* 5, 39.

Erakhrumen, A. and Agbontalor, A. (2007) Review Phytoremediation: an environmentally sound technology for pollution prevention, control and remediation in developing countries. *Educational Research and Review,* 2, 151-156.

Eren, E. and Arguello, J.M. (2004) Arabidopsis HMA2, a divalent heavy metal-transporting P(IB)-type ATPase, is involved in cytoplasmic Zn^{2+} homeostasis. *Plant Physiology,* 136 (3), 3712-3723.

Eren, E., Gonzalez-Guerrero, M., Kaufman, B.M. and Arguello, J.M. (2007) Novel Zn2+ coordination by the regulatory N-terminus metal binding domain of *Arabidopsis thaliana* Zn(2+)-ATPase HMA2. *Biochemistry,* 46 (26), 7754-7764.

Eren, E., Kennedy, D.C., Maroney, M.J. and Arguello, J.M. (2006) A novel regulatory metal binding domain is present in the C terminus of Arabidopsis Zn^{2+}-ATPase HMA2. *Journal of Biological Chemistry,* 281, 33881–33891.

Fan, B. and Rosen, B.P. (2002) Biochemical characterization of CopA, the Escherichia coli Cu(I)-translocating P-type ATPase. *Journal of Biological Chemistry,* 277 (49), 46987-46992.

Faroon, O., Ashizawa, A., Wright, S., Tucker, P., Jenkins, K., Ingerman, L. and Rudisill, C. (2012) Toxicological profile for cadmium.

Felsenstein, J. (1985) Confidence limits on phylogenies: An approach using the bootstrap. *Evolution,* 39 (783-791).

Fernando, N., Panozzo, J., Tausz, M., Norton, R., Fitzgerald, G. and Seneweera, S. (2012) Rising atmospheric CO_2 concentration affects mineral nutrient and protein concentration of wheat grain. *Food Chemistry,* 133 (4), 1307-1311.

Festa, R.A. and Thiele, D.J. (2011) Copper: an essential metal in biology. *Current Biology,* 21 (21), R877-883.

Food, I.O.M. and Board, N. (2001) *DRI, Dietary Reference Intakes for Vitamin A, Vitamin K, Arsenic, Boron, Chromium, Copper, Iodine, Iron, Manganese, Molybdenum, Nickel, Silicon, Vanadium, and Zinc: A Report of the Panel on Micronutrients and of Interpretation and Uses of Dietary Reference Intakes, and the Standing Committee on the Scientific Evaluation of Dietary Reference Intakes*. National Academy Press.

Fu, X. and Harberd, N.P. (2003) Auxin promotes Arabidopsis root growth by modulating gibberellin response. *Nature,* 421 (6924), 740-743.

Fujii, Y., Shimizu, T., Toda, T., Yanagida, M. and Hakoshima, T. (2000) Structural basis for the diversity of DNA recognition by bZIP transcription factors. *Nature Structural & Molecular Biology,* 7 (10), 889-893.

Fukao, Y., Ferjani, A., Tomioka, R., Nagasaki, N., Kurata, R., Nishimori, Y., Fujiwara, M. and Maeshima, M. (2011) iTRAQ analysis reveals mechanisms of growth defects due to excess zinc in Arabidopsis. *Plant Physiology,* 155 (4), 1893-1907.

Fukazawa, J., Sakai, T., Ishida, S., Yamaguchi, I., Kamiya, Y. and Takahashi, Y. (2000) Repression of shoot growth, a bZIP transcriptional activator, regulates cell elongation by controlling the level of gibberellins. *Plant Cell,* 12 (6), 901-915.

Gaetke, L.M. and Chow, C.K. (2003) Copper toxicity, oxidative stress, and antioxidant nutrients. *Toxicology,* 189 (1), 147-163.

Gainza-Cortés, F., Pérez-Dïaz, R., Pérez-Castro, R., Tapia, J., Casaretto, J.A., González, S., Peña-Cortés, H., Ruiz-Lara, S. and González, E. (2012) Characterization of a putative grapevine Zn transporter, VvZIP3, suggests its involvement in early reproductive development in Vitis vinifera L. *BMC Plant Biology,* 12 (1), 1.

Gaither, L.A. and Eide, D.J. (2001) The human ZIP1 transporter mediates zinc uptake in human K562 erythroleukemia cells. *Journal of Biological Chemistry,* 276 (25), 22258-22264.

Galetti, V., Kujinga, P., Mitchikpè, C.E.S., Zeder, C., Tay, F., Tossou, F., Hounhouigan, J.D., Zimmermann, M.B. and Moretti, D. (2015) Efficacy of highly bioavailable zinc from fortified water: a randomized controlled trial in rural Beninese children. *The American Journal of Clinical Nutrition,* 102 (5), 1238-1248.

Gao, M., Zhang, H., Guo, C., Cheng, C., Guo, R., Mao, L., Fei, Z. and Wang, X. (2014a) Evolutionary and Expression Analyses of Basic Zipper Transcription Factors in the Highly Homozygous Model Grape PN40024 (*Vitis vinifera* L.). *Plant Molecular Biology Reporter,* 32 (5), 1085-1102.

Gao, S.X., Liu, D.G., Chen, H. and Meng, X.X. (2014b) Fitness traits and underlying genetic variation related to host plant specialization in the aphid Sitobion avenae. *Insect Science,* 21 (3), 352-362.

Garfinkel, D.J. and Nester, E.W. (1980) *Agrobacterium tumefaciens* mutants affected in crown gall tumorigenesis and octopine catabolism. *Journal Bacteriology,* 144 (2), 732-743.

Genc, Y., Verbyla, A.P., Torun, A.A., Cakmak, I., Willsmore, K., Wallwork, H. and Mcdonald, G.K. (2009) Quantitative trait loci analysis of zinc efficiency and grain zinc concentration in wheat using whole genome average interval mapping. *Plant and Soil,* 314 (1), 49-66.

George, L., Romanowsky, S.M., Harper, J.F. and Sharrock, R.A. (2008) The ACA10 Ca^{2+}-ATPase regulates adult vegetative development and inflorescence architecture in Arabidopsis. *Plant Physiology,* 146 (2), 716-728.

Giaever, G., Chu, A.M., Ni, L., Connelly, C., Riles, L., Veronneau, S., Dow, S., Lucau-Danila, A., Anderson, K., Andre, B., Arkin, A.P., Astromoff, A., El-Bakkoury, M., Bangham, R., Benito, R., Brachat, S., Campanaro, S., Curtiss, M., Davis, K., Deutschbauer, A., Entian, K.D., Flaherty, P., Foury, F., Garfinkel, D.J., Gerstein, M., Gotte, D., Guldener, U., Hegemann, J.H., Hempel, S., Herman, Z., Jaramillo, D.F., Kelly, D.E., Kelly, S.L., Kotter, P., Labonte, D., Lamb, D.C., Lan, N., Liang, H., Liao, H., Liu, L., Luo, C., Lussier, M., Mao, R., Menard, P., Ooi,

S.L., Revuelta, J.L., Roberts, C.J., Rose, M., Ross-Macdonald, P., Scherens, B., Schimmack, G., Shafer, B., Shoemaker, D.D., Sookhai-Mahadeo, S., Storms, R.K., Strathern, J.N., Valle, G., Voet, M., Volckaert, G., Wang, C.Y., Ward, T.R., Wilhelmy, J., Winzeler, E.A., Yang, Y., Yen, G., Youngman, E., Yu, K., Bussey, H., Boeke, J.D., Snyder, M., Philippsen, P., Davis, R.W. and Johnston, M. (2002) Functional profiling of the *Saccharomyces cerevisiae* genome. *Nature,* 418 (6896), 387-391.

Gibson, R.S., Perlas, L. and Hotz, C. (2006) Improving the bioavailability of nutrients in plant foods at the household level. *Proceedings Of The Nutrition Society,* 65 (2), 160-168.

Glover-Cutter, K.M., Alderman, S., Dombrowski, J.E. and Martin, R.C. (2014) Enhanced oxidative stress resistance through activation of a zinc deficiency transcription factor in *Brachypodium distachyon*. *Plant Physiology,* 166 (3), 1492-1505.

Goffeau, A., Barrell, B.G., Bussey, H., Davis, R.W., Dujon, B., Feldmann, H., Galibert, F., Hoheisel, J.D., Jacq, C., Johnston, M., Louis, E.J., Mewes, H.W., Murakami, Y., Philippsen, P., Tettelin, H. and Oliver, S.G. (1996) Life with 6000 genes. *Science,* 274 (5287), 546, 563-547.

Gonzalez-Guerrero, M., Eren, E., Rawat, S., Stemmler, T.L. and Arguello, J.M. (2008) Structure of the two transmembrane Cu transport sites of the Cu-ATPases. *Journal of Biological Chemistry,* 283 (44), 29753-29759.

Graham, R.D. and Stangoulis, J.C. (2003) Trace element uptake and distribution in plants. *The Journal of Nutrition,* 133 (5), 1502S-1505S.

Grass, G., Wong, M.D., Rosen, B.P., Smith, R.L. and Rensing, C. (2002) ZupT is a Zn (II) uptake system in *Escherichia coli*. *Journal of Bacteriology,* 184 (3), 864-866.

Gravot, A., Lieutaud, A., Verret, F., Auroy, P., Vavasseur, A. and Richaud, P. (2004) AtHMA3, a plant P_{1B}-ATPase, functions as a Cd/Pb transporter in yeast. *FEBS Letter,* 561, 22-28.

Greger, M. and Löfstedt, M. (2004) Comparison of uptake and distribution of cadmium in different cultivars of bread and durum wheat. *Crop Science,* 44 (2), 501-507.

Grotz, N., Fox, T., Connolly, E., Park, W., Guerinot, M.L. and Eide, D. (1998) Identification of a family of zinc transporter genes from Arabidopsis that respond to zinc deficiency. *Proceedings of the National Academy of Sciences,* 95 (12), 7220-7224.

Guerinot, M.L. (2000) The ZIP family of metal transporters. *Biochimica et Biophysica Acta (BBA) - Biomembranes,* 1465 (1–2), 190-198.

Günthardt-Goerg, M.S., Matyssek, R., Scheidegger, C. and Keller, T. (1993) Differentiation and structural decline in the leaves and bark of birch (*Betula pendula*) under low ozone concentrations. *Trees,* 7 (2), 104-114.

Günther, V., Lindert, U. and Schaffner, W. (2012) The taste of heavy metals: gene regulation by MTF-1. *Biochimica et Biophysica Acta (BBA)-Molecular Cell Research,* 1823 (9), 1416-1425.

Guo, J., Dai, X., Xu, W. and Ma, M. (2008) Overexpressing GSH1 and AsPCS1 simultaneously increases the tolerance and accumulation of cadmium and arsenic in *Arabidopsis thaliana*. *Chemosphere,* 72 (7), 1020-1026.

Hall, J.L. and Williams, L.E. (2003) Transition metal transporters in plants. *Journal of Experimental Botany,* 54 (393), 2601-2613.

Hansch, R. and Mendel, R.R. (2009) Physiological functions of mineral micronutrients (Cu, Zn, Mn, Fe, Ni, Mo, B, Cl). *Current Opinion in Plant Biology,* 12 (3), 259-266.

Harter, K., Kircher, S., Frohnmeyer, H., Krenz, M., Nagy, F. and Schäfer, E. (1994) Light-regulated modification and nuclear translocation of cytosolic G-box binding factors in parsley. *Plant Cell,* 6 (4), 545-559.

Harwood, W.A. (2014) A protocol for high-throughput Agrobacterium-mediated barley transformation. *Cereal Genomics: Methods and Protocols*, 251-260.

Hasani, M., Zamani, Z., Savaghebi, G. and Fatahi, R. (2012) Effects of zinc and manganese as foliar spray on pomegranate yield, fruit quality and leaf minerals. *Journal of Soil Science and Plant Nutrition*.

Haydon, M.J., Kawachi, M., Wirtz, M., Stefan, H., Hell, R. and Krämer, U. (2012) Vacuolar nicotianamine has critical and distinct roles under iron deficiency and for zinc sequestration in Arabidopsis. *Plant Cell,* 24, 724-737.

He, J., Li, H., Ma, C., Zhang, Y., Polle, A., Rennenberg, H., Cheng, X. and Luo, Z.B. (2015) Overexpression of bacterial gamma-glutamylcysteine synthetase mediates changes in cadmium influx, allocation and detoxification in poplar. *The New Phytologist,* 205 (1), 240-254.

Hegelund, J.N., Schiller, M., Kichey, T., Hansen, T.H., Pedas, P., Husted, S. and Schjoerring, J.K. (2012) Barley metallothioneins: MT3 and MT4 are localized in the grain aleurone layer and show differential zinc binding. *Plant Physiology,* 159 (3), 1125-1137.

Helfenstein, J., Pawlowski, M.L., Hill, C.B., Stewart, J., Lagos-Kutz, D., Bowen, C.R., Frossard, E. and Hartman, G.L. (2015) Zinc deficiency alters soybean susceptibility to pathogens and pests. *Journal of Plant Nutrition and Soil Science,* 178 (6), 896-903.

Hellens, R., Mullineaux, P. and Klee, H. (2000) Technical Focus:a guide to Agrobacterium binary Ti vectors. *Trends Plant Science,* 5 (10), 446-451.

Henriques, A., Chalfun-Junior, A. and Aarts, M. (2012) Strategies to increase zinc deficiency tolerance and homeostasis in plants. *Brazilian Journal of Plant Physiology,* 24, 3-8.

Hindt, M.N. and Guerinot, M.L. (2012) Getting a sense for signals: regulation of the plant iron deficiency response. *Biochimica et Biophysica Acta,* 1823 (9), 1521-1530.

Hirayama, T., Kieber, J.J., Hirayama, N., Kogan, M. and Guzman, P. (1999) RESPONSIVE-TO-ANTAGONIST1, a Menkes/Wilson disease-related copper transporter, is required for ethylene signaling in Arabidopsis. *Cell,* 97, 383-393.

Hirokawa, T., Boon-Chieng, S. and Mitaku, S. (1998a) SOSUI: classification and secondary structure prediction system for membrane proteins. *Bioinformatics,* 14 (4), 378-379.

Hirokawa, T., Boon-Chieng, S. and Mitaku, S. (1998b) SOSUI: classification and secondary structure prediction system for membrane proteins. *Bioinformatics,* 14 (4), 378-379.

Hirschi, K.D., Korenkov Vd Fau - Wilganowski, N.L., Wilganowski Nl Fau - Wagner, G.J. and Wagner, G.J. (2000) Expression of arabidopsis CAX2 in tobacco. Altered metal accumulation and increased manganese tolerance. *Plant physiology*, *124*(1), pp.125-134.

Hoekema, A., Hirsch, P.R., Hooykaas, P.J.J. and Schilperoort, R.A. (1983) A binary plant vector strategy based on separation of vir- and T-region of the *Agrobacterium tumefaciens* Ti-plasmid. *Nature,* 303 (5913), 179-180.

Hofmann, K. (1993) TMbase-A database of membrane spanning protein segments. *The Journal of Biological Chemistry,* 374, 166.

Hogy, P., Wieser, H., Kohler, P., Schwadorf, K., Breuer, J., Franzaring, J., Muntifering, R. and Fangmeier, A. (2009) Effects of elevated CO_2 on grain yield and quality of wheat: results from a 3-year free-air CO_2 enrichment experiment. *Plant Biology,* 11 Suppl 1, 60-69.

Hou, X. and Hou, H.J.M. (2013) Roles of manganese in photosystem II dynamics to irradiations and temperatures. *Frontiers in Biology,* 8 (3), 312-322.

Huala, E., Dickerman, A.W., Garcia-Hernandez, M., Weems, D., Reiser, L., Lafond, F., Hanley, D., Kiphart, D., Zhuang, M. and Huang, W. (2001) The Arabidopsis Information Resource (TAIR): a comprehensive database and web-based information retrieval, analysis, and visualization system for a model plant. *Nucleic Acids Research,* 29 (1), 102-105.

Huang, C., Barker, S.J., Langridge, P., Smith, F.W. and Graham, R.D. (2000) Zinc deficiency up-regulates expression of high-affinity phosphate transporter genes in both phosphate-sufficient and -deficient barley roots. *Plant Physiology,* 124 (1), 415-422.

Huang, M., Zhou, S., Sun, B. and Zhao, Q. (2008) Heavy metals in wheat grain: assessment of potential health risk for inhabitants in Kunshan, China. *Science of the Total Environment,* 405 (1), 54-61.

Huda, K.M.K., Banu, M.S.A., Garg, B., Tula, S., Tuteja, R. and Tuteja, N. (2013) OsACA6, a P-type IIB Ca(2+)ATPase promotes salinity and drought stress tolerance in tobacco by ROS scavenging and enhancing the expression of stress-responsive genes. *The Plant Journal,* 76 (6), 997-1015.

Hulo, N., Bairoch, A., Bulliard, V., Cerutti, L., De Castro, E., Langendijk-Genevaux, P.S., Pagni, M. and Sigrist, C.J. (2006) The PROSITE database. *Nucleic Acids Research,* 34 (suppl 1), D227-D230.

Hussain, D., Haydon, M.J., Wang, Y., Wong, E., Sherson, S., Young, J., Camakaris, J., Harper, J.F. and Cobbett, C.S. (2004) P-type ATPase heavy metal transporters with roles in essential zinc homeostasis in Arabidopsis. *Plant Cell,* 16, 1327–1339.

Imtiaz, M., Alloway, B.J. and Memon, M.Y. (2006) Zinc tolerance in wheat cultivars as affected by varying level of phosphorus. *Communications in Soil Science and Plant Analysis,* 37, 1689-1702.

Imtiaz, M., Alloway, B.J., Shah, K.H. and Siddiqui, S.H. (2003) Zinc Nutrition of Wheat: II: Interaction of Zinc with other Trace Elements. *Asian Journal of Plant Sciences*.

Inaba, S., Kurata, R., Kobayashi, M., Yamagishi, Y., Mori, I., Ogata, Y. and Fukao, Y. (2015) Identification of putative target genes of bZIP19, a transcription factor essential for Arabidopsis adaptation to Zn deficiency in roots. *The Plant Journal,* 84 (2), 323-334.

Inoue, H., Kobayashi, T., Nozoye, T., Takahashi, M., Kakei, Y., Suzuki, K., Nakazono, M., Nakanishi, H., Mori, S. and Nishizawa, N.K. (2009) Rice OsYSL15 is an iron-regulated iron(III)-deoxymugineic acid transporter expressed in the roots and is essential for iron uptake in early growth of the seedlings. *Journal of Biological Chemistry,* 284 (6), 3470-3479.

Ishimaru, Y., Masuda, H., Suzuki, M., Bashir, K., Takahashi, M., Nakanishi, H., Mori, S. and Nishizawa, N.K. (2007) Overexpression of the OsZIP4 zinc transporter confers disarrangement of zinc distribution in rice plants. *Journal of Experimental Botany,* 58 (11), 2909-2915.

Ishimaru, Y., Suzuki, M., Tsukamoto, T., Suzuki, K., Nakazono, M., Kobayashi, T., Wada, Y., Watanabe, S., Matsuhashi, S. and Takahashi, M. (2006) Rice plants take up iron as an Fe^{3+}-phytosiderophore and as Fe^{2+}. *The The Plant Journal,* 45 (3), 335-346.

Ishimaru, Y., Takahashi, R., Bashir, K., Shimo, H., Senoura, T., Sugimoto, K., Ono, K., Yano, M., Ishikawa, S. and Arao, T. (2012) Characterizing the role of rice NRAMP5 in manganese, iron and cadmium transport. *Scientific Reports,* 2, 286.

Ismail, A., Takeda, S. and Nick, P. (2014) Life and death under salt stress: same players, different timing? *Journal of Experimental Botany,* 65 (12), 2963-2979.

Ismail, A.M. and Theodor, P.A. (2012) The effect of heavy metals Zn and Ni on growth of in vitro hairy root cultures of indian mustard *Brassica juncea* L. *International Journal of Advanced Biotechnology and Research*, 688–697.

Izawa, T., Foster, R. and Chua, N.-H. (1993) Plant bZIP Protein DNA Binding Specificity. *Journal of Molecular Biology,* 230 (4), 1131-1144.

Jafarnejadi, A.R., Homaee, M., Sayyad, G. and Bybordi, M. (2011) Large scale spatial variability of accumulated cadmium in the wheat farm grains. *Soil and Sediment Contamination,* 20 (1), 98-113.

Jain, A., Sinilal, B., Dhandapani, G., Meagher, R.B. and Sahi, S.V. (2013) Effects of deficiency and excess of zinc on morphophysiological traits and spatiotemporal regulation of zinc-responsive genes reveal incidence of cross talk between micro- and macronutrients. *Environmental Science & Technology,* 47 (10), 5327-5335.

Jakoby, M., Weisshaar, B., Droge-Laser, W., Vicente-Carbajosa, J., Tiedemann, J., Kroj, T. and Parcy, F. (2002) bZIP transcription factors in Arabidopsis. *Trends Plant Sci,* 7 (3), 106-111.

Johnson, A.A., Kyriacou, B., Callahan, D.L., Carruthers, L., Stangoulis, J., Lombi, E. and Tester, M. (2011) Constitutive overexpression of the OsNAS gene family reveals single-gene strategies for effective iron- and zinc-biofortification of rice endosperm. *PLoS One,* 6 (9), e24476.

Joos, H., Timmerman, B., Montagu, M.V. and Schell, J. (1983) Genetic analysis of transfer and stabilization of Agrobacterium DNA in plant cells. *EMBO Journal,* 2 (12), 2151-2160.

Jorgensen, P.L., Hakansson, K.O. and Karlish, S.J. (2003) Structure and mechanism of Na,K-ATPase: functional sites and their interactions. *Annual Review of Physiology,* 65, 817-849.

Kagaya, Y., Hobo, T., Murata, M., Ban, A. and Hattori, T. (2002) Abscisic acid-induced transcription is mediated by phosphorylation of an abscisic acid response element binding factor, TRAB1. *Plant Cell,* 14 (12), 3177-3189.

Kalai, T., Bouthour, D., Manai, J., Bettaieb Ben Kaab, L. and Gouia, H. (2016) Salicylic acid alleviates the toxicity of cadmium on seedling growth, amylases and phosphatases activity in germinating barley seeds. *Archives of Agronomy and Soil Science,* 62 (6), 892-904.

Karimi, M., Inzé, D. and Depicker, A. (2002) GATEWAY™ vectors for Agrobacterium-mediated plant transformation. *Trends in Plant Science,* 7 (5), 193-195.

Katzen, F. (2007) Gateway® recombinational cloning: a biological operating system. *Expert Opinion on Drug Discovery,* 2 (4), 571-589.

Kavitha, P., Kuruvilla, S. and Mathew, M. (2015) Functional characterization of a transition metal ion transporter, OsZIP6 from rice (*Oryza sativa* L.). *Plant Physiology and Biochemistry,* 97, 165-174.

Kawachi, M., Kobae, Y., Mimura, T. and Maeshima, M. (2008) Deletion of a histidine-rich loop of AtMTP1, a vacuolar Zn(2+)/H(+) antiporter of *Arabidopsis thaliana*, stimulates the transport activity. *Journal of Biological Chemistry,* 283 (13), 8374-8383.

Kawachi, M., Kobae, Y., Mori, H., Tomioka, R., Lee, Y. and Maeshima, M. (2009) A Mutant Strain *Arabidopsis thaliana* that Lacks Vacuolar Membrane Zinc Transporter MTP1 Revealed the Latent Tolerance to Excessive Zinc. *Plant and Cell Physiology,* 50 (6), 1156-1170.

Kaznina, N., Titov, A., Topchieva, L., Batova, Y.V. and Laidinen, G. (2014) The content of HvHMA2 and HvHMA3 transcripts in barley plants treated with cadmium. *Russian journal of plant Physiology,* 61 (3), 355-359.

Kim, D., Gustin, J.L., Lahner, B., Persans, M.W., Baek, D., Yun, D.J. and Salt, D.E. (2004) The plant CDF family member TgMTP1 from the Ni/Zn hyperaccumulator Thlaspi goesingense acts to enhance efflux of Zn at the plasma membrane when expressed in *Saccharomyces cerevisiae*. *The Plant Journal,* 39 (2), 237-251.

Kim, Y.Y., Choi, H., Segami, S., Cho, H.T. and Martinoia, E. (2009) AtHMA1 contributes to the detoxification of excess Zn(II) in Arabidopsis. *The Plant Journal,* 58, 737–753.

Kircher, S., Wellmer, F., Nick, P., Rügner, A., Schäfer, E. and Harter, K. (1999) Nuclear import of the parsley bZIP transcription factor CPRF2 is regulated by phytochrome photoreceptors. *The Journal of Cell Biology,* 144 (2), 201-211.

Kirchoff, B.K. and Claßen-Bockhoff, R. (2013) Inflorescences: concepts, function, development and evolution. *Annals of Botany,* 112 (8), 1471-1476.

Klatte, M., Schuler, M., Wirtz, M., Fink-Straube, C., Hell, R. and Bauer, P. (2009) The analysis of Arabidopsis Nicotianamine Synthase mutants reveals functions for nicotianamine in seed iron loading and iron deficiency responses. *Plant Physiology,* 150 (1), 257-271.

Kobae, Y., Uemura, T., Sato, M.H., Ohnishi, M., Mimura, T. and Maeshima, M. (2004) Zinc transporter of *Arabidopsis thaliana* AtMTP1 is localized to vacuolar membranes and implicated in zinc homeostasis. *Plant Cell Physiology,* 45, 1749-1758.

Kobayashi, F., Maeta, E., Terashima, A., Kawaura, K., Ogihara, Y. and Takumi, S. (2008) Development of abiotic stress tolerance via bZIP-type transcription factor LIP19 in common wheat. *Journal of Experimental Botany,* 59 (4), 891-905.

Kobayashi, Y., Murata, M., Minami, H., Yamamoto, S., Kagaya, Y., Hobo, T., Yamamoto, A. and Hattori, T. (2005) Abscisic acid-activated SNRK2 protein kinases function in the gene-regulation pathway of ABA signal transduction by phosphorylating ABA response element-binding factors. *The Plant Journal,* 44 (6), 939-949.

Koornneef, M. and Meinke, D. (2010) The development of Arabidopsis as a model plant. *The Plant Journal,* 61 (6), 909-921.

Korenkov, V., Park, S.H., Cheng, N.H., Sreevidya, C., Lachmansingh, J., Morris, J., Hirschi, K. and Wagner, G.J. (2007) Enhanced Cd^{2+} selective root-tonoplast-transport in tobaccos expressing Arabidopsis cation exchangers. *Planta,* 225, 403–411.

Korshunova, Y.O., Eide, D., Clark, W.G., Guerinot, M.L. and Pakrasi, H.B. (1999) The IRT1 protein from *Arabidopsis thaliana* is a metal transporter with a broad substrate range. *Plant Molecular Biology,* 40 (1), 37-44.

Kozhevnikova, A.D., Seregin, I.V., Erlikh, N.T., Shevyreva, T.A., Andreev, I.M., Verweij, R. and Schat, H. (2014) Histidine-mediated xylem loading of zinc is a species-wide character in *Noccaea caerulescens*. *The New Phytologist,* 203 (2), 508-519.

Kramer, U. (2010) Metal hyperaccumulation in plants. *Annual Review of Plant Biology,* 61, 517-534.

Krämer, U. and Clemens, S. (2006) Functions and homeostasis of zinc, copper, and nickel in plants IN: Tamas, M.J. and Martinoia, E. (eds.) *Molecular Biology of Metal Homeostasis and Detoxification: From Microbes to Man*. Berlin, Heidelberg: Springer Berlin Heidelberg, 215-271.

Krämer, U., Cotter-Howell, J.D., Charnok, J.M., Baker, A.J.M. and Smith, J.a.C. (1999) Free histidines as metal chelator in plants that accumulate nickel. *Nature,* 379 (6566), 635-638.

Krogh, A., Larsson, B., Von Heijne, G. and Sonnhammer, E.L. (2001) Predicting transmembrane protein topology with a hidden Markov model: application to complete genomes. *Journal of Molecular Biology,* 305 (3), 567-580.

Krysan, P.J., Young, J.C. and Sussman, M.R. (1999) T-DNA as an insertional mutagen in Arabidopsis. *The Plant Cell,* 11 (12), 2283-2290.

Kuhlbrandt, W. (2004) Biology, structure and mechanism of P-type ATPases. *Nature Reviews Molecular Cell Biology,* 5, 282-295.

Kumar, S., Stecher, G. and Tamura, K. (2016) MEGA7: Molecular Evolutionary Genetics Analysis Version 7.0 for Bigger Datasets. *Molecular Biology and Evolution,* 33 (7), 1870-1874.

Kurniawan, T.A., Chan, G.Y., Lo, W.-H. and Babel, S. (2006) Physico–chemical treatment techniques for wastewater laden with heavy metals. *Chemical engineering journal,* 118 (1), 83-98.

Lai, K.T., Berkman, P.J., Lorenc, M.T., Duran, C., Smits, L., Manoli, S., Stiller, J. and Edwards, D. (2012) WheatGenome.info: An Integrated Database and Portal for Wheat Genome Information. *Plant and Cell Physiology,* 53 (2), 7.

Lamesch, P., Berardini, T.Z., Li, D., Swarbreck, D., Wilks, C., Sasidharan, R., Muller, R., Dreher, K., Alexander, D.L. and Garcia-Hernandez, M. (2012) The Arabidopsis Information Resource (TAIR): improved gene annotation and new tools. *Nucleic Acids Research,* 40 (D1), D1202-D1210.

Lanquar, V., Lelièvre, F., Bolte, S., Hamès, C., Alcon, C., Neumann, D., Vansuyt, G., Curie, C., Schröder, A. and Krämer, U. (2005) Mobilization of vacuolar iron by AtNRAMP3 and AtNRAMP4 is essential for seed germination on low iron. *The EMBO Journal,* 24 (23), 4041-4051.

Laurent, C., Lekeux, G., Ukuwela, A.A., Xiao, Z., Charlier, J.-B., Bosman, B., Carnol, M., Motte, P., Damblon, C. and Galleni, M. (2016) Metal binding to the N-terminal cytoplasmic domain of the PIB ATPase HMA4 is required for metal transport in Arabidopsis. *Plant Molecular Biology,* 90 (4-5), 453-466.

Lee, S. and An, G. (2009) Over-expression of OsIRT1 leads to increased iron and zinc accumulations in rice. *Plant Cell and Environment,* 32, 408-416.

Lee, S., Jeong, H.J., Kim, S.A., Lee, J., Guerinot, M.L. and An, G. (2010) OsZIP5 is a plasma membrane zinc transporter in rice. *Plant Molecular Biology,* 73 (4-5), 507-517.

Lee, S. and Kang, B.S. (2005) Expression of Arabidopsis phytochelatin synthase 2 is too low to complement an AtPCS1-defective *Cad1-3* mutant. *Molecules and Cells,* 19 (1), 81-87.

Lee, S., Kim, Y.Y., Lee, Y. and An, G. (2007) Rice P1B-Type Heavy-Metal ATPase, OsHMA9, Is a Metal Efflux Protein. *Plant Physiology,* 145 (3), 831-842.

Lee, S., Persson, D.P., Hansen, T.H., Husted, S., Schjoerring, J.K., Kim, Y.S., Jeon, U.S., Kim, Y.K., Kakei, Y. and Masuda, H. (2011) Bio-available zinc in rice seeds is increased by activation tagging of nicotianamine synthase. *Plant Biotechnology Journal,* 9 (8), 865-873.

Lee, Y., Kim, M., Han, J., Yeom, K.H., Lee, S., Baek, S.H. and Kim, V.N. (2004) MicroRNA genes are transcribed by RNA polymerase II. *EMBO Journal,* 23 (20), 4051-4060.

Lequeux, H., Hermans, C., Lutts, S. and Verbruggen, N. (2010) Response to copper excess in *Arabidopsis thaliana*: Impact on the root system architecture, hormone distribution, lignin accumulation and mineral profile. *Plant Physiology Biochemistry,* 48 (8), 673-682.

Li, D.D., Li, Y.J., Liang, J., Zhao, C.Z., Yin, H.J., Yin, C.Y., Cheng, X.Y. and Liu, Q. (2014) Responses of soil micronutrient availability to experimental warming in two contrasting forest ecosystems in the Eastern Tibetan Plateau, China. *Journal of Soils and Sediments,* 14 (6), 1050-1060.

Li, P.C., Huang, J.G., Yu, S.W., Li, Y.Y., Sun, P., Wu, C.A. and Zheng, C.C. (2016) Arabidopsis YL1/BPG2 Is Involved in Seedling Shoot Response to Salt Stress through ABI4. *Scientific Reports,* 6, 11.

Li, S., Zhou, X., Huang, Y., Zhu, L., Zhang, S., Zhao, Y., Guo, J., Chen, J. and Chen, R. (2013a) Identification and characterization of the zinc-regulated transporters, iron-regulated transporter-like protein (ZIP) gene family in maize. *BMC Plant Biology,* 13 (1), 1.

Li, W., Cowley, A., Uludag, M., Gur, T., Mcwilliam, H., Squizzato, S., Park, Y.M., Buso, N. and Lopez, R. (2015a) The EMBL-EBI bioinformatics web and programmatic tools framework. *Nucleic Acids Research*.

Li, X., Gao, S., Tang, Y., Li, L., Zhang, F., Feng, B., Fang, Z., Ma, L. and Zhao, C. (2015b) Genome-wide identification and evolutionary analyses of bZIP transcription factors in wheat and its relatives and expression profiles of anther development related TabZIP genes. *BMC Genomics,* 16, 976.

Li, Y., Zhang, Y., Shi, D., Liu, X., Qin, J., Ge, Q., Xu, L., Pan, X., Li, W., Zhu, Y. and Xu, J. (2013b) Spatial-temporal analysis of zinc homeostasis reveals the response mechanisms to acute zinc deficiency in Sorghum bicolor. *New Phytologist,* 200 (4), 1102-1115.

Li, Z., Wu, L.H., Zhang, H., Luo, Y.M. and Christie, P. (2015c) Effects of soil drying and wetting-drying cycles on the availability of heavy metals and their relationship to dissolved organic matter. *Journal of Soils and Sediments,* 15 (7), 1510-1519.

Lin, C., Mathad, R.I., Zhang, Z., Sidell, N. and Yang, D. (2014) Solution structure of a 2: 1 complex of anticancer drug XR5944 with TFF1 estrogen response element: insights into DNA recognition by a bis-intercalator. *Nucleic Acids Research*, gku219.

Lin, P.C., Pomeranz, M.C., Jikumaru, Y., Kang, S.G., Hah, C., Fujioka, S., Kamiya, Y. and Jang, J.C. (2011) The Arabidopsis tandem zinc finger protein AtTZF1 affects ABA-and GA-mediated growth, stress and gene expression responses. *The The Plant Journal,* 65 (2), 253-268.

Lin, W., Chai, J., Love, J. and Fu, D. (2010) Selective electrodiffusion of zinc ions in a Zrt-, Irt-like protein, ZIPB. *Journal of Biological Chemistry,* 285 (50), 39013-39020.

Lin, Y.F. and Aarts, M.G. (2012) The molecular mechanism of zinc and cadmium stress response in plants. *Cellular and Molecular Life Sciences,* 69 (19), 3187-3206.

Lin, Y.F., Hassan, Z., Talukdar, S., Schat, H. and Aarts, M.G. (2016) Expression of the ZNT1 Zinc Transporter from the Metal Hyperaccumulator Noccaea caerulescens Confers Enhanced Zinc and Cadmium Tolerance and Accumulation to *Arabidopsis thaliana*. *PLoS One,* 11 (3), e0149750.

Lin, Y.F., Liang, H.M., Yang, S.Y., Boch, A., Clemens, S., Chen, C.C., Wu, J.F., Huang, J.L. and Yeh, K.C. (2009) Arabidopsis IRT3 is a zinc-regulated and plasma membrane localized zinc/iron transporter. *New Phytologist,* 182 (2), 392-404.

Liu, C., Wu, Y. and Wang, X. (2012a) bZIP transcription factor OsbZIP52/RISBZ5: a potential negative regulator of cold and drought stress response in rice. *Planta,* 235 (6), 1157-1169.

Liu, D.J., Wang, Y.B., Guo, C.H., Cong, Q., Gong, X. and Zhang, H.J. (2016) Enhanced Iron and Zinc Accumulation in Genetically Engineered Wheat Plants Using Sickle Alfalfa (*Medicago falcata* L.) Ferritin Gene. *Cereal Research Communications,* 44 (1), 24-34.

Liu, J., Dutta, S.J., Stemmler, A.J. and Mitra, B. (2006) Metal-binding affinity of the transmembrane site in ZntA: implications for metal selectivity. *Biochemistry,* 45 (3), 763-772.

Liu, Q., Liu, Y. and Zhang, M. (2012b) Mercury and cadmium contamination in traffic soil of Beijing, China. *Bulletin of Environmental Contamination and Toxicology,* 88 (2), 154-157.

Liu, X. and Chu, Z. (2015) Genome-wide evolutionary characterization and analysis of bZIP transcription factors and their expression profiles in response to multiple abiotic stresses in *Brachypodium distachyon*. *BMC Genomics,* 16 (1), 1-15.

Liu, X.M., Kim, K.E., Kim, K.C., Nguyen, X.C., Han, H.J., Jung, M.S., Kim, H.S., Kim, S.H., Park, H.C., Yun, D.J. and Chung, W.S. (2010) Cadmium activates Arabidopsis MPK3 and MPK6 via accumulation of reactive oxygen species. *Phytochemistry,* 71 (5-6), 614-618.

Loganathan, P., Vigneswaran, S., Kandasamy, J. and Naidu, R. (2012) Cadmium Sorption and Desorption in Soils: A Review. *Critical Reviews in Environmental Science and Technology,* 42 (5), 489-533.

Lomazzi, M., Borisch, B. and Laaser, U. (2014) The Millennium Development Goals: experiences, achievements and what's next. *Glob Health Action,* 7, 23695.

Lombnaes, P. and Singh, B.R. (2003) Varietal tolerance to Zinc deficiency in wheat and barley grown in chelator-buffered nutrient solution and its effect on uptake Of Cu, Fe, and Mn. *Journal of Plant Nutrition and Soil Science,* 166, 76-83.

Lombnes, P. and Singh, B.R. (2003) Varietal tolerance to Zinc deficiency in wheat and barley grown in chelatorbuffered nutrient solution and its effect on uptake of Cu, Fe, and Mn. *Journal of Plant Nutrition and Soil Science,* 166 (1), 76-83.

Loneragan, J.F. and Webb, M.J. (1993) *Interactions between zinc and other nutrients affecting the growth of plants* Dordrecht, The Netherlands: Kluwer Academic Publishers.

Lowe, J., Vieyra, A., Catty, P., Guillain, F., Mintz, E. and Cuillel, M. (2004) A mutational study in the transmembrane domain of Ccc2p, the yeast Cu(I)-ATPase, shows different roles for each Cys-Pro-Cys cysteine. *Journal of Biological Chemistry,* 279 (25), 25986-25994.

Lu, M., Chai, J. and Fu, D. (2009) Structural basis for autoregulation of the zinc transporter YiiP. *Nature Structural & Molecular biology,* 16 (10), 1063-1067.

Lucca, N. and Leon, G. (2012) Arabidopsis ACA7, encoding a putative auto-regulated Ca^{2+}-ATPase, is required for normal pollen development. *Plant Cell Reports,* 31 (4), 651-659.

Maathuis, F.J. (2009) Physiological functions of mineral macronutrients. *Current Opinion in Plant Biology,* 12 (3), 250-258.

Mackenzie, B., Ujwal, M.L., Chang, M.-H., Romero, M.F. and Hediger, M.A. (2006) Divalent metal-ion transporter DMT1 mediates both H^+ -coupled Fe^{2+} transport and uncoupled fluxes. *Pflügers Archives,* 451 (4), 544-558.

Maldonado-Bonilla, L.D., Eschen-Lippold, L., Gago-Zachert, S., Tabassum, N., Bauer, N., Scheel, D. and Lee, J. (2013) The Arabidopsis tandem zinc finger 9 protein binds RNA and mediates pathogen-associated molecular pattern-triggered immune responses. *Plant and Cell Physiology*, pct175.

Malidareh, H.B., Mahvi, A.H., Yunesian, M., Alimohammadi, M. and Nazmara, S. (2014) Effect of fertilizer application on paddy soil heavy metals concentration and groundwater in North of Iran. *Middle - East Journal of Scientific Research,* 20 (12), 1721-1727.

Mana-Capelli, S., Mandal, A.K. and Arguello, J.M. (2003) *Archaeoglobus fulgidus* CopB is a thermophilic Cu^{2+}-ATPase: functional role of its histidine-rich-N-terminal metal binding domain. *Journal of Biological Chemistry,* 278 (42), 40534-40541.

Mandal, A.K., Cheung, W.D. and Arguello, J.M. (2002) Characterization of a thermophilic P-type Ag^+/Cu^+-ATPase from the extremophile *Archaeoglobus fulgidus*. *Journal of Biological Chemistry,* 277 (9), 7201-7208.

Marschner, P. (2012) Marschner's Mineral Nutrition of Higher Plants, 3rd Edn. Academic Press San Diego, CA.

Marty, F. (1999) Plant vacuoles. *The Plant Cell,* 11 (4), 587-599.

Matsumoto, T., Tanaka, T., Sakai, H., Amano, N., Kanamori, H., Kurita, K., Kikuta, A., Kamiya, K., Yamamoto, M., Ikawa, H., Fujii, N., Hori, K., Itoh, T. and Sato, K. (2011) Comprehensive sequence analysis of 24,783 barley full-length cDNAs derived from 12 clone libraries. *Plant Physiology,* 156 (1), 20-28.

Mayer, K.F., Waugh, R., Brown, J.W., Schulman, A., Langridge, P., Platzer, M., Fincher, G.B., Muehlbauer, G.J., Sato, K., Close, T.J., Wise, R.P. and Stein, N. (2012) A physical, genetic and functional sequence assembly of the barley genome. *Nature,* 491 (7426), 711-716.

Mayer, K.F.X., Rogers, J., Doležel, J., Pozniak, C., Eversole, K., Feuillet, C., Gill, B., Friebe, B., Lukaszewski, A.J., Sourdille, P., Endo, T.R., Kubaláková, M., Číhalíková, J., Dubská, Z., Vrána, J., Šperková, R., Šimková, H., Febrer, M., Clissold, L., Mclay, K., Singh, K., Chhuneja, P., Singh, N.K., Khurana, J., Akhunov, E., Choulet, F., Alberti, A., Barbe, V., Wincker, P., Kanamori, H., Kobayashi, F., Itoh, T., Matsumoto, T., Sakai, H., Tanaka, T., Wu, J., Ogihara, Y., Handa, H., Maclachlan, P.R., Sharpe, A., Klassen, D., Edwards, D., Batley, J., Olsen, O.-A., Sandve, S.R., Lien, S., Steuernagel, B., Wulff, B., Caccamo, M., Ayling, S., Ramirez-Gonzalez, R.H., Clavijo, B.J., Wright, J., Pfeifer, M., Spannagl, M., Martis, M.M., Mascher, M., Chapman, J., Poland, J.A., Scholz, U., Barry, K., Waugh, R., Rokhsar, D.S., Muehlbauer, G.J., Stein, N., Gundlach, H., Zytnicki, M., Jamilloux, V., Quesneville, H., Wicker, T., Faccioli, P., Colaiacovo, M., Stanca, A.M., Budak, H., Cattivelli, L., Glover, N., Pingault, L., Paux, E., Sharma, S., Appels, R., Bellgard, M., Chapman, B., Nussbaumer, T., Bader, K.C., Rimbert, H., Wang, S., Knox, R., Kilian, A., Alaux, M., Alfama, F., Couderc, L., Guilhot, N., Viseux, C., Loaec, M., Keller, B. and Praud, S. (2014) A chromosome-based draft sequence of the hexaploid bread wheat (*Triticum aestivum*) genome. *Science,* 345 (6194).

Mccall, K.A., Huang, C.-C. and Fierke, C.A. (2000) Function and mechanism of zinc metalloenzymes. *The Journal of nutrition,* 130 (5), 1437S-1446S.

Mcgavin, W.J., Mitchell, C., Cock, P.J., Wright, K.M. and Macfarlane, S.A. (2012) Raspberry leaf blotch virus, a putative new member of the genus Emaravirus, encodes a novel genomic RNA. *Journal of General Virology,* 93 (Pt 2), 430-437.

Mcwilliam, H., Li, W., Uludag, M., Squizzato, S., Park, Y.M., Buso, N., Cowley, A.P. and Lopez, R. (2013) Analysis Tool Web Services from the EMBL-EBI. *Nucleic Acids Res,* 41 (Web Server issue), W597-600.

Meharg, A.A., Norton, G., Deacon, C., Williams, P., Adomako, E.E., Price, A., Zhu, Y., Li, G., Zhao, F.-J. and Mcgrath, S. (2013) Variation in rice cadmium related to human exposure. *Environmental Science & Technology,* 47 (11), 5613-5618.

Mei, H., Cheng, N.H., Zhao, J., Park, S., Escareno, R.A., Pittman, J.K. and Hirschi, K.D. (2009) Root development under metal stress in *Arabidopsis thaliana* requires the H^+/cation antiporter CAX4. *The New Phytologist,* 183 (1), 95-105.

Menguer, P.K., Farthing, E., Peaston, K.A., Ricachenevsky, F.K., Fett, J.P. and Williams, L.E. (2013) Functional analysis of the rice vacuolar zinc transporter OsMTP1. *Journal of Experimental Botany,* 64 (10), 2871-2883.

Migocka, M., Kosieradzka, A., Papierniak, A., Maciaszczyk-Dziubinska, E., Posyniak, E., Garbiec, A. and Filleur, S. (2014) Two metal-tolerance proteins, MTP1 and MTP4, are involved in Zn homeostasis and Cd sequestration in cucumber cells. *Journal of experimental botany*, eru459.

Migocka, M., Papierniak, A., Maciaszczyk-Dziubinska, E., Posyniak, E. and Kosieradzka, A. (2015) Molecular and biochemical properties of two P_{1B2}-ATPases, CsHMA3 and CsHMA4, from cucumber. *Plant Cell and Environment,* 38 (6), 1127-1141.

Mikkelsen, M.D., Pedas, P., Schiller, M., Vincze, E., Mills, R., Borg, S., Møller, A., Schjoerring, J.K., Williams, L.E., Baekgaard, L., Holm, P.B. and Palmgren, M.G. (2012a) Barley HvHMA1 is a heavy metal pump involved in mobilizing organellar Zn and Cu and plays a role in metal loading into grains. *PLoS ONE,* 7 (11), 1-13.

Miller, W.A. and Rasochova, L. (1997) Barley yellow dwarf viruses. *Annual Review of Phytopathology,* 35, 167-190.

Mills, R.F., Doherty, M.L., Lopez-Marques, R.L., Weimar, T., Dupree, P., Palmgren, M.G., Pittman, J.K. and Williams, L.E. (2008) ECA3, a Golgi-localized P2A-type ATPase, plays a crucial role in manganese nutrition in Arabidopsis. *Plant Physiology,* 146 (1), 116-128.

Mills, R.F., Francini, A., Ferreira Da Rocha, P.S.C., Baccarini, P.J. and Aylett, M. (2005) The plant P1B-type ATPase AtHMA4 transports Zn and Cd plays a role in detoxification of transition metals supplied at elevated levels. *FEBS Letter,* 579, 783–791.

Mills, R.F., Krijger, G.C., Baccarini, P.J., Hall, J.L. and Williams, L.E. (2003) Functional expression of AtHMA4, a P1B-type ATPase in the Zn/Co/Cd/Pb subclass. *The Plant Journal,* 35, 164-176.

Mills, R.F., Peaston, K.A., Runions, J., Williams, L.E. and Park, S.H. (2012) HvHMA2, a P1B-ATPase from barley, is highly conserved among cereals and functions in Zn and Cd transport. *PLoS ONE,* 7 (8), e42640.

Mills, R.F., Valdes, B., Duke, M., Peaston, K.A. and Lahner, B. (2010) Functional significance of AtHMA4 C-terminal domain in planta. *PLoS ONE,* 5: e13388.

Milner, M.J., Seamon, J., Craft, E. and Kochian, L.V. (2013) Transport properties of members of the ZIP family in plants and their role in Zn and Mn homeostasis. *Journal of Experimental Botany,* 64 (1), 369-381.

Mitaku, S. and Hirokawa, T. (1999) Physicochemical factors for discriminating between soluble and membrane proteins: hydrophobicity of helical segments and protein length. *Protein Engineering,* 12 (11), 953-957.

Mittler, R., Vanderauwera, S., Gollery, M. and Van Breusegem, F. (2004) Reactive oxygen gene network of plants. *Trends Plant Sci,* 9 (10), 490-498.

Miyadate, H., Adachi, S., Hiraizumi, A., Tezuka, K., Nakazawa, N., Kawamoto, T., Katou, K., Kodama, I., Sakurai, K. and Takahashi, H. (2011) OsHMA3, a P1B-type of ATPase affects root-to-shoot cadmium translocation in rice by mediating efflux into vacuoles. *The New Phytologist,* 189 (1), 190-199.

Mobin, M. and Khan, N.A. (2007) Photosynthetic activity, pigment composition and antioxidative response of two mustard (*Brassica juncea*) cultivars differing in photosynthetic capacity subjected to cadmium stress. *Journal of Plant Physiology,* 164 (5), 601-610.

Molins, H., Michelet, L., Lanquar, V., Agorio, A., Giraudat, J., Roach, T., Krieger-Liszkay, A. and Thomine, S. (2013) Mutants impaired in vacuolar metal mobilization identify chloroplasts as a target for cadmium hypersensitivity in *Arabidopsis thaliana*. *Plant Cell and Environment,* 36 (4), 804-817.

Møller, J.V., Juul, B. and Le Maire, M. (1996) Structural organization, ion transport, and energy transduction of P-type ATPases. *Biochimica et Biophysica Acta (BBA)-Reviews on Biomembranes,* 1286 (1), 1-51.

Moreau, S., Thomson, R.M., Kaiser, B.N., Trevaskis, B., Guerinot, M.L., Udvardi, M.K., Puppo, A. and Day, D.A. (2002) GmZIP1 encodes a symbiosis-specific zinc transporter in soybean. *Journal of Biological Chemistry,* 277 (7), 4738-4746.

Morel, M., Crouzet, J., Gravot, A., Auroy, P., Leonhardt, N., Vavasseur, A. and Richaud, P. (2009) AtHMA3, a P1B-ATPase Allowing Cd/Zn/Co/Pb Vacuolar Storage in Arabidopsis. *Plant Physiology,* 149 (2), 894-904.

Moreno, I., Norambuena, L., Maturana, D., Toro, M., Vergara, C., Orellana, A., Zurita-Silva, A. and Ordenes, V.R. (2008) AtHMA1 is a thapsigargin-sensitive Ca^{2+}/heavy metal pump. *Journal of Biological Chemistry,* 283 (15), 9633-9641.

Morina, F., Jovanovic, L., Mojovic, M., Vidovic, M., Pankovic, D. and Veljovic Jovanovic, S. (2010) Zinc-induced oxidative stress in *Verbascum thapsus* is caused by an accumulation of reactive oxygen species and quinhydrone in the cell wall. *Physiologia Plantarum,* 140 (3), 209-224.

Mrízová, K., Holasková, E., Öz, M.T., Jiskrová, E., Frébort, I. and Galuszka, P. (2014) Transgenic barley: A prospective tool for biotechnology and agriculture. *Biotechnology Advances,* 32 (1), 137-157.

Myouga, F., Hosoda, C., Umezawa, T., Iizumi, H., Kuromori, T., Motohashi, R., Shono, Y., Nagata, N., Ikeuchi, M. and Shinozaki, K. (2008) A heterocomplex of iron superoxide dismutases defends chloroplast nucleoids against oxidative stress and is essential for chloroplast development in Arabidopsis. *Plant Cell,* 20 (11), 3148-3162.

Nakanishi, H., Ogawa, I., Ishimaru, Y., Mori, S. and Nishizawa, N.K. (2006) Iron deficiency enhances cadmium uptake and translocation mediated by the Fe2+ transporters OsIRT1 and OsIRT2 in rice. *Soil Science and Plant Nutrition,* 52 (4), 464-469.

Nakase, M., Aoki, N., Matsuda, T. and Adachi, T. (1997) Characterization of a novel rice bZIP protein which binds to the alpha-globulin promoter. *Plant Molecular Biology,* 33 (3), 513-522.

Nantel, A. and Quatrano, R.S. (1996) Characterization of three rice basic/leucine zipper factors, including two inhibitors of EmBP-1 DNA binding activity. *Journal of Biological Chemistry,* 271 (49), 31296-31305.

Negishi, T., Nakanishi, H., Yazaki, J., Kishimoto, N., Fujii, F., Shimbo, K., Yamamoto, K., Sakata, K., Sasaki, T. and Kikuchi, S. (2002) cDNA microarray analysis of gene expression during Fe-deficiency stress in barley suggests that polar transport of vesicles is implicated in phytosiderophore secretion in Fe-deficient barley roots. *The The Plant Journal,* 30 (1), 83-94.

Nevo, Y. and Nelson, N. (2006) The NRAMP family of metal-ion transporters. *Biochimica et Biophysica Acta (BBA)-Molecular Cell Research,* 1763 (7), 609-620.

Nicholas, K.B. and Nicholas Jr, H.B. (1997) GeneDoc: a tool for editing and annotating multiple sequence alignments. Available from: http://www.psc.edu/biomed/genedoc.

Nishiyama, R., Kato, M., Nagata, S., Yanagisawa, S. and Yoneyama, T. (2012) Identification of Zn-nicotianamine and Fe-2'-Deoxymugineic acid in the phloem sap from rice plants (*Oryza sativa* L.). *Plant Cell Physiology,* 53 (2), 381-390.

Nozoye, T., Nagasaka, S., Kobayashi, T., Takahashi, M., Sato, Y., Sato, Y., Uozumi, N., Nakanishi, H. and Nishizawa, N.K. (2011) Phytosiderophore efflux transporters are crucial for iron acquisition in graminaceous plants. *Journal of Biological Chemistry,* 286 (7), 5446-5454.

Oda, K., Otani, M., Uraguchi, S., Akihiro, T. and Fujiwara, T. (2011) Rice ABCG43 is Cd inducible and confers Cd tolerance on yeast. *Bioscience, Biotechnology, and Biochemistry,* 75 (6), 1211-1213.

Ohki (2006) Effect of zinc nutrition on photosynthesis and carbonic anhydrase activity in cotton. *Physiologia Plantarum,* 38, 300-304.

Ok, Y.S., Oh, S.-E., Ahmad, M., Hyun, S., Kim, K.-R., Moon, D.H., Lee, S.S., Lim, K.J., Jeon, W.-T. and Yang, J.E. (2010) Effects of natural and calcined oyster shells on Cd and Pb immobilization in contaminated soils. *Environmental Earth Sciences,* 61 (6), 1301-1308.

Ok, Y.S., Usman, A.R.A., Lee, S.S., Abd El-Azeem, S.a.M., Choi, B., Hashimoto, Y. and Yang, J.E. (2011) Effects of rapeseed residue on lead and cadmium availability and uptake by rice plants in heavy metal contaminated paddy soil. *Chemosphere,* 85 (4), 677-682.

Olesen, C., Sorensen, T.L., Nielsen, R.C., Moller, J.V. and Nissen, P. (2004) Dephosphorylation of the calcium pump coupled to counterion occlusion. *Science,* 306 (5705), 2251-2255.

Ooms, G., Hooykaas, P.J., Van Veen, R.J., Van Beelen, P., Regensburg-Tuink, T.J. and Schilperoort, R.A. (1982) Octopine Ti-plasmid deletion mutants of *Agrobacterium tumefaciens* with emphasis on the right side of the T-region. *Plasmid,* 7 (1), 15-29.

Ooms, G., Klapwijk, P.M., Poulis, J.A. and Schilperoort, R.A. (1980) Characterization of Tn904 insertions in octopine Ti plasmid mutants of *Agrobacterium tumefaciens*. *Journal of Bacteriology,* 144 (1), 82-91.

Orphanides, G., Lagrange, T. and Reinberg, D. (1996) The general transcription factors of RNA polymerase II. *Genes and development,* 10 (21), 2657-2683.

Ouyang, S., Zhu, W., Hamilton, J., Lin, H., Campbell, M., Childs, K., Thibaud-Nissen, F., Malek, R.L., Lee, Y., Zheng, L., Orvis, J., Haas, B., Wortman, J. and Buell, C.R. (2007) The TIGR Rice Genome Annotation Resource: improvements and new features. *Nucleic Acids Research,* 35 (suppl 1), D883-D887.

Palmgren, M.G., Clemens, S., Williams, L.E., Krämer, U., Borg, S., Schjørring, J.K. and Sanders, D. (2008) Zinc biofortification of cereals: problems and solutions. *Trends in Plant Science,* 13 (9), 464-473.

Palmgren, M.G. and Nissen, P. (2010) P-type ATPases. *Annual Review of Biophysics,* 40, 243-266.

Pang, K., Li, Y., Liu, M., Meng, Z. and Yu, Y. (2013) Inventory and general analysis of the ATP-binding cassette (ABC) gene superfamily in maize (*Zea mays* L.). *Gene,* 526 (2), 411-428.

Parinov, S., Sevugan, M., Ye, D., Yang, W.C., Kumaran, M. and Sundaresan, V. (1999) Analysis of flanking sequences from dissociation insertion lines: a database for reverse genetics in Arabidopsis. *Plant Cell,* 11 (12), 2263-2270.

Park, J., Song, W.-Y., Ko, D., Eom, Y., Hansen, T.H., Schiller, M., Lee, T.G., Martinoia, E. and Lee, Y. (2011) The phytochelatin transporters AtABCC1 and AtABCC2 mediate tolerance to cadmium and mercury. *The Plant Journal.*

Patsikka, E., Kairavuo, M., Sersen, F., Aro, E.M. and Tyystjarvi, E. (2002) Excess copper predisposes photosystem II to photoinhibition in vivo by outcompeting iron and causing decrease in leaf chlorophyll. *Plant Physiology,* 129 (3), 1359-1367.

Pedas, P. and Husted, S. (2009) Zinc transport mediated by barley ZIP proteins are induced by low pH. *Plant Signaling & Behavior,* 4 (9), 842-845.

Pedas, P., Schjoerring, J.K. and Husted, S. (2009a) Identification and characterization of zinc-starvation-induced ZIP transporters from barley roots. *Plant Physiology and Biochemistry,* 47, 377–383.

Pedas, P., Schjoerring, J.K. and Husted, S. (2009b) Identification and characterization of zinc-starvation-induced ZIP transporters from barley roots. *Plant Physiology and Biochemistry,* 47 (5), 377-383.

Pedas, P., Ytting, C.K., Fuglsang, A.T., Jahn, T.P., Schjoerring, J.K. and Husted, S. (2008) Manganese efficiency in barley: identification and characterization of the metal ion transporter HvIRT1. *Plant Physiology,* 148 (1), 455-466.

Pedler, J.F., Parker, D.R. and Crowley, D.E. (2000) Zinc deficiency-induced phytosiderophore release by the Triticaceae is not consistently expressed in solution culture. *Planta,* 211 (1), 120-126.

Peiter, E., Montanini, B., Gobert, A., Pedas, P., Husted, S., Maathuis, F.J., Blaudez, D., Chalot, M. and Sanders, D. (2007) A secretory pathway-localized cation diffusion facilitator confers plant manganese tolerance. *Proceedings of the National Academy of Sciences,* 104 (20), 8532-8537.

Pence, N.S., Larsen, P.B., Ebbs, S.D., Letham, D.L., Lasat, M.M., Garvin, D.F., Eide, D. and Kochian, L.V. (2000) The molecular physiology of heavy metal transport in the Zn/Cd hyperaccumulator Thlaspi caerulescens. *Proceedings of the National Academy of Sciences,* 97 (9), 4956-4960.

Persson, D.P., Chen, A., Aarts, M.G., Salt, D.E., Schjoerring, J.K. and Husted, S. (2016) Multi-element bioimaging of *Arabidopsis thaliana* roots. *Plant Physiol*, 770.

Petrov, V.D. and Van Breusegem, F. (2012) Hydrogen peroxide-a central hub for information flow in plant cells. *AoB Plants,* 2012, pls014.

Pieterse, C.M. and Van Loon, L.C. (2004) NPR1: the spider in the web of induced resistance signaling pathways. *Current Opinion in Plant Biology,* 7 (4), 456-464.

Pilon-Smits, E. (2005) Phytoremediation. *Annual Review of Plant Biology,* 56, 15-39.

Pittman, J.K. (2005) Managing the manganese: molecular mechanisms of manganese transport and homeostasis. *The New Phytologist,* 167 (3), 733-742.

Pittman, J.K., Edmond C Fau - Sunderland, P.A., Sunderland Pa Fau - Bray, C.M. and Bray, C.M. (2009) A cation-regulated and proton gradient-dependent cation transporter from Chlamydomonas reinhardtii has a role in calcium and sodium homeostasis. (0021-9258 (Print)).

Pitzschke, A. and Hirt, H. (2010) New insights into an old story: Agrobacterium-induced tumour formation in plants by plant transformation. *EMBO Journal,* 29 (6), 1021-1032.

Podar, D., Scherer, J., Noordally, Z., Herzyk, P., Nies, D. and Sanders, D. (2012) Metal selectivity determinants in a family of transition metal transporters. *Journal of Biological Chemistry,* 287 (5), 3185-3196.

Poschenrieder, C., Tolra, R. and Barceló, J. (2006) Can metals defend plants against biotic stress? *Trends in Plant Science,* 11 (6), 288-295.

Poulsen, L.R., López-Marqués, R.L. and Palmgren, M.G. (2008a) Flip-pases: still more questions than answers. *Cellular and Molecular Life Sciences,* 65, 3119-3125.

Poulsen, L.R., Lopez-Marques, R.L., Pedas, P.R., Mcdowell, S.C., Brown, E., Kunze, R., Harper, J.F., Pomorski, T.G. and Palmgren, M. (2015) A phospholipid uptake system in the model plant *Arabidopsis thaliana*. *Nature Communications,* 6, 7649.

Pourabed, E., Ghane Golmohamadi, F., Soleymani Monfared, P., Razavi, S.M. and Shobbar, Z.S. (2015) Basic leucine zipper family in barley: genome-wide characterization of members and expression analysis. *Molecular Biotechnology,* 57 (1), 12-26.

Printz, B., Lutts, S., Hausman, J.-F. and Sergeant, K. (2016) Copper trafficking in plants and its implication on cell wall dynamics. *Frontiers in Plant Science,* 7.

Raimunda, D., Long, J.E., Sassetti, C.M. and Arguello, J.M. (2012) Role in metal homeostasis of CtpD, a Co(2)(+) transporting P(1B4)-ATPase of *Mycobacterium smegmatis*. *Molecular Microbiology,* 84 (6), 1139-1149.

Ramesh, A., Walker, S.A., Hood, D.B., Guillen, M.D., Schneider, K. and Weyand, E.H. (2004a) Bioavailability and risk assessment of orally ingested polycyclic aromatic hydrocarbons. *International Journal of Toxicology,* 23 (5), 301-333.

Ramesh, S.A., Choimes, S. and Schachtman, D.P. (2004b) Over-Expression of an Arabidopsis Zinc Transporter in *Hordeum vulgare* Increases Short-Term Zinc Uptake after Zinc Deprivation and Seed Zinc Content. *Plant Molecular Biology,* 54 (3), 373-385.

Ranieri, A., Castagna, A., Scebba, F., Careri, M., Zagnoni, I., Predieri, G., Pagliari, M. and Di Toppi, L.S. (2005) Oxidative stress and phytochelatin characterisation in bread wheat exposed to cadmium excess. *Plant Physiology and Biochemistry,* 43 (1), 45-54.

Reeves, P.G. and Chaney, R.L. (2008) Bioavailability as an issue in risk assessment and management of food cadmium: A review. *Science of the Total Environment,* 398 (1), 13-19.

Remans, T., Opdenakker, K., Guisez, Y., Carleer, R., Schat, H., Vangronsveld, J. and Cuypers, A. (2012) Exposure of *Arabidopsis thaliana* to excess Zn reveals a Zn-specific oxidative stress signature. *Environmental and Experimental Botany,* 84, 61-71.

Remy, E., Cabrito, T.R., Batista, R.A., Hussein, M.A., Teixeira, M.C., Athanasiadis, A., Sa-Correia, I. and Duque, P. (2014) Intron retention in the 5'UTR of the novel ZIF2 transporter enhances translation to promote zinc tolerance in arabidopsis. *PLoS Genetics,* 10 (5), e1004375.

Ren, Y., Liu, Y., Chen, H., Li, G., Zhang, X. and Zhao, J. (2011) Type 4 metallothionein genes are involved in regulating Zn ion accumulation in late embryo and in controlling early seedling growth in Arabidopsis. *Plant Cell and Environment,* 35 (4), 770–789.

Rengel, Z. (1995) Carbonic anhydrase activity in leaves of wheat genotypes differing in Zn efficiency. *Plant Physiology,* 147, 251-256.

Rhee, S.Y., Beavis, W., Berardini, T.Z., Chen, G., Dixon, D., Doyle, A., Garcia-Hernandez, M., Huala, E., Lander, G. and Montoya, M. (2003) The Arabidopsis Information Resource (TAIR): a model organism database providing a centralized, curated gateway to Arabidopsis biology, research materials and community. *Nucleic Acids Research,* 31 (1), 224-228.

Ricachenevsky, F.K., Menguer, P.K., Sperotto, R.A. and Fett, J.P. (2015) Got to hide your Zn away: Molecular control of Zn accumulation and biotechnological applications. *Plant Science,* 236, 1-17.

Ricachenevsky, F.K., Sperotto, R.A., Menguer, P.K., Sperb, E.R., Lopes, K.L. and Fett, J.P. (2011) ZINC-INDUCED FACILITATOR-LIKE family in plants: lineage-specific expansion in monocotyledons and conserved genomic and expression features among rice (*Oryza sativa*) paralogs. *BMC Plant Biology,* 11, 20.

Rice, P., Longden, I. and Bleasby, A. (2000) EMBOSS: The European Molecular Biology Open Software Suite. *Trends in Genetics,* 16 (6), 276-277.

Ringli, C. and Keller, B. (1998) Specific interaction of the tomato bZIP transcription factor VSF-1 with a non-palindromic DNA sequence that controls vascular gene expression. *Plant Molecular Biology,* 37 (6), 977-988.

Rodriguez, L., Lopez-Bellido, F.J., Carnicer, A., Recreo, F., Tallos, A. and Monteagudo, J.M. (2005) *Mercury recovery from soils by phytoremediation*. Berlin, Germany: Springer. 197-204.

Rogers, E.E., Eide, D.J. and Guerinot, M.L. (2000) Altered selectivity in an Arabidopsis metal transporter. *Proceedings of the National Academy of Sciences,* 97 (22), 12356-12360.

Roohani, N., Hurrell, R., Kelishadi, R. and Schulin, R. (2013) Zinc and its importance for human health: An integrative review. *Journal of Research in Medical Sciences,* 18 (2), 144-157.

Roosens, N.H., Bernard, C., Leplae, R. and Verbruggen, N. (2004) Evidence for copper homeostasis function of metallothionein (MT3) in the hyperaccumulator *Thlaspi caerulescens*. *FEBS Letters,* 577 (1-2), 9-16.

Rosso, M., Li, Y., Strizhov, N., Reiss, B., Dekker, K. and Weisshaar, B. (2003) An *Arabidopsis thaliana* T-DNA mutagenized population (GABI-Kat) for flanking sequence tag-based reverse genetics. *Plant Molecular Biology,* 53 (1-2), 247-259.

Sadeghzadeh, B. and Rengel, Z. (2011) The Molecular and Physiological Basis of Nutrient Use Efficiency in Crops IN: Hawkesford, M.J. and Barraclough, P. (eds.) *Zinc in Soils and Crop Nutrition*, First ed.: John Wiley & Sons, 40.

Sadeghzadeh, B., Rengel, Z. and Li, C. (2015) Quantitative Trait Loci (QTL) of Seed Zn Accumulation in Barley Population Clipper X Sahara. *Journal of Plant Nutrition,* 38 (11), 1672-1684.

Salama, Z.A., El-Fouly, M.M., Lazova, G. and Popova, L.P. (2006) Carboxylating enzymes and carbonic anhydrase functions were suppressed by zinc deficiency in maize and chickpea plants. *Acta Physiologiae Plantarum,* 28 (5), 445-451.

Saleh, J., Najafi, N., Oustan, S., Aliasgharzad, N. and Ghassemi-Golezani, K. (2013) Effects of silicon, salinity and waterlogging on the extractable Zn, Cu, K and Na in a sandy loam soil. *International Journal of Agriculture: Research and Review,* 3 (1), 56-64.

Samardjieva, K.A., Goncalves, R.F., Valentao, P., Andrade, P.B., Pissarra, J., Pereira, S. and Tavares, F. (2015) Zinc Accumulation and Tolerance in Solanum nigrum are Plant Growth Dependent. *International Journal of Phytoremediation,* 17 (1-6), 272-279.

Sandalio, L.M., Dalurzo, H.C., Gomez, M., Romero-Puertas, M.C. and Del Rio, L.A. (2001) Cadmium-induced changes in the growth and oxidative metabolism of pea plants. *Journal of Experimental Botany,* 52 (364), 2115-2126.

Sasaki, A., Yamaji, N., Mitani-Ueno, N., Kashino, M. and Ma, J.F. (2015) A node-localized transporter OsZIP3 is responsible for the preferential distribution of Zn to developing tissues in rice. *The The Plant Journal,* 84 (2), 374-384.

Sato-Nagasawa, N., Mori, M., Nakazawa, N., Kawamoto, T. and Nagato, Y. (2012) Mutations in rice (*Oryza sativa*) heavy metal ATPase2 (OsHMA2) restrict the translocation of zinc and cadmium. *Plant Cell Physiology,* 53, 213–224.

Sato, K., Tanaka, T., Shigenobu, S., Motoi, Y., Wu, J. and Itoh, T. (2016) Improvement of barley genome annotations by deciphering the Haruna Nijo genome. *DNA Research,* 23 (1), 21-28.

Satoh, R., Fujita, Y., Nakashima, K., Shinozaki, K. and Yamaguchi-Shinozaki, K. (2004) A Novel Subgroup of bZIP Proteins Functions as Transcriptional Activators in Hypoosmolarity-Responsive Expression of the ProDH Gene in Arabidopsis. *Plant and Cell Physiology,* 45 (3), 309-317.

Schaaf, G., Ludewig, U., Erenoglu, B.E., Mori, S., Kitahara, T. and Von Wiren, N. (2004) ZmYS1 functions as a proton-coupled symporter for phytosiderophore- and nicotianamine-chelated metals. *Journal of Biological Chemistry,* 279 (10), 9091-9096.

Schindler, U., Menkens, A.E., Beckmann, H., Ecker, J.R. and Cashmore, A.R. (1992) Heterodimerization between light-regulated and ubiquitously expressed Arabidopsis GBF bZIP proteins. *EMBO Journal,* 11 (4), 1261-1273.

Schiøtt, M., Romanowsky, S.M., Bækgaard, L., Jakobsen, M.K., Palmgren, M.G. and Harper, J.F. (2004) A plant plasma membrane Ca2+ pump is required for normal pollen tube growth and fertilization. *Proceedings of the National Academy of Sciences of the United States of America,* 101 (25), 9502-9507.

Schmidt, R.J., Ketudat, M., Aukerman, M.J. and Hoschek, G. (1992) Opaque-2 is a transcriptional activator that recognizes a specific target site in 22-kD zein genes. *Plant Cell,* 4 (6), 689-700.

Schneider, T., Schellenberg, M., Meyer, S., Keller, F., Gehrig, P., Riedel, K., Lee, Y., Eberl, L. and Martinoia, E. (2009) Quantitative detection of changes in the leaf-mesophyll tonoplast proteome in dependency of a cadmium exposure of barley (*Hordeum vulgare* L.) plants. *PROTEOMICS,* 9 (10), 2668-2677.

Schulte, D., Close, T.J., Graner, A., Langridge, P., Matsumoto, T., Muehlbauer, G., Sato, K., Schulman, A.H., Waugh, R., Wise, R.P. and Stein, N. (2009) The International Barley Sequencing Consortium—At the Threshold of Efficient Access to the Barley Genome. *Plant Physiology,* 149 (1), 142-147.

Schutze, K., Harter, K. and Chaban, C. (2008) Post-translational regulation of plant bZIP factors. *Trends in Plant Sciences,* 13 (5), 247-255.

Seigneurin-Berny, D., Gravot, A., Auroy, P., Mazard, C. and Kraut, A. (2006) HMA1, a new Cu-ATPase of the chloroplast envelope, is essential for growth under adverse light conditions. *Journal of Biological Chemistry,* 281, 2882–2892.

Shanmugam, V., Lo, J.C. and Yeh, K.C. (2013) Control of Zn uptake in *Arabidopsis halleri*: a balance between Zn and Fe. *Frontiers in Plant Science,* 4, 281.

Shanmugam, V., Tsednee, M. and Yeh, K.-C. (2011) ZINC TOLERANCE INDUCED BY IRON 1 reveals the importance of glutathione in the cross-homeostasis between zinc and iron in *Arabidopsis thaliana*,. *The Plant Journal,* 60 (6), 1006–1017.

Shanmugam, V., Tsednee, M. and Yeh, K.C. (2012) ZINC TOLERANCE INDUCED BY IRON 1 reveals the importance of glutathione in the cross-homeostasis between zinc and iron in *Arabidopsis thaliana*. *The Plant Journal,* 69 (6), 1006-1017.

Sharma, S.S., Dietz, K.J. and Mimura, T. (2016) Vacuolar compartmentalization as indispensable component of heavy metal detoxification in plants. *Plant Cell and Environment,* 39 (5), 1112-1126.

Shaver, T.M., Westfall, D.G. and Ronaghi, M. (2007) Zinc fertilizer solubility and its effects on zinc bioailability over time. *Journal of Plant Nutrition,* 30 (1), 123-133.

Shikanai, T., Muller-Moule, P., Munekage, Y., Niyogi, K.K. and Pilon, M. (2003) PAA1, a P-type ATPase of Arabidopsis, functions in copper transport in chloroplasts. *Plant Cell,* 15 (6), 1333-1346.

Shin, L.J., Lo, J.C., Chen, G.H., Callis, J., Fu, H. and Yeh, K.C. (2013) IRT1 degradation factor1, a ring E3 ubiquitin ligase, regulates the degradation of iron-regulated transporter1 in Arabidopsis. *Plant Cell,* 25 (8), 3039-3051.

Siemianowski, O., Mills, R.F., Williams, L.E. and Antosiewicz, D.M. (2011) Expression of the P_{1B}-type ATPase AtHMA4 in tobacco modifies Zn and Cd root to shoot partitioning and metal tolerance. *Plant Biotechnol Journal,* 9 (1), 64-74.

Sievers, F., Wilm, A., Dineen, D., Gibson, T.J., Karplus, K., Li, W., Lopez, R., Mcwilliam, H., Remmert, M., Soding, J., Thompson, J.D. and Higgins, D.G. (2011) Fast, scalable generation of high-quality protein multiple sequence alignments using Clustal Omega. *Molecular Systems Biology,* 7, 539.

Sigurbjorsson, B. and Micke, A. (1969) Progress in mutation breeding. In: Induced mutation in plants *Proceedings of an international symposium on the nature, induction and utilization of mutation in plants*, Vienna. International Atomic Energy Agency, 673-697.

Sinclair, S.A. and Krämer, U. (2012) The zinc homeostasis network of land plants. *Biochimica et Biophysica Acta (BBA)-Molecular Cell Research,* 1823 (9), 1553-1567.

Singh, B., Natesan, S.K.A., Singh, B. and Usha, K. (2005) Improving zinc efficiency of cereals under zinc deficiency. *Current Science,* 88 (1), 36-44.

Singh, D., Yadav, S. and Nautiyal, N. (2014) Evaluation of Growth Responses in Wheat as Affected by the Application of Zinc and Boron to a Soil Deficient in Available Zinc and Boron. *Communications in Soil Science and Plant Analysis,* 45 (6), 765-776.

Singh, K., Foley, R.C. and Onate-Sanchez, L. (2002) Transcription factors in plant defense and stress responses. *Curr ent Opinnion in Plant Biology,* 5 (5), 430-436.

Smeets, K., Opdenakker, K., Remans, T., Van Sanden, S., Van Belleghem, F., Semane, B., Horemans, N., Guisez, Y., Vangronsveld, J. and Cuypers, A. (2009) Oxidative stress-related responses at transcriptional and enzymatic levels after exposure to Cd or Cu in a multipollution context. *Journal of Plant Physiology,* 166 (18), 1982-1992.

Smith, A.T., Smith, K.P. and Rosenzweig, A.C. (2014) Diversity of the metal-transporting P1B-type ATPases. *Journal of Biological Inorganic Chemistry,* 19 (6), 947-960.

Soltangheisi, A., Rahman, Z.A., Ishak, C.F., Musa, H.M. and Zakikhani, H. (2014) Effect of Zinc and Phosphorus Supply on the Activity of Carbonic Anhydrase and the Ultrastructure of Chloroplast in Sweet Corn (*Zea mays* var. saccharata). *Asian Journal of Plant Sciences,* 13, 51-58.

Song, C., Wang, C., Zhang, C., Korir, N.K., Yu, H., Ma, Z. and Fang, J. (2010a) Deep sequencing discovery of novel and conserved microRNAs in trifoliate orange (*Citrus trifoliata*). *BMC Genomics,* 11, 431.

Song, W.Y., Choi, K.S., Kim, D.Y., Geisler, M., Park, J., Vincenzetti, V., Schellenberg, M., Kim, S.H., Lim, Y.P., Noh, E.W., Lee, Y. and Martinoia, E. (2010b) Arabidopsis PCR2 is a zinc exporter involved in both zinc extrusion and long-distance zinc transport. *Plant Cell,* 22 (7), 2237–2252.

Song, W.Y., Martinoia, E., Lee, J., Kim, D., Kim, D.Y., Vogt, E., Shim, D., Choi, K.S., Hwang, I. and Lee, Y. (2004) A novel family of cys-rich membrane proteins mediates cadmium resistance in Arabidopsis. *Plant Physiology,* 135 (2), 1027-1039.

Sonnhammer, E.L., Von Heijne, G. and Krogh, A. (1998) A hidden Markov model for predicting transmembrane helices in protein sequences *Ismb*. 175-182.

Sunkar, R., Kapoor, A. and Zhu, J.K. (2006) Post-transcriptional induction of two Cu/Zn superoxide dismutase genes in Arabidopsis is mediated by downregulation of *miR398* and important for oxidative stress tolerance. *Plant Cell,* 18 (8), 2051-2065.

Sussman, M.R., Amasino, R.M., Young, J.C., Krysan, P.J. and Austin-Phillips, S. (2000) The Arabidopsis knockout facility at the University of Wisconsin-Madison. *Plant Physiology,* 124 (4), 1465-1467.

Suzuki, M., Tsukamoto, T., Inoue, H., Watanabe, S., Matsuhashi, S., Takahashi, M., Nakanishi, H., Mori, S. and Nishizawa, N.K. (2008) Deoxymugineic acid increases Zn translocation in Zn-deficient rice plants. *Plant Molecular Biology,* 66 (6), 609-617.

Swarbreck, D., Wilks, C., Lamesch, P., Berardini, T.Z., Garcia-Hernandez, M., Foerster, H., Li, D., Meyer, T., Muller, R. and Ploetz, L. (2008) The Arabidopsis Information Resource (TAIR):

gene structure and function annotation. *Nucleic Acids Research,* 36 (suppl 1), D1009-D1014.

Szilard, A., Sass L Fau - Deak, Z., Deak Z Fau - Vass, I. and Vass, I. (2007) The sensitivity of Photosystem II to damage by UV-B radiation depends on the oxidation state of the water-splitting complex. *Biochimica et Biophysica Acta (BBA)-Bioenergetics*, 1767(6), pp.876-882.

Tack, F.M.G., Van Ranst, E., Lievens, C. and Vandenberghe, R.E. (2006) Soil solution Cd, Cu and Zn concentrations as affected by short-time drying or wetting: The role of hydrous oxides of Fe and Mn. *Geoderma,* 137 (1–2), 83-89.

Takahashi, R., Ishimaru, Y., Senoura, T., Shimo, H., Ishikawa, S., Arao, T., Nakanishi, H. and Nishizawa, N.K. (2011) The OsNRAMP1 iron transporter is involved in Cd accumulation in rice. *Journal of Experimental Botany,* 62, 4843-4850.

Talano, M.A., Oller, A.L.W., González, P., González, S.O. and Agostini, E. (2014) Effects of arsenate on tobacco hairy root and seedling growth, and its removal. *In Vitro Cellular & Developmental Biology - Plant,* 50 (2), 217-225.

Talke, I.N., Hanikenne, M. and Krämer, U. (2006) Zinc-dependent global transcriptional control, transcriptional deregulation, and higher gene copy number for genes in metal homeostasis of the hyperaccumulator *Arabidopsis halleri*. *Plant Physiology,* 142, 148–167.

Tan, J., Wang, J., Chai, T., Zhang, Y., Feng, S., Li, Y., Zhao, H., Liu, H. and Chai, X. (2013) Functional analyses of TaHMA2, a P_{1B}-type ATPase in wheat. *Plant Biotechnology,* 11 (4), 420-431.

Tanaka, N., Kawachi, M., Fujiwara, T. and Maeshima, M. (2013) Zinc-binding and structural properties of the histidine-rich loop of *Arabidopsis thaliana* vacuolar membrane zinc transporter MTP1. *FEBS Open Bio,* 3, 218-224.

Tapiero, H. and Tew, K.D. (2003) Trace elements in human physiology and pathology: zinc and metallothioneins. *Biomedicine & Pharmacotherapy,* 57 (9), 399-411.

Tapken, W., Ravet, K. and Pilon, M. (2012) Plastocyanin controls the stabilization of the thylakoid Cu-transporting P-type ATPase PAA2/HMA8 in response to low copper in Arabidopsis. *Journal of Biological Chemistry,* 287 (22), 18544-18550.

Tariq, M., Sharif, M., Shah, Z. and Khan, R. (2007) Effect of foliar application of micronutrients on the yield and quality of sweet orange (Citrus Sinensis L.). *Pakistan Journal of Biological Sciences,* 10 (11), 1823-1828.

Tauris, B., Borg, S., Gregersen, P.L. and Holm, P.B. (2009) A roadmap for zinc trafficking in the developing barley grain based on laser capture microdissection and gene expression profiling. *Journal of Experimental Botany,* 60 (4), 1333-1347.

Tennstedt, P., Peisker, D., Bottcher, C., Trampczynska, A. and Clemens, S. (2009) Phytochelatin Synthesis Is Essential for the Detoxification of Excess Zinc and Contributes Significantly to the Accumulation of Zinc. *Plant Physiology,* 149 (2), 938-948.

Thomas, W.T.B., Powell, W. and Wood, W. (1984) The chromosomal location of the dwarfing gene present in the spring barley variety golden promise. *Heredity,* 53 (1), 177-183.

Thomine, S., Lelièvre, F., Debarbieux, E., Schroeder, J.I. and Barbier-Brygoo, H. (2003) AtNRAMP3, a multispecific vacuolar metal transporter involved in plant responses to iron deficiency. *The The Plant Journal,* 34 (5), 685-695.

Thomine, S., Wang, R., Ward, J.M., Crawford, N.M. and Schroeder, J.I. (2000) Cadmium and iron transport by members of a plant metal transporter family in Arabidopsis with homology to Nramp genes. *Proceedings of the National Academy of Sciences,* 97 (9), 4991-4996.

Thompson, J. and Gibson, T. (2002) Multiple sequence alignment using ClustalW and ClustalX. *Curr Protoc Bioinformatics*.

Tiong, J., Mcdonald, G., Genc, Y., Shirley, N., Langridge, P. and Huang, C.Y. (2015) Increased expression of six ZIP family genes by zinc (Zn) deficiency is associated with enhanced uptake and root-to-shoot translocation of Zn in barley (*Hordeum vulgare*). *The New Phytologist,* 207 (4), 1097-1109.

Tiong, J., Mcdonald, G.K., Genc, Y., Pedas, P., Hayes, J.E., Toubia, J., Langridge, P. and Huang, C.Y. (2014) HvZIP7 mediates zinc accumulation in barley (*Hordeum vulgare*) at moderately high zinc supply. *New Phytologist,* 201 (1), 131-143.

Tirado, R. and Allsopp, M. (2012) *Phosphorus in Agriculture, Problems and Solutions. Greenpeace Research Laboratories Technical Report Review*. Amsterdam, The Netherlands

Tottey, S., Block, M.A., Allen, M., Westergren, T., Albrieux, C., Scheller, H.V., Merchant, S. and Jensen, P.E. (2003) Arabidopsis CHL27, located in both envelope and thylakoid membranes, is required for the synthesis of protochlorophyllide. *Proceedings of the National Academy of Sciences,* 100 (26), 16119-16124.

Toyoshima, C. (2009) How Ca^{2+}-ATPase pumps ions across the sarcoplasmic reticulum membrane. *Biochimica et Biophysica Acta,* 1793 (6), 941-946.

Ueno, D., Koyama, E., Yamaji, N. and Ma, J.F. (2011) Physiological, genetic, and molecular characterization of a high-Cd accumulating rice cultivar. *Jarjan. Journal of Experimental Botany,* 62, 2265–2272.

Ueno, D., Yamaji, N., Kono, I., Huang, C.F., Ando, T., Yano, M. and Ma, J.F. (2010) Gene limiting cadmium accumulation in rice. *Proceedings of the National Academy of Sciences,* 107 (38), 16500-16505.

Uno, Y., Furihata, T., Abe, H., Yoshida, R., Shinozaki, K. and Yamaguchi-Shinozaki, K. (2000) Arabidopsis basic leucine zipper transcription factors involved in an abscisic acid-dependent signal transduction pathway under drought and high-salinity conditions. *Proceedings of the National Academy of Sciences,* 97 (21), 11632-11637.

Uraguchi, S., Mori, S., Kuramata, M., Kawasaki, A., Arao, T. and Ishikawa, S. (2009) Root-to-shoot Cd translocation via the xylem is the major process determining shoot and grain cadmium accumulation in rice. *Journal of Experimental Botany,* 60, 2677-2688.

Valdes-Lopez, O., Yang, S.S., Aparicio-Fabre, R., Graham, P.H., Reyes, J.L., Vance, C.P. and Hernandez, G. (2010) MicroRNA expression profile in common bean (*Phaseolus vulgaris*) under nutrient deficiency stresses and manganese toxicity. *The New Phytologist,* 187 (3), 805-818.

Van De Mortel, J.E., Almar Villanueva, L., Schat, H., Kwekkeboom, J., Coughlan, S., Moerland, P.D., Ver Loren Van Themaat, E., Koornneef, M. and Aarts, M.G. (2006) Large expression differences in genes for iron and zinc homeostasis, stress response, and lignin biosynthesis distinguish roots of *Arabidopsis thaliana* and the related metal hyperaccumulator *Thlaspi caerulescens*. *Plant Physiology,* 142 (3), 1127-1147.

Van Der Zaal, B.J., Neuteboom, L.W., Pinas, J.E., Chardonnens, A.N., Schat, H., Verkleij, J.A. and Hooykaas, P.J. (1999) Overexpression of a novel Arabidopsis gene related to putative zinc-

transporter genes from animals can lead to enhanced zinc resistance and accumulation. *Plant Physiology,* 119 (3), 1047-1055.

Vazquez, F., Legrand, S. and Windels, D. (2010) The biosynthetic pathways and biological scopes of plant small RNAs. *Trends in Plant Sciences,* 15 (6), 337-345.

Verret, F., Gravot, A., Auroy, P., Leonhardt, N. and David, P. (2004) Overexpression of AtHMA4 enhances root-to-shoot translocation of zinc and cadmium and plant metal tolerance. *FEBS Letter,* 576, 306–312.

Verret, F., Gravot, A., Auroy, P., Preveral, S., Forestier, C., Vavasseur, A. and Richaud, P. (2005) Heavy metal transport by AtHMA4 involves the N-terminal degenerated metal binding domain and the C-terminal His11 stretch. *FEBS Letter,* 579 (6), 1515-1522.

Verrier, P.J., Bird, D., Burla, B., Dassa, E., Forestier, C., Geisler, M., Klein, M., Kolukisaoglu, Ü., Lee, Y. and Martinoia, E. (2008) Plant ABC proteins–a unified nomenclature and updated inventory. *Trends in Plant Science,* 13 (4), 151-159.

Vert, G., Barberon, M., Zelazny, E., Seguela, M., Briat, J.F. and Curie, C. (2009) Arabidopsis IRT2 cooperates with the high-affinity iron uptake system to maintain iron homeostasis in root epidermal cells. *Planta,* 229 (6), 1171-1179.

Vert, G., Briat, J.F. and Curie, C. (2001) Arabidopsis IRT2 gene encodes a root-periphery iron transporter. *The Plant Journal,* 26 (2), 181-189.

Vert, G., Grotz, N., Dedaldechamp, F., Gaymard, F., Guerinot, M.L., Briat, J.F. and Curie, C. (2002) IRT1, an Arabidopsis transporter essential for iron uptake from the soil and for plant growth. *Plant Cell,* 14 (6), 1223-1233.

Vollenweider, P., Cosio, C., Günthardt-Goerg, M.S. and Keller, C. (2006) Localization and effects of cadmium in leaves of a cadmium-tolerant willow (*Salix viminalis* L.): Part II Microlocalization and cellular effects of cadmium. *Environmental and Experimental Botany,* 58 (1–3), 25-40.

Wang, H., Liu, R.L. and Jin, J.Y. (2009) Effects of zinc and soil moisture on photosynthetic rate and chlorophyll fluorescence parameters of maize. *Biologia Plantarum,* 53 (1), 191-194.

Wang, Y., Itaya, A., Zhong, X., Wu, Y., Zhang, J., Van Der Knaap, E., Olmstead, R., Qi, Y. and Ding, B. (2011) Function and evolution of a MicroRNA that regulates a Ca2+-ATPase and triggers the formation of phased small interfering RNAs in tomato reproductive growth. *Plant Cell,* 23 (9), 3185-3203.

Waters, B.M., Mcinturf, S.A. and Stein, R.J. (2012) Rosette iron deficiency transcript and microRNA profiling reveals links between copper and iron homeostasis in *Arabidopsis thaliana*. *Journal of Experimental Botany,* 63 (16), 5903-5918.

Weast, R.C., Astle, M.J. and Beyer, W.H. (1988) *CRC handbook of chemistry and physics*. CRC press Boca Raton, FL.

Weisany, W., Sohrabi, Y., Heidari, G., Siosemardeh, A. and Ghassemi-Golezani, K. (2012) Changes in antioxidant enzymes activity and plant performance by salinity stress and zinc application in soybean (*Glycine max* L.). *Plant Omics,* 5 (2), 60-67.

Weisshaar, B., Armstrong, G.A., Block, A., Da Costa E Silva, O. and Hahlbrock, K. (1991) Light-inducible and constitutively expressed DNA-binding proteins recognizing a plant promoter element with functional relevance in light responsiveness. *EMBO Journal,* 10 (7), 1777-1786.

Weltmeier, F., Ehlert, A., Mayer, C.S., Dietrich, K., Wang, X., Schütze, K., Alonso, R., Harter, K., Vicente-Carbajosa, J. and Dröge-Laser, W. (2006) Combinatorial control of Arabidopsis proline dehydrogenase transcription by specific heterodimerisation of bZIP transcription factors. *The EMBO Journal,* 25 (13), 3133-3143.

Wessells, K.R. and Brown, K.H. (2012) Estimating the Global Prevalence of Zinc Deficiency: Results Based on Zinc Availability in National Food Supplies and the Prevalence of Stunting. *PLoS ONE,* 7 (11), e50568.

Westin, G. and Schaffner, W. (1988) A zinc-responsive factor interacts with a metal-regulated enhancer element (MRE) of the mouse metallothionein-I gene. *The EMBO journal,* 7 (12), 3763.

White, P.J. and Broadley, M.R. (2009) Biofortification of crops with seven mineral elements often lacking in human diets--iron, zinc, copper, calcium, magnesium, selenium and iodine. *The New Phytologist,* 182 (1), 49-84.

Who (2002) WHO (2002). *The world health report*, 81-92.

Wigge, P.A., Kim, M.C., Jaeger, K.E., Busch, W., Schmid, M., Lohmann, J.U. and Weigel, D. (2005) Integration of spatial and temporal information during floral induction in Arabidopsis. *Science,* 309 (5737), 1056-1059.

Williams, L.E. and Mills, R.F. (2005) P_{1B}-ATPases - an ancient family of transition metal pumps with diverse functions in plants. *Trends in Plant Science,* 10, 491–502.

Williams, L.E. and Pittman, J.K. (2010) Dissecting Pathways Involved in Manganese Homeostasis and Stress in Higher Plant Cells IN: Hell, R. and Mendel, R.R. (eds.) *Cell Biology of Metals and Nutrients*. Berlin: Springer-Verlag Berlin, 95-117.

Wintz, H., Fox, T., Wu, Y.Y., Feng, V., Chen, W., Chang, H.S., Zhu, T. and Vulpe, C. (2003) Expression profiles of *Arabidopsis thaliana* in mineral deficiencies reveal novel transporters involved in metal homeostasis. *Journal of Biological Chemistry,* 278 (48), 47644-47653.

Wong, C.K. and Cobbett, C.S. (2009) HMA P-type ATPases are the major mechanism for root-to-shoot Cd translocation in *Arabidopsis thaliana*. *The New Phytologist,* 181, 71–78.

Wong, C.K., Jarvis, R.S., Sherson, S. and Cobbett, C.S. (2009) Functional analysis of the heavy metal binding domains of the Zn/Cd-transporting ATPase, HMA2, in *Arabidopsis thaliana*. *The New Phytologist,* 181, 79-88.

Wu, C.-Y., Bird, A.J., Chung, L.M., Newton, M.A., Winge, D.R. and Eide, D.J. (2008) Differential control of Zap1-regulated genes in response to zinc deficiency in *Saccharomyces cerevisiae*. *Bmc Genomics,* 9 (1), 1.

Wu, D., Sato, K. and Ma, J.F. (2015a) Genome-wide association mapping of cadmium accumulation in different organs of barley. *The New Phytologist,* 208 (3), 817-829.

Wu, T., Kamiya, T., Yumoto, H., Sotta, N., Katsushi, Y., Shigenobu, S., Matsubayashi, Y. and Fujiwara, T. (2015b) An *Arabidopsis thaliana* copper-sensitive mutant suggests a role of phytosulfokine in ethylene production. *Journal of Experimental Botany*, erv105.

Xiang, C., Miao, Z. and Lam, E. (1997) DNA-binding properties, genomic organization and expression pattern of TGA6, a new member of the TGA family of bZIP transcription factors in *Arabidopsis thaliana*. *Plant Molecular Biology,* 34 (3), 403-415.

Xiang, S., Feng, S., Zhang, Y., Tan, J., Liang, S. and Chai, T. (2015) The N-terminal degenerated metal-binding domain is involved in the heavy metal transport activity of TaHMA2. *Plant cell Reports,* 34 (9), 1615-1628.

Xie, F., Jones, D.C., Wang, Q., Sun, R. and Zhang, B. (2015) Small RNA sequencing identifies miRNA roles in ovule and fibre development. *Plant Biotechnol Journal,* 13 (3), 355-369.

Xiong, J., Lu, H., Lu, K.X., Duan, Y.X., An, L.Y. and Zhu, C. (2009) Cadmium decreases crown root number by decreasing endogenous nitric oxide, which is indispensable for crown root primordia initiation in rice seedlings. *Planta,* 230 (4), 599-610.

Yamaji, N., Xia, J., Mitani-Ueno, N., Yokosho, K. and Ma, J.F. (2013) Preferential delivery of Zn to developing tissues in rice is mediated by a P-type ATPases, OsHMA2. *Plant Physiology*, 113.216564v216561-216113.216564.

Yamasaki, H., Hayashi, M., Fukazawa, M., Kobayashi, Y. and Shikanai, T. (2009) SQUAMOSA promoter binding protein–like7 is a central regulator for copper homeostasis in Arabidopsis. *The Plant Cell,* 21 (1), 347-361.

Yan, J., Wang, P., Wang, P., Yang, M., Lian, X., Tang, Z., Huang, C.F., Salt, D.E. and Zhao, F.J. (2016) A loss-of-function allele of OsHMA3 associated with high cadmium accumulation in shoots and grain of Japonica rice cultivars. *Plant Cell and Environment,* 39 (9), 1941-1954.

Yang, C., Li, D., Mao, D., Liu, X., Ji, C., Li, X., Zhao, X., Cheng, Z., Chen, C. and Zhu, L. (2013) Overexpression of microRNA319 impacts leaf morphogenesis and leads to enhanced cold tolerance in rice (*Oryza sativa* L.). *Plant Cell and Environment,* 36 (12), 2207-2218.

Yang, O., Popova, O.V., Suthoff, U., Luking, I., Dietz, K.J. and Golldack, D. (2009a) The Arabidopsis basic leucine zipper transcription factor AtbZIP24 regulates complex transcriptional networks involved in abiotic stress resistance. *Gene,* 436 (1-2), 45-55.

Yang, Y., Chen, R., Fu, G., Xiong, J. and Tao, L. (2015) Phosphate deprivation decreases cadmium (Cd) uptake but enhances sensitivity to Cd by increasing iron (Fe) uptake and inhibiting phytochelatins synthesis in rice (*Oryza sativa*). *Acta Physiologiae Plantarum,* 38 (1), 1-13.

Yang, Z., Wu, Y., Li, Y., Ling, H.Q. and Chu, C. (2009b) OsMT1a, a type 1 metallothionein, plays the pivotal role in zinc homeostasis and drought tolerance in rice. *Plant Molecular Biology,* 70 (1-2), 219-229.

Yeh, C.M., Chien, P.S. and Huang, H.J. (2007) Distinct signalling pathways for induction of MAP kinase activities by cadmium and copper in rice roots. *Journal of Experimental Botany,* 58 (3), 659-671.

Yesilirmak, F. and Sayers, Z. (2009) Heterelogous Expression of Plant Genes. *International Journal of Plant Genomics,* 2009.

Yi, J. and An, G. (2013) Utilization of T-DNA tagging lines in rice. *Journal of Plant Biology,* 56 (2), 85-90.

Yin, Y., Zhu, Q., Dai, S., Lamb, C. and Beachy, R.N. (1997) RF2a, a bZIP transcriptional activator of the phloem-specific rice tungro bacilliform virus promoter, functions in vascular development. *EMBO Journal,* 16 (17), 5247-5259.

Yruela, I. (2013) Transition metals in plant photosynthesis. *Metallomics,* 5 (9), 1090-1109.

Yuan, L., Yang, S., Liu, B., Zhang, M. and Wu, K. (2012) Molecular characterization of a rice metal tolerance protein, OsMTP1. *Plant Cell Reports,* 31 (1), 67-79.

Zeng, X., Long, H., Wang, Z., Zhao, S., Tang, Y., Huang, Z., Wang, Y., Xu, Q., Mao, L., Deng, G., Yao, X., Li, X., Bai, L., Yuan, H., Pan, Z., Liu, R., Chen, X., Wangmu, Q., Chen, M., Yu, L., Liang, J., Dunzhu, D., Zheng, Y., Yu, S., Luobu, Z., Guang, X., Li, J., Deng, C., Hu, W., Chen, C., Taba, X., Gao, L., Lv, X., Abu, Y.B., Fang, X., Nevo, E., Yu, M., Wang, J. and Tashi, N. (2015) The draft genome of Tibetan hulless barley reveals adaptive patterns to the high stressful Tibetan Plateau. *Proceedings of the National Academy of Sciences,* 112 (4), 1095-1100.

Zhang, B. (2015) MicroRNA: a new target for improving plant tolerance to abiotic stress. *Journal of Experimental Botany,* 66 (7), 1749-1761.

Zhang, H., Liu, Y., Wen, F., Yao, D., Wang, L., Guo, J., Ni, L., Zhang, A., Tan, M. and Jiang, M. (2014) A novel rice C2H2-type zinc finger protein, ZFP36, is a key player involved in abscisic acid-induced antioxidant defence and oxidative stress tolerance in rice. *Journal of experimental botany*, eru313.

Zhang, J.L. and Shi, H. (2013) Physiological and molecular mechanisms of plant salt tolerance. *Photosynthesis Research,* 115 (1), 1-22.

Zhang, M., Zhang, J., Lu, L., Zhu, Z. and Yang, X. (2016) Functional analysis of CAX2-like transporters isolated from two ecotypes of *Sedum alfredii*. *Biologia Plantarum,* 60 (1), 37-47.

Zhao, F.J., Su, Y.H., Dunham, S.J., Rakszegi, M., Bedo, Z., Mcgrath, S.P. and Shewry, P.R. (2009) Variation in mineral micronutrient concentrations in grain of wheat lines of diverse origin. *Journal of Cereal Science,* 49 (2), 290-295.

Zhao, H. and Eide, D. (1996a) The yeast ZRT1 gene encodes the zinc transporter protein of a high-affinity uptake system induced by zinc limitation. *Proceedings of the National Academy of Sciences,* 93 (6), 2454-2458.

Zhao, H. and Eide, D. (1996b) The ZRT2 gene encodes the low affinity zinc transporter in *Saccharomyces cerevisiae*. *Journal of Biological Chemistry,* 271 (38), 23203-23210.

Zhao, H. and Eide, D.J. (1997) Zap1p, a metalloregulatory protein involved in zinc-responsive transcriptional regulation in *Saccharomyces cerevisiae*. *Molecular and Cellular Biology,* 17 (9), 5044-5052.

Zheng, L., Fujii, M., Yamaji, N., Sasaki, A., Yamane, M., Sakurai, I., Sato, K. and Ma, J.F. (2011) Isolation and Characterization of a Barley Yellow Stripe-Like Gene, HvYSL5. *Plant and Cell Physiology,* 52 (5), 765-774.

Zielazinski, E.L., Cutsail, G.E., 3rd, Hoffman, B.M., Stemmler, T.L. and Rosenzweig, A.C. (2012) Characterization of a cobalt-specific P(1B)-ATPase. *Biochemistry,* 51 (40), 7891-7900.

Zielazinski, E.L., Gonzalez-Guerrero, M., Subramanian, P., Stemmler, T.L., Arguello, J.M. and Rosenzweig, A.C. (2013) *Sinorhizobium meliloti* Nia is a P(1B-5)-ATPase expressed in the nodule during plant symbiosis and is involved in Ni and Fe transport. *Metallomics,* 5 (12), 1614-1623.

Zorrig, W., Abdelly, C. and Berthomieu, P. (2011) The phylogenetic tree gathering the plant Zn/Cd/Pb/Co P1B-ATPases appears to be structured according to the botanical families. *Comptes Rendus Biologies,* 334 (12), 863-871.

Zuckerkandl, E. and Pauling, L. (1965) Evolutionary Divergence and Convergence in Proteins *Evolving Genes and Proteins*. Academic Press, 97-166.

Appendix 1

Accession numbers for sequences used in the phylogenetic analysis.

Wheat F group sequences (Li et al., 2015); Rice and Brachypodium (Liu and Chu, 2015); Arabidopsis (Assuncao et al., 2010); Cucumber (Baloglu et al., 2015). The barley sequences used in the phylogenetic tree are mainly those cloned from Golden Promise in this study; the accession numbers given above are for sequences from Morex and Haruna Nijo.

Species	Nomenclature	Accession No.
Wheat	TabZIP4	Traes_1AL_00A8A2030.2
	TabZIP33	Traes_5AS_6F02C9967.1
	TabZIP55	Traes_7AL_A8CAE984E.1
	TabZIP56	Traes_7AL_C7CF7087B.2
	TabZIP62	Traes_1BL_1A885E733.1
	TabZIP79	Traes_3B_34C2CD876.2
	TabZIP97	Traes_5BS_FC54F9BEA.1
	TabZIP120	Traes_7BL_096916DC5.1
	TabZIP150	Traes_5DS_4F7973584.1
	TabZIP179	Traes_7DL_70D4FDB2A.1
	TabZIP180	Traes_7DL_7DDA16622.3
Rice	OsbZIP7	LOC_Os01g58760
	OsbZIP44	LOC_Os05g41540
	OsbZIP53	LOC_Os06g50310
Arabidopsis	AtbZIP19	At4G35040
	AtbZIP23	At2G16770.1
	AtbZIP24	At3G51960
Brachypodium	BdbZIP11	Bradi1g30140.1
	BdbZIP32	Bradi2g21197
	BdbZIP33	Bradi2g21200
	BdbZIP44	Bradi2g52590
Cucumber	CsbZIP59	XP_004147043
	CsbZIP60	XP_004144846
Barley	HvbZIP1	MLOC_2245.1
	HvbZIP10	MLOC_12585.1
	HvbZIP55	MLOC_5655
	HvbZIP56	MLOC_53694.1
	HvbZIP57	MLOC_13410
	HvbZIP58	BAJ85954.1
	HvbZIP61*	BAJ92973.1
	HvbZIP62	MLOC_60894.1

* HvbZIP61 may have been incorrectly annotated as a barley sequence (see main text)

Appendix 2

Coding sequence of barley (Golden Promise) F-group bZIPs based on sequencing results

>HvbZIP1a

ATGGACGACGGGCACCTCGACTGCTCCTCCATCGGCAGCTACTTCGACGACATCCTCATGGACACGGAGCA
GCAGCTTGCGTGCTGTACTCACACCCACACCTGCAACCCGCCCGACCACCACCTCCACCACACCCACACCTG
CCTCCACGTCCACTCCAACTTCACCGCCTCCGCCTCCTCCGACGCCGGCGCCGGCGCCGAGACCCCGGCCG
AGTTCGAGGACGCCCACAACACCTTCAGGAGCAAGAGACGCCGTCCCTCGGGTAATCAGGCGGCCGTGCG
CAAGTACCGGGAGAAGAAGAAGGCGCACACCGTGCTGCTGGAGGAGGAGGCGGCCCGTCTCAGGGCTAT
GAACGAGGAGCTCGGCAAGAAGGTCCAGGATCACGCCGCGCTCGAGGCCGAGGCGGCTAGGCTCCGCTG
CCTGCTCGTCGACGTCAGGGGGAGGATCGAAGGGGAGATCGGCGCCTTCCCTTACCACCGGCGGCCCGCC
AAGGGCGCCGGTCAGGGCGGTGCCCAGATTATGAGTTCATGTGATTTCATAGGAACCTGTGAACAACCTC
ATACGTGTTTTCATTAG

>HvbZIP1b

ATGCTCTCTATGCCCCACCGGCTCTTTTTTCCTATGAAAAAAAGTTGTACCAATATAGATGAAAGAATTTCCC
ATCATGTCGACATCTTGTGCAAAAGTAAAGCAAAACAAAAAAATTTGCAACAGCAAGCAGCACGTGGGCA
CGGCTTAATTAAGCGTCCTCCTGTCTGTCTGCTGCTAATCGCGGCCATGGACGACGGGCACCTCGACTGCTC
CTCCATCGGCAGCTACTTCGACGACATCCTCATGGACACGGAGCAGCAGCTTGCGTGCTGTACTCACACCC
ACACCTGCAACCCGCCCGACCACCACCTCCACCACACCCACACCTGCCTCCACGTCCACTCCAACTTCACCGC
CTCCGCCTCCTCCGACGCCGGCGCCGGCGCCGAGACCCCGGCCGAGTTCGAGGACGCCCACAACACCTTCA
GGAGCAAGAGACGCCGTCCCTCGGGTAATCAGGCGGCCGTGCGCAAGTACCGGGAGAAGAAGAAGGCG
CACACCGTGCTGCTGGAGGAGGAGGCGGCCCGTCTCAGGGCTATGAACGAGGAGCTCGGCAAGAAGGTC
CAGGATCACGCCGCGCTCGAGGCCGAGGCGGCTAGGCTCCGCTGCCTGCTCGTCGACGTCAGGGGGAGG
ATCGAAGGGGAGATCGGCGCCTTCCCTTACCACCGGCGGCCCGCCAAGGGCGCCGGTCAGGGCGGTGCC
CAGATTATGAGTTCATGTGATTTCATAGGAACCTGTGAACAACCTCATACGTGTTTTCATTAG

>HvbZIP10

ATGGACGACAACGGGGACATAGATTTCACCAATCCGGAGACGTACCTGTGCCCAGCCATGGGCGGCGATC
CCCACGACAGTTGCTCCATGTCAATGGACAGCTACTTCGACGACATCCTGAAAGACCCGGAGCACCTCGCA
TGTACTCGGATCCTGCTGGCGGAGTCGGATGATGTCGCCGAGACCTCTGAGTCGCCGCAAGAGGACGGAC
CCAAGAAGAAGCGCCCGCCCGGTAACCGGGCAGCCGTGAGGAGGTACCGTGAGAAGAAGAAGGCCCACA
CGACGCTGCTGGAGGAAGAGGTGGCTCGCCTCAAGGCTCTAAACAAGCAGCTCGTGAGGAGGCTTCAGA
GTCAGTCGTCCCTCGAGGCTGAGGCCTCGAGGCTCCGCTGCCTGCTTGTCGACATTAGAGGGAGGATCGA
AGGGGAGCTCGGTGCTTTCCCTTACCAACGGCCAGTGAAGAACAAGGATTTGGCTGACCAGGGAAGTTCC
CTAGGTATAGGTGGTGCCCAGAAGGTTAGGCTCAGATGCAACAATCCGGTTTACTGCAGTCCAGAGATGC
CGGCCACGACAATGGATGACGATGGTGTTATCAGTGGCGAACTGTTGGGTCAAGGTGCAAATGACAAGTG
GCTCCCAGGTTTGCCAGATGATGTAAAGAGGTGA

>HvbZIP55

ATGGACGACGGACTATACCTTCCGATCCCCAGCCACCTTCTGTTTCCATATCCAGAGATCTCCCACGGCTTC
GATGAGTTCCTAGCGTGCACTCACACACACAGCTGTCCATCGTGGTCGTCGCCGGCCGCGGCGCACACCCA
CACGTGCCTGCATGCGCACACCCAAGTCGTAGCTTCCGGCGAAGACTACGCCGTGGAGCAAGACGAGCTG
AGGAACCCCCGGAAGCCTCTGGGGAACCGGGAGGCCGTGCGCAAGTACCGGCAGAAGAAGAAAGCCCAC
GCAGCCTTCCTCGAGGAGGAGGTCAAGAAGCTCCGCGCCGCCAACCAGCAGCTCCTGAGGCGGCTGCAGG
GCCATGCGGCGCTGGAGGCCGAGGTTGCGAGGCTGACGAGCCTCCTGCTCGACGTCCGAGGCAAGATCG
ACGAGGCCGAGATCGGTGCCCTGCCGTTCGATGAGCGGTGCAGCTTCGGCTCTGTCGTCTGTACTGCTGCA

GAACTCACGCCATGCTTTGACGCTAGCGGTGCTGAGGTAGCAGCGGTCCGGGAGGCTGGCGATGTCGATG
ACGGCGGCATCGTCTCCGGAGAACTCGGTGTTCCTGAAGTGGTGGATGCTGTTGCCAGCTTCGTGAACTCT
GTTGCCTAA

>HvbZIP56

ATGGACGACGGGGACATCGACTTCTCCAACCCGGAGACGTACCTGTGCGAGGCCATGGGCAACGACCCGC
CCGCCAGCTGCTCCATGGGGAGCTACTTCGACGACATCCTCAACAGCGACGCCGACCACCTCGCCTGCACC
CACACCCACACCTGCAACCCGCCCGTCCACGACCTCGCGCACCACACCCATACCTGCGTCCACGTCCACACC
AAGATCCTCTCCGCCTCCGATGACGCCGCCGAGACCTCCGAGTCCCTGCCGGACGCCAAGAAGCAGCGGC
CCTCGGGCAACCGCGCCGCCGTCAGGAAGTACCGCGAGAAGAAGAAGGCCCACACCGCGCTGCTCGAGG
AGGAGGTGGCTCACCTCAAGGCTGTTAATCAGCAGCTCGTGAAGAAGCTCCAGAGCCACTCCGCGCTCGA
GGCCGAGGTGGCCAGGCTCCGCTGCCTGCTTGTTGACATCAGAGGGAGGATCGAAGGGGAGATTGGCAC
TTTCCCTTACCAGCGGTCGGTGAAAAGCAATGAGTTTGTCGACCAGGGGAGCTTTCTTGGTGGTGCGCAGG
TTATGAATTCCTGCGACTTCAGATGCAACGATCAGTTGTACTGCAATCCAGGAATGCAGCAGGCCAGGACA
ATGGACGACGATGGTGTTATGAGTGCTGGACAGGTTTTGGGGCAAGGTGCCGGTGACACTATGGGTTGTG
TAAAACCAGGTTCTTTAAACCCCCCAGGCTGCCGTGGGGGCCAAATGCTGTAA

>HvbZIP57

ATGGACGACGGGGTGGACCTCCCGAGCCAATTCCTCTTCTCCCACCCGGAGATGCCCGGCGCCTTCGACGA
CCTCCTGGCCGACGCCGCCGCGACCTGCACCCACACGCACACCTGCAACCCTCCCGGCCCGTCGGCCGCCA
TGCACACGCACACCTGCCTCCACACGCACACCCACCAGCTCTTCGCCGCCGGCAGCGAGGACGACGACGCG
GCGCGGCCCCGGCGCCCGCTGGGCAACCGGGAGGCCGTGCGCAAGTACCGGGAGAAGAAGAAGGCCCA
CGCCGCGTTCCTGGAGGAGGAGGTCAAGAAGCTGCGCGCCGCCAACCAGCAGCTGCTGCGGAGGCTGCA
GGGCCACGCCACGCTCGAGGCCGAGGTAGCGCGGCTGAGGGGCCTCCTCTCCGACGTCCGGGCCAAGAT
CGACGCGGAGGTCGCCGCCGGCGGTTTCCCGTTCCAGAAGCAGTGCAGCGTCGGCTCCGTGGCGTGCACC
GACCCGACCCTCTGCTTCAACAATGGCAACTCTGAGGTCGGTGGCGCCTGCTGGGGGGACAGCTCTGGGC
CGGCGTCTGCGGATTGCGGGCTCGATGAAGATGCCAATGGCGCCGCTGCGCGGGAGGTCGATGCGCCGG
GACGACCGGTGCGTGCCATGGATGTTGTTGAGCTCTGCTTCCCTAGCTGA

>HvbZIP58

ATGGACGACGGGGACCTGGACTTCTCCTCCATGGGCAGCTACTTCGACTTGGACGTCCTCGGCGACACGGC
GGAGCACCTCGCTCGCTGCACCCACACCCACACCTGCAACCCGCCCGCCCACCACCACCACCCCCACACCCA
CACCTGCCTCCACGTCCACTCCAAGTTCCCCGCCCCCGCCTCCCCCGACGCCGGCGCAGAGACCCCGGCCG
AGTTCGAGGACGCCCACGCCACCTCCAGGACCAATAGGCGCCGCCCGTCGGGCAACCGGGCGGCCGTGCG
CAAGTACCGGGAGAAGAAGAAGGAGCACACGGCGGTGCTGCAGGAGGAGGCGGCCCGCCTCAGGGCTC
TCAACGACCAGCTGGTGAGGAAGGTCCAGGACCACGCCGCGCTTGAGGCCGAGGCGGCCAGGCTCCGCT
GCCTGCTCGTCGACGTCAGGGGCAGGATCGAAGGGGAGATCGGCGCCTTCCCTTACCAGCGCCGGCAGGC
CAAGGGCGACGGCCCGGGCTCCGCTGCTGCTGGTGCTGGTGCTGCCGGCCCGGTCATGATGAGCTCATGT
GGTTTCGTACGAACCTGTGAACAGCCTCCTGTCTGTTTTCGTTAG

>HvbZIP62

ATGGATGACGGGGACCTCGACTTCTCCAACCCGGAGGCGTACCTGGACGCTGCCGGCGGCGGATGCTCCA
TGGACAGCTACTTCGACGGAATCCTCAACGACACGGAGCACCTCGCGTGCACCCACACCCACACCTGCAAC
CCGCCCGTCGACGACAGCTCGCACACCCACACCTGCGTCCACGTCCACACCAAGATCGTCTCGGCGTCCTCC
GACGACTCCCCGGCCGGCAACGGCGCCTCCAAGAAGCGGCCGTCTGGCAACCGGGCGGCCGTGAGGAAG
TACCGGGAGAAGAAGAAGGCCCACACCGCGCTGCTGGAGGAAGAGGTGGTCCGGCTGAAGGCTCTCAAC
AAGCAGCTGCTGAAGAAGCTCCAGAGCCACGCCGCGCTCGAGGCCGAGGCCGCCAGGCTCCGCTGCCTGC
TCGTCGATGTCAGGGGGAGGATCGAAGGGGAGATCGGCGCTTTCCCTTACCAGCGGCCTGCCAAGAACGT
CGATTTGGTTTCTTCTGGTGTTGATCAGGGGGGGTTTCTTGGCAGCGCCCAGGTTACTATTAACTCGTGTGA
TTTCAGATGCAACGATCAGATGTACTGCAATCCAGGGATGCAGATGAGAGCAATGGGCGATGATGGTGCT
ATGAGTGGCCAGATGTTTGGGCAAGGCGCCGGGGATGTTGCAAACATCCAATGCATTGGGAGTGCGAAAT

CTGGGCTCACGATGCCCCCAGGCTGTGGGGGTATGGGGACAATGCCTTCTGGCTGTTTACCCAGTTCCGAA
AAGCAGTGA

Appendix 3

Accession numbers for P_{1B}-ATPAses protein sequences used in the phylogenetic analysis.

A. thaliana, *H. vulgare*, *B. distachyon*, *S. bicolar*, *O. sativa*, and *Z. mays* P_{1B}-ATPAses sequences (Mills et al., 2012); *A. halleri, A. lyrata, B. rapa, E. parvulum, N. caerulescens, O. glaberrima, C. papaya, C. sativus, F. vesca, G. max, J. curcas, M. truncatula, N. tabacum, P. persica, P. trichocarpa, S. tuberosum, S. lycopersicum*, and *V. vinifera* (Zorrig et al., 2011).

Species	Family	Gene name	Status of the sequence	Accession numbers
A. thaliana	Brassicaceae	AtHMA1	Complete	NP_195444
A. thaliana	Brassicaceae	AtHMA2	Complete	AAR10767.1
A. thaliana	Brassicaceae	AtHMA3	Complete	AAL16382.1
A. thaliana	Brassicaceae	AtHMA4	Complete	AAL84162.1
A. thaliana	Brassicaceae	AtHMA5	Complete	NP_176533.1
A. thaliana	Brassicaceae	AtHMA6	Complete	NP_974675.1
A. thaliana	Brassicaceae	AtHMA7	Complete	NP_199292.1
A. thaliana	Brassicaceae	AtHMA8	Complete	NP_001190357.1
A. halleri	Brassicaceae	AhHMA3	Complete	CAD89012.1
A. halleri	Brassicaceae	AhHMA4-1	Complete	ACC68159.1
A. halleri	Brassicaceae	AhHMA4-2	Complete	ACC68152.1
A. halleri	Brassicaceae	AhHMA4-3	Complete	ACC68153.1
A. lyrata	Brassicaceae	AlHMA2	Complete	XP_002867367.1
A. lyrata	Brassicaceae	AlHMA3	Complete	XP_002867366.1
A. lyrata	Brassicaceae	AlHMA4-1	Complete	ADBK01000666
A. lyrata	Brassicaceae	AlHMA4-2	Complete	ADBK01000159
B. rapa	Brassicaceae	BrHMA2	Complete	AC240993
B. rapa	Brassicaceae	BrHMA3-1	Complete	FP017269
B. rapa	Brassicaceae	BrHMA3-2	Complete	AC241039
B. rapa	Brassicaceae	BrHMA4-1	Complete	AC232536
B. rapa	Brassicaceae	BrHMA4-2	Complete	FP102280
E. parvulum	Brassicaceae	EpHMA2	Complete	AFAN01000039
E. parvulum	Brassicaceae	EpHMA3	Complete	AFAN01000039
E. parvulum	Brassicaceae	EpHMA4	Complete	AFAN01000014
N. caerulescens	Brassicaceae	NcHMA4	Complete	CAD98808.1
C. papaya	Caricaceae	CpHMA-A	Complete	ABIM01002425
C. sativus	Cucurbitaceae	CsHMA-A	Complete	ACHR01010422
C. sativus	Cucurbitaceae	CsHMA-B	Complete	ACHR01010422
F. vesca	Rosaceae	FvHMA-A	Complete	AEMH01014081
F. vesca	Rosaceae	FvHMA-B	Complete	AEMH01012163
G. max	Fabaceae	GmHMA-A	Complete	ACUP01005112
G. max	Fabaceae	GmHMA-B	Complete	ACUP01007321
G. max	Fabaceae	GmHMA-C	Complete	ACUP01009759
J. curcas	Euphorbiaceae	JcHMA-A	Partial	BABX01026037
M. truncatula	Fabaceae	MtHMA-A	Complete	AC130275
M. truncatula	Fabaceae	MtHMA-B	Complete	AC135313
N. tabacum	Nicotianeae	NtHMA-A	Complete	HB441191
N. tabacum	Nicotianeae	NtHMA-B	Complete	HB441235

P. persica	Rosaceae	PpHMA-A	Complete	AEKW01008176
P. trichocarpa	Salicaceae	PtHMA-A	Complete	AARH01002993
S. tuberosum	Solanaceae	StHMA-A	Complete	AEWC01030938
S. lycopersicum	Solanaceae	SlHMA-A	Complete	AEKE02004109
V. vinifera	Vitaceae	VvHMA-A	Complete	AM454465
O. glaberrima	Poaceaae	OgHMA2	Complete	ADWL01012616
O. glaberrima	Poaceaae	OgHMA3	Complete	ADWL01013846
O. sativa	Poaceaae	OsHMA1	Complete	XP_015643713.1
O. sativa	Poaceaae	OsHMA2	Complete	ADU53143.1
O. sativa	Poaceaae	OsHMA3	Complete	BAJ25745
O. sativa	Poaceaae	OsHMA4	Complete	XP_015626172.1
O. sativa	Poaceaae	OsHMA5	Complete	XP_015635938.1
O. sativa	Poaceaae	OsHMA6	Complete	XP_015626913.1
O. sativa	Poaceaae	OsHMA7	Complete	XP_015650064.1
O. sativa	Poaceaae	OsHMA8	Complete	EEE58431.1
O. sativa	Poaceaae	OsHMA9	Complete	XP_015643579.1
H. vulgare	Poaceaae	HvHMA1	Complete	BAK06002
H. vulgare	Poaceaae	HvHMA2	Complete	ADG56570.1
H. vulgare	Poaceaae	HvHMA3	Complete	BAK00726
H. vulgare	Poaceaae	HvHMA2/3	Complete	MLOC_52795.2
H. vulgare	Poaceaae	HvHMA4	Complete	BAJ93769
H. vulgare	Poaceaae	HvHMA5	Partial	BAJ93251
H. vulgare	Poaceaae	HvHMA6	Complete	BAK07450
H. vulgare	Poaceaae	HvHMA7	Complete	BAJ87066
H. vulgare	Poaceaae	HvHMA8	Complete	MLOC_58244.3
H. vulgare	Poaceaae	HvHMA9	Complete	BAJ96159
B. distachyon	Poaceaae	BdHMA1	Complete	XP_003560477.1
B. distachyon	Poaceaae	BdHMA2	Complete	XP_003563507.1
B. distachyon	Poaceaae	BdHMA3	Complete	XP_003561282.1
B. distachyon	Poaceaae	BdHMA4	Complete	XP_003571259.1
B. distachyon	Poaceaae	BdHMA5	Complete	XP_003580298.1
B. distachyon	Poaceaae	BdHMA6	Complete	XP_003570214.1
B. distachyon	Poaceaae	BdHMA7	Complete	XP_003574670.3
B. distachyon	Poaceaae	BdHMA8	Complete	XR_137884
B. distachyon	Poaceaae	BdHMA9	Complete	XP_003563343.1
S. bicolor	Poaceaae	SbHMA2	Complete	XP_002438953.1
S. bicolor	Poaceaae	SbHMA3-1	Complete	XP_002459578.1
S. bicolor	Poaceaae	SbHMA3-2	Complete	XP_002459579.1
T. aestivum	Poaceaae	TaHMA2 7AL	Complete	scaffold_556712
T. aestivum	Poaceaae	TaHMA2 7BL	Complete	scaffold_579416
T. aestivum	Poaceaae	TaHMA2 7DL	Complete	scaffold_602651
T. aestivum	Poaceaae	TaHMA3 5AL	Complete	scaffold_375473
T. aestivum	Poaceaae	TaHMA3 5BL	Complete	scaffold_404346
T. aestivum	Poaceaae	TaHMA3 5DL	Complete	scaffold_435190
T. aestivum	Poaceaae	TaHMA2/3 7AL	Partial	scaffold_557470
T. aestivum	Poaceaae	TaHMA2/3 7BL	Partial	scaffold_577252
T. aestivum	Poaceaae	TaHMA2/3 7DL	Partial	scaffold_603863
Z. mays	Poaceaae	ZmHMA2	Complete	AC192236
Z. mays	Poaceaae	ZmHMA3-1	Complete	AC190905
Z. mays	Poaceaae	ZmHMA3-2	Complete	AC190905
Z. mays	Poaceaae	ZmHMA3-3	Complete	AC205008